**Technical Report 242**




# AUTOMATED WEATHER SUPPORT

## PROCEEDINGS OF THE 6th AWS TECHNICAL EXCHANGE CONFERENCE, U.S. NAVAL ACADEMY 21-24 SEPTEMBER, 1970





PUBLISHED BY
AIR WEATHER SERVICE (MAC)
UNITED STATES AIR FORCE
APRIL 1971

# FOREWORD

These pages contain the proceedings of the Sixth of the Technical Exchange Conferences sponsored by the Air Weather Service and hosted by one of the three armed services on a rotation basis. This sixth conference was hosted by the U. S. Naval Weather Service Command in the historic setting of the U. S. Naval Academy grounds at Annapolis, Maryland, during the period 21 - 25 September 1970.

The purpose of this series of conferences is to bring together operational specialists and a distinguished group of research and development experts in order to focus their attention on a facet or problem area within the broad spectrum of aerospace environmental support. The subject addressed by the 1970 conference was restricted in scope. This permitted an in-depth examination of a most important and challenging problem of the weather services: namely, how best to employ computers and automation in weather operations and particularly, how to resolve the thorny question of the optimum "man-machine mix."

The Welcome, Response, and Keynote Addresses of Captain Cook, General Best, and Captain Kotsch set the stage for a most profitable conference. The conference was divided into six separate sessions in which a total of 25 invited papers were presented. These sessions dealt with the following subject areas: Automated analysis and forecasting, Local area forecasting, Tailored meteorological support, Automated processing and application of satellite data, and Environmental simulation. The sixth and final session was devoted to a panel discussion on Automated meteorological support. This panel, chaired by Dr. Karl Johannessen, proved to be a stimulating and innovative finale for the conference

One of the highlights of this conference was the Banquet Address delivered by the Honorable Charles McC. Mathias, Jr., U. S. Senator from Maryland. In his remarks to the conference, Senator Mathias stressed the increasing importance of the rational use of our national resources and commended the assembled conferees on their collective efforts to better observe, understand, and predict one of our valuable environmental resources.

The publication of these proceedings is important for all the attendees and others in the environmental services community. It provides the opportunity to digest carefully the valuable insights and details of work in progress and reported on at the conference. In some cases, the work reported has not appeared in any other publication. A summary by Dr. Fletcher of the highlights of the presentations appears at the end of the report.

The hospitality and use of the facilities of the U. S. Naval Academy are gratefully acknowledged. Mr. Max Edelstein of Headquarters, Naval Weather Service Command, was of immeasurable assistance in the many onerous details of planning and arranging for the conference.

EDWARD O. JESS, Colonel, USAF
Director, Aerospace Services Directorate
DCS/Aerospace Sciences

Distribution: "F" plus Special

TABLE OF CONTENTS


| | Page |
|---|---|
| INTRODUCTORY COMMENTS - Capt Murray C. Cook, Dir, Div of Math and Science, USN Academy | 1 |
| RESPONSE TO WELCOMING ADDRESS - Brig Gen William H. Best, Jr., Commander, USAF Air Weather Service | 3 |
| KEYNOTE ADDRESS - Captain William J. Kotsch, Commander, Naval Weather Service Command | 5 |
| SESSION I - Automated Analysis and Forecasting (Chairman - Colonel Edward O. Jess, Hq Air Weather Service) | |
| Evolutionary Changes in the NMC Primitive-Equation Model and Plans for Future Models - Dr. John D. Stackpole, National Meteorological Center | 9 |
| Fleet Numerical Weather Central's Four-Processor Primitive Equation Model - Lieutenant Philip G. Kesel, Fleet Numerical Weather Central and Frank J. Winninghoff, Naval Postgraduate School | 17 |
| Spectral Models for Global Analysis and Forecasting - Major Thomas W. Flattery, Air Weather Service | 42 |
| Some Primitive-Equation Model Experiments for a Limited Region of the Tropics - Prof R. L. Elsberry and Lt Commander E. J. Harrison, Jr., Naval Postgraduate School | 55 |
| Air Force Global Weather Central Boundary-Layer Model - Lt Colonel Kenneth Hadeen, Air Weather Service | 72 |
| Diagnoses and Prediction of Marine Boundary-Layer Mesoscale-Wind Phenomena - R. V. Cormier and E. C. Kindle, Naval Weather Research Facility | 98 |
| SESSION II - Local Area Forecasting (Chairman - Captain John H. Negele, Naval Weather Service Command) | |
| Predictability of Local Weather - Charles F. Roberts, Forest Service, U. S. Dept of Agriculture | 112 |
| Objective Meso-Scale Analysis of Upper-Air Winds in SEASIA - Marvin J. Lowenthal, U. S. Army Electronics Command | 124 |
| The Development of Automated Short-Range Terminal Forecasting Using Analog Techniques - Lieutenant Carl D. Thormeyer, Fleet Numerical Weather Central | 130 |
| Application of PE-Model Forecast Parameters to Loca-Area Forecasting - Leonard W. Snellman, Weather Bureau Western Region | 151 |
| Preliminary Results of a Program for the Automation of Terminal Forecasts - Harry R. Glahn and Roger A. Allen, Techniques Development Laboratory, ESSA/Weather Bureau | 169 |

Page

SESSION III - Tailored Meteorological Support
(Chairman - Mr. Marvin Diamond, U. S. Army Electronics Command)

An Approach to Automated Support to Field Army Operations - James F. Appleby, U. S. Army Electronics Command 177

Numerical Products as Specific Operational Forecasting Aids - Earl C. Kindle, Richard L. Crisci, and Joseph T. Schafer, Naval Weather Research Facility 183

An Automated Program to Produce and Update Computer Flight Plans - Captain Robert J. LaSure, AFGWC, Air Weather Service 202

Meteorological Support to White Sands Missile Range - Harold M. Richart, U. S. Army Electronics Command 214

The Use of Computer Products in Severe-Weather Forecasting - Robert C. Miller (Colonel, Ret) and Lt Col Arthur Bidner, AFGWC, Air Weather Service 224

SESSION IV - Automated Processing and Application of Satellite Data
(Chairman - Mr. Chankey Touart, Air Force Cambridge Research Laboratories)

Processing of ITOS Scanning Radiometer Data - C. L. Bristor, National Environmental Satellite Center 232

Thoughts on the Second Decade of Navy Satellite - Data Applications - Commander Kenneth W. Ruggles, Navy Weather Research Facility (Project FAMOS) 243

Application of Satellite Data to an Automated Nephanalysis and Forecasting Programs - Major Ralph W. Collins and Major Allen R. Coburn, AFGWC, Air Weather Service 248

The Applications of the Nimbus Meteorological Satellite Data - Lewis J. Allison, Goddard Space Flight Center, NASA 261

Automated Production of Global Cloud-Climatology Based on Satellite Data - Major Donald B. Miller, USAFETAC, Air Weather Service 291

SESSION V - Environmental Simulation
(Chairman - Dr. Lawrence G. Roberts, Advanced Research Projects Agency)

Climate Modification and National Security - Dr. R. R. Rapp, The Rand Corporation 307

Simulation of Ecological Systems - Prof Amos Eddy, Dept of Meteorology, University of Oklahoma 311

Simulation of Weather Sensitive Military Operations - Ralph E. Huschke, The Rand Corporation 323

Environmental Simulation in Air - Pollution Control - George C. Holzworth, National Air Pollution Control Administration 338

Numerical Simulation of Hurricane Development and Structure - Stanley L. Rosenthal, Richard A. Anthes, and James W. Trout, ESSA/National Hurricane Research Laboratory 349

SESSION VI - Panel on Automated Meteorological Support
(Chairman - Dr. Karl Johannessen, Associate Director of Weather Bureau/ESSA)

Prepared Answers to the Set Questions 371

Questions or Comments from the Floor 379

SUMMARY COMMENTS - Dr. Robert D. Fletcher, DCS/Aerospace Sciences, Hq Air Weather Service 382

LIST OF ATTENDEES

Col J. P. Accola, USAF
Capt H. W. Albers, USN
Capt J. M. Alford, USAF
Mr. L. J. Allison, NASA
Mr. J. F. Appleby, USA
Capt C. L. Armstrong, USN
Capt W. S. M. Arnold, USN
Lt J. A. Ashby, USAF
Capt J. P. Ashman, USAF
Maj G. D. Atkinson, USAF
Mr. W. Baginsky, USAF
Mr. J. V. Bassett, USAF
Lt Col K. Bauer, USAF
Mr. R. E. Beck, ESSA
Lt W. N. Benedict, USAF
BGen W. H. Best, Jr., USAF
Capt F. H. Bowers, USAF
Mr. D. D. Bowman, USAF
Mr. C. L. Bristor, ESSA
Cdr D. N. Brown, USN
Dr. J. A. Brown, Jr., ESSA
Maj D. G. Buck, USA
Sgt J. A. Byrnes, Jr., USAF
Mr. K. A. Campana, ESSA
Maj G. C. Carlson, Jr., USA
Mr. A. S. Carten, USAF
Lt Col R. C. Chabot, USA
LCdr E. M. Chase, USN
Mr. H. Chenkin, USN
Maj R. W. Collins, USAF
Mr. W. Collins, ESSA
Mr. R. V. Cormier, USA
LCdr W. N. Cottrell, USN
Lt Col W. Cummins, III, USAF
Mr. A. R. Davis, USAF
Mr. H. O. Davis, USN
Mr. V. J. Descamps, USAF
Capt R. E. DeMichaels, USAF
Mr. A. J. Desmarais, ESSA
Capt N. Detsis, USAF
Mr. M. Diamond, USA
Mr. D. R. Dickson, Univ of Utah
Capt J. Diercks, USAF
Capt C. Dobrot, USAF
Dr A. V. Dodd, USA
Mr. N. L. Durocher, NASA
Mr. D. J. Eddleman, ESSA
Prof. A. Eddy, Univ of Oklahoma
Mr. M. W. Edelstein, USN
Asst Prof R. L. Elsberry, USN
Mr. B. Falzgraf, USAF
Cdr D. M. Farris, USN
Capt J. L. Fenix, USAF
Mr. D. D. Fenn, USAF
Lt. M. E. Fiore, USAF
Dr. R. D. Fletcher, USAF
LCdr D. D. Frame, USN
Mr. J. M. Frosio, USN
Cdr H. A. Galio, Jr., USN
Col N. R. Galligar, USAF
Lt Col A. Gargiulo, USAF
LCdr P. H. Gatje, USN
Dr. R. A. Gentry, Univ of California
Dr. J. P. Gerrity, Jr., ESSA
Mr. T. Gladney, ESSA
Dr. H. R. Glahn, ESSA
Cdr T. J. Glancy, USN
Maj G. L. Glassburn, USAF
MSgt J. Grant, USAF
MSgt G. Grazier, USAF
Ltjg G. L. Greuling, USN
Mr. E. Gross, ESSA
Lt Col K. D. Hadeen, USAF
Prof. G. J. Haltiner, USN
Lt Col J. Hansen, USAF
Lt Col C. R. Harris, USA
Capt E. D. Heath, USAF
Maj K. F. Hebenstreit, USAF
Lt Col M. L. Hershberger, USA
Mr. P. L. Hexter, ESSA
Mr. J. R. Hicks, USA
Mr. R. Hirano, ESSA
Mr. W. B. Hocker, USN
Mr. G. C. Holzworth, NPCA
Lt Col J. J. Hope, USAF
Mr. R. L. Houghton, NASA
Mr. D. C. House, ESSA
Capt W. S. Houston, Jr., USN
Mr. J. G. Howcroft, ESSA
Maj J. P. Huddle, USAF
Cdr R. E. Hughes, USN
Mr. R. E. Huschke, RAND
Dr. C. E. Jensen, ESSA
Col E. O. Jess, USAF
Dr. K. R. Johannessen, ESSA
Mr. K. W. Johnson, ESSA
Cdr J. I. Johnston, USN
Sgt W. W. Jones, USAF
Mr. A. A. Karpovich, USAF
Col W. A. Keils, USAF
Cdr W. H. Keith, USN
Capt J. Kelly, USAF
Mr. R. Kelsey, USA
Lt Col C. D. Kern, USAF
Mr. J. L. Kerr, Dept of Interior
Lt P. G. Kesel, USN
Mr. W. C. Kincannon, USN
Dr. E. C. Kindle, USN
Cdr W. R. King, USN
LCdr R. G. Kirk, USN
Capt J. Klag, USAF
Dr. W. H. Klein, ESSA
Mr. S. J. Knight, USA
Capt W. J. Kotsch, USN
Col A. Kouts, USAF
Cdr A. C. Kranz, USN
Lt Col E. R. Kreins, USAF
Mr. A. D. Kurtz, USA

Capt R. J. LaSure, USAF
Mr. D. A. Lawson, USA
Mr. J. M. Lebedda, USA
Maj L. LeBlanc, USAF
Cdr T.A. Ledew, USN
Mr. M. J. Lowenthal, USA
Lt Col G. L. Luckenbach, USAF
Dr. D. E. Martin, St Louis Univ.
Mr. R. H. Martin, USN
SSgt J. B. Matejceck, USAF
Capt G. W. McCreary, USAF
Capt A. L. McNab, USAF
Dr. R. D. McPherson, ESSA
Mr. L. L. Means, ESSA
Mr. R. Miller, USAF
Col. R. C. Miller, USAF (Ret)
Maj D. B. Miller, USAF
Col D. B. Mitchell, USAF
Mr. L. V. Mitchell, USAF
Maj J. W. Moore, USAF
Capt M. B. Moreland, USN
Mr. C. E. Morrison, USA
Capt J. H. Negele, USN
Capt P. J. O'Reilly, USAF
MSgt W. B. Owings, USAF
Ens J. S. Partesius, USN
TSgt V. L. Patterson, USAF
Mr. A. D. Peterson, USAF
Maj G. Peterson, USAF
Capt G. N. Petregal, USAF
Mr. W. Phillips, UNIVAC
Mr. P. D. Polger, ESSA
Lt Col T.D. Potter, USAF
LCdr R. K. Prien, USN
Cdr P. G. Prokop, USN
Mr. R. T. Quinlan, ESSA
Mr. R. R. Rapp, RAND
Maj M. Reid, USA
Lt Col G. C. Reiter, USAF
Mr. J. Restivo, USAF
Dr. D. F. Rex, NCAR
Mr. O. E. Richard, USAF
Capt T. L. Rish, USAF
Dr. L. G. Roberts, ARPA
Lt Col W. D. Roper, USAF
Dr. S. L. Rosenthal, ESSA
Cdr K. W. Ruggles, USN
Mr. J. D. Rustenbeck, USA
Cdr L. C. Samples, USN
Lt Col R. Sabin, USAF
Mr. M. H. Schefer, USN
LCdr W. Schramm, USN
Mr. M. Schroeder, USA
Lt P. G. Shapin, USAF
Maj E. Shibata, USAF
Dr. F. G. Shuman, ESSA
Lt Col A. L. Shumbera, USAF
Maj J. O. Siebers, USAF
Mr. J. Siderman, USA
Dr. R. H. Simpson, ESSA
Mr. D. H. Slade, AEC
Mr. A. Smith, Jr., ESSA
Mr. L. W. Snellman, ESSA
Mr. I. Solomon, USAF
Capt W. L. Somervell, USN
Mr. G. R. Spalding, USN
Mr. J. D. Stackpole, ESSA
Maj T. E. Stanton, USAF
Col R. J. Steele, USAF
Mr. R. G. Stone, USAF
Lt H. D. Story, USN
Lt Col J. N. Sullivan, USAF
Dr. D. M. Swingle, USA
Cdr R. F. Thomas, USN
Lt C. D. Thormeyer, USN
Mr. C. N. Touart, AFCRL
Capt C. Tracy, USAF
Capt B. D. Underwood, USAF
Cdr L. J. Underwood, USN
Dr. T. Vonderhaar, Colorado State Univ
Capt J. R. Walton, USAF
LCdr R. C. Warren, USN
TSgt R. L. Williams, USAF
Cdr W. E. Willingham, USN
Lt Col S. R. Withrow, USAF
Capt P. M. Wolff, USN
Lt E. L. Worsham, USAF
Mr. M. J. Young, USAF
Dr. M. A. Alaka, ESSA
Col. Howard G. Allbee, USAF
Mr. P. W. Allen, ESSA
Mr. Leo Alpert, USA
Mr. Sumner Barr, Drexel University
Mr. C. S. Barrientos, ESSA
Mr. L. Belanger, General Dynamics
Mr. R. J. Bermowitz, ESSA
Col. J. M. Bird, USAF
Mr. J. R. Bocchieqi, ESSA
Mr. E. Bollay, EG & G
Lt Col W. R. Brett, USAF
Lt Col W. I. Caristensen, Jr., USAF
Mr. P. F. Clapp, ESSA
Maj Allen R. Coburn, USAF
Mr. H. B. Cole, ESSA
Dr. D. S. Cooley, ESSA
Mr. T. C. Council, FAA
Mr. K. S. Durham, USAF
Lt Col R. C. Erickson, USAF
Mr. C. R. Dunn, ESSA
Col. J. M. Dunn, USAF
Cmdr. E. J. Fischer, USN
Maj. T. W. Flattery, USAF
Capt R. J. Fleming, USAF
Lcdr D. D. Frame, USN
Mr. J. M. Frosio, USN
Lcdr H. A. Galio, Jr., USN
Mr. J. B. Galipault, Profile Inc.
Mr. J. G. Gamble, FAA
Lcdr P. H. Gatje, USN
Col. L. A. Gazzaniga, USAF
Mr. F. Godshall, ESSA
Cmdr G. D. Hamilton, USN
Mr. G. A. Hammons
Capt P. J. Havanac, USAF
Lt Col M. L. Hershberger, USAF
Mr. Arthur Hilsenrod, FAA
Mr. F. L. Horning, USA
Dr. F. House, Drexel University

Col. A. R. Hull, USAF
Capt. J. A. Jepson, USN
Mr. J. D. Johnson, USCG
Mr. J. Keating, Mitre Corp
Mr. James E. Demper, ESSA
Mr. J. J. Keyser, USN
Mr. A. F. Korte, ESSA
Dr. C. W. Kreitzberg, Drexel Univ.
Mr. M. H. Kulawiec, ESSA
Mr. Frank Lewis, ESSA
Dr. F. Y. Lin, St. Louis Univ.
Capt. F. J. Luna Jr., USAF
Mr. F. V. Melewicz, FAA
Mr. H. Michael Mogil, ESSA
Maj. G. Mushalko, USAF
Dr. T. H. R. O'Neill
Mr. F. P. Ostby, ESSA
SSgt. J. M. Park, USAF
Col. J. W. Park, Jr, USA
Lcdr L. J. Pingel, USN
Mr. J. Pinkerton, Drexel Univ.
Mr. M. Plattner, USAF
Mr. N. A. Pore, ESSA
Lcdr A. W. Pruitt, USN
Capt. J. W. Purdom, USAF
Mr. R. M. Reap, ESSA
Mr. H. M. Richart, USA
Mr. C. Roberts, Forest Service
Mr. W. Cary Robinson, USA
Lcdr J. W. Robinson, USN
Cmdr. F. J. Schatzle, USN
Mr. R. S. Seaman
Mr. Warren Smith, ESSA
Mr. A. E. Snider
Mr. R. L. Sorey, ESSA
Mr. J. F. Sowar, FAA
Mr. K. C. Spengler, AMS
Mr. W. C. Spreen, ESSA
Mr. R. Talley, USA
Capt. J. L. Thomas, USAF
Mr. P. F. Twitchell, USN
Dr. H. M. E. Van de Boogarard, NCAR
Mr. J. C. West, USN
Mrs. F. L. Whedon, ESSA
Mr. Scott L. Williams, ESSA
Mr. R. J. Younkin, ESSA
Mr. W. W. Vaughan, NASA
Mr. A. H. Murphy, Univ. of Michigan

# INTRODUCTORY COMMENTS TO THE METEOROLOGICAL TECHNICAL EXCHANGE CONFERENCE ON 21 Sep 1970

Captain Murray C. Cook

Director, Division of Mathematics and Science, USNA

Thank you, Captain Armstrong.

General Best, Captain Kotsch, Distinguished Guests. On behalf of the Superintendent, Vice Admiral James Calvert, it is my pleasure to welcome you to the United States Naval Academy and the start of the Sixth Annual Meteorological Technical Exchange Conference. It is our hope that you will have an interesting and productive conference during your four-day stay. And, judging from the agenda which I have seen, it will indeed be a most interesting conference; the productivity is up to you. If this beautiful weather is any indication of your capability, the conference will also be quite productive.

I personally feel there is a very strong need for the continuing exchange of information--in conferences such as this--between people working in the same field at different locations. This is particularly true among the services, although the need is just as great in our society as a whole, and within each of the individual services. Reading something in the technical journals is just not the same as discussing the matter with the people involved.

Just this past Saturday, on the way up to a very unpleasant afternoon at Penn State (like Navy being on the short end of a 55-7 football stick unpleasantness), the ex-Air Boss of the Shangri La and I were recalling the many occasions during our naval careers when we had visited other activities and found that: on occasion, they did things in a way which was superior to the way in which we were doing them; on occasion, they did things in a way which was inferior to the way in which we were doing them; and sometimes they were doing things which we were not doing at all. Regardless of the outcome, the visit always ended with each of the participants gaining from the exchange of information.

The Naval Academy, in its one hundred twenty-fifth year as an academic institution--dedicated to the development of professional Navy and Marine Corps officers--is also very much interested in the exchange of information. The Naval Academy has always had a strong interest in the field of meteorology. From the time the discipline first became identified as a discrete science, meteorology has been a required part of the instruction of midshipmen at the Naval Academy. Although meteorology is not offered as one of our 24 majors, it is offered as an option to the oceanography major. You might be interested to know that roughly one-eighth of the entire brigade are oceanography majors.

For those students majoring in oceanography, even though they may not be in the meteorology option, there is a requirement to take a minimum of two courses in meteorology—a course in general meteorology and a course in environmental dynamics. In our undergraduate program in oceanography we consider the air-ocean environment as a continuum—from the medium of the hydrosphere, through the surface interface, to the less dense medium of the atmosphere—and investigate the interactions within that continuum.

Those students who do not major in oceanography are introduced to the subject of meteorology through a Fundamentals of Naval Science course in which one-sixth of the course is devoted to a study of the air-ocean environment. Subsequently, the midshipmen have an opportunity to observe the collection and dissemination of meteorological data, and the various means by which this is accomplished, during their at-sea training periods.

We encourage our oceanography majors—after they leave the Naval Academy—to participate in a meteorological and oceanographic observation program, especially if they happen to be assigned to a ship in which there is not a regularly assigned aerologist or oceanographer. Fortunately, they have not been expected to interpret the data and make local area forecasts—a topic which I note is in the agenda for tomorrow morning. I would venture that this subject has about an

80 percent chance of being the most difficult topic of the conference to pin down. I hope you have invited the Weather Board Girls from the local TV stations for this discussion, although I will have to admit that they have been doing better of late. Perhaps it is because we have been in a stable air mass.

Looking into the not too distant future, I can envision the day when we will have an array of sensors permanently installed in all major metropolitan areas, and on major combatants. These instruments will sense the parameters which affect local meteorological conditions and feed the information to a computer where it will be matched against a bank of historical data, and a 100 percent reliable forecast coughed out automatically.

However, I can also see that, just when such a program starts to come to fruition, those meteorologists who are working on another of your agenda items—climate modification—will make a break-through and then it will be back to the drawing boards in the forecasting business.

In reviewing the agenda for the conference, I was surprised to note that you have not included anything on the physiological aspects of meteorology. I have had a little personal experience in this area, but I don't have an answer for a problem which I observed. On every occasion in which I have been deployed to WESTPAC aboard an aircraft carrier, I have noted a strange anomaly. When a pilot would return from a flight on a balmy, sunny day, he would report his squadron call sign, the side number of his aircraft, the fact that he had the "meatball" in sight, and his fuel state in an even, steady voice. Invariably, however, when the same pilot would return to the carrier on a dark, rainy night, with the deck moving all over the place, his voice would be two to three octaves above its normal level. As I said, I can't solve that one; but I guess it must have something to do with the rarefied air which he was flying through, coming down the glide slope on a dark, rainy night. I will leave that one for you to solve.

Well, you are already fifteen minutes into your conference and still on schedule, which is a good start. Once again, welcome to the Naval Academy. If there is any way that the staff may be of assistance, do not hesitate to let us know. LCDR Pete Gatje is our liaison officer for this conference and will be glad to help you with any problems which you may have. Thank you.

Brigadier General William H. Best, Jr.
Commander, USAF Air Weather Service

Thank you, Captain Cook, for your kind words of welcome. These annual meetings with our sister meteorological services have become one of the high spots of the year for us in the Air Force Weather Service. And certainly, our meetings on Navy territory have been among the most memorable and pleasant.

It is always profitable for us in the Air Force to discuss our common problems with our ground- and water-borne colleagues. Though "meteorologists" differ from "aerologists" in name, we usually find ourselves facing the same problems in but slightly differing guises. Today the central problem for all our services is to reconcile the growing gap between expanding tasks and diminishing resources. We are into new and heretofore esoteric areas: weather modification, space environmental support (with "space" defined as beyond 50 km), atmospheric sampling, to name a few. At the same time, we find that we must support sophisticated automated command control systems without downgrading the personal attention to individual decision-makers that must be the hallmark of a military environmental service. Moreover, we must solve these problems with fewer dollars and people.

Mechanisms have evolved to meet these challenges. Some are based on a judicious division of functions between man and machine, alloting to each the job he does best. As an inevitable consequence, we have each brought more and more of our mechanized functions to one or a few physical locations to make cost-effective use of scarce and expensive resources. Thus these two ideas -- automation and centralization -- have been guiding forces of operational meteorology in the last decade. It is therefore appropriate that as we face a new decade we address ourselves to them once again.

But the austerity of the 1970's must emphasize yet another idea. Faced by similar problems and common poverty, all our services must continue to conscientiously seek ways in which resources and expertise can be shared to enable each to perform its unique functions better and at less cost. Many examples come to mind, already existing, as evidence that this can be done:

1. As proposed by the Naval Weather Service there will soon be a computer-to-computer link between the Fleet Numerical Weather Central at Monterey and the Air Force Global Weather Central at Offutt.

2. We now have an exchange of officers between Monterey and Offutt, with two Navy aerologists at GWC and two Air Weather Service meteorologists at Monterey. Commander Morford was Project Officer on AFGWC Manual 105-1, our Products Manual. He was a natural for this task because the Navy has traditionally produced outstanding manuals.

3. At the Joint Typhoon Warning Center on Guam, AWS and NWS personnel work jointly.

4. In the Pacific we use Pearl Harbor products to support Air Force flight operations, products that come to our units on Guam and Hickam through extensions of the Naval Environmental Weather Data Network (NEDN).

5. In the D. C. area, the Naval Weather Service handles autodin traffic for my AWS units.

6. Our automated weather network (AWN) distributes weather data for the nation. Among other things it keys fleet weather broadcasts from Norfolk, Alameda, Rota, Sangley Point and Yokosuka. Navy now has a liaison officer at our AWN hub at Carswell to coordinate Navy requirements supported by this Air Force communications system.

Nor are cooperative programs limited to the Air Weather Service-Naval Weather Service interface:

1. With ESSA and the Navy we have a joint manual on satellite data interpretation.

2. Our Solar Forecast Center at Colorado Springs has access to ESSA Research Laboratories' time-share 940 computer at Boulder.

These are only a few examples of arrangements that are cost-effective. And they do not usurp organizational responsibilities and prerogatives.

Now with these proven accomplishments, when a Congressman or a Congressional investigator says, "Why do we have all these 'overlapping, duplicating weather services?'" our answer should be an explanation of the unique requirements each of us faces, and how we are cooperating (and succeeding) to avoid unnecessary redundancy and duplication.

In this connection, it is interesting to read the Fitzhugh Blue Ribbon Defense Panel Report, examining the organization and management of the DOD, which was submitted to President Nixon in July. In the letter of transmittal, Mr. Fitzhugh wrote, "The Panel found many things that we believed should be corrected, but believes, and I agree, that many of the difficulties result from the structure of the Department of Defense itself, which almost inevitably leads people into 'adversary' relationships rather than toward cooperation in the interest of the department — and the Nation — as a whole. /Speaker's underline./ I hope the Panel's recommendations will not be considered criticisms of individuals, but will help to restructure the department and 'the bureaucracy' so that the talent and dedication of the fine people, both military and civilian, can be unleashed and redirected to accomplish more effectively the basic objectives of the Department of Defense and the Nation."

The changing pattern of functions within each of our services and the increasing number of shared activities between us reemphasize the complexity of environmental support functions today. No aspect of this support is more replete with potentials and pitfalls than the subject of our conference this week -- Automated Meteorological Support. The most cursory inspection of this theme boggles the mind with questions and ideas. Who automates? What do we automate? Do we allocate computers one per forecaster, one per service, or one per nation? The first and last alternatives are probably equally wrong for different reasons. But in between lies a universe of tradeoffs subject to cold, hard analysis. In these days when our decisions are increasingly subject to objective scrutiny by the watchdogs of the public purse, and rightly so, our decisions can stand only if they are the consensus of our organizations, not merely the Utopian "druthers" of one or another isolated group of staff planners.

Clearly we cannot hope to plot the entire future course of our discipline in these few short days. But I hope that the presentations and discussions will bring us all closer to a common understanding of our common problems. Automation, centralization, and cooperation mean more than hardware, rooms full of light tables, and smoky committee rooms. They are ideas. And as Alfred North Whitehead wrote, "Ideas won't keep. Something must be done about them."

KEYNOTE ADDRESS
FOR THE
1970 METEOROLOGICAL TECHNICAL EXCHANGE CONFERENCE

Captain William J. Kotsch

Commander, Naval Weather Service Command

Captain Cook, General Best, distinguished guests and fellow meteorologists:

It is my pleasure and privilege to expound on the theme of the Sixth Technical Exchange Conference sponsored this year by the Naval Weather Service Command, and hosted by the United States Naval Academy. As most of you know, these conferences were conceived by the Air Weather Service, and are being conducted annually to promote the exchange of information within the Department of Defense concerning new developments and techniques in meteorology. Participation by other government agencies and the academic community is also encouraged. This year our subject is "Automated Meteorological Support". I propose to discuss the history of this topic briefly, and provide you with recent examples of what the Air Force, Army and Navy are doing in this challenging field. Then I will venture my personal views as to where we in the Department of Defense should emerge at the end of this decade employing the "man-machine mix" concept of environmental support.

Nearly fifty years ago Richardson published his famous monograph, "Weather Prediction by Numerical Process". Although at that time the basic principles underlying numerical weather prediction were known, manual computations lasting several months were necessary for each forecast. Due to imperfections in the early model, the results were often grossly in error. Twenty years ago Charney, Fjortoft and Von Newmann published the first successful numerical predictions using Rossby's model. The success of these experiments resulted in the formation of the Joint Numerical Weather Prediction Unit (JNWP) which was established in 1954 and staffed by many of you here from the Air Force, Navy and Weather Bureau.

One year later, in 1955, routine operational numerical products were produced by JNWP. In the ensuing fifteen years, there have been many advances and changes. To meet specialized and unique military requirements, the Air Force Global Weather Central at Offutt, and the Navy Fleet Numerical Weather Central at Monterey, were established. Meanwhile the Weather Bureau's National Meteorological Center at Suitland has continued to provide basic numerical weather products for the nation.

We have witnessed many other major advances since the establishment of these three major numerical weather centrals. First, there has been a rapid growth in computer power -- from the first generation computers used in the mid 1950s to the third and fourth-generation computers now in use, or programmed in the near future. Next, we have seen a significant growth in our observational networks and data-gathering systems. Ground based, aircraft and ship reports have improved both in quantity and quality. The explosive input of our newest data source, the meteorological satellite, has threatened to swamp even the most sophisticated computer envisioned in this decade. Other new data sources are evolving, employing such new technology as lasers and infra-red sensors. We are measuring input from solar activity, and are making better use of oceanographic observations in recognition of the interdependence of the motions of the air and the sea. Keeping pace with these many advances, vastly improved numerical models have evolved, and even better ones are in the offing.

I note from the outstanding program of papers to be presented during this conference, that all of these factors will be discussed in detail. However, there is one facet that I would like to elaborate upon which relates directly to the theme of our meeting, "Automated Meteorological Support". The conotation of this theme, as applied to the Air Force, Army and Navy, can best be explained by discussing recent programs of these three services where automation of meteorological predictions is integral to the support of aircraft, missiles and ships.

For my first example, the Air Force Global Weather Central has developed a route forecast model. This integrated package of computer programs is designed to simulate the response of an aircraft

to the environmental conditions likely to occur during a given flight. The model uses forecast data which have been pre-computed and stored within the Global Weather Central's data base.

The customer provides essential data elements, such as flight altitude, true air speed and time of departure. Using the stored data base of forecast environmental conditions for the track and time period, the route-forecast model prints out a prediction along the aircraft's route. Nearly fifty meteorological and navigational parameters can be specified at each leg point, and, in addition, segment summaries may also be made. Meteorological parameters which can be printed out include: wind direction and speed, wind factor, accumulated wind factor, temperature, d-value, accumulated temperature deviation, density altitude, base and top of contrails, and tropopause height and temperature.

Time, distance, true course, magnetic heading, sun angle, air distance, gross weight and fuel are a partial list of the available navigational options.

The route forecast model provides maximum support for the user. It is available in near real-time on a global basis and incorporates flexibility, timeliness and responsiveness. Any requestor: Command Control Center, Aircrew or Weather Detachment, can be provided operational forecasts of pertinent meteorological elements. By including navigational data, the program will provide complete tailored forecasts for any Air Force flight.

As a second example, The U. S. Army Electronics Command Atmospheric Sciences Lab. at White Sands Missile Range has under development a prelaunch real-time impact prediction system for unguided rockets. Most of these missiles, such as the Athena, Arpat, Little Joe-2 or Aerobee-350, are fin-stabilized, therefore turn into the wind during their burning phase. The amount of turning, or wind sensitivity of the rocket, is a major factor in trajectory and impact prediction.

To obtain real-time data input for impact prediction, a new generation automatic data collection and processing system has been developed. The system includes a 500-foot wind tower, three automatic (T-9) radars, three FPS/16 radars, a gun probe system, a vacuum launcher system and associated digital computers and high speed printers.

The 500-foot tower is instrumented at eight levels. Measurements obtained include data which are edited and programmed to retain the latest sixty seconds of tower data for wind calculation procedures. The T-9 radars track parachutes in the 500- to 20,000-foot region. These parachutes are delivered at points in space close to the rocket trajectory by means of a vaccum launcher. To obtain winds above 20,000 feet, three FPS/16 radars are used to track simultaneously deployed parachutes from 200,000, 100,000 and 50,000 feet. A gun probe is used to place the parachutes at the three FPS-16 altitudes. By the use of vacuum launchers and gun probes, it has been possible to decrease count-down time to 100 minutes -- instead of the 280 minutes formerly needed when raobs were used.

The impact prediction system has many advantages: The number of rockets which must be "cut down" for safety reasons should be reduced — there should be a decrease in the number of cancellations due to meteorological conditions — the cost of each firing should be minimized — and there should be an increase in the number of rockets which can be safely fired in a given time period.

For my third example, the Naval Environmental Watch System (NEWS) has been developed to provide a capability, within the Naval Weather Service Command, to automatically and continuously monitor and forecast environmental factors affecting operational capabilities of surface ships under U.S. Navy control anywhere in the world's oceans. The first phase - the "NEWS" program is now operational at Fleet Weather Central Pearl Harbor. All U.S. Navy, U.S. Coast Guard, Military Sealift Command, and Navy contract ships operating in the Pacific Ocean are monitored by the operational "NEWS" program.

Inputs to the "NEWS" program consist of ship locator files on magnetic tape provided by the Pacific Fleet Operations and Control Center — and grid fields of environmental parameters for the latest synoptic time — and for the next forty-eight hours — provided by the Fleet Numerical Weather Central.

The outputs of the system consist of a computer prepared plot of the current positions of all ships underway in the Pacific, and their expected positions every twelve hours for the next sixty hours. There is also a printout of the name and designator, position of departure point, latitude and longitude of destination, course and speed, date-time-group of the latest ship

movement report received. Present ship's position and positions every twelve hours for the next forty-eight hours are listed — and the environmental conditions at the present position, and those forecast to exist at future positions, are computed. An alert list depicts all ships that are forecast to encounter winds in excess of twenty-five knots — or a combined sea height in excess of ten feet — or visibility of one mile or less during the next forty-eight hours. The computer also prints out a plain-language message giving the range of conditions forecast for the next twenty-four hours for all ships that have requested enroute weather forecasts — as well as forecasts for all Pacific Ocean Station Vessels and selected Pacific Islands for the next forty-eight hours.

The environmental parameters included in the "NEWS" output are degree of cloud cover or precipitation, visibility, surface wind direction and speed, wave height, swell direction and height, and combined sea height and direction. At present the various programs that constitute the "NEWS" are all run on a computer at Fleet Weather Central Pearl Harbor. The basic steps are the "Navigate Section" — which computes ship's positions — The "Environmental Section" — which matches the ship's position with the appropriate Fleet Numerical Weather Central grid field and extracts the required environmental data — and the "Output Section", which formats and plots or prints the various outputs.

Future refinements will include a provision for using the latest weather report from the ships to correct their computed position and for comparison with the analysis fields for quality control purposes. The updated positions based on the weather reports will also provide input to the Fleet's ship locator files.

Before giving you my views as to the expected developments in the "man-machine mix" concept of environmental support, I would like to point out some of the similarities in the three programs I have just described. All three require the rapid collection and assimilation of very large quantities of data using automated weather network systems — supplemented by position data for the aircraft, missile or ship being supported. All three employ high speed computers for the data processing and analysis phase, and provide for skilled analysts to monitor the product. All three integrate the prediction of movement of the aircraft, missile or ship and couple it with the environmental prediction that is applicable in time and space. Once again the high-speed computer provides optimum service in this area. All three in the final link of the system of providing operational products to the consumer — the packaging and delivery phase — print out by message or chart — information which responds to a wide variety of situations and environmental conditions.

Looking ahead to the future, I do not envision any great changes in procedures for the first three phases of automated environmental support, namely collection of data, processing and analysis of data, and prediction. By this I do not mean that there will not be significant advances in these three areas. I am certain that improved data collection networks will evolve — communications satellites will undoubtedly play a key role in this program. Processing and analysis of data will progress as new computers gain in speed — and the models provided enable us to develop techniques for the mesoscale — and possibly some of the microscale — forms of analyses. Prediction will certainly advance with development of such models as the "Primitive Equation" where dramatic increases in hemispheric prediction accuracy have already become apparent.

However, it is in the packaging and delivery phase that I look for the most exciting advances. The packaging of synoptic analyses and prognoses is conveniently and rapidly performed by computers. Changes of projection and scale — interpolation of data at specific points — and preparation of messages — are simple operations on a computer. But to alter these operations so as to obtain a different projection, scale or interpolated point, a change in the program may be required. These changes are often extremely time consuming, and are not compatible with rapidly changing military operations. Although the majority of environmental support requirements are stable — very often the most important operational support is in response to an urgent one-time request for information — not immediately available or accessible in the computer. And it is not habit forming to advise a military Commander that "It will take two weeks to write a program for information that he wants right now". The responsiveness demanded by changing military commitments will, for a long time, require assignment of competent forecasters, together with adequate resources, close to the field of operations.

There is also the problem of the lack of the computer's personality. The human forecaster, in preparing forecasts for aircraft, missiles and ships and particularly for briefing a Commander

in planning a critical operation, adds that crucial ingredient which is completely lacking in the computer product — the personal touch. For example, in the NEWS program the forecasts are packaged in a standard form and transmitted to the ship — all of this is done without any human intervention. But alas, the forecasts have no charisma. They are completely sterilized of any personality. To use the forecasts, it has been found necessary for the forecaster to monitor and rework them. Then the Commanding Officer of the ship knows that some person back on shore is watching him and is concerned about his ship. Letters of appreciation are received every day for this extra touch, and it is not only due to forecast accuracy. The last sentence of a letter of appreciation recently received by one of our Pacific weather centrals reads, "It is certainly comforting to a ship of the Fleet to know that such total support is provided by the shore-based Navy".

In conclusion, I would like to reiterate that ours is a multi-faceted business which has its reward for a job properly performed — customer satisfaction. Just as the brilliance of a diamond is tarnished by a single dull facet, so also is our service derogated by poor quality in a single phase of the total production process. We must take care not to become so enraptured with the computers' impressive success in certain phases that we overextend it into those areas wherein its capabilities are limited or non-existent. Highly trained human forecasters will, for a long time to come, and certainly during this decade, be required to monitor, interpret, package, and deliver computer products. This requires that trained meteorologists closely oversee the operation of computers that perform analysis and prediction. It also requires that competent forecasters — with access to the complete line of computer products — be assigned in close proximity to primary customers. If we are to continue achieving our goal — the satisfaction of our customers — these manual functions must be accommodated in our grand design for tomorrow.

# EVOLUTIONARY CHANGES IN THE NMC PRIMITIVE-EQUATION MODEL AND PLANS FOR FUTURE MODELS

John D. Stackpole

National Meteorological Center, Washington, D. C.

## Abstract

Current developments in the NMC operational 6-layer forecast model are discussed with particular reference to the quantitative precipitation forecast section. The salient features of the proposed new NMC operational 9-layer global forecast model are discussed with particular reference to the development of the finite difference system.

## I. INTRODUCTION

That's a very long title which, even in its length, is perhaps a little misleading in its generality. My concerns here will be only with the current operational PE model (the 6-layer model as described by Shuman and Hovermale [1] in 1968 as amended since) and the current plans and stage of development of the model to replace the 6-layer model. Numerous other plans and models could be discussed — limited area models, implicit time differencing work, studies of various grids, spectral analysis and forecasting, etc. — but these, of course, will be left for those most involved with them to talk about.

Another possibly misleading element in the title is the use of *Evolutionary* — the root meaning "to roll out" is fine, implying one change following smoothly from another, but the strong connotation of progress and improvement in the rolling out process should not be assumed a priori.

A case in point is the development of the precipitation forecasting section of the 6-layer model and the associated vagaries, and this topic will constitute the initial portion of the present discussion.

## II. NUMERICAL QUANTITATIVE-PRECIPITATION FORECASTING

Those readers familiar with the vertical resolution of the current operational model (Fig. 1) will no doubt know that up until 00Z October 29, 1969 the QPF section of the forecast model had no resolution in the vertical — the quantity actually forecast was the total precipitable water (W) of the lowest three layers of the model.

The forecast equation was simply

$$\frac{\partial W}{\partial t} + \nabla \cdot W\tilde{\underline{V}} = 0 \tag{1}$$

where $\tilde{\underline{V}}$ was an appropriately weighted vertical mean wind combining the values of the three layers.

An obvious and quite evolutionary change was the introduction of a degree of vertical resolution in the precipitable water modeling. We then have an equation to forecast precipitable water in each layer:

$$\frac{\partial W}{\partial t} + \nabla \cdot W\underline{V} + \left( \frac{qp_\sigma}{g} \dot{\sigma} \right)_A - \left( \frac{qp_\sigma}{g} \dot{\sigma} \right)_B = 0 \tag{2}$$

where the new vertical advection terms involve the specific humidity q, pressure derivative $p_\sigma$, vertical velocity $\dot{\sigma}$ and gravity g, evaluated at the surfaces above (subscript A) and below (subscript B) the layer in question. Equation (2) is applied to each of the three lowest layers. Analogous to before with the single lamination of moisture, precipitation is assumed to form whenever the forecast W exceeds the saturated value $W_s$ for the layer. The amount of excess, $W-W_s$, is directly the amount of rain and indirectly the amount of latent heat released. The

latter, of course, is a contribution to the temperature forecast for the layer in which the condensation is modeled to occur.

With the laminated moisture, it is also possible to add further reasonable (evolutionary) changes, to wit: If an upper layer is saturated with precipitation forming while the layer below is not saturated, we can model evaporation and evaporative cooling by requiring the lower layer to become saturated, at the expense of the falling rain, before any rain can pass out through the lower layer. This cascade continues to the ground.

It also seemed that the introduction of the laminated moisture would be a good opportunity to delete the *reduced saturation* feature of the one layer model. This was the device that caused precipitation to begin to form at W values less than 100% of saturation, usually at 80% or 70% relative humidity.

These changes all seem quite reasonable, quite evolutionary if you will, and the unfortunately rather limited number of tests did nothing to discourage operational implementation.

The availability of forecasts of three layers of precipitable water, generally presented in terms of layer mean relative humidities, have proven to be quite useful. A number of Weather Bureau offices have devised local precipitation and cloud forecast techniques based on the laminated humidity information. Also, the forecasters at NMC have noted that the humidity forecasts they use, generally the mean humidity of all three layers together, have been as valuable in their more general guidance forecasting as the one layer model was, or more so.

The actual quantitative precipitation forecasting, as opposed to the relative humidity, however, has shown a bias to be too dry. A bias of this sort will have a pronounced effect upon typical precipitation verification scores such as the threat score — the ratio of the number of correctly forecast points to the sum of all the forecast and all the observed less the overlapped duplicates. Fig. 2 is a relatively long history of the 12- to 24-hour precipitation threat score for the PE model (marked PEP for Primitive Equation Precipitation) and the Techniques Development Laboratory SAM precipitation model [2]. The latter has been included as a control in that it has undergone no development since its inception. It's quite apparent that the score deteriorated on October 29, 1969 when the laminated model was initiated. There was just not enough rain falling from the model — this was substantiated by other scores not shown here, the bias in particular.

Our efforts since the time we realized the nature of the problem have been directed towards getting more rain out without unduly disturbing the relative humidities. Because of this last constraint, we initially avoided the relatively obvious rainmaking procedure of returning to the device of reduced saturation. The structure of the model was investigated carefully to see if there were physical or numerical processes neglected which if included would induce more rain.

Three interrelated rain sources were turned up and incorporated in the model:

1. The saturation precipitable water is computed every other timestep rather than hourly as previously done. This, in conjunction with Item 3 below, would allow for precipitation from air that was undergoing a short-term cooling and warming cycle.

2. The moist convective adjustment was expanded to include the boundary layer. In that the effect of such an adjustment would always be to cool the boundary layer, and possibly also the layer above it, this, in conjunction with Item 3, will augment the rain.

3. Orographically and convectively induced supersaturation was retained. If a layer in the model is cooled (by any means), its relative humidity, upon recomputation of the saturation precipitable water, will increase. In former procedures, any supersaturation that resulted was suppressed - this was for reasons of stability in the one-layer moisture model; with the elimination of this constraint, more rain can and indeed does fall from the model.

These changes were introduced 12Z March 19, 1970.

A fourth potential source of rain (at least for the first 24 hours or so of the forecast) was uncovered in the handling of the initial relative humidity analysis. The analysis is designed to give values of nearly 100% for areas of present observed rain. These are frequently small-scale. In the manipulations of the initial humidity analysis, to prepare it for the model's use, a considerable smoothing of the analysis occurred that reduced these small-scale areas to well below saturation. Thus, the model would fail to forecast rain even in its initial stages,

where precipitation was occurring at the initial time. By bypassing the smoothing procedure, a gratifying increase of rainfall was forecast in areas observed to be raining at the initial time. This procedure became operational 12Z June 1, 1970.

It is apparent from Fig. 2 that these changes have not had a clear cut effect upon the scores. It's rather difficult to draw firm conclusions because of the rather severe deterioration of the predictability of precipitation during the late spring and summer months - those who work with these scores suggest that we could well be in the noise level during these months.

Some bias still remained - more recently, we have redeployed the reduced saturation, this time setting it at 90% relative humidity. A reduced saturation is a physically reasonable thing - it's unlikely that an entire column of the atmosphere must reach saturation before precipitation may start - the only arbitrary item is the selection of the appropriate value for the reduced saturation. The most feasible way to determine this is to select a reasonable number and watch the subsequent operational performance of the model and the verification statistics. 90% was selected on the basis of the numerical value of the bias in the forecasts and on the physical basis that since the laminations of moisture are thinner than before the reduction of saturation need not be as severe. The use of 90% for saturation began 12Z September 8, 1970.

The concern over the precipitation sections of the model, although obviously important for its own right, is also of interest because these developments and any further ones are going to be carried over as directly as possible into the new operational model. This is obviously in line with the consciously evolutionary procedures being followed. To this model and its major changes, we shall now turn our attention.

## III. THE NEW NMC OPERATIONAL MODEL

As implied above, one of the guidelines for the development of the model to replace the currently operational 6-layer model is that of evolutionary continuity. We wish, therefore, to keep intact as much of the physics currently in the model as possible while making those changes required of us to meet new requirements placed upon NMC both as a national center and as the analysis and forecast arm of the Washington World Meteorological Center. This is not to say that research and development will take place only in response to outside requirements, but that resulting changes (internally or externally generated) will be introduced in as orderly a manner as possible.

This new model is intended to make it possible for NMC to take full advantage of the next generation of computers as soon as they are available. It also is designed to run on the currently available machines with only slight modifications of the original design. The overall plan is to complete the research and development work necessary to construct and use the model with the currently available machines and then move to the new with a minimum of trouble.

Even with the modifications necessary to run on current machines, the new model will offer an increase in both resolution and forecast domain over the present one - any forecast improvements will of course be welcomed. What then are the changes to be introduced in going from the current to the new model?

Two items in particular: the vertical resolution and the horizontal grid.

First, the vertical structure. With reference to Fig. 3, the principal changes are seen to be the addition of two more forecast information layers — one in the stratosphere allowing us to extend the top of the model to greater heights to accommodate possible aircraft flights up there, and one tentatively in the boundary layer. This latter is not final — we are planning to experiment with this layer also as a fourth troposphere layer or possibly doing away with the constant pressure thickness boundary layer altogether and having five troposphere layers, not necessarily of equal pressure thickness. The moisture computation will be in all five troposphere/boundary layers and is going to be in terms of q, specific humidity, rather than W, precipitable water, for reasons relating to the finite difference system. That's about all there is to say about the vertical resolution — the horizontal is something else again.

In order to meet our responsibilities as a World Meteorological Center, we should have a global forecast model. To accomplish this, we have left the polar-stereographic projection behind and after considerable experimentation with variations have settled on an even latitude-longitude finite difference grid with the equations of motion written in spherical coordinates. Initially, the forecast domain will be limited to the (entire) northern hemisphere with simple boundary conditions at the equator, e.g., symmetry, but the full global extension will present no problems, once machines with sufficient capacity and speed become available.

The first (and quite appropriate) question to ask is what about the pole point where, in spherical coordinates, terms such as

$$u \frac{\partial v}{r \cos \phi \partial \lambda}$$

$r$ = earth radius
$\phi$ = latitude
$\lambda$ = longitude

or

$$\frac{uv}{r} \tan \phi \text{ become infinite.}$$

The apparently successful resolution of these difficulties and other related ones is what Lloyd Vanderman [3] has accomplished in his design of a finite-difference system for the equations. The difference system and what is done at the pole are related — indeed doing what has to be done at the pole puts certain constraints on the form of the differencing system and is what motivated Vanderman to develop the particular form.

To see what's going on, consider a particular term such as

$$u \frac{\partial v}{\partial x} \qquad \partial x \equiv r \cos \phi \partial \lambda$$

If we use Shuman's finite difference notation, i.e.,

$$f_x = \frac{f_{i+.5} - f_{i-.5}}{\Delta x} \qquad \Delta x = r \cos \phi \Delta \lambda$$

$$f_y = \frac{f_{j+.5} - f_{j-.5}}{\Delta y} \qquad \Delta y = r \Delta \phi$$

$$\overline{f}^x = .5\left( f_{i+.5} + f_{i-.5} \right)$$

$$\overline{f}^y = .5\left( f_{j+.5} + f_{j-.5} \right)$$

the advection term goes over to

$$\overline{\overline{u}^x v_x}^y$$

and a typical metric term becomes

$$\overline{\frac{\overline{u}^x \overline{v}^y}{r} \tan \phi}^y .$$

The advective term here may be compared with what is used in the current polar stereographic model — the *semi-momentum* form:

$$\overline{u}^{xy} \overline{v_x}^y .$$

If we look at a grid box numbered thusly


we can write (disregarding the .5 and $\Delta x$ factors)

$$\overline{u}^{xy} \overline{v_x}^y \equiv [(u_1 + u_2 + u_3 + u_4)(v_2 - v_1 + v_3 - v_4)]$$

$$= \overline{\overline{u}^x v_x}^y + [(u_1 + u_2)(v_3 - v_4) + (u_3 + u_4)(v_2 - v_1)]$$

The latter terms, cross product terms, are what Vanderman neglects. This neglect, with the consequent change in the form of the advection term, is the first major element of the differencing system. The reasons for the neglect arise from the polar considerations.

These advection terms constitute a portion of the tendency terms $\partial u/\partial t$ etc., and are appropriately considered as belonging in the center of the box. Consider the particular case when the box we are looking at is the first box south of the north pole, i.e., points 3 and 4 are both pole points but at a slightly different longitude; here $v_x$ is infinite for the point 4 minus point 3 difference because $\Delta x$ is zero. To eliminate the infinity, the tendencies are averaged vectorially all around the pole for this particular grid box row. This is the second major element. A moment's consideration will show that this procedure causes all the infinite terms to add to precisely zero, provided that the u and v winds at the pole are but components of a single vector wind. This additional constraint represents the third major element of Vanderman's system. Note that if the cross product terms of the semimomentum form were retained, the infinite terms would not necessarily add to exactly zero (although there would presumably be considerable cancellation).

The means of obtaining the single polar vector wind must also be considered: we do not make a forecast of the wind(s) at the pole point(s) but instead specify the single vector wind at the pole as the vector mean of the v (northward) component wind previously forecast at all the points one row south of the pole. By using the locally northward components only, we satisfy at least intuitively a feeling for continuity of the wind structure across the pole.

The convergence of the meridians near the pole introduces another problem to be dealt with: the Courant-Friedrichs-Levy type instability. It is taken care of by the device of averaging the tendencies longitudinally over a distance on the earth equal to the distance between the grid latitude circles. The further north one goes the larger, in terms of longitude, is the average length. It is evident that this averaging will not always include an integral number of meridians — early tests indicated that it was absolutely essential to include the appropriate fractional portion of the ultimate tendency-containing grid box. A sketch may help to clarify this.

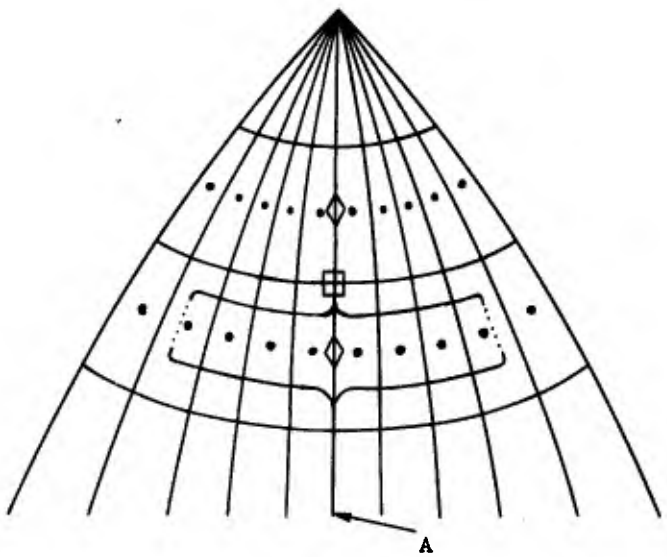


Fig. 4 Longitudinal Averaging of Tendencies

The dots · indicate the location of the computed tendencies which we wish to average to meridian A, the curly brackets the horizontal extent of the averaging, and the diamond ◇ the location of the result on the central meridian. Note in the sketch that the ultimate boxes are not completely enclosed in the averaging brackets — it is this fractional portion of which cognizance must be taken. After the east west averaging of the tendencies to the meridians, a simple north-south averaging of the ◇ values returns the tendencies to the grid points ( □ ) and the time step is complete.

The data source for the global or northern hemisphere model will be the spectral analyses described elsewhere in this volume by Major T. Flattery.

At present, the plans for initialization or balancing of the data are not specific - the spectral analysis procedure implies a wind-geopotential relationship of some sort and we can only tell by experimentation if further manipulation of the data will be necessary. In this line we have included capability for Euler-Backward time differencing as well as centered steps and are prepared for various self-adjustment procedures such as restoring the heights (or winds) after each time step to their prior values for an appropriate initializing period. All this will be subject to experimentation.

Other plans relating to further developments in the physics incorporated in the model are not lacking. We wish to include a long wave radiation calculation taking account of clouds, assuming a simple relationship between clouds and relative humidity; a radiative equilibrium calculation of surface temperature over land; perhaps some sort of stability dependent vertical diffusion to replace the rather abrupt convective adjustment currently in use; the precipitation process (our old friend) is not lacking in places for refinement; and so on.

There seems no lack of work to be done.

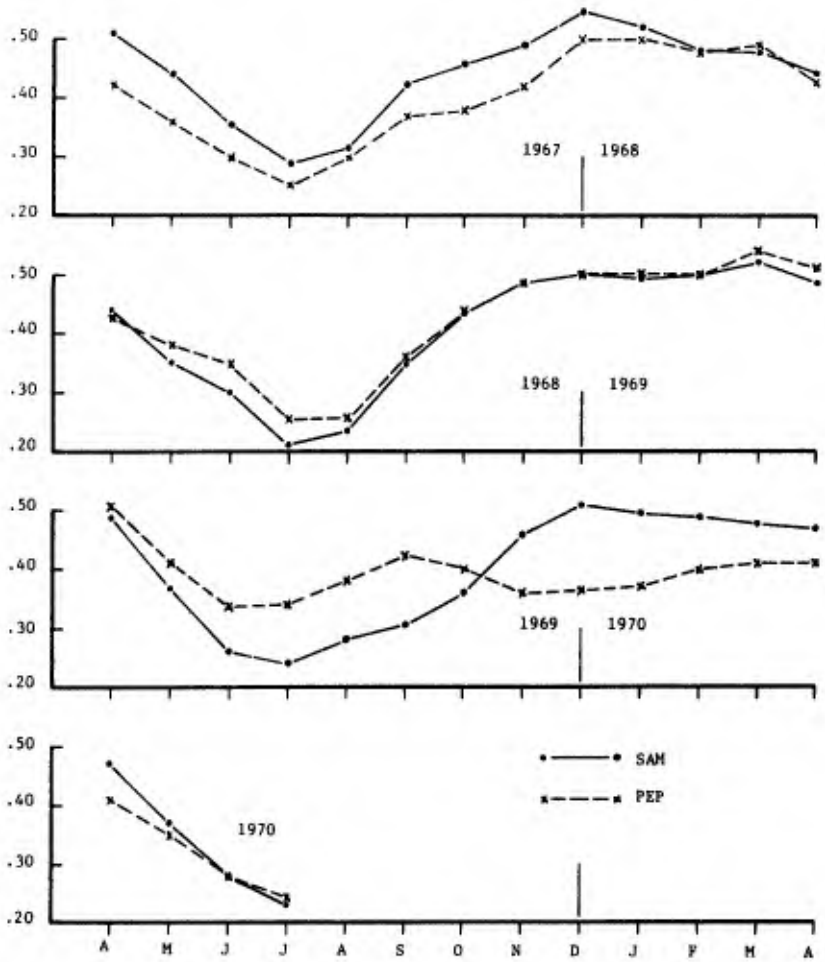


Fig. 2 — SAM and PEP Threat Score

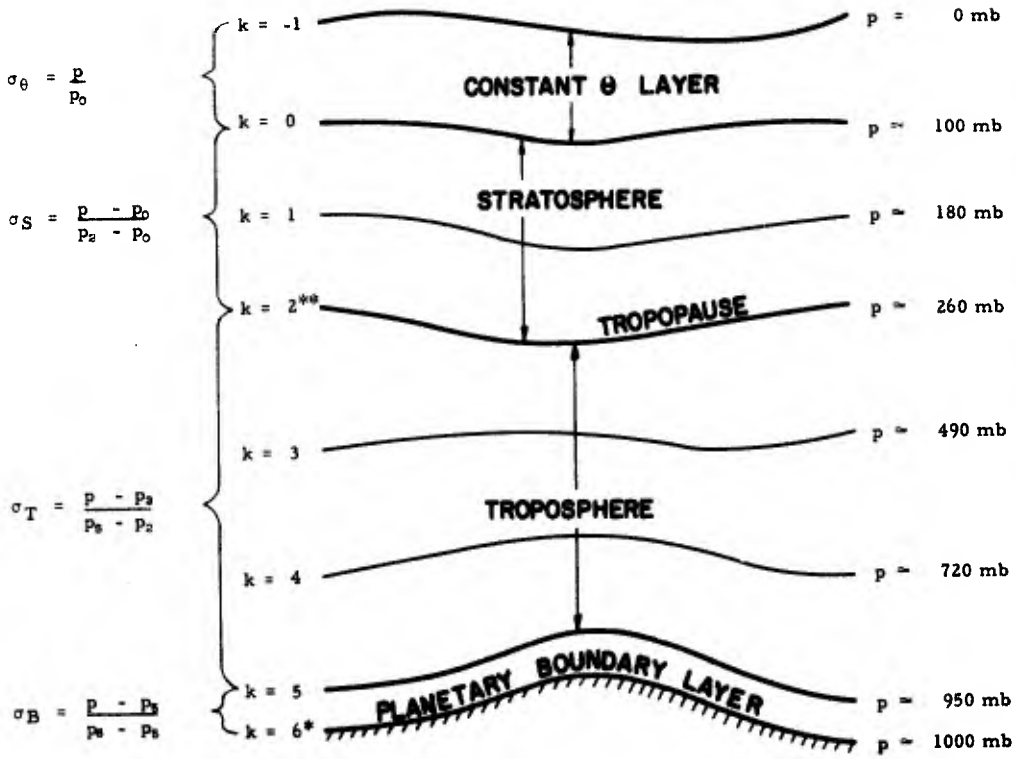


Fig. 1 — Vertical Structure of 6-Layer PE Model.

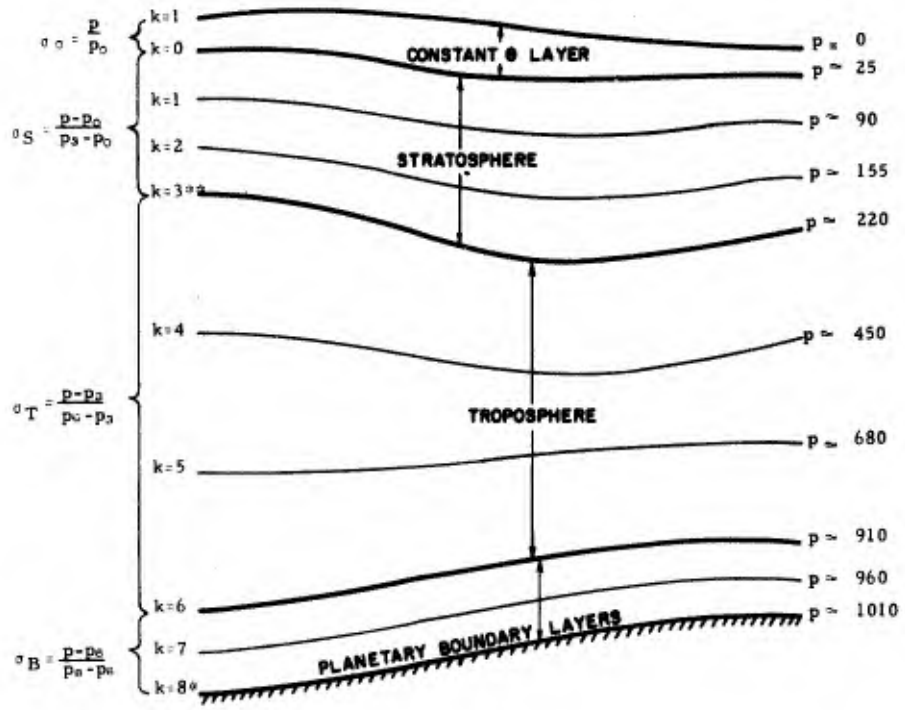


Fig. 3 — Vertical Structure of 8-Layer PE Model.

## REFERENCES


1. Shuman and Hovermale, J. App. Meteor., v. 7, p. 525, 1968.

2. Glahn, Lowery and Hollenbaugh, ESSA Tech. Memo. WBTM TDL-23, July 1969.

3. Vanderman, ms. to be published in the Proceedings of Regional Seminar on Synoptic Analysis and Forecasting in the Tropics for WMO Regions III and IV, Campinas, S.P., Brazil, September 1969. (See also Bulletin of A.M.S., v. 51, p. 594, 1970).

# FLEET NUMERICAL WEATHER CENTRAL'S FOUR-PROCESSOR PRIMITIVE EQUATION MODEL

Philip G. Kesel
Fleet Numerical Weather Central
Monterey, California

Frank J. Winninghoff
U. S. Naval Postgraduate School
Monterey, California

## Abstract

The Fleet Numerical Weather Central, Monterey, multi-layer primitive-equation atmospheric prediction model has been under development by the authors since late 1968. The current version is executed using four central processing units simultaneously on FNWC's two dual-processor CDC 6500 computers. Partitioning the model reduced the running time by a 3.1 factor. Seventy-two hour prognoses are generated twice daily, requiring two hours per run.

The conservation forms of the difference equations are based on the Arakawa technique and integrated, using a 381 kilometer space step (at 60 North) and a ten-minute time step, on sigma surfaces. Realistic FNWC-Clarke mountains are used. Pressure- force terms are replaced by a single geopotential gradient on pressure surfaces synthesized locally (after Kurihara) to reduce inconsistent truncation error. Lateral diffusion is performed on forecast difference fields to prevent systematic distortions of sigma-surface state parameter distributions. Stress is applied at the lowest level. We use constant flux, restoration boundaries. Centered time differencing is used, but integrations are re-cycled each six hours with an Euler-backward step to reduce solution separation.

The moisture and heat source and sink terms are fashioned after the Mintz and Arakawa representations mainly. Terms representing evaporation and large-scale condensation, sensible heat exchange, a parameterization of cumulus convection and precipitation, and solar and terrestrial radiation are included. Dry-convective adjustment precludes hydrostatic instability.

Initialization of the model is based on FNWC's Northern Hemisphere objective analyses of the state parameter structure from the surface to 50 MBS. Non-divergent initial wind fields are obtained from solution of a linear balance equation.

Interim verification results are encouraging. In winter the 36-hour PEM sea-level pressure prognoses exhibit about twice the skill (RMS sense) of the operational thickness-advection model (SLP). Summer scores show little increase in skill over the SLP. The model's ability to simulate the generation of new storms in the October 1969 - April 1970 period was noteworthy. Problem areas include a tendency toward over-development of continental anticyclones of small horizontal scale, some difficulty in controlling the heat release from the parameterization of cumulus, and under movement of small-scale features (truncation problem).

## 1. INTRODUCTION

An important responsibility of the Fleet Numerical Weather Central, Monterey, is to provide numerical meteorological analyses and forecasts, on an operational basis, according to the needs of the U. S. Navy. In addition to this, FNWC is also responsible for the development and test of meteorological techniques applicable to Navy prediction problems. Perhaps the most recent

accomplishment of this development program has been the design and development of the FNWC five-layer, atmospheric prediction model, based on the so-called "primitive equations" (PEM).

The PEM was initially programmed as a single-processor version to be executed in one of the two FNWC CDC 6500 Computer Systems. In 1969 the emphasis was on boundary conditions, initialization procedures, the elimination of inconsistent truncation errors, the introduction of stress and diffusion terms, the inclusion of source and sink terms in the moisture and thermodynamic equations, and the stability of solutions. By early 1970, the development reached a point at which the complete model was rather skillfully simulating the essential distributions of the state parameters for forecast periods from one to three days. Its ability to predict the generation of new storms was particularly encouraging, especially those storms which developed just off the east coast of Asia.

The FORTRAN coded, single-processor PEM, however, required over three hours of computer time to output a set of 36-hour predictions. In the period from May 1970 to August 1970 the FNWC primitive equation model was partitioned and programmed to run simultaneously in all four central processing units of the two CDC 6500 computers. The execution time for a three-day forecast run has been reduced by a factor of 3.1 to just under two hours. Further speedups will be made as computational routines for which the physics is firm are coded in machine language. At present, the Four-Processor Model is being run to 72 hours twice daily.

The main purpose of this paper is to describe, in moderate detail and in a qualitative way, the FNWC Four-Processor Primitive-Equation Model. It is also important, we feel, to outline the approach taken to exploit the parallelism in the equation set, as well as to take advantage of the total system capability in order to make this model operationally useful.

Section 2 contains the description of the model. The special treatment of the heating and moisture source and sink terms is described in Section 3. The Four-Processor Model design is contained in Section 4. Sections 5 and 6 are devoted to interim verification results and discussion of future model development, respectively.

## 2. MODEL DESCRIPTION

The governing differential equations, written in flux form, are similar to sets used earlier by Smagorinsky (1965), Mintz and Arakawa (1968), and others. The conservative-type difference equations are based on the Arakawa technique (1966). A rather complete description of both the continuous forms and finite difference forms of the equations will be found in a forthcoming paper by Kesel and Winninghoff (1970). At this time, let it suffice to list the continuous equations in Figure 1.

The difference equations preclude nonlinear computational instability by requiring that the horizontal and vertical flux terms conserve the square of any advected parameter, if one assumes continuous time derivatives. Total energy conservation is ensured by requirements placed upon the vertical differencing; specifically, by use of a special form of the hydrostatic equation. The latter condition may be relaxed, however, without perceptible bad effects. The integrated mass is conserved.

### 2.1 Domain, Variables

Integrations are performed on Phillips' (1957) sigma surfaces in which pressure (p) is normalized with the underlying terrain pressure ( $\pi$). The horizontal wind components (u, v), temperatures (T), and heights (z), are carried at levels where sigma equals 0.9, 0.7, 0.5, 0.3, and 0.1. The moisture variable (q) is carried at the lower three of these surfaces. For convenience, the vertical velocity variable (w) is defined as minus sigma dot and is calculated diagnostically from the continuity equation for the layer interfaces (sigma = 0.8, 0.6, 0.4, and 0.2). Other symbols used are: diabatic heating (H), moisture source and sink (Q), and surface stress (F). Figure 2 applies.

A. East - West Momentum Equation

$$\frac{\partial \pi u}{\partial t} = -m^2 \left\{ \frac{\partial}{\partial x} \left( \frac{uu\pi}{m} \right) + \frac{\partial}{\partial y} \left( \frac{uv\pi}{m} \right) \right\} + \pi \frac{\partial (wu)}{\partial \sigma}$$

$$+ \pi vf - m \left\{ \frac{\partial \phi}{\partial x} + RT \frac{\partial \pi}{\partial x} \right\} + K \nabla^2 u\pi + F_x$$

B. North-South Momentum Equation

$$\frac{\partial \pi v}{\partial t} = -m^2 \left\{ \frac{\partial}{\partial x} \left( \frac{uv\pi}{m} \right) + \frac{\partial}{\partial y} \left( \frac{vv\pi}{m} \right) \right\} + \pi \frac{\partial wv}{\partial \sigma}$$

$$- \pi uf - m \left\{ \pi \frac{\partial \phi}{\partial y} + RT \frac{\partial \pi}{\partial y} \right\} + K \nabla^2 v\pi + F_y$$

C. Thermodynamic Energy Equation

$$\frac{\partial \pi T}{\partial t} = -m^2 \left\{ \frac{\partial}{\partial x} \left( \frac{\pi uT}{m} \right) + \frac{\partial}{\partial y} \left( \frac{\pi vT}{m} \right) \right\} + \pi \frac{\partial (wT)}{\partial \sigma} + H\pi$$

$$K \nabla^2 \pi T + \frac{RT}{c_p \sigma} \left\{ -w\pi + \sigma \left( \frac{\partial \pi}{\partial t} + m \left( u \frac{\partial \pi}{\partial x} + v \frac{\partial \pi}{\partial y} \right) \right) \right\}$$

D. Moisture Conservation Equation

$$\frac{\partial e\pi}{\partial t} = -m^2 \left\{ \frac{\partial}{\partial x} \left( \frac{\pi ue}{m} \right) + \frac{\partial}{\partial y} \left( \frac{\pi ve}{m} \right) \right\} + \pi \frac{\partial (we)}{\partial \sigma} + Q\pi$$

where Q = moisture source/sink term

E. Continuity Equation

$$\frac{\partial \pi}{\partial t} = -m^2 \left\{ \frac{\partial}{\partial x} \left( \frac{u\pi}{m} \right) + \frac{\partial}{\partial y} \left( \frac{v\pi}{m} \right) \right\} + \pi \frac{\partial w}{\partial \sigma}$$

F. Hydrostatic Equation

$$\frac{\partial \phi}{\partial \sigma} = - \frac{RT}{\sigma}$$

Figure 1. THE DIFFERENTIAL EQUATION SET.

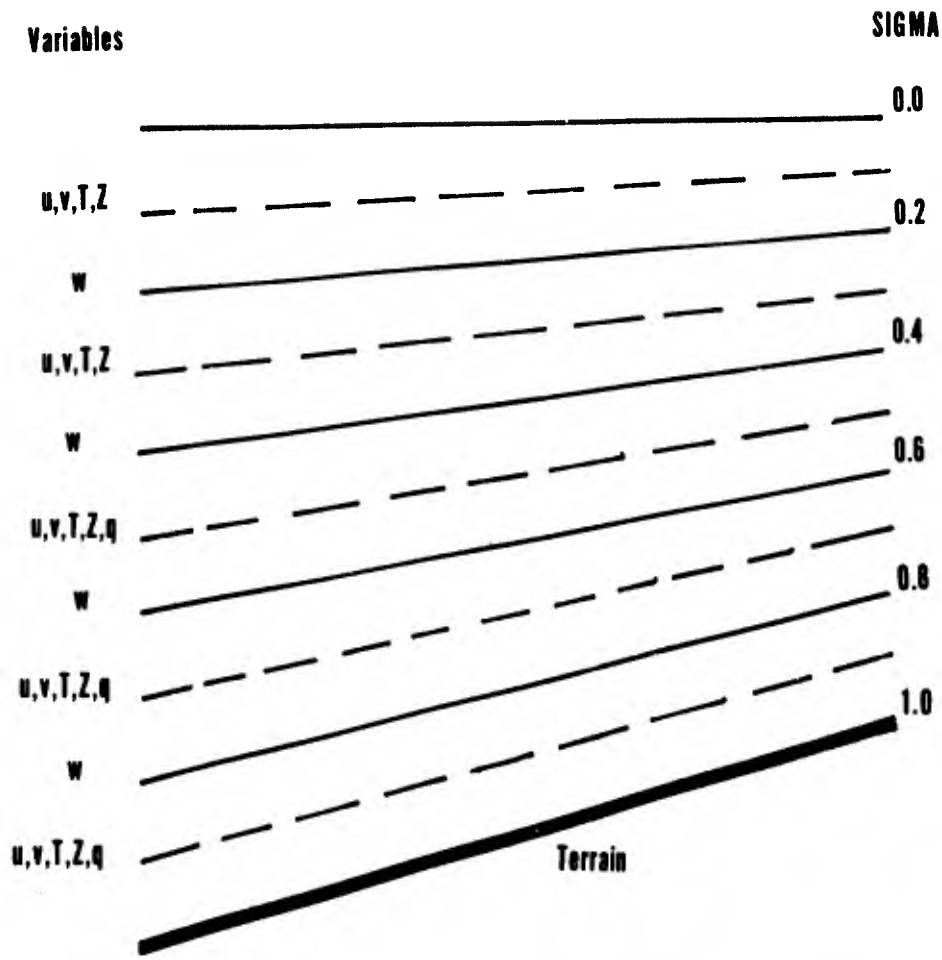


Figure 2. DIAGRAM OF LEVELS AND VARIABLES. The terrain pressure (pi) is carried at sigma = 1.0. The vertical velocity (w) vanishes at the top and bottom of the column. Horizontally, we use a 63 x 63 array in which the equator is an inscribed circle.

The earth is mapped onto a polar stereographic projection of the Northern Hemisphere. In the calculation of map factor (m), and Coriolis parameter (f), the sine of the latitude ($\phi$) is not permitted to take on values less than that value corresponding to 23 degrees latitude. This restriction arose from the attempt in practice to produce more realistic initial winds in the subtropics and tropics. The horizontal domain consists of a 59 x 59 subset of the standard 63 x 63 FNWC grid. The geographical equator is an inscribed circle of the latter.

## 2.2 Time Differencing, Solution Separation

The Richtmyer centered-time differencing method is used for all but the initial ten-minute step of each six-hour integration cycle. The initial step in each integration cycle involves a Matsuno (Euler backward) step which possesses more desirable stability properties than does a forward step. The combination of Matsuno initial steps and six-hour recycling maintains the desired stability and greatly reduces solution separation in so doing. Test runs were made using an iterative scheme to initialize the model. In runs of this type, Matsuno time differencing was used throughout, but this will be discussed in the section on initialization.

## 2.3 Terrain, Truncation Error

A rather realistic specification of the underlying terrain is used at FNWC. Studies at Monterey have indicated the sensitivity of the model to variations in the height and character of the terrain. As a consequence, a more detailed terrain set based on values at 10-minute latitude-longitude intersections is being completed by Mr. Leo Clarke for use in an 89x89 fine-mesh model which will be programmed later this year. At the risk of over-simplification, it appears as though it is less deleterious to a forecast to reduce terrain heights in a region (or omit minor mountain ranges) than it is to increase terrain heights (both of which arise when one generates a highly stylized mountain set).

Since more realistic terrain has been used, a Kurihara (1968) type of modification was made in the pressure-force terms to reduce the inconsistent truncation error (and the resulting stationary noise patterns over high irregular terrain). Instead of evaluating both the gradient of the geopotential distribution on a sigma surface and the terrain pressure gradient (invariant with altitude), geopotential correction fields are computed at neighboring points to each point to enable one to compute the geopotential gradients on pressure surfaces which are "synthesized" locally in the process. (A special type of lateral diffusion should be used in conjunction with this Kurihara modification to redistribute the remaining high frequency elements at the higher altitudes.)

## 2.4 Lateral Diffusion

Lateral diffusion is applied to redistribute the unwanted high frequencies in both the mass and motion fields, regardless of their origin. If diffusion operators are applied to sigma surface temperatures, however, systematic warming results from the numerical procedure over mountain tops (ridges). with the opposite taking place in valleys. The same type of unrealistic redistributions of winds occur to a lesser extent, but in regions characterized by strong vertical wind shear the effect is both detectable and deleterious.

To avoid this difficulty, lateral diffusion is performed on the (forecast) difference fields as appropriate, rather than on sigma surface distributions. By so doing, the gross character of the sigma-surface distributions of temperature and winds is left essentially unaltered.

## 2.5 Boundary Conditions

Two types of lateral boundary conditions have been studied very carefully in the past two years at FNWC. The first to be used with some success was two-way cyclic continuity. This approach was discarded in favor of a type of constant flux, restoration boundaries devised by the authors in January 1970.

Two-way cyclic continuity was computationally stable for long-term integrations, but required flattening and blending of the tropical regions at initialization time. In general, the adjustment processes in the lower latitudes were both aggravated and delayed by this restructuring technique, and sometimes led to poor forecasts in the region from 40 North and southward.

The constant flux, restoration boundary (CFRB) technique is described below. At initial time, all of the distributions of temperature, moisture, winds, and terrain pressure are saved. Next, a field of restoration coefficients which vary continuously from unity(at and south of 4 North) to zero (at and north of 17 North) is computed and saved. At the end of each ten-minute time step the new values (just obtained) of the aforementioned variables are restored back toward their initial values (in the region south of 17 North) according to the amount specified by the field of restoration coefficients. See Figure 3. The net effect of this procedure is to produce a fully dynamic forecast north of 17 North, a persistence forecast south of 4 North, with a blend in between. The mathematical-physical effect of the technique is that the blend region acts as an energy "sponge" for outwardly propagating inertio-gravity oscillations. The initial fluxes on the grid square boundary are preserved. No restructuring of the tropics is necessary. These boundaries have been used routinely for integrations to three days with no perceptible difficulties in the products.

## CONSTANT FLUX, RESTORATION BOUNDARIES (KESEL AND WINNINGHOFF)

1. Save initial values of winds, temperatures.

2. Compute restoration coefficients (RC).

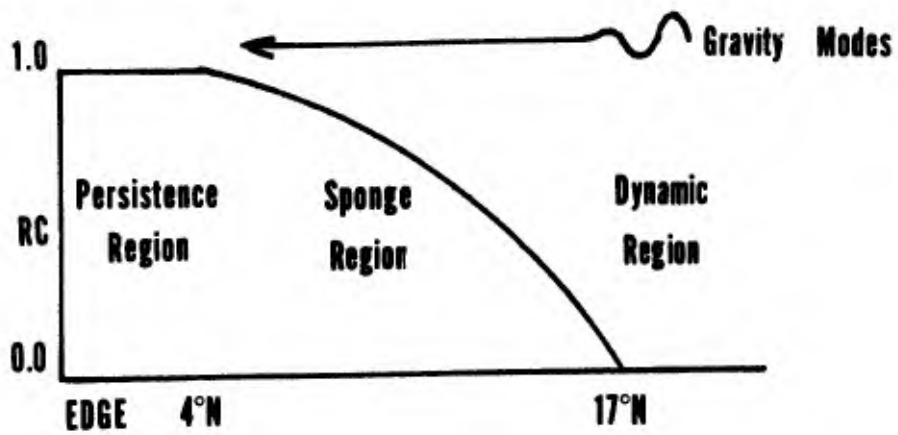


3. After integration, restore variables 'RC' amount toward initial values.

Figure 3. CONSTANT FLUX, RESTORATION BOUNDARIES. The values of the variables obtained in each time step are returned toward their initial values, in the latitudes indicated, an amount indicated by the field of restoration coefficients.

2.6 Initialization Procedures

For basic inputs to the model we use the virtual temperature analyses for the Northern Hemisphere at 12 constant pressure levels distributed from 1000 MBS to 50 MBS, height analyses at seven of these levels, and moisture analyses at four levels from the surface to 500 MBS. In addition, we use a terrain field, sea-level pressure and sea-surface temperature analyses. Monthly mean surface-temperature fields are used at present to compute an albedo field.

The initial non-divergent wind components are obtained from solution of the so-called linear balance equation on pressure surfaces, with interpolation to sigma surfaces. These appear to be satisfactory for two to three day predictions. Early experimentation with winds from the

full balance equation led to the tentative conclusion that little or no statistically meaningful improvement in the forecasts resulted (compared to the linear balance equation).

Plans are underway to shift to an iterative procedure for initializing the model following the guidelines of Winninghoff (1968). Although Winninghoff found that an iteration period equivalent to a 36-hour forecast might be necessary to effectively "adjust" the model, some type of compromise might be possible. That is, one might iterate only until such time as a reasonable set of dry omegas is generated.

### 2.7 Surface Stress

Frictional dissipation is accounted for in the gross boundary layer (sigma = 1.0 to 0.8) only. The stress is assumed to vanish at the top of this layer. The stress terms are the same as those used by Shuman and Hovermale (1968). The drag coefficient ($C_d$ = .0015) is, for the present, taken to be a constant. The surface wind speeds are obtained by extrapolation from neighboring sigma surfaces.

## 3. HEATING EFFECTS AND MOISTURE

The heating functions used in the model represent, in some measure, both an adaptation and extension of the work of Mintz and Arakawa, as reported by Langlois and Kwok (1969). Essentially, we incorporate terms representing evaporation and condensation processes, sensible heat exchange, solar and terrestrial radiation, and an Arakawa-Katayama-Mintz (1968) parameterization of cumulus convection and precipitation.

For background information, note that we use a gross albedo distribution determined as a function of the mean monthly surface temperature, based on the work of Dickson and Posey (1967). A Smagorinsky parameterization of "middle" cloudiness is used in the gross layer between sigma (0.8) and sigma (0.4) based on the relative humidity.

We compute radiation, sensible heating, and evaporation once each hour. Condensation, both large-scale and cumulus-type, is considered each time step. Both moisture and heat are redistributed for the lower three layers in the Arakawa cumulus parameterization (referred to as "moist-convective adjustment" in this paper). Dry-convective adjustment is performed at the conclusion of each step. Brief discussions of each of these physical processes, and the methods by which they are evaluated numerically, are given in the next few sections.

### 3.1 Radiation Processes

Radiative fluxes, both solar and terrestrial, are computed at levels where sigma takes on values, 1.0, 0.6, and 0.2, with flux divergences (and heating rates) then being calculated for the two gross layers thus defined. Temperature changes appropriate to the lower of these two gross heating layers are assigned arbitrarily to the model's levels where sigma = 0.9 and 0.7. The temperature changes appropriate to the uppermost gross layer are assigned to the levels where sigma = 0.5, 0.3, and 0.1.

Solar radiation is modeled using the Mintz and Arakawa approach as developed by Joseph (1966). We compute both the insolation (S) at the top of the atmosphere, and the precipitable water in the column. S is assumed to be in two parts: .349S which is subject to absorption and reflection, but not to scattering; and .651S which is subject to scattering, but not absorption. Considering the degree of middle cloudiness, we are then able to calculate the heating rates by making the additional assumptions that: in-cloud path length is 1.66 the normal length; an arbitrary amount of water vapor is added to account for the presence of clouds; the reflected radiation for cloud tops is subject to absorption only; and that the cloud albedo is 0.5. Finally, we determin the solar radiation reaching the ground to be used later in the calculation of sensible heat and evaporation.

In the long-wave radiation computations, we use the FNWC analyzed sea surface temperatures (holding these constant in time). Over land, temperatures are obtained from a heat balance equation. Employing Danard's method (1969) and Kuhn's data (1963) for emissivities, the flux divergences (and heating rates) may be calculated. As before, we use the degree of cloudiness to apportion the rates for the "clear" and "overcast" conditions.

### 3.2 Sensible Heat and Evaporation

Sensible heating is determined as a function of the air temperature-surface temperature difference, and may lead to some difficulties because we do not carry temperatures, winds, and moistures sufficiently close to the surface. Evaporation over water is computed as a function of the saturation moisture at the surface and the moisture near the surface. To overcome the difficulty, the air near the surface is assumed to be a very thin boundary layer which does not absorb or store a significant amount of heat or moisture. The fluxes of moisture and heat, therefore, are the same through the top and bottom of this thin layer.

Evaporation over land is calculated from a Bowen ratio, using data from Budyko as given in Sellers (1965).

### 3.3 Condensation

The release of latent heat is based on an approximate, but economical, solution given by Langlois and Kwok, to the equation

$$c_p (T_{new} - T_{old}) = L (q_{old} - q_{new})$$

Where q is the moisture variable, $c_p$ is the specific heat at constant pressure, and L is the latent heat.

If supersaturation exists at the lowest computational level, then the excess is precipitated. At the same time, the temperature will rise (from $T_{old}$ to $T_{new}$). This process is modified slightly at higher levels. We check the possibility of evaporating precipitated water into the next lower level and let rain fall to the ground only if that next lower level also becomes (is) saturated.

### 3.4 Moist-Convective Adjustment

Three types of convection are considered: high thin cumulus (involving levels where sigma = 0.5 and 0.7): deep penetrating convection (involving levels where sigma = 0.9, 0.7, and 0.5); and low thin cumulus (involving levels 0.9 and 0.7). Precipitation may result from the first two types. Two energy parameters,

$$h = c_p T + gz + Lq$$

and

$$E_n = c_p T + gz + Lq_s$$

are used in conjunction with measures of the total upward convective mass flux, as well as the entrainment, to determine the degree of conditional instability of the column. Note that $E_n$ is conserved along a moist pseudo adiabat, and the difference (h - Lq) is conserved along a dry adiabat.

Some undesirable results occurred with the initial implementation of this routine. In general, it tended to over-precipitate in the southwestern portions of the subtropical highs, and over mountainous areas in the tropics and subtropics. The effect of this was the gradual decrease in surface pressure as a consequence of this heating, usually producing pressures on the order of 4 to 8 millibars too low in the associated areas. In a few instances, closed cyclonic circulations were developed in the latitude band from 20N to 30N. Subsequent testing and modification of this scheme have eliminated many of these difficulties.

## 4. FOUR-PROCESSOR PARTITIONED MODEL

In the period from May until August 1970 the FNWC Primitive Equation Model was programmed to run in a four-processor mode using both dual-processor CDC 6500 computers. To do this required answers to three different types of questions:

a. How to partition the computational segments of a system of differential equations into four approximately equal time lapse segments?

b. How to modify the standard Scope 3.2 Operating System to enable four programs on two computers to communicate with each other via Extended Core (ECS), while at the same time preventing other programs from interfering?

c. How to design an efficient and foolproof program-synchronization mechanism to ensure that all four programs start and remain in correct time phase?

It is beyond the scope of this paper to treat questions b. and c. This will be covered in considerable detail in a forthcoming paper by Beckett, Kesel, Winninghoff, Wolff, and Morenoff. The following section will describe the way in which the computational load was partitioned to permit the four-way parallel execution of the programs.

First, the problem was envisioned as being divisible into three main categories: initialization section; the typical time step; and the output section. The overall model partition structure is shown in Figure 4.

In the input/initialization section, the computational burden was split three ways: Processor 2 and Processor 3 each solve the balance equation on one-half of the required pressure surfaces (from 1000 MBS to 50 MBS); Processor 1 takes care of I/O and initializes everything else (temperatures, terrain pressure, moisture, etc.).

In a typical time step, a three-way split is accomplished first, and then a four-way split takes place. See Figure 5. First, consider the three-way split. Processor 1 integrates the continuity equation to obtain the local change in terrain pressure, and the vertical velocity fields at the layer interfaces. Processor 2 computes the geopotential field correction terms for the five computational levels (for the north-south momentum equation Kurihara modification), while Processor 3 computes these same five geopotential correction fields for the east-west momentum equation. Secondly, a four-way split is possible once the aforementioned fields are available. In Processor 1 the N/S momentum equation is integrated at five levels. The E/W momentum equation is integrated in Processor 2 at five levels. The thermodynamic energy equation is put into Processor 3 to obtain the five new levels ot temperatures. And integrating the moisture continuity equation yields three new levels of moistures in Processor 4. Interspersed with the three levels of moistures in Processor 4 is the routine for: large-scale condensation; the evaporation of this precipitation into layers beneath (where appropriate); and the associated temperature changes. To do this in proper time phase, an intra-step second level of synchronization is required between Processor 3 and Processor 4. Since Processor 4 handles only three levels of moistures, and since the first three levels of new temperatures are available concurrently with the three levels of moistures, it is possible for Processor 4 to commence the moist convective adjustment routine while Processors 1, 2, and 3 are working on their assignments at level 4. At the conclusion of the fifth level of temperatures (and at very nearly the same instant that the moist convective adjustment is completed), the dry convective adjustment (involving five levels of new temperatures) routine is started in Processor 4. When the final temperature distributions are available from this routine, the new geopotential fields are computed in Processor 4 by integrating the hydrostatic equation.

A three-way partition is effected in the output section (which is entered every six hours during the forecast period). Processor 1 outputs those fifty-four fields (mostly on sigma surfaces) required to restart the model from any output tau (if necessary). Processors 3 and 4 postprocess the output fields (transformation of coordinates; fill in values under terrain; filter) and output about 58 data fields each output tau to the disk (tape). See Figure 6.

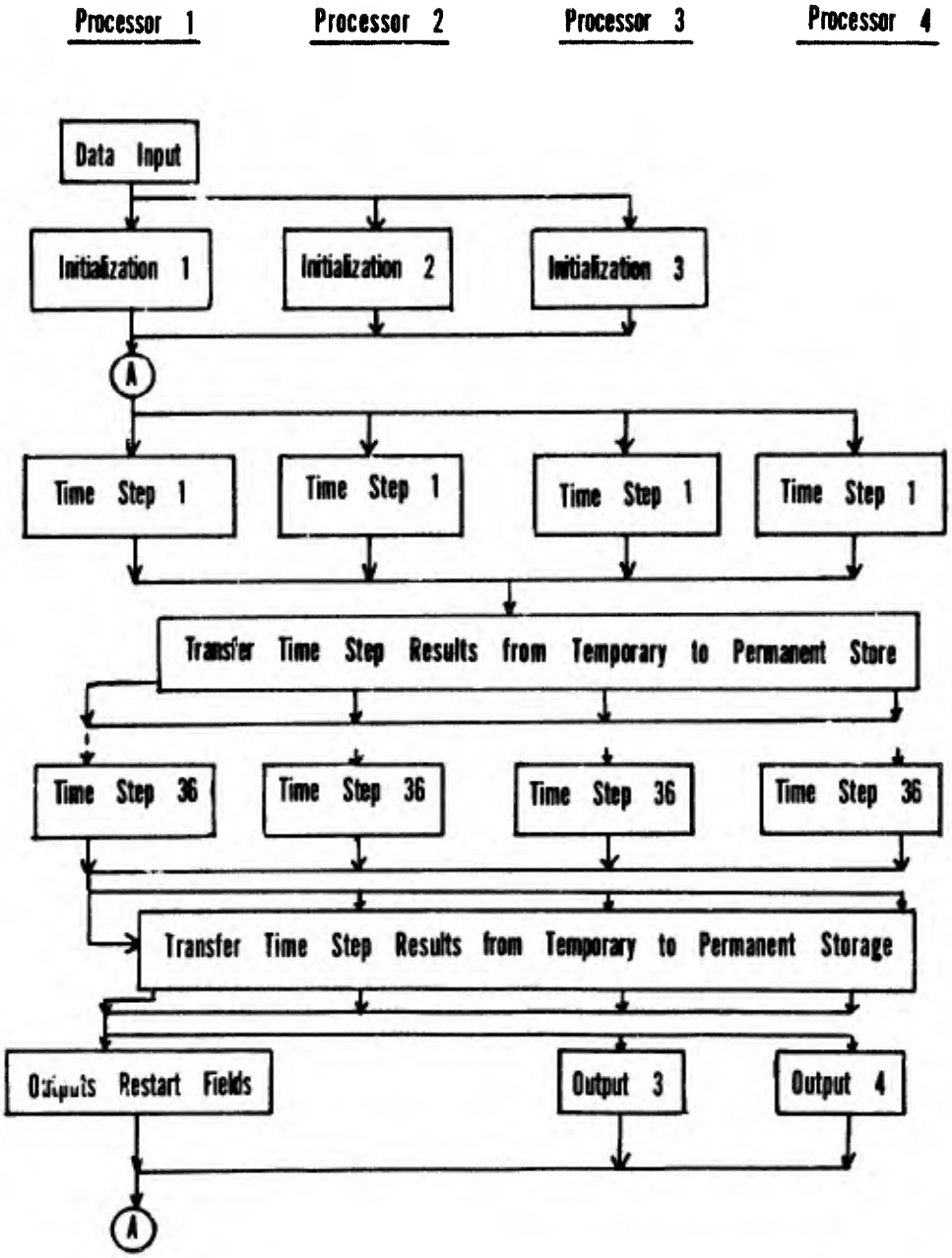


Figure 4. OVERALL MODEL PARTITION STRUCTURE

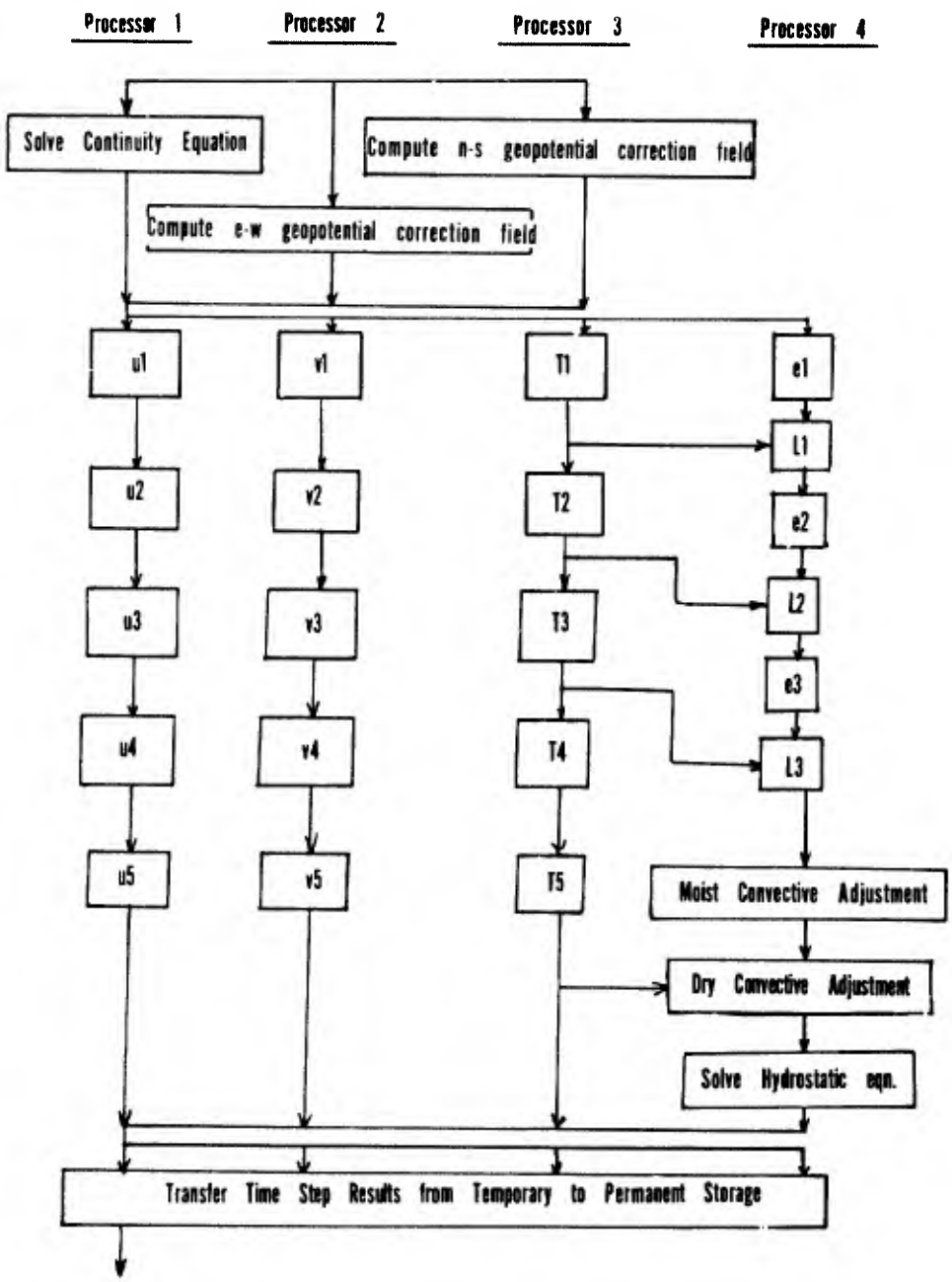


Figure 5. TYPICAL TIME-STEP PARTITION STRUCTURE

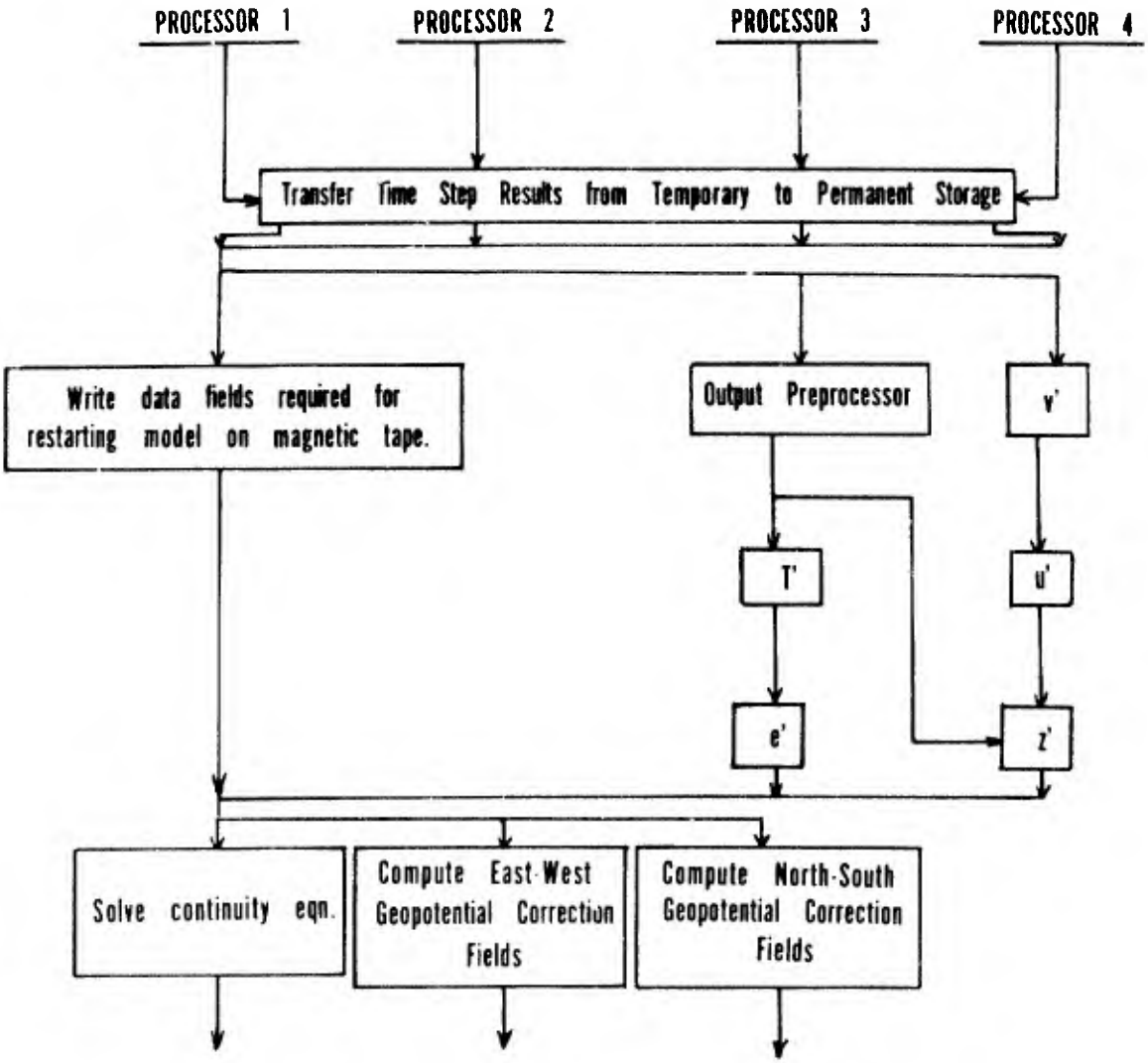


Note: Primes (') indicate that output variables are on pressure surfaces.

Figure 6. OUTPUT PARTITION STRUCTURE

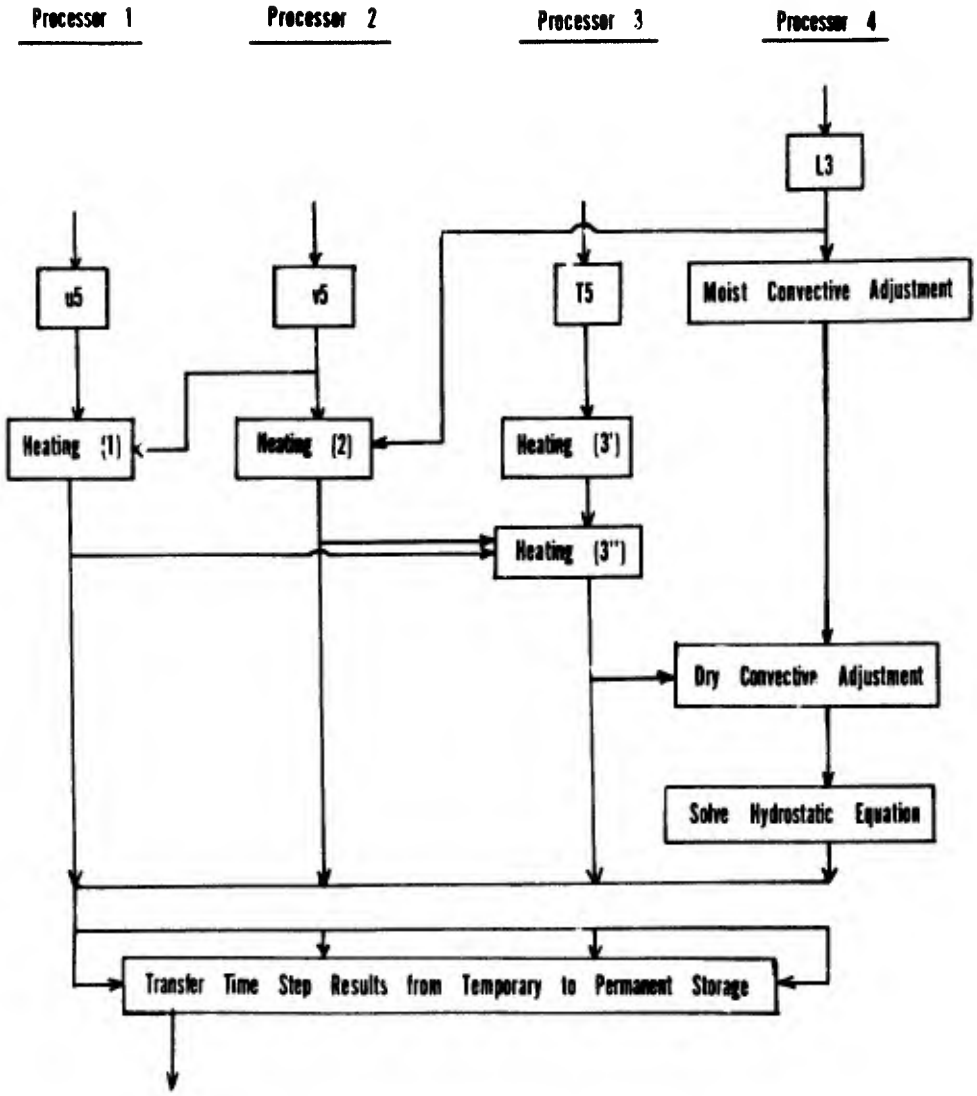


Figure 7. INFLUENCE OF HEATING ON TIME-STEP COMPUTATION

Once each six time steps, the so-called "heating package" is evaluated. This results in a three-way partition of the computational segments pertaining to solar radiative and terrestrial radiative fluxes, evaporation from the underlying surface, and sensible heat exchange. These segments go in Processors 1, 2, and 3, just after the new winds and temperatures are completed for level 5, but before the dry convective adjustment routine is started in Processor 4. See Figure 7.

## 5. INTERIM RESULTS

The application of the primitive-equation model to numerical weather prediction during the past year led to an unqualified improvement in the capability at FNWC, particularly in the winter half of the year. Figure 8 shows the comparative results for a typical early spring month and for an early summer month. The persistence error curve is denoted by "P", the FNWC thickness-advection surface model error is indicated by "SLP", and the PE model error is so marked. All values are in terms of root-mean-square, in millibars, with verification taken over month long series of 36-hour forecasts (in this instance we show the results in the "action" latitudes, from 35N to 65N). In general, the PE surface progs were about two times as skillful as the operational SLP model during the winter half of the year. In summer, on the other hand, the improvement was proportionately less as fewer and fewer baroclinic situations prevailed. In terms of hemispheric RMS scores the results are about the same. During the winter month discussed earlier, for example, the persistence RMSE was 5.56, the SLP was 4.61, and the PE was 3.94 millibars. This suggests that the PE contained about 1.7 times the skill of the SLP on a hemispheric basis. (Note that the 12-hour SLP forecasts were used as guess fields for the surface analyses.)

In addition to reproducing the essential features of the verification analyses, both at sea level and at 500 MBS, the model shows considerable promise in its ability to simulate the growth of baroclinic waves. This is particularly true in the western Pacific Ocean, where most of last year's storms were successfully predicted. About half of the east coast (U.S.) storms were missed, although the data base was comparable.

### 5.1 A Winter Case Study

A very interesting case of cyclogenesis occurred in late January 1970 in the western Pacific. In 36 hours the low pressure center south of Japan deepened from 1005 MBS to about 965 MBS. We were curious as to the effects of varying one thing at a time in the model during this cyclogenetic event. Figures 9 through 15 show the outcome. Figures 9 and 10 contain the initial and verification sea-level pressure analyses. Figure 11 is the standard run, and has all diabatic terms included, initial winds from the linear balance equation, idealized mountains, and uses constant flux, restoration boundaries. This version deepened the new storm to 962 MBS. Figure 12 contains the output from a model which differs from the standard only in the lateral boundary conditions used; that is, we used two-way cyclic boundaries which required considerable alteration of the meridional components south of 23 degrees North. The storm was deepened to 961 millibars, or only one millibar different from the standard with restoration boundaries. In Figure 13, we show the adiabatic version which only deepened the storm to 991 MBS (which was comparable to the SLP (thickness advection model) value of 994 MBS. We varied the initial winds in the version shown in Figure 14, using geostrophic winds (constant f) and deepened the storm to 981 MBS. Finally, Figure 15 shows the result when we used a better specification of the terrain. The result was 968 MBS, or about 3 millibars too high. Recall that the idealized terrain produced a low about 3 millibars too deep.

In any event, this map set can be perused at the reader's leisure. We feel it constitutes a very interesting, but by no means, complete treatment of this type of event.

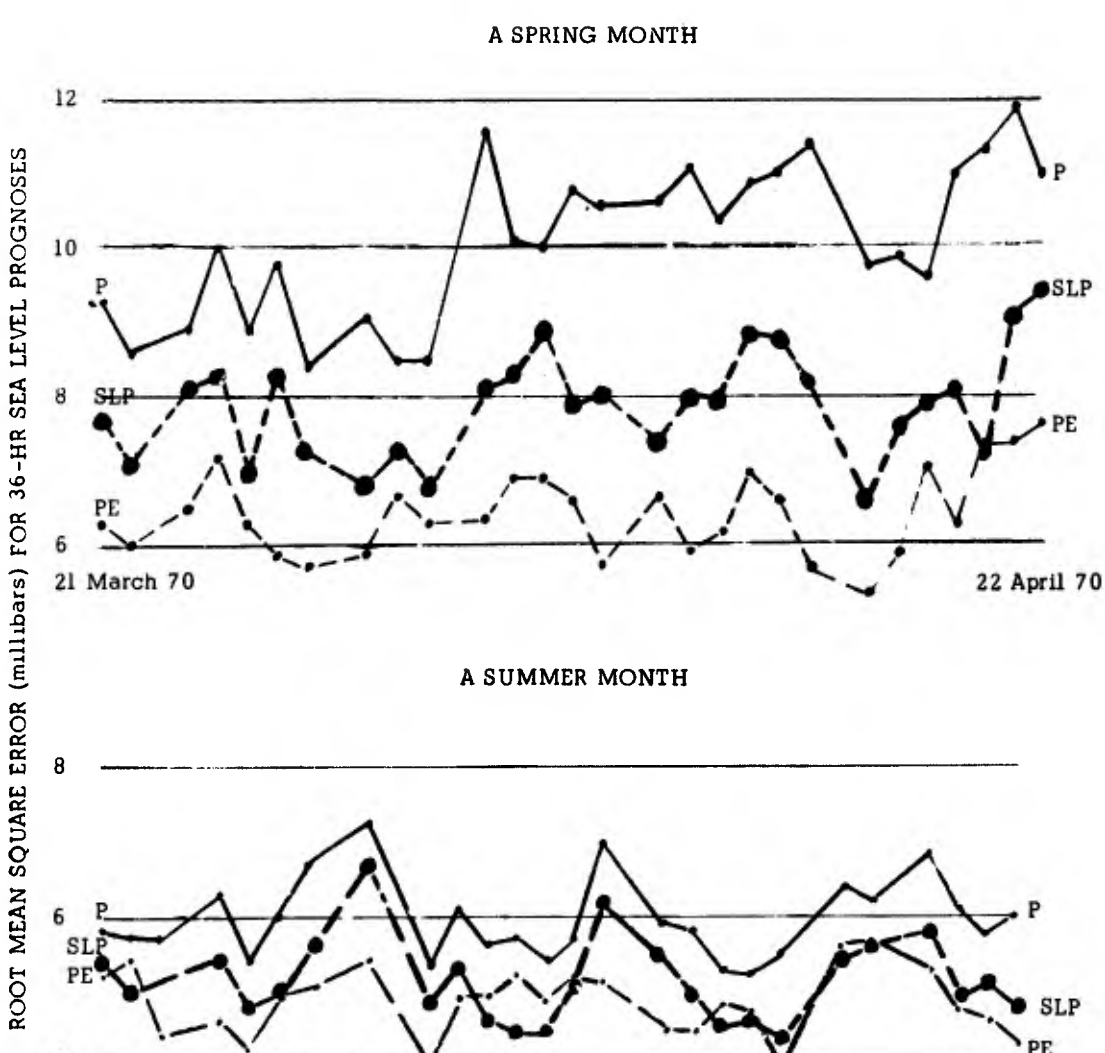


Figure 8. RMSE OF FNWC PRIMITIVE EQUATION MODEL 36-HR SEA LEVEL PRESSURE PROGNOSES FOR TYPICAL MONTHS IN SPRING AND SUMMER 1970. Values are computed for the latitude band between 35°N and 65°N.

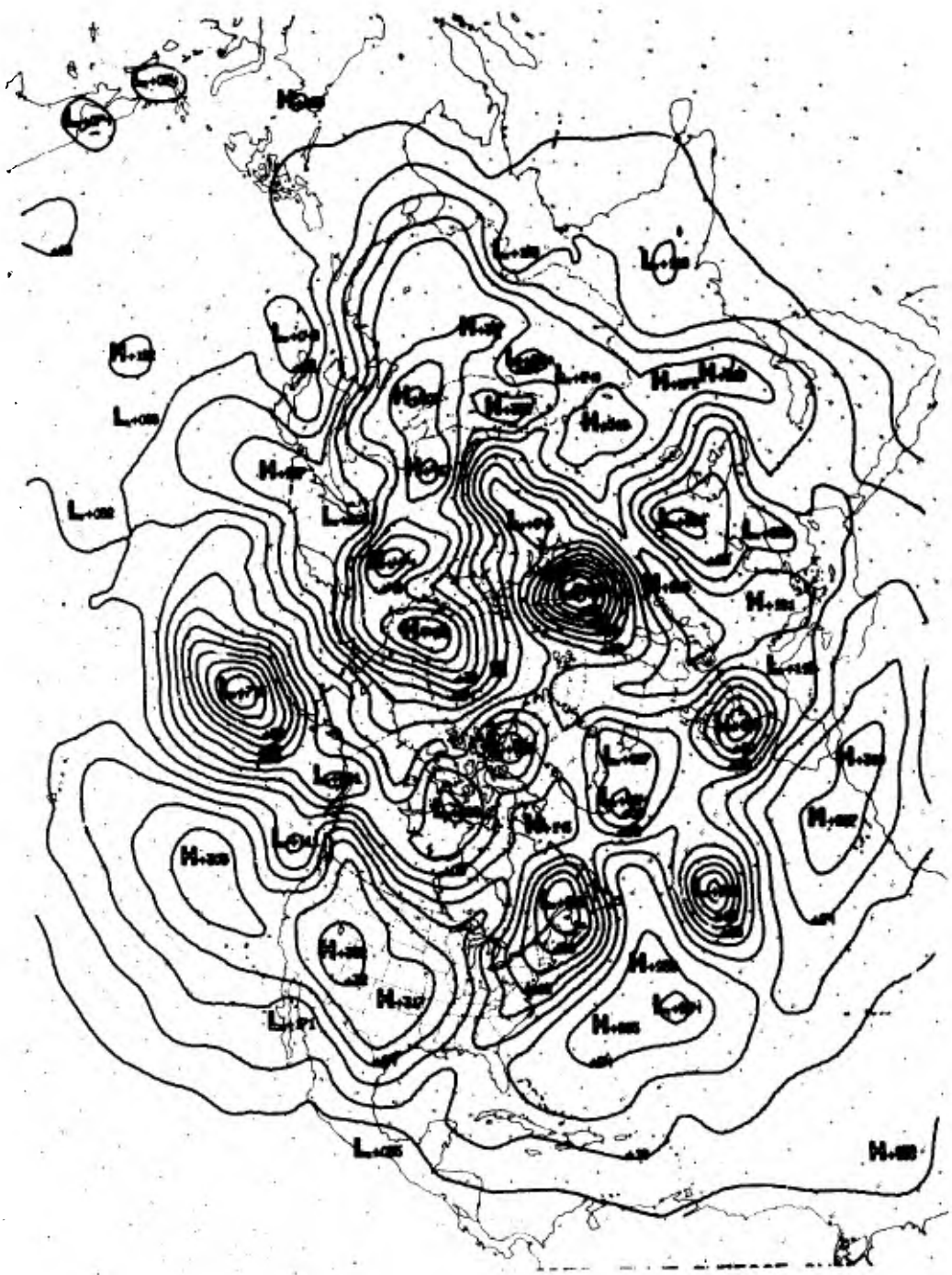

Figure 9. INITIAL ANALYSIS DATED 0000Z, 30 JANUARY 1970.
Note the weak 1004.8 MB low south of Japan.

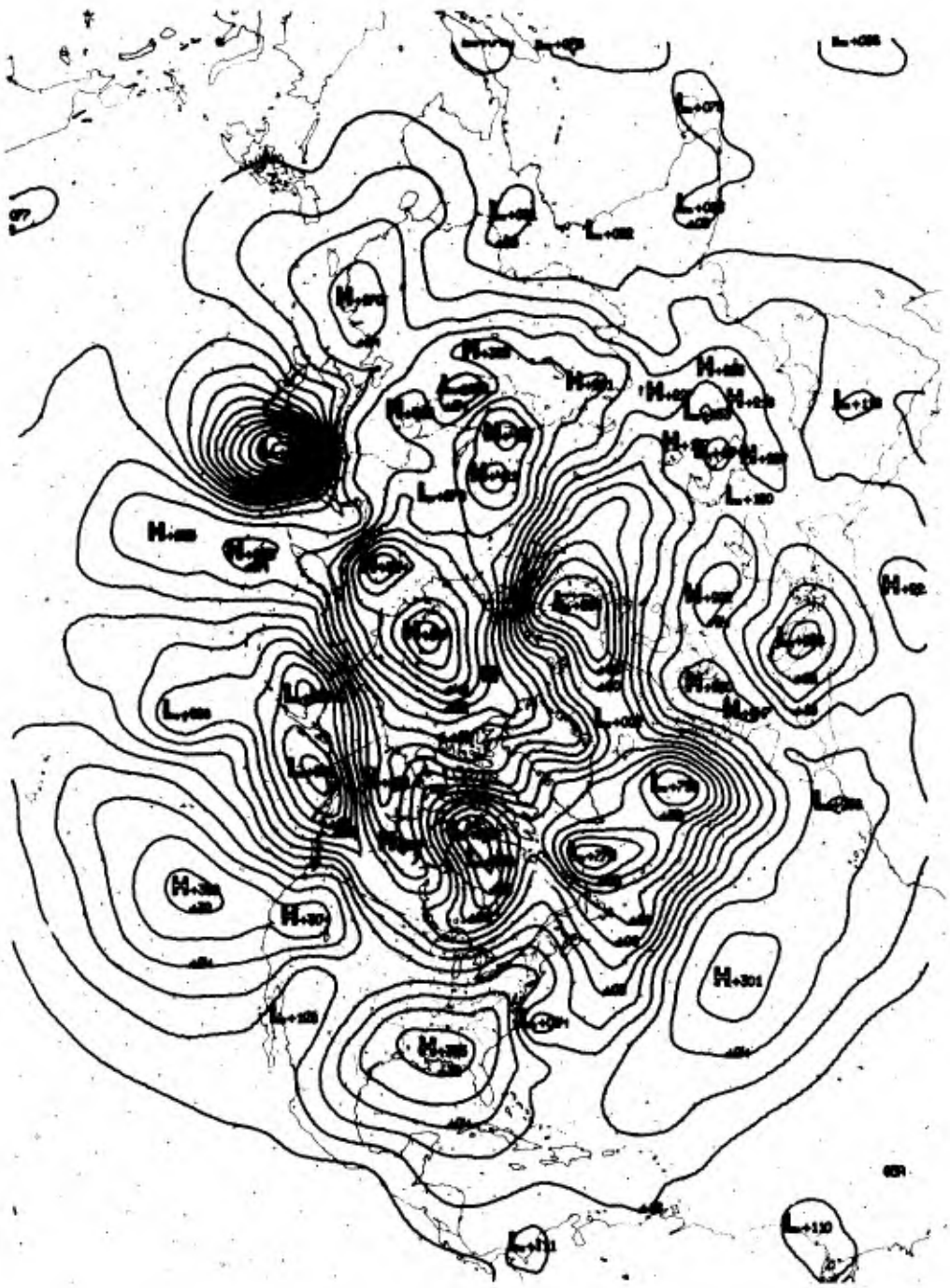

Figure 10. VERIFICATION ANALYSIS DATED 1200Z, 31 JANUARY 1970.

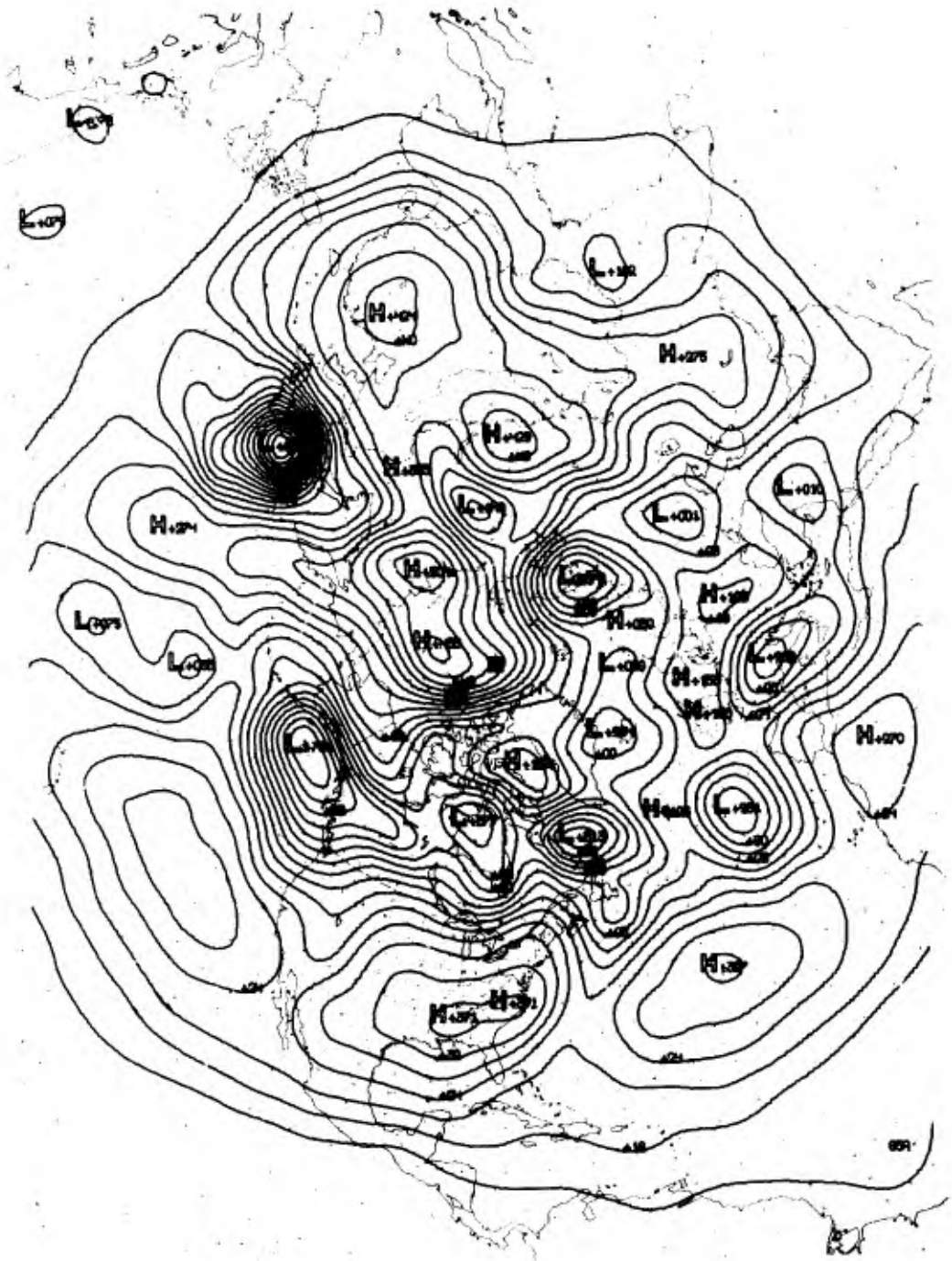

Figure 11. THE "STANDARD" FORECAST.
Model uses restoration boundaries, initial winds from linear balance equation, idealized terrain, and all diabatic heating terms.

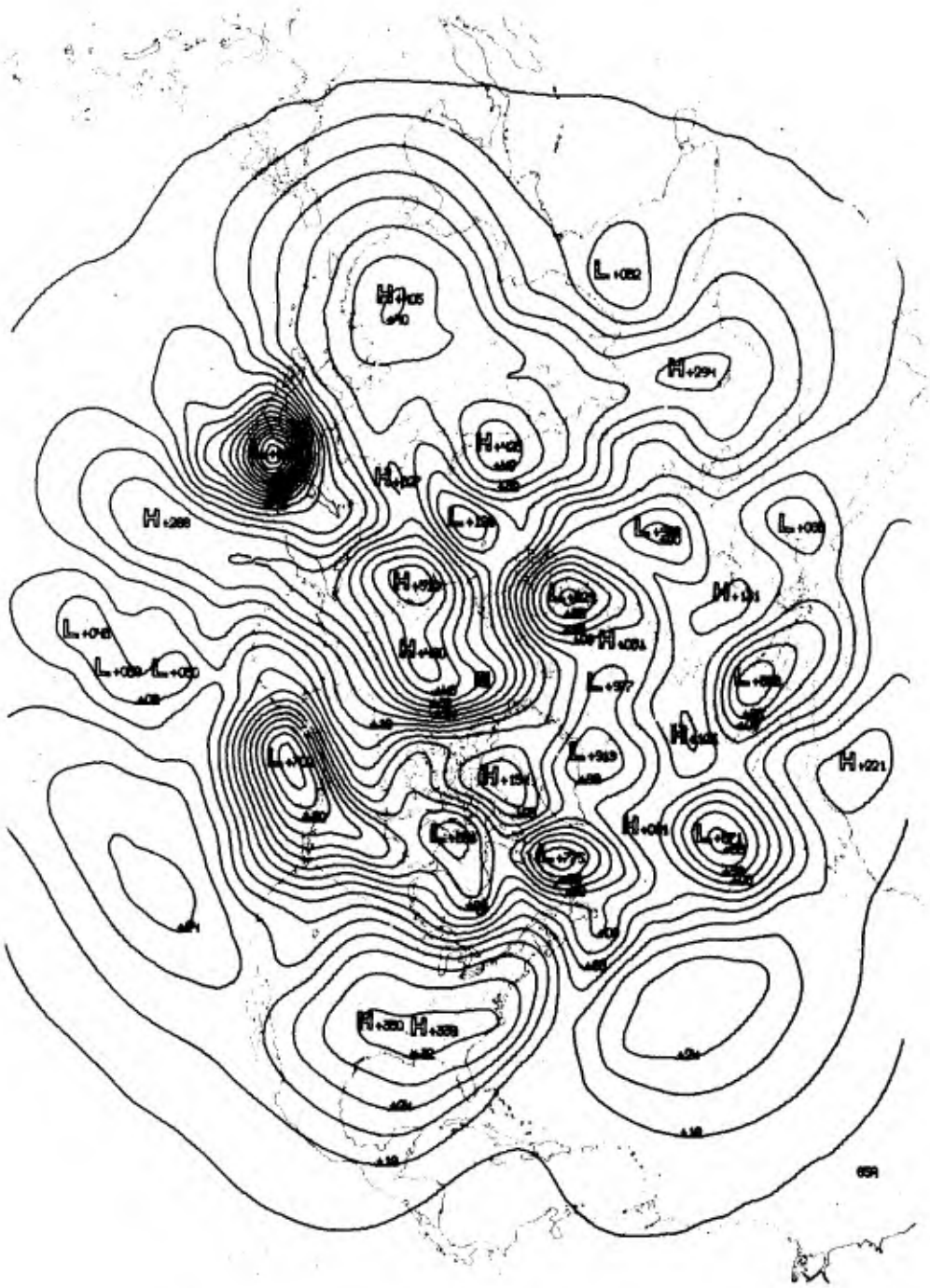

Figure 12. CYCLIC BOUNDARIES MODEL.
Identical to standard run in other ways.

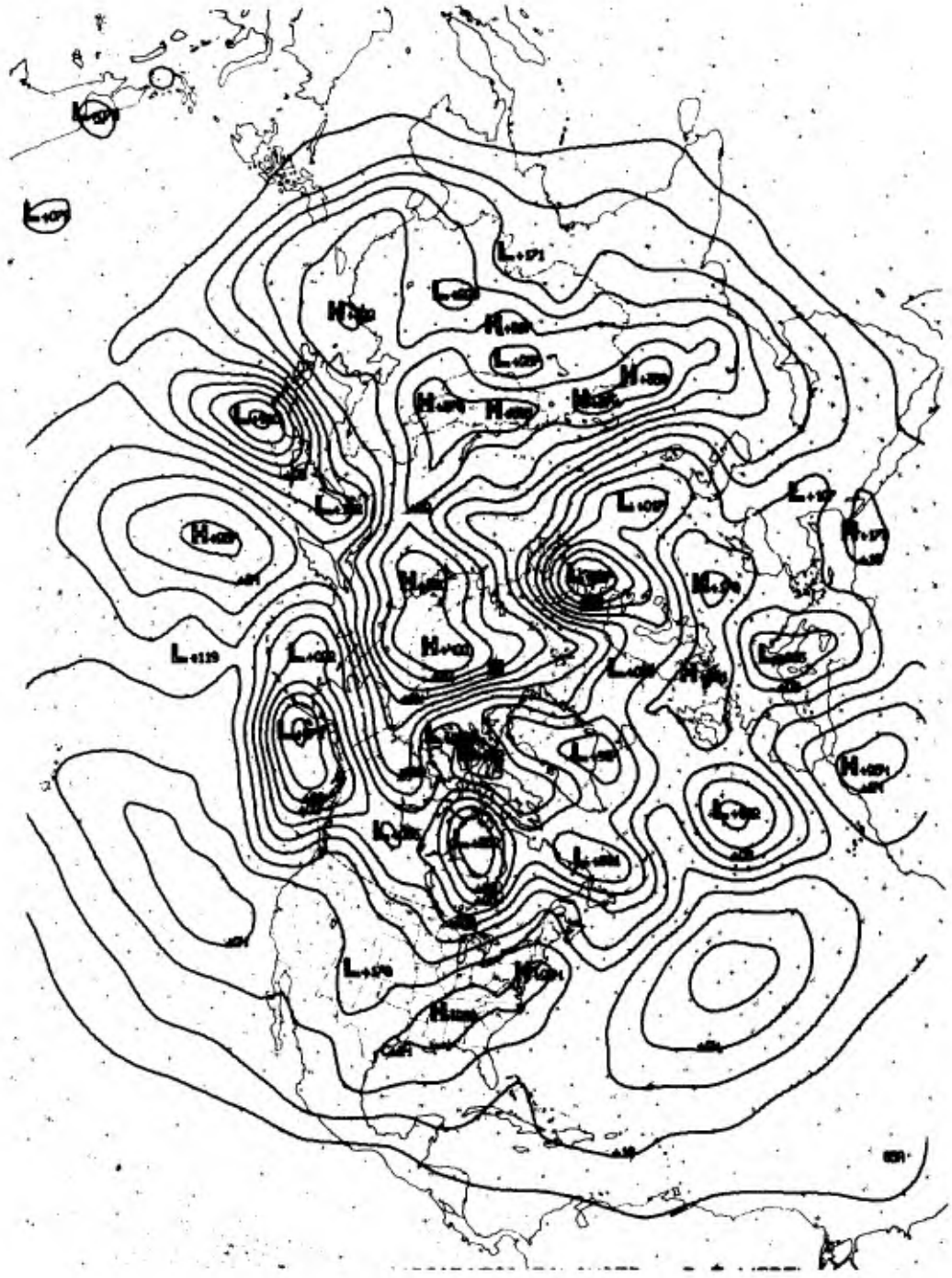

Figure 13. ADIABATIC MODEL.
Identical to standard run
in other ways.

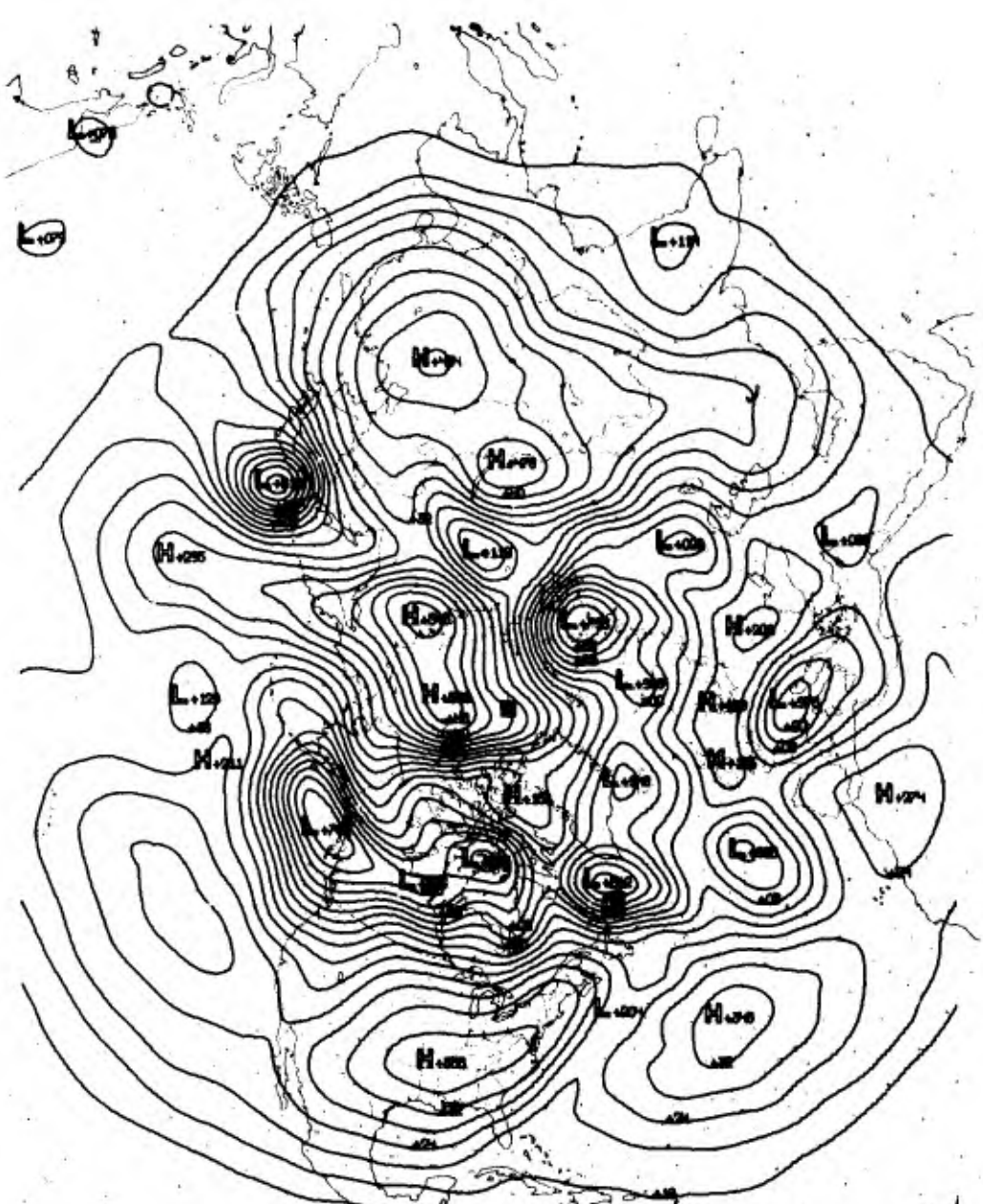

Figure 14. GEOSTROPHIC WIND MODEL.
Identical to standard run in other ways.

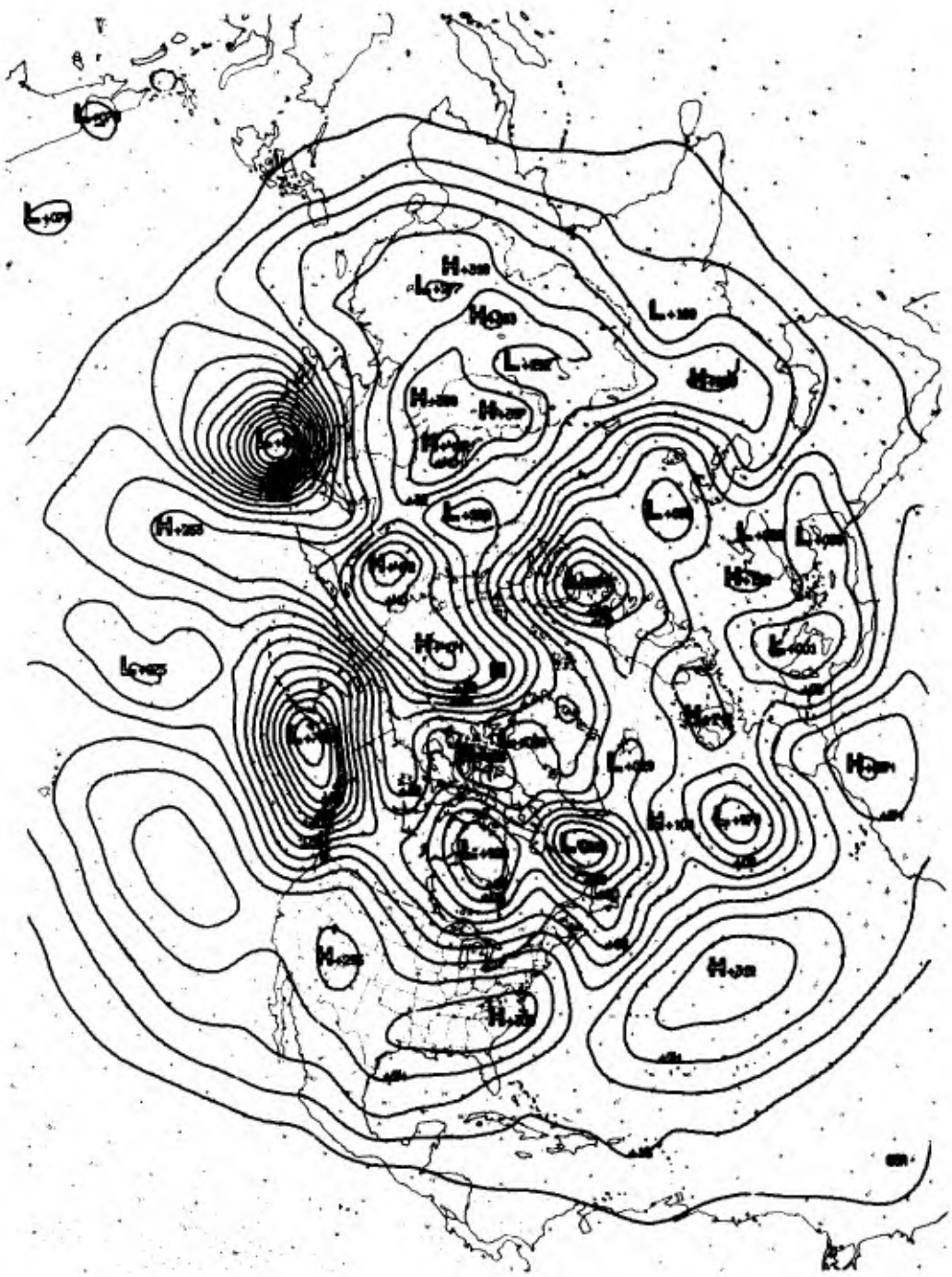

Figure 15. REALISTIC MOUNTAIN MODEL.
Identical to standard run in other ways.

## 6. FUTURE DEVELOPMENT

Those study areas in which real hope exists appear to be related to the reduction of truncation error by shifting to a finer mesh, and to the reduction of initialization error by improvements in the data base or analysis scheme. Other improvements of a more minor nature will no doubt result from refinements in numerical techniques or in the formulation of specific terms (such as the heating functions).

There are several aspects to the initialization problem. These include, but are not limited to: the number, distribution, type and quality of observations; to the manner in which these observations are employed to model the state parameter structure. Although the first of these constitutes an acute problem, it is not a legitimate pursuit for the authors. We feel rather hopeful though, that satellite-sourced soundings will be available in large numbers in the coming years. Rather, we can concentrate our efforts on analysis models which dynamically condition the state parameter structure, and on techniques which derive from these structures the initial wind distributions, and the like. Since our experience level with baroclinic primitive equation models is still limited, we feel also a need to examine the implied phase relationships to determine which perturbations, real or fictitious, lead to baroclinic developments. Further, can the fictitious perturbations be quality controlled out of the initial analyses?

As to the matter of truncation error, one can fall back on recognizable constraints. How much time can I take to produce a three-day forecast? How many points can I have in my grid? How many levels? Do I possess the computer power to do the type of job that is required? Looking into the very early 1970's, it appears as though we may be able to afford to predict on an 8000-point grid rather than on our current 4000-point grid. For the immediate future, we feel reasonably satisfied with five-layer resolution in the vertical. To help pay for this "growth" we developed the Four-Processor Model. In addition, those computational segments for which the physics is reasonably firm can be coded in machine language. The fixed-point arithmetic problem can be studied, too. At the current time, we use 100% of our CDC 6500 computer capability and 50% of our Extended Core capacity. To shift to an 8000-point grid, additional central memory would ordinarily be required, necessitating a different approach to partitioning the model. In this version, we plan to partition the horizontal domain into fourths (instead of the computational burden). In the net, this will actually cut the central memory requirement by 15% since we'll use one-fourth the points in fields twice their current size. Further, the scheme will allow a 72-hour prog to be executed in four hours vice 5 hours and 20 minutes, as required by the current partitioning scheme.

## REFERENCES


Arakawa, A.,
1966 Computational Design for Long-term Numerical Integration of the Equations of Fluid Motion: Two Dimensional Incompressible Flow, Part 1, Journal of Computer Physics, 1, pp. 119-143.

Arakawa, A., Katayama, A., and Mintz, Y.,
1968 Numerical Simulation of the General Circulation of the Atmosphere. (Appendix 1, A. Arakawa: Parameterization of Cumulus Convection), Proceedings of the WMO/IUGG Symposium on NWP, Tokyo, 14 pages.

Beckett, W., Kesel, P., Winninghoff, F., Wolff, P., and Morenoff, E.,
1970 Four-Way Parallel Processor Partition of an Atmospheric Primitive-Equation Prediction Model, September 1970 (submitted to ACM).

Danard, M.,
1969 A Simple Method of Including Long-Wave Radiation in a Tropospheric Numerical Prediction Model, Monthly Weather Review, 97, 1, pp. 77-85.

Dickson, R. R. and Posey, J.,
1967 Maps of Snow-Cover Probability for the Northern Hemisphere, Mo. Wea. Rev. Vol. 95, No. 6, pp. 347-353, June 1967.

Haltiner, G. J.,
1968 Numerical Weather Prediction, U. S. Naval Postgraduate School (unpublished manuscript).

Joseph, J.,
1966 Calculation of Radiative Heating in Numerical General Circulation Models, Department of Meteorology Technical Report No. 1, UCLA, 60 pages.

Kesel, P. G.,
1968 Experiments with Atmospheric Primitive-Equation Models, U. S. Naval Postgraduate School, Monterey, California (unpublished Master's Thesis).

Kesel, P. G., and Winninghoff, F. J.,
1970 Development of a Multi-Processor Primitive-Equation Atmospheric Prediction Model, Fleet Numerical Weather Weather Central, Monterey (unpublished manuscript).

Kuhn, P. M.,
1963 Soundings of Observed and Computed Infrared Flux, Journal of Geophysical Research, 68, 5, pp. 1415-1420, March.

Kurihara, Y.,
1968 Note on Finite-Difference Expressions for the Hydrostatic Relation and Pressure Gradient Force, Monthly Weather Review, 96, 9, September.

Langlois, W. E., and Kwok, H. C. W.,
1969 Description of the Mintz-Arakawa Numerical General Circulation Model, Department of Meteorology, UCLA Technical Report No. 3, 95 pages.

Miyakoda, K., Smagorinsky, J., Strickler, R. G., and Hembree, G. D.,
1969 Experimental Extended Predictions with a Nine-Level Hemispheric Model, Monthly Weather Review, 97, 1, pp. 1-76.

Phillips, N. A.,
1957 A Coordinate System having some Special Advantages for Numerical Forecasting, Journal of Meteorology, 14, 4.

Sellers, W.,
1965 Physical Climatology, The University of Chicago Press, Chicago and London.

Shuman, F. G., and Hovermale, J. B.,
1968 An Operational Six-Layer Primitive-Equation Model, Journal of Applied Meteorology, 7, pp. 527-547.

Smagorinsky, J., Manabe, S., and Holloway, L. L.,
1965 Numerical Results from a 9-Level General Circulation Model of the Atmosphere, Monthly Weather Review, 93, 12, pp. 727-768.

Winninghoff, F. J.,
1968 On the Adjustment Toward a Geostrophic Balance in a Simple Equation Model with Application to the Problems of Initialization and Objective Analysis, UCLA, unpublished Doctoral Thesis.

# SPECTRAL MODELS FOR GLOBAL ANALYSIS AND FORECASTING

Major Thomas W. Flattery, USAF

Operating Location H, Hq Air Weather Service

## Abstract

Although spectral methods offer several advantages for use in meteorological prediction, they have proved too costly to use on an operational basis. The use of Hough functions (the eigenfunctions of Laplace's tidal equation) offers the possibility, not only of making spectral prediction practical, but of performing spectral meteorological analysis directly on observed data. Hough functions can be used to define a wind law valid over the entire sphere. The tropics can thus be treated in the same manner as the mid- and high-latitudes. Because Hough functions can be divided into gravitational and rotational modes, they can be used to "filter" the primitive equations, and thus permit longer time extrapolations when they are used in a spectral forecasting model.

## I. INTRODUCTION

Spectral methods have been used for the investigation of a number of meteorological problems in the past. Spectral analysis has been discussed by Haurwitz and Craig [1], Ellsaesser [2], Eliasen and Machenhauer [3], and others. The application of spectral methods to forecasting has been discussed by Silberman [4], Platzman [5, 6], Baer and Platzman [7], Baer [8], Ellsaesser [9], Robert [10, 11], and others. However, techniques in operational use today are almost exclusively based upon finite-difference operations on arrays of data. These data are specified at regularly spaced grid-points within the area or volume being analyzed or forecast.

The reasons for this lack of application are not difficult to find. The typical spectral analysis procedure requires that the data to be analyzed be specified at a regular network of points — thus, a conventional meteorological analysis of observed data must previously have been performed. A spectral analysis of this type is therefore only useful if such a representation is more accurate, or yields new information not explicitly available in the grid-point data. Such information would of course include coefficient values for a spectral forecast. However, such forecasts have been considered too costly to perform routinely when the numerical techniques described in [4 - 11] are employed.

This paper reports on an attempt to avoid the major difficulties which have hindered the application of spectral techniques and to devise a scheme which is suitable for operational use.

## II. SYMBOLS

| | |
|---|---|
| $a$ | radius of earth |
| $a^{\ell}_{m,n}$ | expansion coefficient in (2.5) |
| $A_n$ | normalization factor (see (3.2)) |
| $b^{\ell}_{m,n}$ | expansion coefficient in (2.5) |
| $f$ | non-dimensional frequency, $f \equiv \sigma/2\Omega$ |
| $g$ | gravity |

| | |
|---|---|
| $G_n^\ell$ | orthogonal pressure function |
| $H_m^\ell$ | Hough function |
| h | equivalent depth, $h \equiv 4\Omega^2 a^2/g\beta$ |
| I | integral defined by (2.6) |
| k | weighting factor for winds vs heights |
| $\ell$ | longitudinal wave number |
| L | truncation limit for $\ell$ |
| m | order of Hough function |
| M | truncation limit for m |
| n | index for pressure functions |
| N | truncation limit for n |
| p | pressure |
| S | mean static stability (see (2.3)) |
| u,v | eastward and northward velocity components |
| $U_m^\ell$, $V_m^\ell$ | velocity functions related to $H_m^\ell$ by (2.4) |
| z | height of a constant-pressure surface |
| $\alpha_o$, $\alpha$ | mean and perturbation specific volumes |
| $\beta$, $\beta_n$ | eigenvalue of (2.2) or (2.3) |
| $\Theta_o$ | mean potential temperature |
| $\lambda$ | longitude |
| $\mu$ | sine of latitude |
| $\sigma$ | angular frequency of an atmospheric oscillation |
| $\phi$ | latitude |
| $\omega$ | total rate of change of pressure dp/dt |
| $\Omega$ | angular frequency of earth's rotation |

## III. METEOROLOGICAL ANALYSIS USING HOUGH FUNCTIONS

As the spectral method is based upon the representation of pertinent variables in series of functions, the choice of which functions to employ is of considerable importance. A basic constraint is that the functions be capable of satisfying any boundary conditions associated with the variables to be represented. Furthermore, it is highly desirable that the functions used be complete, or at a minimum, capable of representing arbitrary fields to within some specified accuracy. In general, surface spherical harmonics, the eigenfunctions of Laplace's equation on a sphere, have been the functions used for hemispheric or global spectral analysis and prediction. (For numerical reasons, Robert 10 used special combinations of spherical harmonics rather than the functions themselves.) These functions satisfy the horizontal boundary conditions for the atmospheric mass field (regularity at the poles and cyclic continuity in longitude). They do not satisfy the required conditions for the velocity components but can be made to do so by a simple modification. For vorticity models, where the one

predicted variable is the stream function, spherical harmonics possess a special advantage. They are themselves the eigenfunctions of the linearized vorticity equation, and their selection is therefore indicated not only for numerical simplicity, but because they are associated naturally with the physical problem itself.

The determination of "natural" functions to employ when considering the full set of meteorological equations, or "primitive" equations, would be difficult indeed. We therefore consider a simplified version of this set — that governing the linear behavior of an atmosphere which is in a basic state of rest:

$$\frac{\partial u}{\partial t} - 2\Omega\sin\phi\, v = -\frac{\partial gz}{a\cos\phi\partial\lambda}$$

$$\frac{\partial v}{\partial t} + 2\Omega\sin\phi\, u = -\frac{\partial gz}{a\partial\phi}$$

$$\frac{\partial gz}{\partial p} = -\alpha \qquad (2.1)$$

$$\frac{\partial u}{a\cos\phi\partial\lambda} + \frac{\partial v\cos\phi}{a\cos\phi\partial\phi} + \frac{\partial\omega}{\partial p} = 0$$

$$\frac{d(\ln\theta)}{dt} = 0$$

We postulate that the solution of these equations will constitute particularly efficient functions for the representation of the state of the atmosphere, since they would exactly represent the state of an idealized atmosphere.

Equations (2.1) can be combined after substitution of a factor $e^{i(\sigma t+l\lambda)}$, and separation of variables employed to give

$$\frac{d}{d\mu}\left(\frac{1-\mu^2}{f^2-\mu^2}\frac{dH}{d\mu}\right) - \frac{l^2 H}{(f^2-\mu^2)(1-\mu^2)} - \frac{l}{f}\frac{(f^2+\mu^2)H}{f^2-\mu^2} + \beta H = 0 \qquad (2.2)$$

$$\frac{d}{dp}\left(\frac{1}{S}\frac{dG}{dp}\right) + \beta G = 0 \qquad S \equiv -\alpha_o\frac{\partial(\ln\theta_o)}{\partial p} \qquad (2.3)$$

where $\beta$ is a separation constant, H and G are the latitudinal- and pressure-dependent parts of z, and the other symbols are as found in the list of symbols in Section II.

Equation (2.2) is Laplace's tidal equation and its regular eigenfunctions are known as Hough functions. Their properties are described by Flattery [12] and Longuet-Higgins [13]. They are functions of three parameters — f, $l$, and $\beta$, and an infinite set of $H_m^l(\mu)$ exists for each $\beta$ (or f) and each $l$.

In principle, values of $\beta_n$ must be determined by solving (2.3). A spectrum of eigenvalues $f_m$ and associated eigenfunctions $H_m^l(\mu)$ can then be determined for each $\beta_n$. The relation between $\beta$ and f for $l=1$ is shown in Figure 1. A similar relationship exists for other wave numbers. Each of the curved lines in Figure 1 represents a mode of oscillation of the model atmosphere (2.1). The modes divide into four categories - two sets of fast-moving modes ($m>0$) and two sets of slower modes ($m<0$). The fast modes correspond to gravity waves moving west ($f>0$) or east ($f<0$). The slower modes with $f>0$ are manifestations of meteorological type waves or Rossby waves. The fourth category with $f<0$ and $\beta<0$ are not associated with any known observed phenomenon. A set of $H_m^l(\mu)$ is determined by the intersections of the vertical line through a chosen value of $\beta$ with the curved lines.

Figure 2 illustrates the behavior of the $H_m^l(\mu)$ of rotational type for wave numbers $l=1$ to 24. This set of functions is associated with $\beta \sim 8.8$. The parameter $\beta$ is often expressed as an an equivalent depth h, where h is related to $\beta$ by $\beta \equiv 4\Omega^2a^2/gh$. Equations (2.1) can be used to relate the height function $H_m^l$ to wind component functions $U_m^l$ and $V_m^l$:

$$\sqrt{1-\mu^2}\,U_m^\ell = \frac{1}{f^2-\mu^2}\left\{\mu(1-\mu^2)\frac{d}{d\mu} - \ell f\right\} H_m^\ell$$

$$\sqrt{1-\mu^2}\,V_m^\ell = \frac{1}{f^2-\mu^2}\left\{\ell\mu - f(1-\mu^2)\frac{d}{d\mu}\right\} H_m^\ell \qquad (2.4)$$

These relations constitute a "wind law." They reduce to the geostrophic relation as $f \to 0$, but for any finite f, are valid over the whole sphere. Figures 3 and 4 show $U_m^\ell$ and $V_m^\ell$ corresponding to the height functions in Figure 2.

The solution of (2.3) is complicated by the difficulty of specifying a satisfactory upper boundary condition. In any case, the existence of a discrete spectrum of eigenvalues $\beta_n$ is questionable. We will therefore not use (2.3) and instead will use empirical pressure functions for the vertical representation of the atmosphere. This does not eliminate the necessity for choosing a value or values of $\beta$, since the horizontal functions depend on this parameter. Fortunately, most $H_m^\ell(\mu)$ do not vary rapidly in character as $\beta$ is varied, so the choice cannot be of critical importance to the spectral representation. Reference to atmospheric tidal theory [14, 15] suggests a value $\beta = 9$ as appropriate for the atmosphere. However, as a set of functions with $\beta = 59$ had been computed in connection with a related project, and were readily available, it was used in the experiments discussed below. The determination of an optimal choice for $\beta$ is a subject for future investigation.

A set of vertical functions was obtained, using the method of Obukhov [16] and Holmstrom [17], from operational analyses made at the National Meteorological Center during the month of April 1970. One-level analyses using Hough functions were performed at each of 15 pressure levels from 1000 to 10 millibars and empirical orthogonal functions were obtained using the coefficients of the Hough function series expansions as the dependent variables. A total of 19 days of analyses were used. The coefficients were grouped by longitudinal wave numbers, to admit the possibility that the vertical structure of the very-large-scale atmospheric waves may be markedly different from that of the shorter waves. Some evidence that this is true was found in the results, but definitive conclusions await the examination of a larger sample of analyses. The set of pressure functions obtained was adequate for testing the analysis procedure.

As the atmosphere is observed to be in quasi-geostrophic balance, we choose only the rotational modes to include in a spectral representation. Then z, u, and v can be expressed as

$$z \sim \sum_{\ell=0}^{L}\sum_{m=\ell}^{M}\sum_{n=1}^{N}\left(a_{m,n}^\ell \cos\ell\lambda + b_{m,n}^\ell \sin\ell\lambda\right)H_m^\ell(\mu)G_n^\ell(p)$$

$$u \sim \sum_{\ell=0}^{L}\sum_{m=\ell}^{M}\sum_{n=1}^{N}\left(a_{m,n}^\ell \cos\ell\lambda + b_{m,n}^\ell \sin\ell\lambda\right)U_m^\ell(\mu)G_n^\ell(p) \qquad (2.5)$$

$$v \sim \sum_{\ell=0}^{L}\sum_{m=\ell}^{M}\sum_{n=1}^{N}\left\{a_{m,n}^\ell \sin\ell\lambda - b_{m,n}^\ell \cos\ell\lambda\right\} V_m^\ell(\mu)\, G_n^\ell(p)$$

where the $G_n^\ell(p)$ are the empirical orthogonal functions described above. To signify rotational modes, it is desirable in principle to use notation with m negative as in Flattery [12]. However, as we will be concerned here only with rotational modes, we omit the negative designation, since no ambiguity can result.

We wish to minimize the integral

$$I = \int_V \left\{(z_{obs} - z_{anal})^2 + k\left[(u_{anal} - u_{obs})^2 + (v_{anal} - v_{obs})^2\right]\right\}dV \qquad (2.6)$$

over the volume being analyzed. The weighting factor k determines the relative importance to be given to the height observations compared to the wind observations.

The condition that I be minimized is given by

$$\frac{\partial I}{\partial a^{\ell}_{m,n}} = \frac{\partial I}{\partial b^{\ell}_{m,n}} = 0 \qquad \begin{matrix} \ell = 0,\ldots,L \\ m = \ell,\ldots,M \\ n = 1,\ldots,N \end{matrix} \qquad (2.7)$$

where L, M. N are the truncation limits of the series

In order to solve (2.7), it is necessary to know $Z_{obs}$, $U_{obs}$, and $V_{obs}$ over the volume to be analyzed, which is of course the object of the procedure. We therefore start with a "guess field," as is presently done in grid-point procedures, and divide the volume to be analyzed into cubes, in order to numerically evaluate the integrals which arise from (2.7). If an observation is present in the cube, it is used; otherwise, the guess field is substituted. Equation (2.7) can then be solved. If observations were available in every cube, the result would be a least-squares fit to the observed data. However, since data is distributed unevenly, the resultant least-squares fit minimizes a combination of departures from data and from guess-field values. In general, the observed data will not be well analyzed after this procedure is applied once. It is therefore necessary to iterate: After each iteration, the guess field has been altered in regions where data are available, so that a new least-squares problem is posed. The procedure converges until the data are analyzed to within the resolution of the series (2.5).

The rate of convergence of this procedure is dependent upon the number of cubes into which the atmosphere is divided. The larger the number, the slower the convergence. The integrity of the original guess field is also better maintained if the number of cubes is large. However, overemphasis on the guess field can be disastrous, since corrections would be limited to the smallest scales. The number of volume elements used in evaluating (2.7) must therefore represent a compromise. We wish to select the smallest number possible in order to hasten convergence, but at the same time maintain continuity through the guess field. Empirical evidence indicates that the number of cubes should be of the same order of magnitude as the number of observations available. However, the analysis is relatively insensitive to this number.

An example of the application of this procedure to data for 1200Z, 17 December 1967 is shown in Figure 5. In this case, the first guess field was a flat pressure surface, and a one-level analysis performed at 500 mb [$G^{\ell}_{n}(p)\equiv 1$]. Figure 6 shows the corresponding operational National Meteorological Center analysis. Agreement is evident except in the polar region, where no data were available, and in the mid-Pacific, where a deep low center appears. This feature was "bogused," that is, monitoring analysts inserted fictitious data to force it into the analysis. The Hough analysis apparently requires a more precise relationship between height and wind data, and bogusing techniques would have to be somewhat altered to obtain a desired response. The truncation limits for (2.5) were in this case L=24, M=12 (only symmetric Hough functions were used to procure a hemispheric, rather than global, analysis).

Figure 7 illustrates the capabilities of the analysis procedure when data are relatively sparse, but distributed over the whole hemisphere. The Hough analysis (Figure 7b) used only SIRS data — soundings recovered from infrared satellite observations. A total of 322 soundings covering a 24-hour period were used. Clearly, the resulting analysis lacks certain details of the operational NMC analysis (Figure 7a) which used all available data and continuity, but the basic flow pattern has been recovered. Some of the differences between the two analyses can be attributed to the time difference -- the NMC analysis is synoptic, while the Hough analysis used data valid between 1600 GMT 19 August and 1600 GMT 20 August, 1969. The resolution of the Hough analysis is L-16, M-12.

A significant potential advantage of the Hough analysis is its ability to specify both height and winds at all latitudes. As the wind law (2.4) is continuous over the sphere, tropical data enter naturally, and in the same manner, as mid- and high-latitude data. Evidence thus far obtained indicates that the analysis gives reasonable height and wind fields, even at the equator. The introduction of Hough heights and winds as initial conditions for a primitive equation hemispheric forecast model has not presented problems in the tropics.

The wind law (2.4) is linear, and is therefore inaccurate in those regions where trajectories havelarge curvature. To compensate for this, a modification can be made in the analysis procedure. Two separate sets of coefficients can be retained — one for heights and one for

wind components. In solving (2.7), the weighting factor k can be made small when height coefficients are being considered, and large for the wind coefficients. This procedure has been found to produce more realistic wind fields at a modest increase in expense.

A number of experiments have been performed using all available data between 1000 and 10 millibars to obtain a three-dimensional spectral analysis. The technique appears to converge well and give reasonable analyses at all levels. Some problems are present at the lowest and highest levels, but these are believed due to the inadequacy of the $G_n^\ell(p)$ as presently determined. The procedure performs a complete hemispheric analysis in approximately 10 minutes on the CDC 6600 computer, which is comparable to the time taken for the operational grid-point procedure when performed on the standard NWP octagon.

## IV. FORECASTING WITH HOUGH FUNCTIONS

Spectral forecasting techniques offer several advantages over grid-point methods. Spatial truncation can be limited to scales smaller than those being forecast; smoothing is not required, and spectral coefficients provide a particularly efficient means of storing information. However, spectral techniques are in general quite costly in terms of computer time when compared to those utilizing grid points.

Similar statements apply to a comparison between "primitive equation" atmospheric models (those which utilize the full set of hydrostatic meteorological equations) and "filtered" or "vorticity" models. The former allow a more general relationship to exist between mass and velocity fields, and permit a natural incorporation of forcing due to heating and friction. However, finite-difference extrapolations in time must be made several times more frequently because of the existence of high-frequency motions in such models, and they therefore require much more computer time.

The use of Hough functions offers the possibility of retaining many of the advantages noted above, while reducing the cost to a level acceptable for operational use. Consider the primitive equations for a barotropic fluid covering the (spherical) rotating earth:

$$\begin{aligned} \frac{du}{dt} - 2\Omega\sin\phi\, v &= -\frac{\partial gz}{a\cos\phi\,\partial\lambda} \\ \frac{dv}{dt} + 2\Omega\sin\phi\, u &= -\frac{\partial gz}{a\,\partial\phi} \\ \frac{dz}{dt} + z\nabla\cdot\vec{v} &= 0. \end{aligned} \tag{3.1}$$

We assume that a Hough one-level analysis has been performed so that the dependent variables u, v, and z are expressed as in (2.5) with $G_n^\ell(p)\equiv 1$, and N=1.

Equations (3.1) permit gravity waves as well as the desired meteorological (Rossby) waves, and therefore numerical stability considerations dictate that a small time step be used for time extrapolation. However, the linear behavior of the fields represented by (2.5) is rotational; gravity waves are not present because the gravitational Hough functions were not included in the series expansions. The time step can be increased to that which is used for vorticity models.

The general technique used for spectral calculations is to substitute the series (2.5) into (3.1) and, effectively, to express the non-linear terms in series of the same form as (2.5). This procedure is facilitated if the expansion functions are orthogonal. For the case of Hough functions with $\beta$ = constant, the orthogonality relationship is

$$\int_{-1}^{1} H_m^\ell H_n^\ell + \beta\left(\frac{U_m^\ell U_n^\ell + V_m^\ell V_n^\ell}{1-\mu^2}\right)d\mu = A_m\,\delta_{m,n} \tag{3.2}$$

where $\delta_{m,n}$ is the Kroneker delta and $A_m$ is a normalization factor. This relationship does not lend itself to simple application if the dependent variables are kept in spectral form. We therefore adopt an alternative approach.

Consider a latitude-longitude grid covering the globe (or hemisphere). If the points are equally spaced, the analysis procedure described in Section 3 becomes a true least-squares fit. No iteration is required. We therefore calculate $\partial u/\partial t$, $\partial v/\partial t$, and $\partial z/\partial t$ at the points of such a grid by summing the series (2.5). We can then extrapolate at each grid-point to obtain future values of u, v, and z. We then perform an analysis on this new field to return to a spectral representation. Because only rotational Hough functions are included, those gravitational waves present in the new field are left out, and only the rotational part is retained. This procedure can then be repeated until the desired forecast is obtained.

A number of experiments have been conducted using such a model over the Northern Hemisphere. The program requires approximately one minute for each 12-hour forecast period when run on the CDC 6600 computer to produce forecasts with resolution L=24, M=12. This resolution has been found to be similar to that obtained from the standard NWP octagon. The forecasts themselves appear to be similar to those produced by other barotropic models, but exact comparisons are difficult due to the present lack of forcing terms in the Hough forecast model. Further evaluation of the quality and usefulness of the forecasts is in progress. The forecasting procedure described above can be easily extended to three dimensions and a model using this technique is now being developed.

## V. SUMMARY

The use of Hough functions for meteorological analysis offers several possible advantages over present techniques:

a. A global analysis of the atmosphere is easily accomplished as the tropics can be treated in the same manner as other latitudes.

b. The scale of the analysis can be easily controlled so that data sparse regions blend naturally with those where observations are plentiful. The Hough procedure can analyze satellite data, which is observed in widely separated swaths, without introducing unrealistic short-wave features.

c. Since Hough functions arise from the study of atmospheric oscillations, they should be particularly efficient for the representation of observed mass and velocity fields.

The use of Hough functions for numerical prediction is also potentially advantageous. By utilizing them, it is possible to retain the form of the primitive equations while suppressing the non-meteorological part of their solution.

## VI. REFERENCES


[1] Haurwity, B, and Craig, R. A., Atmospheric Flow Patterns and Their Representation by Spherical Surface Harmonics, Geophysical Research Paper No. 14, ARDC, AFCRC, Cambridge, 1952, 78 pp.

[2] Ellsaesser, H. W., "Expansion of Hemispheric Meteorological Data in Antisymmetric Surface Spherical Harminic (Toplace) Series," Journal of Applied Meteorology, Vol. 5, No. 3, June, 1966, pp 263-276.

[3] Eliasen, E., and Machenhauer, B., "On the Observed Large-Scale Atmospheric Wave Motions," Tellus, Vol. 21, pp. 149-166, 1969.

[4] Silberman, I., "Planetary Waves in the Atmosphere," Journal of Meteorology, Vol II, No. 1, Feb. 1954, pp.27-34.

[5] Platzman, G. W., "The Spectral Form of the Vorticity Equation," Journal of Meteorology, Vol. 17, No. 6, Dec, 1960, pp. 635-644.

[6] Platzman, G. W., "The Analytical Dynamics of the Spectral Vorticity Equation," Journal of the Atmospheric Sciences, Vol. 19, No. 4, July 1962, pp. 313-328.

[7] Baer, F., and Platzman, G. W., "A Procedure for Numerical Integration of the Spectral Vorticity Equation," Journal of Meteorology, Vol. 18, No. 3, June 1961, pp. 393-401.

[8] Baer, F., "Integration with the Spectral Vorticity Equation," Journal of the Atmospheric Sciences, Vol. 21, No. 3, May, 1964, pp. 260-276.

[9] Ellsaesser, H. W., "Evaluation of Spectral Versus Grid Methods of Hemispheric Numerical Weather Prediction," Journal of Applied Meteorology, Vol. 5, No. 3, June 1966, pp. 240-262.

[10] Robert, A. J., "The Integration of a Low Order Spectral Form of the Primitive Meteorological Equations," Journal of the Meteorological Society of Japan, Vol. 44, No. 5, Oct. 1966, pp. 237-245.

[11] Robert, A. J., "Integration of a Spectral Barotropic Model from Global 500-mb Charts," Monthly Weather Review, Vol. 96, No. 2, Feb. 1968, pp. 83-85.

[12] Flattery, T. W., "Hough Functions," Technical Report No. 21 to the National Science Foundation (Grant NSF-GP-471), University of Chicago, Department of the Geophysical Sciences, March, 1967.

[13] Longuet-Higgins, M. S., "The Eigenfunctions of Laplace's Tidal Equation on a Sphere," Translations of the Royal Society of London, Vol 262, Feb 1968, pp. 511-607.

[14] Weekes, K. and Wilkes, M. V., "Atmospheric Oscillations and the Resonance Theory," Proceedings of the Royal Society of London, Vol A 192, 1947, pp 80-99.

[15] Siebert, M., "Atmospheric Tides," Advances in Geophysics, Vol. 7, 1961, pp. 105-187.

[16] Obukhov, A. M., "The Statistically Orthogonal Expansion of Empirical Functions," Izvestia, Atmospheric and Oceanic Physics (AGU translation), Series 1960, pp. 288-291.

[17] Holmstrom, I., "On a Method for Parametric Representation of the State of the Atmosphere," Tellus, Vol. 15, No. 2, 1963, pp. 127-149.

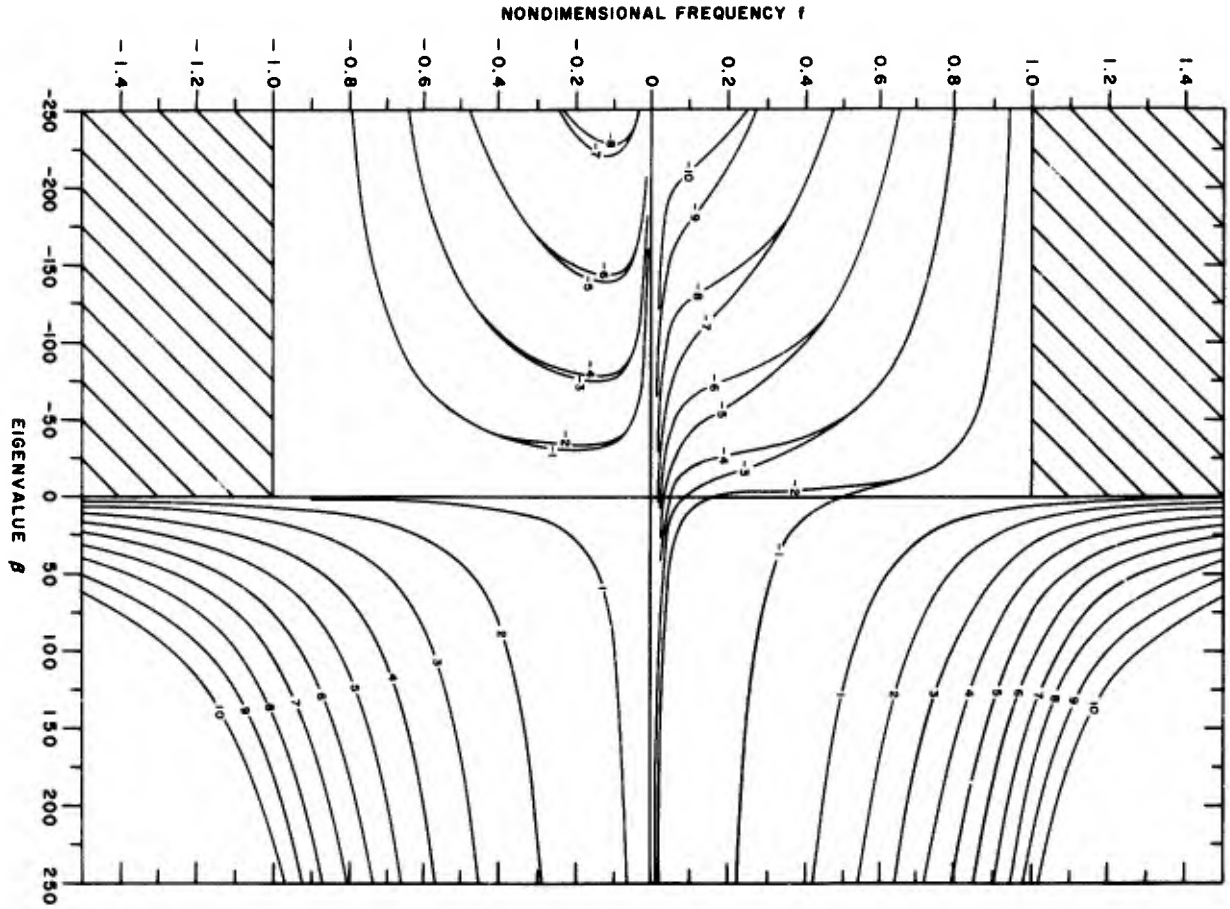


Figure 1. The relationship between eigenvalue β and non-dimensional frequency f for wave number $\ell = 1$.

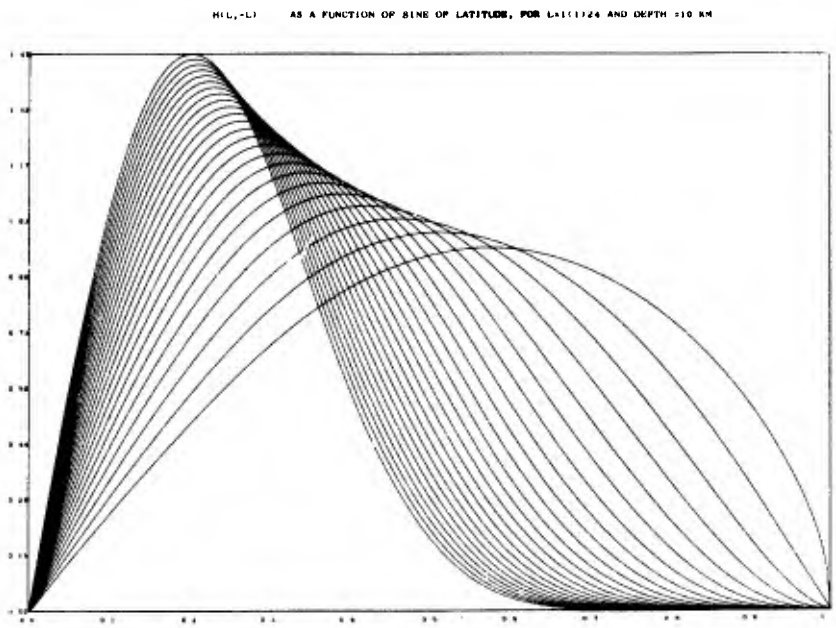

Figure 2. Latitudinal variational of $H_\ell^p(\mu)$ for $\beta = 8.8$ and wave number $\ell$ = to 24.

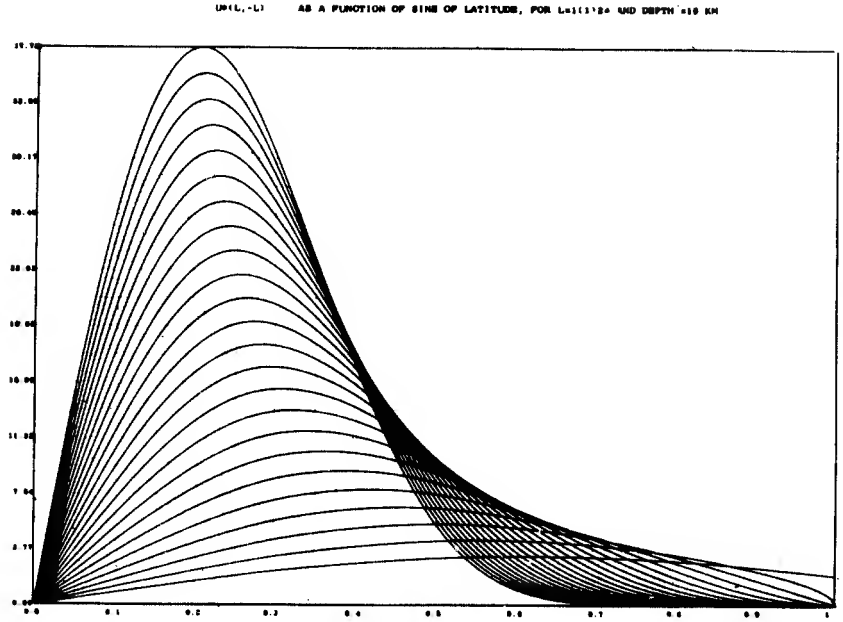

Figure 3. Latitudinal variation of $U_{\ell}^{\mu}(\mu)$ for $\beta = 8.8$ and wave number $\ell = 1$ to 24.

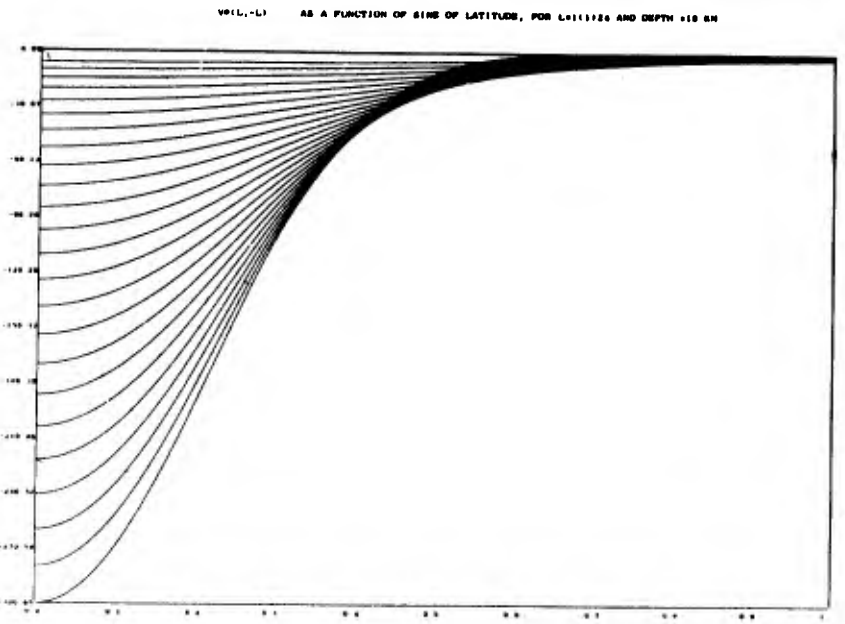

Figure 4. Latitudinal variation of $V_{\ell}^{p}(\mu)$ for $\beta = 8.8$ and wave number $\ell = 1$ to 24

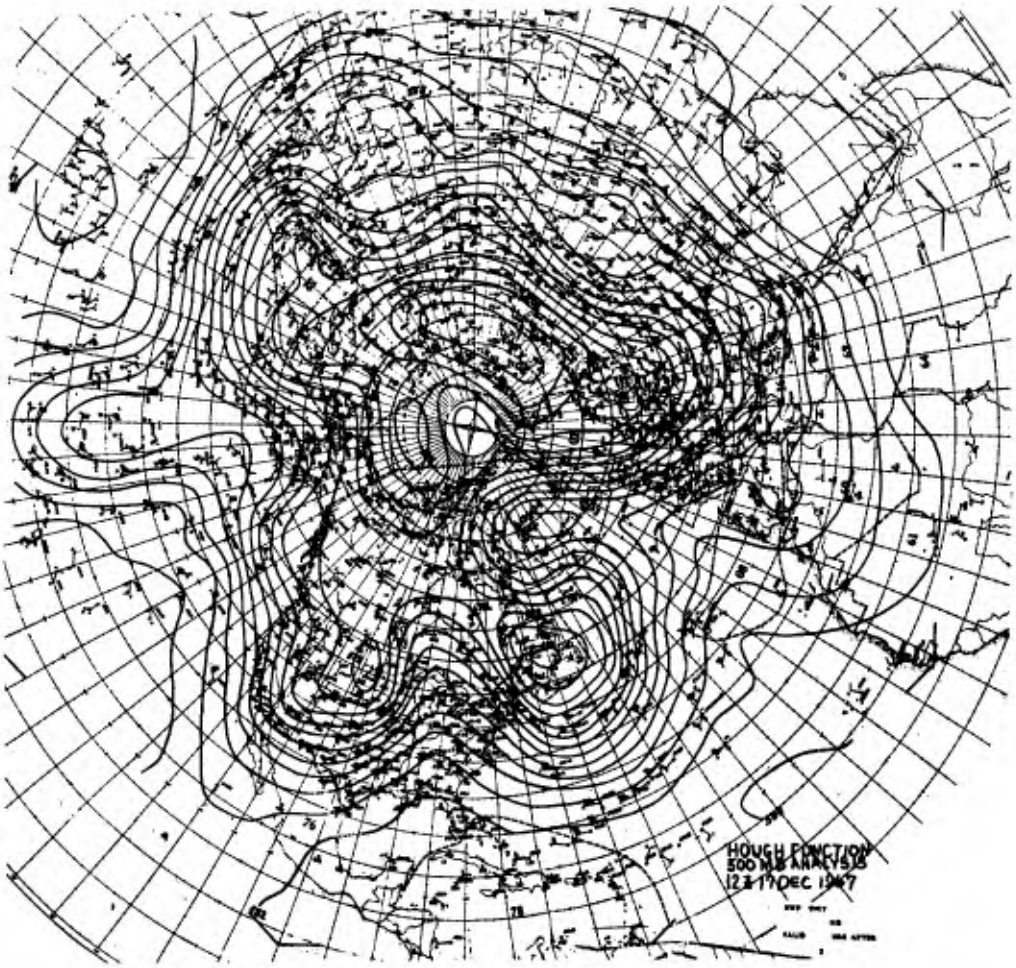


Figure 5. Hough-function 500-mb analysis for 1200 GMT, 17 December 1967.

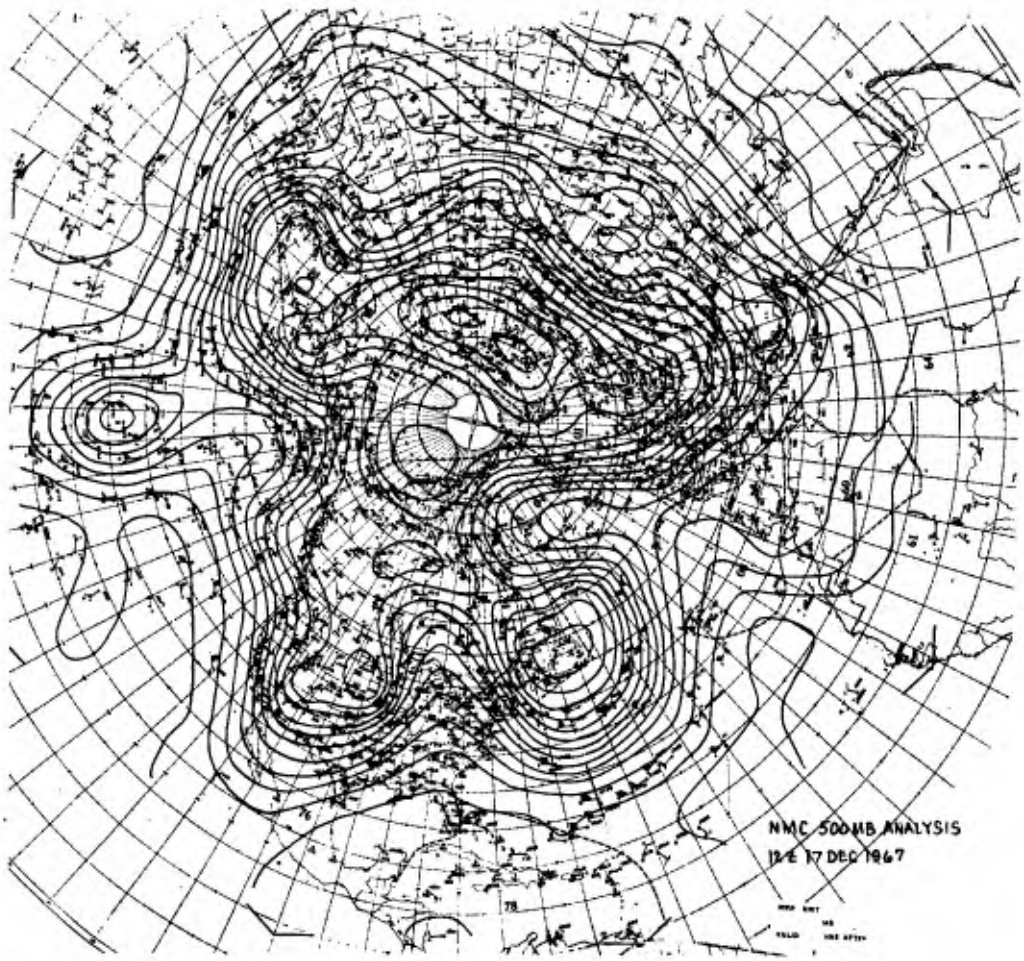


Figure 6. National Meteorological Center 500-mb analysis for 1200 GMT, 17 December 1967

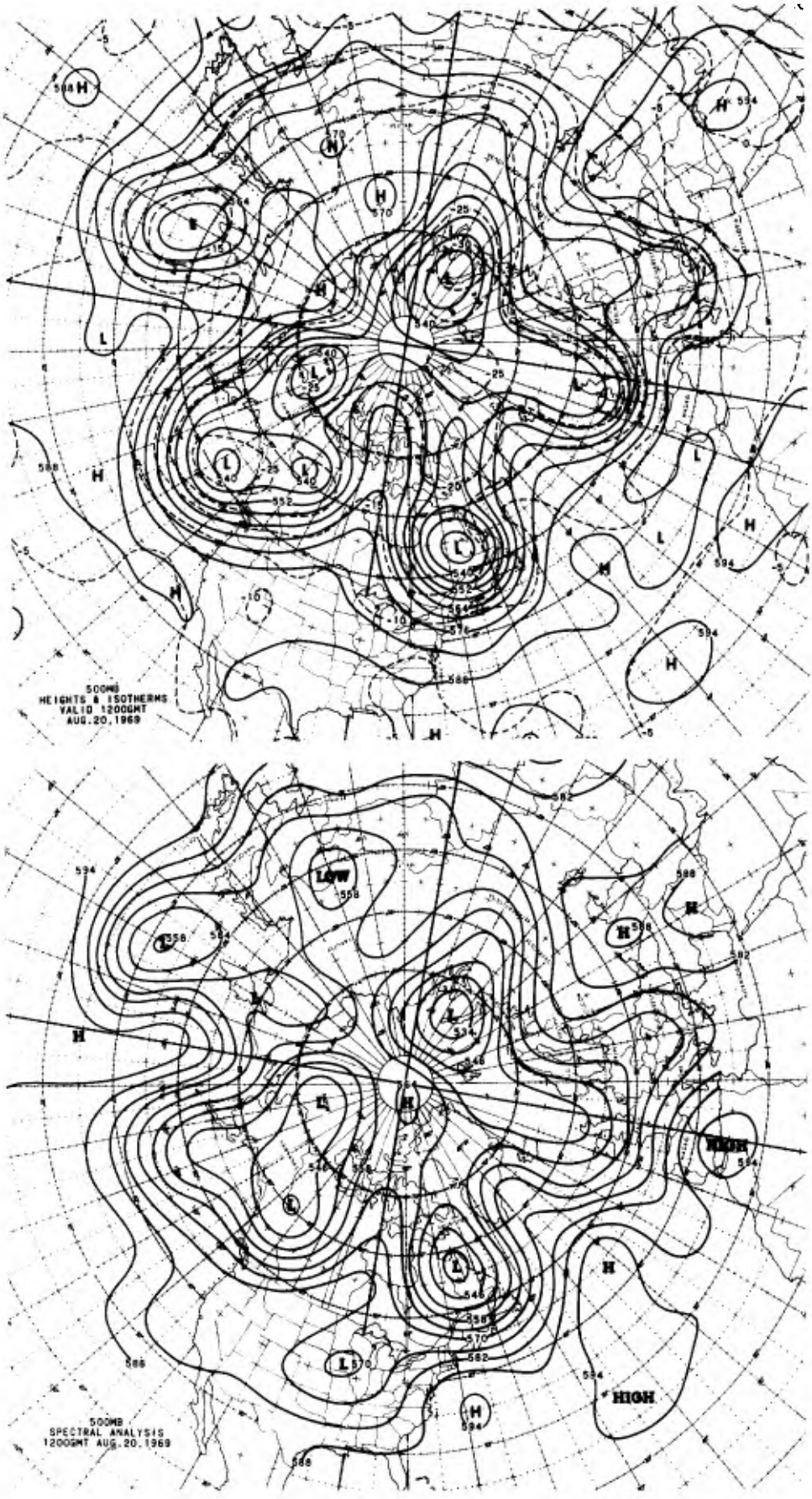


Figure 7. (a) National Meteorological Center 500-mb analysis for 1200 GMT, 20 August 1969

(b) Hough-function analysis using infra-red satellite data obtained from 1600 GMT, 19 Aug 1969 to 1600 GMT, 20 August 1969.

# SOME PRIMITIVE-EQUATION MODEL EXPERIMENTS FOR A LIMITED REGION OF THE TROPICS

Prof. R. L. Elsberry and LCdr. E. J. Harrison, Jr.

Naval Postgraduate School
Monterey, California 93940

Abstract

A nine-layer primitive equation model designed to test the effect of various latent heat parameterization schemes on the prediction of tropical circulations is described. The model is initialized from wind information. Two types of oscillations arose from the imposed horizontal boundary conditions — a short-period height oscillation and a longer period kinetic-energy oscillation. The character of the two oscillations and the required boundary conditions to remove the oscillations are described. Tests of the model with three parameterization schemes are compared by means of latent and sensible heat balances, a kinetic energy balance, and the predicted distribution of precipitation over a 24-hour period.

## 1. INTRODUCTION

As we move into the 1970's we presumably have the capability of integration of the equations of motion for global forecasting. Still there is considerable justification for integrating limited region models. This is particularly true in the tropics where conventional data coverage is rather limited. Furthermore some of the knowledge accumulated about primitive equation models needs to be tested in three-dimensional tropical models.

In the research reported here there were three objectives: 1. To examine problems resulting from initialization based primarily on wind information. 2. To test the effect of various techniques for incorporating latent heat of condensation. 3. To predict development of tropical circulations. Experiments concerned with the first two of these objectives are briefly discussed below.

Although the prognostic model described here is separate from the Fleet Numerical Weather Central (Monterey) model described by Lt. Kesel in an earlier paper in these proceedings, the finite difference forms used are rather similar. The model differs from the FNWC model in that the equations are in pressure coordinates, and are for nine layers. The upper and lower pressure levels are 100 mb and 1000 mb, respectively. Values of the potential temperature ($\theta$), geopotential ($\varphi$), and vertical velocity ($\omega$) are carried at 1000 mb. Vertical velocity is carried at intermediate 100 mb levels, with all other variables staggered at the mid-levels.

Before discussing the modifications in the equations required for the various latent-heat parameterization schemes, we describe some oscillations which arose from the horizontal boundary conditions.

## 2. DATA INITIALIZATION

The prognostic model is kept as simple as possible to isolate the effects of various types of latent heating parameterization. The equations and the initial experiments with a parameterization due to Kuo [7] are described in detail by Harrison [4]. In general the equations are expressed in pressure coordinates, and use the flux form of finite-differencing described by Arakawa [1] with the lower boundary condition

$$\frac{d\Phi_{1000}}{dt} = 0 \tag{1}$$

where $\varphi_{1000}$ is the 1000-mb geopotential. The vertical velocity in pressure coordinates at each level is computed from the continuity equation integrated downward from 100 mb where the vertical velocity is assumed to be zero.

Tw portant features of the prognostic model are matched by the diagnostic model. The flow in the zonal direction is made cyclic by extending the grid five points in the manner of Krishnamurti [6]. In effect this eliminates the need for specifying boundary conditions in the zonal direction. Along the northern and southern boundaries of the channel, insulated, free-slip walls are assumed. For example, at the wall placed midway between the northern-most gridpoints, with the index j increasing northward,

$$v_{j+1} = -\frac{m_{j+1}}{m_j} v_j \tag{2}$$

where v and u are the meridional and zonal wind components, and m is the map factor. Thus in the diagnostic model the wall is a streamline, requiring that $\psi$ = constant. Conservation of kinetic energy in the finite difference formulation requires

$$\Phi_{j+1} = \Phi_j \text{ at the northern wall}$$

and this condition is imposed in solving for the geopotential ($\Phi$) from the balance equation. This condition implies that the potential temperature is also constant across the walls. Note that the conditions chosen here are those required to match the prognostic equations, and differ from those of Hawkins and Rosenthal [5], which are designed to produce an accurate representation of the original winds. The compromise between accuracy and consistency with the prognostic equations is an important aspect in the limited-region model. Hawkins and Rosenthal [5] show that inclusion of the divergent portion of the wind improves the representation of the actual wind field, but experiments in which the initialization included divergent components are not discussed here.

## 3. SHORT-PERIOD HEIGHT OSCILLATIONS

Examination of the total kinetic energy led to discovery of a kinetic energy oscillation and prompted a detailed analysis of the height fields at various subintervals of the period. In the frictionless adiabatic version of the model, the geopotential averaged over each pressure surface varied by less than 10 $m^2 sec^{-2}$, as might be expected from Eq. (1). Calculation of the root mean square deviation (RMSD) of the geopotential from the area-averaged mean did illustrate a short-period oscillation. Some indication of a longer-period variation in the RMSD of geopotential appears in Fig. 1, but the dominant period for Experiment I is about four hours. The amplitude of the oscillation decreases from 1000 mb to 650 mb, then increases again to 250 mb, although the phase is different. An oscillation of 100 $m^2 sec^{-2}$ represents a significant distortion of the geopotential on the pressure surface, especially at 1000 mb.

The evolution of deviations from the initial 1000 mb height field during the first cycle of the oscillation is shown in Fig. 2. The positive center to the right of the middle of the grid corresponds to the position of Tropical Storm Betsy, the main synoptic feature of interest. By the end of the first hour (Fig. 2a) the storm has been predicted to fill nearly 25 meters from an

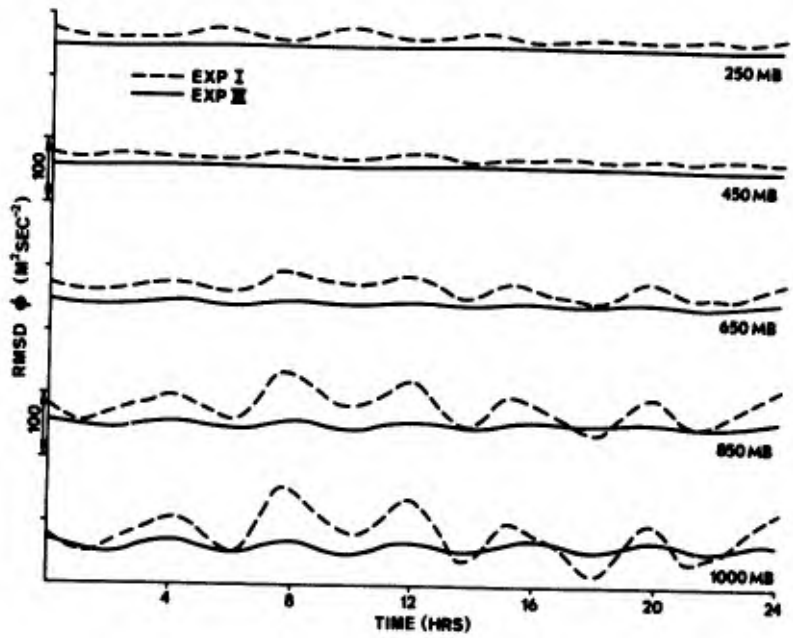


Fig. 1 Time variation of the root-mean-square deviations of the geopotential for selected levels. Each of the curves is to the same scale with the ordinates displaced.

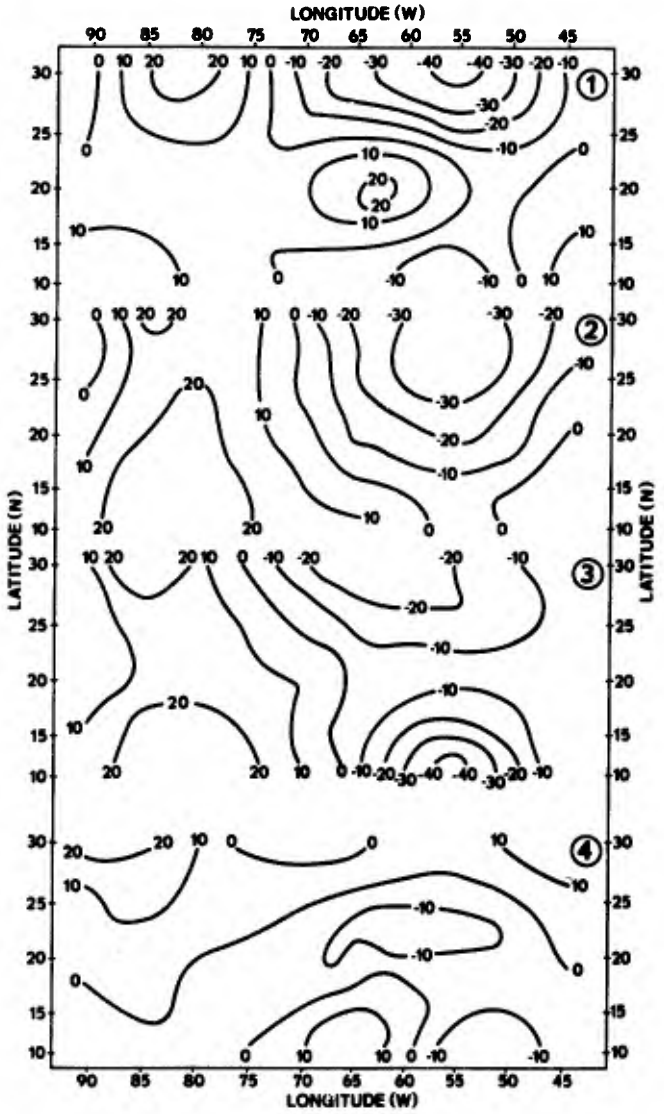


Fig. 2 Deviations from the initial 1000-mb height (m) field at: (a) 1 hour, (b) 2 hours, (c) 3 hours, (d) 4 hours from initial time of 1200 GMT on 29 August 1965.

initial 1000-mb height value of 98 meters. To the northeast the extension of the Bermuda high has deepened more than 25 meters from a value of 175 m. Compensation occurs farther to the west, where the pressures are predicted to rise 25 m in one hour, so the area-averaged height changes by only 0.1 m. The rapid evolution of the rise and fall centers is evident in Fig. 2b-2d. At various times in the cycle the centers near the northern and the southern boundaries dominate, but near the end of the cycle (Fig. 2d) the magnitude of the deviations is diminishing. It is then easy to see why 12-hour and 24-hour predicted height fields appeared quite reasonable and masked the existence of the oscillation.

Deviations from the initial height fields at other levels (not shown) closely reflect those in Fig. 2a-2d, but with larger amplitudes as suggested by the theory of Benwell and Bretherton [2].

It should be noted that the character of the oscillation is quite distinct from that found by Benwell and Bretherton [2]. In their model the heights are fixed on the boundaries and the maximum amplitude is in the center of the region. With no compensation between pressure rises and falls, large height variations occur even when averaged over the entire region. As Benwell and Bretherton [2] point out, the oscillation was produced by a systematic bias due to the omission of the linear terms in the balance equation. For the experiment with height variations shown in Fig. 2a-2d, these terms are included. Experiments with other forms of the balance equation produced no change in the oscillation, although slightly different initial fields resulted.

The apparent origin of the height oscillation on the boundaries of the region suggested that matching of boundary conditions in the diagnostic phase to those in the prognostic phase may not be sufficient. For example at the northern wall, the tendency was to rapidly reduce the height gradient along the wall. In the first experiment (I) the first-guess field for relaxation of the initial pressure-height fields was obtained by differential analysis building upward from the surface pressure field. Values on the boundaries were computed with the hydrostatic equation using preliminary temperature analyses. In Experiment II the heights along the walls were set equal to constant values derived by averaging the initial guess heights along the walls. This restriction further deteriorates the representativeness of the initialization, particularly in the upper levels. Examination of height deviation fields for Experiment II showed that large height rises and falls on the walls were eliminated. The deviations which remained were nearly uniform along the walls and represent a slow "sloshing" from one wall to the other with a maximum value of about eight meters at 1000 mb.

Another detrimental aspect of the computationally-produced oscillation is shown in Fig. 3. Because of the cyclic continuity in the zonal direction and Eq. (2), the area average of the vertical velocity is zero. However, the root-mean-square of the vertical velocity at the 1000, 500 and 200-mb levels rapidly oscillates in Experiment I, especially at 1000 mb. The median RMS value of about $6 \times 10^{-4}$ mb/sec at 1000 mb is also significant, as most latent heat parameterization schemes depend on the vertical velocity at the top of the boundary layer. At higher levels the median RMS values are larger, but the dominant variations appear to have longer periods. In Experiment II these longer period variations at upper levels remain, but with smaller median values. The RMS vertical velocity at 1000 mb has approximately the same amplitude with a shift to slightly lower frequency. It is clear that removal of the short-period height oscillation does not completely eliminate the large vertical velocity variations. This periodicity of $\omega$ is related to the kinetic energy oscillation.

## 4. KINETIC ENERGY OSCILLATION

Early tests of the computational scheme with barotropic analytical fields verified the conservation of kinetic energy properties of the finite-difference scheme. However, both adiabatic and diabatic experiments with real data produced a kinetic energy oscillation with a period of 19 hours. The amplitude of the kinetic energy oscillation was large relative to

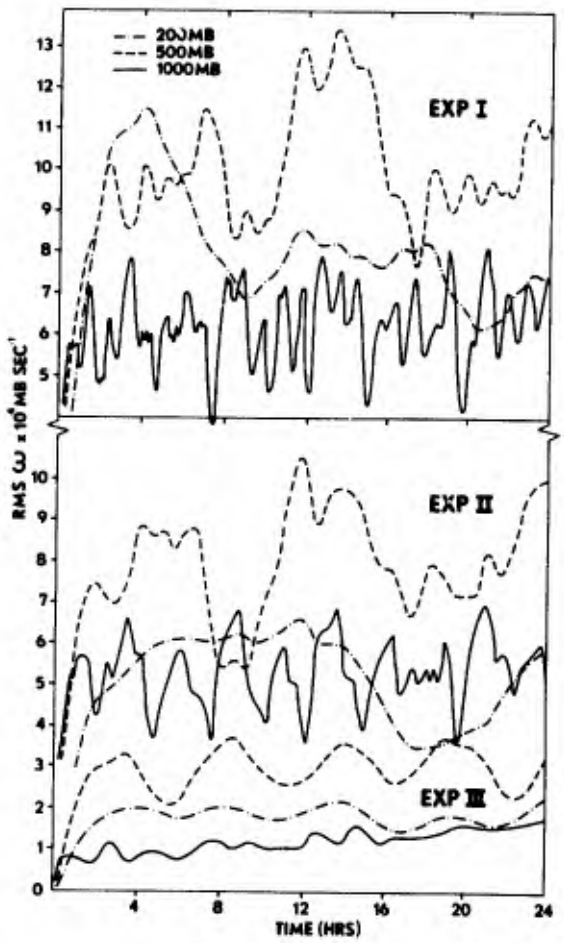


Fig. 3 Root-mean-square $\omega$ ($10^{-4}$mb $sec^{-1}$) as a function of time at: 1000 mb (solid line), 500 mb (dashed line), 200 mb (dot-dash line). (a) Original experiment including both the short-period height oscillation and long-period kinetic-energy oscillation. (b) With height oscillation removed. (c) With kinetic energy oscillation removed.

changes induced by baroclinic processes enhanced by diabatic heating, and thus could not be ignored.

Figs. 4a and 4b illustrate the kinetic energy oscillation at selected levels in Experiments I and II, respectively. The kinetic energy variation with time in Experiment II is smoother and has a slightly smaller amplitude. Most of the variation occurs at 150 mb, the level of maximum westerlies, and at 950 mb, the level of maximum easterlies. Intermediate layers have small fluctuations which suggests an oscillation in the kinetic energy of the zonal component.

The character of the wind oscillation indicates an imbalance between the north-south gradients of height and of the streamfunction $\psi$. As shown in Fig. 5 for Experiment II, where the two gradients are constant for each level, most of the levels within the easterly basic flow fall along the line corresponding to a geostrophic initial basic current. In the upper levels with westerly flow the gradient is reversed, and the corresponding points are not "balanced" with the stream function gradient between the walls. Both the first-guess height field, which is used to estimate the constant boundary heights, and the initial wind field, which is based on rather few reports at upper levels, contribute to the imbalance. After completion of the relaxation for the initial heights, the meridional pressure-height gradients at individual points are only slightly out of balance with the winds. However, the error is generally uniform across the channel. The initial kinetic energy is fixed, by using winds for initialization, and the total height gradient is imposed. As these boundary heights are not fixed in time, an adjustment occurs which tends to balance wind and height gradients. As the boundary heights vary under the constraint that the mean height be conserved, the north-south height gradient will tend to change in the same sense at all points. Thus there is a net change in the kinetic energy rather than a shift from zonal to meridional types of kinetic energy associated with the height oscillation.

Forcing the initial streamfunction boundary values and height to be balanced in a quasi-geostrophic sense eliminates the long-period kinetic energy oscillation (Experiment III in Fig. 4c). The temperature lapse rates at both the north and south walls are quite sensitive to small variations in the heights, or the thickness between the layers. Some vertical smoothing of the basic current, or equivalently the stream function difference between the north and the south walls, was necessary. Then the corresponding height gradients were chosen to assure smoothly varying temperature profiles. At the southern wall the lapse rates were made to approximate the mean tropical sounding (Riehl, [10]). A colder, but smooth temperature profile results on the northern wall when the required horizontal height gradient between the walls is imposed. A rather marked decrease in the RMS $\omega$ is noted in Fig. 3c for Experiment III. The long period oscillation at 200 mb is eliminated, as well as most of the shorter period variations. A periodicity of about five hours remains in the 500-mb and 200-mb RMS $\omega$ values. This upper tropospheric oscillation is not too important, at least in the tests of the latent-heat parameterization schemes.

## 5. DIABATIC EXPERIMENTS

Three latent-heat parameterization schemes, due to Kuo [7], Rosenthal [13], and Pearce and Riehl [9], have been tested. Most of the details and modifications needed to adapt these schemes to the model cannot be covered here. In some cases these changes are significant and it may not be justifiable to designate the modified scheme by the name of the original author. The objective of the various schemes is to evaluate vertical flux of heat and moisture on a scale smaller than the grid scale, i.e. an attempt to evaluate the terms

$$\frac{\partial \widetilde{\omega\theta}}{\partial p} = \frac{\partial \tilde{\omega}\tilde{\theta}}{\partial p} + \frac{\partial \widetilde{\omega^* q^*}}{\partial p}$$

$$\frac{\partial \widetilde{\omega q}}{\partial p} = \frac{\partial \tilde{\omega}\tilde{q}}{\partial p} + \frac{\partial \widetilde{\omega^* q^*}}{\partial p}$$

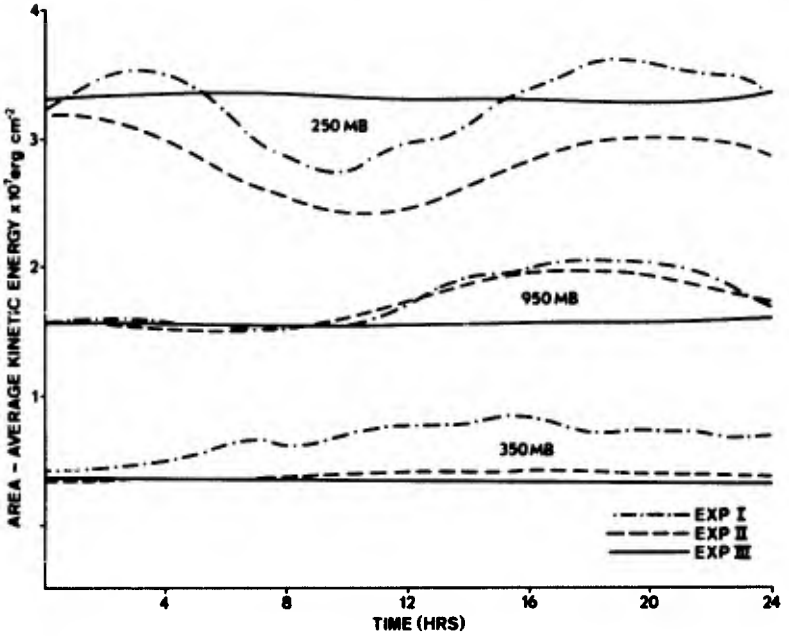


Fig. 4 Area-averaged kinetic energy ($10^7$ ergs $cm^{-2}$) at: 950 mb (solid line), 550 mb (dashed line), 150 mb (dot-dash line). (a) Experiment I, (b) Experiment II, (c) Experiment III.

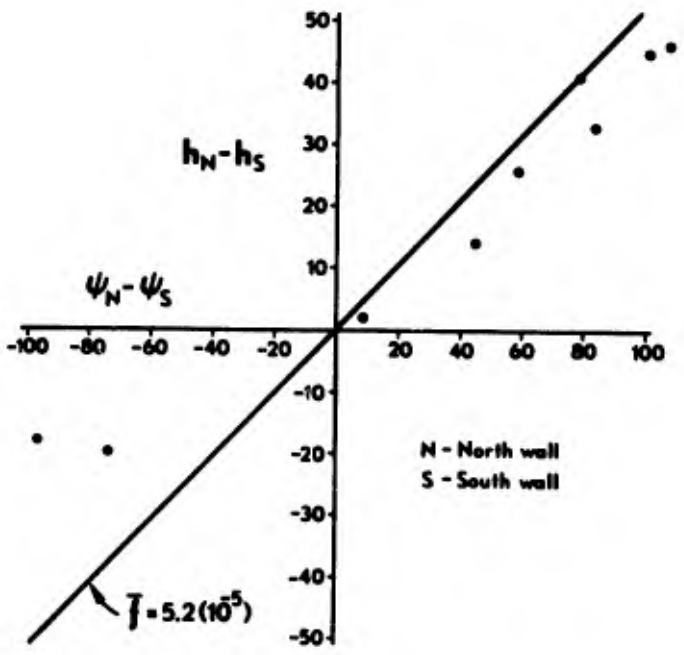


Fig. 5 Difference in stream function ( $x10^{-5} m^2 sec^{-1}$) and heights (h) in meters between the north (N) and south (S) walls for Experiment II. The solid line represents a geostrophic relation using the mean Coriolis acceleration for the channel.

where ~ denotes an average over the area of the grid and * denotes a deviation from the area average. Thus the first term on the right is the normal large scale convection and the second term represents convection of all scales smaller than that of the grid. In the cases to be described, the cumulonimbus is the only type of convection which is represented. The convection is presumed to penetrate to a height where the moist adiabat from the cloud base intersects the environmental sounding, which normally is above 250 mb in the tropics.

It should be emphasized that the $\omega^*$ represents an updraft concentrated in a small area within cloud and compensating descent over a large area outside cloud. The parameterization schemes generally involve a convective mass flux which is expressed in terms of the large-scale parameters of the model. In each of the cases, ascent of the convective flux is assumed to be along a moist adiabat from cloud base. Since the active convection generally occupies less than two per cent of the area, the environmental thermodynamic properties are taken to be those calculated by the normal finite difference equations.

Two crucial features are the mass flux and the "trigger" for the convection. In general the schemes depend on low-level convergence of moisture into the convective plume. The Rosenthal and the Pearce-Riehl schemes consider convection will occur if there is ascent at the top of the boundary layer. For the Kuo scheme, positive net integrated moisture convergence into the column is required, but the main contribution to the convergence is in the lowest layer.

In the Kuo scheme the total convergence of moisture into a column by large-scale advection, and evaporation from the sea surface, is designated by C. Two other quantities, C1 and C2, which are the amounts of moisture required to bring the environmental specific humidity q and temperature T to the moist-adiabat values $q_s$ and $T_s$, are also computed. Thus C1 and C2 represent the amount of moisture that would be required to produce a cloud in the time step $\Delta t$, while C is the amount of moisture actually available. The per cent of the area covered by active convective elements is then

$$a = \frac{C}{C1+C2}$$

and typically less than 1 or 2 per cent.

The net effect of the convection on the environment is twofold: (1) The specific humidity of the layer is increased by $a(q_s-q)$, presumably by lateral mixing of decaying convective elements. (2) The temperature of the layer is similarly increased by $a(T_s-T)$.

The Rosenthal scheme is somewhat simpler as the moisture distribution is not predicted. I.. the above expression for a, the only term in the denominator is that involving the amount of moisture (C2) which must be condensed to heat the entire column from the environment temperature T to the moist adiabat temperature $T_s$. Also the available moisture supply C is assumed to be the upward flux at the top of the boundary layer due to frictional convergence. Values of a are generally larger than in the Kuo scheme, although the available moisture supply is assumed to be only the vertical mass flux at the 900 mb level induced by convergence in the 1000-900 mb layer. This mass flux is assumed to reach saturation at the 900 mb level.

The Pearce and Riehl scheme is more physically-inclined in that it considers fluxes inside and outside of a model cloud. Fig. 6 illustrates the fluxes of moisture and temperature. Horizontal advection occurs at the boundary of the grid square and detrainment or entrainment effects are included at the sides of the model cloud. Continuity equations for the fluxes can be written to express the net effect on the moisture in the layer. These expressions are shown schematically in Fig. 6; the actual equations are derived by Pearce and Riehl (1968). One of the important features of the scheme is the expression for the precipitation. Substitution in the moisture equation leads to cancelling of the vertical fluxes within the cloud. Similar expressions for the net temperature change in the layer include a positive effect due to latent heat of condensation. The assumption that the incloud properties of the cloud are moist

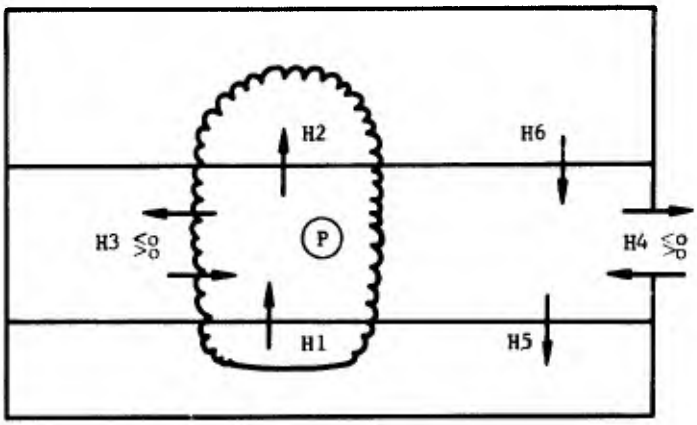


$$\omega^* = \omega - \omega_e \qquad \omega_e = -\Gamma\omega$$

$$\frac{H1}{H2} = \omega^* q^* \qquad H3 = q^* \frac{\partial\omega}{\partial p}^* \qquad H4 = \nabla\cdot W_2 q$$

$$\frac{H5}{H6} = \omega_e q \qquad P = -(H1 - H2) + H3$$

$$\frac{\Delta q}{\Delta t} \alpha - (H1 - H2) - (H5 - H6) - H4 - P$$

$$\frac{\Delta q}{\Delta t} \alpha - (H5 - H6) - H4 - H3$$

$$\frac{T1}{T2} = \omega^*\theta^* \qquad T3 = q^* \frac{\partial\theta}{\partial p}^* \qquad T4 = \nabla\cdot W_2 \theta$$

$$\frac{T5}{T6} = \omega_e\theta \qquad -\frac{L}{Cp} P = -(T1 - T2) + T3$$

$$\frac{\Delta\theta}{\Delta t} \alpha - (T1 - T2) - (T5 - T6) - T4 + \frac{LP}{Cp}$$

$$\frac{\Delta\theta}{\Delta t} \alpha - (T5 - T6) - T4 - T3$$

Fig. 6 Schematic illustration of the fluxes of moisture and temperature for the Pearce-Riehl scheme. Exact expressions may be found in Pearce and Riehl (1968).

adiabatic requires that the latent heat energy released be equal to the heat required to offset adiabatic expansion and to increase the potential energy of the convective parcels. This is also assumed to be true for entraining parcels. Thus the latent heat release does not appear explicitly in the temperature equation (see Fig. 6). The detrainment of cloudy air results in lateral mixing of properties, as are also assumed in the Kuo and the Rosenthal schemes. However, the dominant effects are due to clear air fluxes which are induced by the cloud.

The induced clear air fluxes ($\omega_e$) are proportional to the computed large-scale vertical velocity. The proportionality constant $\gamma$ is empirically derived from observations in several Caribbean easterly waves (Pearce and Riehl [9]; Riehl and Pearce [12]). The environmental vertical velocity is at most equal to one-half of the large-scale vertical velocity, and is required to be subsident. Compensating ascent is within cloud, so mass balance is maintained. Temperature and moisture changes are determined by flux convergence of $\omega^*$ and $\omega_e$, which are directly related to convergence of the large-scale motion. This is an important concept but it has not been widely tested.

Let us look first at the effect of the different parameterization schemes on the synoptic features for a single set of initial data. These will be compared with a frictionless, adiabatic prognosis from the same initial conditions. Fig. 7 is an illustration of the intensity changes and displacement of the 1000-mb pressure centers. There are two weak low-pressure centers in the trough along the southern wall, and two high cells in the subtropical ridge. However, the important translating feature is Tropical Storm Betsy ($L_1$). In each case the predicted displacement of Betsy is to the west-northwest rather than to the north-northwest as was observed. This is likely due to the presence of the walls. The predicted differences in displacement of the tropic storm are rather small; probably because the weak storm interacts very little with the basic current.

Examination of the magnitude of the pressure centers also shows little difference between the schemes. In every case the principal low center is filled by 10-17 m ($\approx$2 mb). The actual disturbance intensified early in the period, but decreased later to nearly the initial value. The other centers are in regions of weak gradients and the changes are rather small. Of course these results are from a single experiment — they only indicate that uncontrollable development does not occur in the model even though the necessary conditions seem to be present. We now look in more detail at the effects of the parameterization schemes on the large scale fields.

Inspection of the latent and sensible heat budgets of the entire region is one of the possible means of describing the role of the precipitation computed by the different schemes. The total heat energy is conserved by the computational scheme, except that advection is allowed through the 1000-mb surface. For comparison we include the comparable 24-hour balances of a frictionless, adiabatic version of the model.

The latent heat balance for the region is shown in Table 1 with units of cal $cm^{-2}$. In the frictionless, adiabatic model the total moisture remains constant, at least to small truncation error. No explicit moisture is carried in the Rosenthal scheme, but the evaporation in latent heat units ($Q_e$) in the subcloud which would be necessary to offset the precipitation (LP) is shown in parentheses. By comparison with the evaporation term computed in the other schemes, we see that the necessary evaporation is not excessive.

Because the advection (Adv) is small the main balance is between the evaporation in latent heat units and the precipitation. The values of $Q_e$ near 120 cal $cm^{-2}$ represent an evaporation in 24 hours of about 0.2 gm of liquid water. About one-half of the evaporation is precipitated with the Kuo scheme. The evaporation enters directly in the moisture available for convection in columns with net moisture convergence, but in the convective process only approximately one-third is condensed as the remainder goes to increase the specific humidity. The main feature to be seen in the latent-heat balance is the inability of the

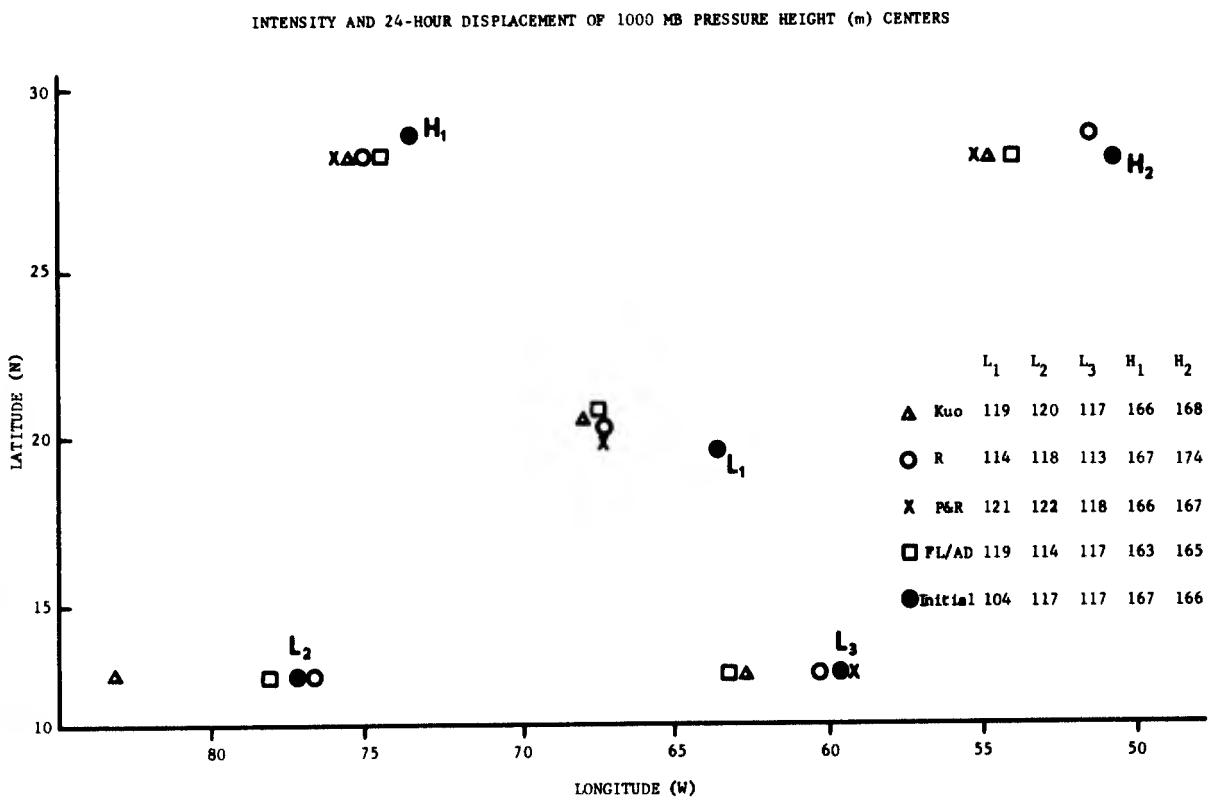


Fig. 7 Initial positions of 1000 mb pressure-height centers and displacement and intensity of the centers at the end of the 24 hours for the various models. The low pressure center ($L_1$) represents Tropical Storm Betsy (1965).

TABLE 1

LATENT-HEAT BALANCE
($cal/cm^2$)
t = 24 hours

| | $\Delta(L_g)$ | $Q_e$ | LP | Adv | Truncation |
|---|---|---|---|---|---|
| Frictionless, Adiabatic | 1 | | | 0 | 1 |
| Kuo | 53 | 121 | -68 | 2 | -2 |
| Rosenthal | | (107) | -107 | | |
| Pearce-Riehl | 107 | 125 | -15 | 0 | -3 |

TABLE 2

SENSIBLE-HEAT BALANCE
($cal/cm^2$)
t = 24 hours

| | $\Delta(c_pT)$ | $Q_s$ | LP | $Q_r$ | Adv | Truncation |
|---|---|---|---|---|---|---|
| Frictionless, Adiabatic | -2 | | | | 1 | -3 |
| Kuo | -67 | 13 | 68 | -146 | 16 | -18 |
| Rosenthal | -20 | | 107 | -128 | -14 | 15 |
| Pearce-Riehl | -116 | 18 | 15 | -146 | 19 | -22 |

TABLE 3

KINETIC-ENERGY BALANCE
($10^4$ $ergs/cm^2$)
t = 24 hours

| | $\Delta$(KE) | Gen | Adv | Dissipation | Truncation |
|---|---|---|---|---|---|
| Frictionless, Adiabatic | 101 | 86 | 15 | | 0 |
| Kuo | 70 | 1614 | 1 | -1545 | 0 |
| Rosenthal | 2765 | 5044 | 2 | -2281 | 0 |
| Pearce-Riehl | -925 | 832 | -2 | -1755 | 0 |

schemes, particularly Pearce-Riehl, to precipitate sufficient amounts of moisture to offset the evaporation.

Condensation, or in this case, precipitation heat tends to offset the radiation loss included in the sensible heat balance in Table 2. The assumed radiative cooling varies only with height, with values of 0.7°C/day in low layers to a small heating in the 100-200 mb layer. The profile generally approximates that found by Riehl [11] for this region. A lower radiative cooling ($Q_r$) for the Rosenthal scheme results as the 950 mb and 1000 mb temperatures are fixed for this scheme. Although the advection (Adv) is not small, the main balance should again be precipitation heating offsetting radiational cooling. However, as we noted above in the latent heat balance, the precipitation heating is too small. The sensible heat flux from the sea also contributes to offsetting the loss due to radiation. It is of some interest that the ratio of sensible heat flux to latent heat flux is 11 per cent and 14 per cent for the Kuo and the Pearce-Riehl schemes respectively. These are computed from actual sea-surface temperatures (Landis and Leipper, [8]) with the usual bulk transport equations, which are velocity dependent.

Truncation errors are rather large in all of the schemes. These errors accumulate in replacing vertical flux expressions that correspond to the large-scale horizontal fluxes with less exact convective-scale fluxes. As the truncation errors are of the same magnitude as the advection term, the errors do not change the physical interpretation of the sensible heat balance.

In summary each of the schemes results in precipitation which is too small. As a result the total moisture tends to increase and the temperatures tend to drop. Examination of the six-hourly balances showed even larger deficits of precipitation in the early periods with precipitation becoming more dominant near the end of the day. All the schemes depend directly on the vertical velocity which initially is zero. For the Rosenthal scheme the velocity at the top of the boundary layer due to frictional convergence is the crucial input to the latent heating, whereas in the Kuo scheme evaporation also contributes. The Pearce-Riehl scheme is even more directly related to vertical velocity at all levels. It takes some time for the vertical velocity at upper levels to respond to the heating, which only gradually extends to upper levels. However, once the heating does become significant in the Rosenthal and the Pearce-Riehl schemes, the coupling with the vertical velocity is too strong and single grid-point instability can develop. For this reason it was necessary to smooth the heating over surrounding points.

Our basic hypothesis is that latent heat release is important in the prediction of developing tropical circulations. The above results point out the importance of proper initialization for such circulations. Each of the schemes underestimates the precipitation in the first six hours, and the model with the Pearce-Riehl method is only becoming organized at the end of the 24-hour period.

Table 3 is a summary of the changes in kinetic energy summed over the entire volume. In the frictionless, adiabatic version the total kinetic energy increased about one per cent in the 24-hour period, mainly as a result of conversion from potential energy. The same order of magnitude of kinetic energy increase occurs with the Kuo scheme, but in that case the time change is a small residual between generation and dissipation terms. In the other two schemes these two terms do not offset each other, resulting in a very large kinetic energy increase with the Rosenthal scheme and a large decrease in the Pearce-Riehl model.

In the model the dissipation is entirely in the lowest layer, and the large dissipation also implies a large frictional convergence in this layer. Particularly in the Rosenthal method, the increased frictional convergence in the boundary layer leads to increased moisture supply to convective heat release. This is the conditional instability of the second kind (CISK) discussed by many authors. The same type of reasoning holds in general for the Kuo model. However, the effect of integrating the moisture convergence over the entire depth and use of some

of the moisture for redistribution makes the relation less direct.

A superficial view of the Pearce-Riehl scheme would suggest less precipitation heating results in less generation of kinetic energy. However, the relation may not be this simple as several runs in which the precipitation heating was doubled by mistake resulted in less generation of kinetic energy. Not only is the total amount of heat release important, but its horizontal distribution must be such as to increase the horizontal pressure gradient in the proper sense for increased potential-energy release.

The most important comparison between the schemes is the horizontal distribution of the precipitation, or the diabatic heating. Fig. 8 is the comparison in units of mm/day averaged over the 154 km square; areas with precipitation of less than 0.05 mm/day are shaded. The larger amounts of precipitation with the Kuo scheme are concentrated well to the north of the position of Tropical Storm Betsy. However, two additional centers appear, including one at the eastern end of the grid where the adjustment for cyclic continuity induces a trough in the easterlies. The required cyclic continuity also contributes to a large moisture convergence in this region as the western end of the grid is quite moist but the eastern end of the trades is dry.

The model with the Rosenthal scheme produces a generally similar distribution and amount in the region of the tropical storm, but the maximum is in advance of the trough axis. More precipitation is released along the southern wall where the low-level flow is convergent, but the maximum at the eastern end of the grid is missing. This occurs because the Rosenthal scheme is not dependent on horizontal moisture convergence.

A striking difference is seen in the distribution of precipitation for the Pearce-Riehl scheme. The amounts are generally uniform and small throughout the region. Minimum values are located on the southern wall where the other schemes have maximum values. The small maximum near the storm is also directed opposite that of the other two schemes. As we indicated above, the model with the Pearce-Riehl scheme is slow to organize the vertical motion fields and the 24-hour values are not a fair test of the ability of this particular scheme to represent the small scale convection.

## 6. CONCLUSIONS

Specifying inconsistent height boundary conditions to initialize a ten-level primitive equation model generated two separate types of oscillation which mask the meteorological developments in the tropical model. The height oscillation has a vertical structure similar to the inertio-gravity wave produced in a middle-latitude model, as discussed by Benwell and Bretherton (1968). Elimination of the height oscillation is achieved by setting boundary conditions that the initial heights along the northern and southern walls are constant.

The oscillation in the total kinetic energy is not easily detected on the synoptic maps, as the variation is in the basic current. This arises from an imbalance between the initial basic current and the specified height gradient between the northern and the southern walls. When quasi-geostrophic height gradients between the walls are specified in the initialization, the kinetic energy oscillation is eliminated.

We are of course hesitant to choose a particular latent heat parameterization scheme without a test which includes a developing disturbance. It is clear that large differences in precipitation do occur with the three schemes discussed. The release of latent heat does not lead to uncontrollable development of the storm, although a very marked increase in kinetic energy occurs with the Rosenthal scheme. And the movement, if not the intensity, is fairly well predicted by all the schemes for this single case.

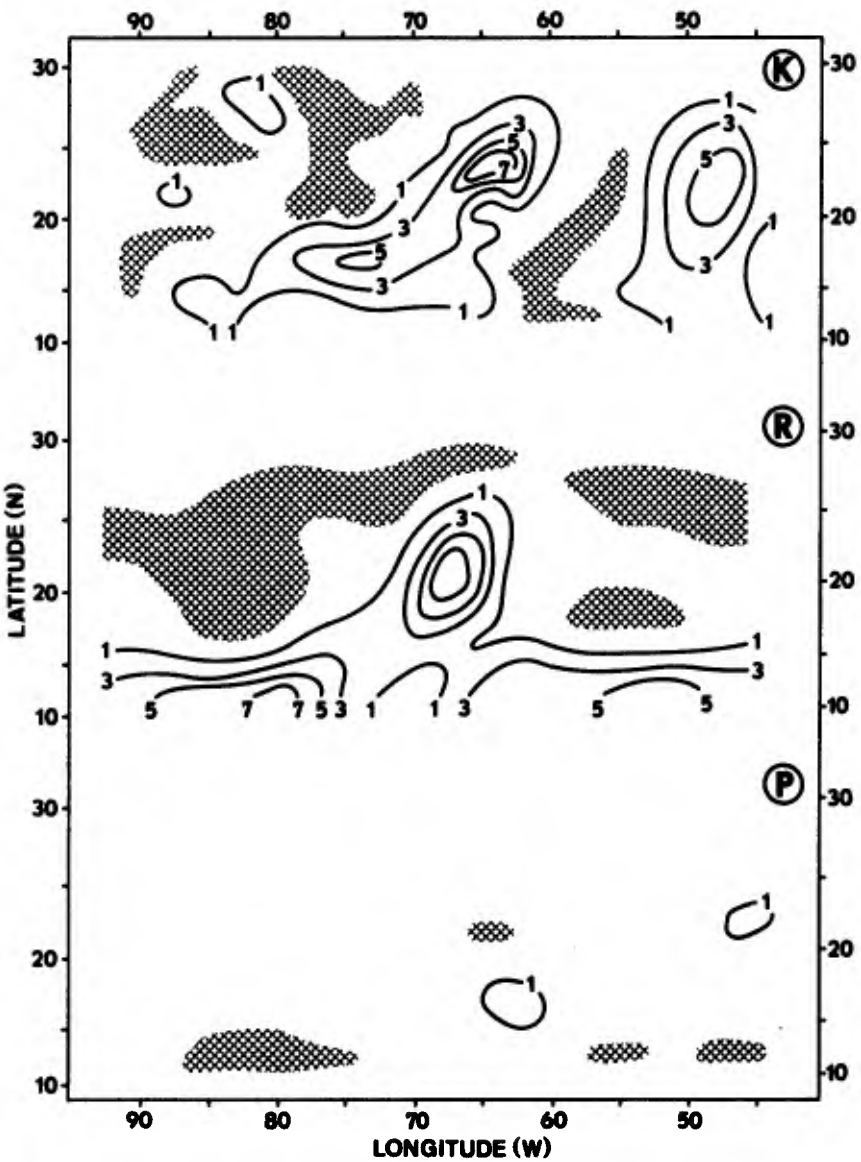


Fig. 8 Distribution of 24-hour precipitation (mm/day) for the Kuo (K), the Rosenthal (R), and the Pearce-Riehl (P) schemes. For amounts greater than 1 mm/day the interval is 2 mm/day; areas with less than 0.05 mm/day are shaded.

## 7. REFERENCES


1. Arakawa, A., 1966: Computational design for long-term numerical integration of the equations of fluid motion: Two-dimensional incompressible flow. Part I. J. Computational Physics, 1, 119-143.

2. Benwell, G. R. R., and F. P. Bretherton, 1968: A pressure oscillation in a 10-level atmospheric model. Quart. J. Roy. Met. Soc., 94, 123-131.

3. Charney, J. and A. Eliassen, 1964: On the growth of the hurricane depression. J. Atmos. Sci., 21, 68-75.

4. Harrison, E. J., Jr., 1969: Experiments with a primitive-equation model designed for tropical application. M. Sc. Thesis, Naval Postgraduate School, 54 pp.

5. Hawkins, H. F., and S. L. Rosenthal, 1965: On the computation of stream functions from the wind field. Mon. Wea. Rev., 93, 245-252.

6. Krishnamurti, T. N., 1969: An experiment in numerical prediction in equatorial latitudes. Quart. J. Roy. Met. Soc., 95, 594-620.

7. Kuo, H. L., 1965: On formation and intensification of tropical cyclones through latent heat release by cumulus convection. J. Atmos. Sci., 22, 40-63.

8. Landis, R. C., and D. F. Leipper, 1968: Effects of Hurricane Betsy upon Atlantic Ocean Temperature. J. Applied Met., 4, 554-562.

9. Pearce, R. P., and H. Riehl, 1968: Parameterization of convective heat and momentum transfer suggested by analysis of Caribbean data. Proc. WMO-IUGG Symposium on Num. Wea. Prediction, Tokyo, I, 75-84.

10. Riehl, H., 1954: Tropical Meteorology. McGraw-Hill (New York).

11. Riehl, H., 1962: Radiation measurements over the Caribbean during the autumn of 1960. J. Geophy. Res., 67, 3935-3942.

12. Riehl, H., and R. P. Pearce, 1968: Studies on interaction between synoptic and mesoscale weather elements in the tropics. Atmospheric Science Paper No. 126, Colorado State Univ., 64 pp.

13. Rosenthal, S. L., 1968: Numerical experiments with a multilevel primitive equation model designed to simulate the development of tropical cyclones, Experiment I. ESSA Tech. Memo. ERLTM-NHRL 82, 36 pp.

# AIR FORCE GLOBAL WEATHER CENTRAL BOUNDARY-LAYER MODEL

Kenneth Hadeen, Lt Col, USAF

Air Force Global Weather Central
Offutt Air Force Base, Nebraska

## Abstract

An eight level physical-numerical prediction model for the lower troposphere (SFC - 1600m) has been developed for application over limited areas of high operational interest. This model is an integral part of the complete AFGWC effort in meso-scale (sub-synoptic) numerical analysis and prediction with the goal of providing greater horizontal and vertical resolution in both the numerical analysis and forecast models.

Important features of this boundary-layer model include a completely automated objective analysis of input data, transport of heat and moisture by three-dimensional wind components, terrain and frictionally induced vertical motions, heat and mass exchange in water-substance phase changes and eddy flux of heat and moisture.

Examples are shown to demonstrate the potential of this model to realistically simulate and accurately predict the actual behavior of the atmosphere in the boundary layer region.

AIR FORCE GLOBAL WEATHER CENTRAL BOUNDARY-LAYER MODEL

It is a distinct pleasure for me to have this opportunity to briefly describe the Air Force Global Weather Central's (AFGWC) Boundary-Layer Model. In the next few minutes I would like to place the model in perspective, describe the operation of the model, and show examples of the output from the model. This boundary-layer model has been in operational production for approximately one and a half years.

To place the model in prespective, we first note that physical-numerical models for the prediction of macro-scale motion in the free atmosphere have proven to be of considerable value as objective aides for flight forecasting. However, operational requirements exist for local and terminal forecasts which require initial specification and subsequent prediction of smaller scale, sub-synoptic atmospheric perturbations. To meet this requirement, a "window" concept has been in existence at the Air Force Global Weather Central for several years. This concept is commonly referred to in recent literature as "grid-nesting", "grid telescoping", or as "limited-area" forecasting.

Essentially, this concept is to use the output from macro-scale numerical models as time variant boundary conditions for a subregion or "window" of high operational interest. Over this "window" a fine-mesh numerical analysis, and forecast is produced using a higher grid density and a shorter time step than the hemispheric macro-scale model. The fine-mesh analysis is made for each mandatory level (i.e., 1000-850-700-500-300mb); the fine-mesh forecast is generated for the four mandatory levels of the free atmosphere from 850 to 300mb.

The AFGWC Boundary-Layer Model is used to provide a more detailed analysis and forecast in the complex region adjacent to the earth's surface. By using the fine-mesh analysis at mandatory levels as first-guess fields and the output from the fine-mesh prediction model as time-variant upper-boundary conditions, a consistent and powerful forecast system is obtained.

The first figure shows the current, operational North American Window. The region contained within the black outline (outer rectangle) represents the area covered by the fine-mesh analysis, fine-mesh forecast, and boundary-layer analysis. This is a (37 x 39) grid. The region covered by the Boundary-Layer Forecast model is outlined in Red (inner rectangle). This is a (29 x 27) grid. The grid interval is ($\frac{1}{2}$) one-half the AFGWC or NMC macro-scale grid (approximately 100 nautical miles depending upon latitude).

Current plans are to have several forecast "windows" over data-dense regions (land areas) and a relocatable window capability. A second "window" for Eurasia is shown in the next figure (2). This window is now being run in a semi-operational configuration. Of interest here is the fact that although the fine-mesh analysis and forecast area (outer rectangle) has eight less grid points than the North American Window, it has two radiosonde reports for each one in the North American window. Also a large percentage of the reporting stations have four upper-air observations per day compared to one every twelve hours over the North American Window. The grid interval used over this window is one-half the GWC macro-scale, however data density is sufficient to support a higher grid density.

A third window is scheduled to go into semi-operational production 60 days after the second window becomes fully operational. This East Asian Window is shown in the next figure (3). As in the previous figures the area outlined in black (outer rectangle) is the region covered by the fine-mesh analysis, fine-mesh forecast model and the boundary-layer analysis. The forecast region of the BLM is outlined in red (inner rectangle).

The model is designed to have flexibility in the number of levels and thickness between levels. The next figure (4) shows the vertical depiction of the model in its current operational mode. There are seven layers (8 levels) in the vertical.

Initial specification of the temperature and moisture structure is obtained by a completely automated numerical analysis. This objective analysis technique makes optimum use of surface and upper-air reports to form a consistent, high-resolution, three-dimensional analysis. Initial conditions of geostrophic wind components(Vg, Vg) at 1600m AGL are obtained from the fine-mesh analysis. Upper time-variant boundary conditions of geostrophic wind (Vg, Vg) and an estimate of the cloudiness above the B.L. region are required in the execution of the model. The parameters derived from the forecast model at each level include the three wind components, temperature, specific humidity and specific moisture. Post-processing yields D-value for each level and an objective turbulence number.

The model is a hybrid model which uses the detailed thermal structure and pertinent geophysical parameters (terrain elevations, roughness) to diagnose the fields of motion within the boundary-layer region and forecast techniques to solve tendency equations for temperature and moisture. The decision not to integrate the momentum equations was made because of the large horizontal and vertical gradients found near the Earth's surface, unrepresentative data, computer time required, and finally, the desire to obtain a realistic and representative flow without smoothing either the terrain or the data. Examples of the diagnostic flow are given later as part of a case study.

The next figure (5) is an abbreviated schematic of the operational flow of the model. Briefly the operational flow is as follows:

a. Initial conditions of temperature, specific humidity, and specific moisture for each grid point and level as well as fixed field-data of surface elevation, surface roughness and radiational coefficients are brought into the model. Horizontal wind components (Vg Vg) at 1600m AGL are read from drum data base into the model (computed by the Fine-Mesh, Free-Atmosphere Prediction Model).

b. Geostrophic wind components for each lower level are computed using the detailed thermal structure and terrain elevations.

c. Eddy viscosity, angle of geostrophic deviation, and wind speed at the 50m level are computed using equations derived from the work of many scientists (Lettau, Blackadar, Monin, and Obukhov, Priestly, Lumley, Panofsky) and are dependent upon stability, roughness and wind speed.

d. Kinematic balance equations which are a modified set of Ekman equations to obtain balance among coriolis, pressure, and frictional forces are solved.

e. With the horizontal wind components available, a vertical velocity is determined by integrating the continuity equation and determing a terrain-induced vertical motion.

f. The prognostic portion of the model begins with the forecast of surface temperature and specific humidity for the next time step. (Based on advection including adiabatic effects radiational climatology, modified by cloudiness within and above the boundary-layer region).

g. Tendency equations which use tnree-dimensional flow, adiabatic changes, eddy transport of heat and moisture (using Estoque formulation of eddy coefficients of diffussion and conductivity depending on free or forced convection) are next solved.

h. Latent-heat computation with associated heat and mass exchange in water-phase change (work by McDonald) completes the forecast for this time step and the model is ready to compute new diagnostic winds and recycle.

i. Displays are output on a high-speed printer at desired forecast intervals.

j. On completion of the desired forecast, post-processing to obtain D-values at each level and storage into the AFGWC drum data base is accomplished.

The remainder of the presentation deals with a case study starting at 00Z on 16 January 1970. Rather than present a superficial examination of several cases, it is felt that more can be learned in a short time about the model by a more thorough examination of one case. It's purpose is to demonstrate the detailed initial analysis, the applicability of the diagnostic procedures to flow in the boundary-layer region at initial and forecast times, and the detailed thermal structure which when placed in the hands of talented forecasters will yield meso-scale weather predictions of consistently good and occasionally exceptional quality. The performance of the model on this particular case isn't any better or worse than can be expected on a particular day.

The general synoptic situation at 0000Z on 16 January 1970 is shown in the next figure (6). The main storm track was through the southern portion of the United States as evidenced by the occluded system approaching the west coast, the remains of an occluded system along the New Mexico-Texas border and the wave disturbance off the south-east tip of Florida. Arctic and modified Arctic air dominated Canada and the northern regions of the United States. The cold Arctic high over western Canada has been nearly stationary the previous 24 hours.

Figures 7, 8, 9 and 10 show the rapid wave development and formation of an occlusion in the Great Lakes Region, the cold penetration of arctic air along the eastern slopes of the Rocky Mountains, the development of a wave along the front in Eastern Colorado and the movement of the occluded system into the western United States.

How did the boundary-layer model handle this system? First the wind flow as diagnosed by the model is investigated. The next figure (11) has a few streamlines depicting the wind flow at 1600m above the terrain. This wind field was derived from height fields interpolated from the 850-700-500mb fine-mesh analyses. The diagnosed flow at 50m is shown in the next figure (12). The isobaric pattern with fronts, highs and lows were obtained from the NMC analysis as indicated on a previous figure (6). Of interest, is the outflow around the high located along the Virginia coast, the high over eastern Canada, the inflow in the vicinity of the inverted trough through Iowa into north western Wisconsin and across the western end of Lake Superior, flow associated with the arctic high over western Canada and especially the flow in the vicinity of the 1016mb isobar over Nevada, Idaho, Wyoming and Colorado.

The 12-hour forecast of winds at 1600m and 50m AGL are depicted in figures 13 and 14 respectively. Without discussing the validity of the NMC analysis, it is apparent that the model showed a more open wave in the Great Lakes Region with the warm-frontal trough over Lake Huron and Lake Ontario. The model tended to push the cold air southward along the mountains faster than was indicated on the analysis and eastward in Wisconsin slightly slower than what occurred. The flow in the vicinity of the high centered over the four corners area of Colorado, New Mexico, Arizona and Utah was very good.

The 24-hour forecast of winds at 1600m and 50m are shown in figures 15 and 16 respectively. Of interest is that the 50m wind field indicates that the frontal system over Nevada should be nearer the Utah border. Surface observations shown in figure 10 indicate that the model forecast may be the better placement of this system. The model forecast of the winds associated with the leading edge of the arctic high trailed the actual frontal position by a full grid length by the end of the 24-hour forecast. The lee-side trough over eastern Colorado with associated perturbation on the arctic front in the Nebraska panhandle was well represented by the model, the trough associated with the weak occlusion moving into the Pacific north-west was well represented.

The frontal positions from figures 6, 8 and 10 were consolidated into a continuity chart which is depicted by the next figure (17). Time cross-sections of winds and temperatures for a grid location near Medford, Oregon and for a location in eastern Colorado to demonstrate how the model forecast the movement of these systems will be presented next.

The winds displayed in the next figure (18) are grid winds and it is necessary to subtract 45° from the direction to obtain wind direction in relation to true north. Of interest, is the development of the wind max at approximately 300m above the surface at the 4-6 hour forecast period coincident with the frontal passage and the relative homogeneous air mass behind the front.

An entirely different situation is depicted in the next figure (19) which is a time cross-section at a grid location in eastern Colorado. At initial time relatively warm air was over the grid point, the arctic air over Nebraska moved southward bringing cold air over the grid point, a wave perterbation developed on the arctic boundary and the cold air receded. The westerly winds then caused strong adiabatic warming associated with the down slope winds at the end of the forecast period.

A visual presentation of the vertical temperature structure at initial time, the change which occurred with the eastward movement of the arctic high and the rapid occlusion of the frontal system is depicted in the next series of figures. Figures 20, 21 and 22 are for grid row 11 through the arctic high. Figures 23, 24 and 25 are for grid row 14 and shows the penetration of the cold air as it moved south and eastward. It should be noted that the scale in these figures is greatly distorted. The vertical coordinate is approximately two miles while the abscissa is nearly 3000 miles. The station call letters are only approximate locations and may be either north or south of the actual grid row.

D-values computed in the post-processing phase of the operational run have proven very useful in locating and predicting frontal movements. An interpolated D-value field for 1600m AGL (obtained from the free atmosphere fine-mesh model) is shown in the next figure (26). D-values are computed at each lower level by building down from the 1600m level, level-by-level using the specific temperature anomaly between levels. An analysis of the surface D-value is given in the next figure (27). Frontal positions, highs and lows were added to show the correlation with the surface analysis. This case shows that large variations of D-value can occur in the boundary-layer region. An example of this change is demonstrated over western Canada where the D-value at 1600m AGL is approximately +40 feet and at the surface for the same location the D-value is +690 feet.

Although the case presented here was an intense system the model has correctly diagnosed smaller scale, organized flows correctly that were not in evidence at the upper boundary. As seen from this case study, the model tends to be slightly slow on fast-moving systems. However, the model on several occassions correctly forecast the cyclogenesis and movement of lows in the Gulf of Mexico into the eastern portion of the United States; it has held frontal troughs quasis-stationary for several forecast cycles and correctly forecast the movement when it did occur.

Although there is need for much refinement in the model, the diagnostic technique for wind flow over variable terrain has wide application for use with free-atmosphere dynamic models. A free-atmospheric dynamic model coupled with the boundary-layer model for the lowest 100-150mb of the troposphere would be an extremely powerful forecast tool.

REFERENCES

1. Barnes, S.L., "Technique for Maximizing Details in Numerical Weather Analysis," Journal of Applied Meteorology, 3(4), Aug 1964.

2. Estoque, M.A., "The Sea Breeze as a Function of the Prevailing Synoptic Situation," Journal of the Atmospheric Sciences, 19(3): 425-437, Sept. 1962.

3. _____, _____, "A Numerical Model of the Atmospheric Boundary Layer," Journal of Geophysical Research, 68(4): 1103-1113, Feb. 1963.

4. Gerrity, J.P., "A Physical Low-Cloud Prediction Model, "423L System Program Office, Electronics Systems Division, Air Force Systems Command, United States Air Force, L.G. Hanscom Field, Bedford, Mass., Oct. 1965.

5. _____, "A Physical-Numerical Model for the Prediction of Synoptic-Scale Low Cloudiness," Monthly Weather Review, 95(5): 261-282, May 1967.

6. McDonald, J.E., "The Saturation Adjustment in Numerical Modelling of Fog," Journal of the Atmospheric Sciences, 20(5): 476-478, Sept. 1963.

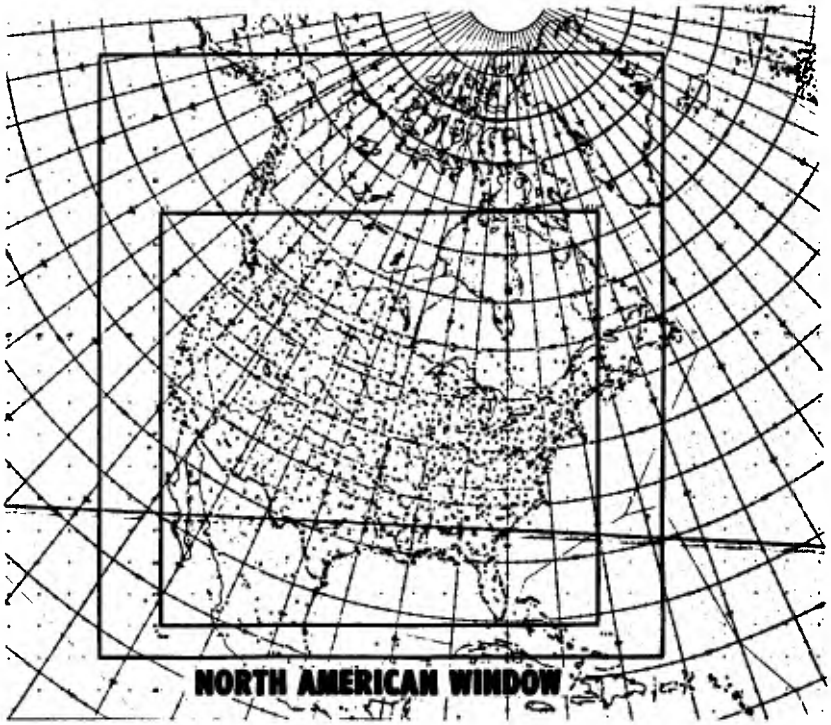


Figure 1

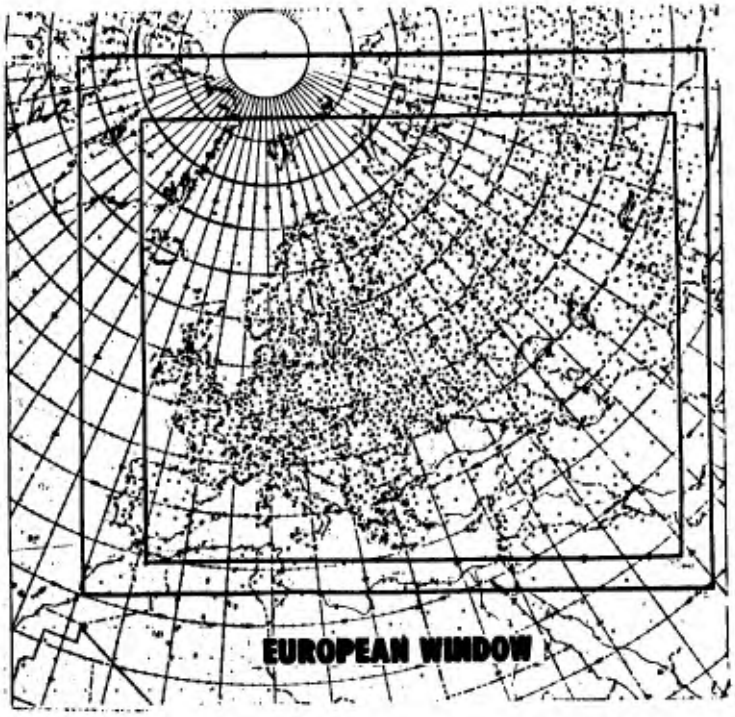


Figure 2

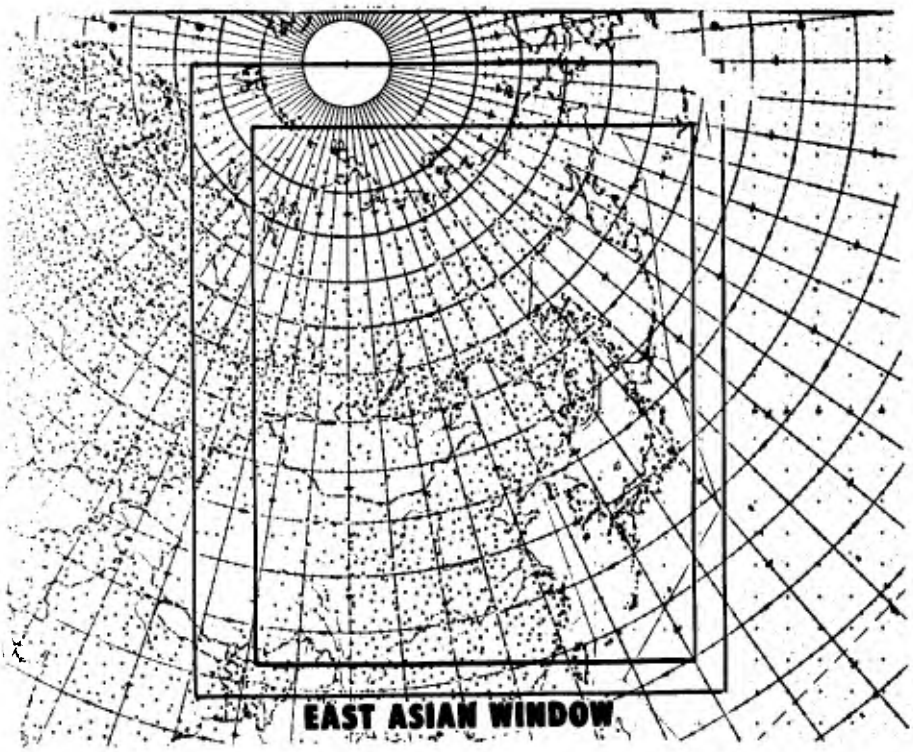


Figure 3

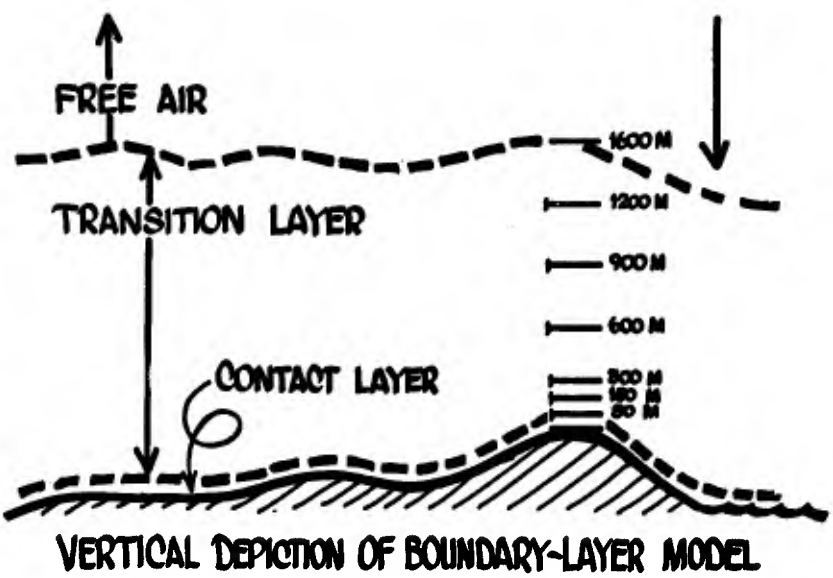


Figure 4

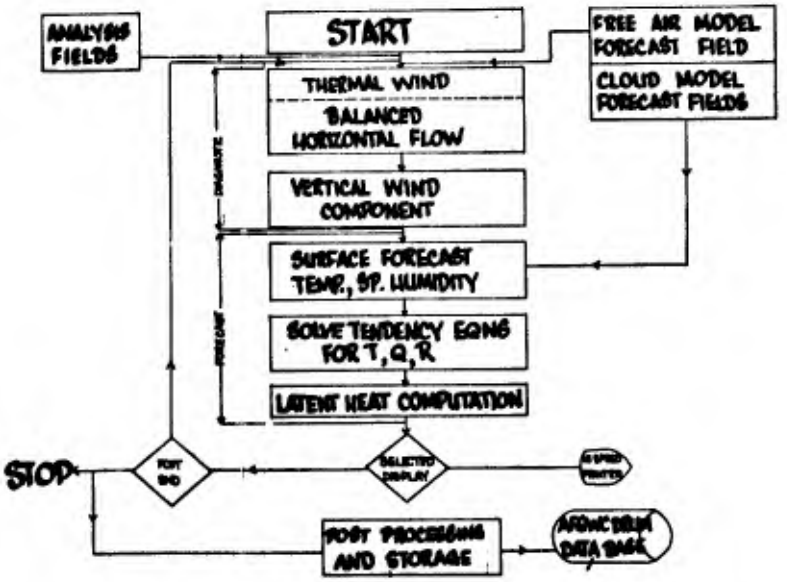


Figure 5

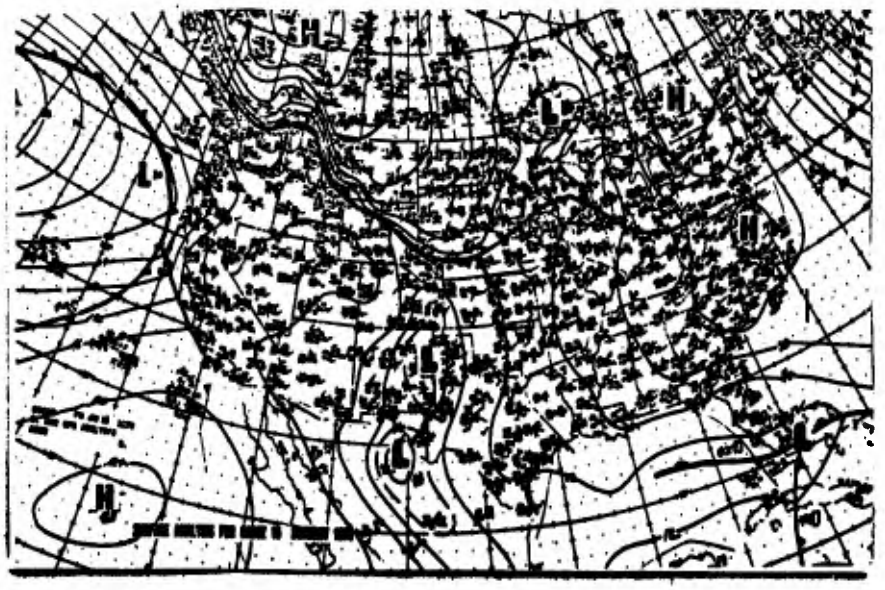

Figure 6

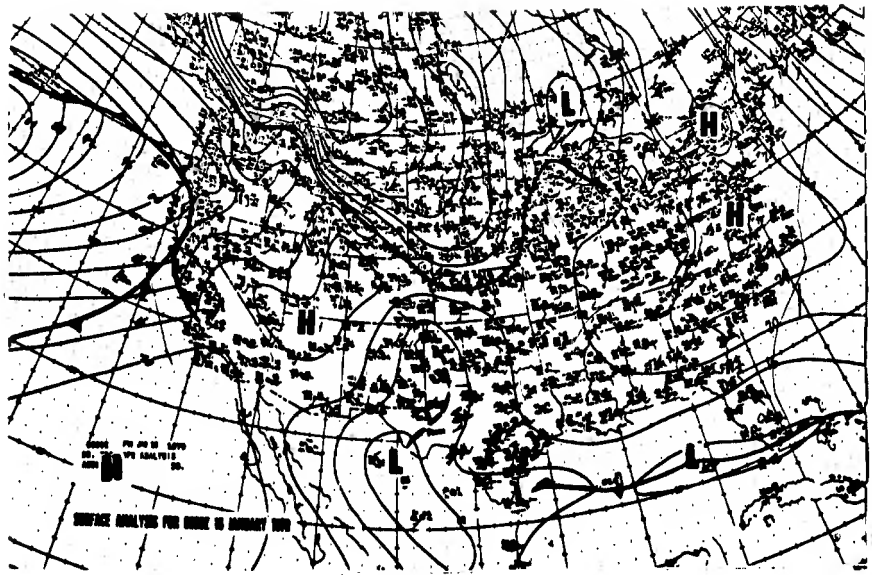


Figure 7

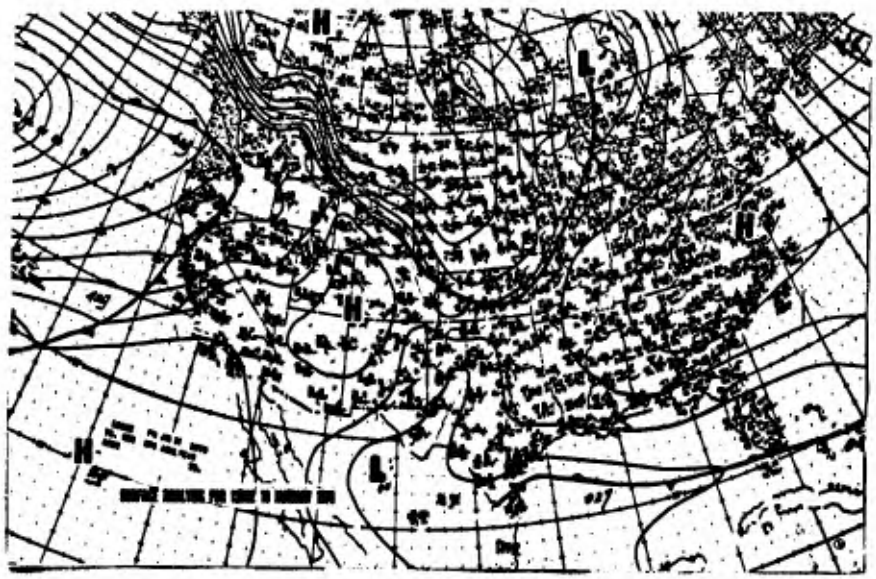


Figure 8

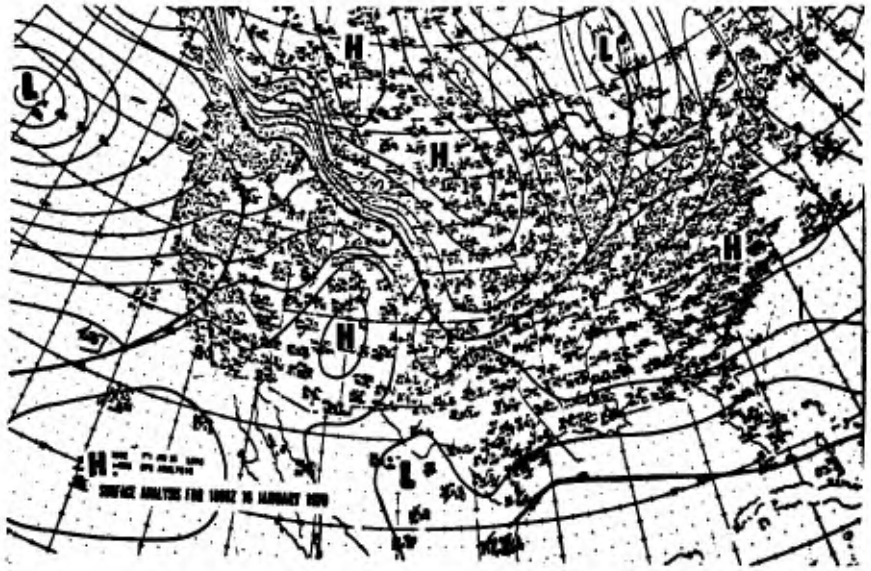

Figure 9

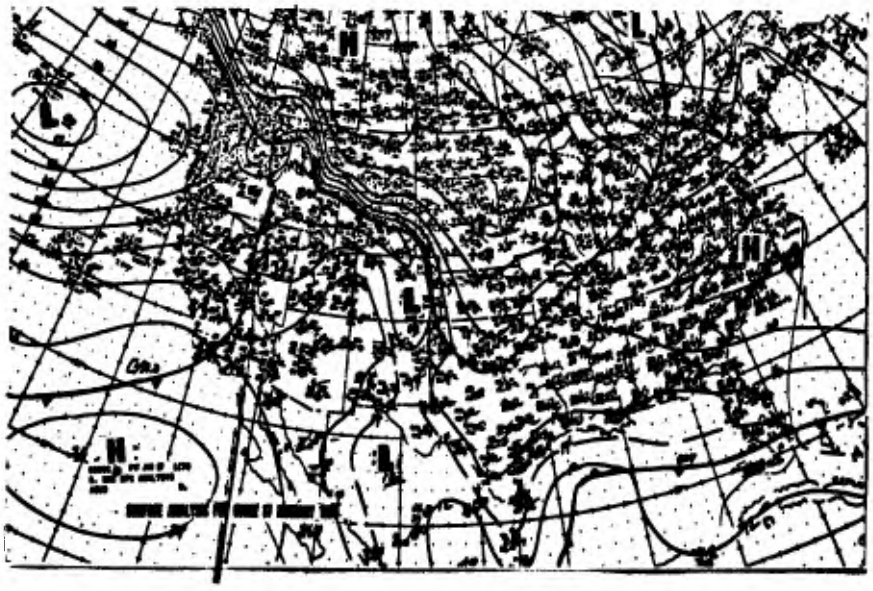

Figure 10

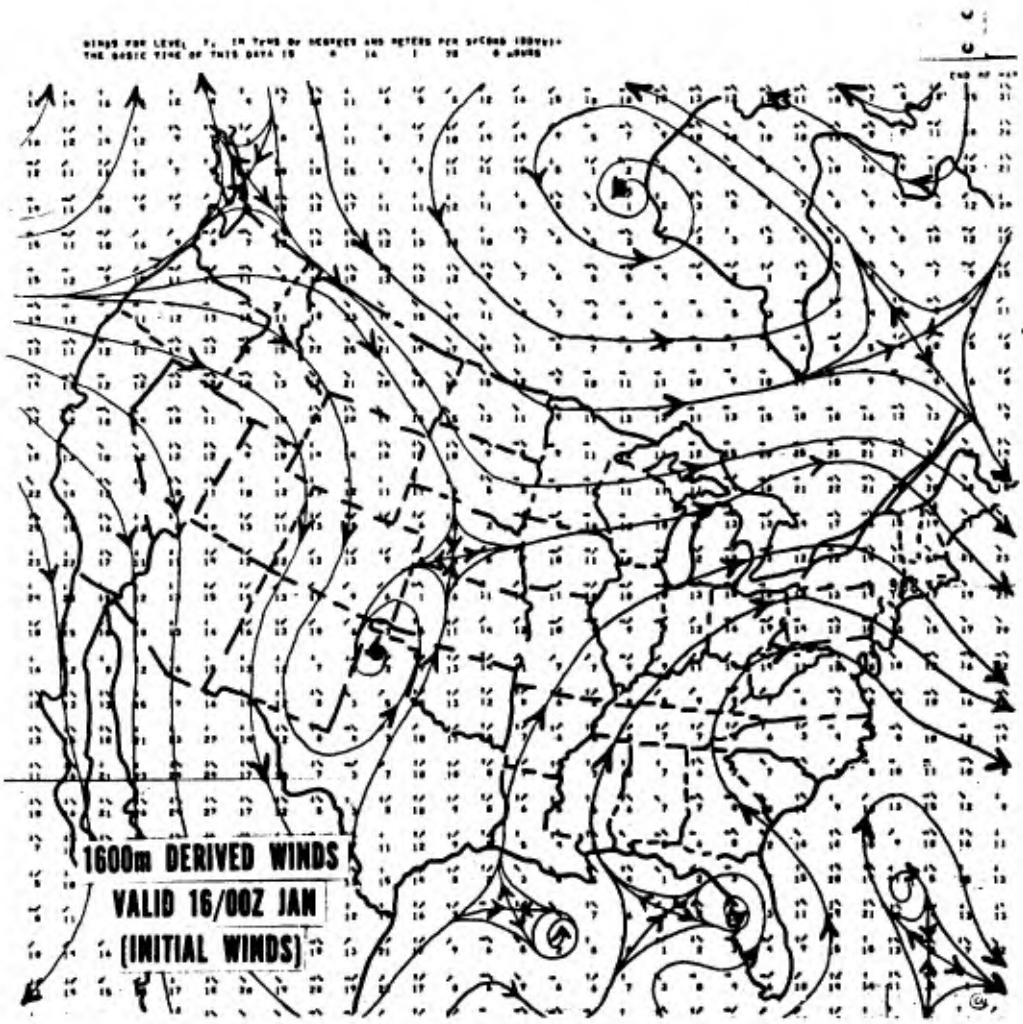


Figure 11

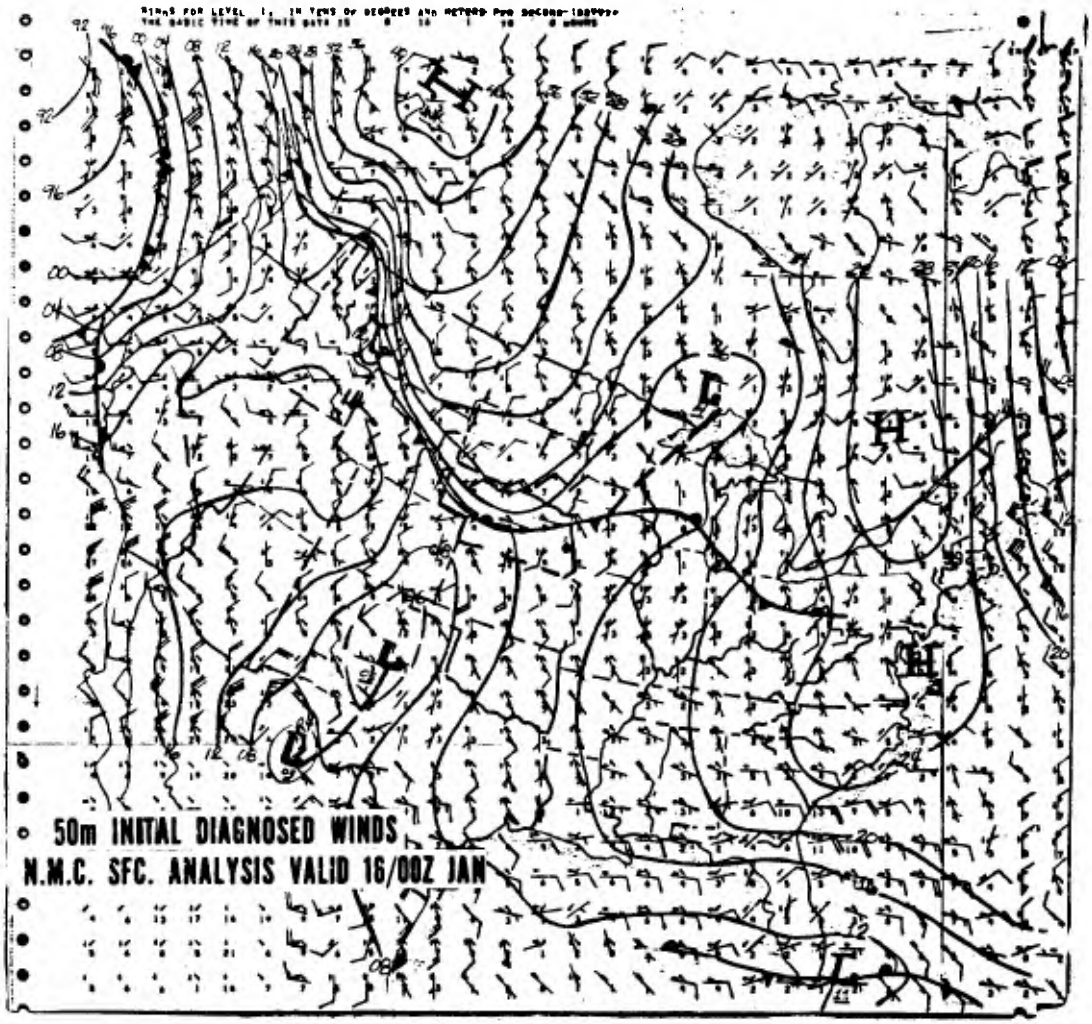
50m INITAL DIAGNOSED WINDS
N.M.C. SFC. ANALYSIS VALID 16/00Z JAN

Figure 12

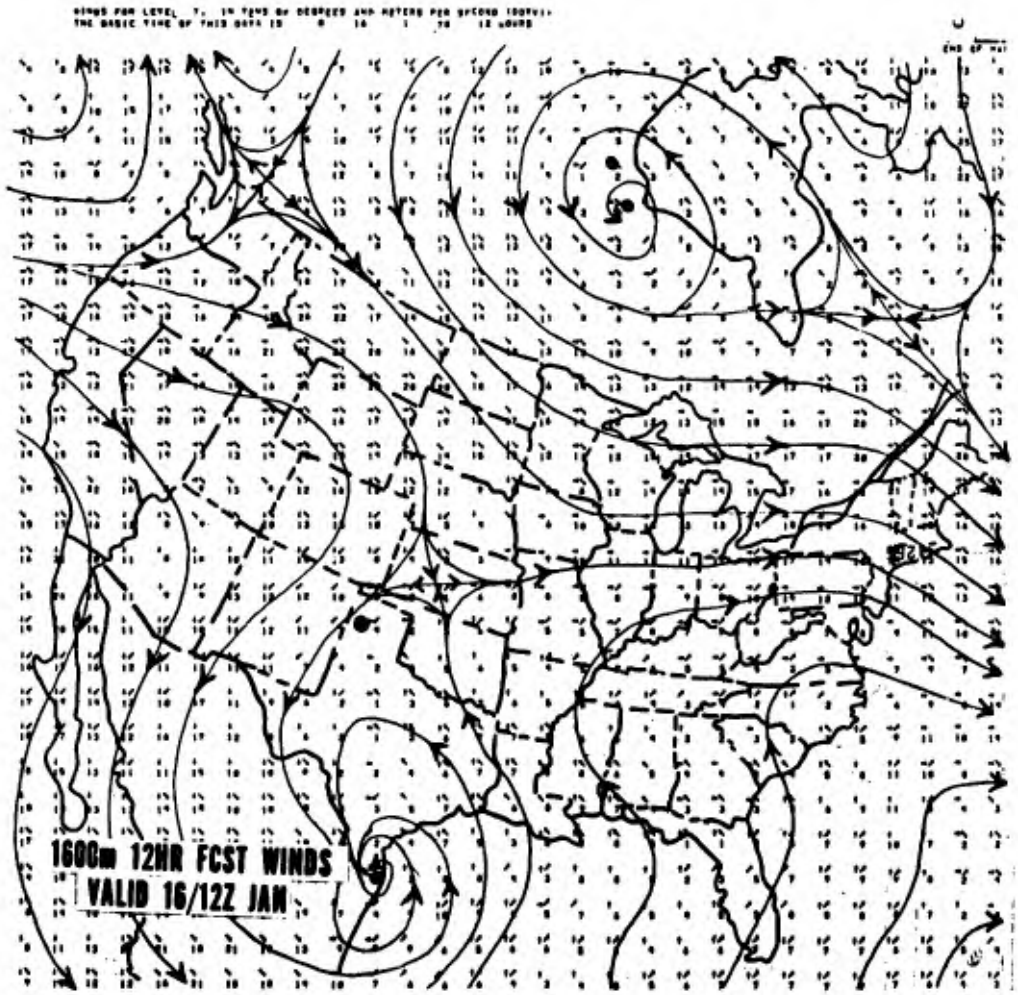


Figure 13

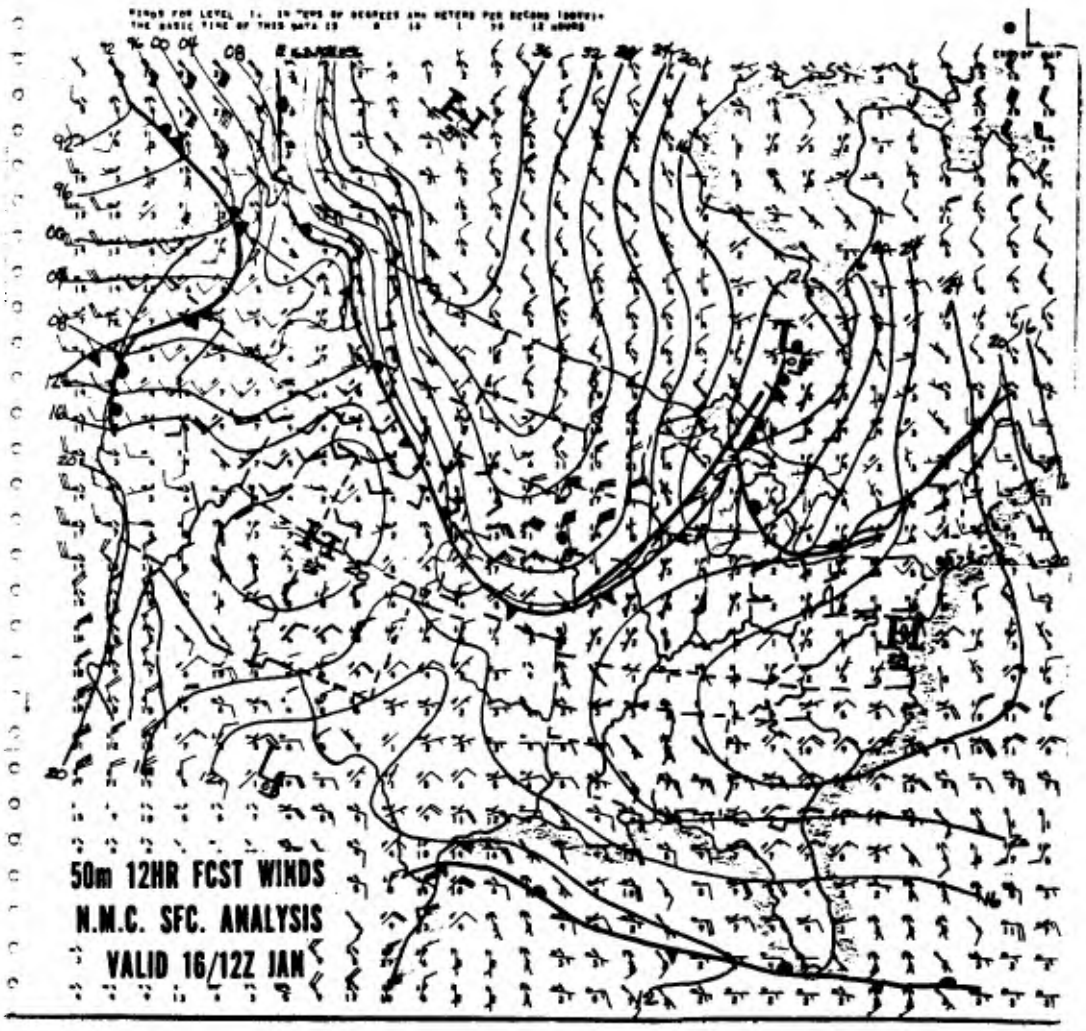


Figure 14

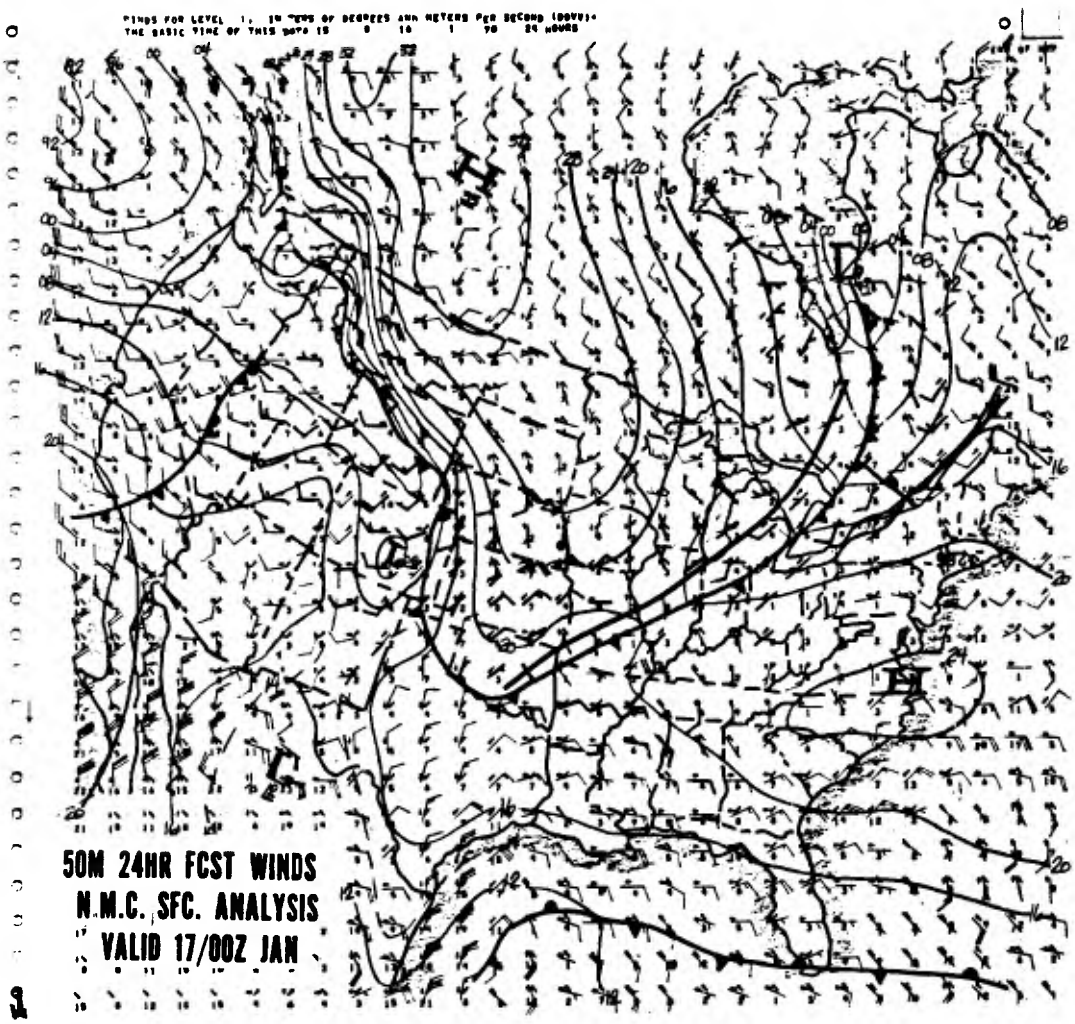


Figure 15

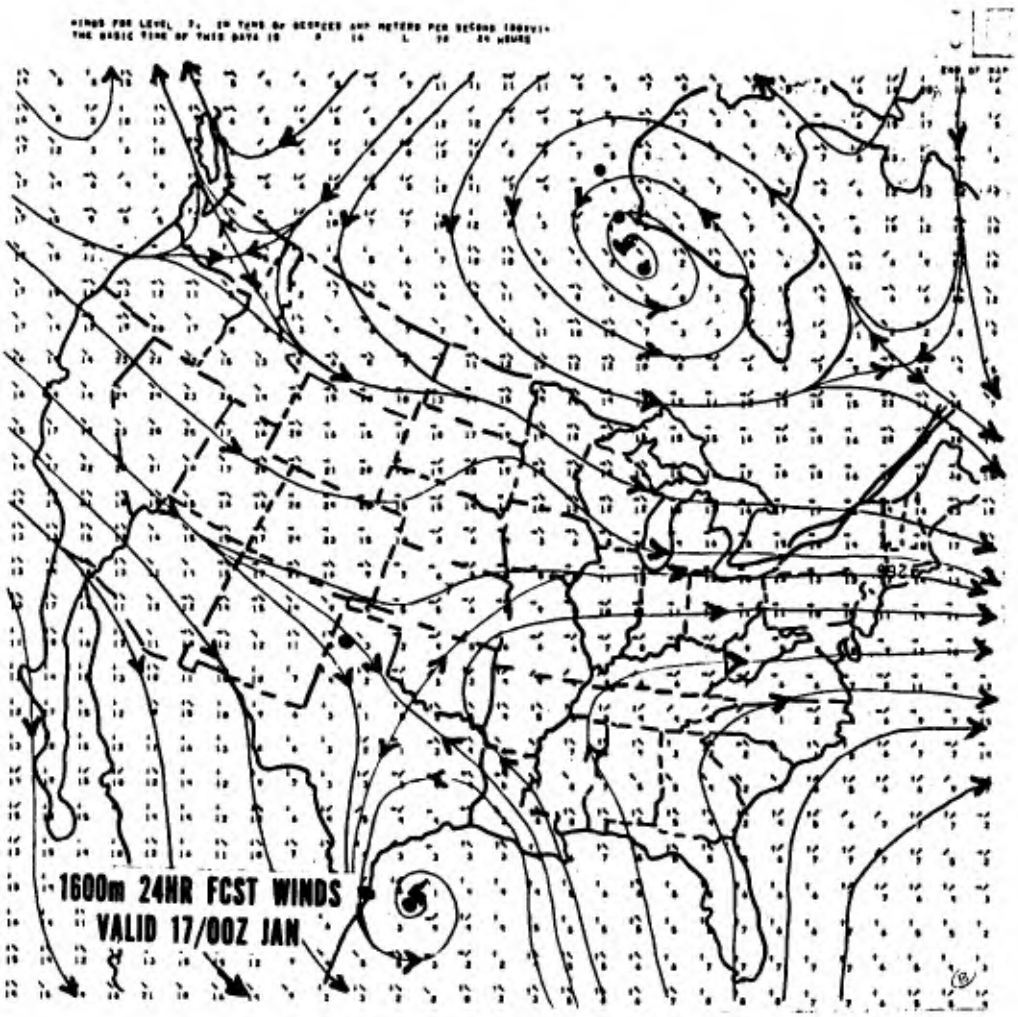


Figure 16

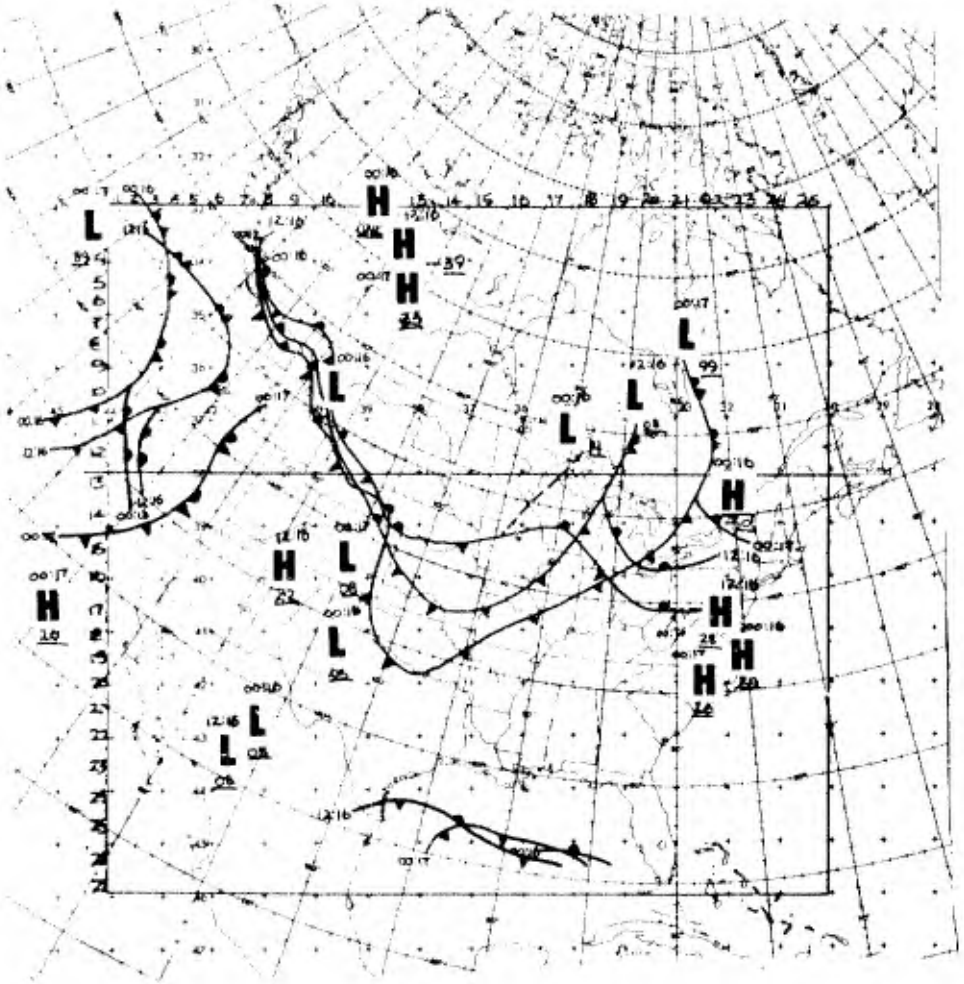

FRONTAL CONTINUITY CHART FOR 16/0000Z TO 17/0000Z JANUARY 1970

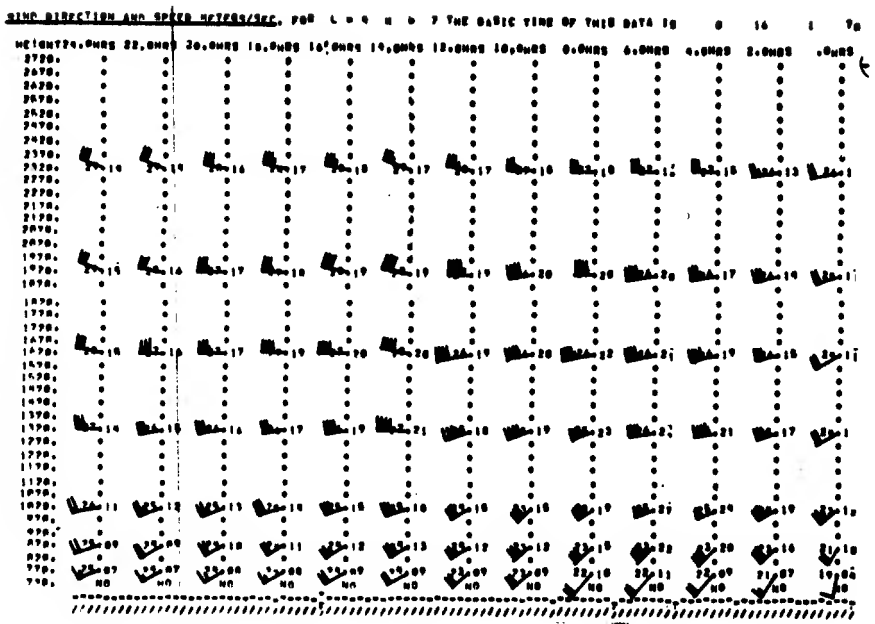

SUBTRACT 45 DEG FROM WIND DIRECTIONS SHOWN
TO OBTAIN TRUE DIRECTIONS.

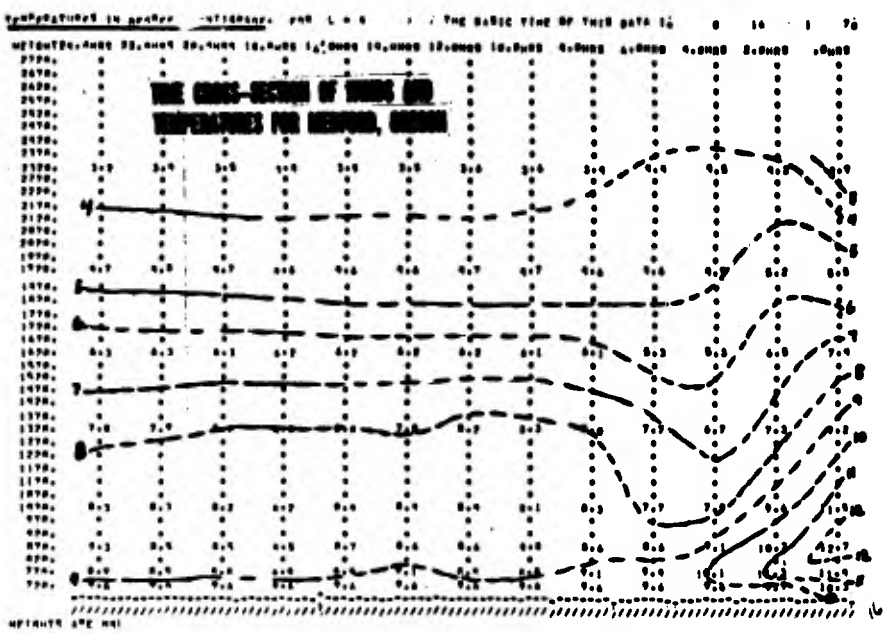

Figure 18

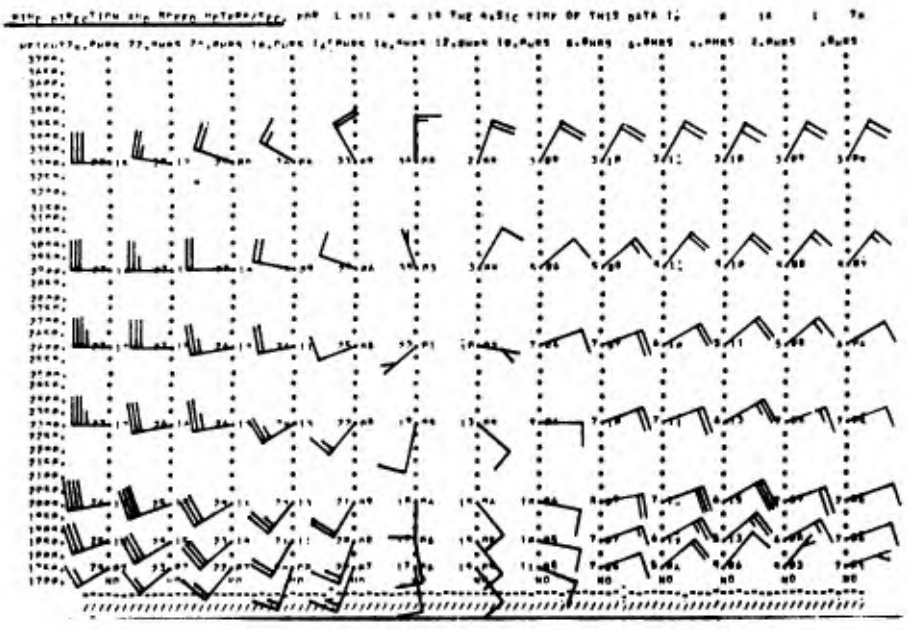

SUBTRACT 25 DEG FROM WIND DIRECTIONS SHOWN
TO OBTAIN TRUE DIRECTIONS.

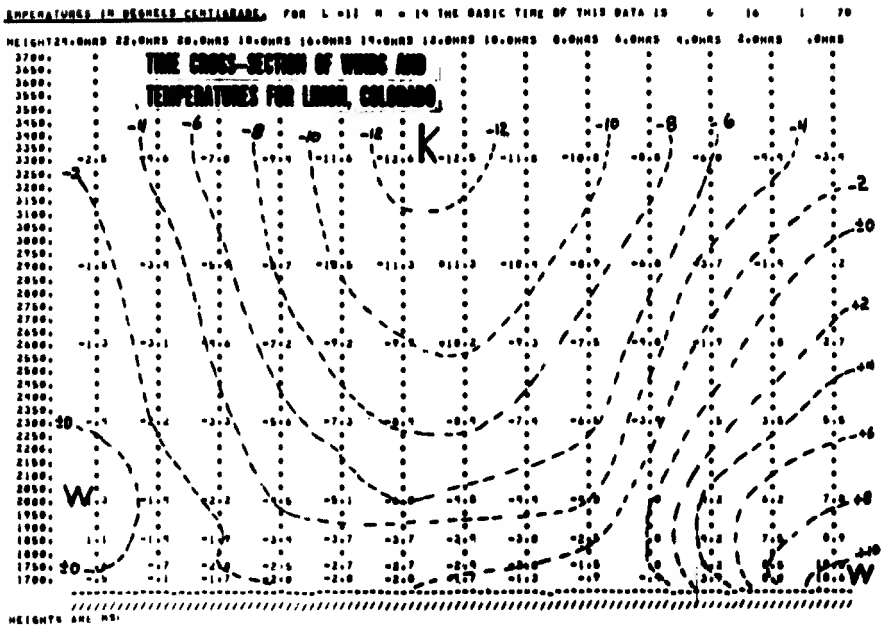


Figure 19

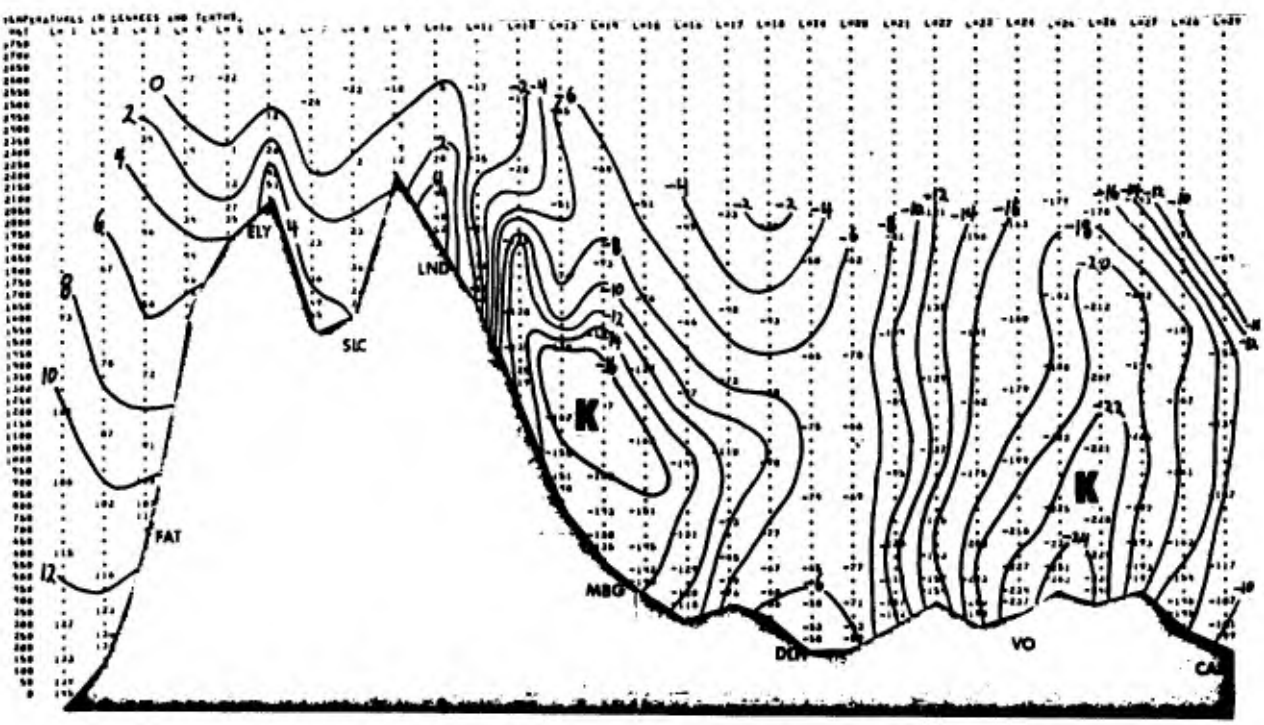


TEMPERATURE CROSS-SECTION (ROW 11)
VALID 0000Z 16 JANUARY 1970

Figure 20

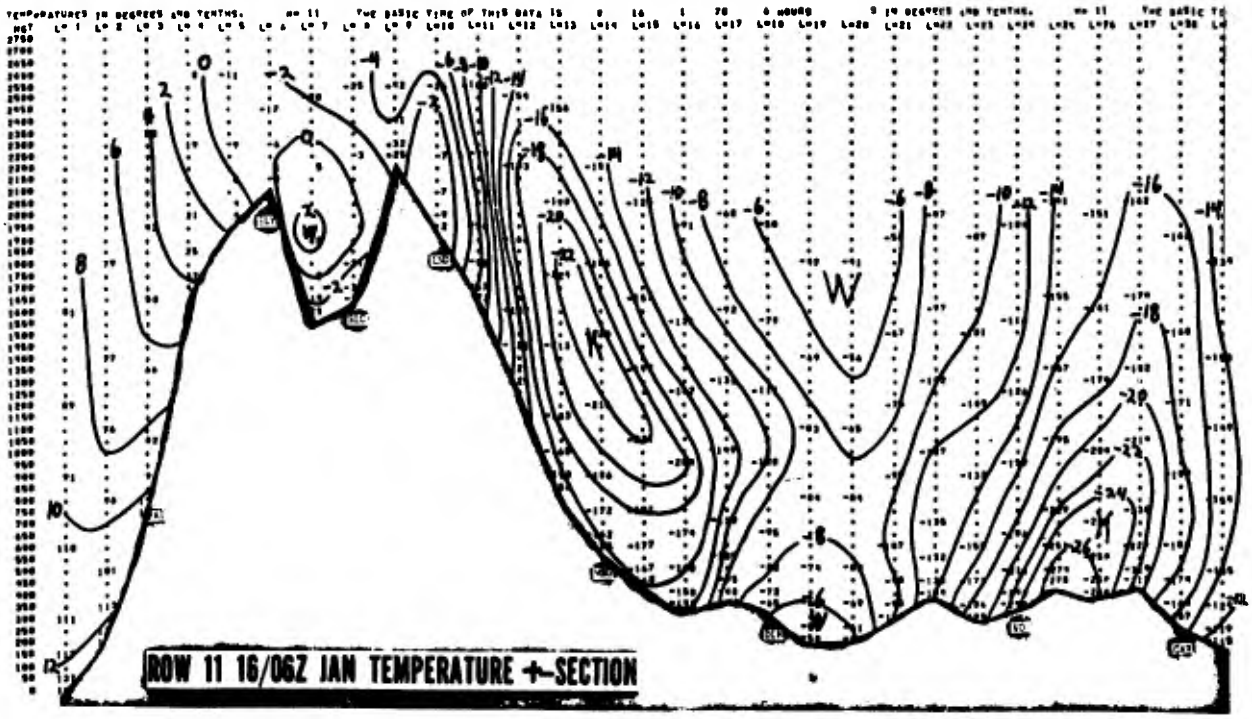


21

Figure 21

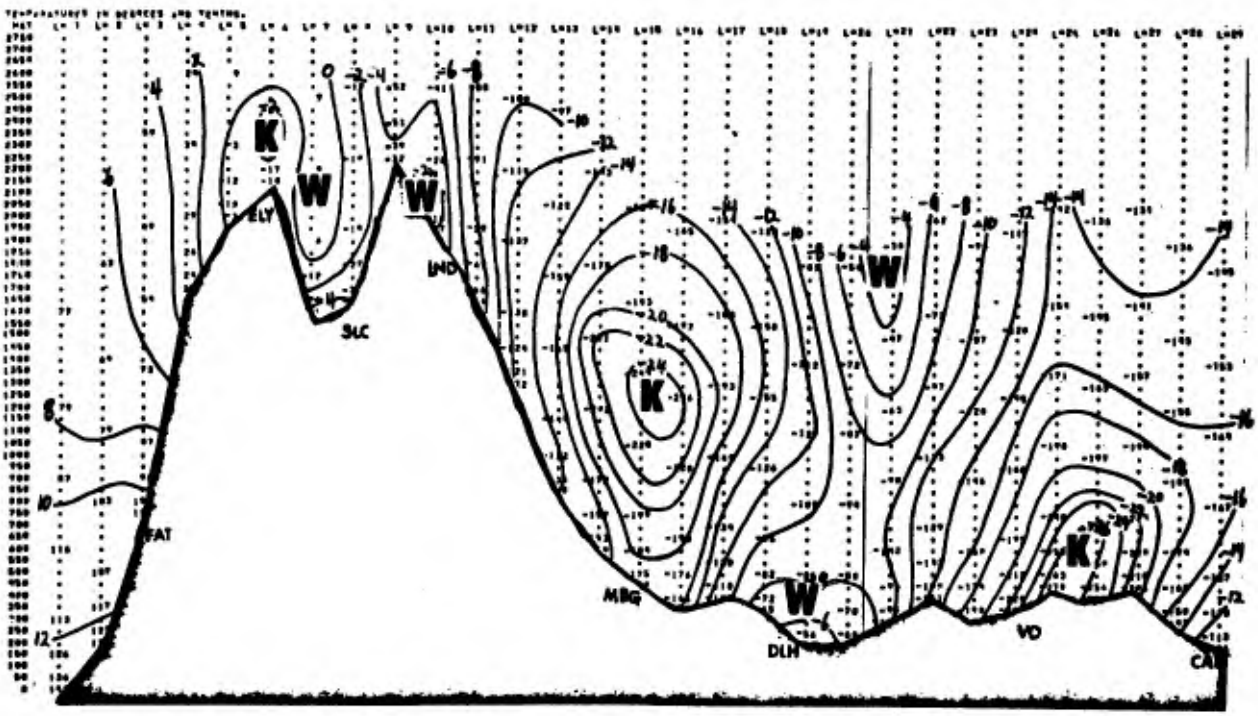


12 HOUR FORECAST TEMPERATURE CROSS-SECTION (ROW 11)
VALID 12002 16 JANUARY 17 1970

Figure 22

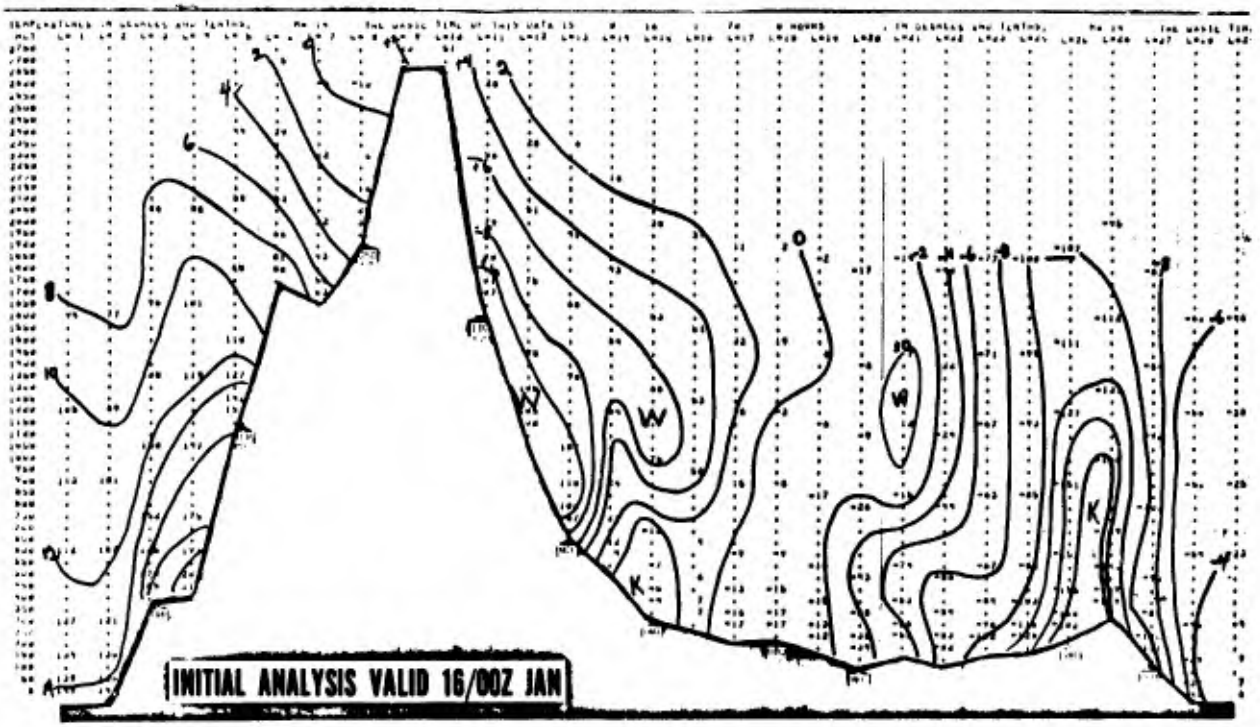


Figure 23

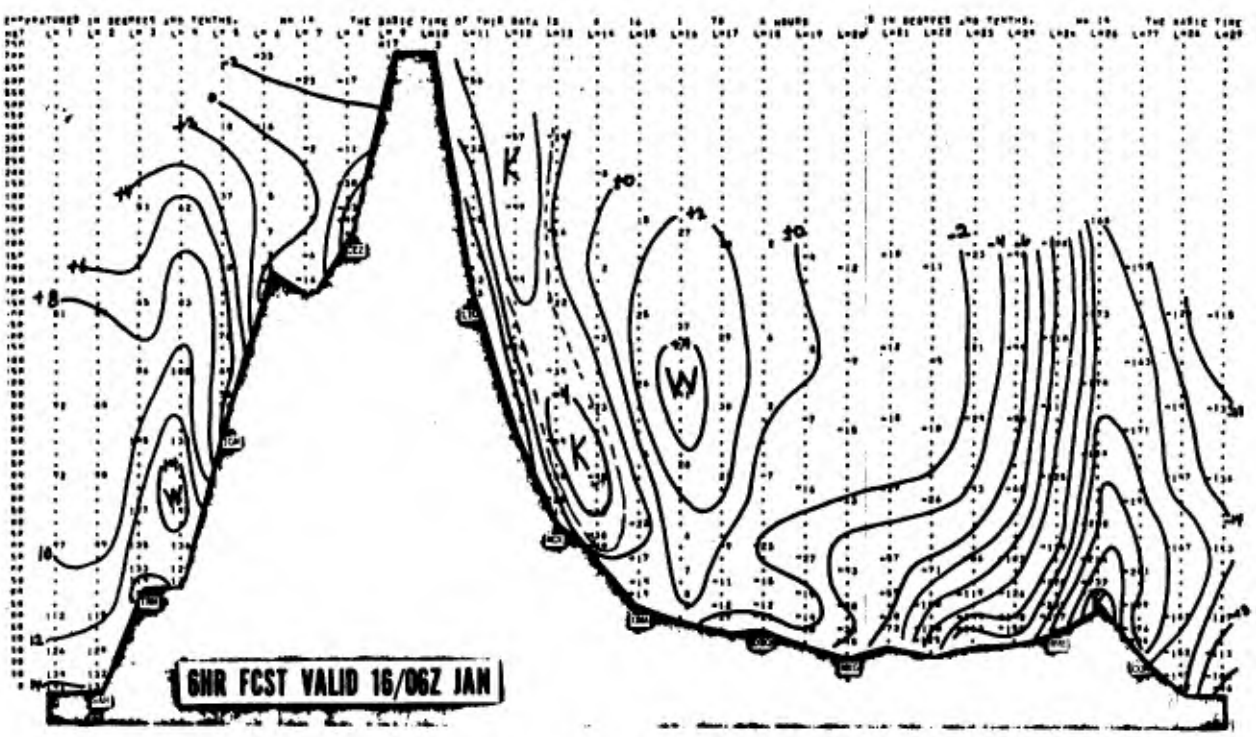


Figure 24

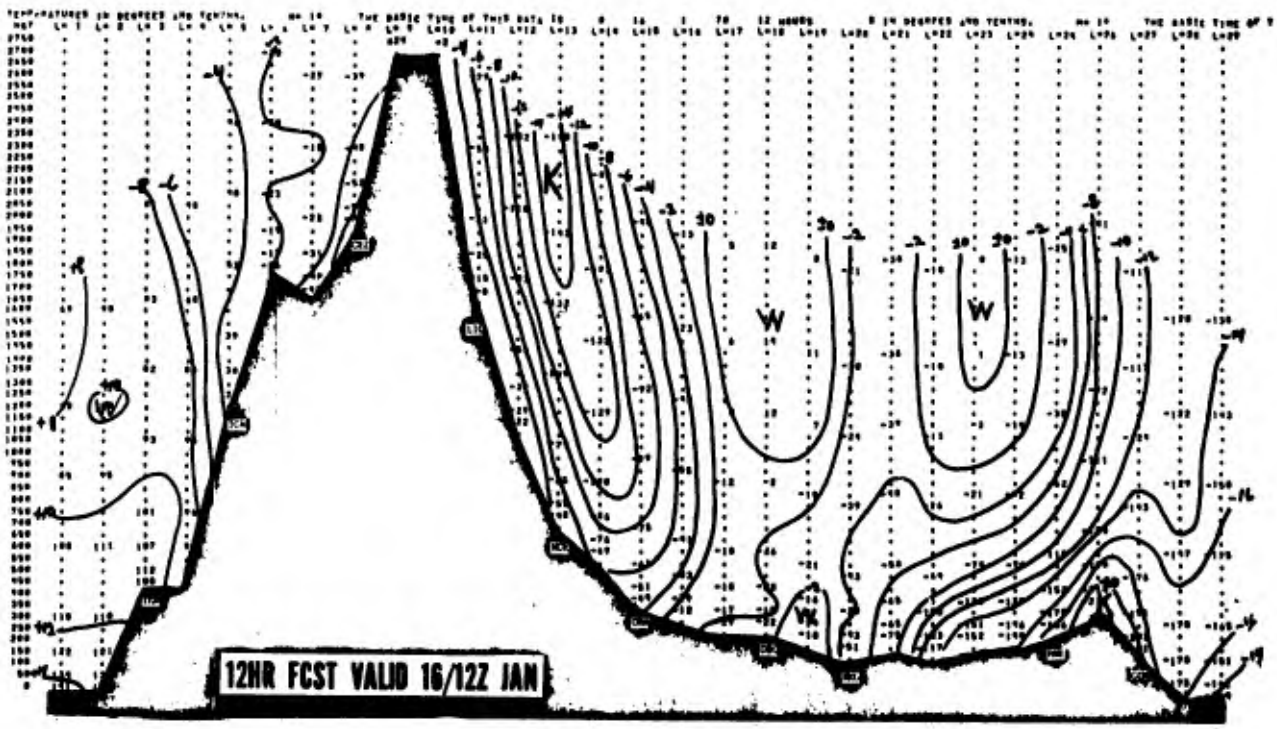


Figure 25

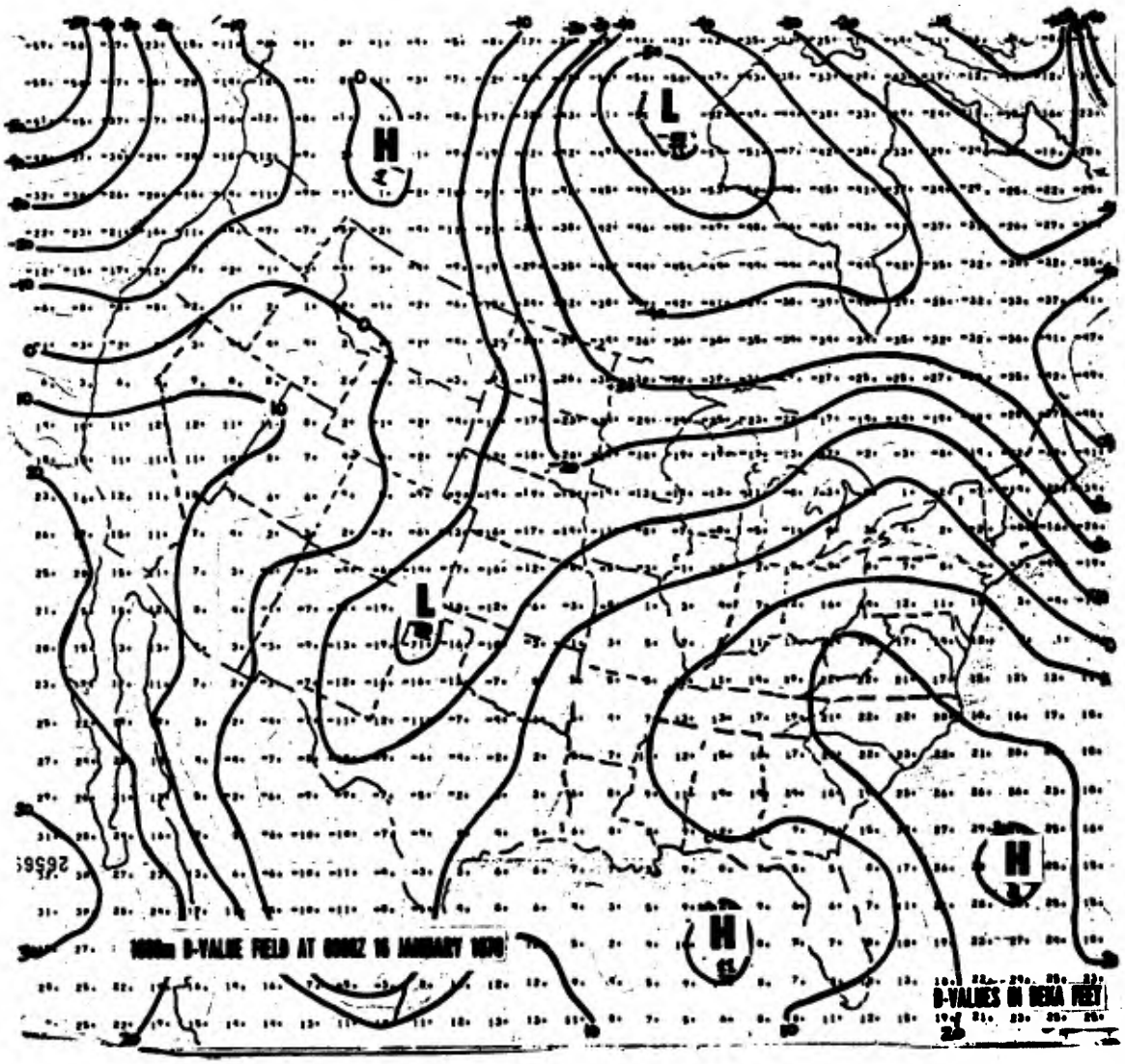


Figure 26

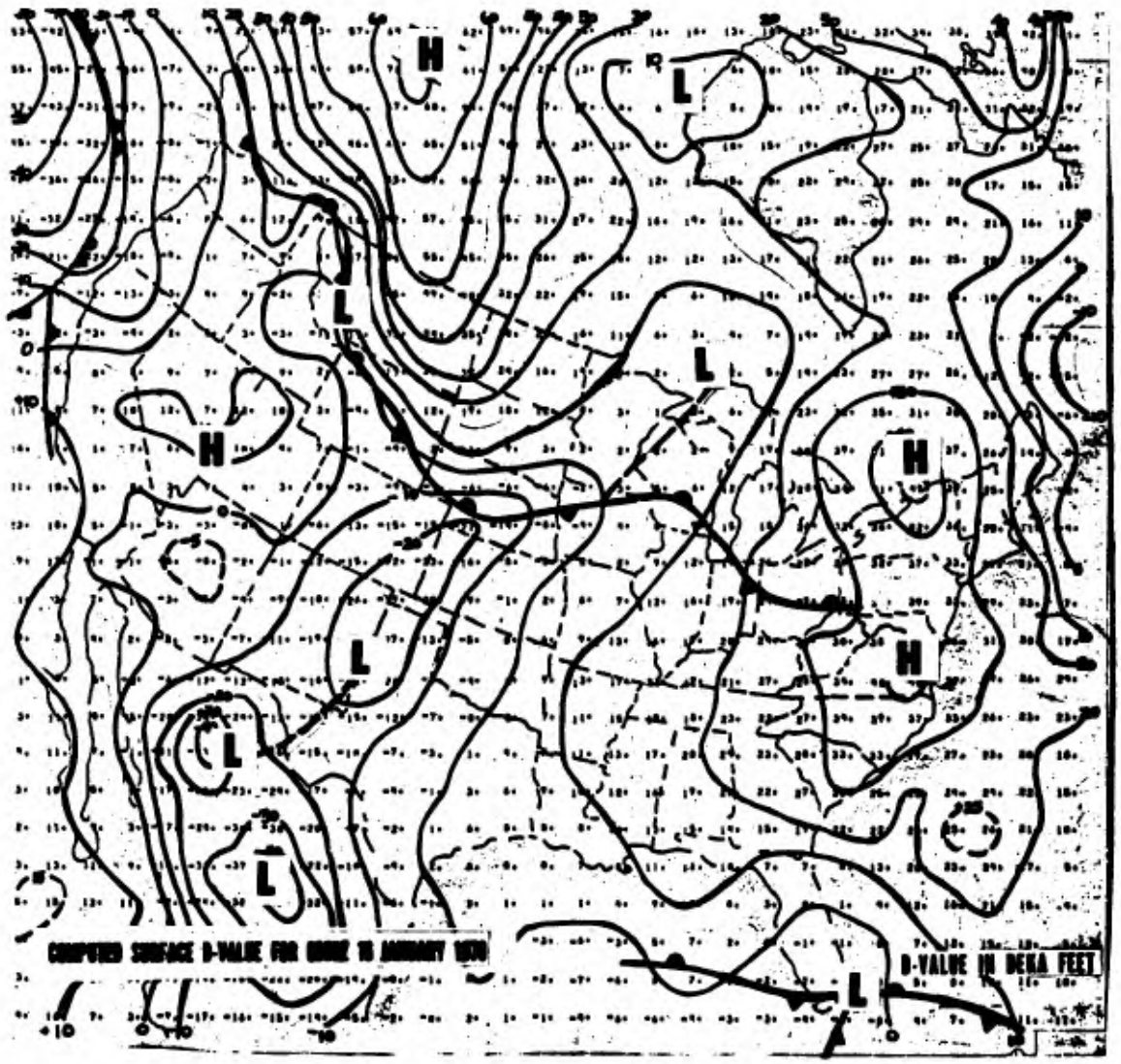


Figure 27

# DIAGNOSES AND PREDICTION OF MARINE BOUNDARY-LAYER MESOSCALE-WIND PHENOMENA

R. V. Cormier and E. C. Kindle

U.S. Navy Weather Research Facility
Norfolk, Virginia

## Abstract

A rationale for the prediction of the operationally-significant surface weather elements is presented wherein boundary-layer mesoscale forecast rules would be developed by running, in a research environment, existing mesoscale boundary-layer models with varying synoptic and mesoscale initial conditions. The Navy Weather Research Facility's initial attempts in this direction have been aimed at diagnosing the unusual and sometimes strong winds observed in the marine boundary layer. Preliminary modelling runs of these winds although encouraging, point to the need for more realistic simulation of heat and momentum-transfer processes.

## 1. A RATIONALE

The development of improved prediction of operational weather is the major problem facing the meteorological community today. While the marked strides that have been made in hemispheric prediction of the hydro- and thermodynamic parameters have created a potential for a marked improvement in forecasting, they do not guarantee it.

As pointed out by Kindle (1969) at last years' Technique Exchange Conference, a long-overdue development, that is critical to significant improvement of operational forecasts, is an organized rationale for predicting the operationally-significant weather. This requires an extensive effort in developing principles and techniques relating cumulus and mesoscale processes to predictable synoptic-scale features.

With the recent and projected developments in data sources, physical theory and computational capabilities, the development of a comprehensive forecasting rationale can be realized with the appropriate dedication of research resources. A quite vulnerable (and also quite important) area in such a program is the interpretation and integration of the effects of high-resolution surface conditions interacting with the predictable synoptic-scale features. These effects are most significant in the vicinity of intense gradients of surface properties such as along the east coasts of continents during the winter, at the cold edges of the Gulf Stream and Kuroshio Current, in the South China Sea, at the north coasts of the Mediterranean, etc. Based on these observational facts, the Navy Weather Research Facility has undertaken the development of a diagnostic and prediction program for the operational phenomena characteristic of these regions.

The ideal objective of such a program would of course be the development of high-resolution, prognostic, primitive-equation, numerical models that could be applied operationally with boundary conditions being provided by operational large-scale models. While such an end product will be sought through the adaption of contemporary models, our diagnosis of the current problems of boundary-layer primitive equations (and their prospects for solution) such as initialization, integration of boundaries with larger-scale models, and high-resolution computational costs, indicate that the prospects of immediate success for such a direct approach are slim.

Another approach which is undergoing diagnosis is the application of sophisticated diagnostic-numerical models. However, here the addition of the required reality and resolution to such a model necessary to accommodate the complexity of processes involved, would present computational problems that are very difficult to resolve within the criteria for operational application. Although both of these approaches present computer time and numerical computational problems that limit their current wide-spread operational use, for the prediction of high-resolution/mesoscale phenomena, their prospects for usefulness in a research environment as diagnostic devices is more promising. In this phase, the models would be run or re-run with a range of degrees of freedom in the various mesoscale conditions within a realistic range of the various large-scale synoptic features. The results of these experiments would provide a basis to permit the subjective superimposition of these local effects on the operational synoptic-scale products and should provide a series of useful prediction techniques beginning by the fall of 1971.

## 2. UNUSUAL AND/OR INTENSE MESOSCALE MARITIME WINDS

In addition to diagnoses of contemporary numerical-model applicability, the initial phase of the program has been concerned with the development of a clearer understanding of the descriptive and physical nature of unusual and intense maritime mesoscale winds.

The occurrence of unusual and/or strong, mesoscale, maritime, surface winds are particularly important to Naval operations and their prediction cannot be left to simple extrapolations from the lower tropospheric synoptic scale numerical predictions, since these winds do not follow the classical relationship that exist relating surface winds to gradient-level winds.

The existence of such winds has been known for some time. As early as 1953, a frequent strong decrease of boundary layer winds with height, rather than the expected increase, at North Atlantic weather ship locations, was noted by Jones (1953).

Table 1. Frequency (Per Cent) of Wind Speed Increase (Decrease) With Altitude Over the Sea [Data from Jones (1953), rearranged by Roll (1965)].

| Wind levels (meters) | Wind speed difference (knots) | | | | |
|---|---|---|---|---|---|
| | Decrease | | Increase | | Number of cases |
| | <-10 | -9 to 0 | 1 to 10 | >10 | |
| 600-300 | 1 | 46 | 48 | 5 | 797 |
| 300-surface | 3 | 40 | 46 | 11 | 793 |

Table 1 shows that in 40% of the cases studied, the winds decreased by 0 to 9 knots from the surface to 300 m.; and in 3% of the cases, the wind decrease was in excess of 10 knots.

Table 2. Frequency (Per Cent) of Wind Speed Increase (Decrease) From the Surface to 600 Meters Over the Sea as Related to Thermal Stratification [Data from Jones (1953), rearranged by Roll (1965)].

| Wind Speed | Air-sea temperature difference (°F.) | | | | | | Number of cases | Per Cent |
|---|---|---|---|---|---|---|---|---|
| | >+2 | +1 to -2 | -3 to -7 | -8 to -12 | -13 to -17 | <-17 | | |
| Decreasing | 0 | 20 | 36 | 45 | 40 | 32 | 247 | 32 |
| Unchanged | 3 | 6 | 6 | 7 | 7 | 8 | 47 | 6 |
| Increasing | 97 | 74 | 58 | 48 | 53 | 60 | 490 | 62 |
| Number of cases | 67 | 176 | 258 | 166 | 77 | 40 | 784 | 100 |

Table 2 shows the cases stratified according to air-sea temperature difference or stability. We note that the greatest percent of boundary layer winds decreasing with height — 45% — occurred with boundary-layer cold-air advection when the air temperature was 8 to 12° F. colder than the water temperature.

Marine meteorologists have reported frequent trouble forecasting winds at the northern edge of the Gulf Stream during cold air outbreaks in early winter (Crozier, 1969). Surface winds frequently in excess of, and up to twice the computed surface gradient value have been noted within apparently very limited regions at and along the Gulf Stream North Wall.

The possibility of unique winds and/or wind circulation patterns along boundaries between water masses of significantly different temperatures has also been shown in satellite photographs (Warnecke, et al., 1969). Figure 1 is a view photographed by the satellite ATS III on 11 March 1968. It shows the clear skies within the cold Humboldt Current off the west coast of South America, and also shows a band of clouds at the western edge of the current. This suggests the existence of a superimposed mesoscale thermal circulation (and wind field) between the cold and warm-water regions, similar to the land-sea breeze phenomenon.

Canadian meteorologists have documented a fairly frequent occurrence of "supergeostrophic" surface winds during the winter off the coast of Nova Scotia (Dexter, 1959). Figure 2 presents the speed difference between the surface geostrophic wind and the observed surface wind at Lurcher Lightship located off of Yarmouth, Nova Scotia, plotted against the surface geostrophic wind under conditions of northwest flow. Any negative value, that is, any point plotted below the zero line marks the occurrence of a "supergeostrophic" wind. One can see that these occurrences make up a large number of the cases studied.

More recently, Mendenhall (1967) has shown that the behavior of wind direction within the boundary layer, in addition to that of wind speed, can also depart from the classical picture of winds veering with height. Figure 3 shows the observed change of direction of wind with height in the lowest kilometer at ship Nan (30° N., 140° W.) during August 1960. Negative values of "veering" indicate a backing of the wind with increasing height, which is contrary to classical Ekman behavior.

This negative wind-veering with height, that is backing with height, may be related to strong superadiabatic lower boundary-layer lapse rates. Figure 4 shows time-series of one-hour averaged data of boundary layer observed wind veering and concurrent lapse rates taken from a TV tower in Oklahoma City during the period 9-12 March 1967. We note that the backing wind regimes correspond to some degree with the periods of superadiabatic lapse rates.

Kuettner (1959), in studying low-level roll-clouds over the ocean showed some very interesting distributions of the vertical wind-speed variability in the boundary layer. Figure 5 shows a boundary-layer profile of wind speed versus height when low-level cloud bands or cloud streets were widespread. The profile shows a wind maximum of 45 knots below 1000 feet and a relative wind minimum of 22 knots located near the inversion base. Also plotted at each point on the wind profile is the wind direction which is near constant with height. In this case if the wind were geostrophic above the inversion, the low-level wind could have been indeed "supergeostrophic."

Other cases of strong ageostrophicity of wind such as in the South China Sea during the Northeast Monsoon or during the mistral in the western Mediterranean are also enigmas which cannot be explained by the classical gradient-level/surface wind relationship.

This search for observational evidence of these unusual wind regimes, which is still going on, has thus already uncovered quite a bit of documentary data and descriptions of unusual winds.

Further, to minimize the chances of discarding the key factors when making the physical compromises in the models often necessary for computational solvency, the potential causal processes for these wind regimes are being isolated and tested as part of our boundary-layer modelling.

## 3. PRELIMINARY DIAGNOSES

As a result of a preliminary diagnoses, the Navy Weather Research Facility has deduced that these unusual and strong wind regimes might be created by one or a combination of three major mesoscale processes which can occur with given synoptic flows. These are:

(1) Sudden changes in surface friction,
(2) Sudden inversion breakthroughs,
(3) Enhanced momentum exchange through cold-air advection in the boundary layer.

A sudden change in friction, that is, in eddy viscosity takes place as air moves from coastal areas, especially when mountainous, to adjacent ocean areas. Here not only do we get an increase of wind because of less frictional retardation, but because of the inertial adjustment of the velocity field toward its new equilibrium value as a result of the sudden release of friction, one could in theory obtain the "supergeostrophic" winds found by the Canadians, much in the same way that Blackadar (1957) postulated as the explanation for the nocturnal low-level jet.

The sudden breaking through of strong subsidence inversions, characteristic of equatorward moving polar air, brought about by strong heating of an air mass over warmer oceans, will enable the sudden mixing of air with potentially different moments. Depending upon the relative directions of the flows above and below the inversion, this could cause either an acceleration or a deceleration of the surface wind. Figure 6 schematically depicts these conditions. The top view shows the case where the surface air could be accelerated by an inversion breakthrough; whereas the bottom view shows the reverse, where the surface wind speed would decrease.

This latter case — a sudden decrease of surface winds due to an inversion breakthrough can take place during slow surges of the South China Sea Northeast Monsoon where the winds near the surface are strong northeasterly while the air above the inversion is west to west southwesterly. The inversion breakthrough can be seen in satellite photographs because the breakthrough allows the convective processes to change the cloudiness to convective elements smaller in size than the resolution capability of the satellite sensor. Figure 7 shows an example of this situation. The sudden beginning of the clear air on this cloud photograph taken over the South China Sea shows the line along which the inversion breakthrough occurs. An analysis of the wind field corresponding to this time shows a wind-speed minimum just south of this same line (U.S. Navy Weather Research Facility, 1969).

Cold air moving over warm water creates strong vertical exchanges of heat and momentum in the boundary layer, thereby causing surface winds to be stronger than in neutral or warm-advection environments. With, in addition, the presence of a post-cold-frontal type inversion in the lower troposphere, which would limit the downward flux of momentum from above, conditions may be proper for the occurrence of low-level wind maxima. A schematic portrayal of such a situation is shown on figure 8.

The upper portion of the figure, part (a), shows the characteristic low-level (of the order of 4,000 feet) inversion, and the postulated surface and inversion-base geostrophic winds, under conditions of exaggerated cold-air advection. Part (b) to the left snows a postulated surface wind, $\underline{V}(1)$, and the balance of forces that would result in the absence of the eddy flux of momentum from the upper backed winds. We see that the resultant of the surface Coriolis Force, (CF), and the surface frictional force, (FF), balances the surface pressure-gradient force, (PGF), resulting in the wind, $\underline{V}(1)$.

Part (c) on the lower right shows, that now considering a downward flux of momentum from the upper backed winds, an additional force component, labeled M, is provided to the surface air, causing it to blow more toward low pressure and be thus accelerated to a higher wind speed than would be the case if cold-air advection were not present. We have, for this schematic illustration, assumed that the additional force component, M, is in the direction of the vertical shear within the layer. We now have a new balance of forces, as indicated on the figure, with an indicated increase in the surface wind, $\overline{V}(1)$. Under these postulated conditions, without any appreciable flux of momentum through the inversion from above, the wind just below the inversion would tend to decelerate and the resulting wind-speed profile would show a low-level maxima as both Jones (1953) and Kuettner (1959) found.

A given surface, maritime wind could be the complex result of all of these processes interacting with the synoptic flow. Thus, a wide range of variability in the resultant maritime low-level wind is possible not only in different locations but at different times in the same location.

## 4. INITIAL WEARSCHFAC MODELLING EFFORTS

Initial Navy Weather Research Facility numerical modelling efforts have been aimed at trying to numerically simulate the previously mentioned, intense winds found at the North Wall of the Gulf Stream. The realistic simulation of this phenomena could lead to the development of forecast rules for these difficult to predict winds which would make use of only synoptic scale prognoses.

The basic model being used is a simplified version of a two-dimensional primitive equation, boundary-layer model, developed by Estoque and Bhumralkar (1968). Initial runs of this version have been promising but the increases of wind at the northern edge of a simulated Gulf Stream are less than observed.

Figure 9 presents the results of one of these runs, and shows the vertical and horizontal distribution of wind speed along a line perpendicular to the Gulf Stream. For this run, the following initial conditions were postulated: (1) an exaggerated 20° C. ocean temperature difference across an east-west oriented Gulf Stream; (2) a subsidence inversion with its base at 210 meters and top at 460 meters; and (3) northerly geostrophic winds of 10 m./sec. (20 knots) below the inversion and 20 m./sec. (40 knots) above the inversion. The model was run until a steady state was achieved for the given initial conditions.

This figure shows that at the Gulf Stream North Wall and at a height of 10 meters, the steady state wind was 11.1 m./sec. (22.2 knots), somewhat stronger than the given 10 m./sec. geostrophic wind; and that upstream, the wind at the same level was 9.9 m./sec. We thus have realized an increase of 1.2 m./sec. at the North Wall — a value much smaller than observed.

Recent conversations with personnel of the Fleet Weather Central Norfolk have indicated that strong winds at the North Wall of the Gulf Stream are most noticeably realized when the isobars intersect the North Wall at an oblique angle rather than at a 90° angle. Modelling runs, conducted last week using such a geostrophic wind distribution, showed that wind direction was indeed important, and a greater increase of wind than previous runs was realized at the North Wall; but this increase was still below observed values and located further downstream than observed.

Our diagnoses of this lack of complete realistic simulation by the current model indicate that the fluxes of heat and momentum allowed by the eddy-transfer coefficients are too small. Accordingly, we are presently investigating alternative eddy-tranfer coefficient formulations and also questioning the magnitudes of the transfers allowed by these formulations in the upper levels of the boundary layer, where large transfers must occur as evidenced by the infrequent observance of superadiabatic lapse rates there.

Another feature of maritime winds which is being investigated through modelling, is the behavior of winds downstream of coastlines with rough terrain. Our initial efforts make use of a simple particle/Lagrangian dynamics approach to the problem wherein the surface frictional force is assumed to be proportional and opposite in direction to the wind velocity vector. A similar model has recently been used by Gordon and Taylor (1966) in an investigation of low-latitude convergence zones. Although this approach does not accommodate all of the physical processes involved, it does permit the study of the inertial adjustment of an air parcel to a sudden change of frictional forcing. Such an adjustment is dependent on the initial (over land) velocity of an air parcel, as well as latitude and the friction proportionality constant. Initial runs of this model have been aimed at obtaining realistic values for this constant. Figure 10 shows some results of these runs. We have assumed on east-west coastline located at 45° N. latitude with isobars running north-south with a northerly geostrophic wind of 20 m./sec. (40 knots). A typical land-wind speed under these conditions of 12.5 m./sec. (25 knots) making a 45° angle to the isobars is also assumed. Under these assumtions, the friction coefficient over land, $K_{LAND}$, obtained through calculations is $1.0X10^{-4}$ $sec.^{-1}$. The upper curve shows the inertial adjustment of a parcel of air after leaving the coast if the friction force is reduced nearly one order of magnitude; the lower curve shows the behavior if friction is reduced one half. Because inertial oscillations of the magnitude shown on the upper curve have not been observed in the boundary layer, we accept the lower curve as being more reasonable. Here the wind approaches the geostrophic and stays near this value for some time (following the parcel). Although not all physical processes are included here, an effect of this nature must be present in the real atmosphere.

And that gentlemen is the current status and the guiding rationale of one aspect of the Navy Weather Research Facility's attempts at providing Naval meteorologists with guidance and tools to forecast the operationally significant weather elements.

REFERENCES


BLACKADAR, A. K., "Boundary-Layer Wind Maxima and Their Significance for the Growth of Nocturnal Inversions." Bulletin of the American Meteorological Society, Vol. 38, No. 5, pp 283-290, May 1957.

CROZIER, J., "Investigation of Supergradient Winds in North Wall of Gulf Stream." U.S. Navy Fleet Weather Central, Norfolk, Virginia, Unpublished Manuscript, March 1969.

DEXTER, R. V., "Preliminary Report on Winter Wind Speed Versus Pressure Gradient at Sea Off the Nova Scotia Coast." Meteorological Branch, Dept. of Transport, Canada, CIR-3213, TEC-304, 10 June 1959.

ESTOQUE, M. A., and C. M. BHUMRALKAR, "Theroetical Studies of the Atmospheric Boundary Layer." U.S. Army Electronics Command, Fort Huachuca, Arizona, ECOM-67G2-F, June 1968.

GORDON, A. H., and R. C. TAYLOR, "Lagrangian Dynamics and Low-Latitude Weather." Hawaii Institute of Geophysics, University of Hawaii, HIG-66-12, August 1966.

JONES, D. R., "Note on Observed Wind Shear at Low Levels Over the Ocean." Bulletin of the American Meteorological Society, Vol. 34, pp 393-396, 1953.

KINDLE, E. C., "The Navy Weather Research Facility Program for Development of a Functional Display and Presentation System." Proceedings of the 5th AWS Technical Exchange Conference, Air Weather Service (AWS) Technical Report, 1969.

KUETTNER, J., "The Band Structure of the Atmosphere." Tellus, Vol. 11, No. 3, pp 267-293, Aug 1959.

MENDENHALL, B. R., "A Statistical Study of Frictional Wind Veering in the Planetary Boundary Layer." Dept. of Atmospheric Science, Colorado State University, Fort Collins, ASP Paper No. 116, December 1967.

ROLL, H. U., Physics of the Marine Atmosphere. Academic Press, New York, 1965.

WARNECKE, G., et al., "Ocean Current and Sea Surface Temperature Observations From Meteorological Satellites." NASA, Goddard Space Flight Center, Greenbelt, Maryland, NASA TN D-5142, November 1969.

U.S. NAVY WEATHER RESEARCH FACILITY, "The Diagnosis and Prediction of SEASIA Northeast Monsoon Weather." U.S. Navy Weather Research Facility, NWRF 12-0669-144, June 1969.

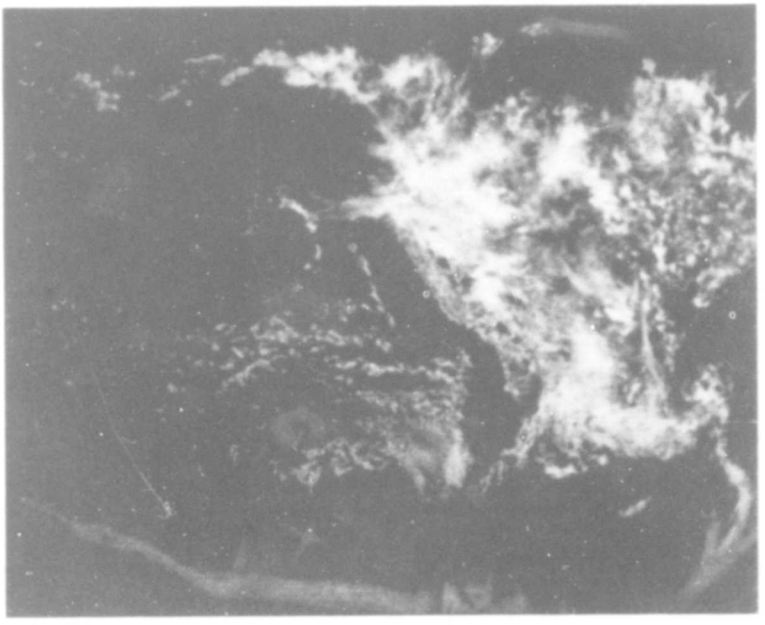

Figure 1. ATS-III(IDCS) Photograph Taken on March 11, 1968, 1622 GMT, Showing Cloud-Free Area Over Humboldt Current [From Warnecke, et al, 1969)].

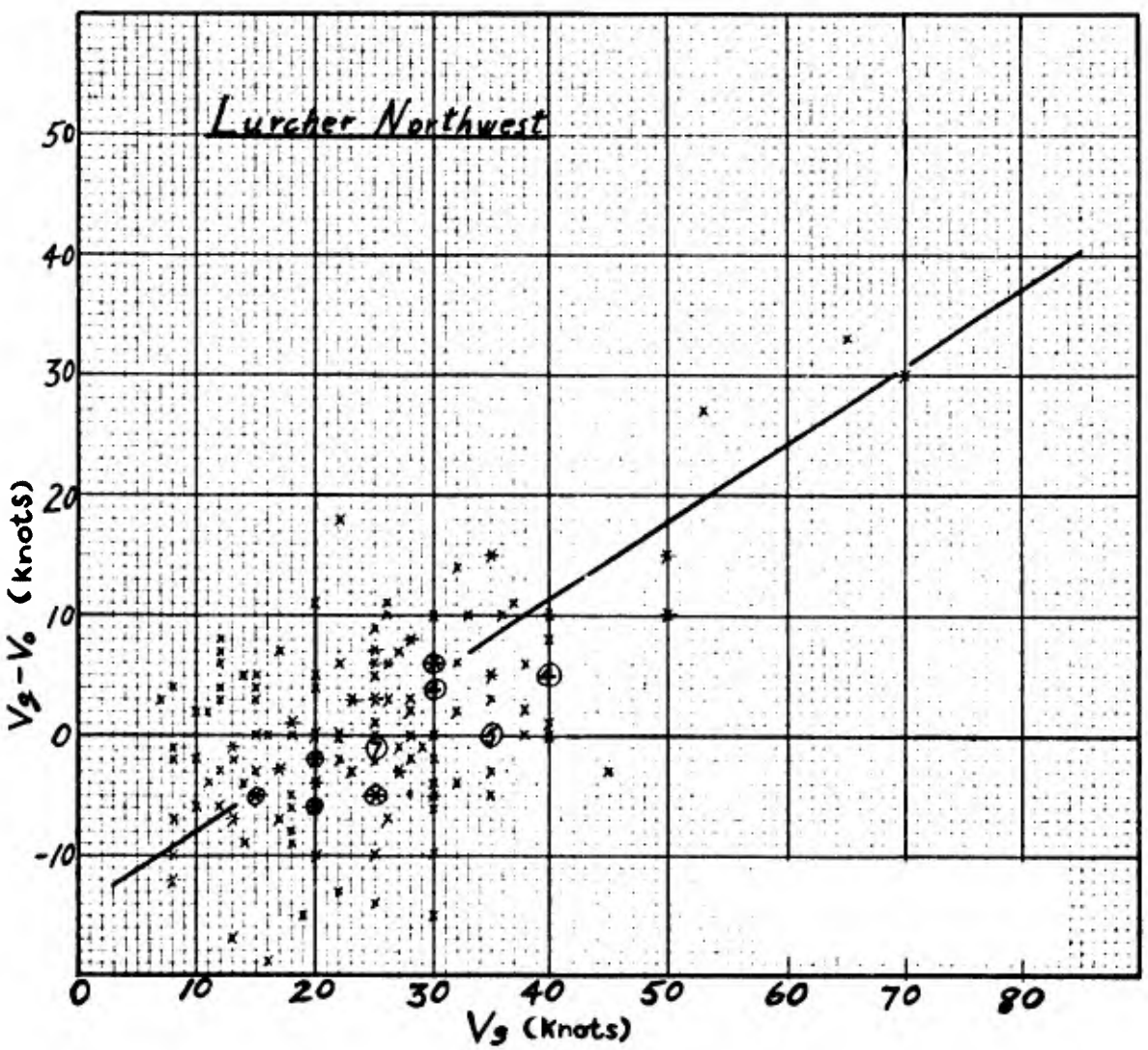


Figure 2. Surface Geostrophic Wind Minus the Observed Wind Plotted Against the Surface Geostrophic Wind at Lurcher Lightship (Near Yarmouth, Nova Scotia) Under Conditions of Northwest Flow (From Dexter, 1959).

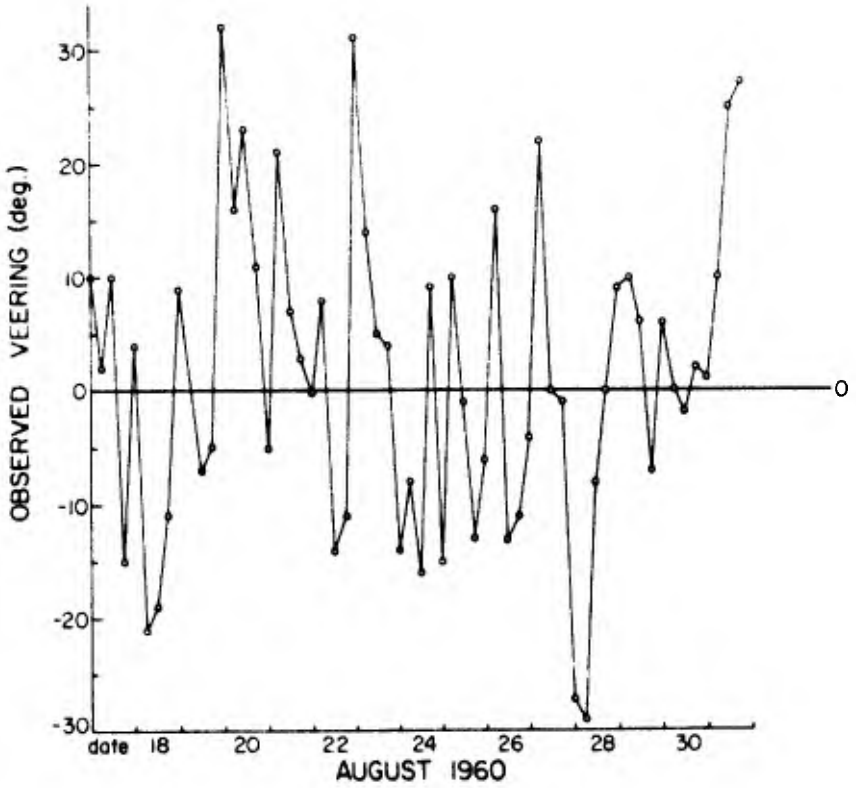


Figure 3. Observed Clockwise Turning (Veering) of the Wind Direction With Increasing Height in the Lower Kilometer at Ship Nan (30° N., 140° W.) During August 1960 (From Mendenhall, 1967).

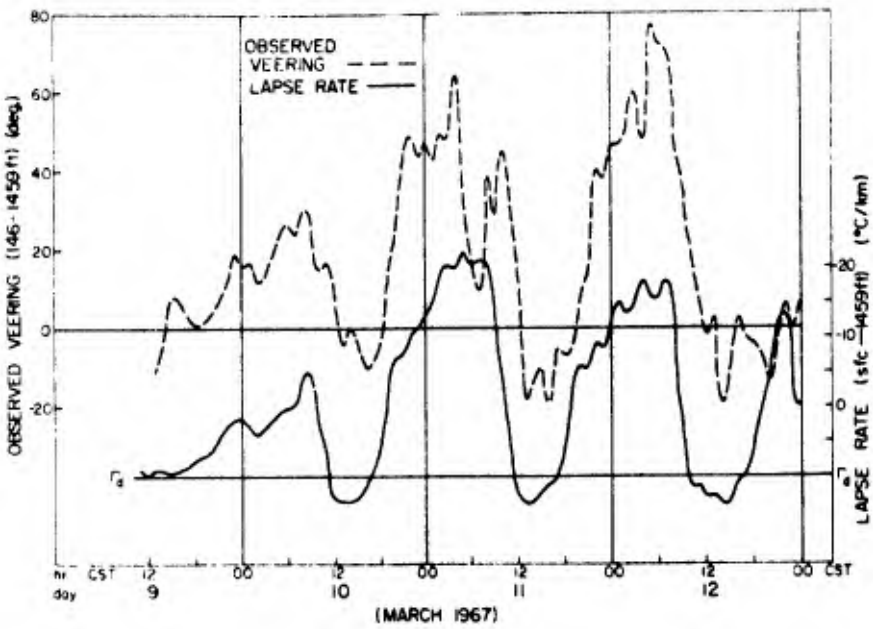


Figure 4. Observed Clockwise Turning of Wind With Increasing Height (Veering) and Observed Lapse Rate From a TV Tower in Oklahoma City (From Mendenhall, 1967).

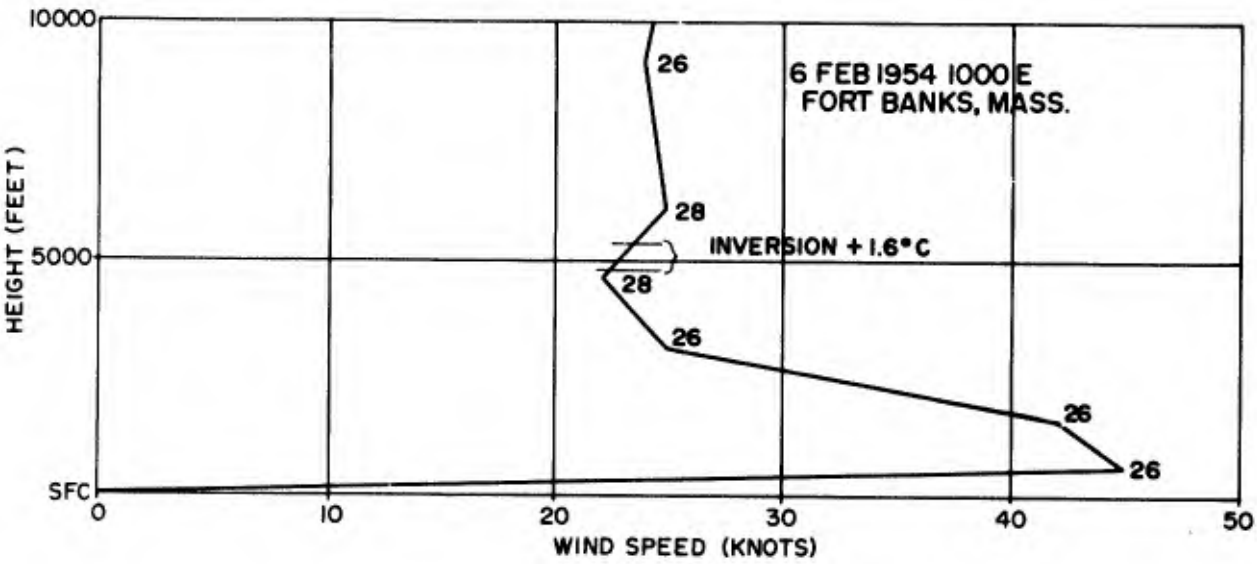


Figure 5. Observed Wind-Speed Profile When Clouds Bands Were Widespread (From Kuettner, 1959).

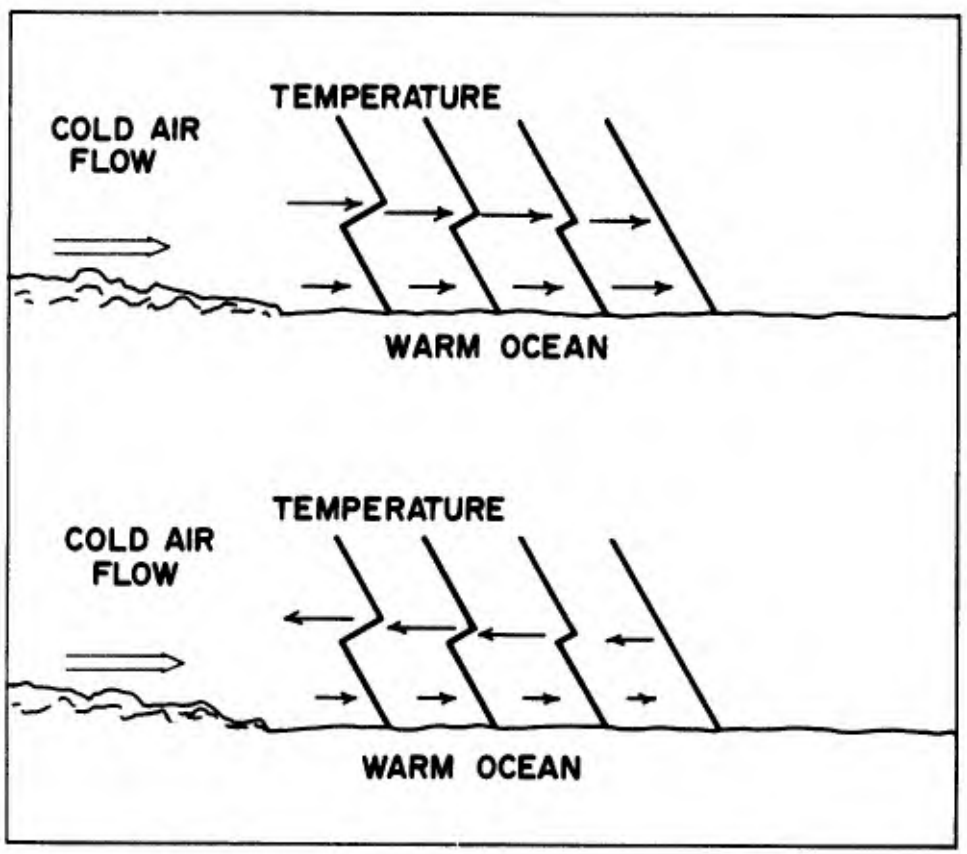


Figure 6. Schematic Portrayal of the Potential Effect of an Inversion Breakthrough on the Low-Level Wind.

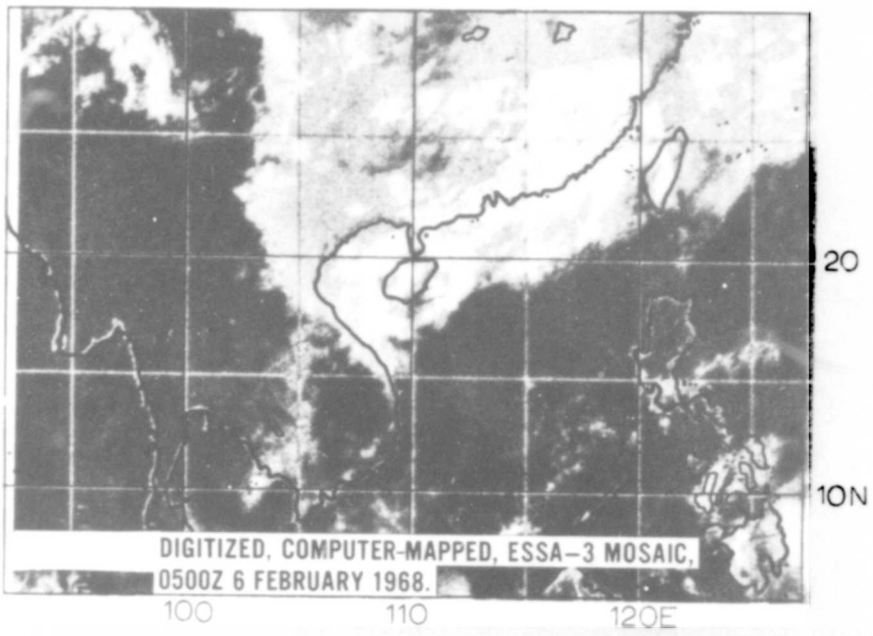


Figure 7. Example of an Inversion Breakthrough During a Slow Surge of the Northeast Monsoon Producing a Decrease in Low-Level Winds.

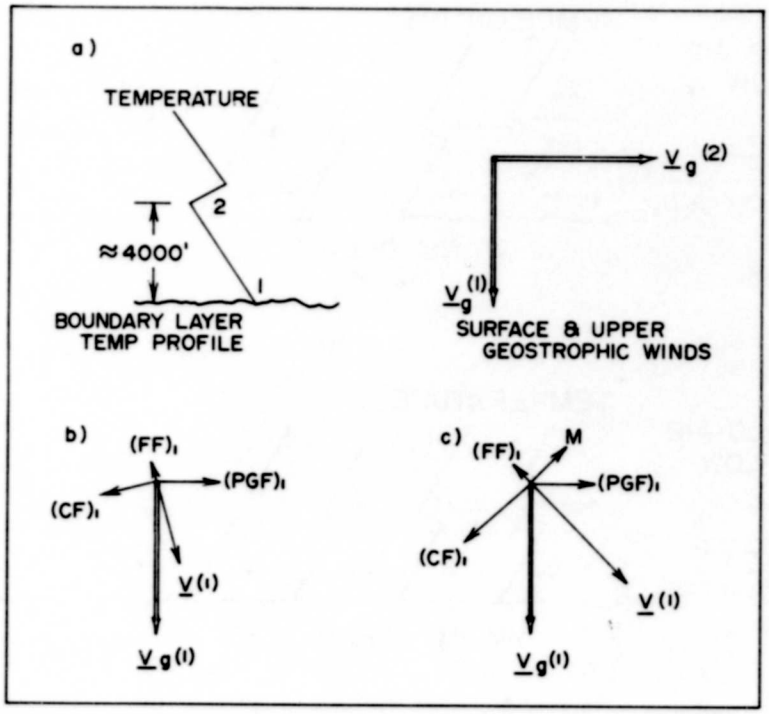


Figure 8. Schematic Example of a Situation Which Could Cause a Low-Level Wind Speed Maximum (See text for explanation of vectors).

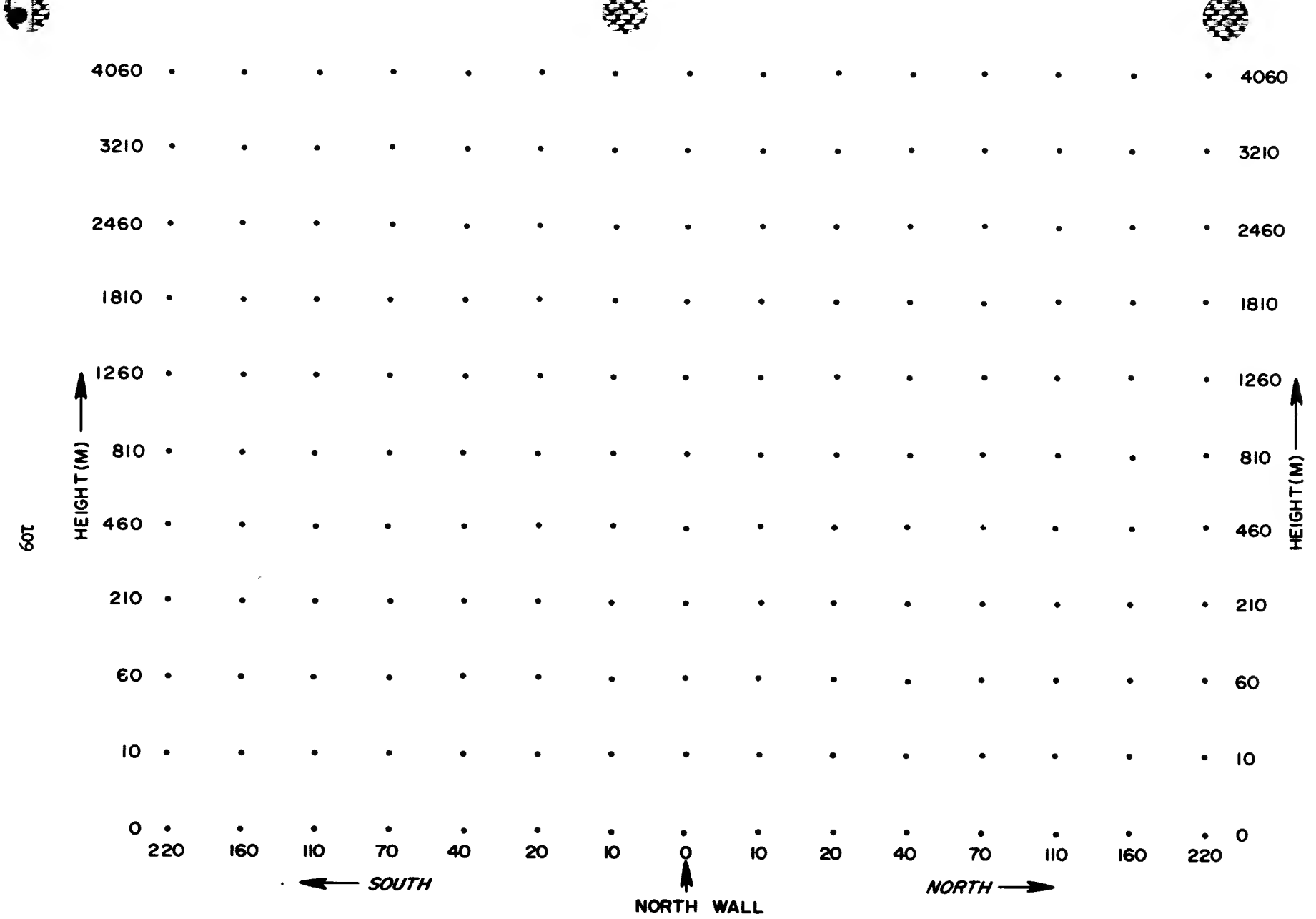


Figure 9. Predicted Wind Speed (m./sec.) From a Numerical Model Simulating Increase of Winds at Northern Edge of Gulf Stream.

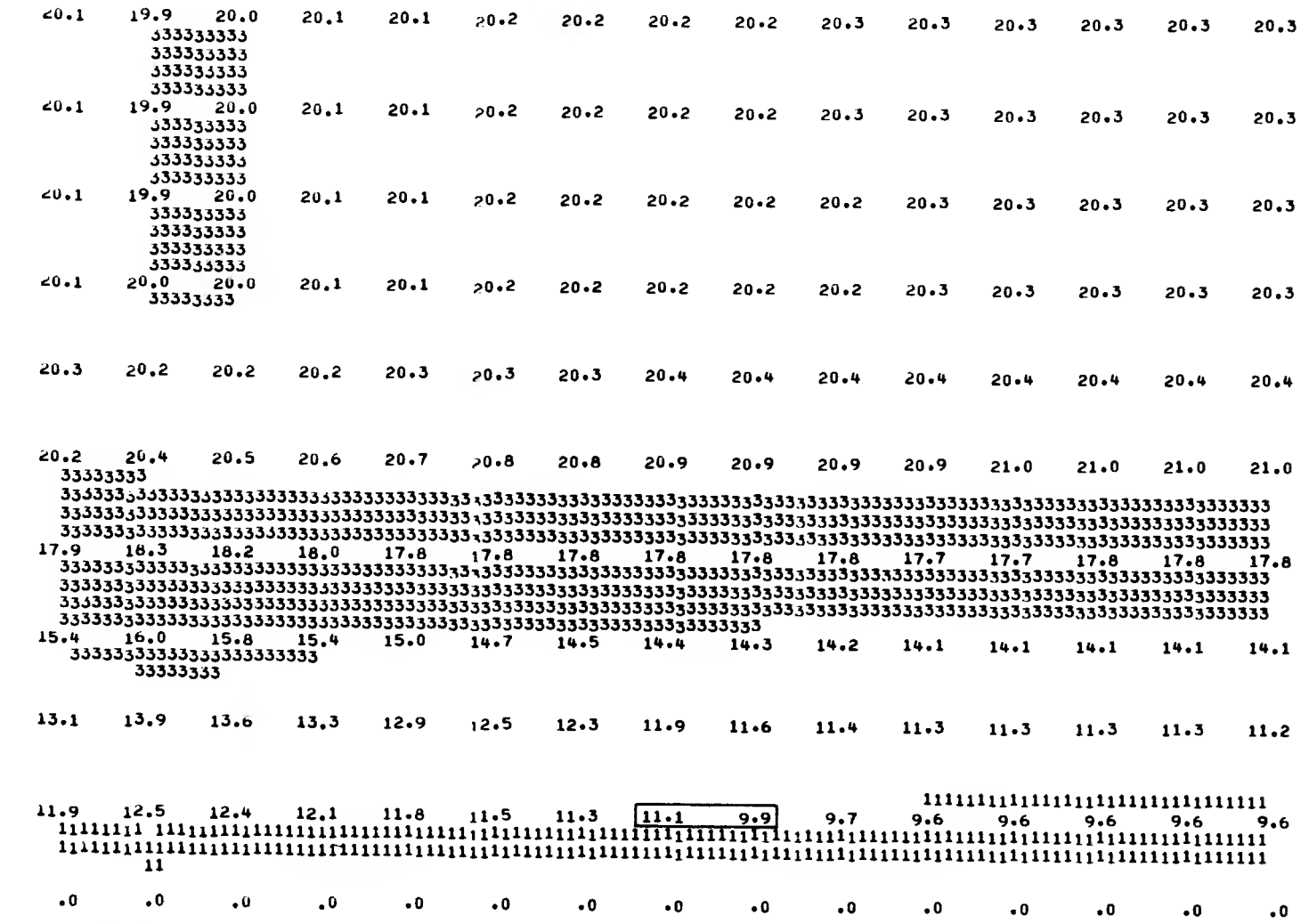


DATO SCALED BY .10U-01, CONTOUR INTERVAL IS 5
ROWS 1 THRU 11, COLUMNS 1 THRU 15.

*IND SPEED

RUN 4 ITERATION 900 T = .1500+02

← AIR FLOW →

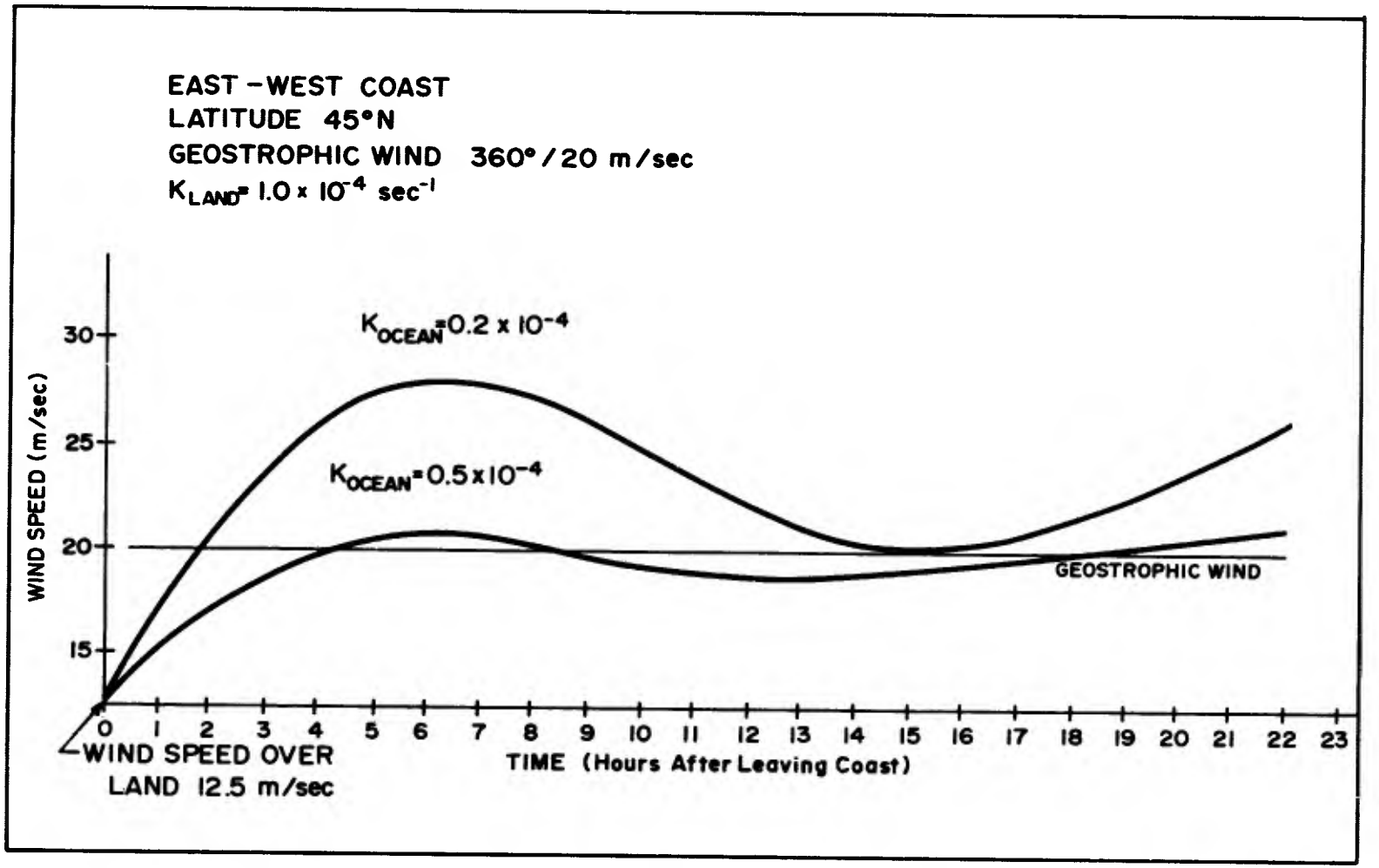


Figure 10. Effect of the Variation of the Friction Proportionality Constant on the Inertial Adjustment of an Air Parcel.

# PREDICTABILITY OF LOCAL WEATHER

Charles F. Roberts

Division of Forest Fire and
Atmospheric Sciences Research
Forest Service
U.S. Department of Agriculture

Abstract

The general problem of predictability is defined. The limitations on predictability arising from methodology and physical laws as expressed in the Lorenz-Robinson hypothesis are reviewed. Scale factors are derived for local weather events and theoretical predictability is tested. Comparisons between predictability limitations and accuracy of operational forecasts are made through an attempt at spectral decomposition of forecast skill.

## 1. BACKGROUND

The question of the ultimate limits on the predictability of the atmosphere is being studied rather seriously for the first time in connection with the cost-benefit analyses of the world weather watch program. Over the last decade or so, meteorologists have formulated programs and plans on the assumption that there are no inherent limitations to the predictability of the atmosphere or else the gap between its predictability with current methods and data, and what might ultimately be obtained, is so great that it is not worthy of practical considerations.

It is only when we attempt to justify, on a purely economic basis, the expenditure of several hundred million dollars in support of the development and operation of a global weather-prediction system that we are forced to state what credibility we can anticipate in weather forecasts produced by such a system. Since the best studies available on predictability have indicated that the gap between what we might ultimately expect to achieve and what we are currently able to deliver may not be as large as we had assumed, the question of predictability has become a matter of major concern to the World Weather program and especially the GARP Committee. A summary of the studies on predictability has been provided by Charney [1] in a recent report of that Committee.

The question which actually underlies these cost-benefit studies, and the one which must ultimately be answered, is not the predictability of the physical state of the atmosphere, but rather the predictability of the time sequence of weather variations at specific locations and over finite areas of the earth's surface. Insofar as this writer is aware, none of the present GARP studies have addressed this question directly, and none of the completed studies provide the information from which a usable answer can be formulated.

Of course, the whole scientific basis of modern weather forecasting rests on the assumption that there exists a unique transformation between physical state of the atmosphere and the occurrence of weather phenomena. For some elements this transformation is obvious, but it must be kept in mind that the cloudiness, precipitation and other phenomena which the man on the street loosely groups under the term "the weather" results from the very subtle interaction between the fields of physical-state variables and the geography of the area in question, including man-made features. This fact is well known by those weather forecasters who use the "perfect prog" approach to weather forecasting, in which the attempt is made to derive statistical specifications of weather from measured data-fields. Forecasters who have experimented extensively with this method are painfully aware of the fact that physical-state variables are generally only sufficient to provide a general probability distribution for weather elements and events. Furthermore, it is a rather common experience of forecasters that two synoptic situations which appear to differ by an insignificant degree statistically will often evolve through widely differing modes in terms of the resulting weather phenomena. The importance of establishing the limits of the predictability of the weather and weather phenomena suggests that the problem ought to be studied in depth. I have undertaken only a preliminary empirical study of some elementary aspects of the problem.

## 2. PROBLEM DEFINITION

I shall treat the prediction problem in a stochastic framework; that is to say, I assume that the output of a prediction is the specification of the probability function of some element or phenomena in the positive time axis. The diagrams in figure 1 will help make my definition clear.

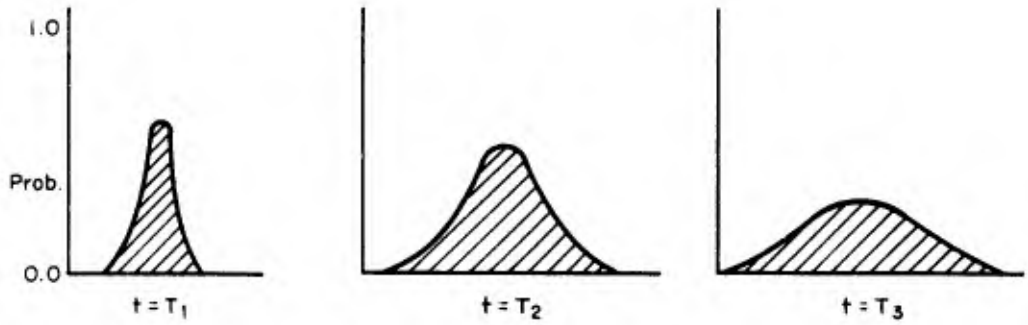


Figure 1 - An illustration of the decay of information with forecast period.

At each future time, $T_i$, the prediction yields a probability function. As time increases, the spread of the probability function increases until at some more or less distant future time it approaches a limiting function which is the "climatological" probability distribution or the unconditional probability function.

The information provided by the prediction is inversely related to the spread of the probability distribution. When the probability distribution reaches its limiting function the information content is identical to that provided by estimation based on the statistical compilation of past observations. The predictability of the atmosphere should be expressed in terms of a measure of the increase in information which results from the prediction.

There is, of course, a practical side to the predictability question which the above definition has not recognized. The use of our definition of predictability allows a forecast to provide information even though, from a utilitarian point of view, the forecasts might be worthless. But if we are to introduce such practical considerations, the economics of the forecast situation would have to be taken into account. From this point of view, weather would lose all predictability when the cost of producing the forecast just equalled the value of the information yielded by the forecast, but we shall not pursue these economic considerations in the present discussion.

Limitations on predictability arise from several sources: (1) methodology: the methods and equations employed are incorrect or inadequate; (2) data: the data available either do not define conditions in the manner required by the governing physical laws or the data contain errors which lead to incorrect specifications; and (3) the physics of the prediction problem: the governing physical laws may limit the information content of the specification. In considering the limitations on the predictability of the weather, we are certainly confronted with two of the above problems, and there are some, Robinson [2] for example, who believe that (3) may also be operative.

We shall first look briefly at methodology and some of its deficiencies. There are two methods which are customarily used to predict the future state or behavior of organized systems. The first, which we can call the physical method because of the prevalence with which it is used in the prediction of physical systems, involves the statement of the fundamental physical laws in the form of time-dependent mathematical equations which can be solved by known methods. A simple, but classic example of the physical prediction method is provided by the prediction of the trajectory of a particle traveling through a force field which is defined in both space and time coordinates. When the prediction problem is considered in this framework, it often boils down to a problem in solving a multivariate differential equation.

The meteorological prediction problem differs from the classical problem largely because the mathematical statements of the meteorological equations are of a form which is rather difficult to solve. Furthermore, some of the data required by the equations cannot be obtained from existing measurements. To work with the meteorological equations, they must be simplified in a manner which (1) eliminates the need for measurements that are not made, (2) will also make the equations amenable to practical solution, and (3) preserve all of the important physics that govern atmospheric processes. The entire science of numerical weather forecasting has grown up around efforts to achieve these ends.

## 3. STATISTICAL WEATHER PREDICTION

The second prediction method which has been widely used in weather forecasting is the statistical method. The statistical prediction method is essentially empirical in that a large volume of historical data which presumably describe the time history of atmospheric behavior in a meaningful way is analyzed to isolate prediction relationships. The statistical method for weather prediction is an attempt to derive empirically, a simple simulation model for a system governed by a rather complex set of differential equations. The limitations to predictability when a purely statistical method is used are obviously quite severe.

The prediction equation which must be derived by statistical analysis consists of a relationship of the form

$$Y_t = F(X_1, X_2, X_3, \ldots X_n)_{t=0} \qquad (1)$$

where $Y_t$ is the value of the dependent variable, often called the "predictand," at a future time t, and the $X_i$ are the independent variables or "predictors" measured at some past time, say t = 0. In reality, the form of the function F can be completely general.

Considering the characteristics of F, it is obvious that the function must be defined over an n-dimensional space. The generation of the function exactly over this space from empirical data alone requires filling the entire space with measured data points. The n- dimensional space is a discrete space, and we may imagine it to be made up of boxes or compartments, each compartment representing a location defined by simultaneous measurements of each of the $X_i$ independent variables. If the function F is single-valued and well behaved each compartment will be characterized by a unique value for $Y_t$. The task of mapping the function F over the n- dimensional space consists of filling each compartment with at least one measurement and fitting a mathematical function identically to each point. If the independent variables are themselves independent, all possible combinations of the values for the $X_i$ are realizable. The number of the compartments thus formed and hence the magnitude of the data requirement and the fitting problems are easily computed.

If the forecasting equation has n independent variables, each variable having k discrete classes or values then there are $N = (k)^n$ possible combinations or compartments which make up the hyperspace. For example, if we are dealing with an equation with 6 variables, each with 6 classes, then $N = (6)^6 = 46{,}656$, a number which represents 60 years of data if two observations per day are assumed.

If measured data points are randomly distributed throughout the predictor space (this is the most favorable condition) the probability that a given number of the compartments will not contain a data point is given by the Poisson probability function

$$P(m,\mu) = \frac{e^{-\mu}\mu^m}{m!} \qquad (2)$$

where $\mu = Ne^{-r/N}$ and m is the number of compartments that are empty after r observations have been randomly distributed. For example, if 8,000 observations are distributed through 1,000 compartments, the probability of one or more empty compartments is about 0.3. If the $X_i$ are not independent it is much more difficult to fill all compartments. If the data contain errors, several observations are needed in each compartment to reduce error by smoothing. For statistical weather forecasting, the above argument implies that available data samples will define a complex process over only a small portion of the domain of its existence.

The question may be properly asked as to how, under such serious constraints, simple statistical schemes have been developed that will yield predictions on each and every occasion. The explanation lies in the fact that most of the statistical analysis procedures which are applied in the

development of prediction equations are little more fitting techniques which automatically interpolate across the vast number of empty compartments in the n- dimensional predictor space. Generally, the fitting techniques employ a linear function such as a hyperplane or a simple, low degree, polynomial for interpolation or extrapolation through the empty spaces.

## 4. LIMITATIONS OF THE PHYSICAL METHODS OF PREDICTION

In considering the limitations inherent in physical prediction methods, we shall neglect the obvious difficulties that arise from numerical approximations. These omissions will serve to focus the discussion on limitations that arise from the fundamental physical laws or the mathematical statements of these laws.

Theoretical considerations of this problem have pursued somewhat different lines of investigation. Robinson [3] who was perhaps the first to point out the devastating consequences of inherent predictability limitations for practical weather forecasting examined the problem from the point of view of the adequacy of the mathematical statements of the physical laws as prediction equations.

Lorenz [4] on the other hand, considers the growth in prediction error in a two-dimensional model which arises from the laws governing spectral transfer of energy in a two-dimensional model of the atmosphere. Lorenz's analysis concludes that the atmosphere loses predictability in those scales associated with weather producing systems at a rate which depends on the functional form of the spectrum, not in the amplitude of the initial error in the scales which are nonobservable.

Both the Lorenz and Robinson analyses show a very strong relationship between the predictability at points in time and the scale of the phenomena, the smaller scales losing predictability at a much more rapid rate than the larger-scale systems.

A little better physical insight into the situation discussed by Lorenz is obtained through the use of the diagram in figure 2. Let's visualize the prediction model as an electronic system through which we are passing information in the form of signals. We construct a wave number spectrum for the atmospheric data which represents the input. The output at any future time has a wave number spectrum which is essentially a mathematical transformation of the input spectrum, the transformation process depending on the frequency or wave number response of the processor we are using. For weather prediction, we, of course, hope and expect our processor to be a perfect analogue of atmospheric behavior.

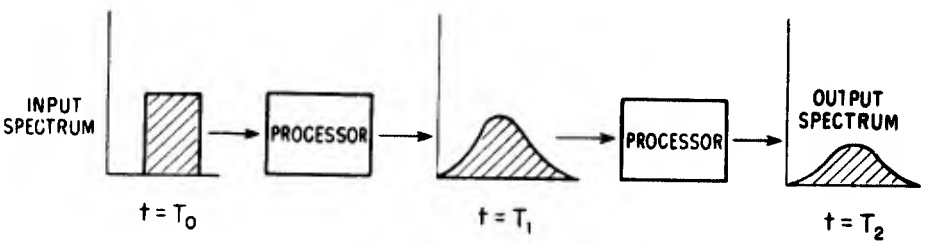


Figure 2 - Prediction as an input-output process for a nonlinear system.

If the input spectrum consists of both information and error and if the processor is linear, the error energy in the output remains as a constant multiple of the signal energy in each frequency or wave-number band. If the processor is nonlinear, which is the case with the physical mechanisms of the atmosphere, the error is exchanged in time throughout the entire spectrum in a manner specified by the transfer function governing the processor. This is essentially the concept which Lorenz has analyzed in his study of predictability.

Ideally speaking, for our purposes, the results of predictability studies should appear in the form of a table which shows the time and wave-number dependence of the systems transfer function. I have constructed an example of the type of table I have in mind.

Table 1. — Wave-number response function for error energy transfer

| Wave Number | 1 | 2 | 3 | 4 | 5 | 6 | 7 | 8 | 9 | 10 | 11 | 12 |
|---|---|---|---|---|---|---|---|---|---|---|---|---|
| 1 hr. | 0 | 0 | 0 | 0 | 0 | 0 | 0 | 0 | 0 | 0 | 0 | 0.50 |
| 5 hr. | 0 | 0 | 0 | 0 | 0 | 0 | 0 | 0.05 | 0.75 | 1.0 | 1.0 | 1.0 |
| 24 hr. | 0 | 0 | 0 | 0 | 0.05 | 0.25 | 1.0 | 1.0 | 1.0 | 1.0 | 1.0 | 1.0 |
| 72 hr. | 0 | 0 | 0.01 | 0.20 | 1.0 | 1.0 | 1.0 | 1.0 | 1.0 | 1.0 | 1.0 | 1.0 |
| 120 hr. | 0 | 0.05 | 0.60 | 1.0 | 1.0 | 1.0 | 1.0 | 1.0 | 1.0 | 1.0 | 1.0 | 1.0 |

The data are obtained from a rather crude "eyeball" interpolation of Lorenz's predictability diagram reproduced in figure 3. With response function and the true spectral distribution of energy in the various atmospheric scales, one could derive the total performance of a "perfect" forecasting system. We shall make use of this information for this purpose in Section 6.

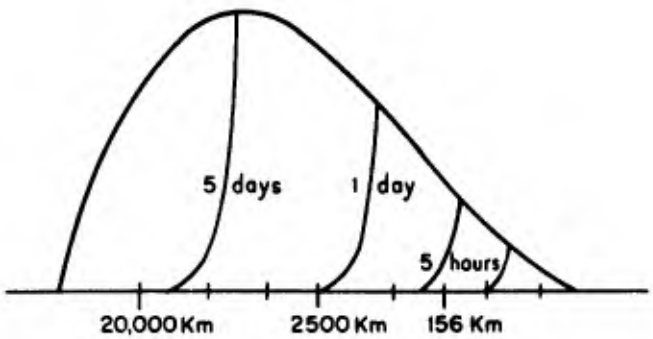


Figure 3 - Error and atmospheric energy spectra for predictions of varying lengths resulting from Lorenz's two-dimensional vorticity model (from Lorenz [1969]).

## 5. CHARACTERISTIC SPACE SCALES AND PREDICTABILITY OF LOCAL WEATHER

In defining predictability limitations for local weather phenomena, forecasters find it quite natural to consider the problem in the light of the Lorenz-Robinson results. For the remainder of this paper, therefore, I shall present data which will provide indications of the scale characteristics of local weather phenomena with attendant implications on predictability. Finally, I shall show data relating present forecasting skill and the scale of the phenomena being predicted.

## Scale Factors for Precipitation

Among the common local weather phenomena, precipitation probably commands the widest interest from most agencies and activities concerned with the weather. We shall consider two aspects of precipitation; precipitation amount or the accumulation of rainfall during a storm period; and precipitation events, the occurrence of precipitation in an amount greater than some threshold valve during a definite period of time. We shall determine the scale and hence something about the predictability of these features of precipitation as a local weather phenomena.

The most definitive studies of precipitation characteristics are those of Huff [5] and his colleagues from the Illinois State Water Survey, where several dense networks of rain gages covering a number of areas in the State of Illinois have been in operation for almost fifteen years.

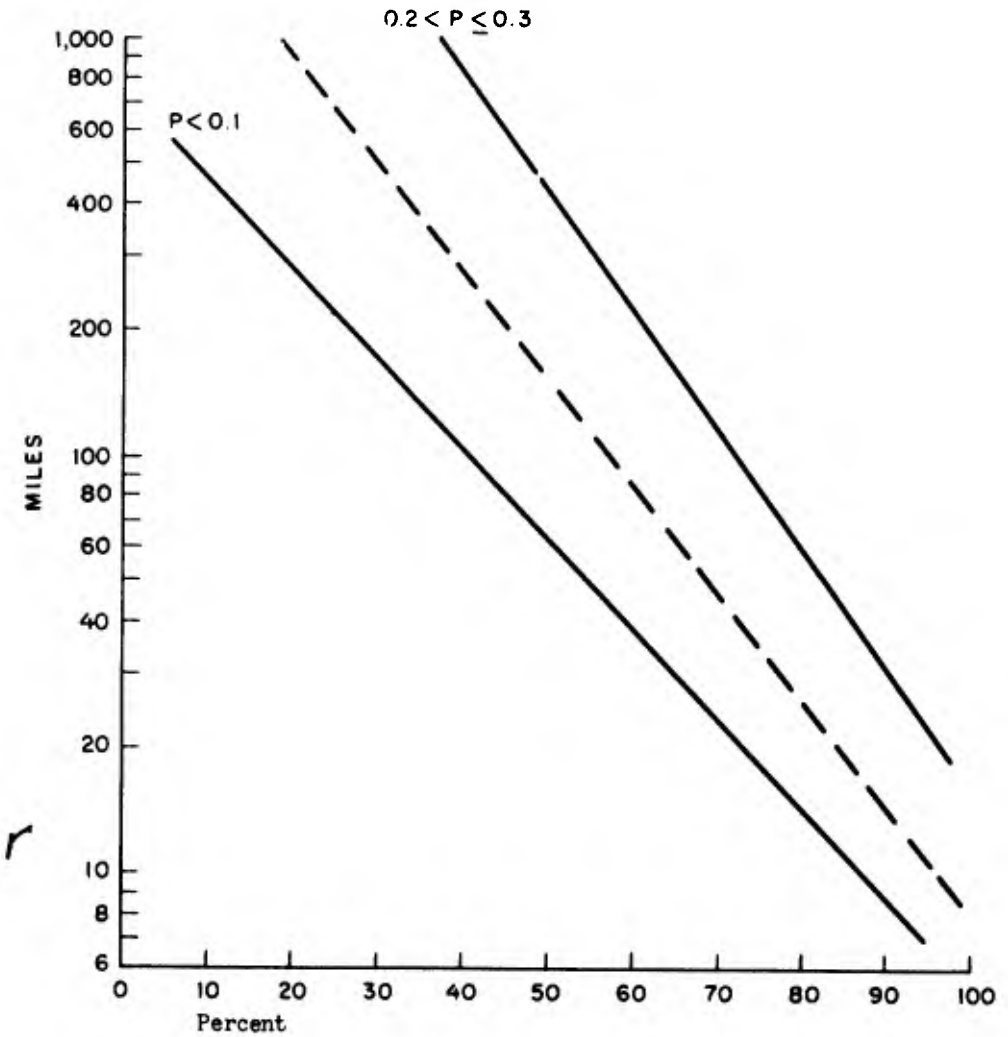


Figure 4 - Distribution function for radius of equivalent circular area for various classes of precipitation events, P less than 0.1 inch, P between 0.21 and 0.30. The dashed line is the average of the two. P is storm total precipitation and r is radius in miles.

An indirect measure of scale characteristics can be obtained from Huff's data giving the conditional areal coverage of precipitation events on the central Illinois networks. From a model which treats precipitation occurrence at points over an area as a random process, I have devel-

oped a relationship [6] between point frequency and a scale factor, r defined as the radius of the circle of area equivalent to that swept out by a precipitation event

$$r = R\left(\frac{f + \sqrt{f}}{1 - f}\right)$$

where R is a constant equal to the radius of the rain-gage network area and f is the conditional relative point frequency of precipitation.

Assuming that the conditional relative point frequency is equal to the conditional areal coverage, I have transformed Huff's data into a scale measure. The results which are the distribution functions for area radii of the precipitation events tabulated by Huff are given in figure 4.

These results show that the "typical" midwestern "storm," defined as precipitation accumulation from outset to ending, ranges in size from an area having a radius of 20 miles at the 10 percentile to one about 1,000 miles at the 90th percentile. The median radius occurs at about 150 miles.

This result can be interpreted to say that about 30 percent of all storms in the midwest have characteristic scales of less than 225 miles, and larger than 1,000 miles. This scale measure, defined as a wave length, is obtained by assuming that the precipitation covers about one-half of the wave length.

When these data are passed through the scale predictability relationship derived by Lorenz, we find that the ultimate predictability of the majority precipitation events (scale $\leq$ 2,000km) is limited to time periods of less than 2 days.

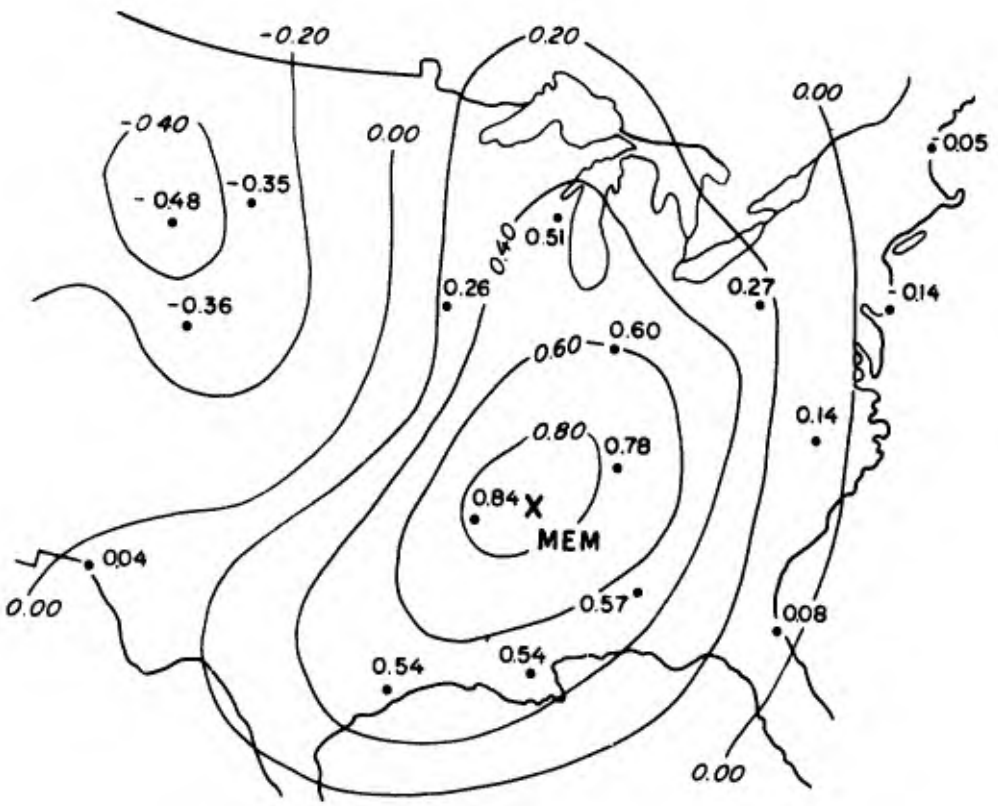


Figure 5 - Correlation function for 24-hour maximum temperature change for Memphis, Tennessee.

I carried out a scale analysis on summertime precipitation events defined as the occurrence of more than 0.09 inch of precipitation in 24 hours in central Kentucky and found that the radius of the average area covered by an event is about 80 miles [6]. Put into a measure which can be applied in Lorenz's analysis this would yield a scale factor of 160 miles. These systems would then have a theoretical upper limit of predictability of 6-9 hours.

The Characteristic Scale of Temperature Change

The second most important element routinely covered in local weather forecasts is the 24-hour temperature change, generally including both maximum and minimum temperatures. To pursue the analysis of the predictability of local weather, I have analyzed the scale of the weather event "24-hour change in maximum temperature." The analysis consisted of computing the spatial correlation function for temperature change. From this, one can obtain the wave length of the predominant scale. The Fourier transform of the space correlation function would be required to establish the spectrum of scale. My analysis is limited to the characteristic scale which is determined by the first zero-crossing of the space correlation function.

The analysis consisted of computing the space correlation function for maximum temperature change for two locations, Memphis and Pittsburgh. The field for Memphis is shown in figure 5. Both fields yielded a characteristic wave length or scale for the transient disturbance controlling the 24 hours maximum temperature change of about 3,500 km. According to Lorenz's analysis, this scale would be predictable up to about 3 days. Let me emphasize again that I have been talking about characteristic sizes. Remember, that the disturbances we are talking about have a distribution of scales, some predictable for much longer and shorter time periods than others. Operational weather forecasting deals with all of the scales and hence forecasting performance is a composite of the skill attained in each scale.

## 6. SCALE ANALYSIS OF THE PERFORMANCE OF OPERATIONAL WEATHER FORECASTS

So far, we have been talking about the limitations on the performance of "perfect" forecasting systems. It would be instructive to compare the relationship between what we are currently able to do and what theory suggests may ultimately be possible. To facilitate this comparison, I have prepared the diagrams in figures 6 and 7. Figure 6 shows the performance of current operational temperature forecasts issued by 50 Weather Bureau forecast offices scattered throughout 48 States. The skill in capturing the variability in particular scales is expressed in terms of the correlations between the predicted temperature difference for two points separated in space and the observed temperature difference for the same two points. Smooth curves fitted by eye have been drawn for the data points representing a wide range of separation distances.

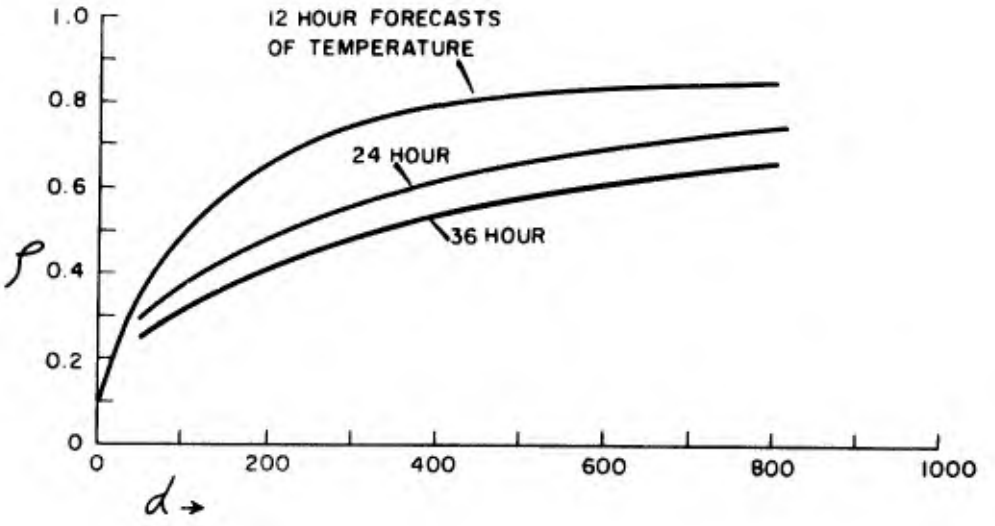


Figure 6 - Correlation between forecast and observed temperature difference for varying separation distances. P is the correlation and d is separation distance in miles. (Curves were filled by eye to some 50 data points.)

These curves depicting the relationship between forecast skill and space scale merely confirm what we have suspected all along; current weather forecasts derive most of their skill in dealing with disturbances in the upper portion of the so-called synoptic scale.

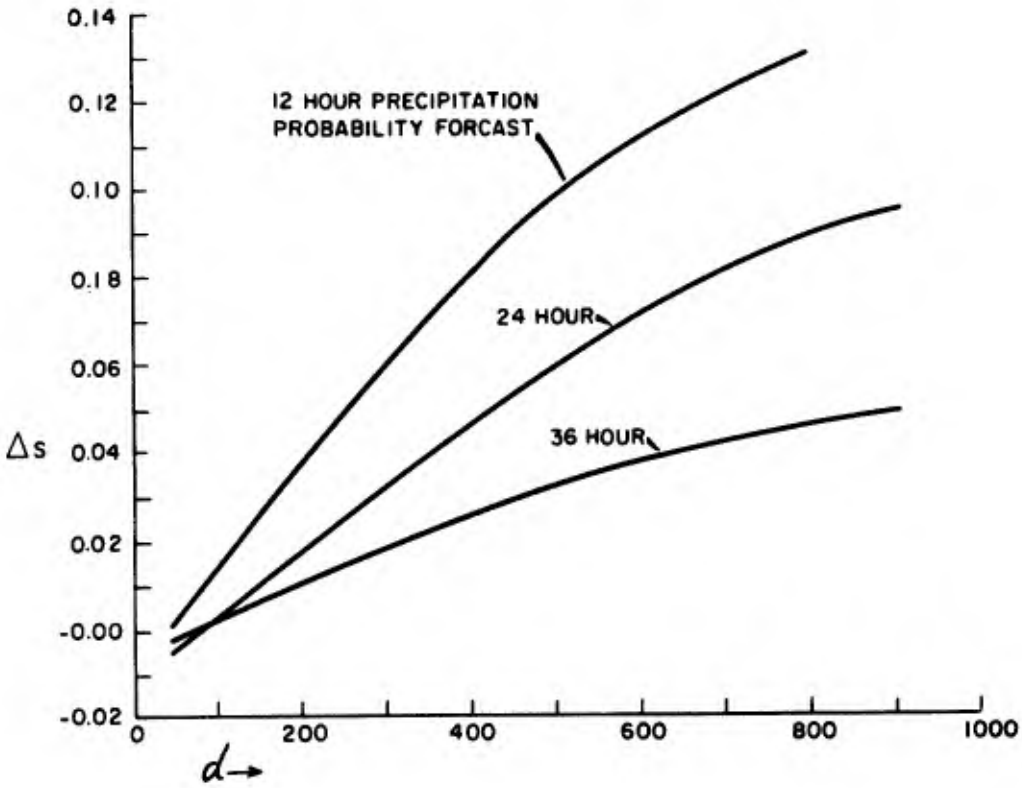


Figure 7 - Difference between the Brier score for a given point and those made by transposing the forecast to another location across a separation distance d. $\Delta S$ is Brier score difference and d is separation distance in miles.

A little different picture is obtained from an analysis of precipitation forecasts shown in figure 7. The scale analysis for precipitation probability prediction shows more skill in the shorter scale than would have been expected by using the results of Lorenz's theoretical analysis. The performance curves are depicting the difference in Brier Score [7] , between forecasts which have skill in discriminating spatial variations in precipitation probability on the scale represented by abscissa and those which have no skill. As was mentioned, these curves show that the difference between skilled and unskilled forecasts is much greater in the smaller scales than might have been expected. The explanation is probably dependent on two facts:

(a) Much of the variability in precipitation probability is found in wave lengths representing the lower portion of the synoptic scale and the sub-synoptic scale. The analysis of the scale of precipitation events has shown this to be the case.

(b) A part of the variability in precipitation probability is forced on the atmosphere from external sources such as terrain features and diurnal variability, to mention two obvious influences.

One of the most interesting comparisons to be made is between present forecasts and the performance of a "perfect" forecasting system. I have made such a comparison by computing the correlation coefficient for the stream function field in Lorenz's model for various prediction periods

from the assumption that the total error in the stream-function field at any time is made up from the energy in those scales which have lost or are in the process of losing predictability.

Figure 8 shows the manner in which the time decay of correlation between forecast and "observed" geopotential in a "perfect" prediction system contrasts with the operational 500-mb geopotential forecasts produced by the National Meteorological Center (NMC). The implication of the comparison are, if valid, rather disturbing since they seem to suggest that the ultimate limit on the predictability of the physical state of the atmosphere may not be too far above what we are presently able to achieve with routine operational numerical forecasting. I must qualify this result by cautioning that the correlations are not strictly comparable since the NMC correlations refer to time changes in the geopotential field.

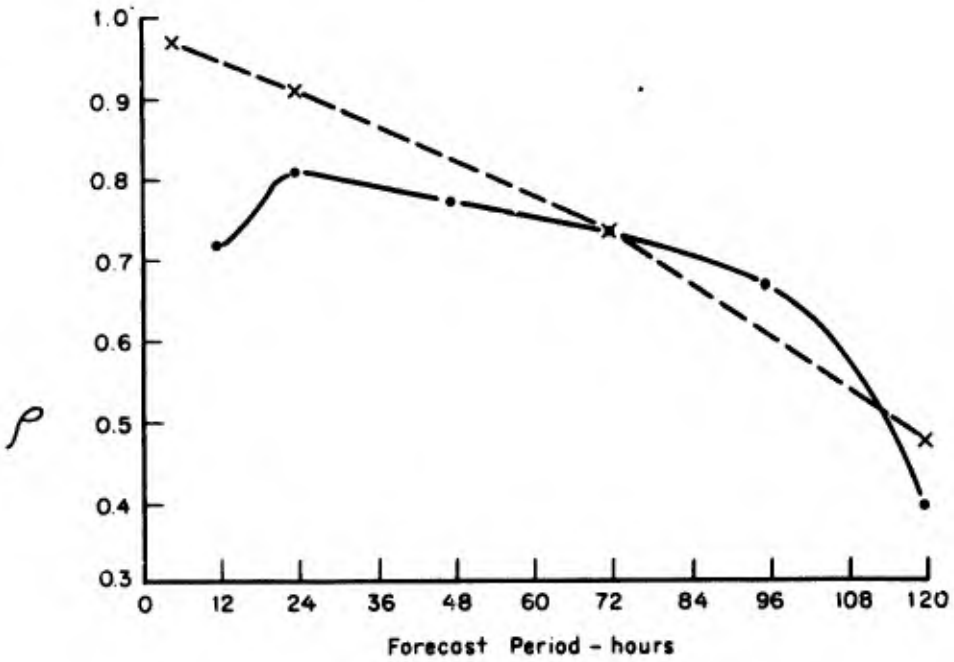


Figure 8 - Correlation between predicted and observed stream function for Lorenz model (dashed line). The solid line is the correlation between predicted and observed geopotential changes at 500 mb for the NMC operational models. (PE to 48 hours, barotropic to 120 hours.)

An interesting feature of the curves in figure 8 is the apparent minimum in correlation for the NMC predictions at 12 hours. This minimum probably arises from a combination of two effects: (1) the diurnal changes in geopotential that are not accounted for in the NMC model and (2) the filtering properties of the time-difference operator which at 12 hours strongly amplifies the very-short-wave disturbances. The general properties of the wave-number response of the time-difference operator are shown in figure 9.

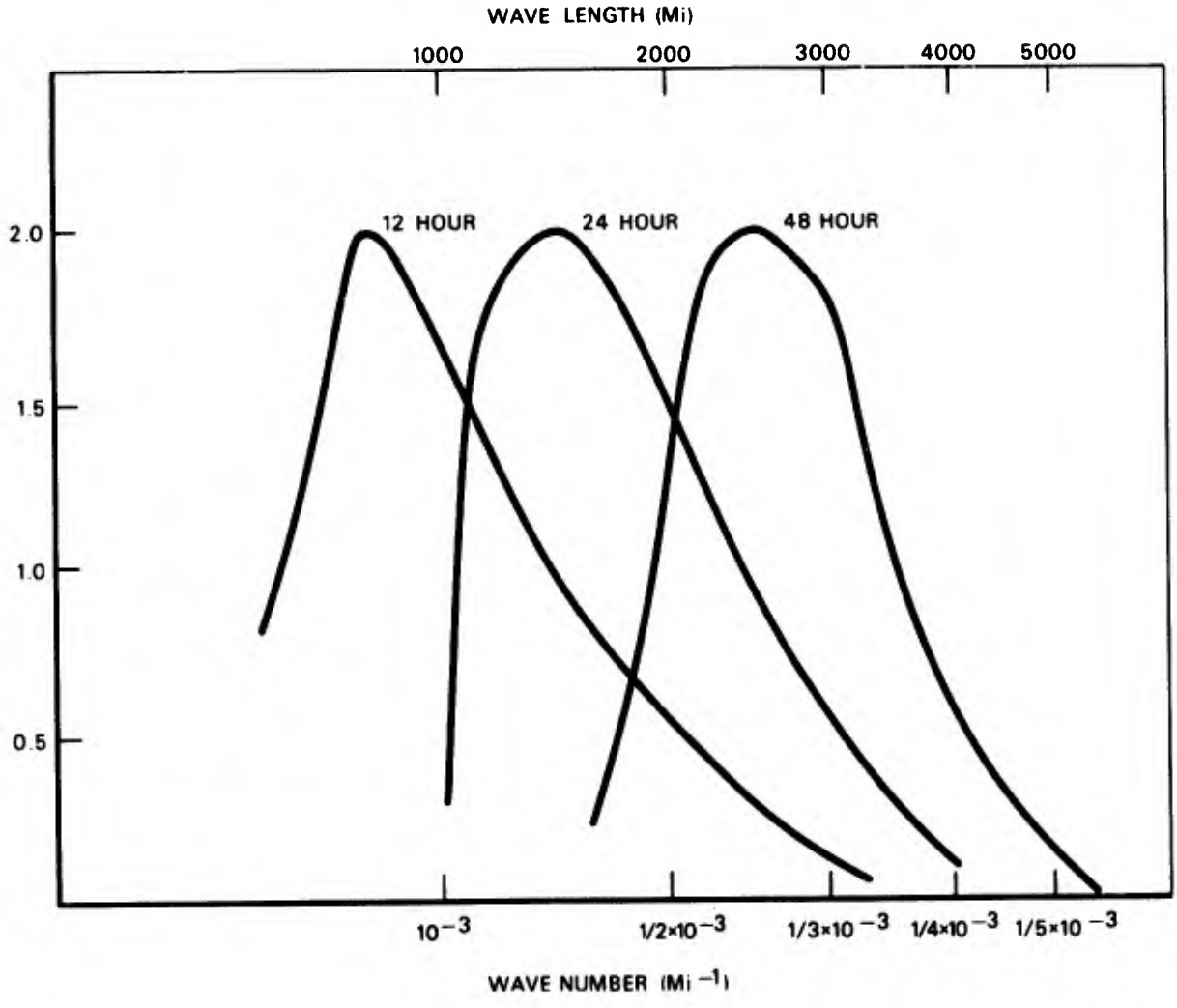


Figure 9 - Frequency response for a time-difference operator applied to traveling, Rossby-type waves.

## 7. SUMMARY, CONCLUSIONS AND SUGGESTIONS FOR FURTHER WORK

We have examined some of the limitations on forecasting accuracy that arise both from the methodology of prediction and the physical laws governing atmospheric behavior.

The analysis has been based on both the theoretical relationships between scale and predictability derived by Lorenz, and the derived information on scale factors for local weather events, including precipitation and temperature change. The predictability consequences of these scale measures which for the common weather events of precipitation and temperature change lie in the lower portion of the synoptic scale, appear to limit completely useful predictions of these events to 2 to 3 days. However, predictions of these events will continue to show some positive skill out to several days in advance, because of the contribution of the very-long-wave disturbances. If these conclusions are valid, they provide rather depressing indications for future major improvements in weather forecasting accuracy, because the present skill in weather forecasting appears to resemble quite closely that which we infer to be theoretically obtainable.

Perhaps, the most useful result of these conclusions is to acquaint researchers with the urgent need to validate or modify the Lorenz analysis with a more complete and correct model of atmospheric behavior. At the same time, it would seem to be worthwhile to undertake studies which would provide good data on the economic utility of weather information. Sooner or later, we shall be faced with some tough economic decisions regarding the potential payoff of a more expensive world meteroological network. We ought to be prepared to provide decision makers on the national level with guidance on where it is best to invest our scientific and technical resources to improve weather services of our nation and those of the other nations of the world.

## REFERENCES


1. Charney, J. A. 1969. "Predictability."In:National Academy of Sciences Plan for U.S. Participation in GARP.

2. Robinson, G. D. 1968. "A Seminar on Predictability." Office of Met. Ops. Colloquium, Weather Bureau.

3. Robinson, G. D. 1967. "Some Current Projects for Global Meteorological Observations and Experience." Quarterly Journal of the Royal Met. Society. October 1967.

4. Lorenz, E. N. 1969. "The Predictability of a Flow Which Possess Many Scales of Motion." Tellus, 1969.

5. Huff, F. A. and P. T. Schickedanz. 1970. "Rainfall Evaluation Studies." Final Report NSF GA-1360. Illinois State Water Survey. Urbana, Illinois.

6. Roberts, C. F. 1970. "The Derivation of a Scale Measure for Precipitation Events." Unpublished manuscript.

7. Brier, G. 1950. "A Skill Score for the Evaluation of Probability Forecasts." Monthly Weather Review, 1950.

# OBJECTIVE MESO-SCALE ANALYSIS OF UPPER-AIR WINDS IN SEASIA

Marvin J. Lowenthal

Atmospheric Sciences Laboratory
US Army Electronics Command
Fort Monmouth, New Jersey

Abstract

Using data from artillery meteorological sections in Vietnam, an objective analysis program has been developed that permits observational wind data to be converted into a fine-mesh mesoscale grid with a spacing of 1/4 degree (about 15 miles).

Wind analyses are made at 6-hour intervals for mean layer winds using the normal artillery zone structure. If observations for a station are missing, a linear or quadratic interpolation is made. The wind vector field and isotachs are presented on a cathode-ray tube which is photographed to obtain a permanent record.

Films have been made to show typical wind analyses for a weekly period during the summer and winter monsoon. The films demonstrate the internal consistancy of the data as well as the diurnal variations of winds.

## 1. INTRODUCTION

At the last session of the Technical Exchange Conference in Colorado Springs, attention was drawn to the vast amount of upper data that was being taken by U. S. Army Artillery Metro Sections in South Vietnam. It was pointed out that here was the only truly functional meso-scale radiosonde network that operated daily throughout the year. Soundings are normally taken four times a day, in some cases as often as six daily, as the operations require.

In the beginning the data were discarded after the ballistic applications were completed, but for the past four years the data have been preserved and eventually find their way to ETAC. But in these days of economic belt tightening, the monumental task of reducing all the data to punched cards was impossible. Our laboratory did manage to have the data for 1967, 1968, and part of 1969, placed on punched cards by the National Weather Records Center, Asheville, North Carolina, and the data are available for research purposes.

## 2. DISCUSSION

The primary purpose of the soundings is the correction of Artillery Fire for Non-Standard Atmospheric Conditions that exist at the battery. Where units are stationed some distance from the Metro Section, the application of the received metro message may cause significant errors due to the spatial variation of the atmospheric parameters – especially winds.

Stanford Research Institute has been involved in developing objective analysis techniques for the Tropics for our laboratory for some time. Objective techniques are necessary to eliminate the need for a trained meteorologist skilled in tropical analysis, and to ensure uniformity of analysis at all times. In addition to being applicable in the Tropics, we specified that the grid size must be small enough for Army usage, no greater than 30 km.

The computer program that evolved can either produce winds at given locations or as vectors centered on grid points which are spaced at 1/4 degree intervals.

An example is shown below on the first slide.

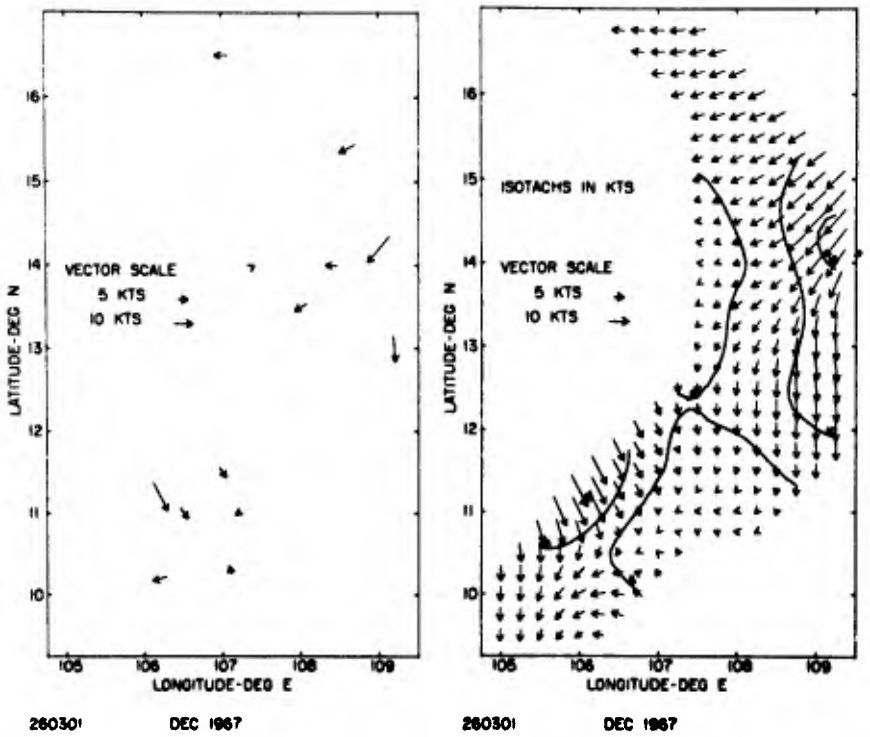


On the left we see the observed winds for Dec. 26, 1967, from artillery metro soundings between 1200 and 1800 Local Time. These represent the mean winds for the lowest artillery zone — surface to 200 meters above the ground as determined from Rawin Set AN/GMD-1(A)'s. For easy reference, these winds may be considered as occurring at the mid-point of the zone —i. e., 100 meters above the ground. It is noted that the station density is highest in the south around Saigon (10. 5°N - 106. 5°E) and more sparse elsewhere. Nevertheless the coverage in both time and space is unusually complete when compared with data in the United States. For example, the State of California, roughly similar in size and shape to South Vietnam, has but three radiosondes with data only every 12 hours.

On the right of the slide we see the objective analysis at grid-point intervals of 1/4 degree. This analysis fits the data very well, with some smoothing evident where the data are very densely spaced.

The analyses are made by a computer that determines the wind values at the five nearest stations, weighting the observed values inversely as their distance from the grid point. The

program automatically generates the vector and isoline displays on a cathode-ray tube, which is subsequently photographed to produce a permanent hard copy.

In the film that follows, wind analyses for the period 23-31 December 1967 will be shown for the various artillery levels from 100 meters above the surface to 7000 meters above ground. They represent the mean winds in layers of varying thickness, starting with 200 meters near the ground, then 500 meters up to 2000 meters elevation, then 1000 meters up to 6000 meters, finally 2000 meters thick thereafter.

The film shows conditions typical of the winter season — the so-called northeast monsoon time. It is not possible to comment on all the mesoscale features that appear on the maps as the film progresses. However, some highlights and background are provided to provide focal points for observing the wind flow. It will be noted that streamlining the maps becomes relatively simple, and a tropical meteorologist would have an easy time drawing lines of convergence, divergence, neutral points, etc. A few of these will be pointed out in the course of the film.

Before showing the film, it would be wise to review the topography of South Vietnam since the terrain has such an important influence on the wind flow at lower levels. The second slide shows the main terrain features.

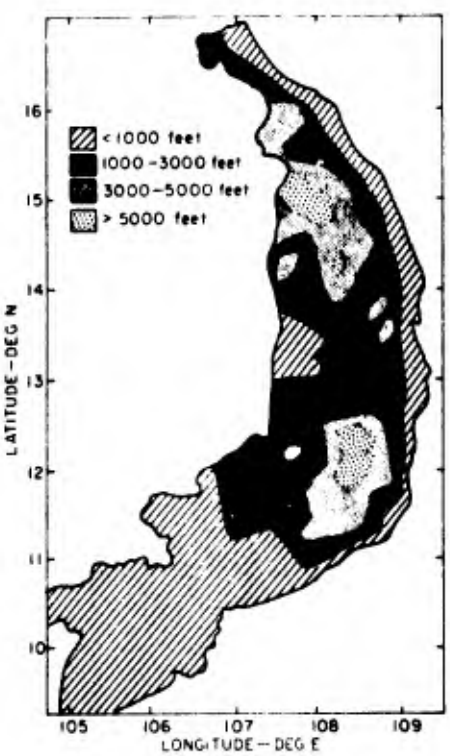


Low lands exist along the coast and in the Delta regions (South of 11°N). Elevation increases westwards from the coast to the Annamite Highlands that roughly parallel the coastline with maximum elevations above 6000 feet. The highlands are not continuous; there is a gap between 12.5°N and 14°N (approximately) where elevations are 3000 feet or less. Moist low-level northeast winds impinging on the exposed northeasterly coast are constrained to flow east of the mountains until they reach the break. They can then pour westwards and southward into the Mekong Lowlands. Example of this flow will be evident on the film.

## 3. COMMENTARY ACCOMPANYING FILM

### Comments on Zone 1 (0-200 meters above the ground)

23 December 1967

As series opens there has been a good surge of polar air from Siberia that has pushed down the Indochina region. The surface analysis of Professor Scherhag shows a cold front terminating off shore in the South China Sea near 12°N latitude. Our first map would seem to indicate the trough, if not the front, probably extends across South Vietnam near 11°N. Winds to the north are the normal outflow from the high. The gap in the highlands between 13° and 14°N allows low level northeasterly winds to penetrate the western portion of South Vietnam. Generally, the flow parallels the mountains, then circles out anti-cyclonically westwards as the highlands end near 11°N. The two air flows – northerly thru the gap and southerly from the Delta region, tend to converge in the southwesterly portion of our map. The convergence line will be evident on many of the low-level maps. On occasions small meso systems or neutral points in the streamlines can be drawn. Strong deep northerly flows that penetrate the entire country destroy these circulations, as will be seen on the maps.

24 December

By the 24th the trough has continued south to clear the peninsula as northerly winds appear throughout. By the end of the day, in the extreme south, winds veer to west, become very light and variable on the 25th, eventually becoming southeasterly. The high has become more shallow and winds to the west of the mountains are much lighter than the on-shore winds.

The high center is retreating northwards. Late on the 25th the convergent zone appears as the return flow of south to southwest winds over the Delta meets the northeasterly or direct flow west of the mountains. As the southerly flow increases, the position of the convergent line moves west or north, depending on whether the northerly winds remain moderate or become light. By the 26th, the original surge is gone. In the northern part, light winds become easterly. The strongest winds are on the east coast 13-15°N due to a westward extension of a Pacific high with circulation down to 10°N by late afternoon. This new surge of northeasterlies on the 26th briefly destroys the convergence zone, but when the stronger winds funnelling thru the gap in the mountains recurve to become northwesterly at 11°N-12°N, 105°E-107°E, the zone is restored.

A similar situation occurs on the 28th. Strengthening southeasterlies near 10°N force the zone westwards until it moves off the map early on the 29th. A neutral point and a meso-low are just on the SW edge of the map.

A new Siberian high has begun to move southwards. By the morning of the 29th the winds north of 16° have all shifted to N or NW from their previous SE. By the end of the day, winds have backed as far south as 13°, but not until the 31st do the northerlies push down to 10°N. Again a meso system is apparent in the SW. Note again, how the air on the 29th pours thru the gap in the mountains between 13° and 14°N with velocity maxima due to the funnelling action.

### Zone 2 (200 - 500 m above the ground)

These maps are essentially the same as Zone 1 and exhibit the same overall patterns. It will be noted, however, that the convergent zone in the SW is more sharply defined, and small scale circulations in area between 10°N-12°N, 106°E-107°E abound.

The convergent zone is most noticeable on the 24th and 25th, a small closed circulation on the 25th and 26th.

Zone 3 (500 m - 1 km)

The patterns are somewhat simpler here with northeast winds to 11°N then light variable winds. When the winds in the extreme south turn and become westerly on the 24th, and the familiar convergence pattern appears that lasts until the 26th, when the new northeasterly surge again simplifies the pattern. By the morning of the 30th, northeasterlies cover the whole area 12 hours earlier than at the lower levels. Likewise, they persist for a shorter time retreating northwards by the 31st.

Zone 4 (1 - 1.5 km)

Smoother, larger-scale flow patterns are more noticeable here with generally coherent circulations even with very light winds. Few convergent zones or meso systems appear. Northereasterlies cover the entire map on the 29th from the polar air mass — 12 hours earlier than at the next lower level.

Zone 5 (1.5 - 2 km) near 850 mb

The 850-mb map of Prof. Scherhag for this period shows a high in the Pacific extending across Indochina to the Indian Ocean. This accounts for the northeasterly winds that prevail from the 23rd to the 25th. The eastward retreat of the limb of the high to the coast of Vietnam on the 25th causes the diminishing of the wind velocities and the shift to southeast in the north. A col area is established with a small high circulation near 15°N, 107.5°E that rapidly moves southwards and westwards off the map in 24 hours, leaving indifferent general circulation over Vietnam. Early on the 27th circulation with the winds spirally anti-cyclonically appears on the early map but disappears six hours later as northeasterly flow is established on the east coast.

The 850-mb 0000Z map of the 28th shows a cold front reaching the east coast near 14°N, and the corresponding wind map does indicate a shear line there that can be picked up near 13.5°N six hours later before disappearing in the generally lightening northeasterly flow.

A strengthening of the Pacific High again causes predominantly northeasterlies over the whole region on the 29th, with conditions rather similar to those at the beginning of our study period.

Zone 6 (2 - 3 km)

The beginning of the series Dec. 23-26 show, as before, the influx of northeasterly winds from the Pacific, the circulation around the westerly limb of the high, then the development of a high to the west that predominates thru the 28th, until displaced by the new Pacific circulation on the 29th. By the end of the period a new high has formed to the west, with strong circulation around it.

Zone 7 (3 - 4 km)

A predominance of large scale circulations — around a high to the west on Dec. 23rd and 24th; around the Pacific high Dec. 25th to the 27th, followed by reestablishment of the circulation around a new high to the west for the remainder of the period (Dec. 28 - 31). The first indication of the change is the formation of a meso high in the south that moves rapidly westwards.

Zone 8 (4 - 5 km)

Zone 8 circulations are similar to those of Zone 7, allowing for the slope of the axis of the Pacific high to the south. The circulation around the high in the west is much stronger than in Zone 7. The change occurs about 18 hours earlier than in Zone 7. The meso high formation prior to the change is similar to that observed in Zone 7.

Zone 9 (5-6 km) and 10 (6-8 km)

These zones emphasize the two circulations of the immediately lower levels with transitions from the flow around a high to the east to that around a high to the west taking place in 6-12 hours. The pattern in the closing days of the period is most pronounced at these levels.

The preceding film, while displaying the wind field at discrete time periods of six hours, was not in any sense an animated film. To animate the wind flow requires a presentation of winds at many intermediate times. If we interpolate between the observed winds and present the patterns at 10 or 15 intervals, the animation process becomes possible. In the very short film that follows, such a procedure has been followed.

The winds at the 1000-meter level have been used to show the wind patterns for a seven-month sequence — July 1967 to January 1968 — at an extremely rapid speed. Two three-day sequences, 24-26 September 1967 and 8-11 November 1967 are also recorded.

# THE DEVELOPMENT OF AUTOMATED SHORT-RANGE TERMINAL FORECASTING USING ANALOG TECHNIQUES

Carl D. Thormeyer, Lieutenant, U. S. Navy

Fleet Numerical Weather Central
Monterey, California

## Abstract

An analog approach to automated short-range terminal forecasts is being developed at Fleet Numerical Weather Central. The selection model will take current meteorological analyses and prognoses (employing the FNWC primitive equation model) of 500-mb, 1000-mb, and 500-1000 mb thickness fields, comparing them with historical weather sequences over an optimum-sized area about 20 degrees latitude by 30 degrees longitude. Hourlies from the station in question which are associated with the one best analogous weather pattern can then be issued as a terminal forecast. Tests of a modified version of this approach show considerable promise, with unexpected initial skill.

## I. INTRODUCTION

The phenomenal increase in aviation activity over the last 25 years has had at least two effects on the forecasting of aviation terminal weather. First, it has generated a requirement for increasingly accurate aviation terminal forecasts. Secondly, the scope and volume of such forecasts have increased to the point where some degree of automation would considerably lessen the workload.

Provision of a detailed aviation terminal forecast which shows consistent accuracy regardless of weather conditions has often been one of the more frustrating problems encountered by the experienced meteorologist. As a result of this and the increasing workload involved, some degree of automation in terminal forecasting has been necessary for some time; and becomes increasingly necessary as time goes on. Nonetheless, attempts at automating terminal forecasts have shown little or no success during the past 10 years, with little additional success anticipated over the next five years [1].

Military installations are particularly affected by the terminal forecast problem, as associated weather detachments often must depend on guidance from terminal forecasts provided by the U. S. Weather Bureau for nearby civilian terminals. Such guidance may or may not be applicable for these military installations at any given time, depending on local topography and on effects of mesoscale weather phenomena.

Many military installations rely heavily on local forecasting aids, which usually are essentially a compilation of climatological data at that station assembled into probability statistics; these statistics are then often translated into words and related to synoptic events. Such forecasting aids serve to put in writing the "human memory" aspect of an experienced forecaster; e.g., statements like "it usually rains when the wind is from the southeast." Due to frequent turnover of personnel, this kind of compilation of information is vital for the weather detachment at a military installation.

Since information from station forecasting aids (even when supplemented by aviation forecasts provided by the Weather Bureau for civilian terminals) is not fully sufficient for weather forecasts for nearby military installations, an additional and more comprehensive approach is desirable. Further, automated terminal forecasts, despite recent advances in the fields of dynamics and statistics, have in general not yet become reality in routine operations. Therefore, Fleet Numerical Weather Central (FNWC) is now developing an automated terminal forecast program, using an analog approach. The technique is based on a modification of the FNWC hemispheric analog selection model described by Wolff and Thormeyer [2], and on initial concepts described by Wolff and Woodworth [3]. This new technique, the first prototype of which should have initial operational applications in the autumn of 1970, is formulated on the selection of regional analogs. This is accomplished by matching current analyses and primitive equation model prognoses with historical synoptic patterns. The computer can thus recall the historical weather patterns most similar to those of today, and subsequently output corresponding historical hourlies as a terminal forecast. In doing so, the computer acts as the "memory" of an experienced forecaster, but with the advantage of having complete total recall at all times; and as such surpasses forecasting aids in this regard.

At best, this analog technique (once fully developed) will solve the problem of automated terminal forecasts. At worst, it will be a valuable added forecast tool; giving a degree of "experience" to the forecaster that he might not otherwise have. This endeavor is part of the overall Naval Weather Service goal of eventually attaining as highly an automated forecast system for naval operations as is possible.

## II. MODEL APPROACH

### A. Justification

A forecaster who is experienced in the weather types affecting a given station can often remember some past weather situations which are similar to the one currently occurring, and hence can consider these analogous situations when formulating his forecast. A large high-speed digital computer (such as the CDC 6500 at FNWC) can simulate this human element to a much greater degree, finding analogous weather patterns with considerably increased accuracy. Specifically, given a data base sufficiently long enough to account for most known possible cyclic effects (at least 22 years), one can find in the history analogous weather patterns over any regional area of the globe which closely resemble current patterns. Unlike hemispheric analogs, these historical patterns have consistently shown higher numerical correlations with current weather than has 24-hour persistence. Further, at least one of these local-area analogs can be expected to closely resemble current patterns throughout at least a 24-hour period in all but the most extreme cases. This matching ability thus justifies the computer extraction of the associated historical hourly weather, issuing it as a 24-to-48-hour terminal forecast.

### B. Background

A 24-year data bank (1946-1969) of key hemispheric analyses, as well as complete historical aviation hourly files at 15 Naval installations for the same time period, is now available in the FNWC archives as part of the development of an automated climatology service. This development has been described elsewhere [2, 3, 4].

Initial tests had indicated that unlike the hemispheric analog (which must normally go out beyond three days before surpassing persistence in skill), a regional area analog routinely correlates at a higher value with current data than does 24-hour persistence. This is true, regardless of the degree of uniqueness of the current synoptic pattern; providing the size of the regional area to be correlated is optimum. In other words, a forecast of hourly weather using this technique, regardless of skill, should be superior to using yesterday's weather to forecast that of today (i.e., persistence).

The problem then becomes one of developing a model which will achieve the desired skill in the most efficient manner. Although the final goal is total automation, the initial prototype will require some manual quality control.

## C. The Basic Screen

The short-range forecast model under development at FNWC employs a selective screening technique similar to the one used for hemispheric analog selection [2], but covers a regional area only. The model searches 24 years of historical analyses within ±45 days of the current date, correlating over an area approximately 20 degrees latitude by 30 degrees longitude. On the initial screen, both 500-mb and 1000-mb total disturbance fields (analyses with a common zonal component removed) are searched and correlated; an average of the two correlation values taken, and the lowest 99 percent eliminated. Thus, approximately 40 dates remain as analog candidates at the conclusion of this first screen. The second pass screens out 50 percent of the remaining candidates (leaving 20 dates), using the 500-1000 mb thickness analysis (zonal component removed). This screening process is then repeated, correlating 24-hour primitive equation model prognoses of current data with the remaining analog dates plus 24 hours. Each pass again eliminates 50 percent of the remaining candidates, leaving five final possibilities. At this point, until a total automation can be attained, qualified meteorologists could select the one best analog for each regional area involved; once historical charts and associated hourly weather have been examined in light of current trends. Once this step has been automated (plans are described in Section IV.B), a second computer program will search the historical file for the appropriate hourlies, outputting them as terminal forecasts.

While several variations of this screen have been tested, the model as described above has been the most efficient and accurate approach so far; given the volume of data involved and computer hardware/software considerations. This model is diagrammed in Figure 1.

## D. Model Considerations

In developing the above model, there have been four special considerations. These are as follows: determining the most efficient screen while encompassing all necessary meteorology; determining the optimum area size for each regional analog; eliminating outside influences on the optimum area selected; and determining the seasonal zone of the historical data base which must be searched.

### 1. Meteorologically-Efficient Screening

The first model consideration, that of a meteorologically-sound yet efficient screen, is dictated by the accuracy desired and the "real-time" that is available to produce this accuracy. If specific weather occurrences (wind, rain, fog, thunder, etc.) are to be accurately forecasted for a station, then the associated synoptic patterns in the region surrounding that station must be matched as exactly as possible; both for upper air (500 mb) and surface (1000 mb). Further, if temperature forecasts are to be reasonable, and a delineation of rain vs. snow is to be made in borderline situations, then the matching of thermal patterns is also important.

Due to the limited time available for searching 24 years of data for matching patterns (with the present FNWC schedule and priorities, it is six-to-seven hours after analysis time before all current analyses and prognoses are ready for historical searching), the model must be a high-speed one. Although both large- and small-scale patterns are important in this matching, "real-time" considerations do not allow searching of these ranges of scale separately. However, the entire pattern can be effectively matched when all ranges of scale are considered at once. Thus, the synoptic patterns and associated thermal structure over a properly-sized region can be most efficiently described at any given time by the 500-mb, 1000-mb, and 500-1000 mb thickness values within that region. Removing a common zonal component from these

parameters prior to correlation (the same zonal value is removed from each chart) further enhances the delineation of the patterns, allowing a more "normalized" distribution of correlation values; with possible range from -1.00 to +1.00.

It would not be necessary to describe the thickness parameter if the matches at 500 mb and 1000 mb could approach perfection. Since this is rarely the case, however, thickness becomes a good eliminator when "zeroing in" on a given weather pattern. While it might be desirable to correlate at other levels or on other variables, the length of the data base involved is generally only five to nine years. Further, operational considerations preclude such additional searching, even if data were available for a sufficient period of record.

Since it cannot be said at the outset whether synoptic patterns at 500 mb or 1000 mb (or both) are most important in describing local weather, both must be equally considered in the model. Therefore, once zonal influences have been removed, the correlations at 500 mb and 1000 mb are averaged. The screen then eliminates all but a predetermined number of the highest averages; the idea being that it is most important to match the existing pressure-height weather pattern on the initial screen before going on to thickness.

As stated earlier, regional matches of synoptic patterns rarely approach perfection; yet this is desirable if an accurate terminal forecast is to be made. In determining the percentage of dates that can be eliminated on the first screen, tests have shown that needed accuracy normally occurs only in the top one percent of the historical data. Thus, 99 percent of the historical weather patterns can be eliminated on the first pass through the screen. Other testing has shown that a 50 percent cut on further passes through the screen is the most efficient, while being least likely to eliminate good analogs or allow bad analogs to survive.

2. Optimum Area Size

The second model consideration, that of determining the optimum area size for the region affecting each station, is largely dictated by the degree of skill desired. The area size must be large enough to adequately portray the synoptic weather patterns currently affecting (or expected to be affecting within 24 hours of analysis time) the station for which the forecast is being made. It further must be large enough to minimize influences outside of the area correlated. On the other hand, the size of the area chosen must not be so large as to miss the pattern details and exact locations of these synoptic systems. It must not be so large that correlation with 24-hour-old persistence would produce values routinely exceeding that of the best analog candidates, if one expects to attain forecast skill superior to using yesterday's weather for today's forecast. Although hemispheric analogs are normally inferior to persistence out to three days, this inferiority diminishes as progressively smaller portions of the hemisphere are correlated. At some point, there is an optimum area size which will routinely produce analog candidates having correlation values superior to 24-hour persistence. This optimum size, however, is not normally small enough to depict small-scale or rapidly-moving features with sufficient accuracy. Thus, the optimum area size ultimately selected must be small enough to account for this requirement, if associated analogous weather is to be skillful as a terminal forecast. This area must not be so small, however, that a synoptic system cannot be adequately represented by the FNWC grid spacing (grid points are 200 nm apart at 60°N). The dilemma in these optimum-area-size criteria is then as follows — the larger the area, the less the explained variance; the smaller the area, the more difficult it is to adequately depict the principal influencing synoptic patterns.

It is desirous to choose an optimum area size using the above criteria in which correlations of 0.90 or greater (on a scale from -1.00 to +1.00) can be routinely attained on all parameters correlated, once zonal components have been removed. Such a value would account for at least 80 percent of the variance, and would adequately represent large-and-small-scale synoptic patterns in the area of question. Regretfully, attainment of this correlation value cannot always be realized if the other criteria set forth above are to be met. A correlation of 0.90 would

be more easily attainable if historical and current charts were, say, one hour apart rather than 12 or 24 hours. Since this is not the case, nor is it likely to be the case in the foreseeable future, a more realistic correlation range of 0.80 to 0.90 is sought in the model. Such values are routinely superior to 24-hour persistence, while normally being high enough to adequately describe the details of the synoptic patterns being correlated. In the more common and/or quasi-stationary weather situations, the best analogs attain correlation values of 0.95 routinely; while in more unique or rapidly changing situations, correlation values of the best analogs may be as low as 0.70. In either event, these extreme values still exceed those of their respective 24-hour persistences. This sometimes rapid fluctuation in correlation values explains why, when screening, it is important to ascertain the best analogs by saving a percentage of those correlating highest, rather than attempting to save all those above a certain value.

The optimum area size which at present seems to meet most closely all of the above criteria has been found to be approximately 20 degrees latitude by 30 degrees longitude in temperate zones; or about 50 - 55 FNWC gridpoints. Two such areas selected for initial testing are shown in Figure 2.

3. Eliminating Outside Influences

It is intuitively obvious that outside influences could destroy an initially good regional analog match within 24 hours. Further, the smaller the region correlated, the more likely this is to occur. Therefore, the third major model consideration is the elimination of these outside influences, once an optimum area size has been ascertained. This problem can be minimized by selecting a large enough area; as discussed above. However, increasing the area size allows increased erosion of weather patterns by small-scale features within the area itself; i.e., patterns which become less adequately depicted as the area size increases. Hence, the required accuracy becomes more difficult to realize. There are two possible approaches in avoiding this dilemma: a less-strict initial screen can be made over a larger area using large-scale parameters, or dynamic models may be brought into play. Testing and experience have dictated that the latter approach is the more satisfactory solution.

Initial experimentation on the elimination of historical dates for regional analogs not reasonably matching in the hemispheric large-scale failed for three reasons: (1) the increased running time and loss of model efficiency was unsatisfactory; (2) the best regional analogs seldom correlated well in the large-scale at hemispheric level, thus good local area analogs were prematurely eliminated; and (3) even the best hemispheric large-scale correlations explain only 50-65 percent of the variance (which is inferior to 24-hour persistence), thus they too are open to outside influences.

Therefore, it was decided that the best attributes of both analog and dynamic approaches to forecasting should be combined into a single model which could most accurately select local area analogs for use in automated terminal forecasting. As such, the FNWC Primitive Equation (PE) dynamic forecast model initially described by Kesel [5], and later by Kesel and Winninghoff [6] is being incorporated into the FNWC local-area analog selection scheme. Under this arrangement, not only must the best analog candidates correlate highly with the current weather pattern in the optimum area; these surviving analog candidates plus one day must also correlate highly with the predicted weather pattern as depicted on the 24-hour PE prognoses. For example, if 12Z 03 Jan 1956 correlates highly with 12Z 15 January 1970, then 12Z 04 Jan 1956 must also correlate well with the 24-hour PE progs verifying at 12Z 16 Jan 1970; if the hourlies from that date in 1956 are to be considered as a 1970 forecast.

4. Seasonal Searching

The fourth model consideration, that of determining the seasonal zone of the historical data base which must be searched, is dictated by the extent of seasonal weather variations at the stations being considered. For example, while bitter cold in the Northeast U. S. normally

occurs only between about 15 Dec and 20 Feb, a heavy wet snowstorm might occur any time from mid-November to early-April. A search of ±30 days is not adequate in the latter instance; however, a search of ±45 days has so far been found sufficient in all but the most extreme situations.

E. Model Limitations

Aside from the limitations implied in the discussion of model considerations above, there are two additional inherent limitations: excessive lag time, and the possibility of up to 12 hours of phase error in the pattern match and hence hourly weather.

1. Excessive Lag Time

This limitation results from the fact that, due to current FNWC schedules and priorities, it is nearly ten hours after observation time by the time the raw data can be gathered, the analysis performed, the primitive equation model and subsequent local-area analog selection model run to completion; and formal selection of the best historical weather sequence for issuance as a terminal forecast. Hence, the 24-hour analog search period is nearly half gone by the time the forecast can be received.

2. Phase Errors in Time and Space

This second limitation results from the fact that historical maps are separated by 12 or 24 hours, making possible up to a 12-hour phase-error in synoptic patterns and hence associated weather. This would be avoidable only if historical data were available on an hourly basis, and it were possible to run the model hourly using 12 to 24 times as much data and time. This is of course unattainable with current resources and equipment. Although historical charts only 12 hours apart will allow a maximum phase error of but six hours, any phase error is complicated by diurnal effects. For instance, 12Z current data which correlates best with a 00Z historical chart fails to account for such diurnal effects as air-mass thunderstorms, ground fog, and temperature variations. Thus, the user may have to adjust the phasing of the predicted weather forward or backward up to 12 hours in time; depending on the current local weather sequence as compared to the automated terminal forecast which has been issued.

## III. TEST CASES

Several test dates are currently being examined, with the intent to simulate automated terminal forecasts for several geographically-close NEDN stations using the same analogous weather sequence. Specifically, the two optimum areas shown in Figure 2 were considered initially; with Alameda, California and Washington, D. C. (Andrews Air Force Base) as the specific terminals. Through this testing, the present approaches to the previously discussed model considerations emerged as described above. For testing purposes, however, the actual final current analyses were used in the selection model, rather than the 24-hour progs from the initial time.

Although other test data is available, results from but one representative test date (12Z 09 February 1970) are presented below. This date involves a moderately difficult terminal forecasting situation at both stations. The conclusions to be drawn from these results, and the degrees of skill shown in them, are typical

A. Washington, D. C. - 12Z 09 February 1970

The Washington case involved a fast-moving developing storm in the Middle Atlantic States which subsequently moved out to sea. Development at 500 mb was still occurring during the period. The storm spread rain, drizzle and fog across the Washington area; while dropping heavy wet snow in Central Pennsylvania. The forecast problem then was one of precipitation

type and associated temperature, and restrictions to vision with associated visibilities. This "current" period (12Z 09 February 1970 to 12Z 10 February 1970) best matched with the 24-hour historical period starting at 00Z 14 January 1968, and ending at 00Z 15 January 1968. Correlation values of the various parameters within this match ranged from 0.80 to 0.90. Although the diurnal times do not match in this instance (00Z vs. 12Z), insistence upon two corresponding 12Z times would have eliminated this best historical date as a candidate.

Figures 3-6 show the synoptic situation and best overall match for the initial time, and for the initial time plus 24 hours; both at 500 mb and the surface. The actual situation is shown in the top half and the analogous situation in the bottom half of each figure, with the area correlated enclosed by a dashed line.

The sequence of hourly weather taken from this analogous synoptic pattern (forecasted weather), with an associated listing of the weather actually occurring (verifying weather), is shown in Figure 7. For comparative purposes, both listings are extended backwards 12 hours from the time of the initial match. Several strengths and limitations of this forecast emerge from these listings. Cloud types, ceilings, visibilities, weather and obstructions to vision are very much comparable, including precipitation types and timing. Winds are reasonably comparable. Temperatures are comparable during precipitation, but not before or after; partially due to matching a 12Z time with a 00Z time. In addition, heavy snow did fall in Central Pennsylvania out of this analogous system. Regretfully, however, this analog would not have produced a good forecast for Jacksonville, Florida or Brunswick, Maine; demonstrating the need for separate optimum areas for these stations.

B. Alameda, California - 12Z 09 February 1970

The Alameda case involved a stagnant but somewhat anomalous weather pattern along the U. S. West Coast. A small-scale 500-mb low and associated weak surface development just offshore produced heavy rain at San Diego, but only a light shower at Alameda. The forecast problem was one of whether or not precipitation would occur, and of what cloud types, ceilings, and visibility restrictions would affect the station regardless. In this instance, several analog candidates emerged with high correlation values, but largely centered on adjacent dates in sequences from 1961 and 1965. The best analogous pattern matching the "current" period (12Z 09 February 1970 to 12Z 10 February 1970) was the historical period from 12Z 21 Jan 1961 to 12Z 22 January 1961. Correlation values of the various parameters ranged from 0.90 to 0.95. For this example, matching the clock time (12Z) was vital, since much of the associated weather was diurnal in nature.

Figures 8-11 show the synoptic situation and best overall match for the initial time and initial time plus 24 hours at 500 mb and the surface. Again, the actual situation is shown in the top half and the analogous situation in the bottom half of each figure; with the area correlated enclosed by a dashed line.

Figure 12 shows the sequence of hourly weather taken from this analogous synoptic pattern (forecasted weather), with the associated listing of weather actually occurring (verifying weather). Again, both listings are extended backward 12 hours for comparative purposes.

Several strengths and weaknesses emerge from these listings also. Occurrence and timing of cloud types, ceilings, visibilities and obstructions to vision are handled well, although cloud cover is underpredicted. Diurnal effects were handled correctly. Winds and temperatures were somewhat off, however; and the one rain shower that occurred was not predicted. Unfortunately, heavy rain did not occur at San Diego from this analogous pattern. However, a second highly-correlating analog from 12Z 15 January 1965 (although not quite as good a numerical match as 1961) would have predicted that event. Regretfully, the forecast accuracy of the terminal weather at Alameda from the 1965 sequence was not adequate for aircraft operations; although cloud types, ceilings and specific restrictions to vision were similar. In particular, visibilities were

much lower than those in either 1961 or 1970, and for a much longer period of time. This, coupled with the East Coast experience, pointed out the inadequacy of lumping all stations up and down an entire coastline into one area for the purpose of short-range terminal forecasting. Such a conclusion was not wholly unexpected, given the optimum area size required for reasonable accuracy at a single station.

## IV. OPERATIONAL AND DEVELOPMENTAL PLANS

### A. Operational Plans

It is planned to eventually make totally-automated short-range terminal forecasts available on a daily basis for most Naval Environmental Data Network (NEDN) Tieline stations on the U. S. east and west coasts. In the meantime, FNWC will have the capability in the autumn of 1970 to at least provide the dates of the five best analogous patterns. Until total automation of this scheme can be implemented, station personnel would thus be able to consider the hourly weather associated with the five best analogous weather patterns when preparing a terminal forecast. Historical hourly weather in airways format, if not available locally, can be obtained for most tieline stations from FNWC's automated climatology archives.

Initially, forecast availability will be limited to five stations — Alameda, Moffett Field and Monterey in Central California; Washington, D. C. and Norfolk, Virginia along the U. S. East Coast. The number of stations for which these forecasts will be available will increase as additional optimum areas are defined and tested. Specifically, new areas are planned for the southeast U. S., New England, Northwest U. S., Southern California; and Keflavik, Iceland.

### B. Developmental Plans

#### 1. Composite Approach

For various reasons (inexact analyses, historical or current; imperfect prognoses, unique or extreme weather situations, uncontrollable or unknowable outside influences, etc.), the best analog match does not always produce the best terminal forecast; although one of the top five matches usually can. Hence, a composite approach at terminal forecasting using the weather associated with the top five analogous synoptic patterns will be investigated. As previously mentioned, a predecessor to any composite could be the provision of hourlies from each of the top five analogous patterns; or the dates themselves from which to look up the associated historical hourlies (as discussed above).

#### 2. More Sophisticated Model

There has been some indication in the testing that a screen which starts out with a larger region (but not hemispheric), and then zooms in on specific stations for various parameters might be a superior method of local area analog selection in certain instances. The volume of data searched, as well as the internal bookkeeping required, has made this approach prohibitive in the initial prototype model, however.

#### 3. Automation

As described earlier, the initial terminal forecast model will be only semi-automated. In order to totally automate, it will be necessary to numerically compare the analogous historical hourlies with current incoming raw data at each station for which forecasts are to be issued. Since current data is used for routine FNWC analyses, it is available continually in the computer. A certain amount of historical hourly data for each station can also be kept in the same computer for these comparative purposes.

Three difficulties — phasing problems (diurnal and otherwise), the problem of missing hourly data (both historical and current), and the problem of permanent bulk storage within the machine — must be considered in any attempt at total automation. Once these and other problems involved in automatically comparing historical and current hourlies (and relating these comparisons to synoptic patterns) have been solved, it is a seemingly simple additional step to automatically update these forecasts as required and as available data permits — perhaps at six-hourly intervals.

## V. CONCLUSIONS

Despite restrictions, the analog approach toward automation of short-range terminal forecasts shows considerable promise. At worst, this technique will offer a new tool to the short-range forecaster, giving him a degree of "experience" he might not otherwise have had. At best, this approach will ultimately solve the automated terminal forecast problem.

## ACKNOWLEDGEMENTS

Sincere appreciation is extended to Mr. Richard G. Elms, who wrote the computer program for the Selection Model; and to CAPT P. M. Wolff, CAPT W. S. Houston, and LCDR H. Lewit for reviewing the manuscript.

## REFERENCES

1. Snellman, L. W., Man-Machine Mix in Applied Weather Forecasting in the 1970's, Technical Memorandum WBTM WR-40, Environmental Science Services Administration, Weather Bureau Western Region, Salt Lake City, Utah, August 1969.

2. Wolff, P. M. and C. D. Thormeyer, Extended Range Analog Forecast Program at Fleet Numerical Weather Central, Technical Note #49, Fleet Numerical Weather Central, Monterey, California, September 1969.

3. Wolff, P. M. and W. C. Woodworth, Hourly Point Forecasting at FNWF, Technical Memo #16, Fleet Numerical Weather Facility, Monterey, California, September 1966.

4. Wolff, P. M., A Proposal for Modern Computer Climatology Service, Technical Memo #8, Fleet Numerical Weather Facility, Monterey, California, 15 June 1965.

5. Kesel, P. G., Experiments with Atmospheric Primitive Equation Models, M.S. Thesis, U. S. Naval Postgraduate School, Monterey, California, December 1968.

6. Kesel, P. G. and F. J. Winninghoff, Development of a Multi-Processor Primitive-Equation Atmospheric Prediction Model (to be published).

FLOW DIAGRAM

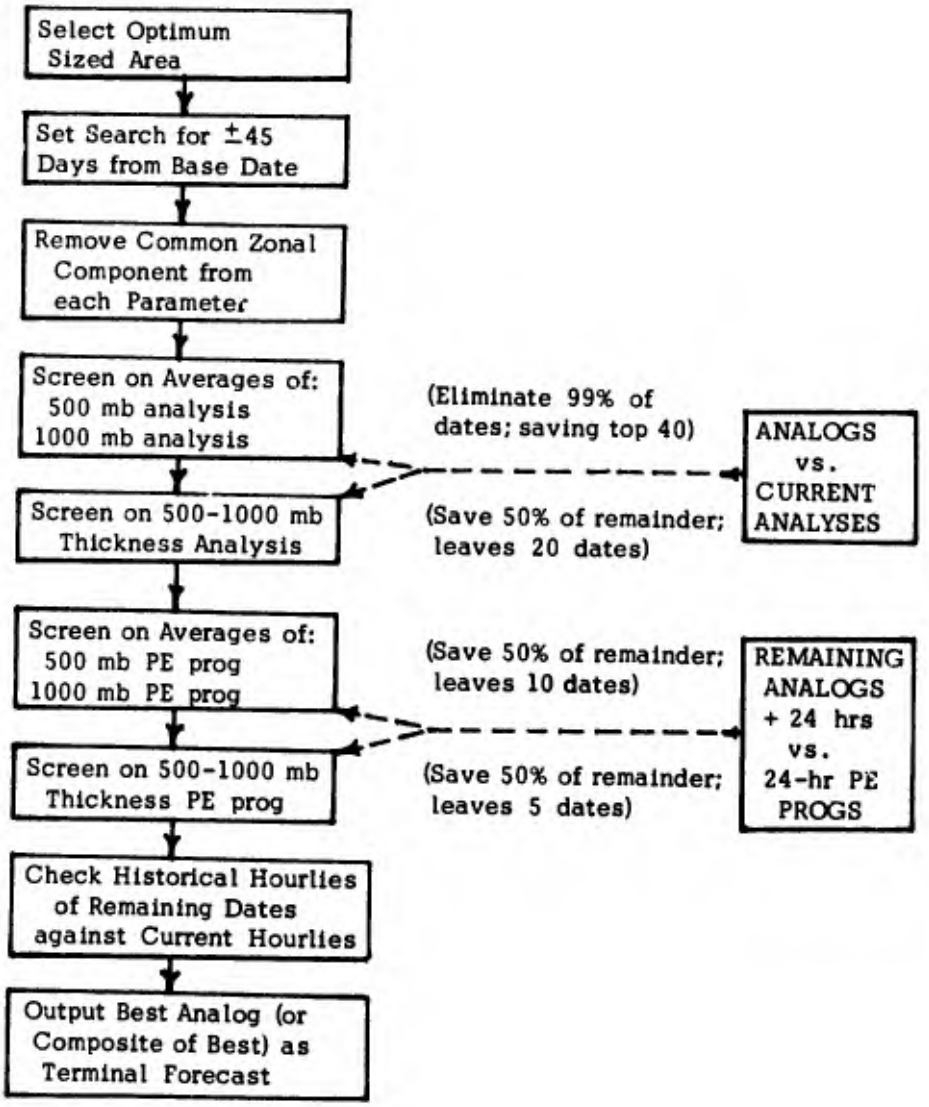


Figure 1. Flow Diagram of Automated Terminal Forecast Model

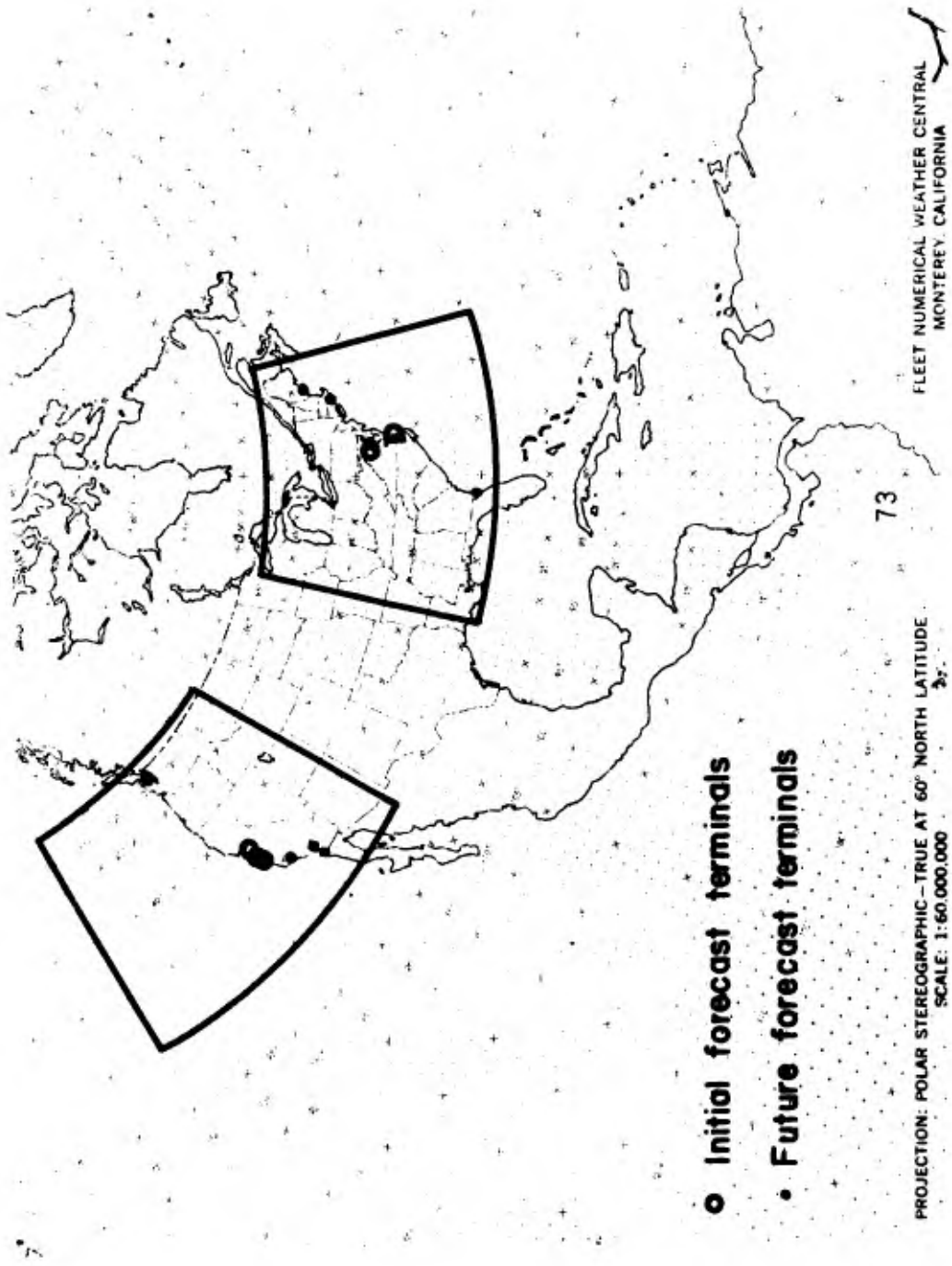


Figure 2. Initial Optimum-Sized Areas for Local-Area Analog Selection

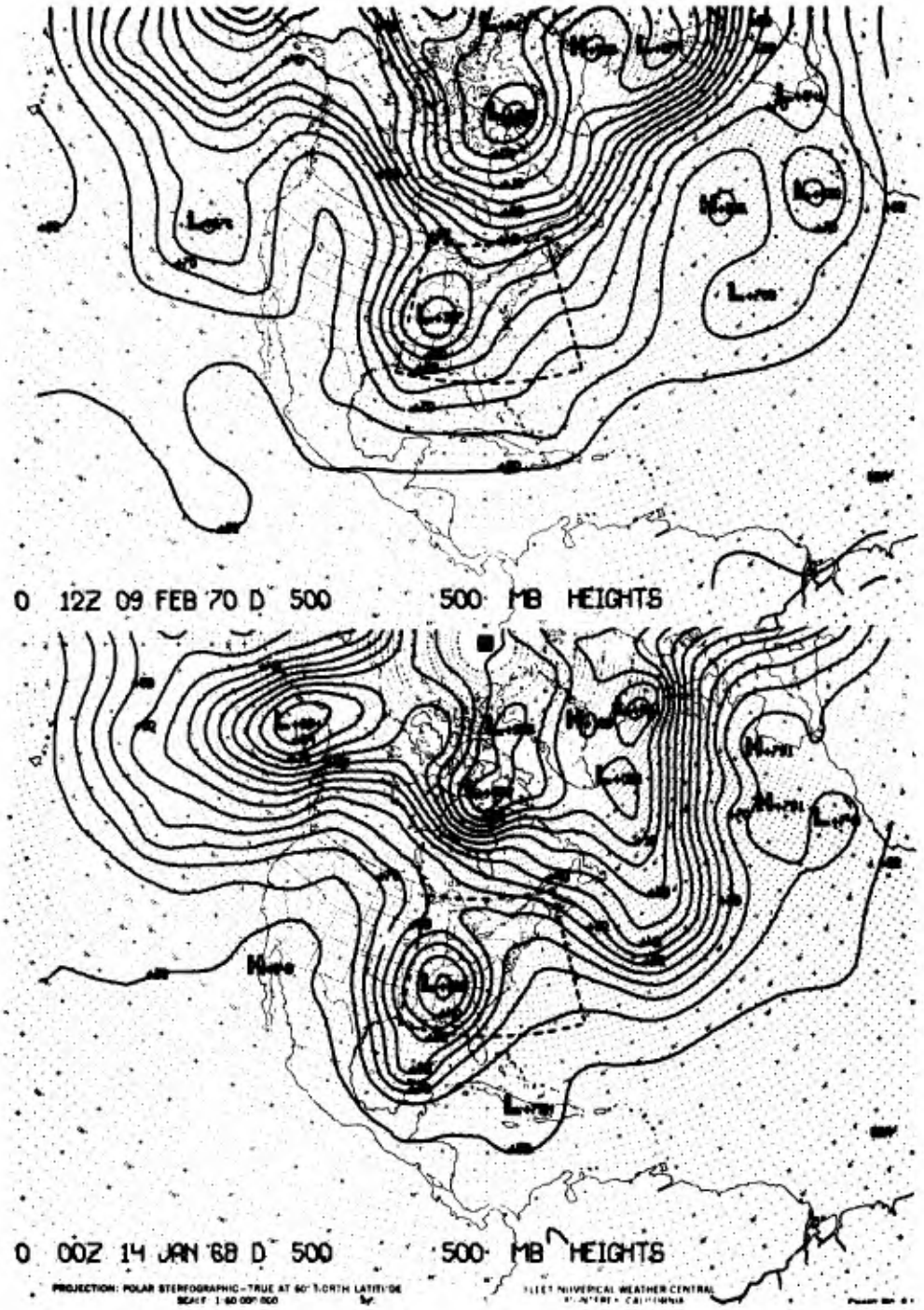


Figure 3. Initial 500-mb Match vs. Best Overall Analog: Washington

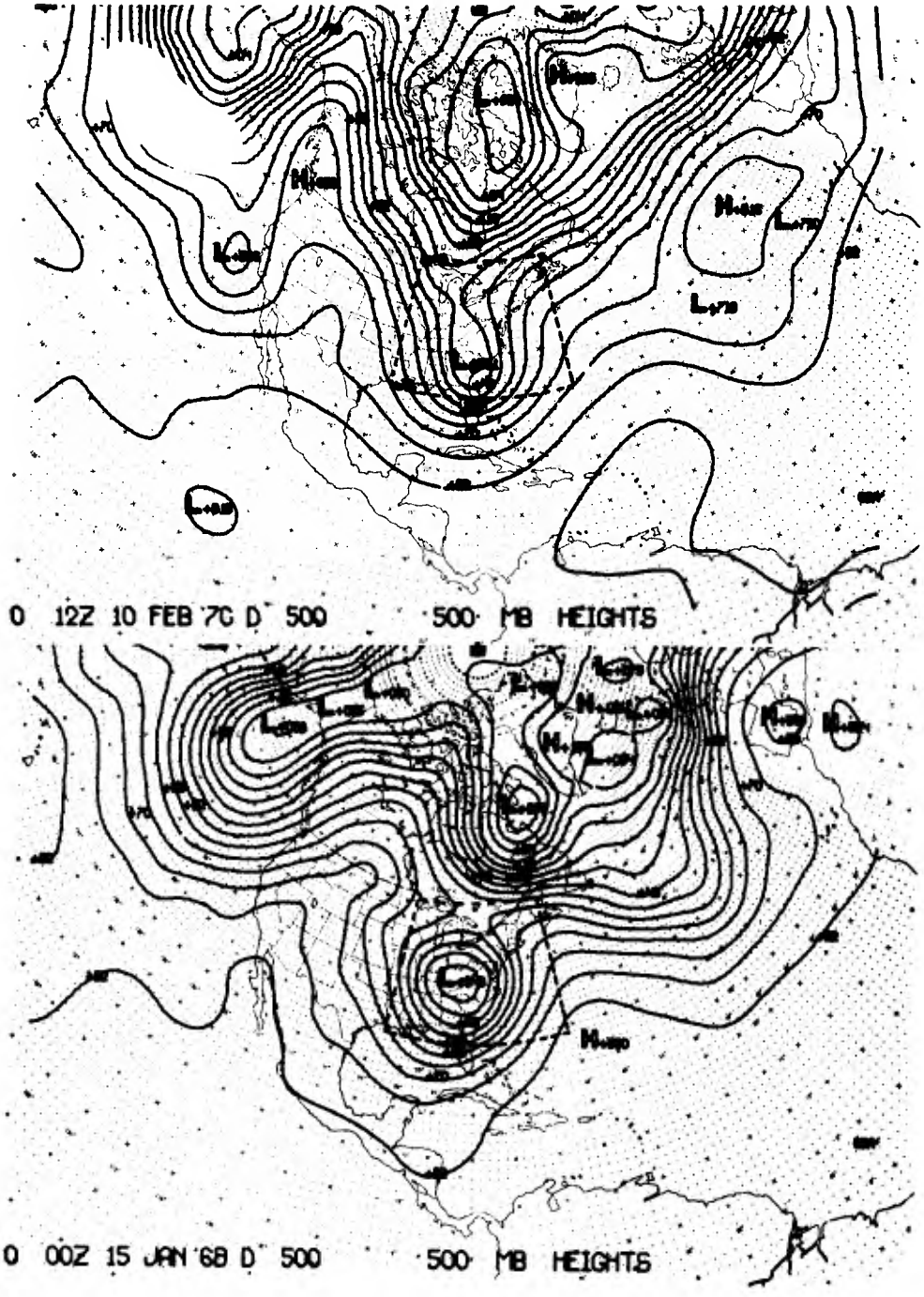


Figure 4. Initial Time plus 24 hours (Actual) vs. Analog plus 24 hours: 500 mb, Washington

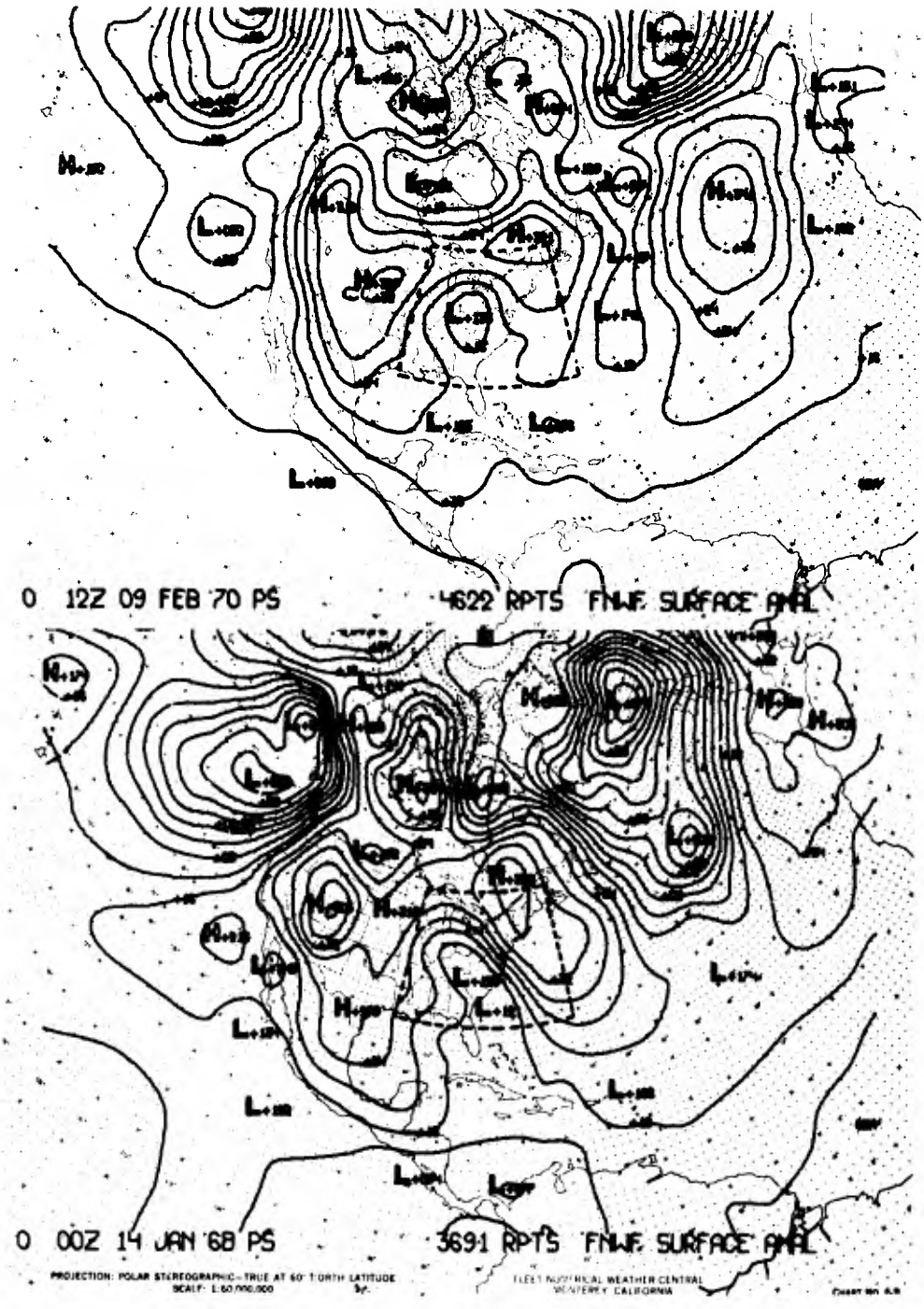


Figure 5. Initial Surface Match vs. Best Overall Analog: Washington

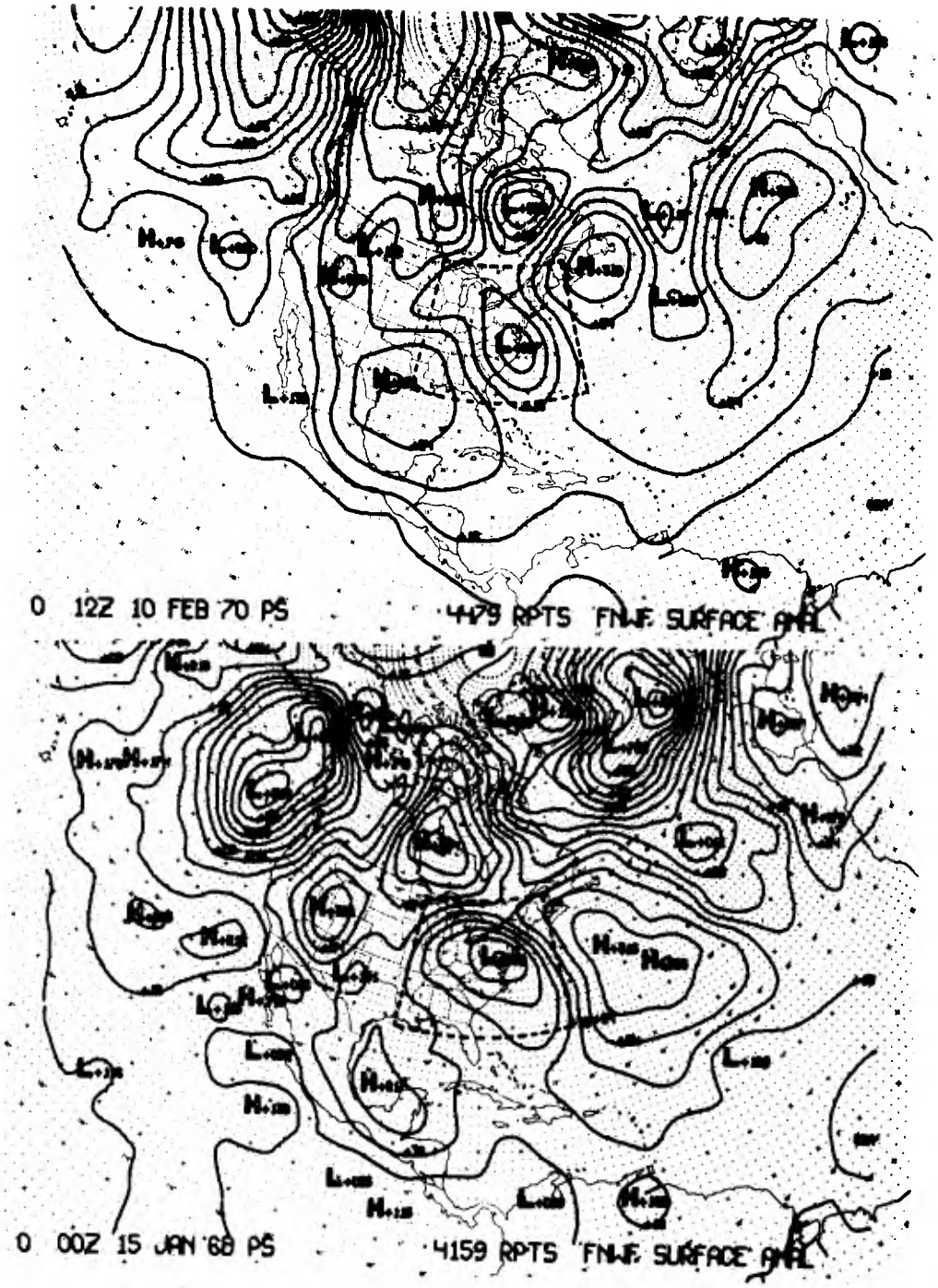


Figure 6. Initial Time plus 24 hours (Actual) vs. Analog plus 24 hours: Surface, Washington

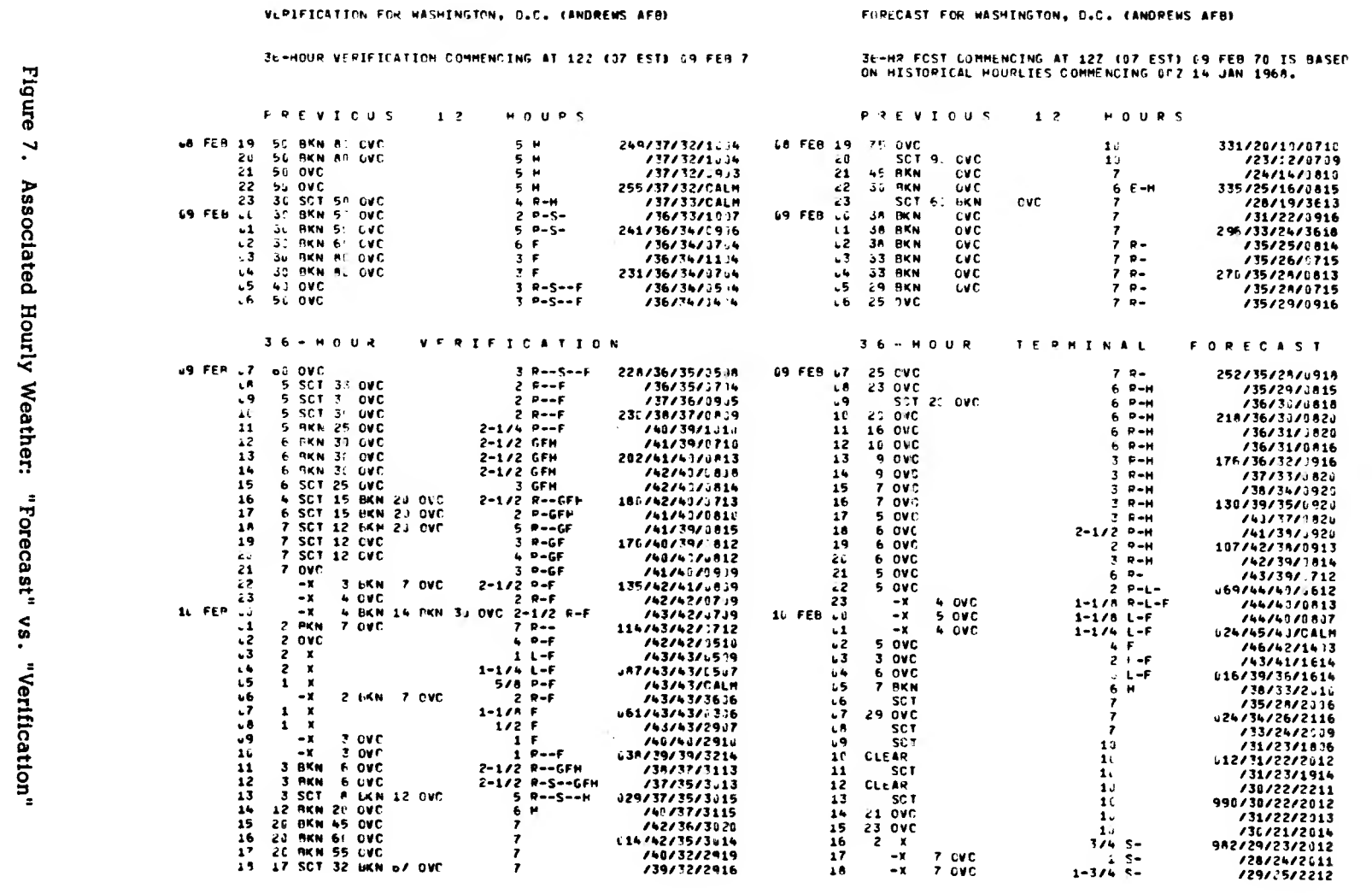

VERIFICATION FOR WASHINGTON, D.C. (ANDREWS AFB)

36-HOUR VERIFICATION COMMENCING AT 12Z (07 EST) 09 FEB 7

PREVIOUS 12 HOURS

| | | | | | | | | |
|---|---|---|---|---|---|---|---|---|
| 08 FEB | 19 | 50 | BKN | 8[illegible] | OVC | | 5 H | 249/37/32/1[illegible]34 |
| | 20 | 50 | BKN | 80 | OVC | | 5 H | /37/32/1[illegible]04 |
| | 21 | 50 | OVC | | | | 5 H | /37/32/[illegible]903 |
| | 22 | 50 | OVC | | | | 5 H | 255/37/32/CALM |
| | 23 | 30 | SCT | 50 | OVC | | 4 R-H | /37/33/CALM |
| 09 FEB | 00 | 30 | BKN | 5[illegible] | OVC | | 2 R-S- | /36/33/1007 |
| | 01 | 30 | BKN | 5[illegible] | OVC | | 5 R-S- | 241/36/34/0906 |
| | 02 | 30 | BKN | 6[illegible] | OVC | | 6 F | /36/34/0704 |
| | 03 | 30 | BKN | 8[illegible] | OVC | | 3 F | /36/34/1104 |
| | 04 | 30 | BKN | 8[illegible] | OVC | | 3 F | 231/36/34/0704 |
| | 05 | 40 | OVC | | | | 3 R-S--F | /36/34/0[illegible]04 |
| | 06 | 50 | OVC | | | | 3 R-S--F | /36/34/1[illegible]04 |

36-HOUR VERIFICATION

| | | | | | | | | | | |
|---|---|---|---|---|---|---|---|---|---|---|
| 09 FEB | 07 | 60 | OVC | | | | | 3 | R--S--F | 228/36/35/0508 |
| | 08 | 5 | SCT | 35 | OVC | | | 2 | F--F | /36/35/0714 |
| | 09 | 5 | SCT | 3[illegible] | OVC | | | 2 | P--F | /37/36/0905 |
| | 10 | 5 | SCT | 3[illegible] | OVC | | | 2 | R--F | 230/38/37/0809 |
| | 11 | 5 | BKN | 25 | OVC | | 2-1/4 | P--F | /40/39/1010 |
| | 12 | 6 | BKN | 30 | OVC | | 2-1/2 | GFH | /41/39/0710 |
| | 13 | 6 | BKN | 3[illegible] | OVC | | 2-1/2 | GFH | 202/41/40/0813 |
| | 14 | 6 | BKN | 3[illegible] | OVC | | 2-1/2 | GFH | /42/40/0818 |
| | 15 | 6 | SCT | 25 | OVC | | | 3 | GFH | /42/40/0814 |
| | 16 | 4 | SCT | 15 | BKN | 20 OVC | 2-1/2 | R--GFH | 186/42/40/0713 |
| | 17 | 6 | SCT | 15 | BKN | 20 OVC | | 2 | P-GFH | /41/40/0810 |
| | 18 | 7 | SCT | 12 | BKN | 20 OVC | | 5 | P--GF | /41/39/0815 |
| | 19 | 7 | SCT | 12 | OVC | | | 3 | R-GF | 176/40/39/[illegible]812 |
| | 20 | 7 | SCT | 12 | OVC | | | 4 | P-GF | /40/40/[illegible]812 |
| | 21 | 7 | OVC | | | | | 3 | P-GF | /41/40/0909 |
| | 22 | | -X | 3 | BKN | 7 OVC | 2-1/2 | P-F | 135/42/41/[illegible]859 |
| | 23 | | -X | 4 | OVC | | | 2 | R-F | /42/42/0709 |
| 10 FEB | 00 | | -X | 4 | BKN | 14 BKN 30 OVC | 2-1/2 | R-F | /43/42/[illegible]709 |
| | 01 | 2 | BKN | 7 | OVC | | | 7 | R-- | 114/43/42/[illegible]712 |
| | 02 | 2 | OVC | | | | | 4 | P-F | /42/42/0510 |
| | 03 | 2 | X | | | | | 1 | L-F | /43/43/[illegible]509 |
| | 04 | 2 | X | | | | 1-1/4 | L-F | 087/43/43/[illegible]507 |
| | 05 | 1 | X | | | | 5/8 | P-F | /43/43/CALM |
| | 06 | | -X | 2 | BKN | 7 OVC | | 2 | R-F | /43/43/3636 |
| | 07 | 1 | X | | | | 1-1/4 | F | 061/43/43/[illegible]836 |
| | 08 | 1 | X | | | | 1/2 | F | /43/43/2907 |
| | 09 | | -X | 3 | OVC | | | 1 | F | /40/40/2910 |
| | 10 | | -X | 3 | OVC | | | 1 | P--F | 038/39/39/3214 |
| | 11 | 3 | BKN | 6 | OVC | | 2-1/2 | R--GFH | /38/37/3113 |
| | 12 | 3 | BKN | 6 | OVC | | 2-1/2 | R-S--GFH | /37/35/3[illegible]13 |
| | 13 | 3 | SCT | 8 | BKN | 12 OVC | | 5 | R--S--H | 029/37/35/3015 |
| | 14 | 12 | BKN | 20 | OVC | | | 6 | H | /40/37/3115 |
| | 15 | 20 | BKN | 45 | OVC | | | 7 | | /42/36/3020 |
| | 16 | 20 | BKN | 60 | OVC | | | 7 | | 014/42/35/3[illegible]14 |
| | 17 | 20 | BKN | 55 | OVC | | | 7 | | /40/32/2919 |
| | 18 | 17 | SCT | 32 | BKN | 60 OVC | | 7 | | /39/32/2916 |

FORECAST FOR WASHINGTON, D.C. (ANDREWS AFB)

36-HR FCST COMMENCING AT 12Z (07 EST) 09 FEB 70 IS BASED ON HISTORICAL HOURLIES COMMENCING 07Z 14 JAN 1960.

PREVIOUS 12 HOURS

| | | | | | | | | |
|---|---|---|---|---|---|---|---|---|
| 08 FEB | 19 | 75 | OVC | | | | 10 | 331/20/10/0710 |
| | 20 | | SCT | 9[illegible] | OVC | | 10 | /23/[illegible]/0709 |
| | 21 | 45 | BKN | | OVC | | 7 | /24/14/1810 |
| | 22 | 30 | BKN | | OVC | | 6 E-H | 335/25/16/0815 |
| | 23 | | SCT | 6[illegible] | BKN | OVC | 7 | /28/19/3613 |
| 09 FEB | 00 | 38 | BKN | | OVC | | 7 | /31/22/0916 |
| | 01 | 38 | BKN | | OVC | | 7 | 296/33/24/3618 |
| | 02 | 38 | BKN | | OVC | | 7 R- | /35/25/0814 |
| | 03 | 33 | BKN | | OVC | | 7 R- | /35/26/0715 |
| | 04 | 33 | BKN | | OVC | | 7 R- | 270/35/28/0813 |
| | 05 | 29 | BKN | | OVC | | 7 R- | /35/28/0715 |
| | 06 | 25 | OVC | | | | 7 R- | /35/29/0916 |

36-HOUR TERMINAL FORECAST

| | | | | | | | | |
|---|---|---|---|---|---|---|---|---|
| 09 FEB | 07 | 25 | OVC | | | | 7 R- | 252/35/29/0918 |
| | 08 | 23 | OVC | | | | 6 R-H | /35/29/0815 |
| | 09 | | SCT | 25 | OVC | | 6 R-H | /36/30/0818 |
| | 10 | 20 | OVC | | | | 6 R-H | 218/36/30/0820 |
| | 11 | 16 | OVC | | | | 6 R-H | /36/31/0820 |
| | 12 | 10 | OVC | | | | 6 R-H | /36/31/0816 |
| | 13 | 9 | OVC | | | | 3 R-H | 176/36/32/0916 |
| | 14 | 9 | OVC | | | | 3 R-H | /37/33/0820 |
| | 15 | 7 | OVC | | | | 3 R-H | /38/34/0920 |
| | 16 | 7 | OVC | | | | 3 R-H | 130/39/35/0920 |
| | 17 | 5 | OVC | | | | 3 R-H | /41/[illegible]/0820 |
| | 18 | 6 | OVC | | | | 2-1/2 R-H | /41/39/[illegible]920 |
| | 19 | 6 | OVC | | | | 2 R-H | 107/42/38/0913 |
| | 20 | 6 | OVC | | | | 3 R-H | /42/39/1814 |
| | 21 | 5 | OVC | | | | 6 R- | /43/39/[illegible]712 |
| | 22 | 5 | OVC | | | | 2 R-L- | 069/44/40/[illegible]612 |
| | 23 | | -X | 4 | OVC | | 1-1/8 R-L-F | /44/43/0813 |
| 10 FEB | 00 | | -X | 5 | OVC | | 1-1/8 L-F | /44/40/0807 |
| | 01 | | -X | 4 | OVC | | 1-1/4 L-F | 024/45/43/CALM |
| | 02 | 5 | OVC | | | | 4 F | /46/42/1403 |
| | 03 | 3 | OVC | | | | 2 [illegible]-F | /43/41/1614 |
| | 04 | 6 | OVC | | | | [illegible] L-F | 016/39/36/1614 |
| | 05 | 7 | BKN | | | | 6 H | /38/33/2[illegible]16 |
| | 06 | | SCT | | | | 7 | /35/28/2[illegible]16 |
| | 07 | 29 | OVC | | | | 7 | 024/34/26/2116 |
| | 08 | | SCT | | | | 7 | /33/24/2[illegible]09 |
| | 09 | | SCT | | | | 10 | /31/23/1[illegible]36 |
| | 10 | CLEAR | | | | | 10 | 012/31/22/2012 |
| | 11 | | SCT | | | | 10 | /31/23/1914 |
| | 12 | CLEAR | | | | | 10 | /30/22/2211 |
| | 13 | | SCT | | | | 10 | 990/30/22/2012 |
| | 14 | 21 | OVC | | | | 10 | /31/22/2013 |
| | 15 | 23 | OVC | | | | 10 | /30/21/2014 |
| | 16 | 2 | X | | | | 3/4 S- | 982/29/23/2012 |
| | 17 | | -X | 7 | OVC | | 1 S- | /28/24/2011 |
| | 18 | | -X | 7 | OVC | | 1-3/4 S- | /29/25/2212 |

Figure 7. Associated Hourly Weather: "Forecast" vs. "Verification"

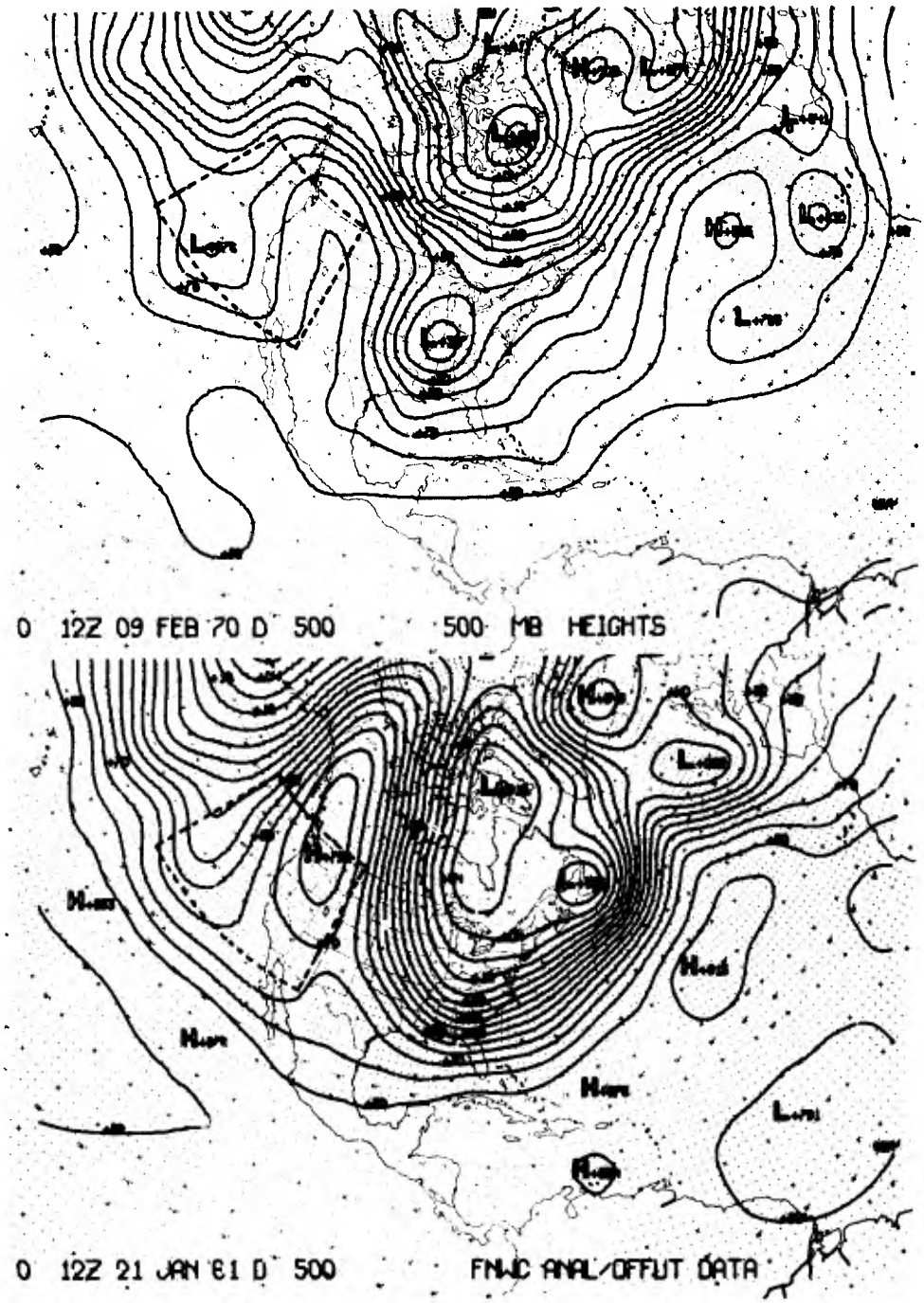


Figure 8. Initial 500-mb March vs. Best Overall Analog: Alameda

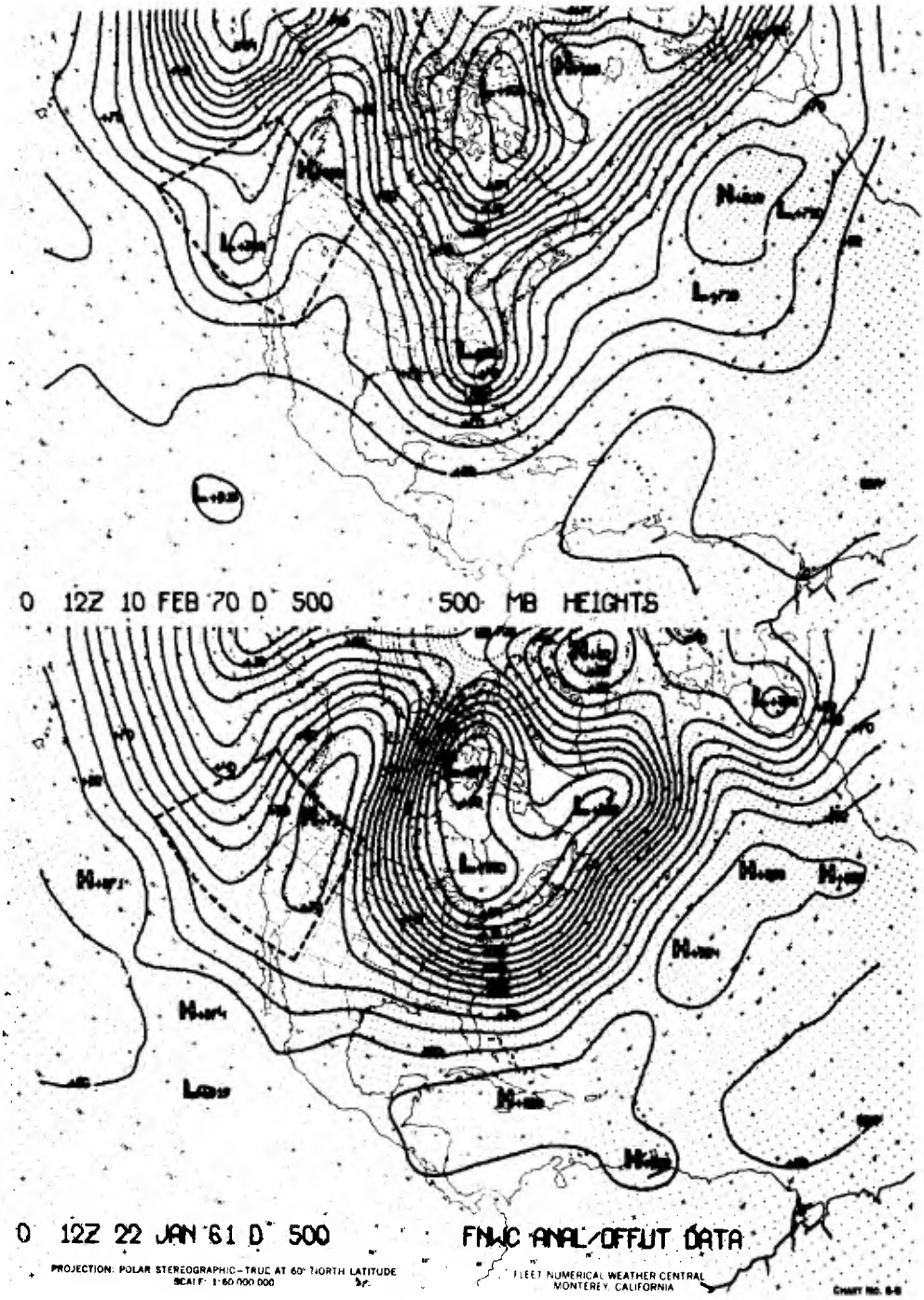


Figure 9. Initial Time plus 24 hours (Actual) vs. Analog plus 24 hours: 500 mb, Alameda

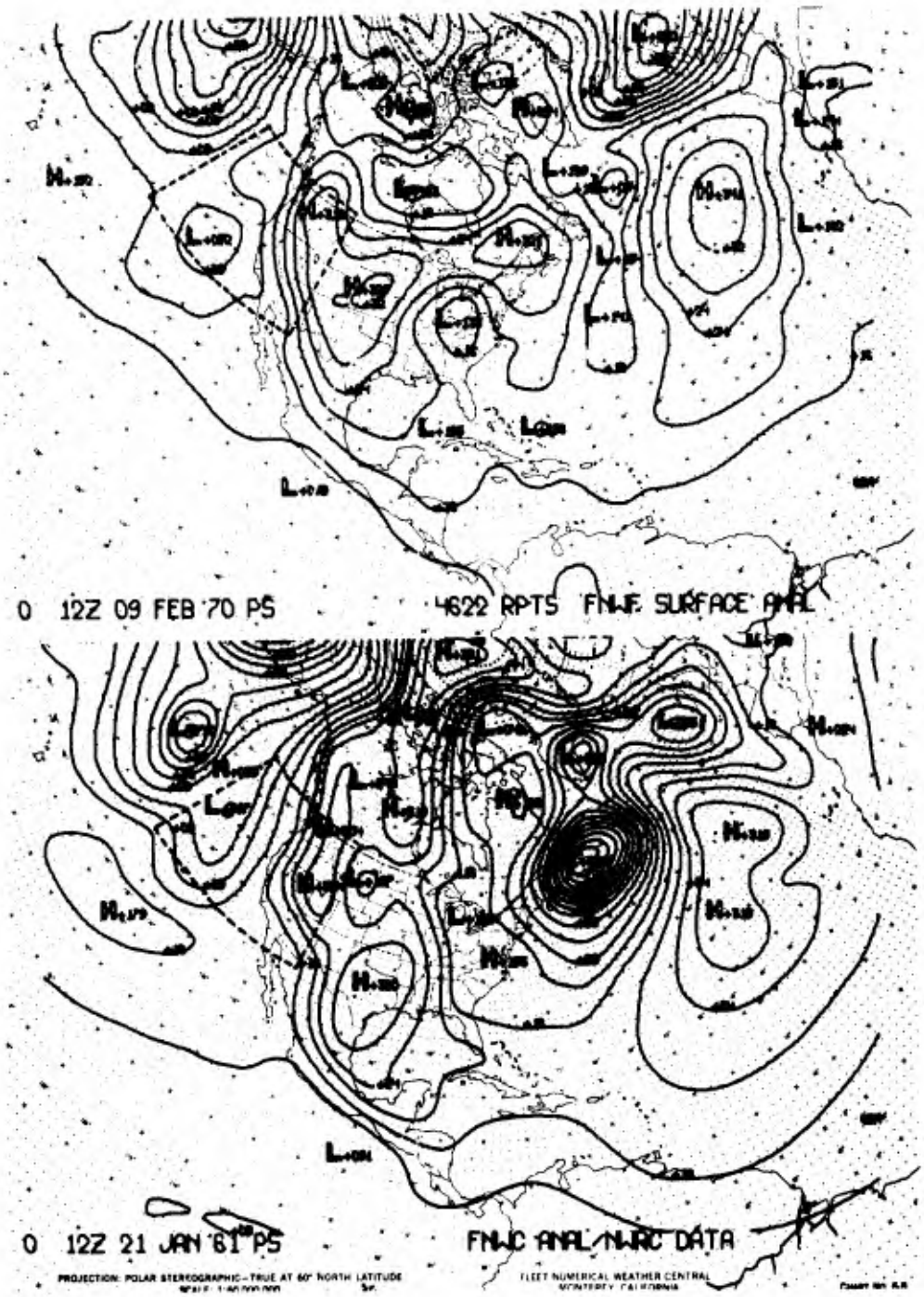


Figure 10. Initial Surface Match vs. Best Overall Analog: Alameda

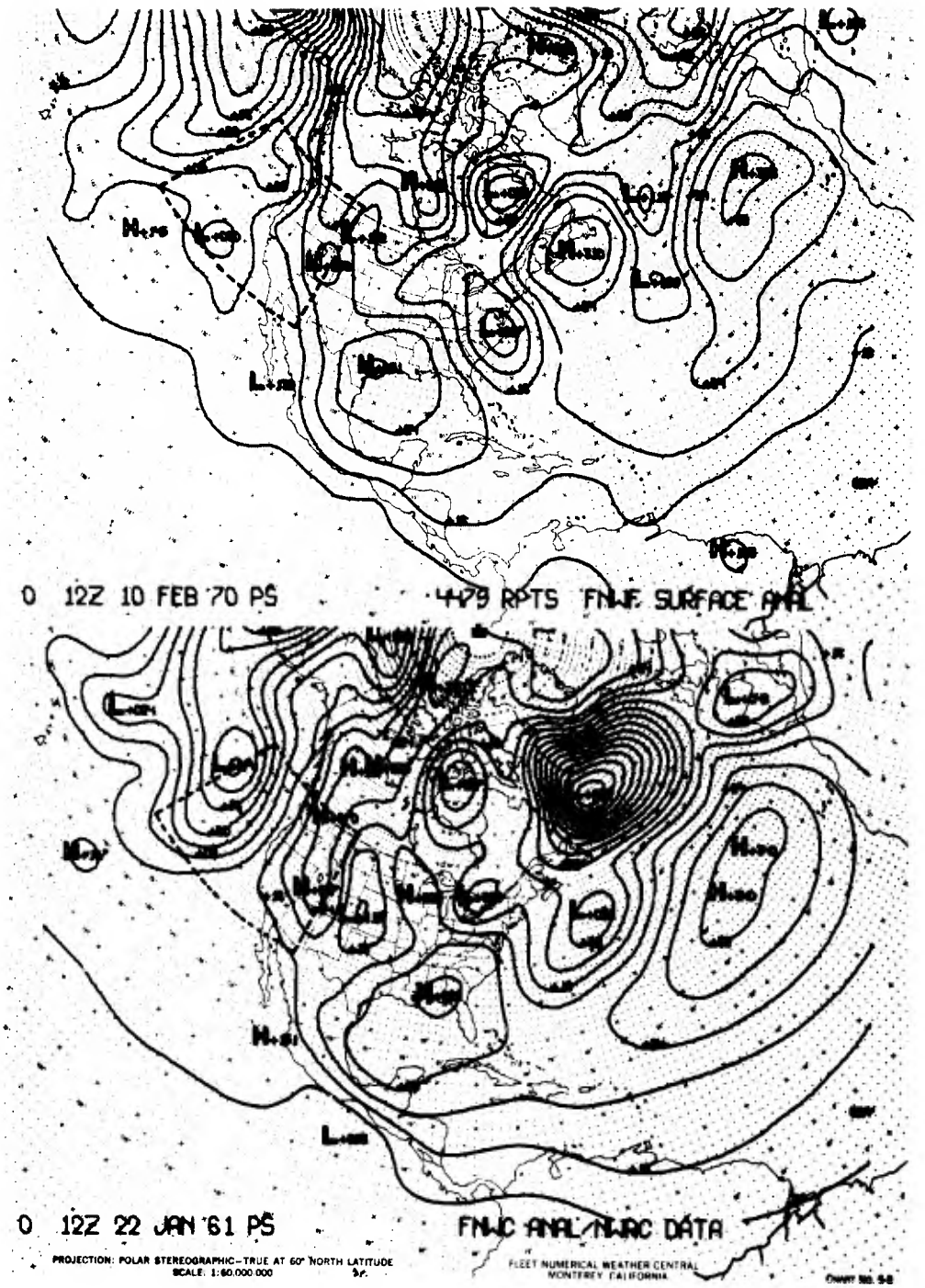


Figure 11. Initial Time plus 24 hours (Actual) vs. Analog plus 24 hours: Surface, Alameda

VERIFICATION FOR ALAMEDA, CALIF.

36-HOUR VERIFICATION COMMENCING AT 12Z (04 PST) 09 FEB 70.

| | | PREVIOUS 12 HOURS | | | VERIFICATION | | | 36-HOUR TERMINAL FORECAST |
|---|---|---|---|---|---|---|---|---|
| 08 FEB | 16 | U OVC | | 10 | 129/71/39/0636 | 08 FEB 16 | / - SCT | 5 HK 159/52/40/3108 |
| | 17 | 150 SCT U OVC | | 10 | 130/68/38/0705 | 17 | / - BKN | 6 HK 159/50/40/3408 |
| | 18 | 150 SCT U BKN | | 10 | 130/67/36/CALM | 18 | / - BKN | 7 155/50/40/3108 |
| | 19 | U BKN | | 10 | 131/59/46/2204 | 19 | / - SCT | 7 153/49/41/3104 |
| | 20 | U OVC | | 10 | 135/58/47/2662 | 20 | CLEAR | 7 150/48/40/3608 |
| | 21 | U OVC | | 10 | 133/58/46/3533 | 21 | CLEAR | 7 148/46/43/3606 |
| | 22 | U OVC | | 10 | 132/57/45/2902 | 22 | CLEAR | 5 GF 149/45/41/3405 |
| | 23 | U BKN | | 10 | 131/57/45/3534 | 23 | / - SCT | 4 GF 148/44/42/3608 |
| 09 FEB | 00 | U OVC | | 10 | 137/56/46/0204 | J9 FEB 00 | / - BKN | 4 GF 148/44/41/3406 |
| | 01 | 150 SCT U OVC | | 10 | 131/55/47/CALM | 01 | / - SCT | 6 HK 149/43/43/3608 |
| | 02 | 150 SCT U OVC | | 10 | 129/55/47/3032 | 02 | CLEAR | 6 HK 148/43/40/3408 |
| | 03 | 25 SCT 150 SCT U OVC | | 10 | 121/54/47/0010 | 03 | CLEAR | 8 148/43/40/3408 |
| 09 FEB | 04 | 150 SCT U OVC | | 10 | 113/53/47/3132 | 09 FEB 04 | CLEAR | 8 146/42/39/3408 |
| | 05 | 150 SCT U BKN | | 10 | 114/54/47/CALM | 05 | CLEAR | 7 146/42/39/3406 |
| | 06 | 150 SCT U BKN | | 10 | 111/53/46/CALM | 06 | CLEAR | 8 146/42/39/3408 |
| | 07 | 150BKN / OVC | | 6 H | 108/53/46/3034 | 07 | CLEAR | 7 144/42/39/3411 |
| | 08 | 150 BKN / OVC | | 5 H | 105/54/47/3235 | 08 | / - SCT | 4 HK 149/42/38/3112 |
| | 09 | 133 BKN / OVC | | 5 H | 105/56/47/3134 | 09 | / - SCT | 4 HK 152/42/36/3410 |
| | 10 | 35 SCT 100 BKN | / OVC | 5 H | 101/57/47/3404 | 10 | / - SCT | 5 HK 155/44/37/3112 |
| | 11 | 50 SCT 100 BKN | / OVC | 5 H | 102/58/47/2412 | 11 | / - SCT | 5 HK 154/45/37/3112 |
| | 12 | -X 50 SCT 100 BKN | / OVC | 4 H | 099/61/46/CALM | 12 | / SCT | 5 HK 142/49/40/3110 |
| | 13 | -X 100 BKN | / OVC | 4 H | 096/61/46/2102 | 13 | 160 SCT / SCT | 4 HK 135/47/40/3114 |
| | 14 | -X 100 BKN | / OVC | 4 H | 105/59/51/1505 | 14 | 160 BKN | 5 HK 131/50/39/2910 |
| | 15 | -X 100 BKN | / OVC | 4 H | 100/63/46/1204 | 15 | 160 BKN | 5 HK 130/50/39/3110 |
| | 16 | 100 BKN | / OVC | 7 | 110/63/45/CALM | 16 | 100 BKN 160 OVC | 6 HK 136/50/40/3408 |
| | 17 | 50 SCT 140 BKN | / OVC | 7 | 105/62/47/3213 | 17 | 100 BKN 160 OVC | 6 HK 139/50/40/3608 |
| | 18 | 50 SCT 100 SCT | U BKN | 8 | 107/59/47/2905 | 18 | 100 OVC | 8 141/49/43/3106 |
| | 19 | 50 SCT 100 SCT | / SCT | 8 | 109/57/46/3204 | 19 | 100 OVC | 8 145/49/43/3406 |
| | 20 | 100 SCT | / SCT | 8 | 116/56/47/1304 | 20 | 100 OVC | 10 140/49/43/3436 |
| | 21 | 100 SCT | U OVC | 7 | 132/57/48/1310 | 21 | 90 BKN | 10 151/48/42/3406 |
| | 22 | 100 OVC | | 5 RW- | 143/56/49/1210 | 22 | 90 BKN U BKN | 10 151/48/42/3436 |
| | 23 | 2. SCT 100 BKN | | 8 | 139/55/51/1616 | 23 | 90 BKN U OVC | 12 156/48/43/3606 |
| 10 FEB | 00 | 100 BKN | | 10 | 136/55/49/0602 | 10 FEB 00 | 90 BKN U OVC | 12 159/48/42/3606 |
| | 01 | 100 OVC | | 10 | 144/54/49/1104 | 01 | 100 OVC | 12 156/49/41/3432 |
| | 02 | 100 OVC | | 10 | 145/54/49/2902 | 02 | 100 OVC | 12 160/49/41/3605 |
| | 03 | 100 OVC | | 10 | 146/54/49/3508 | 03 | 100 BKN | 8 162/49/41/3604 |
| | 04 | 100 OVC | | 10 | 149/53/49/3435 | 04 | 100 SCT | 8 163/48/40/3407 |
| | 05 | 100 OVC | | 7 | 156/53/49/3136 | 05 | 70 SCT 100 SCT / SCT | 8 160/47/41/3406 |
| | 06 | 100 OVC | | 6 H | 154/53/49/3336 | 06 | 140 SCT U BKN | 8 166/47/41/3608 |
| | 07 | 100 BKN | | 5 H | 155/52/49/3603 | 07 | 140 SCT U BKN | 8 172/46/41/3607 |
| | 08 | 100 BKN | / BKN | 5 H | 156/53/49/3105 | 08 | 140 SCT U BKN | 7 173/46/41/3606 |
| | 09 | 100 BKN | / BKN | 4 GFHK | 159/55/51/CALM | 09 | 140 BKN U OVC | 5 HK 177/49/41/3604 |
| | 10 | 100 BKN | | 4 HK | 161/57/50/1535 | 10 | 120 BKN U BKN | 5 HK 181/52/41/CALM |
| | 11 | 80 BKN | | 6 HK | 163/57/51/1553 | 11 | 100 BKN U OVC | 4 HK 184/52/42/3406 |
| | 12 | 30 SCT 80 BKN | / BKN | 5 HK | 159/62/51/1721 | 12 | 100 SCT 150 BKN | 4 HK 175/52/39/3108 |
| | 13 | 100 BKN | / BKN | 5 HK | 151/61/50/0705 | 13 | 120 OVC | 3 HK 171/54/45/3110 |
| | 14 | 30 SCT 100 BKN | / BKN | 5 HK | 141/63/51/3206 | 14 | 45 SCT 120 BKN | 3 HK 168/55/45/3110 |
| | 15 | 40 SCT 70 BKN | / BKN | 5 HK | 139/63/51/3406 | 15 | 45 BKN 120 OVC | 3 HK 167/54/46/3112 |

FORECAST FOR ALAMEDA, CALIF.

36-HR FCST COMMENCING AT 12Z (04 PST) 09 FEB 70 IS BASED ON HISTORICAL HOURLIES COMMENCING 12Z 21 JAN 1961.

Figure 12. Associated Hourly Weather: "Forecast" vs. "Verification"

# APPLICATION OF PE-MODEL FORECAST PARAMETERS TO LOCAL-AREA FORECASTING

Leonard W. Snellman

Chief, Scientific Services Division
Weather Bureau Western Region
Salt Lake City, Utah

## I. INTRODUCTION

My approach to the subject of application of P.E. model forecast parameters in local-area forecasting will be to discuss the philosophy that is developing in operational use of dynamic predictions. Illustrations of current use of P.E. model products will also be given. During this discussion I hope to bring out the changing role of the meteorologist in local-area forecasting because there is no doubt in my mind that the forecast structure of the 1970s should be the man-machine mix. It is also important at this time that we emphasize the role of the forecaster because many forecasters are interpreting the considerable work being done in automation as efforts to eliminate their jobs rather than to help them do a better job. Unfortunately, this erroneous interpretation is affecting forecaster morale, and such work should really be improving morale.

Since evidence to date indicates that a completely automated local-area forecast is not in the foreseeable future, I suggest that our development efforts be directed toward projects that will help the forecaster provide better weather service to his users, rather than automating forecasting functions for automation's sake. I put the recent work of producing worded local forecasts by computer in this latter category [1].

There is considerable evidence to show that present local-area forecasting routines are closely tied to the P.E.-model forecast output and that this tie is increasing. Over the past four years, operational forecasters have developed increased confidence in using NMC guidance to prepare their local forecasts. A large surge of this confidence came after the 6-layer P.E. model became operational in 1966. This confidence was earned by the model's excellent handling of routine as well as some difficult synoptic regimes such as the formation of cut-off lows along the West Coast and certain types of deepening troughs. Furthermore, useful numerical forecasts of moisture and thermal parameters were made available for the first time. These were soon used both qualitatively and quantitatively in preparing precipitation and temperature forecasts.

Most operational forecasts are now so closely tied to P.E.-model outputs that the accuracy of local forecasts rises and falls to a large extent with the accuracy of P.E.-model prognoses. As Dr. Stackpole pointed out yesterday, the P.E. model was not quite as good in handling many important precipitation situations last winter as it was in the winter of 1968-69. Verification data show that this resulted in decreased accuracy of local forecasts too.

## II. VERIFICATION COMPARISONS

This first slide (Figure 1) shows the verification by threat score of the P.E.-model measurable-precipitation forecasts (so-called PEP forecasts) and the final NMC manual products based on this P.E. guidance. The higher the threat score the better the forecasts. Note that the manual improvement over PEP is essentially constant and that it is in phase with the rise and fall of accuracy of the P.E. product.

The next slide (Figure 2) shows the marked changes in the PEP forecasts from the winter 1968-69 to last winter [2,3]. The two charts on the left give the threat score as a function of geography. The stippled areas indicate threat scores of over 50, i.e., relatively good forecasts, and the cross-hatched areas locate scores of less than 20, or rather poor forecasts. Note that the good (stippled) areas decreased and the poor (cross-hatched) areas increased from 1968-69 to last winter. The charts on the right of the figure give the bias of the PEP forecasts. One hundred percent signifies no under- or overforecasting of the frequency of precipitation. The stippling shows areas where the PEP model forecast precipitation more frequently than was observed. Note how dry the 1969-70 P.E. model was east of the Rockies with most biases less than 60%.

The slip in accuracy of the P.E. model last winter also shows up in both local temperature and precipitation forecasts. This slide (Figure 3) shows the temperature forecast verification for October-March (winter) 1968-69 (solid lines), and 1969-70 (dashed), for the Western Region of the Weather Bureau (eight most western states of contiguous 48 states). The periods refer to essentially 12-, 24-, and 36-hour forecasts of maximum and minimum temperatures. The right graph gives the verification of NMC forecasts. These NMC forecasts were man-machine mix products with the objective temperature-forecast guidance being the so-called Klein temperatures [4]. The middle graph is the verification of Weather Bureau forecast office temperature predictions and the left graph shows the verification of locally-prepared local forecasts. Note that these data show better performance in 1968-69 than last year. They also show that field offices considerably improved the guidance that they received from NMC.

This slide (Figure 4) is a similar verification of measurable precipitation forecasts using the threat score. The same things are evident although the improvement over NMC guidance by regional and local forecasts is much less. However, the best forecast for all three periods is still the locally-prepared forecast.

Dr. Stackpole indicated that the slip in performance of the P.E. model probably resulted from changing the handling of moisture in the model. Of course part of the deterioration could have been the result of a recurrence of synoptic regimes last winter that are not well handled by the current P.E. model. Nonetheless, the close tie between local forecasts and P.E.-model forecasts suggests that changes in the model should be made only after careful albeit limited testing to be reasonably certain that there will be no deterioration in operational output. If we are to promote maximum utilization of P.E. products by operational forecasters, model changes must be made with more discretion in the future. This is in contrast to the situation that existed 5 years ago when model changes could be made without too much regard for the operational forecaster because in those days his final forecast output was not so closely tied to the NWP output as it is today.

## III. USE OF P.E.-MODEL OUTPUT

The present P.E.-model output is used in essentially three ways in producing operational forecasts:

1) Directly. A few P.E. forecast parameters are given directly to the user. These are mostly upper-air parameters used by aviation interests. To my knowledge there are no P.E. forecasts given directly to the public in local forecasts.

2) As Guidance. Some P.E. products are available in final user form but the forecaster uses them only as guidance in preparing his forecast. Examples are QPF, boundary-layer winds, etc. Probably the most useful form in which this P.E. forecast guidance reaches the field forecaster is in the so-called FOUS teletype bulletin, i.e., the 48-hour forecast of selected P.E. parameters printed out at 6-hourly intervals for about 100 cities.

3) As Forecast Aids. Some P.E. forecast parameters are used both qualitatively and quantitatively in preparing the local forecast; but

in contrast to the uses just mentioned, the parameters are not explicitly a part of the final forecast. Examples are vertical motion, lifted-index, etc.

The general high quality of the forecast of these parameters has resulted in a significant increase over the past two years in the development and use of statistical studies that tie these P.E. forecast parameters to local weather conditions. Development of such studies is still in the ascendant and I think it will continue that way for many years.

The resulting local-area forecasting scheme that is evolving could be called a dynamic-statistical-manual scheme. A man-machine mix where the only manual input into the process is the local forecaster. This means that local forecasters are looking to the P.E. model to provide the general meteorological prognosis and statistical studies, or as I prefer to call them conditional-climatology studies, to refine the P.E. products to their particular local area. Therefore, our most productive use of P.E. data will be the dynamic-statistical approach, and we should probably judge the models in terms of its contribution to this type of forecast rather than the categorical indication of precipitation.

There is some controversy regarding the best technique to use in developing conditional climatologies when P.E.-model forecast parameters are used. One approach is to develop the statistics using observed parameters, i.e., the perfect-prog technique. The other is to develop them using P.E. forecast parameters, i.e., the imperfect-prog technique. I lean toward the use of the perfect-prog technique, because the results of such studies improve as the P.E. forecasts are improved. In any case there are merits to both approaches, and we are encouraging the development of both types of studies.

## IV. EXAMPLES OF STATISTICAL STUDIES

At this point, it might be good to look at a few examples of these approaches now in operational use. Many forecasters are using P.E. mean relative-humidity forecasts as input variables to their precipitation forecast studies. This slide (Figure 5) gives the start of a study for Astoria, Oregon using 12- and 24-hour P.E. forecasts of relative humidity and vertical-motion to get the probability of precipitation. The area above the heavy line indicates over 50% occurrence of precipitation [5].

Another example is this study (Figure 6) developed by the Southern Region of the Weather Bureau for stations in the southeastern part of the country. P.E. forecasts of relative-humidity, vertical-motion, and lifted index are related to frequencies of measurable precipitation occurrence within the next 6 hours.

An example of a perfect-prog study is that which we have developed for our region using a set of 500-mb flow types and the conditional climatologies of measurable precipitation occurring at each of our stations [6]. By this technique we are trying to add objectively a measure of detail to the weather implications of the P.E. 500-mb forecast. This slide (Figure 7) shows the probability of precipitation over western United States associated with this particular flow pattern. This program is now operational in that 500-mb P.E. initial, 12-, 24-, 36-, 48-, and 72-hour prognoses are typed by computer at NMC twice per day and the types are transmitted over teletype Service "C" for use by our forecasters. The end result is conditional climatological expectancies of precipitation for each 12-hour period of the 72-hour forecast for specific stations. Because the types are aimed at relating the probability of precipitation to the large-scale forecast flow, our next step in this study is to refine these probabilities using other P.E. forecast parameters within types. Since the history tape of the P.E. prognosis is used in the typing, we look for NMC to do the computer work, rather than doing it locally. I think most studies will eventually be based on P.E. forecast parameters and computed routinely at NMC with the end results sent to the field.

Another example of an operational dynamical-statistical program based on the perfect-prog technique is the so-called Klein max/min temperature forecasts. This is the temperature-

forecast guidance produced totally by machine using P.E.-model forecast parameters in regression equations [4]. NMC now transmits these temperatures to the field twice daily via teletype and facsimile.

It is interesting to note that many field forecasters are much happier with this totally machine-produced guidance, than the previous man-machine mix temperature guidance that was previously transmitted. Forecasters prefer the machine output because they can learn and take into account the biases and systematic errors in objectively-derived guidance for their particular area. When a centrally-prepared man-machine-mix product is used, the biases, etc., of the manual input are unknown. The success of P.E.-model forecasts is resulting in forecasters giving less weight to NMC man-machine-mix forecast guidance and more to purely machine products.

## V. PROBLEMS WITH COMPUTER FORECASTS

This is not to say that I am advocating machine-produced local-area forecasts—far from it. There are too many unacceptable aspects of a pure machine product of this type. For example:

1) Insensitivity. Insensitivity to critical values that may exist on a given day. For example, if fruit is in a certain stage of development, a temperature of 26 may be more significant than a temperature of 28. It is true that such critical temperatures could be put into a central computer program, but the local and changing character of such critical values makes this impractical. A man can do jobs of this type much better than a computer.

A forecaster often takes the existing and recent-past local weather into account in preparing and packaging his temperature and/or precipitation forecasts. The computer can't do this because significant local data will not usually be available. For example, he may highlight or play down a changing trend after a rainy spell depending on the state of local rivers or farms.

Objective forecasts as well as centrally-prepared man-machine-mix products can change the forecast for a specific location significantly every 12 hours such that "yo-yo" forecasts result much more frequently than they do now. "Yo-yo" forecasting is very disturbing to users and erodes confidence the user has in weather forecasts.

2) Time Lag. Computer-produced forecasts based on the P.E. model have a large lag-time (over 6 hours after data time) before reception in the field. For example we don't get the 12-hour P.E. forecast until 6 hours of that 12-hour period have passed. Twice each day the only P.E. guidance available is 18 hours old!

3) Detailed Information Missing. It is difficult to see how important detailed information such as radar and GOES-type satellite observations can get into the computer in time to be incorporated into short-range (<18 hours) forecasts. Many important weather changes that require warnings are the result of rapidly developing situations.

4) Computer Failure. A big problem at times is missing NWP products due to computer failure. As models become more sophisticated and computers get bigger, the use of back-up will be more difficult.

5) Normal Input-Data Missing. Missing input data can cause important forecast errors. Once a procedure is automated, the time period for accepting input data becomes very rigid. Should these data be only slightly delayed, they may not be used in the forecast computations.

A dramatic example of what can happen when there are data-input problems occurred last May. Important input temperatures for the Klein temperature equations were missed causing serious forecast errors for several days. This slide (Table 1) shows 48 hours of this period. Note that Klein temperatures for New York City were consistently in error 10 to 20 degrees. See Appendix I for further explanation of the forecast failure.

Therefore, there is now and will continue to be a need for the machine product to be processed by man before giving it to the public. This manual massage can best be done by the local or regional forecaster rather than by a distant forecast central. The local forecaster is often in the best position to take into account shortcomings in the physics of the model that affect his area. History shows that in large scale at least, manual adjustments to the NWP forecasts are decreasing and the time is only a few years away when operational forecasters will be able to accept NWP upper-air flow prognoses without modification. I believe other P.E. outputs, however, will continue to be modified by forecasters applying known systematic errors or biases of the forecasts for their local areas. Modification by intuition is no longer acceptable. This may still be done on occasion but it is not justified. Explicit P.E. forecasts in user format can best be tailored to local uses locally. For example the NWP meteorological input to air-pollution forecasts, soil-temperature forecasts, QPFs for water-supply regulation need local adaptation, especially in western United States.

And lastly, the local forecaster can take into account the latest local data to improve the machine forecast, which may be based on data as much as 18 hours old. The importance of use of the latest data was indicated by Mr. Roberts' discussion [7].

## VI. EXAMPLES OF MANUAL MASSAGE

An example of the type of physical reasoning that can be done locally is illustrated in this slide (Figure 8). At times there are strong diurnal changes of relative humidity (RH) that the model doesn't take into account. The solid line is the observed mean 1000-500 mb RH; the broken lines are three consecutive P.E. FOUS forecasts. Note that the 00Z input data are low and remain low; the 1200Z input data are high and the forecasts in general remain high. This could cause quite different objectively determined probabilities of precipitation. However, a man knowing of this diurnal change would modify the machine forecast accordingly. Also since the trends of the FOUS forecasts are more useful than the absolute forecast values, the forecaster can easily consider these trends in his massaging of the machine product.

History shows that manual massage by local forecasters is justified with regard to temperature. This slide (Table 2) shows two recent verifications which support this point.

During a two-week period last February, forecasters at 19 stations in the Weather Bureau's Southern Region, from Phoenix in the west to Atlanta and Miami in the east, improved on objective temperature forecasts by significant amounts. The left side of the slide (Table 2) gives the mean forecast errors for both types of forecast. The right side of the slide shows verification data for Missoula, Montana for last winter. The local forecasters, several of whom are meteorological technicians, through manual massage, made significant improvements in both maximum and minimum temperature forecasts.

When discussing the need for manual override, there is one factor that must be considered, but which has never really been documented: namely, exactly what are the desired accuracies and lead times for the many forecasts which are issued? Obviously these will vary from place to place and with the season and type of weather. But it is difficult to know how or what to automate until the limits of the results are defined.

## VII. SUMMARY

Operational forecasters are very much pleased with the substantial improvements in forecast accuracy over the last several years of P.E.-model forecast guidance. However, many forecasters, like myself, are not very optimistic about significant breakthroughs in accuracy of machine products in the future even with the use of finer-mesh and global P.E. models. Rather

it looks like slow, steady progress for the next decade. Therefore, I would like to revise the forecast of NWP improvement which I made at last year's conference as shown on this slide (Figure 9). The dot-dash line is the original forecast and the dashed line the revision showing steady but much slower progress. Certainly finer-mesh and global models should increase the accuracy of many parts of the P.E.-model forecast output. However significant progress in forecasting such parameters as temperature and moisture in the detail needed will probably be much slower. As Russell Younkin, Chief of the Quantitative Precipitation Forecast Branch of NMC, and one of the most knowledgable and capable precipitation forecasters in the country, pointed out in a recent consultant visit, "We usually make a significant step forward when we first incorporate gross features of the atmosphere into dynamic models, but we run into trouble and progress is much slower when we start introducing details." This certainly appears to have been the case when the P.E. model was modified from a single to multi-layered moisture model.

Therefore, the answer to the role of automation in production of local-area forecasts, at least for the next decade or so, seems to be through the use of dynamically-forecast parameters used in conditional climatologies (statistical studies) to produce more specific guidance. This guidance can then be used to provide high-quality local forecasts by manual adaptation. The statistical studies can be automated for operational use at either a central location like NMC or a regional forecast center or locally. Some type of computer link between the NMC computer and small regional-center computer appears to be most desirable. Also, the use of such studies gets away from categorical forecasts of dynamic prediction and gives us forecast guidance in probabilistic terms if we want it. This slide (Figure 10) depicts this idea graphically.

I would like to close by strongly endorsing Captain Kotch's statements which said to me, "Let's centralize the computer facilities and decentralize the manual effort. Let's transmit machine-produced meteorological products to the man on the forecast firing line for adaptation, packaging and delivery to the user" [8]. This type of man-machine mix will make the 1970s the golden decade for the operational forecaster. He will be close enough to the user to feel the pressure of his weather service needs, but so well supported by machine products that his productivity and job satisfaction will be increased and occasions of poor meteorological advice will be limited.

## VIII. ACKNOWLEDGMENTS

I gratefully acknowledge the generous response of my Weather Bureau colleagues, Dr. Ed Diemer, Alaskan Region; Mr. Ed Carlstead, Pacific Region; Mr. Carlos Dunn, Eastern Region; Mr. Larry Hughes, Central Region; and Mr. Paul Moore, Southern Region, to a request for their ideas on the subject of this paper.

I also appreciate the Weather Bureau's giving me the privilege of accepting the invitation to participate in this conference. However, the ideas expressed are my own and should not be considered as Weather Bureau policy.

## IX. REFERENCES

[1] Glahn, H. R., "Computer-Produced Worded Forecasts" ESSA Technical Memorandum WBTM TDL 32, June 1970.

[2] Numerical Weather Prediction Activities, National Meteorological Center, First Half 1969, July 1969, pages 26-31.

[3] Numerical Weather Prediction Activities, National Meteorological Center, First Half 1970, July 1970, pages 25-29.

[4] Klein, W. H.; Lewis, F.; and Casely, G. P., "Automated Nationwide Forecasts of Maximum and Minimum Temperature," Journal of Applied Meteorology, Vol. 6, No. 2, April 1967, pages 216-228.

[5] Williams, P., "Objective Forecasts from P.E. Output," Western Region Technical Attachment, No. 70-11, March 24, 1970 (U.S. Weather Bureau Manuscript).

[6] Augulis, R. P., "Precipitation Probabilities in the Western Region Associated with 500-mb Map Types," ESSA Technical Memorandum WBTM WR 45, parts 1, 2, 3, and 4. December 1969.

[7] Roberts, C. F., "Predictability of Local Area Weather." In these Proceedings.

[8] Kotsch, W. J., "Keynote Address for the 1970 Meteorological Technical Exchange Conference." In these Proceedings.

## APPENDIX 1

The following explanation of the large errors in the Klein maximum-and minimum-temperature forecasts for New York City during the period May 8-11, 1970 was given by Mr. Gordon A. Hammons of the Techniques Development Laboratory of Weather Bureau Headquarters:

> "Study of the observed and forecast temperature data during the period in question indicates that the large forecast errors are mainly due to missing computer runs, missing reports from New York City, and a large temperature increase in the same time interval.
>
> "There were three cases when no computer run was made: 12Z/9th, 12Z/11th, and 00Z/12th. In addition to the missing runs, the NYC observation was missing on 12Z/8th and on 12Z/12th. So, in this four-day period, there were five cases out of ten in which the latest min was not available to the system.
>
> "The May-June equations for New York City use the min temperature as a predictor for both the max and min forecast. The weight on this term is .44 for the min forecast and .88 for the max forecast. The large weights on the NYC min term will give a tendency to forecast persistence. Now, during the period in question, the temperatures warmed up considerably. The max went from the 60s to around 90, and the mins had about ten-degree increase.
>
> "It seems that the problem is a combination of a large temperature change at a time when runs were missed and reports were missing. The result is that, in these cases, the most current min was not used in an equation in which the min is an important factor. The unfortunate part is that the field does not know when a guess is used instead of a report. However, in the case of a back-up transmission, NYC should be made aware of the hazards of using the back-up transmission if the air mass at NYC has just changed."

TABLE 1

NEW YORK CITY MAY 1970

| INITIAL DATA | KLEIN FORECAST | OBSERVED MAX/MIN |
|---|---|---|
| May 8 00Z | 66 - 48 - 68 | 72 - 56 - 90 |
| May 8 12Z | 48 - 69 - 50 | 56 - 90 - 70 |
| May 9 00Z | 73 - 52 - 69 | 90 - 70 - 93 |
| May 9 12Z | 52 - 69 - 52 | 70 - 93 - 69 |
| May 10 00Z | 73 - 56 - 74 | 93 - 69 - 88 |

TABLE 2

KLEIN TEMPERATURE FORECASTS

Avg. 24-Hour Forecast Errors (°F)
19 SR Stations
10 - 28 February 1970

| | Max | Min |
|---|---|---|
| Obj. | 5.3 | 5.8 |
| Lcl. | 3.5 | 3.6 |

Avg. 24-, 36-, 48-Hour Forecast Errors (°F)
Missoula, Montana
December 1969 - February 1970

| | Max - Min - Max | | | Min - Max - Min | | |
|---|---|---|---|---|---|---|
| Obj. | 5.0 | 5.9 | 6.3 | 5.0 | 5.8 | 5.8 |
| Lcl. | 2.7 | 4.4 | 4.3 | 3.7 | 3.8 | 5.3 |

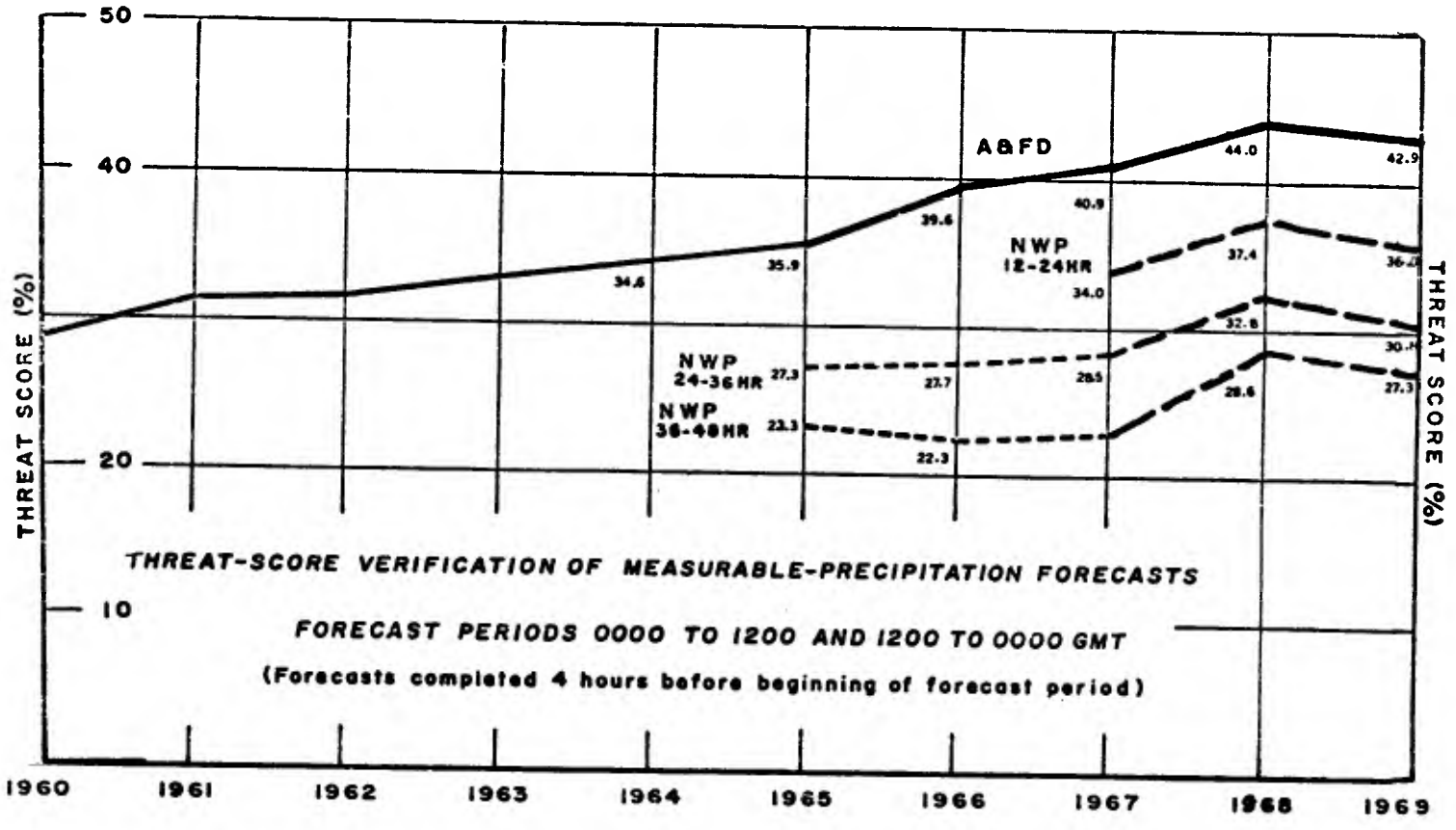


Figure 1. Threat-score verification of Measurable-Precipitation Forecasts 1960 through 1969. A&FD curve reference to subjective man-machine-mix forecast prepared by Analysis and Forecast Division of NMC.

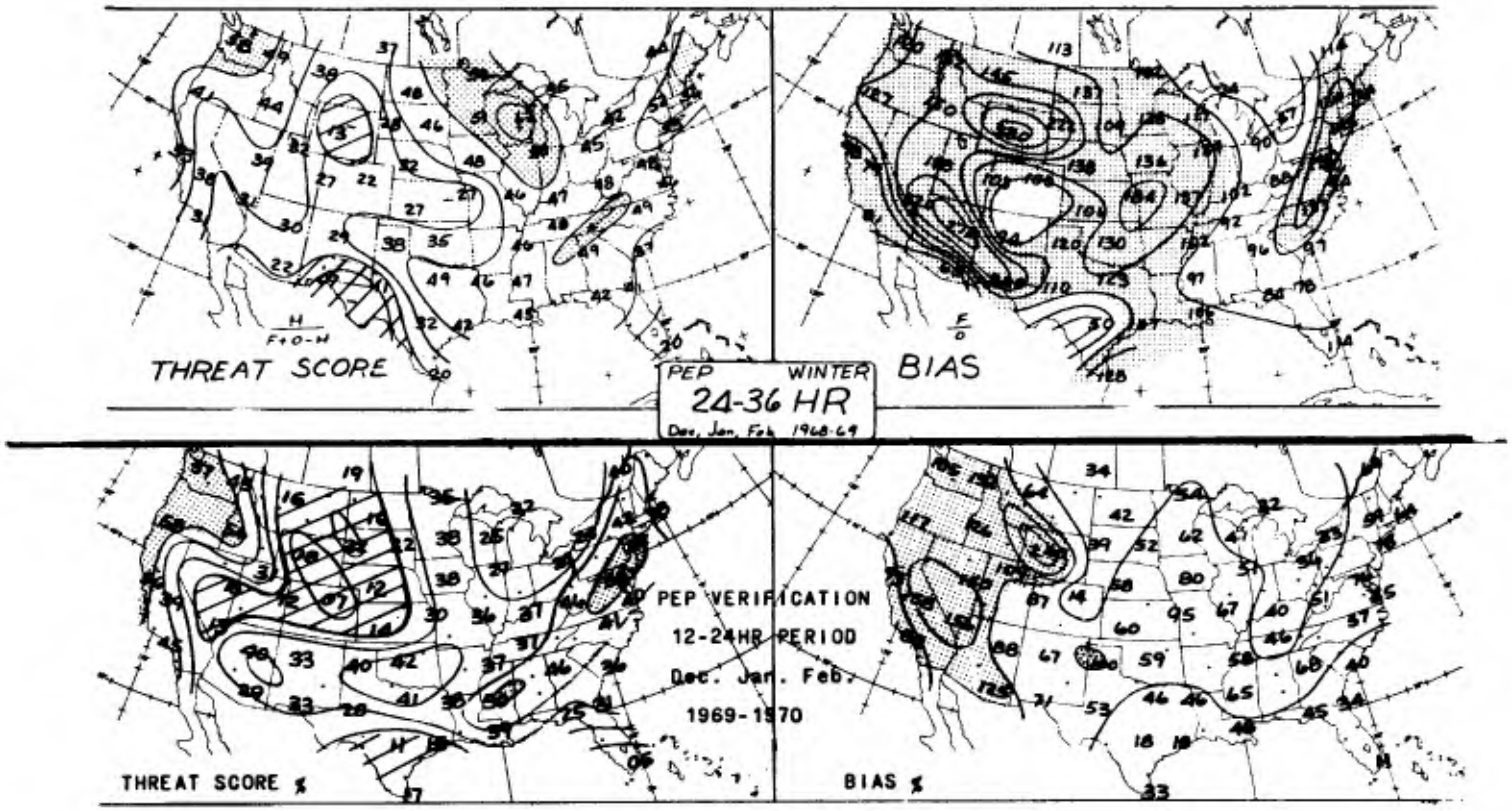


Figure 2. P.E. precipitation verification for forecasts of measurable precipitation (>.01") for 1968-69 and 1969-70 winter months (December, January, February). Threat score is:

$$\frac{\text{Hits}}{\text{Fcst} + \text{Obs} - \text{Hits}} \times 100$$

scores >50% are stippled; scores <20% cross hatched. Bias is:

$$\frac{\text{No. of Fcst Occurrences}}{\text{No. of Observed Events}} \times 100;$$

>100% is stippled. Charts taken from [2] and [3].

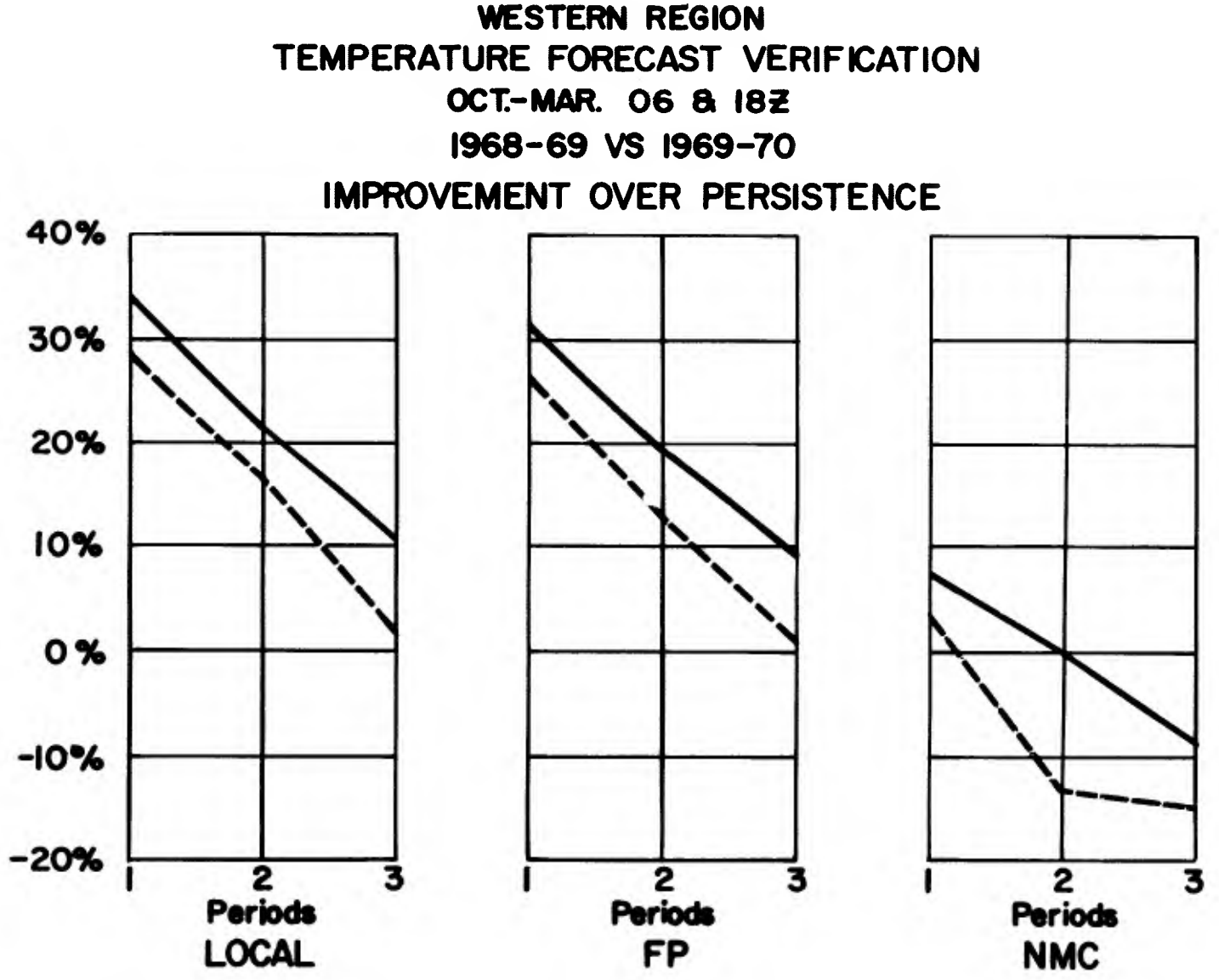


Figure 3. Verification of Western Region local maximum and minimum 12-, 24-, and 36-hour temperature forecast as improvement over 24-hour persistence for 1968-69 (solid) and 1969-70 (dashed) winters (October-March).

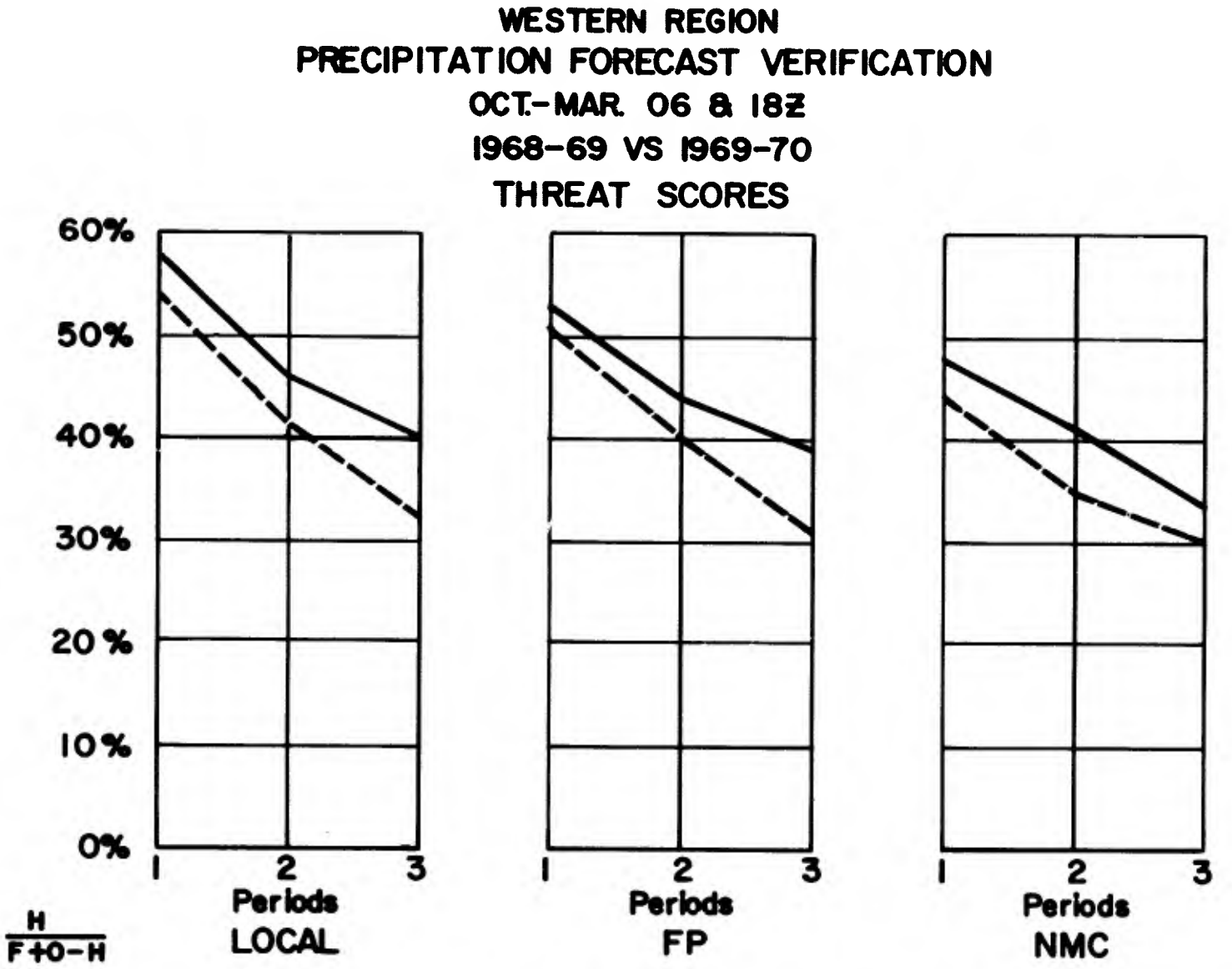


Figure 4. Verification of Western Region 12-, 24-, and 36-hour precipitation forecasts by threat score for 1968-69 (solid) and 1969-70 (dashed) winters.

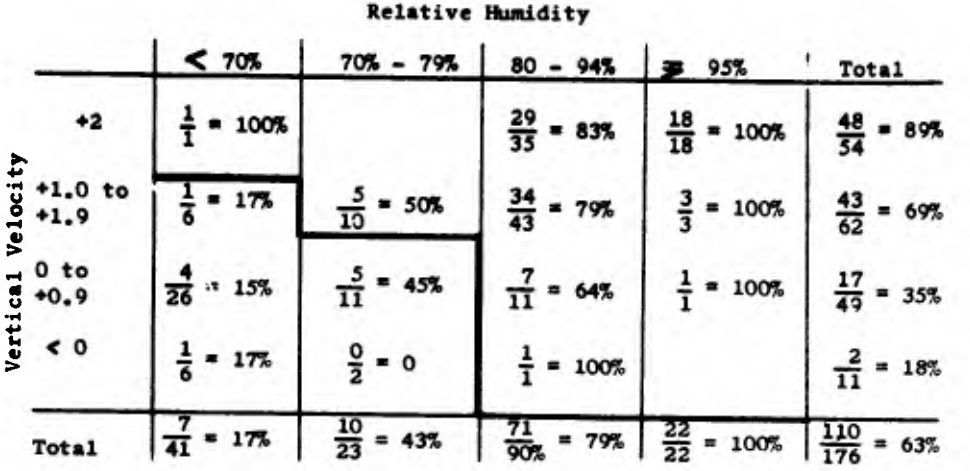


Figure 5. Relationship of RH and VV to occurrence of precipitation at Astoria, Oregon (12- to 24-hour forecast).

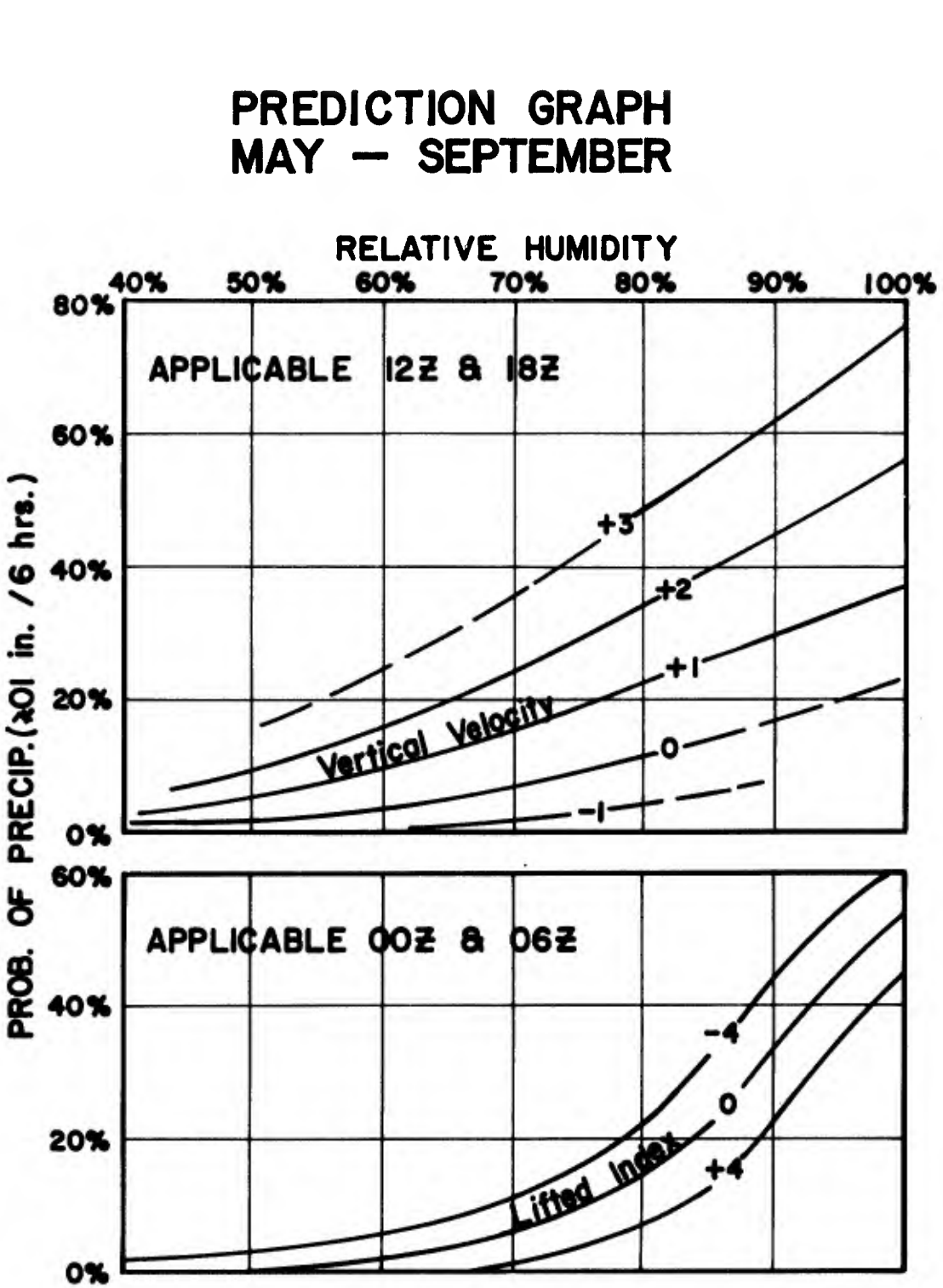


Figure 6. Southern Region statistical forecast aid for summer using P.E. parameters as input. Top graph is for the prediction of precipitation occurring midnight to noon -- 6-hour periods ending at 1200Z and 1800Z. Bottom graph is for the 6-hourly periods in afternoon and evening ending 0000Z and 0600Z.

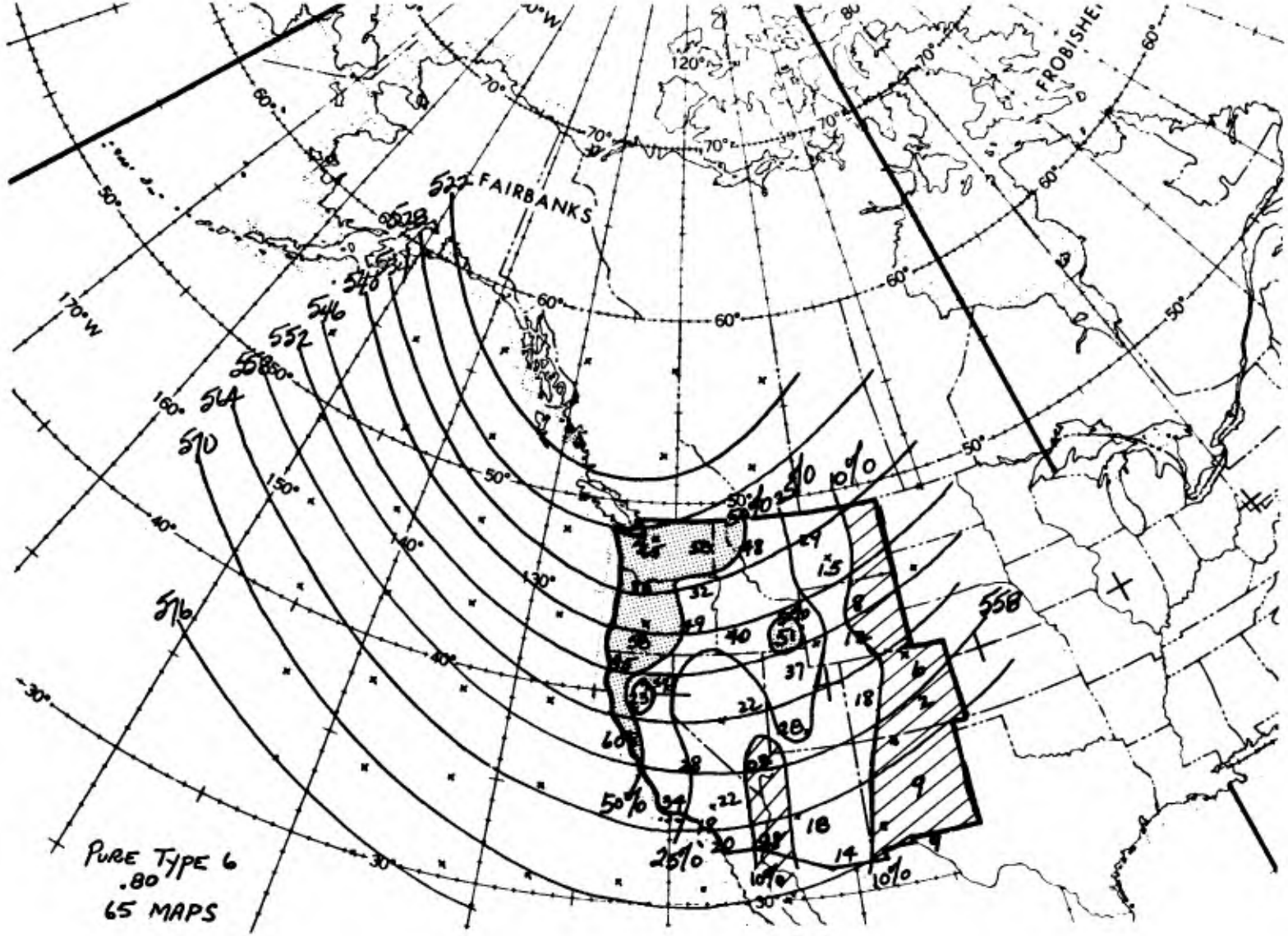


Figure 7. Western Region 500-mb winter type map 6 with probabilities of precipitation for 12-hour period after map time. Stippling indicates probabilities ≥50%; cross hatching indicates probabilities <10%.

# DIURNAL RELATIVE HUMIDITY CHANGES

## (Data from NAFAX NOS. 234-85 and Fous-2 Forecast Bulletins)

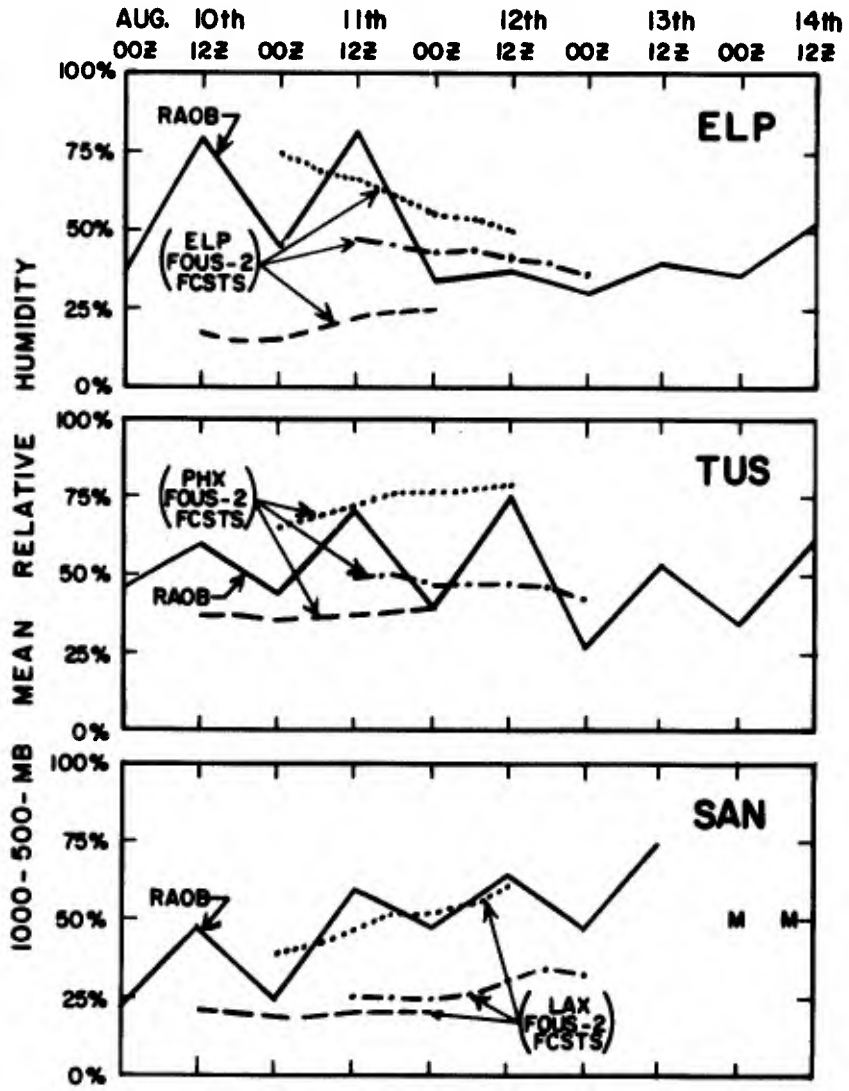


Figure 8. Plot of mean 1000-500-mb relative humidity for El Paso, Texas (ELP), Tucson (TUS), and San Diego (SAN) August 11-14, 1970 and related FOUS-2 mean relative-humidity forecasts for El Paso; Phoenix, Arizona (PHX); and Los Angeles, California (LAX). FOUS forecast starts with 12-hour forecast. Forecasts based on 0000Z P.E.-forecast runs are dash and dot-dash lines.

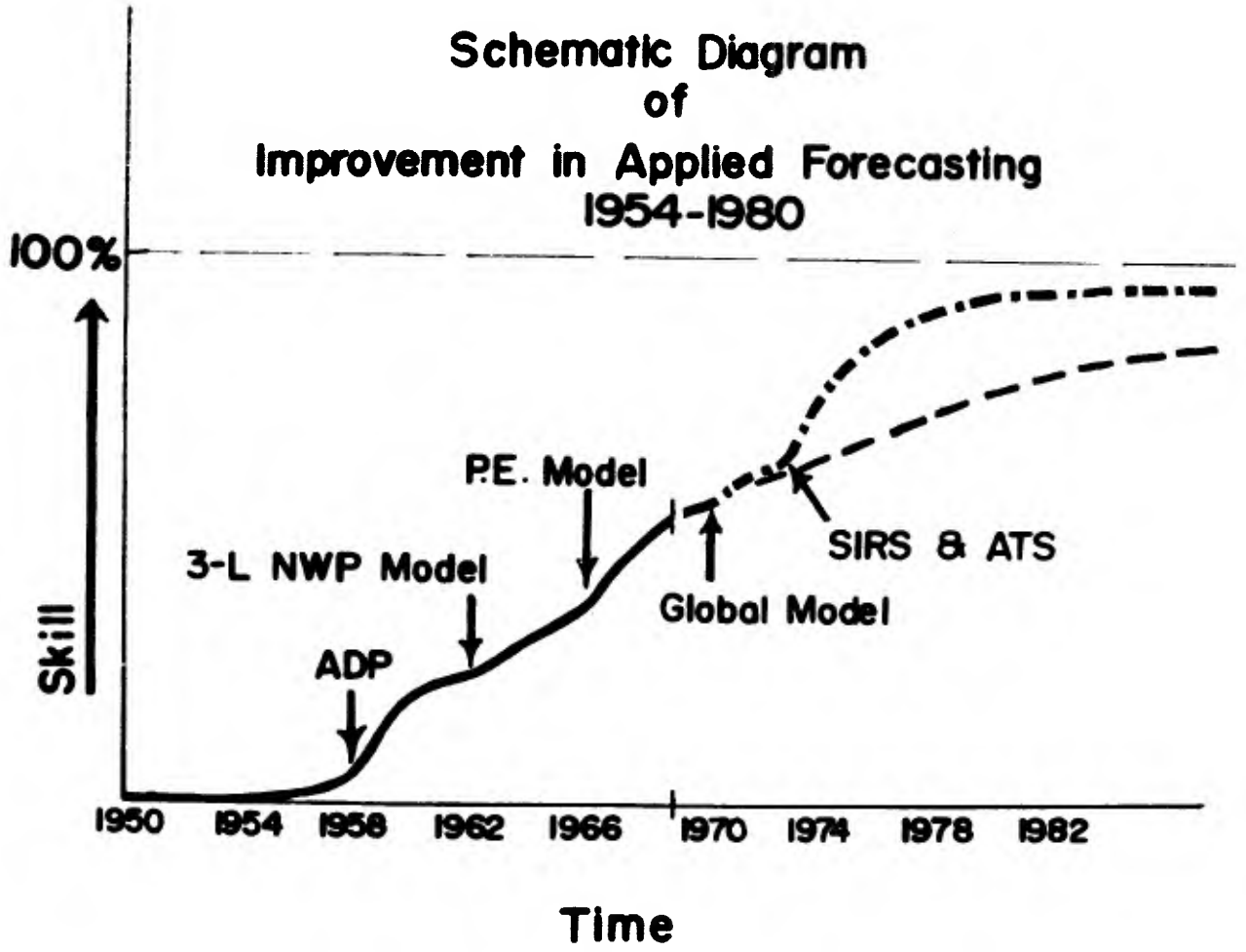


Figure 9. Schematic trend of improvement in applied forecasting, 1954-1982 revised. Dashed curve is revision of original forecast (dash-dot) from AWS TR 217, page 162.

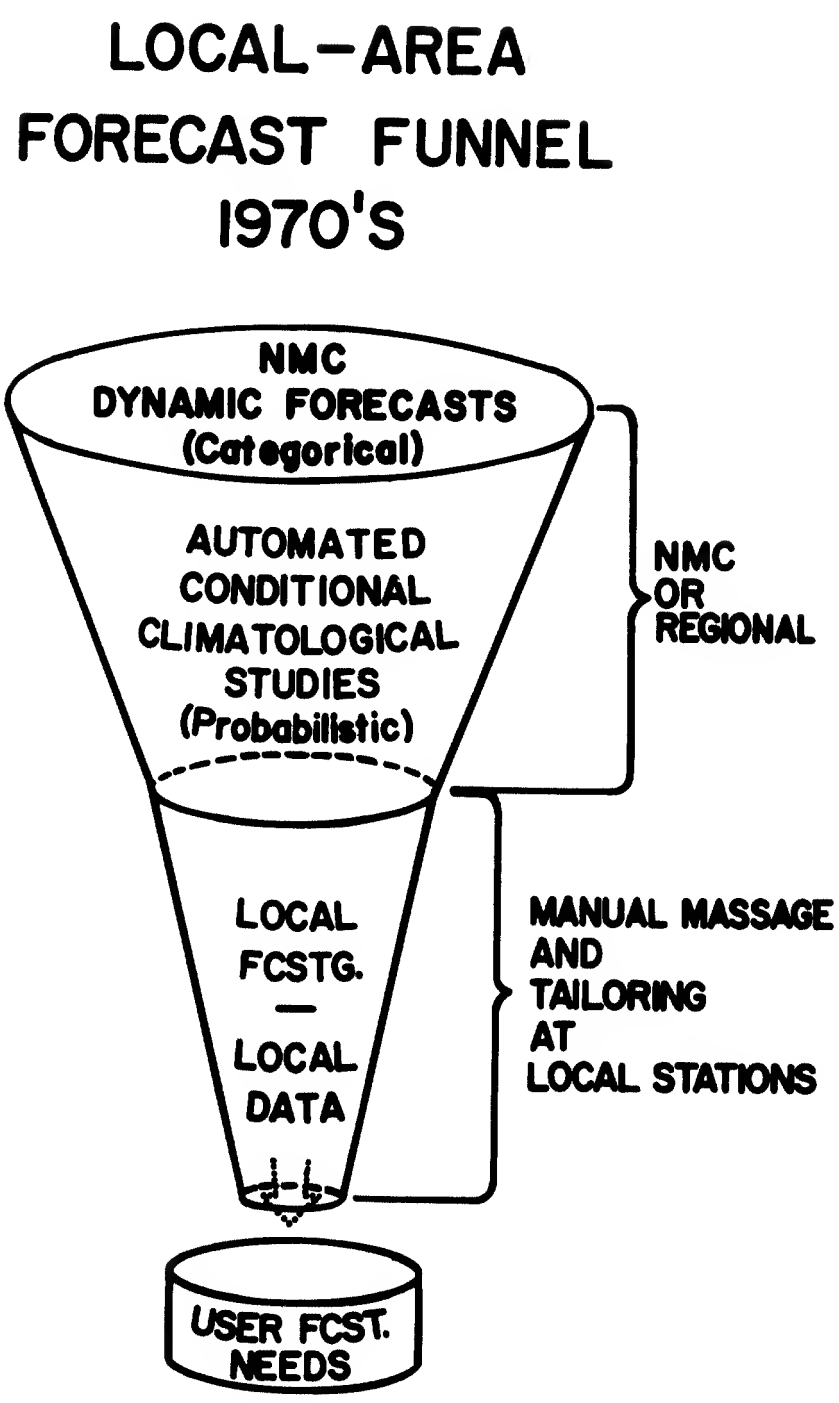


Figure 10. Graphical summary of machine-statistical-manual scheme of preparing local forecasts.

# PRELIMINARY RESULTS OF A PROGRAM FOR THE AUTOMATION OF TERMINAL FORECASTS[1]

Harry R. Glahn and Roger A. Allen

Techniques Development Laboratory, ESSA Weather Bureau
Washington, D.C.

## Abstract

The Weather Bureau's effort in terminal weather prediction for aviation is discussed. The REEP technique has been used for forecasting the probability of ceiling and visibility in each of 5 categories. After numerous experiments, it has been concluded that the use of data from a network of stations surrounding the predictand station provides better forecasts than the use of data from only the predictand station; however, the increase in accuracy probably does not justify the large increase in development costs.

At present we are working to develop and implement single-station equations at about 150 terminals. Objective forecasts of surface wind are now being transmitted to 79 stations in the eastern U. S. In the future, we plan to use the output from numerical models for ceiling and visibility forecasting as well as for wind estimation.

## OBJECTIVE

The Weather Bureau's present R&D program in terminal weather prediction is aimed at automating the principal parts of the terminal-forecast message. This means, of course, developing objective forecasting techniques which can be put into operation on a computer. This activity has been going on for quite a few years in a gradually evolving program. Most of the work has been on ceiling and visibility prediction, and, more recently, on wind. The program has evolved from the statistical development efforts carried on by Travelers Research Center some years ago, to an approach which is still largely statistical but incorporates the output of numerical prediction models. We anticipate, that, as numerical prediction results improve and include more details of the lower atmosphere, the prediction of cloud bases, fog, wind, ceiling, and visibility will also improve.

Our immediate objective is to automate the forecasting of ceiling, visibility, and wind at selected terminals and to transmit these forecasts to the Weather Bureau Forecast Offices which prepare the terminal forecasts (FT's) for transmission. It is planned ultimately to include additional information on weather, particularly severe weather, and to be able to provide a complete terminal forecast by computer techniques. Needless to say, this goal is still a long way off.

---

[1] This work has been supported by the Federal Aviation Administration, Department of Transportation.

## METHODS OF APPROACH

The method of approach has been primarily statistical. Forecast equations have been derived by developing a set of possible predictor variables, then screening these to select a subset to use in a linear multiple-regression equation.

Variations in the method of approach have been primarily in the kinds of predictors used—whether binary predictors or continuous variables. The predictand has been categorized into binary variables in the case of ceiling and visibility where it was desired to produce probability forecasts. For wind prediction, the predictand has been left in continuous form.

The ceiling and visibility predictands are shown in table 1. Each is divided into 5 categories which roughly provide the kind of detail needed for operational decisions. The narrow categories at low values of ceiling and visibility have the disadvantage of being extremely difficult to forecast, and the result is that the forecasts are not very good in the lower ranges of the scale. This is one reason for providing probability forecasts—whatever ability the prediction equations have to discriminate among categories will be represented in the probabilities.

Table 1. The five predictand categories of ceiling and visibility.

| Category | Ceiling | Visibility |
|---|---|---|
| | Feet | Miles |
| 1 | ≤ 100 | ≤ 3/8 |
| 2 | 200 - 400 | ½ - 1 3/8 |
| 3 | 500 - 900 | 1½ - 2½ |
| 4 | 1000 - 2900 | 3 - 4 |
| 5 | ≥ 3000 | ≥ 5 |

The statistical screening procedure used for ceiling and visibility has become known as the Regression Estimation of Event Probabilities (REEP) [1]. This technique screens binary predictors to produce a set of 5 equations which give the probability of each predictand category. A sample set of equations is given in table 2.

## OPERATIONAL TEST

An operational test of a system for providing guidance to field forecasters in ceiling and visibility forecasting was conducted during the 7-month period September 1965 through March 1966 [2]. REEP equations were developed for 3-, 5-, and 7-hour projections for airports at Albany (ALB), Baltimore (BAL), Washington (DCA), New York (JFK), Los Angeles (LAX), Chicago (ORD), Seattle (SEA), and San Francisco (SFO). Predictors in these equations were simple, observed variables from a network of stations surrounding the predictand station put into binary form. Forecasts were made from these equations at the National Meteorological Center four times a day and sent by teletype to the forecast offices.

Table 2. Eight-hour visibility prediction equations for Chicago O'Hare Airport.

| Order of Selection | Predictor | Regression Coefficients for Five Categories | | | | |
|---|---|---|---|---|---|---|
| | | ≤ 3/8 | ½-1 3/8 | 1½-2½ | 3 - 4 | ≥ 5 |
| | Constant | .034 | .120 | .181 | .259 | .405 |
| 1 | ORD VIS ≥ 5 | -.012 | -.036 | -.034 | -.062 | .144 |
| 2 | MLI WEA NONE | .002 | -.027 | -.042 | -.039 | .106 |
| 3 | RAN VIS ≤ 3/8 | .139 | .002 | -.040 | -.064 | -.037 |
| 4 | DSM VIS ≤ 7/8 | .116 | .067 | .004 | .066 | -.252 |
| 5 | MDW VIS ≥ 5 | -.014 | -.027 | -.055 | -.040 | .137 |
| 6 | MKE VIS ≤ 3/8 | .121 | -.005 | .054 | -.079 | -.091 |
| 7 | MSN WEA NONE | -.008 | -.022 | -.026 | -.067 | .124 |
| 8 | TOD 05-08 CST | -.012 | -.018 | -.033 | -.042 | .105 |

The forecast offices made ceiling and visibility probability forecasts before receiving the guidance (PRE-REEP forecasts). They also made probability forecasts after receiving the guidance (POST-REEP forecasts). The three sets of forecasts—REEP, PRE-REEP, and POST-REEP—were then compared, in terms of the P-Score [3], as to their improvement over Climatological Expectancy of Persistence (CEP). CEP is a probability forecast based only on the initial value of the predictand variable, time of day, and day of year [4]. The verification statistics are shown in table 3.

Table 3. Comparison of REEP and subjective forecasts. Average of about 5550 forecasts for ALB, BAL, DCA, JFK, LAX, ORD, SEA, SFO.

| | | % Improvement over CEP | | |
|---|---|---|---|---|
| | | REEP | PRE-REEP | POST-REEP |
| CIG | 3-Hour | 9.7 | 15.3 | 16.4 |
| | 5-Hour | 11.4 | 14.1 | 16.3 |
| | 7-Hour | 8.9 | 11.3 | 14.7 |
| VIS | 3-Hour | 4.6 | 7.4 | 10.6 |
| | 5-Hour | 5.3 | 4.1 | 7.4 |
| | 7-Hour | 7.6 | 3.1 | 7.4 |

It was concluded that the REEP forecasts were of some value as guidance in preparing terminal forecasts, but the value was rather small and irreguiar due to the inability of these particular equations to present the forecaster with high probabilities of forthcoming low ceiling and low visibility conditions in difficult forecasting situations. The experiment demonstrated the feasibility of computing and distributing such automated forecasts from a central computer and also showed that the statistical equations were stable when applied to a completely independent sample of data.

## BOOLEAN PREDICTOR TEST

A Boolean predictor is one that has been derived from two or more binary predictors by means of the logical operators "AND" and "OR". Using Boolean predictors in a linear regression equation is a way of taking into account complex and physically meaningful relationships. In this test, predictors were developed for Seattle 3-hour ceiling and visibility prediction which were Boolean combinations of the simple weather elements observed at a network of stations [5]. These Boolean predictors were intended to provide a more complete formulation of the conditions which precede specified categories of the predictand than was possible with the simple predictors used in the previous experiment.

An example Boolean predictor is shown in figure 1. In order for this predictor to have the value of 1, the specified conditions must be satisfied; otherwise, it will take the value of 0. It is intended to specify a weather situation occurring between 9:00 P.M. and 5:00 A.M. inclusive and during the period September 15 to November 15. The situation is characterized by low ceiling and low visibility at one or more of the stations Seattle, Paine Field, and McCord AFB or by relative humidity $\geq$ 90 percent and low wind speed at Seattle, or drizzle at Seattle.

| | |
|---|---|
| DOY | 259-074 and TOD 2100-0500 |
| AND | ( SEA CIG 200-900 AND SEA VIS $\leq$ 4) |
| OR | ( PAE CIG $\leq$ 900 AND PAE VIS $\leq$ 4 ) |
| OR | ( TCM CIG $\leq$ 900 AND TCM VIS $\leq$ 4 ) |
| OR | ( SEA RLH $\geq$ 90 AND SEA WSD 5-9 ) |
| OR | SEA WEA L, ZL ) |

Figure 1. A sample Boolean Predictor used for Seattle 3-hr. ceiling.

Table 4 shows the improvement of the P-Score over climatology (not CEP) for Boolean and simple predictors on development data. Although the 10,000 case samples for the Boolean and simple predictor experiments were both drawn from the same 10-year period, they were not identical and, therefore, the comparison is not as good as might be desired. Even so, it seems clear that the Boolean predictors, when applied to a network of surrounding stations, have little or nothing to offer in ceiling and visibility prediction over and above simple predictors from a similar network of stations. This conclusion, together with the fact that the definition of the complicated Boolean predictors is very time consuming and expensive, led us to abandon this particular approach.

Table 4. Comparison of simple and Boolean predictor results for Seattle 3-hour ceiling and visibility. 8172 development cases and 1800 test cases are combined.

| | % Improvement over Climatology | | | | | |
|---|---|---|---|---|---|---|
| CIG | ≤100 | 200-400 | 500-900 | 1000-2900 | ≥3000 | Total |
| Simple Predictors | 39 | 10 | 14 | 29 | 39 | 32 |
| Boolean Predictors | 38 | 12 | 14 | 25 | 39 | 30 |
| VIS | | | | | | |
| Simple Predictors | 41 | 12 | 10 | 12 | 44 | 30 |
| Boolean Predictors | 38 | 11 | 8 | 8 | 38 | 26 |

## SINGLE-STATION TEST

Because of the great difficulties encountered in processing data from a network of stations and in defining predictors from that network (which would be different for each network) it seemed desirable to see how much accuracy would be lost by using predictors from only the predictand station. Accordingly, single station equations were derived for 3-, 6-, 9-, and 12-hr. ceiling and visibility for New York (JFK), New Orleans (MSY), Chicago (ORD), and Seattle (SEA) [6]. A set of 339 simple and Boolean predictors were specified which were used for both ceiling and visibility, and for all projections and stations. Also, stratifications were made by season (winter and summer) and by time of day (A.M. and P.M.) in order to compare equations based on stratified samples with those based on the unstratified sample.

Table 5 gives the improvement in the P-Score over climatology for the stratified and unstratified samples. These results indicate that stratification does yield slightly better forecasts; however, the additional developmental effort required is probably not justified.

Table 5. Comparison of stratified and unstratified single-station forecast techniques. Average of CIG and VIS, 4 terminals, 3952 test cases.

| | % Improvement over Climatology | | |
|---|---|---|---|
| | Type of Stratification | | |
| | Season and Time of Day | Season | Unstratified |
| JFK | 22.4 | 22.8 | 22.6 |
| MSY | 10.1 | 9.6 | 8.6 |
| ORD | 19.5 | 19.6 | 20.0 |
| SEA | 12.7 | 12.1 | 10.3 |
| AVERAGE | 16.0 | 15.8 | 15.2 |

Table 6. compares the reduction of variance (which is inversely related to the P-Score) on dependent data for single-station equations and equations using a network of stations. Again, the same period of record (10 years) was used, but the samples were not identical. As might be expected, the network equations were better than the single station equations.

Table 6. Comparison of Network and Single-Station Equations on development data. Average of JFK, MSY, ORD, and SEA.

| | | % Reduction of Variance | |
|---|---|---|---|
| | | Network | Single Station |
| CIG | 3-Hour | 30.2 | 26.8 |
| | 5, 6-Hour | 21.6 (5-hr) | 16.8 (6-hr) |
| | 8, 9-Hour | 15.6 (8-hr) | 11.8 (9-hr) |
| | 12-Hour | 11.8 | 9.6 |
| VIS | 3-Hour | 22.4 | 20.2 |
| | 5, 6-Hour | 15.6 (5-hr) | 11.0 (6-hr) |
| | 8, 9-Hour | 10.4 (8-hr) | 6.8 (9-hr) |
| | 12-Hour | 7.8 | 5.6 |

## SURFACE WIND

Probably the best way to arrive at an objective estimate of the surface wind is to statistically relate the observed wind to the forecasts of wind, and perhaps other variables, obtained from numerical (dynamic) models. In order to use this Model-Output Statistics (MOS) technique, a sample of forecasts from the model must be collected for analysis. Such a sample of predictor data, as well as predictand data, was available from TDL's SAM Project [7].

Separate regression equations were developed for estimating the U and V wind components and the wind speed valid at 1200 and 1800 GMT for each of 10 stations in the eastern U. S.—Albany, Atlanta, Baltimore, Cleveland, Cincinnati, Washington, New York, New Orleans, Chicago, and St. Louis [8]. Data for April through September 1967 and 1968 were used.

The equations were evaluated for each day in April and May 1969 for which SAM data tapes were available. The wind forecasts in the FT's made at the Weather Bureau Offices were used for comparison. Since the FT's do not mention wind if the speed is expected to be less than 10 kts, the comparison was made in two ways.

For all those cases where the FT's included wind, and objective forecasts were available, the root mean square error (RMSE) of direction (computed from the U and V equations) and speed were computed. Also, contingency tables for speed were prepared by considering the FT forecast of wind to be under 10 kts when wind was not mentioned. From these contingency tables, skill scores and percent correct were computed. These scores are shown in table 7.

Table 7. Comparison of official FT and Objective Wind Forecasts for 10 stations in the eastern U.S. for April and May 1969.

| VALID TIME (GMT) | PROJECTION (HR) | FORECAST | DIRECTION RMSE (DEG) | SPEED (kts) | | |
|---|---|---|---|---|---|---|
| | | | | RMSE | SKILL SCORE | PERCENT CORRECT |
| 12 | 5 | OBJECTIVE U,V EQUATIONS | 35 | | | |
| | 5 | OBJECTIVE SPEED EQUATION | | 3.5 | .37 | 76 |
| | 3 | FT | 33 | 3.6 | .36 | 71 |
| 18 | 11 | OBJECTIVE U,V EQUATIONS | 47 | | | |
| | 11 | OBJECTIVE SPEED EQUATION | | 3.5 | .29 | 54 |
| | 9 | FT | 50 | 4.3 | .24 | 49 |

Table 7 indicates that the directions from the objective forecasts were as good as those from the FT's and that the speeds from the objective were better than those from the FT's. The projections of the objective forecasts (5 and 11 hours) refer to the latest data used (0700 GMT). Actually the forecasts could be available to the field forecasters before 0900 GMT. The FT's were prepared with 0900 and perhaps 1000 GMT data available; transmission time for the forecasts is 1045 GMT.

## FUTURE PLANS

Future plans for our aviation weather program are based on the realization that forecasting for aviation has much in common with forecasting for other purposes. Although there is a difference in emphasis, the overlap with public weather forecasts is considerable. The same observations are available and must be processed for each forecast. We are depending more and more on numerical models and we must use the forecasts from one or two of these for several purposes.

Consequently, we are pursuing a more integrated program within TDL. The SAM model, originally designed for public weather purposes, is being extended to the West Coast and is being tailored to provide numerical input to the aviation forecasts. Also, we intend to investigate the critical problem of severe convective weather in the terminal area—a different emphasis, but not unrelated, of course, to our severe-storm work for non-terminal areas.

These are rather long-range efforts. In the more immediate future we plan to develop single station equations for ceiling and visibility for about 150 terminals and transmit forecasts from them over teletype to be used as guidance. At the same time, we will be experimenting with the output from the numerical models used operationally by the Weather Bureau in order to determine the usefulness of this type of information in ceiling and visibility forecasting. Surface wind forecasts are already being made for the eastern one-third of the U. S. and transmitted to the field as part of the SAM bulletin. This work will be extended when the data become available from the revised model and will eventually form a part of an automated FT.

## ACKNOWLEDGMENTS

The authors wish to thank the many members of TDL who contributed in various ways to this report.

## REFERENCES


1. Miller, R. G., "Regression Estimation of Event Probabilities." Tech. Report No. 1, Contract Cwb-10704, The Travelers Research Center, Hartford, Conn., 1964, 153 pp.

2. Allen, R. A., "Operational Evaluation of a Ceiling and Visibility Prediction Technique." Report No. FAA-RD-70-17, The Federal Aviation Administration, Washington, D. C., Dec. 1969, 19 pp.

3. Brier, G. W., "Verification of Forecasts Expressed in Terms of Probability." Monthly Weather Review, 78(1), 1950, pp. 1-3.

4. Enger, I., Russo, J. A., Jr., and Sorenson, E. L., "A Statistical Approach to 2-7-hr Prediction of Ceiling and Visibility." Tech. Report No. 2, Contract Cwb-10704, The Travelers Research Center, Inc., Hartford, Conn., Sept. 1964, 48 pp.

5. Allen, R. A., "Predicting Ceiling and Visibility with Boolean Predictors." Report No. FAA-RD-70-37, The Federal Aviation Administration, Washington, D. C., May 1970, 37 pp.

6. Allen, R. A., "Single Station Prediction of Ceiling and Visibility." Report No. FAA-RD-70-26, The Federal Aviation Administration, Washington, D. C., April 1970, 48 pp.

7. Glahn, H. R., Lowry, D. A., and Hollenbaugh, G. W., "An Operational Subsynoptic Advection Model." ESSA Technical Memorandum WBTM-TDL 23, July 1969, 26 pp.

8. Glahn, H. R., "A Method for Predicting Surface Winds." ESSA Technical Memorandum WBTM-TDL 29, March 1970, 17 pp.

# AN APPROACH TO AUTOMATED SUPPORT TO FIELD ARMY OPERATIONS

James F. Appleby

Atmospheric Sciences Laboratory
US Army Electronics Command
White Sands Missile Range, New Mexico

## INTRODUCTION

At the last Technical Coordination Conference, Dr. Swingle,[1] Atmospheric Sciences Laboratory (ASL), discussed a Qualitative Material Development Objective[2] for an Automatic Meteorological System for 1985 (AMS-85). He discussed in detail the philosophy and design concept of such a system. This afternoon I would like to discuss an approach to the development of such a system and briefly outline a study that is being conducted to determine if this approach is feasible.

The Army has requirements for meteorological information in many types of operations, including Army aviation, chemical defense, radiological and bacteriological defense, artillery fire support, amphibious assaults, river crossing operations, and trafficability. Automatic Met System 85 must be designed to fulfill all these requirements. Its role will be to provide the best possible information to meteorologically dependent or affected weapon systems and tactics. In other words, it should supply current meteorological information tailored to meet the requirements of the user.

Many Army units involved in the operations I mentioned above have meteorological equipment on their TO and E's and take routine observations in support of their own operations. Our approach to an automated support system will be to investigate the feasibility of using these data to develop a small-scale data base of meteorological information which can be used to supply tailored information to Army operational units.

Our concept of the development of AMS-85 is to begin with a relatively simple system with limited capabilities, but including all the functions of AMS-85— collecting, editing, storing, analysing, predicting, and distributing of atmospheric information. This initial system will be incrementally expanded in a hierarchy of atmospheric support systems, each of increased capability and complexity, culminating in 1985 with AMS-85. Under this concept the meteorological service could progressively improve as the state-of-the-art in small-scale meteorology advances and more efficient systems can be devised.

The relationship of the AMS to the Air Force Global Weather System is shown in Fig.1.

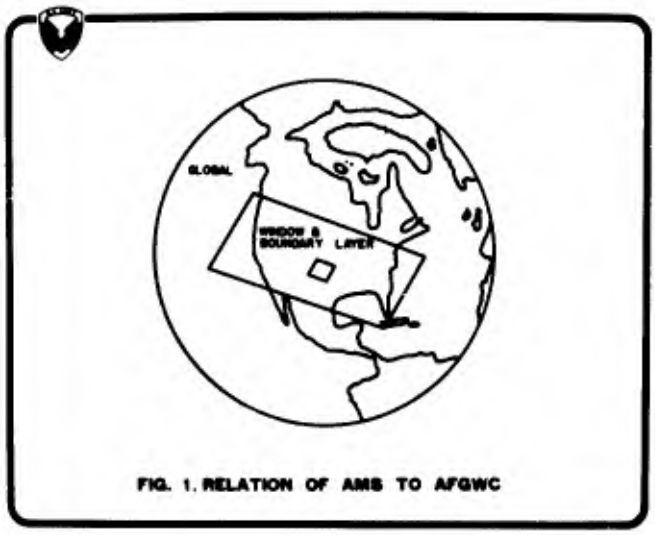


FIG. 1. RELATION OF AMS TO AFGWC

The system would begin where the global, window and boundary-layer models leave off and cover only the Field Army's specific area of interest. Local Army observations would be used to provide greater detail in the Army area. Schematically, the AMS-85 would look like Fig.2.

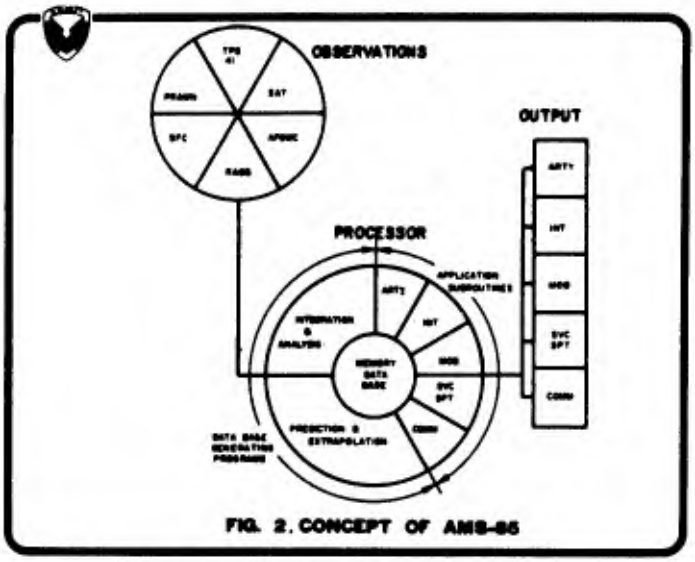


FIG. 2. CONCEPT OF AMS-85

Inputs to the system are shown in the circle labeled Observations. The basic framework of the system would be the Air Force Global Weather Central Data Base for the Army area. This data base would give the system a finished product based on the world-wide data analysis and prediction system. The radiosonde stations of the artillery would provide current data to increase the density and update predictions that are several hours old. Surface observations from air strips, chemical smoke battalions and other units with meteorological equipment on their TO and E's are another source of meteorological data. In the future, portable radar wind equipment (PRAWN) and the TPS-41 radar would be another source of observational data. Satellite systems could also contribute information for the system. The heart of the system would be the processor which contains the computer programs which would integrate these data into a data base of meteorological parameters. It would also contain a means of making short-range extrapolations or predictions to keep the data base current between observations and application subroutines which would extract data from the base and format it in a form the user requires.

This approach presupposes that communication and facilities for rapid data processing and analysis will be available. At this time it is premature to state specific requirements, since the technical feasibility of the approach has not been proven. However, in the future (approximately 1977) the first increment of the Tactical Operation System (TOS)[3] will be deployed in the Field Army. "The TOS is a modern data processing system using high speed electronic computers and efficient means for user communications. It is designed to process vast amounts of data to enable commanders and their staffs to base decisions on information that is complete, correct, and timely." As initially conceived, TOS encompasses 18 functional areas, including weather. Fig. 3 shows the equipment configuration of the TOS[4].

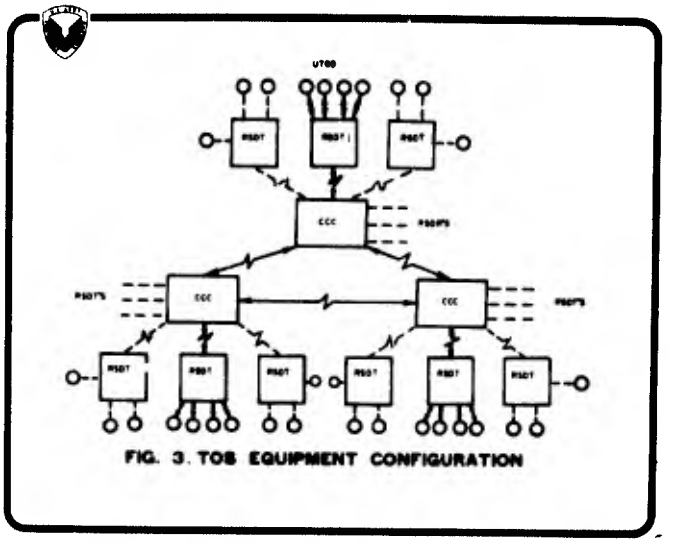

FIG. 3. TOS EQUIPMENT CONFIGURATION

Each Central Computer Center (CCC) is interconnected and is capable of managing 16 full duplex communication channels. Remote Station Data Terminals (RSDT) serve 8 input/output devices (UIOD) and will have some computation capability. Thus, if the software for an operational meteorological support proves feasible, much of the hardware required by the system is already scheduled to be deployed in the Field Army.

## THE INITIAL SYSTEM

The initial system will be limited in scope; it will deal primarily with the area of artillery operations. Artillery meteorological requirements are clearly defined and recognized by Command and Staff. The system will include the basic function of collection, analysis and distribution of meteorological information, functions which must be included in AMS-85. The data base required for artillery support is essentially the same as that needed for general Army support, and the existing artillery meteorological system will serve as a base from which to work. The scope of the initial AMS is indicated in Fig.4 by the hatched areas.

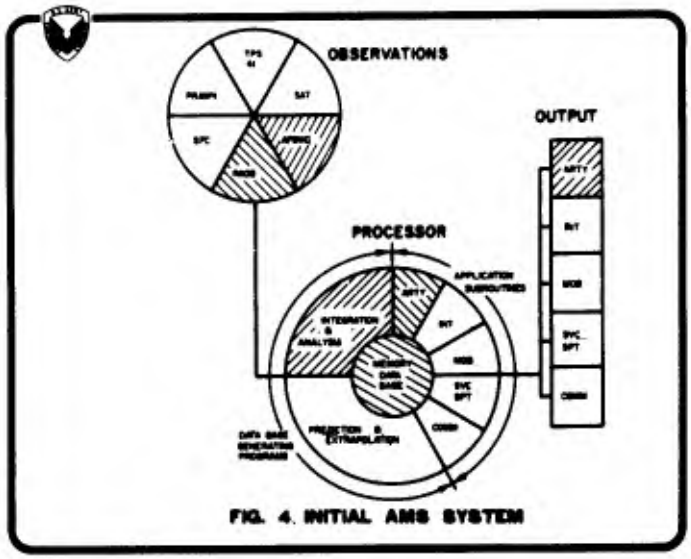


FIG. 4. INITIAL AMS SYSTEM

The essential concept of the initial system is the "synthetic ballistic observation." Each user (normally fire direction centers) will be able to ask TOS for a ballistic Metro message valid for a given place at the current time, and the system will synthesize the required message from meteorological data stored in TOS.

The basic weather data stored in TOS will be the regional analyses and forecasts furnished by the Air Weather Service, supplemented with the upper-air observations taken by the artillery meteorological sections. The data base would be updated as new upper-air observations become available.

## FEASIBILITY OF SUCH A SYSTEM

There are some fundamental questions that should be investigated to determine if this approach to automatic support to artillery is feasible. First and foremost, we must prove that an analyzed field is more representative of the ballistic state of the atmosphere along the trajectory of a projectile than a single sounding.

The method now used by artillery smooths the single sounding in the vertical by determining mean ballistic parameters for a zone. These zones range from 200 meters to 1000

meters in depth. A recent study[5] sponsored by the Atmospheric Sciences Laboratory indicates that objective techniques can be used with some success to derive the horizontal distribution of ballistic parameters from synoptic soundings. Deflection errors in artillery firing were on the average smaller when corrections were computed from the analyzed data than those from single soundings. This study and the success of the present artillery system tend to justify a horizontal as well as vertical smoothing of synoptic observations.

Another factor to be considered is the vertical and horizontal resolution required in the data banks to satisfy the artillery's requirements. To some extent, the horizontal resolution will be limited by the spacing of the Artillery Meteorological Sections. However, computation time for the analysis and the amount of data storage must be considered. It remains to be seen if an optimum balance can be reached that will satisfy the requirements and still be within a reasonable limit for a time-sharing computer system. We will investigate problems of this type.

## APPROACH

To investigate these problems, we will build a data base of wind, temperature and moisture for a single time period over a simulated Army area (approximately a square of 500 km on a side). This data base will be developed from real data using state-of-the-art techniques. We will test the results derived from the data base against the requirements being determined under a separate study on information criteria for artillery.

During the tornado season, the National Severe Storms Laboratory (NSSL) operates a dense network of meteorological observing stations in Oklahoma, including nine rawinsonde stations. During storm periods, the rawinsonde stations take observations at intervals of three hours or less, analogous to artillery metro-section operations. We have a cooperative arrangement with NSSL whereby they will furnish two weeks of data taken this past spring. In addition, the AWS Global Weather Central at Offutt AFB has furnished its data base (observations, analyses, and forecasts) for the midwestern part of the United States for the same period. This will be the first increment of our basic meteorological data for use in the tests.

Additional data of the same type will be gathered next year, and other data will be obtained as needed. The area covered by the National Severe Storms Network is small in comparison to the area normally considered to be occupied by a Field Army; however, it should be adequate to apply and test fine-mesh analysis techniques[6]. The upper air network is more dense than is usually employed in the Field Army. The approximate spacing is 25 km as compared to approximately 35 km in Viet Nam. This is an advantage, since observations can be omitted from the analysis for testing purposes. The Army Ballistics Laboratory has furnished another tool which we intend to use. It is a computer program for simulating artillery fire which includes the meteorological corrections. In this way the effect of analysis as function of distance from an observation can be assessed in terms of its effect on the impact of the projectile.

## PROGRESS

Our major progress to date has been to develop the capability to read the Air Force Global Weather Central tapes on our computer system. This may sound trivial to those of you who have never exchanged data tapes with people working with different computer systems. We have tentatively selected a horizontal grid spacing of 1/8 of the global weather northern-hemisphere grid (approximately 45 km) for a data base. The vertical spacing will be the same as that used in the AFGWC data base over the United States.

Several techniques have been selected to develop data bases. One is an adaptation of schemes used in the initialization for numerical prediction. Observations will be used to update and increase the detail of the first-guess AFGWC predictions. The fine-mesh analysis procedure of successive corrections with a variable scan radius used by GWC[7] will be used. A second approach based on fitting the data with polynomial fits to scalar fields will also

be tried. In this approach observations will be weighted more heavily than predicted data. Computer programs for these have been prepared. A third approach based on the objective-analysis method of Endlich and Mancuso[8] for examining environmental conditions associated with severe storms is being programmed. In October when we are scheduled to receive the radiosonde data from the Severe Storms Laboratory, a comparison of the methods will be made.

Some work has been done on examining the effects of the vertical resolution of meteorological parameters used to correct artillery fire with the simulation program. Preliminary results indicate that doubling the depth of the present artillery zones for computer messages causes a displacement of 15 meters; a second doubling of the zones gave no appreciable change over a 9000-meter range. More complex vertical and horizontal meteorological structures will have to be investigated with this program.

## SUMMARY

The deployment of the Army Tactical Operation System in the Field Army will provide a means of exploiting many of the technical advances of the past few years and those that will be made in the near future. Military Commanders and weapon systems can have rapid access to meteorological data that it has not been practical to provide before. I have outlined briefly a concept of an approach to operational weather support and a limited study to determine if a suitable data base can be established to support artillery fire. It may be possible to develop an automated meteorological system to serve Army operations in the field without increasing personnel or materiel requirements or the burden on Army units now providing their own meteorological support. If we find an automated support to artillery is feasible, the concept will be extended to other requirements.

## REFERENCES

1. Swingle, Don: "The Army's Automatic Meteorological System," Oct 69, Proceedings of the AWS Technical Exchange Conference, 14-17 July 1969, AWS Tech Report 217.
2. QMDO Plan 1512b(6): "Automatic Meteorological System," Revision 1 April 1970.
3. Government Affairs Institute: "Tactical Operations System (TOS)," Interim Report, Tech Info Rpt 6.2.11. Prepared for the US Army Materiel Command, Contract DAAG39-69-C-001, Washington, DC, Feb 1969.
4. Computer Systems Command: Software Design Concept, TOS Operating System, Annex C to the Initial System for the Provisional Automated Tactical Operation System, Nov 1968.
5. Ostby, F. P. Jr.; Pandolfo, J. P.; Veigns, Keith W.; Spiegler, David B.: "Ballistic Wind Study," Final Report No. 4, Tech Report ECOM 01377-F, Contract DA 28-043-AMC-01377(E).
6. Techniques Development Laboratory: "An Operational Oriented Small Scale 500 Millibar Height Analysis Program," Mar 1969, WBTM TDL 19, US Dept Commerce/ESSA.
7. Fleming, CPT Rex J.: "Air Force Global Weather Central Fine-Mesh Upper Air Analysis Model," Dec 1969, AFGWC, AWS(MAC) Offutt AFB, AFGWC Tech Memo 69-2.
8. Endlich, R. M., and Mancuso: "Objective Analysis of Environmental Conditions Associated with Severe Thunderstorms and Tornados, Jun 1968, MWR, Vol.96, No. 6, Pg 342-350.

# NUMERICAL PRODUCTS AS SPECIFIC OPERATIONAL FORECASTING AIDS

Earl C. Kindle, Richard L. Crisci, and Joseph T. Schaefer

Navy Weather Research Facility

The use of discrete horizontal slices for analyzing and predicting the atmosphere has developed from the weather-data collection and processing capabilities which evolved through the first 40 years of this century.

The introduction of the electronic-computer capability presented a whole new dimension in the potential approach to analysis and forecasting. However, it has for the most part, and with few exceptions, been used to present an increased and confusing number of horizontal slices which differ little from those used during WW II.

Until recently, the pre-1940 technique of weather forecasting had not changed much. It can be described as two simple steps.

First: Make a projection of a horizontal slice of the atmospheric parameters.

Second: Fit a model of weather phenomena to this projection.

Prior to 1950, the major problem in this two-step operation was reliable prediction of the horizontal slices; and quite appropriately, the dominant proportion of research effort was directed accordingly. However, the advent of numerical prediction has markedly improved the quality of the predicted horizontal slices and now the stumbling block to improved forecasting is the filling in of weather phenomena once the predicted slabs of winds, pressures and temperature have been provided. Yet, inertia momentum has left the old proportion of research efforts still with us.

Unquestionably, as a result of the marked improvement in operational prediction of the horizontal slabs, some improvement has filtered down to the actual forecasting—"trickle" is probably a better word. Nevertheless, despite the fact that a great deal of serious weather is independent of frontal activity, the primary formal rationale available to the forecaster today for filling in the weather on the predicted horizontal slices is a simple, obsolescent, overworked, frontal-cyclone model. It is no surprise that verifications of actual weather forecasts have a hard time beating persistence.

Based upon this low level of success, the managerial levels, prompted by the prospects of bigger computers, and continually striving for administrative hygiene, are naturally attracted to arguments for a womb-to-tomb automated system. If you can't be accurate, you may as well be neat. But the use of a larger computer would amount to just sweeping our failures under a bigger rug.

A growing consensus of our profession concludes that the major problem in improved prediction of the operationally significant phenomena is specification of the mesoscale processes from predictable synoptic-scale parameters. Given the synoptic-scale numerical predictions, it is presumed that the development and intensity of the operationally-significant mesoscale phenomena evolve through two major processes:

First: Interaction within the large-scale processes "per se" producing such features as squall lines, isolated but intense rain, clear-air turbulence, sudden wind shifts, etc.

And Second: Interaction of the larger-scale flow with high-resolution topographic features, such as Mr. Cormier discussed yesterday afternoon.

With regard to the latter, these influences, being fixed and knowable to a fair degree of precision, can be incorporated at the time of availability of the operational numerical product. The results of efforts to date are quite promising for the early realization of this capability.

With regard to the former (interaction within the large-scale processes), the determination of specific mesoscale features that ensue from the cascading

effects of discrete scale interactions is not so promising. While the recent research programs and laboratory operation of some higher-resolution models indicate promise for a collective prediction of these resulting mesoscale consequences (such as characteristic frequencies, and intensity of the variability over a large domain), the timing and intensity of specific events is not likely to be predictable in the same way.

But looking at resources available to us, it seems plausible that these mesoscale features could become predictable on a short-range basis if a facile means could be developed to compare the way the numerical models develop smaller-scale features with the way the atmosphere is actually behaving during the early period of the forecast. This could be done, for example, by comparing and diagnosing overlays of space and time cross-sections of the predicted and observed wind, temperature, moisture and weather events in the context of satellite, radar and other observed data. This procedure would require the availability of special computation procedures used in a specially-tailored data storage, retrieval and display system.

For example, convective activity is generally the atmosphere's response to large-scale processes which destroy the static stability and is generally proportional to the rate at which the large-scale processes would drive the atmosphere unstable, ranging from small cumulus to a large area of tornadoes. Of course, this response is in turn affected by other properties of the atmosphere, such as vertical wind-shear, surface vorticity and vertical distribution of stability.

To estimate the extent and character with which atmospheric instability will be released over a given domain, a meaningful "weather watch" program would permit frequent computation and a comparative display of the predicted and observed rates at which the atmosphere is creating instability (through differential advection, diabatic heating, etc.), and of the character, intensity and scale of the mesoscale cells that release it by diagnosing such other data as synchronous satellite pictures, radar and conventional observations.

These convective processes are not captured by the operational numerical models. Some special versions attempt to parameterize the effect of convection on the synoptic scale, but neglect specification of the convection itself.

Many models, to maintain dynamic stability, arbitrarily readjust lapse rates to acceptable values. The magnitude of this adjustment could be an important forecast output; since it is a measure of what the convective scale has to accomplish to keep the atmosphere realistic, and is also a measure of a "weather producer".

There are many currently-known physical principles which could be used now to improve forecasts, if the predicted and observed parameters could only be made readily available and in the proper format. For example;

The prediction of strong convective instability, induced by differential advection in the vertical, is not likely to be reflected in conventional forecasts—nor even in the diagnoses of predicted static stability. However, the predicted development of such a regime in sea-breeze convergence domains would clearly indicate prospects for very heavy precipitation and squally weather which might otherwise occur as a "sleeper".,---or,

The predicted occurrence of high moisture content in the lower few thousand feet, separated by an inversion from dry, clear air above, will favor strong nocturnal fog formation. The inversion will protect the moist air from dry-air mixing from above, and favor strong nocturnal radiation from the moist layer. However, the existence of strong divergence (in the boundary layer) in a warm, moist-air-over-cold-water advection situation will favor a dry-air flux into the boundary layer and prevent the formation of fog, even with strong advection taking place; —another example;

In a rain environment, the predicted presence of above-freezing temperatures below 800 mb, would indicate that falling snow will be changed to rain before reaching the surface. However, if the temperatures below 800 mb are not much above freezing, continual precipitation will cool the lower air and produce a surface snow condition.

In this case, the forecaster should have a capability for determining the extent to which the lower air will be exposed to the cooling precipitation.

Precipitation falling from the middle or upper troposphere should be diminished if a decrease of wet-bulb temperatures is expected in the lower levels.

Similarly, in a rain domain produced by continuous overrunning, the low ceilings and visibilities characteristic of such a regime should deteriorate if the temperature of the rain increases or from a decreased wet-bulb temperature in the colder air below.

Fog will form more readily during the night when the surface geostrophic flow is advecting air of higher dew-point temperature, and will burn off very slowly, with a low ceiling forming, in the forenoon dissipation process.

Since all of these types of rules are based upon physical principles, they should be adaptable to magnitude computations and quantitative applications.

The Air Weather Service 1967 Winter Trajectory Test Program confirmed clearly that terminal ceiling and visibility forecasts could be improved by providing numerically-derived predictions of the low-level moisture and temperature distribution in a time-space domain. Their report on this program showed that the use of these specially-predicted data permitted a general improvement in terminal forecasts for a large number of selected stations, but was most striking at Scott AFB where a more effective subjective integration and override was possible. The special products provided for that test were only a small fraction of the total information that is potentially available and potentially useful in making actual weather forecasts, and would have been even more useful had they been available in a more digestible format.

The potentially useful and predictable information, and the optimum format for its delivery, vary extensively over a diverse range of possible forecasts, and are also dependent upon the given weather situation. Yet, we can't deluge the forecaster with more charts. He's up to his eyeballs now. Rather, the ready availability of the information on demand and its adaptability to forecasting judgements is the key.

The ability to make such judgements as the examples just mentioned must be provided at various echelons in the weather-service chain according to their contributions to the effectiveness of the pertinent operation. The obligation of a major numerical-predicting center to monitor its product as generated, and to interrupt the dissemination process long enough to introduce corrections, should physical reality be lost, represents an entirely different requirement from that which exists near the end of the chain where operational decisions are made on the basis of the information delivered—and where the optimum decision may require the user and the forecaster to carry out a short-fused dialogue as to weather effects on several markedly different options.

It would be premature to specify the "where and what" of such a program at this time. The nature of the specific techniques developed and logistic feasibility will be factors to contend with; but the following guidelines have been adopted by the Navy Weather Research Facility as basic design tenets for the ultimate system.

First and foremost, the forecast-judgement capability available aboard a particular ship, installation, or center, must be commensurate with the nature and consequences of the command judgements made there and must be able to accommodate the incorporation of additional information as it becomes available near the end of the chain that is not considered in the basic numerical product, and which we cannot afford to disregard.

By the same token, and this is our third tenet, data-processing capabilities are unlikely to be extensive at forward echelons, so the on-scene forecaster must be provided with those processed analyses, diagnoses and judgements which can better be generated higher up the chain—but care must be exercised that creeping paternalism (an inseparable ailment of major computer complexes) does not presume that the infinite wisdom at the tail is better able to judge the needs of the beast than requirements expressed from the end where the teeth are.

In a fast-moving situation, a commander should not be expected to delay an imperative decision while his forecaster calls mother to obtain a variation in the duty prediction.

A significant portion of our resources at the Navy Weather Research Facility is concerned with designing the optimum mix between the preprocessed basic numerical products from high up in the delivery chain, and the on-scene information available locally, such as pilot reports, radar data, direct readout satellite data, the most recent synchronous-satellite pictures, or—equally important—a peek out the porthole, which must be utilized to quantitatively re-evaluate the computer-predictable parameters in the light of this ground-truth information.

We believe we're fairly close to being able to make recommendations concerning those components which would prove advantageous to the Fleet Numerical Weather Central and to a computer-equipped weather central; but for most important link in the chain, the forecaster aboard a fleet flagship or attack carrier, we are handicapped by insufficient information as to those meteorological computer and communication facilities which will be available aboard ship.

We have just completed the second phase in the development of an evolving, versatile display-and-presentation system. This is the computer interface which links the expanded human judgement made possible by modern data-storage, retrieval, and display capabilities with marked development in computer diagnosis and processing capabilities.

We have completed the basic elements of software for the first phase of our technique and principle development program.

We have initiated a series of research programs to extract from current knowledge and to develop the principles needed for forecasting judgements.

This system, as it is presently configured, will permit the following type operations in the not too distant future:

Push-button availability of radarscope mosaic and synchronous satellite picture sequences.

Computer interrogation by the forecaster for additional computations, or analogs of weather sequences from similar previous situations.

Overlay comparison of the analogs, and the differences between the physical parameters of the analog and the predicted parameters to permit deduction of the forecast differences in weather events.

Animation of predicted space and time cross-sections for routes and locations of interest, which provides a very dramatic portrayal of the forecast sequence of weather events.

Direct-readout of synchronous-satellite pictures overlayed on the corresponding predicted fields of temperature, humidity and vertical velocity.

The limitation of diagrams and illustrations, as well as our present state of development, prevent us from showing you examples of all the foregoing; however, we believe the results of an experiment conducted this spring will show some of the potential for this program.

During the month of February, we arranged to receive history tapes from the NMC P. E. model, on a pseudo-real time basis. From these, we prepared a series of predicted space and time cross-sections of moisture, temperature, clouds, winds, etc., for stations in the east coast area. We've selected and reproduced some of these which were computed for display with our system.

At 1900 EST on the 16th of February, a frontal system along the east coast with a developing low just south of the Florida panhandle was evident from the surface pressure analysis, which is shown in figure 1(a). Figure 1(b) (24-hour surface "prog") showed this low moving to about a hundred miles east of the North Carolina coast, with rain extending through eastern North Carolina and Southeastern Virginia up to the southern tip of New Jersey. By 36 hours (fig. 1(c)) the low was forecast to have moved to the northeast, well off the coast, and a general anticyclonic regime was expected to dominate the whole east coast area.

Figure 2 shows a 30-hour predicted time cross-section for Norfolk. Time runs from left to right, beginning at 0100 EST on the 17th. The dashed lines are values of predicted condensation pressure spread (in millibars), and the solid lines are predicted vertical velocities in millibars per hour. Notice that a near-saturated condition (that is, condensation pressure spread values less than 30 millibars, shown by the shaded area) prevails for the first half of the period from the surface to 500 millibars, and that it begins to dry out aloft with the dry air coming lower as the period progresses.

The vertical-velocity field shows strong upward motion during the first twelve hours, decreasing and reversing itself by the end of 16 hours. From this it would be logical to expect continued heavy clouds and rain throughout the first 12-15 hours, with the rain ending by about 1300 EST on the 17th and the heavy clouds remaining throughout the period. With the low-level moisture remaining through at least 0700 EST on the 18th and the increasing clear dry air above (aiding nocturnal radiation), one would have to expect low ceilings and fog to remain throughout the night.

The actual weather that ensued is shown along the bottom. Notice that the rain did decrease (ending about 1000 EST), and that low ceilings and fog continued throughout the whole period.

Figure 3(a) shows the synoptic situation for the 24-hour-later period, which indicates a good verification of the previous centrally-prepared product. The 12- and 24-hour surface forecasts, figures 3(b) and 3(c), show the region coming under the influence of a high-pressure system, with the southwesterly flow returning by the end of the 24-hour period.

Figure 4 shows the 36-hour-predicted cross-section of condensation-pressure spread, which shows the first 12 hours to be consistent with the previous 30-hour forecast showing clearing aloft, but with near-saturated conditions remaining in the lowest layers well into the next forenoon. The drying out of the upper levels during the night would re-support a forecast for fog and low ceilings to continue throughout the night period, but burn off in the early forenoon the next day as clear skies in the upper levels permit uninhibited solar heating.

The verifying data are again shown along the bottom. Notice that the fog continued through the night with some breaks, but burned off by 1300 the next afternoon.

In the next situation we see that on 18 February 1900 EST (fig. 5(a)) there was a cold front moving across the middlewest. The 24-hour surface and weather-distribution progs (figs. 5(b) and 5(c)) showed the front going by Norfolk within 24 hours, with broken to overcast lower clouds extending over the whole domain and broken to overcast upper clouds covering the eastern Virginia-North Carolina area.

Figure 6 shows the 36-hour prediction of potential temperature in the time cross-section for Norfolk which presents clear evidence of a very strong frontal passage at about 1500 on the 19th.

The predicted CPS values corresponding to figure 6, are shown in figure 7 and indicate that the only cloudiness that should be predicted would be some scattered to broken low clouds for a few hours during the afternoon and early evening. The verification of these data is provided along the bottom of figure 7. Notice that the 3500-foot to 5000-foot broken cloud cover is the only significant weather that occurred during this frontal passage.

The next case that was studied presented a rather dramatic event, in which a very strong frontal passage occurred in the Norfolk area resulting in an abrupt strong wind shift and a sudden change from rain to moderate and blowing snow. The stage for this event is set at 1900 EST on the 24th of February. In figure 8 we see a rather complex frontal situation that is about to affect the east coast. There is a low over the Great Lakes sweeping a strong cold outbreak toward the southeast. Another developing low is in the East Texas area and moving rapidly to the east-northeast.

Figure 9 shows the 24- and 36-hour predictions of both the surface and 500-millibar charts. The 24-hour forecast predicts the low in Texas to develop and move just to the east of the North Carolina coast, drawing the Arctic front from the north in behind it.

In 36 hours the low was predicted to move well off the east coast. From the 24-hour 500-millibar and surface forecasts, the prospect of a sharp active cold front moving through the Norfolk area about 4 hours later is not very apparent.

Figure 10 shows the 36-hour prediction of the time cross-section of potential temperature for Norfolk beginning at 1900 on the 24th of February. Notice here that the temperature starts to drop slowly in the afternoon of the 25th, but does not start dropping rapidly until about 2200 or 2300 EST at which time it drops very rapidly, indicating a strong cold frontal passage.

Figure 11 shows the 36-hour prediction of the condensation-pressure spread values and the vertical velocities with the same code used previously. Notice that upper cloudiness is expected to prevail early in the period, dropping down below 700 millibars by 1300 EST and down to very low levels by 1900 EST, but rising again after 0100 EST. Notice the dry wedge of air that is predicted to occur between 850 and about 600 millibars after 0100 EST. With these predicted vertical velocities and moisture values, one would expect precipitation to begin somewhere around noon on the 25th and continue until about midnight, being perhaps most intense around 1900 EST.

Comparing the moisture and vertical-velocity predictions with the predicted zero-degree isotherm (the heavy black line on fig. 11), shows a marked drop in temperature occurring while precipitation should still be occurring (about 2200 to 2300 EST)—which would be a distinct indication for the rain to change to snow. Notice further that although there is still heavy moisture

above 700 millibars and upward vertical velocities after 0100, the presence of the dry air below 700 millibars would have a definite diminishing influence on the precipitation.

The verifying weather is shown along the bottom of the chart. Attention is invited to the moderate rain which occurred in the afternoon with a prediction of strong upward velocities and marked lowering of the condensation layers. The rain activity continued until about 2100 EST where it changed to snow, and became very light after 0100 (corresponding to the cold-dry wedge mentioned before) with skies going broken sometime before 0700 the next morning.

Figure 12 shows the 36-hour cross-section prediction of the north-south wind component, with the total predicted wind speed on the next to last line along the bottom of the chart. Notice that the switch from south to north took place in the afternoon at approximately the same time as the gradual temperature drop took place; and the increase of stronger northerlies coincided with the strong temperature change that took place later in the evening, but was not as precise an indicator of a sharp frontal passage as the temperature profile was.

The verification of these wind forecasts is shown on the last line at the bottom of the chart, with gusts indicated by parentheses. Notice that there is the tendency to overpredict the wind speed with a southerly flow ahead of the front and to underpredict the wind speed significantly with northerly flow, which is consistent with the findings discussed yesterday by Mr. Cormier.

We have done some work in the animation of space cross-sections during this time, and this technique revealed some very interesting sequences in the significant weather events taking place during a forecast period. It is not possible to show any of these animations on a printed page, but figure 13 is the 36-hour space cross-section forecast of condensation-pressure spread and potential temperature selected from the end of an animated sequence. This cross-section extends from central Pennsylvania through Norfolk to about 300 miles southeast of Hatteras.

Notice that by 36 hours the intense cold front is past Hatteras, but the heavy-moisture domain is more extensive and deeper than when the front passed Norfolk, and the atmosphere became much more unstable between 850 and 500 millibars. This would lead one to predict much heavier precipitation and squally weather as the system moves to sea, but no snow since the air will have been dried considerably before the cold air domain prevails.

This intensification forecast would have verified quite well. Continuous moderate rain was reported as the front passed Frying Pan Shoals south of Hatteras, and ships reported 40-50 knot surface winds and continuous moderate rain at the time corresponding to this cross section.

We plan to expand these experiments this winter, and to operate closer to a real-time basis by using the output from the Fleet Numerical Weather Central. We are investigating the possibility of having the computation of the predicted values accomplished at Monterey, to avoid transmitting of history tape data. At the present time, we're still using the three-dimensional kinematic trajectories to predict our moisture and temperature. This will probably be necessary until we get into higher-resolution models, when it is hoped that we can go directly from the model predicted values to the predicted parameters of consequence to the weather forecaster.

Thank you.

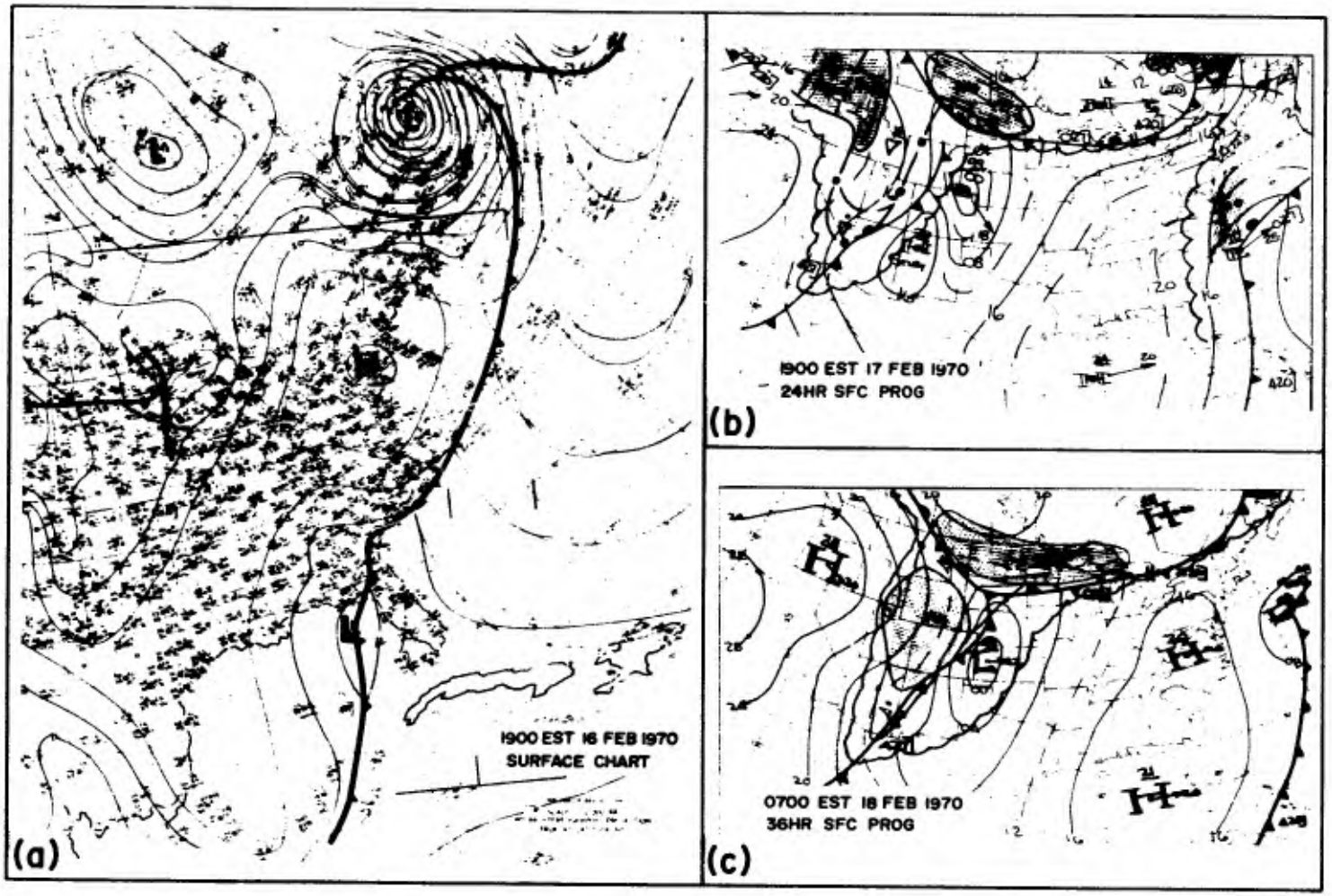


Figure 1. (a) Surface Pressure Analysis 1900 EST 16 Feb. 1970; (b) 24-Hr. Surface Pressure/Weather Prognosis; (c) 36-Hr. Surface Pressure/Weather Prognosis.

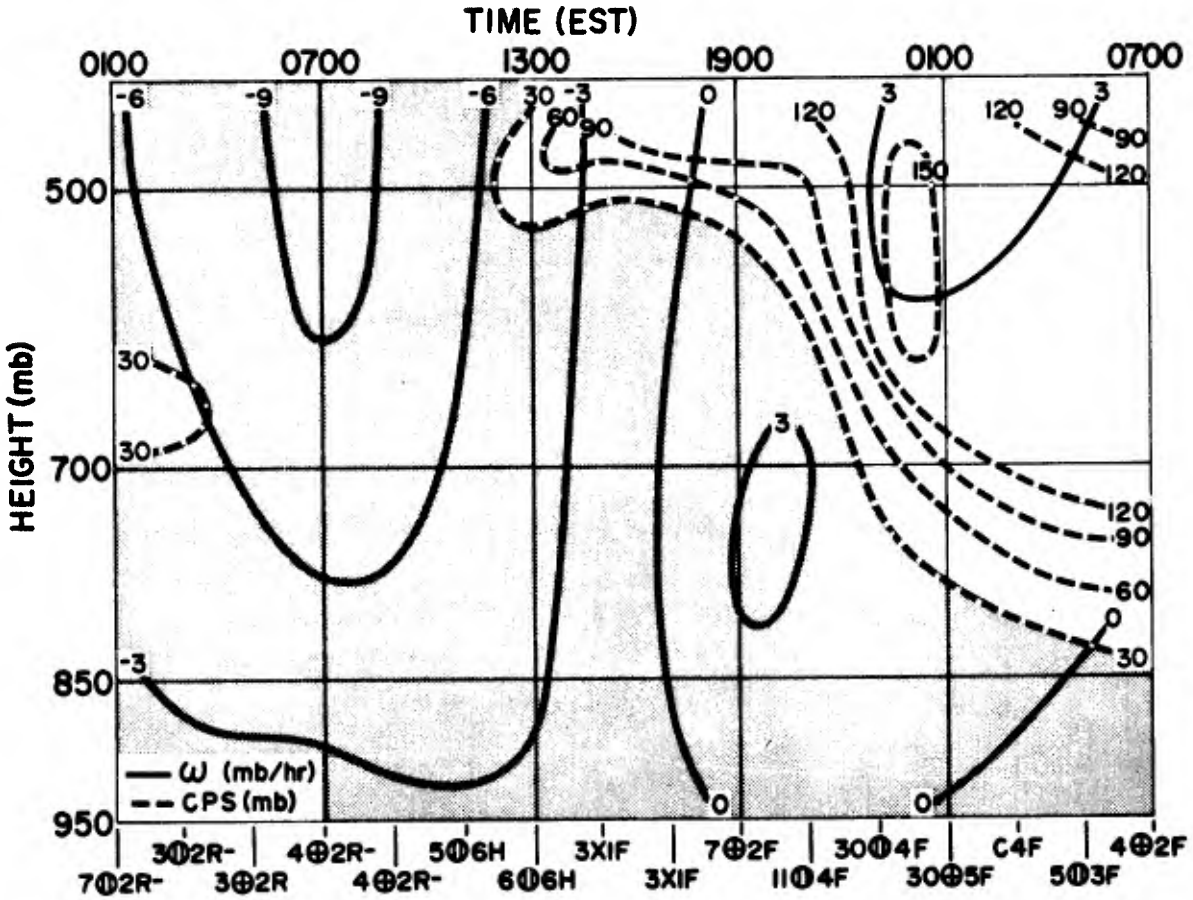


Figure 2. 30-Hr. Time Cross-Section Forecast for Norfolk, Va. Prepared From Data Observed at 1900 EST 16 Feb. 1970.

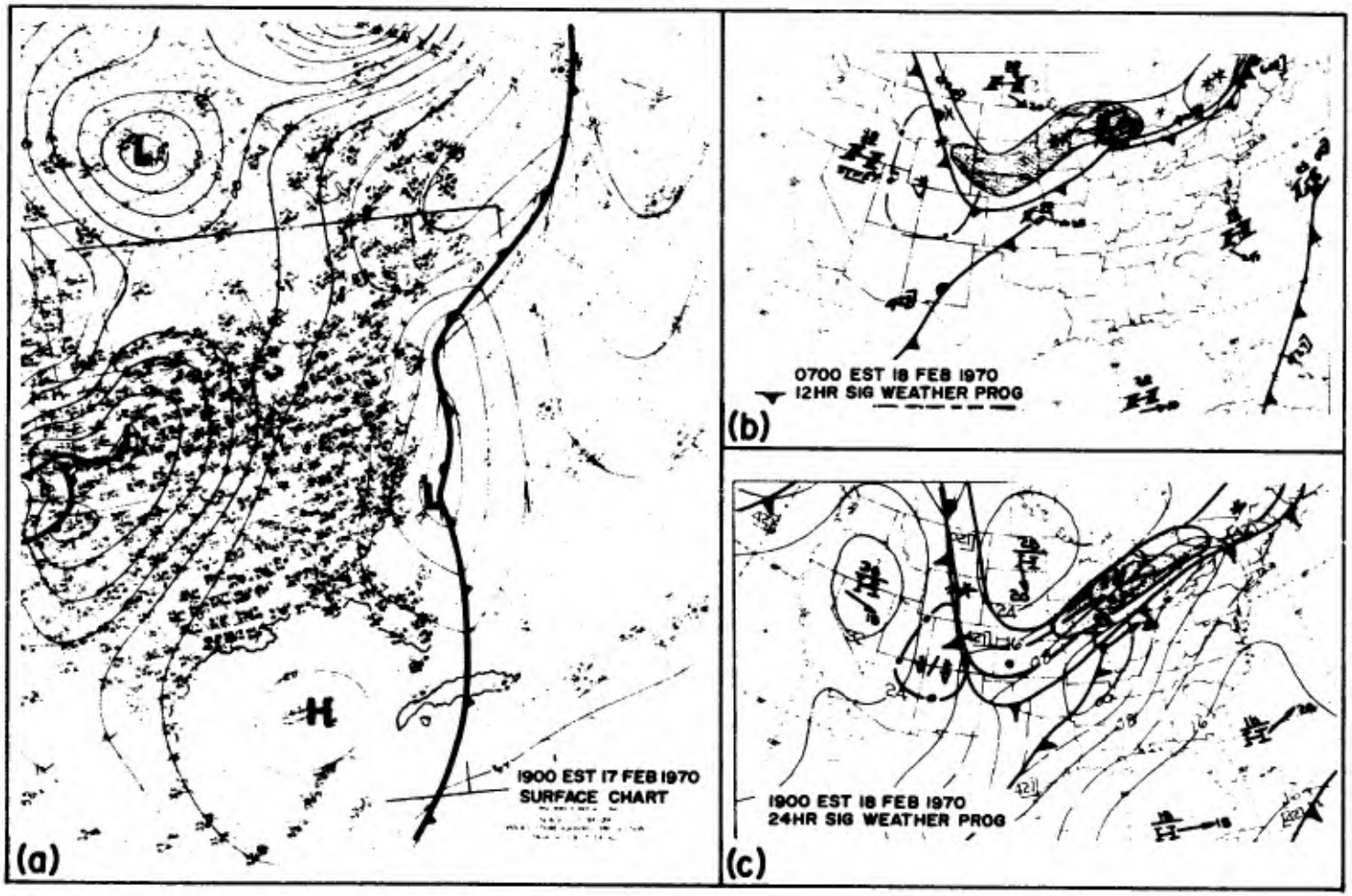


Figure 3. (a) Surface Pressure Analysis 1900 EST 17 Feb. 1970; (b) 12-Hr. Weather Prognosis; (c) 24-Hr. Surface Pressure/Weather Prognosis.

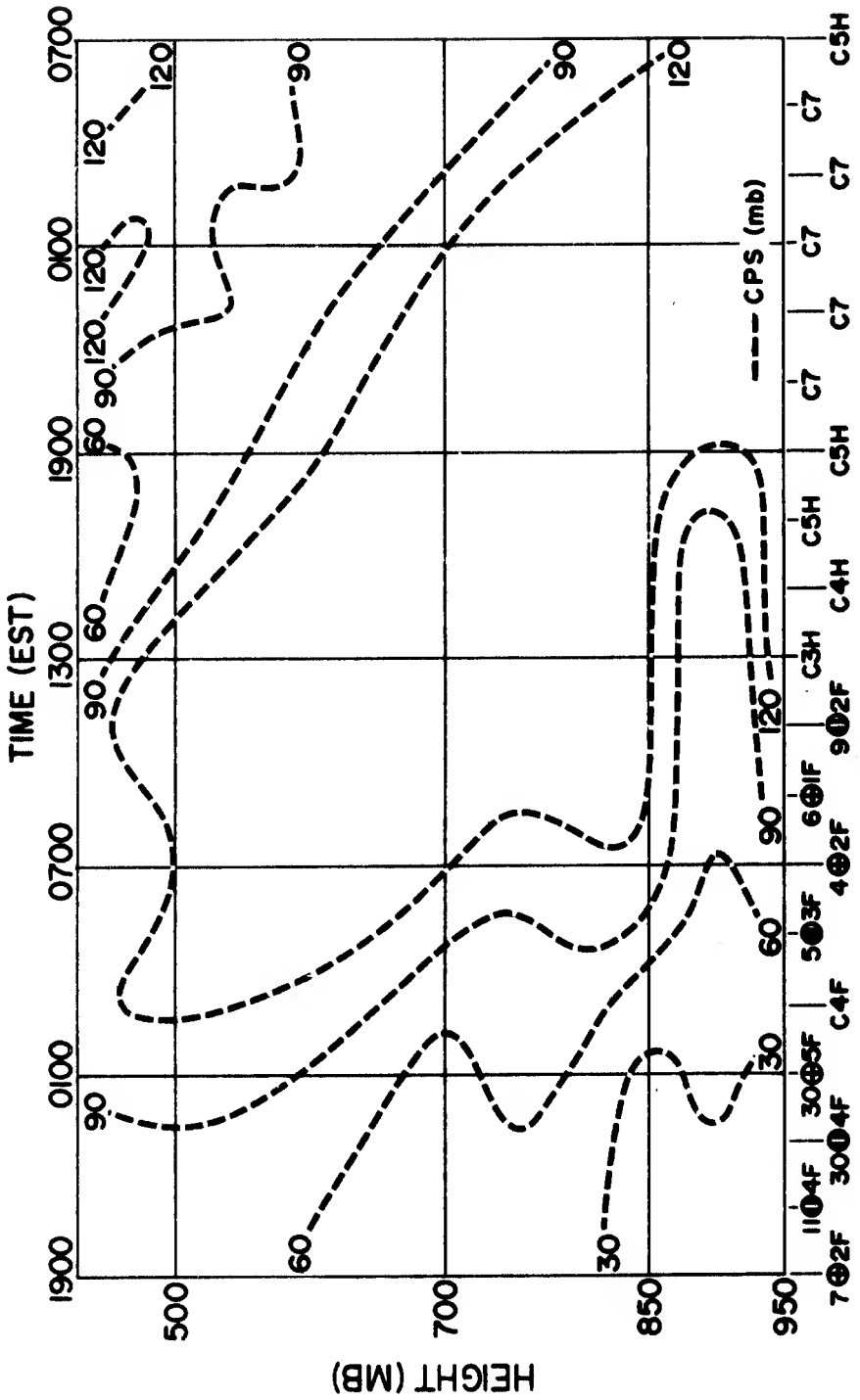


Figure 4. 36-Hr. Time Cross-Section Forecast for Norfolk, Va. Prepared From Data Observed at 1900 EST 17 Feb. 1970.

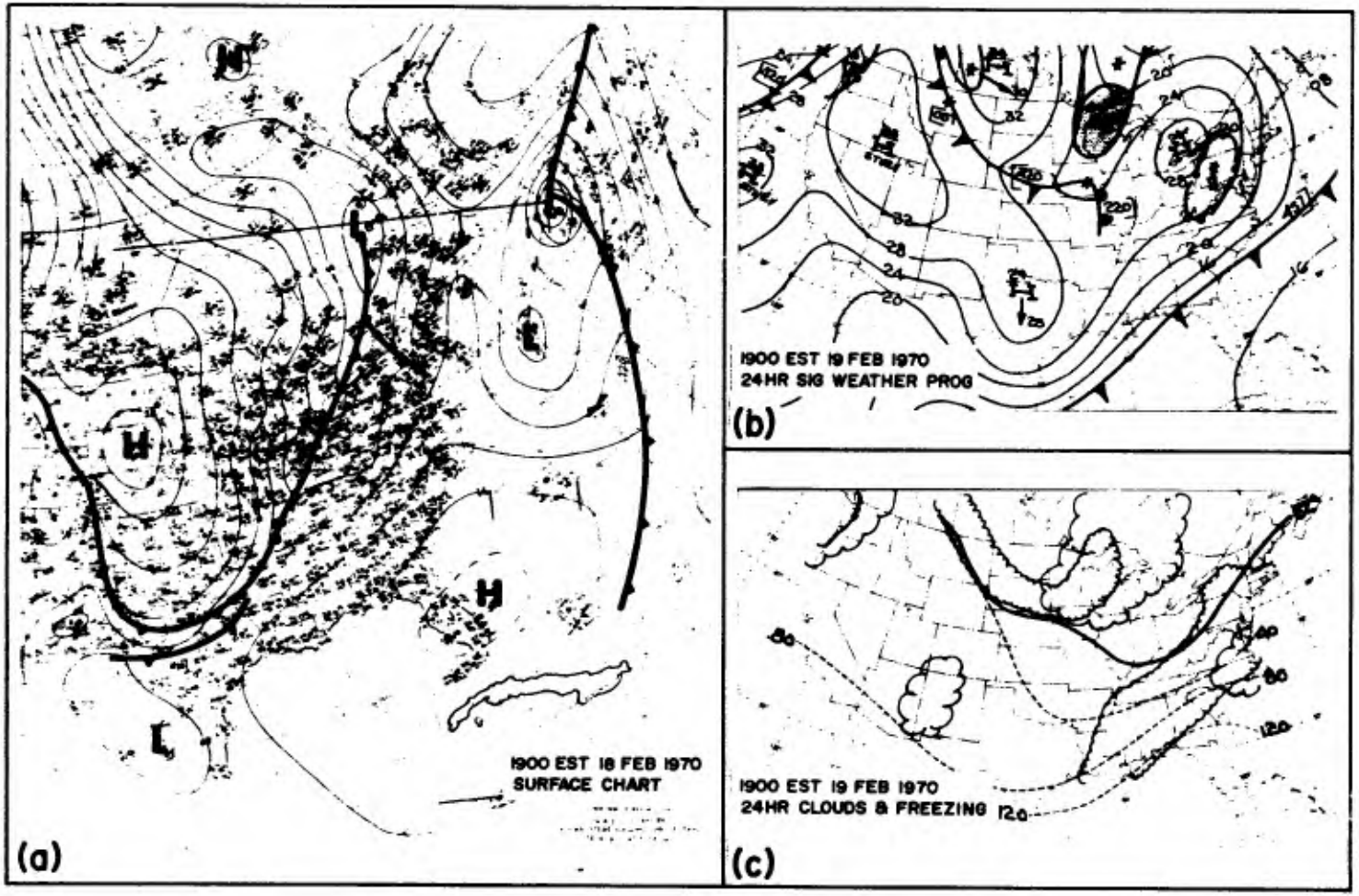


Figure 5. (a) Surface Pressure Analysis 1900 EST 18 Feb. 1970; (b) 24-Hr. Surface Pressure/Weather Prognosis; (c) 24-Hr. Clouds/Freezing Level Prognosis.

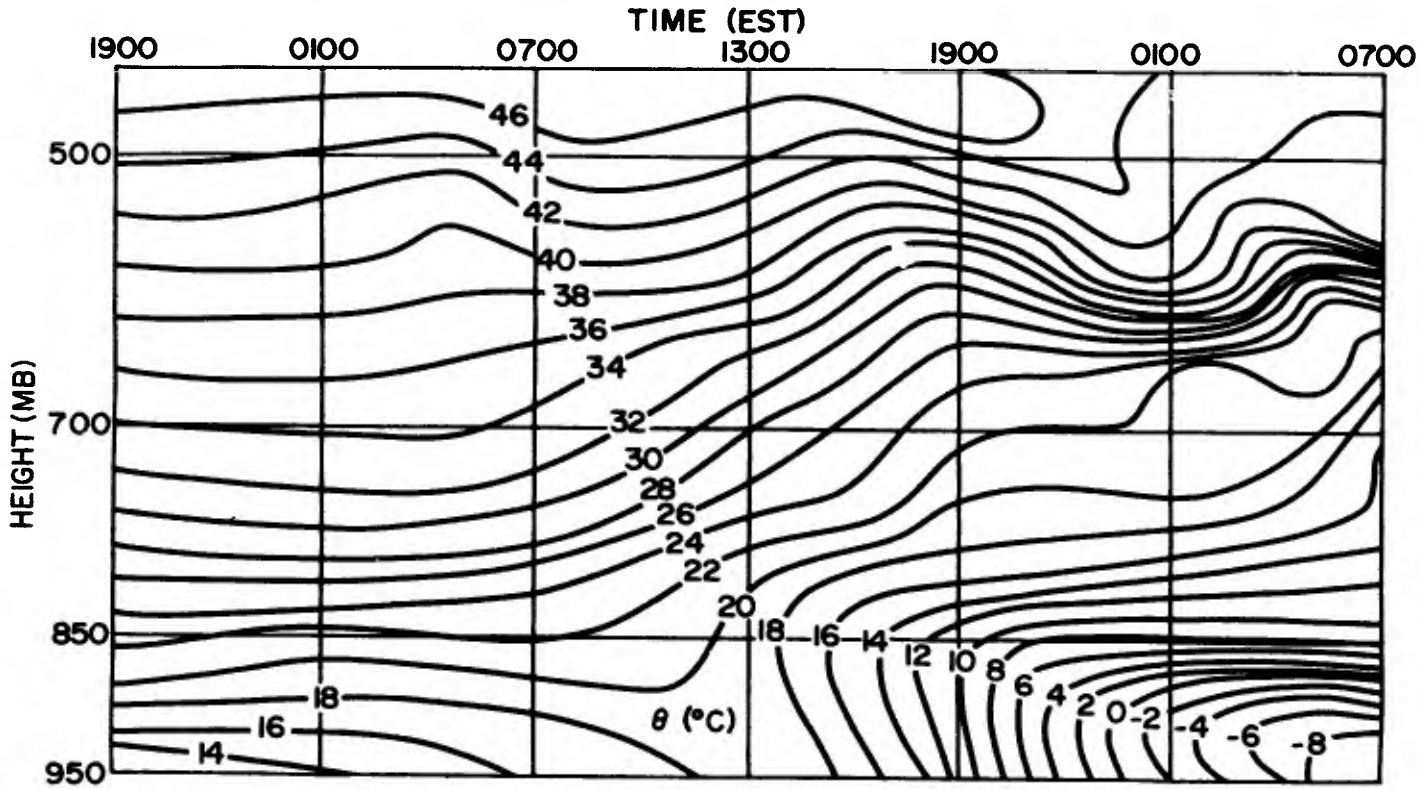


Figure 6. 36-Hr. Potential Temperature Time Cross-Section Forecast for Norfolk, Va. Prepared From Data Observed at 1900 EST 18 Feb. 1970.

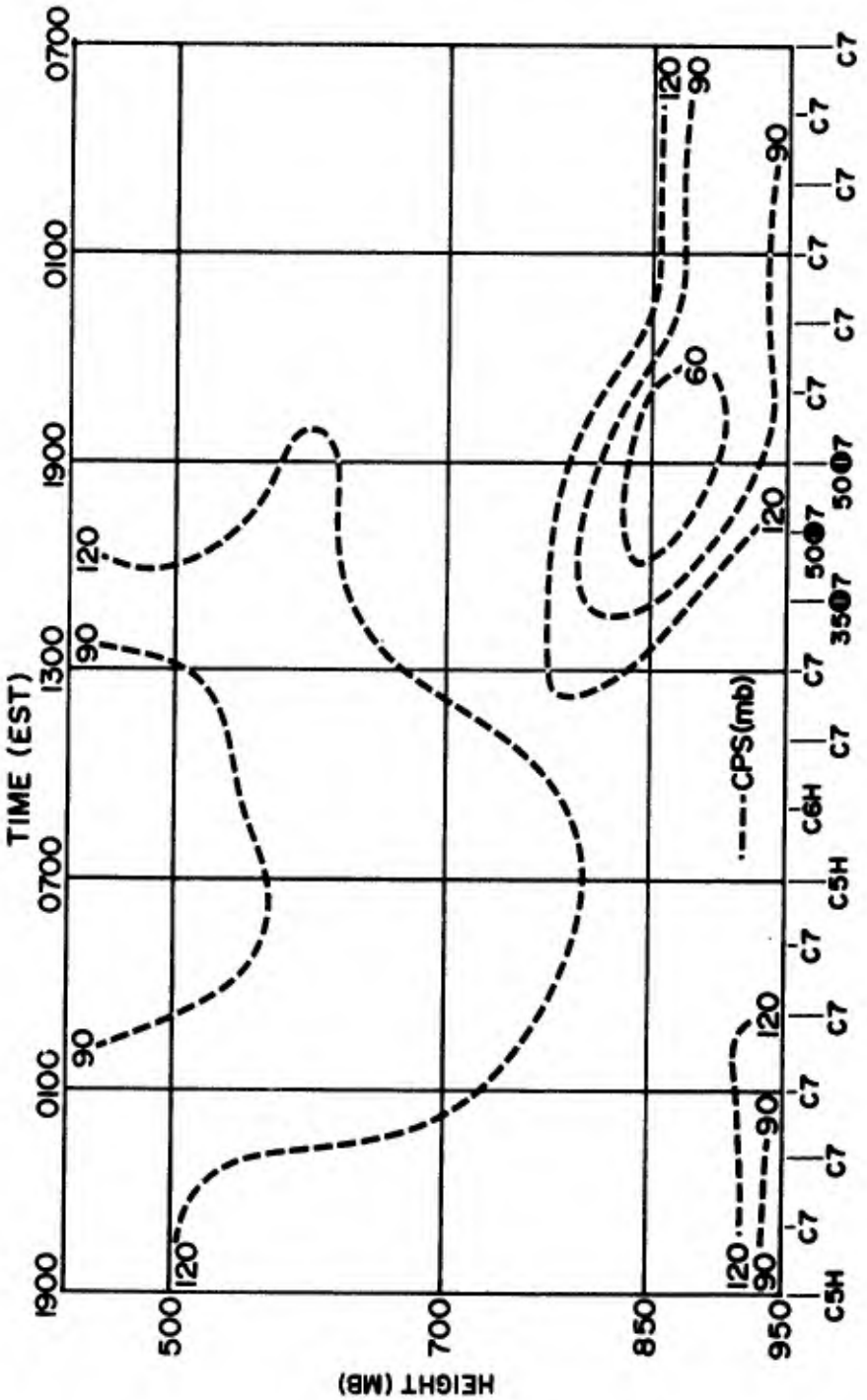


Figure 7. 36-Hr. CPS Time Cross-Section Forecast for Norfolk, Va. Prepared From Data Observed at 1900 EST 18 Feb. 1970.

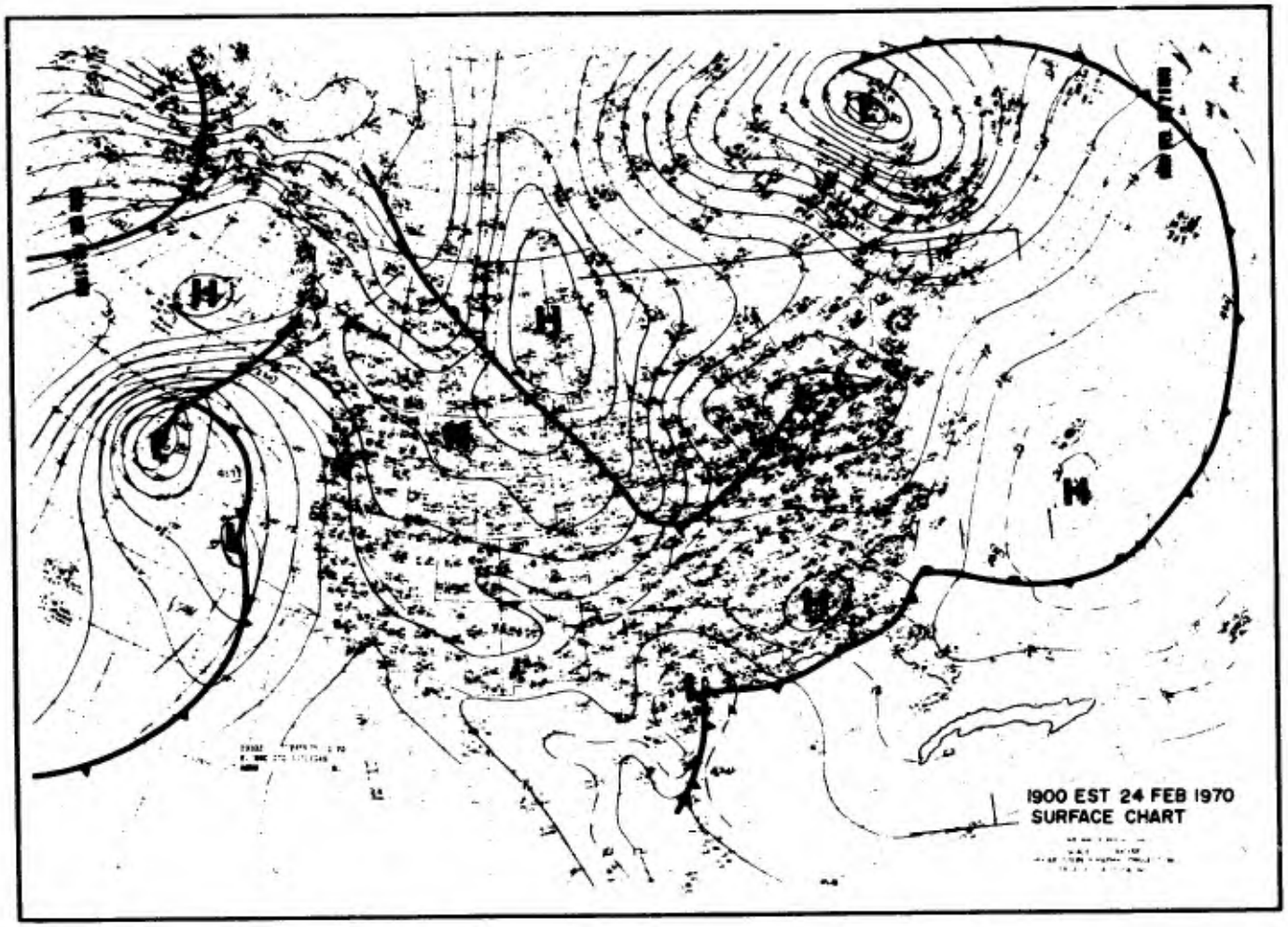


Figure 8. Surface Pressure Analysis 1900 EST 24 Feb 1970.

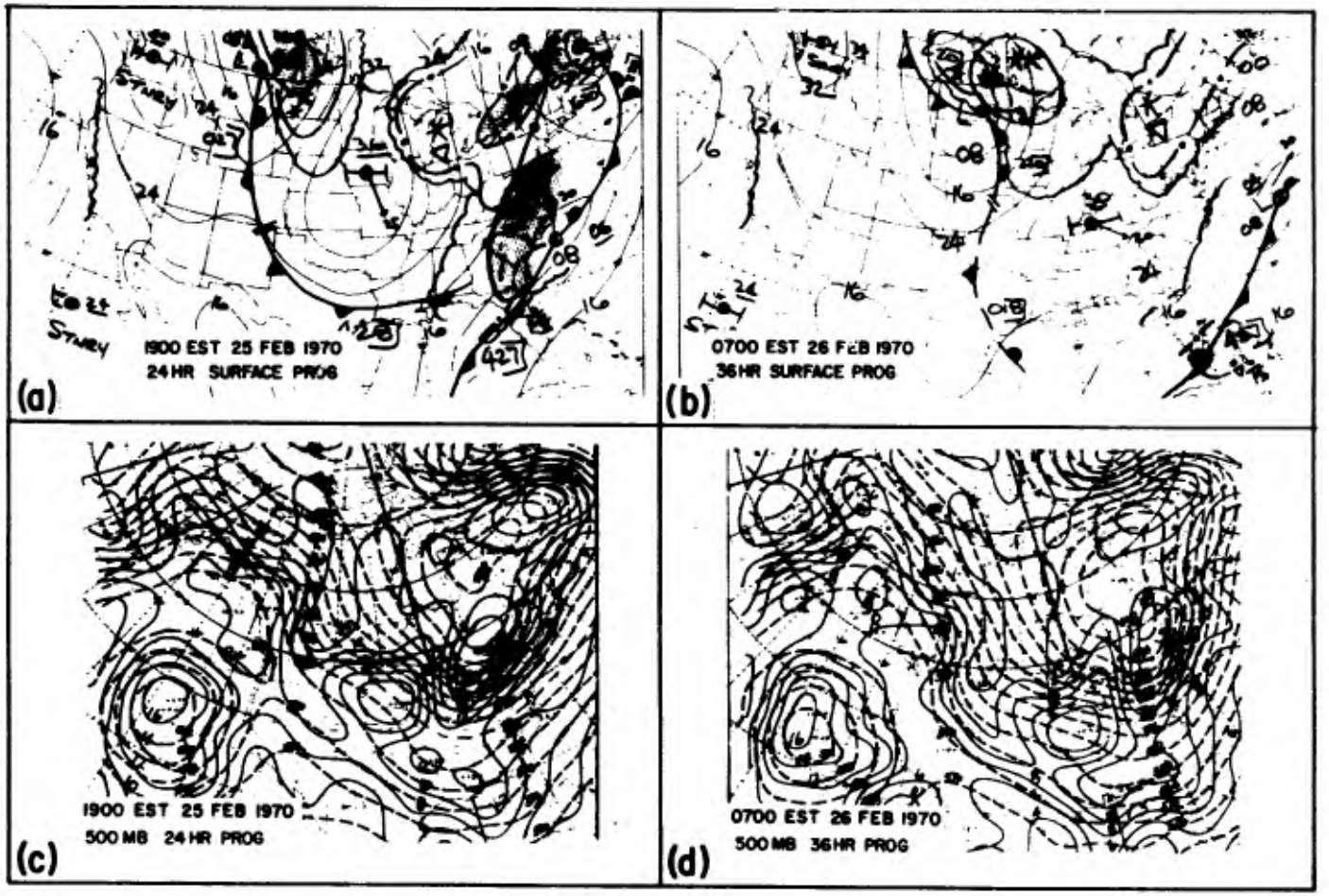


Figure 9. (a)/(b) 24/36-Hr. Surface Pressure/Weather Prognosis; (c)/(d) 24/36-Hr. 500-Mb. Height/Vorticity Prognoses.

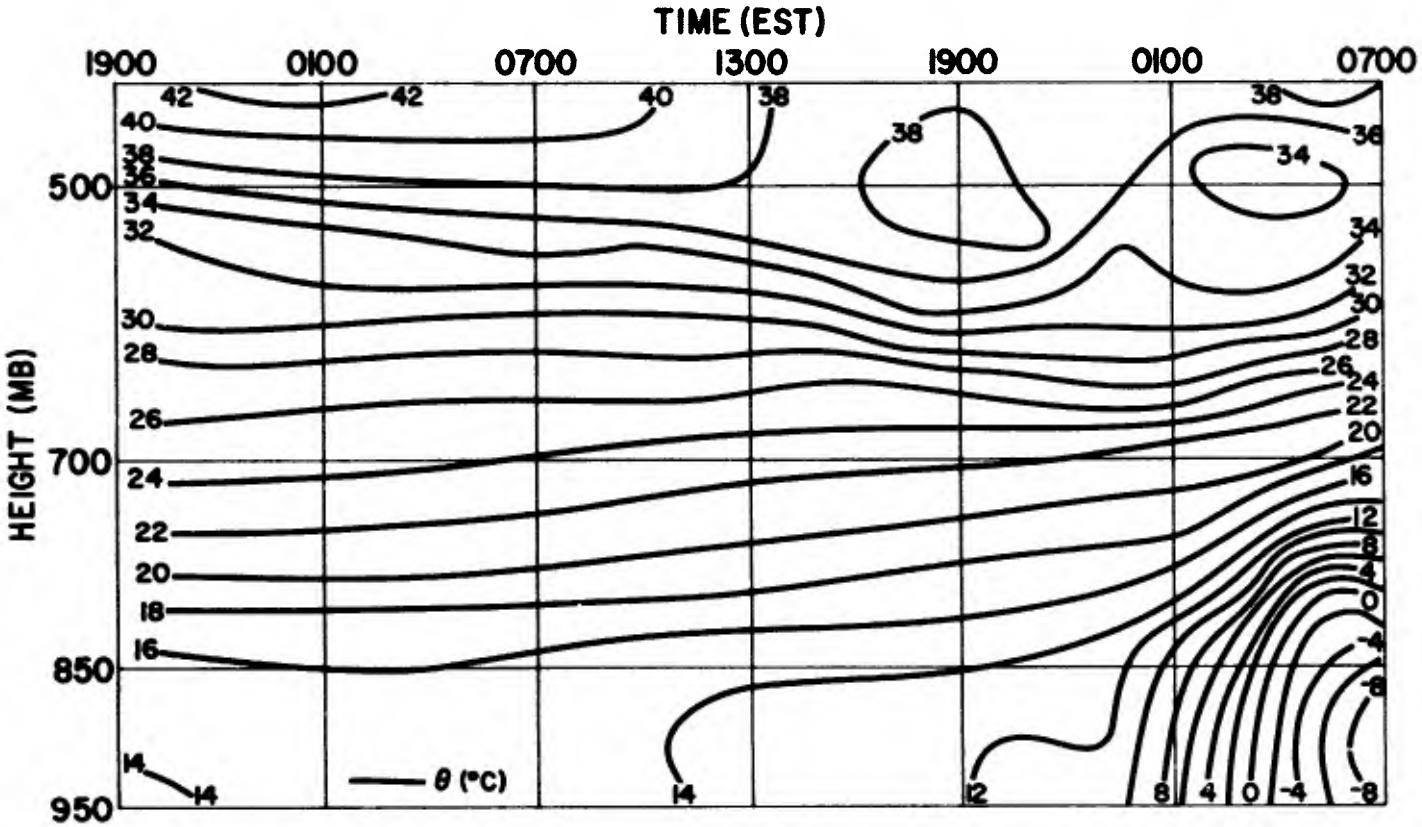


Figure 10. 36-Hr. Potential Temperature Time Cross-Section Forecast for Norfolk, Va. Prepared From Data Observed at 1900 EST 24 Feb. 1970.

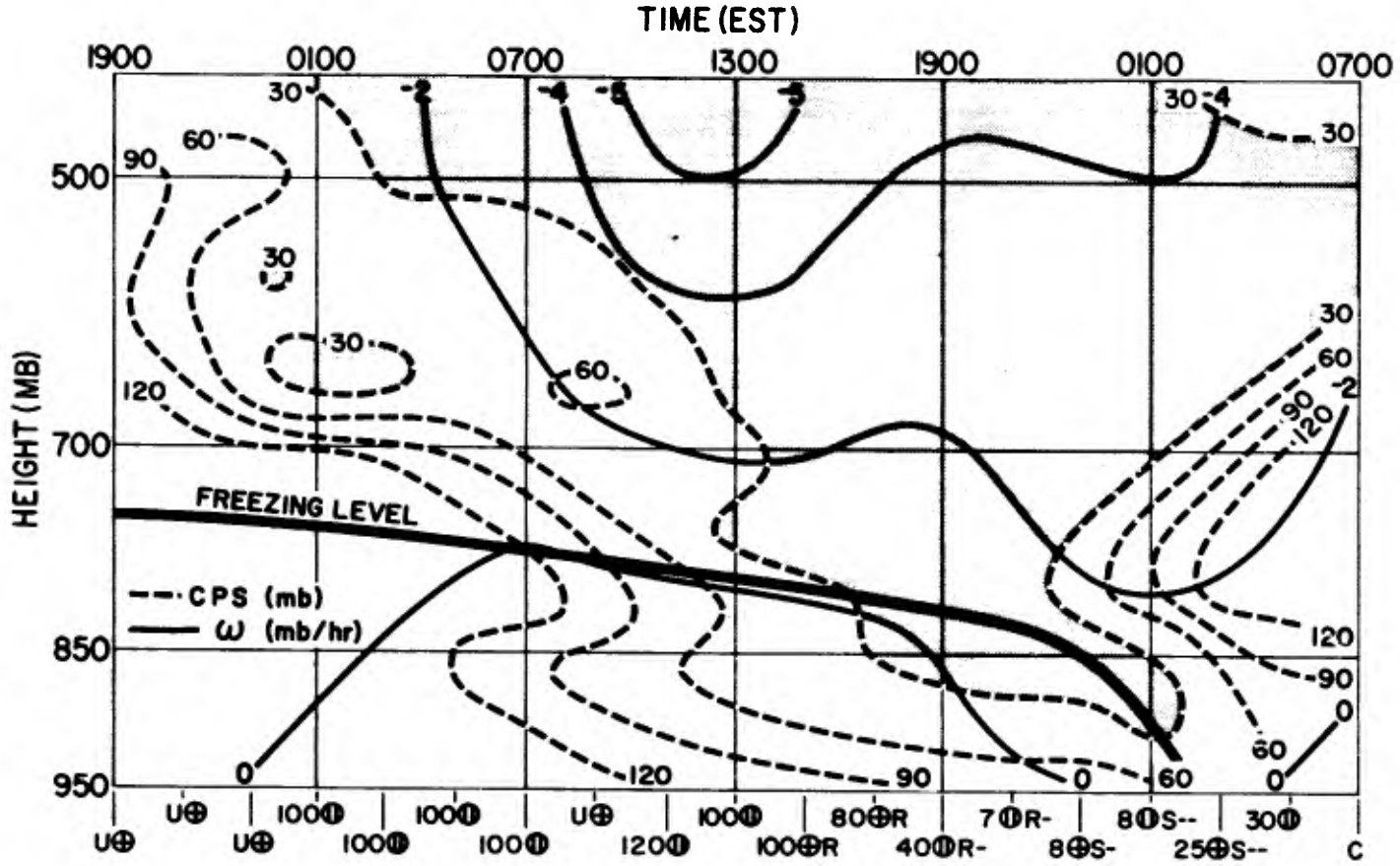


Figure 11. 36-Hr. Time Cross-Section Forecast for Norfolk, Va. Prepared From Data Observed at 1900 EST 24 Feb. 1970.

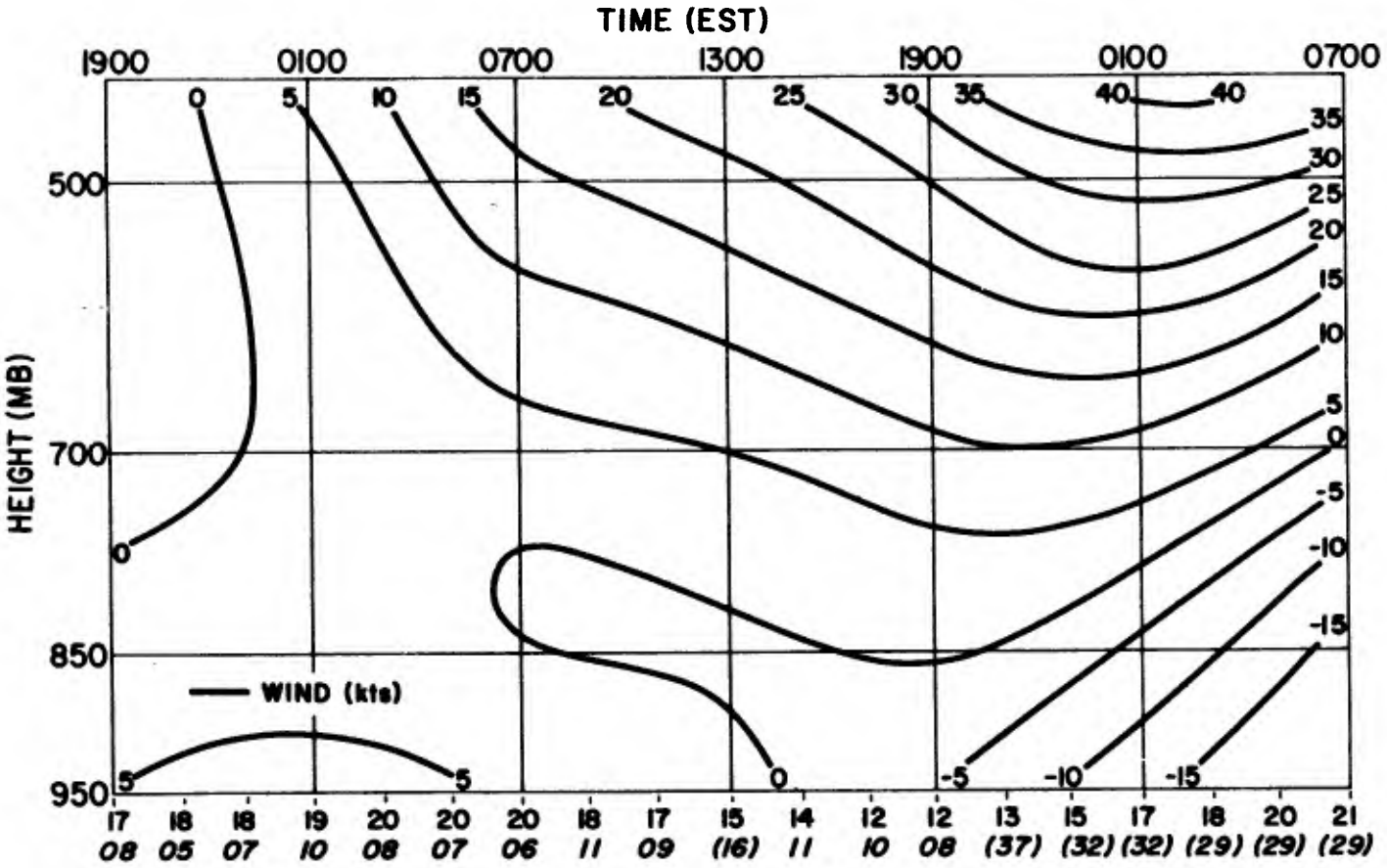


Figure 12. 36-Hr. N-S Wind Component (v) Time Cross-Section Forecast for Norfolk, Va. Prepared From Data Observed at 1900 EST 24 Feb. 1970.

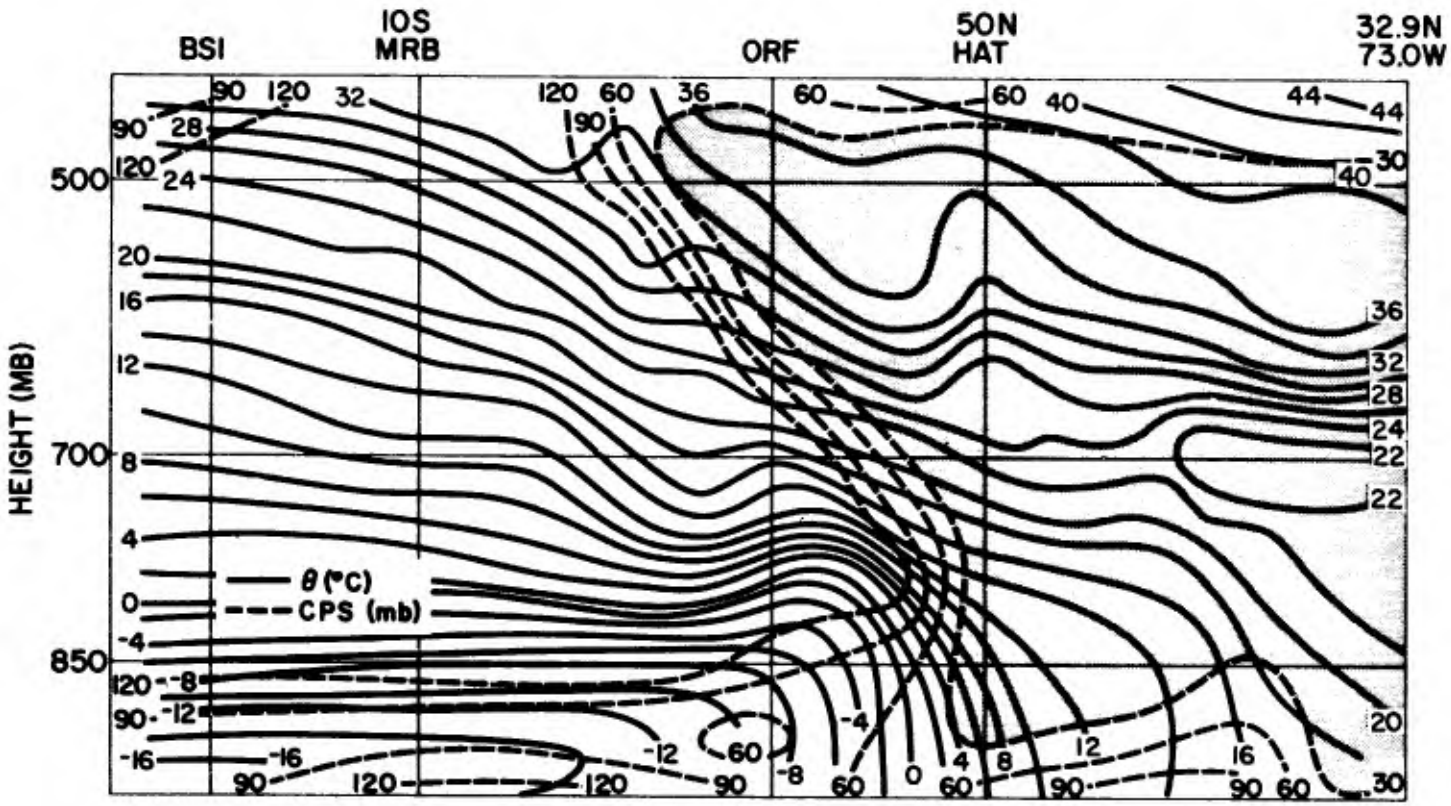


Figure 13. 36-Hr. Forecast Space Cross-Section Prepared From Data Observed at 1900 EST 24 Feb. 1970.

# AN AUTOMATED PROGRAM TO PRODUCE AND UPDATE COMPUTER FLIGHT PLANS

Capt Robert J. LaSure

Air Force Global Weather Central
Offutt Air Force Base, Nebraska

## Abstract

The Route Forecast Model is a computer program executing at the Air Force Global Weather Central designed to produce operational Route Forecasts and Computer Flight Plans. The program itself has no forecasting ability but relies upon pre-computed analysis and forecast fields residing in a data base. Utilizing a complete meteorological data base and specific route, track, and fuel libraries, computer flight plans complete with wind-temperature forecasts, navigation parameters, and a time-fuel analysis are produced routinely and on a demand-response basis. Flight-plan requests are received on a real-time basis, processed by the Route Forecast Model and transmitted to world-wide DOD users.

## 1. INTRODUCTION

The Route Forecast Model (RFM) is an operational computer program that produces route forecasts, point forecasts, and computer flight plans (CFP) at the Air Force Global Weather Central (AFGWC). Historically, the first program designed to apply winds and wind factors to a route processing simple route forecasts began more than six years ago. The current production program executing today is an extension of that simple program, expanded and modified as required to meet the demands of additional DOD agencies. Today, a computer flight plan is based on a route forecast but is expanded to include all navigation and fuel parameters required for complete mission-tailored support.

## 2. DATA BASE

The Route Forecast Model does not make forecasts as its name implies. Instead, meteorological analysis and forecast programs are executed and their output, gridded wind, temperature, and pressure fields, are stored in a data base residing on mass storage devices. The Route Forecast Model merely extracts and interprets data-base fields as required to produce a meteorological route forecast.

The basic technique exploited by the Route Forecast Model is one of interpolation in space and time. As an aircraft progresses along a route, the route is subdivided into flight/grid legs such that a minimum relation between leg distance and grid spacing is maintained. A unique set of meteorological parameters is then interpolated horizontally, vertically, and in time to each flight/grid leg forming RFM forecast values. Fixed-time and time-phased forecasts result from interpolation in space and time.

The Route Forecast Model requires that a fully global data base be available prior to its execution. The data-base parameters required are gridded winds, temperature, and pressure fields arranged in a rectangular grid system. In addition, a complete set of climatic fields for both hemispheres is also required.

Macro-scale (approx 200-mile grid spacing) fields are the most commonly used and form the basis of the data base at AFGWC. Above 20 degrees north latitude, the GWC Northern Hemisphere analysis and forecast fields provide wind, temperature, and pressure forecasts from 1000 to 10 MB on an octagonal 47x51 grid. Analysis fields are retained for 24 hours and forecast fields extend from 6 to 72 hours. Between 20 degrees North and 40 degrees South latitude, a tropical analysis field provides the wind and temperature data source.

Below 40 degrees south, or on an optional world-wide basis, climatic mean winds and temperatures provide RFM with its data source. Standard deviations are also available and can be applied by RFM to produce a route forecast based on any level of probability. Climatic fields are available by season in the Southern Hemisphere and by month in the Northern Hemisphere for the 850 to 100 MB levels.

Meso-Scale (approx 100-mile grid spacing) fields are optionally available depending on the location, time, and altitude of the air mission being supported. Meso-scale fields such as the Fine-Mesh analysis and forecast fields are located within selected windows and are produced only for selected vertical levels. The Boundary-Layer analysis and forecast fields are also available within the fine-mesh windows and are applicable to the lower 5000 feet of the atmosphere in a terrain following mode.

## 3. INPUT SPECIFICATIONS

The Route Forecast Model is designed to produce mission-tailored forecast support. By utilizing RFM, one computer program must perform all required tasks to support all users. The technique employed for producing mission-tailored products is one of stating required display parameters at the time of initial route submission. Thus, every route input into the flight planning system must state its final display description.

Route input to RFM is composed of route specifications and track descriptions. The route specifications state explicitly the options desired, the product addressing, the appending text messages, and the required aircraft specifications if fuel computations are required. The track description can be of two forms — route or track/profile.

Track description supplied via route input is a complete list of locations by latitude, longitude, air speed, and altitude describing the route to be flown. In example 1, the aircraft will depart KMER 3723N 12034W at a true air speed of 355 knots, and a departure altitude of 5000 feet. The aircraft then climbs to 14000 ft at 3715N 12045W, to 26000 ft at 3716N 12220W and to 28000 ft at 3635N 12405W. The aircraft will thereafter cruise at 28000 ft, and a true air speed of 458 via the indicated locations to PHIK at 2118N 15754W.

Track descriptions supplied via track/profile parameters provide individual descriptions of the aircraft track over the earth's surface via latitude and longitude and of its vertical profile which specifies air speed and altitude by time intervals. Example 5 depicts a track description from Torrejon (4029N 00327W) to Dover (3908N 07528W) via the indicated locations. The vertical structure is described by the profile and climb options. The profile states for 0000 time (departure) the true air speed will be 370 knots and an altitude of 1000 feet. Thereafter until 3 hr 07 min, the true air speed will be 427 knots at an altitude of 35000 ft and thereafter until 14 hr 37 min, the true air speed will be 425 knots at an altitude of 39000 ft. The climb options state that a climb from Torrejon will occur for 23 minutes to an altitude of 35000 feet.

## 4. DISPLAY PRODUCT

The output product is composed of columnar or summary, or a combination of columnar and summary, displays as shown in example 2. Columnar options appear vertically under a header identifing the option requested. The complete product is arranged sequentially by flight leg from departure to destination or from destination to alternate. All forecast options are computed on a leg by leg basis and are displayed in columnar format as requested. Enroute summaries are displayed beneath the columnar forecast and provide overall-to-destination or route-segment summaries of columnar data.

## 5. COLUMNAR OPTIONS

The columnar options available in RFM are as many and varied as route-forecast users. The forecast product is formed by selecting from the list of options, those options required in the desired sequence for the product display. The columnar options listed below are available in the current version of the Route Forecast Model. The options available for S segment summaries, O overall summaries, and P point summaries are so indicated. Alternate

spellings and columnar headings are listed in parenthesis to the right of the option.

LOCATION OPTIONS:

| OPTION NAME | SUMMARY | OPTION DESCRIPTION |
|---|---|---|
| LG | S O P | Flight leg number |
| LAT | S O P | Latitude in degrees and minutes |
| LONG | S O P | Longitude in degrees and minutes |
| FLAT | S O P | Latitude in degrees and tenths |
| FLONG | S O P | Longitude in degrees and tenths |
| ICAO | | ICAO location identifier |
| LOCID | S O P | 5 character location identifier |
| LOCATION | | 14 character location identifier |
| TAC | | TACAN Channel (if supplied) |
| VOR | | VORTAC frequency (if supplied) |
| CAL | | Collective Addressee List (if supplied) |
| ALT | P | Altitude in feet*100 |

WEATHER PARAMETERS:

| | | |
|---|---|---|
| WIND | P | Wind direction and velocity as DDD/VVV |
| DDVVV | P | Wind direction and velocity as DDVVV |
| WF | S O | Wind factor (+ is tailwind, - is headwind) knots |
| TTT (ZT) | P | Temperature in deg C |
| DVAL | P | Pressure D-value in feet*10 |
| TD | P S | Temperature deviation from standard, in deg C |
| ATD | O | Accumulated temperature deviation from standard |
| DA | P S | Density altitude |
| SA | | Sun angle |
| BCTC | P | Base-top contrails in feet*100 |
| TROP | P | Tropopause height (ft*100) and temperature (deg C) |
| WFPXX | S | Wind factor at altitude plux XX,000 feet |
| WFMXX | S | Wind factor at altitude minus XX,000 feet |
| TPXX | S | Temperature at altitude plus XX,000 feet |
| TMXX | S | Temperature at altitude minus XX,000 feet |

CLIMATIC PARAMETERS:

| | | |
|---|---|---|
| SVD | S | Standard Vector deviation |
| ASVD | O | Accumulated standard vector deviation |
| WWF | S | Worst wind factor (headwind), knots |
| AWWF | O | Accumulated worst wind factor |
| TSD | S | Temperature standard deviation |
| ATSD | O | Accumulated temperature standard deviation |
| WTT | S | Worst temperature (warmest),deg C |
| AWTT | O | Accumulated worst temperature |
| WTIM | | Worst time on flight leg in minutes |
| WETE | | Worse time enroute (accumulated worst time as HHMM) |

TIME SPEED DISTANCE PARAMETERS:

| | | |
|---|---|---|
| TIM(ZT) | S | Time of flight leg in minutes |
| ATIM (TT, ETE) | O | Accumulated time as HHMM |
| ETA | O | Estimated time of arrival |
| TTR | | Total time remaining as HHMM |
| TAS | | True air speed in knots |
| CAS | | Calibrated air speed in knots |
| MACH | | Mach number (xxx implies x.xx mach) |
| GS | | Ground speed in knots |
| DIS (ZD) | S | Flight leg distance in nautical miles |

| | | |
|---|---|---|
| TDIS | O | Total or accumulated leg distance |
| ADI | S | Air distance |
| TADI | | Total or accumulated air distance |
| TDR | | Total distance remaining |

NAVIGATION PARAMETERS:

| | | |
|---|---|---|
| TCS (TC) | | True course (arrival) |
| THD (TH) | | True heading |
| MV | | Magnetic variation |
| MCS (MC) | | Magnetic course |
| MHD (MH) | | Magnetic heading |
| GCS | | Grid course |
| GHD | | Grid heading |
| GWD | | Grid wind |
| GV | | Grivation |

FUEL PARAMETERS:

| | | |
|---|---|---|
| FLCHG | S | Leg fuel change/burn in pounds*100 |
| AFLCHG | O | Accumulated fuel change/burn |
| FLREM | | Fuel remaining |
| GWT | | Aircraft gross weight |

UTILITY PARAMETERS:

| | | |
|---|---|---|
| BLANK | | Blank column |
| ELEV | S P | Maximum terrain elevation |
| MODE | | Flight mode |
| LGTYPE | | Flight leg type |
| FOLD | | Vertical page fold |
| FOLDH | | Horizontal page fold |
| 2SPACE | | Double space |

A simplified method exists for selecting columnar and summary options in standard option formats. A standard option format is but itself an option representing a series of fixed options in a fixed sequence. Example 5 utilizes the standard option format CFP2 for requesting the options of LOCATION, ALT, WIND, TAS, GS, DIS(ZD), TIM(ZT), ATIM(TT), TDR, TCS(TC), MCS(MC), MHD(MH), CAL, FOLDH, LAT, and LONG.

Columnar fuel displays and the time-fuel analysis summary are dependent upon user input parameters. Two different fuel computations exist within RFM. The first technique utilizes fuel manuals reduced to equations residing within the fuel programs. With this technique, fuel computations are based upon forecast temperature, speed, flight mode, and forecast gross weight. Departure input parameters required are gross weight and fuel onload. The alternate fuel technique is the submission of fuel tables containing the accumulated burnoff per hour as part of the route specifications (example 5). The submission of fuel tables as part of the route specifications allows immediate computation of fuel for any aircraft, but requires the user to consider temperature, gross weight, and flight mode. Additional options and computations allow for air-refueling, ground-refueling, weight adjustment, fuel degradation, reserve computations and holding.

## 6. SUMMARIES

Columnar forecasts may be summarized, as required, by defining options and points over which the summary is to occur. An alternate method as used in examples 1 and 2 is the use of pre-defined summary options. Segment summaries are summaries between any two route definition points and are identified on the submitted route by the insertion of the summary name immediately following the point at which the summary is to occur. Overall summaries are indicated in a similar manner unless the pre-defined overall to to destination summary is desired (OVERALLS). An overall summary is simply a segment

summary with the departure point fixed as the first summary point.

Specialized summaries such as temperature deviation (TDSUM) produce an overall to destination forecast of temperature from standard. The equal-time point (ETP) summary (ETPSUMMARY) produces a series of three wind-factor forecasts surrounding the computed ETP (FWF is forecast wind factor, WF1 is the first-half-wind factor, and WF2 is the second-half-wind factor) and the time and distance from departure to the computed equal-time point. The ETP summary option may be controlled via route input to specify the area in which the ETP computation is to occur. Also available are the mid-time and mid-distance summaries similar to the ETP summary above. The time-fuel analysis summary is also available providing required fuel input parameters are supplied. The time-fuel analysis will be computed via MAC or Air Force standards depending on the fuel analysis requested.

## 7. LIBRARIES

At a user's request, route specifications and track descriptions, in a combined form (ready for processing), may be stored on a Route Library maintained by the Route Forecast Model. After the insertion of a route into the Route Library, a simplified request may be submitted to extract and process that route by the Route Forecast Model. Additional functions of library updates, deletions, listings, and accounting are also performed by RFM and its associated programs.

Additional libraries are maintained as part of the MAC-CFP system at AFGWC for the storage, update, and retreival of individual tracks, profiles, and destination alternates. Under the MAC-CFP system, individual tracks, profiles, and alternates are selected at the time of request and formed into complete routes as part of the execution of the Route Forecast Model. This allows for the possible combination of any track with any profile and any of the possible alternates with a total combination exceeding 2 million routes. Use of these libraries however is limited to the MAC-CFP users only.

## 8. CFP SYSTEM

The operation of the computer flight-planning system at the Air Force Global Weather Central (AFGWC) is completely automated and is initiated by the submission of a request into the CFP system. Examples 5 and 6 represent actual results of support derived from the MAC-CFP system.

A flight planner at the MAC Area Command Post at Lindsey Air Station, Germany requires CFP support for a C141 aircraft from Torrejon, Spain to Dover AFB. At departure time minus six hours, a Flight Plan Request Message is encoded at Lindsey and transmitted to AFGWC via the common-carrier Autodin. Within 20 minutes, that same flight plan request message is received at AFGWC by its autodin facility and punched onto paper tape. Moments later, the paper tape is read directly into the computer system by an on-line teletype with paper-tape attachments.

The raw autodin input message is accepted within the computer system by the Real-Time Operating System. Upon receipt and recognition of the autodin input message, an acknowledgement is transmitted to the teletype input device. Since the Real-Time Operating System can not decode the raw input message, the complete message is passed directly to the MAC Control program for input decoding.

The MAC Control program must decode and recognize all Autodin input messages since several types of input messages are possible. Upon recognizing the message as a flight plan request, individual requests are generated corresponding to individual computer flight plan demands. Total system capability allows for library updates and multiple CFP demands to be submitted within the same autodin input message. The individual request for CFP support generated by the MAC Control program identifies the route to be flown by track, alternates, and profile library labels and is generated complete with all addressing required for product dissemination. The request thus generated is passed back to the Real-Time Operating System for computation by the Route Forecast Model.

The Real-Time Operating System is the basic control program operating within the computer system. It receives raw autodin input messages, weather observations, and requests from AFGWC in-house devices and computer programs. Flight-plan requests, whether generated by a computer program or submitted by a Route Forecaster are passed directly to the Route Forecast Model for computation.

Once activated by the Real-Time Operating System, the Route Forecast Model recovers and analyzes the input-request message. Upon recognizing a requirement for MAC-CFP support, the CFP demand itself is decoded. In example 5, the CFP demand 172N6RPL0022 represents a request for track 172N, alternate code 6, aircraft R, profile RPL, no extra fuel, and a departure time of 2200Z. Based on the required track, profile, aircraft, and alternates, the route input as shown in example 5 is constructed and processed. If the request required a route from the Route Library, it would merely be extracted and processed directly. All computer flight plans generated are formated for the transmission device and are complete with addressing headers and trailer entries. The completed product is passed to the Real-Time Operating System for the actual product transmission.

The Real-Time Operating System receives and transmits the computer flight plan generated by the Route Forecast Model to a high-speed paper-tape punch located within AFGWC's Autodin facility. The CFP on paper tape is then transmitted directly via autodin to the requesting Area Command Post (Lindsey AS) and the aircraft departure base (Torrejon). The elapsed time from the transmission of the flight-plan-request message from the MAC Area Command Post to the receipt of the completed Computer Flight Plan at the departure base is basically a function of communications time and the tasks currently within the CFP system. Total throughput time is often under 45 minutes.

## 9. CONCLUSION

The Route Forecast Model is the computational portion of a computer flight planning system operational at the Air Force Global Weather Central. The program is constantly under development as new applications and options are discovered. The flexibility and usefulness of the products generated are limited only by the ingenuity of its requestor.

```
DATED 70 SEP 14  AT 1906@157
LABEL        2-YOUNGTIGER
ORIGINATOR   OPB2D2
COMMAND      SAC
UNIT         KMER
AUTHORITY    YOUNG TIGER
LAST REQUESTED       TOTAL REQUESTS      TIME USED   DATE CREATED
 70 SEP 14                  35             1170/0189   70 MAR 23
***1  UNCLASSIFIED
   2  COMM  CAS00
   3  COMM  CAS01
   4  COMM  FAF10
   5  COMM  SAC10
   6  PRINT YOUNG TIGER SUPPORT
   7  PRINT CASTLE TO HICKAM VIA ALFA ROUTE
   8  LG
   9  LAT
  10  LONG
  11  TCS
  12  THD
  13  MV
  14  MHD
  15  DDVVV
  16  ALT
  17  TTT
  18  TAS
  19  GS
  20  DIS
  21  TIM
  22  ATIM
  23  OVERALLS
  24  ROUTE
  25  KMEP     3723   12034   355   300     5000
  26  SEGSUM
  27           3715   12045                14000
  28           3716   12220                26000
  29           3635   12405   458          28000
  30           3615   12450
  31           3440   13000
  32           3255   13500
  33  140W     3100   14000
  34  SEGSUM
  35           2837   14500
  36           2600   15000
  37           2327   15355
  38           2300   15439
  39           2231   15605
  40           2108   15752
  41  PHIK     2118   15754
  42  SEGSUM
  43  RTEND
```

Example 1

YOUNG TIGER SUPPORT
CASTLE TO HICKAM VIA ALFA ROUTE

AFGWC TIME PHASED ROUTE FORECAST ROUTE 2-YOUNGTIGER
DEPARTURE POINT KMER
LAT 3723N LONG 12034W DEPT ALT 5000FT ETD 70 SEP 14 2330Z
ACCUMULATED TIMES ADJUSTED FOR 1 PCT ROUTE DEVIATIONS

| LG | LAT | LONG | TCS | THD | MV | MHD | DDVVV | ALT | TTT | TAS | GS | DIS | TIM | ATIM |
|---|---|---|---|---|---|---|---|---|---|---|---|---|---|---|
| 1 | 3715N | 12045W | 228 | 230 | -17 | 213 | 35012 | 140 | 5 | 355 | 360 | 12 | 2 | 0002 |
| 2 | 3716N | 12220W | 271 | 275 | -17 | 258 | 32029 | 260 | -18 | 355 | 336 | 76 | 14 | 0016 |
| 3 | 3635N | 12405W | 244 | 250 | -17 | 233 | 33034 | 280 | -32 | 355 | 350 | 93 | 16 | 0032 |
| 4 | 3615N | 12450W | 242 | 246 | -17 | 229 | 33031 | 280 | -35 | 458 | 456 | 41 | 5 | 0037 |
| 5 | 3440N | 13000W | 251 | 254 | -17 | 237 | 34023 | 280 | -35 | 458 | 457 | 270 | 36 | 0113 |
| 6 | 3255N | 13500W | 249 | 250 | -17 | 233 | 35012 | 280 | -36 | 458 | 460 | 270 | 36 | 0149 |
| 7 | 3100N | 14000W | 247 | 247 | -16 | 231 | 02004 | 280 | -35 | 458 | 461 | 279 | 37 | 0226 |
| 8 | 2837N | 14500W | 243 | 242 | -15 | 227 | 09006 | 280 | -35 | 458 | 463 | 297 | 39 | 0305 |
| 9 | 2720N | 14732W | 241 | 239 | -14 | 225 | 09010 | 280 | -34 | 458 | 467 | 155 | 20 | 0325 |
| 10 | 2600N | 15000W | 239 | 238 | -13 | 225 | 07012 | 280 | -35 | 458 | 470 | 154 | 20 | 0345 |
| 11 | 2327N | 15355W | 235 | 235 | -13 | 222 | 04011 | 280 | -35 | 458 | 468 | 263 | 34 | 0419 |
| 12 | 2300N | 15439W | 236 | 237 | -12 | 225 | 02009 | 280 | -34 | 458 | 465 | 49 | 6 | 0425 |
| 13 | 2231N | 15605W | 250 | 251 | -12 | 239 | 36009 | 280 | -34 | 458 | 461 | 84 | 11 | 0436 |
| 14 | 2108N | 15752W | 230 | 231 | -11 | 220 | 34008 | 280 | -33 | 458 | 461 | 129 | 17 | 0453 |
| 15 | 2118N | 15754W | 350 | 349 | -11 | 338 | 33007 | 280 | -33 | 458 | 452 | 10 | 1 | 0454 |

OVERALL TO PHIK AWF 3 TDIS 2182 ATIM 0454 ETA 0424Z
SEGSUM SEGMENT SUMMARY

| LOCID/LOCID | WF | DIST | TIM | LOCID/LOCID | WF | DIST | TIM |
|---|---|---|---|---|---|---|---|
| KMER 140W | -1 | 1041 | 0226 | 140W PHIK | 7 | 1141 | 0228 |

Example 2

```
DATED 70 SEP 14  AT 17229477
LABEL        E5-E23
ORIGINATOR   GWC201
***1   UNCLASSIFIED
    2   COMM   XXXXAT DET2 6WEAWG ANDREWS AFB MD
    3   COMM   XXXXAT DET40 2WEASQ HIGH WYCOMBE ENGLAND
    4   COMM   XXXXAT EUROPE/AFRICA ALFCP TORREJON AB SPAIN
    5   PRINT E-5/E-23 ANDREWS TO LONDON VIA GOOSE/PRESTWICK
    6   PRINT THIS FLT PLAN COMPUTES A TAS ON CLIMB 360KTS CRUISE 470KTS
    7   DISPLAY      ETP
    8   ACTYPE       VC135B
    9   DEGRAD       -06
   10   NAV          MIDPOINT
   11   DISPLAY      LEVELOFF
   12   LG
   13   LOCID
   14   LAT
   15   LONG
   16   FOLOH
   17   MODE
   18   DDVVV
   19   MCS
   20   GS
   21   DIS
   22   TIM
   23   ATIM
   24   TOP
   25   FLPEM
   26   ALT
   27   WFM04
   28   WF
   29   WFP04
   30   OVERALLS
   31   TDSUM
   32   ETPSUMMARY
   33   MACTIMEFUELANALYSIS
   34   ROUTE LOCATION          LAT     LON   DIST   TAS   ALT1   ALT2   ALT3 TAC VORT
   35   KADW                   3849   07652   900    360   5000
   36   START CLIMB 0022                              470  33000
   37   SEA I                  3906   07448
   38   PUTNA                  4157   07151
   39   KENNE                  4326   07037
   40   BANGO                  4451   06852
   41   PRESQ                  4646   06806
   42   MTJOL                  4832   06822
   43   L EON                  5151   06317
   44   GOOSE                  5317   06021
   45   START ETP
   46   CYQX                   5530   05659
   47                          5800   05000
   48   PRINC                  6004   04310
   49   EGPX                   5900   03000
   50   EGPX                   5600   01000
   51   SKIP                   5545   00532
   52   PREST                  5529   00436
   53   STOP  ETP,
   54   NEW G                  5511   00410          470  33000
   55   DEAN                   5443   00326
   56   POLE                   5345   00206
   57   LICHF                  5245   00143
   58   DAVEN                  5211   00107
   59   GARST                  5141   00025          360
   60   LONDO                  5128   00027                5000
   61   ALTERNATE
   62   LONDO                  5128      27               21000
   63   MILDE                  5222  -00028
   64   RTEND
```

Example 3

```
E-5/E-23 ANDREWS TO LONDON VIA GOOSE/PRESTWICK
THIS FLT PLAN COMPUTES A TAS ON CLIMB 360KTS CRUISE 470KTS

AFGWC TIME PHASED ROUTE FORECAST                          ROUTE E5-E23
DEPARTURE POINT KADW
LAT 3849N  LONG 07652W DEPT ALT   5002FT  ETD 70 SEP 14 2300Z
FUEL COMPUTATIONS BASED ON A/C VC135B, DEPT GWT 2355, DEPT FUEL 1200
NAVIGATION PARAMETERS ARE BASED ON LEG MIDPOINTS
ACCUMULATED TIMES ADJUSTED FOR 1 PCT ROUTE DEVIATIONS
LG  LOCID    LAT    LONG
MODE DDVVV MCS   GS DIS TIM ATIM  TOR FLREM ALT WFM04   WF WFP04
  1 SEA I 3906N 07448W
C    27023 089  382  98  15 0015 3324  1130 250    18   22    25
  2 LVLOF 3941N 07414W
C    28039 047  377  44   7 0022 3280  1109 330    16   17    16
  3 PUTNA 4157N 07151W
     28052 051  492 174  21 0043 3106  1069 330    22   22    20
  4 KENNE 4326N 07037W
     28065 047  491 104  13 0056 3002  1044 330    21   21    18
  5 BANGO 4451N 06852W
     28076 060  527 114  14 0110 2888  1017 330    37   37    33
  6 PRESQ 4646N 06806W
     28089 036  472 119  15 0125 2769   989 330     4    2    -1
  7 MTJOL 4832N 06822W
     28097 016  439 107  15 0140 2662   961 330   -27  -31   -34
  8 L EON 5151N 06317W
     28102 071  525 279  32 0212 2383   902 330    52   55    54
  9 GOOSE 5317N 06021W
E    28079 082  523 137  16 0228 2246   873 330    50   53    54
 10 CYQX  5532N 05659W
E    27051 075  521 178  22 0250 2068   834 330    28   31    32
 11       5802N 05022W
E    23029 092  499 274  33 0323 1794   776 330    27   29    31
 12 PRINC 6024N 04310W
E    20052 095  511 245  29 0352 1549   724 330    39   41    40
 13 ETP   5944N 03643W
E    26069 129  536 195  22 0414 1354   685 330    65   66    59
 14 EGPX  5900N 03200W
E    26068 131  534 210  24 0438 1144   643 330    63   64    56
 15 EGPX  5600N 01200W
E    31046 126  512 667  79 0557  477   511 330    39   42    37
 16 SKIP  5545N 00532W
E    24028 108  493 151  19 0616  326   480 330    21   23    22
 17 PREST 5529N 00436W
E    23039 128  485  35   4 0620  291   474 330    13   15    16
 18 NEW G 5511N 00410W
     23044 151  466  23   3 0623  268   469 330    -4   -4    -1
 19 DEAN  5443N 00326W
     23049 148  465  38   5 0628  230   461 330    -5   -5    -1
 20 POLE  5345N 00206W
     23055 150  461  75  17 0638  155   445 330   -10   -9    -4
 21 LICHF 5245N 00143W
     23059 176  438  62   9 0647   93   430 330   -33  -32   -27
 22 DAVEN 5211N 00107W
     23061 155  456  47   5 0652   53   422 330   -14  -14    -9
 23 GARST 5141N 00025W
     23062 147  465  40   5 0657   13   414 330    -6   -5    -1
 24 LONDO 5128N 00027W
T    23048 196  323  13   6 0703    0   405  50   -31  -37   -41
TEMPERATURE DEVIATION SUMMARY FOR ROUTE IS   5
ETP SUMMARY      FWF  41, WF1  41, WF2  41, TIME 0414, DIST 2068
OVERALL TO LONDO  AWF   30  TDIS  3422  ATIM 0703  ETA 0603Z
 AFGWC TIME AND FUEL ANALYSIS (MAC)
  1-ENROUTE              0703  079520   2-RESERVE          0042  000000
  3-ENROUTE + RESERVE    0745  079500   4-ALTERNATE        0000  000000
  5-HOLDING              0045  006023   6-APP/LANDING      0015  002400
  7-TOTAL/FLAPS UP       0845  087923   8-ACCELERATION             001500
  9-ID EXTRA FUEL              000000  10-TAXI/RUNUP              002000
 11-PLANNED RAMP               091423  12-TAKE OFF FUEL           120000
    BURN OFF FUEL              081900     ENDURANCE       1138

AFGWC TIME PHASED ALTERNATE ROUTE FORECAST
DEPARTURE POINT LONDO
LAT 5128N  LONG 00027W DEPT ALT  21000FT  ETD 70 SEP 15 0603Z
LG  LOCID    LAT    LONG
MODE DDVVV MCS   GS DIS TIM ATIM  TOR FLREM ALT WFM04   WF WFP04
 25 MILDE 5222N 00028E
     22045 040  404  64  10 0713    0   391 210    37   44    50
TEMPERATUPE DEVIATION SUMMARY FOR ROUTE IS   5
OVERALL TO MILDE  AWF   30  TDIS  3486  ATIM 0713  ETA 0613Z
 AFGWC TIME AND FUEL ANALYSIS (MAC)
  1-ENROUTE              0703  079500   2-RESERVE          0042  000000
  3-ENROUTE + RESERVE    0745  079500   4-ALTERNATE        0010  001400
  5-HOLDING              0045  006023   6-APP/LANDING      0015  002400
  7-TOTAL/FLAPS UP       0855  089323   8-ACCELERATION             001500
  9-ID EXTRA FUEL              000000  10-TAXI/RUNUP              002000
 11-PLANNED RAMP               092823  12-TAKE OFF FUEL           120000
    BURN OFF FUEL              081900     ENDURANCE       1138
```

Example 4

```
                    THIS MESSAGE IS
                * * * U N C L A S S I F I E D * * *
              REFERENCE REQRF                          650

DATED 70 SEP 14  AT 16298047
LABEL       172N6PPL0022
ORIGINATOR  OPS207
***1  UNCLASSIFIED
    2  CFP2
    3  ETD           2202Z14SEP70
    4  STRUCTURE     172N RPL LETO KDOV  48N          E     H
    5  IDPROFILE     RPL
    6  TEMPPROFILE   STD
    7  PROFILE       0000        T370        1000
    8  PROFILE        307        T427       35000
    9  PROFILE       1437        T425       39000
   10  ACTYPE        C-141A
   11  FUELMANUAL    55-20 6MAR69
   12  FUELPAGE      011
   13  FUELDATA       17800       30200       42000       53200       63700
   14  FUELDATA       73800       83800       93700      103000      112200
   15  FUELDATA      121300      129800      138200      146300      154300
   16  TOGWT         310000
   17  TAXIFUEL        1900
   18  LANDINGTIME   15
   19  MAXFUEL       153352
   20  NAV           MIDPOINT
   21  FORMAT        CFP
   22  DISPLAY       LEVELOFF
   23  ETPSUMMARY
   24  MIDTIMESUMMARY
   25  MACTIMEFUELANALYSIS
   26  RTREV         0
   27  IDTRACK       172N
   28  TRACK LOCATION******  **LAT  **LONG DIST   ALTCON CAL
   29  LETO  TOPREJON         4029     327 9999
   30  START CLIMB   23                          T427 35000
   31        MOSTOLES         4020     347
   32        NAVAS DEL REY    4022     415
   33        ZAMORA           4132     538
   34        SANTIAGO         4256     826
   35  START RES
   36        EGPX/LECM        4500    1200                  AB2
   37                         4700    2000                  AC1
   38        CYQX/EGPX        4800    3000                  AC1
   39                         4800    4000                  AB1
   40                         4800    4500
   41        ADI7             4800    4700
   42                         4800    5000                  AB1
   43        ADI7/CYQX        4800    5100
   44        ST JOHNS RBN     4740    5249
   45  STOP  RES
   46        CYQM/CYQX        4636    5810
   47        SYDNEY           4609    6003
   48        HALIFAX          4455    6324
   49        YARMOUTH         4350    6605
   50        CYQM             4315    6700
   51        DAVEY            4257    6731
   52        NANTUCKET        4117    7002
   53        091R/79 JFK      4050    7206
   54        KENNEDY          4038    7346
   55        COYLE            3949    7426
   56        KENTON           3914    7531
   57  KDOV  DOVER            3908    7528          D
   58  ALTERNATE
   59  KDOV  DOVER            3908    7528    84X
   60  KWRI  MCGUIRE          4001    7436
   61  START HOLD  45
   62  ALTERNATE
   63  KDOV  DOVER            3908    7528    78X
   64  KADW  ANDREWS          3849    7652
   65  START HOLD  45
   66  ALTERNATE
   67  KDOV  DOVER            3908    7528   138X
   68  KLFI  LANGLEY          3705    7621
   69  START HOLD  45
   70  RTEND
```

**Example 5**

```
MAC COMPUTER FLIGHT PLAN     172N6RPL0022
172N RPL LETO KDOV  48N          E     H L/O 23   0/0 C-141A 14/19Z-01Z
TORREJON            ALT    WIND   TAS  GS   ZD   ZT    TT   TDR   TC   MC   MH CAL
  4029N  0327W                                              3295
MOSTOLES            060 294/  4  370 366   18   03    03  3277  240  247  247
  4020N  0347W
NAVAS DEL REY       120 230/ 10  370 363   21   04    07  3256  275  283  282
  4022N  0415W
ZAMORA              350*269/ 29  370 350   94   16    23  3162  318  326  322
  4132N  0538W
SANTIAGO           +350 275/ 57  427 376  150   24    47  3012  304  313  309
  4256N  0826W
EGPX/LECM           350 267/ 65  427 376  198   32   119  2814  309  320  313 AB2
  4500N  1200W
4700N  2000W        350 283/ 52  427 375  354   57   216  2460  290  304  303 AC1

CYQX/EGPX           390 308/ 59  427 375  409  106   322  2051  278  297  301 AC1
  4800N  3000W
4800N  4000W        390 282/ 38  425 388  401  102   424  1650  270  294  295 AB1

4800N  4500W        390 279/ 49  425 377  201   32   456  1449  270  296  297

ADIZ                390 277/ 65  425 360   80   13   509  1369  270  297  298
  4800N  4700W
4800N  5000W        390 267/ 76  425 349  120   21   530  1249  270  298  297 AB1

ADIZ/CYQX           390 264/ 80  425 345   40   07   537  1209  270  298  297
  4800N  5100W
ST JOHNS RBN       +390 265/ 79  425 347   76   13   550  1133  255  282  284
  4740N  5249W
CYQM/CYQX           390 269/ 80  425 347  228   40   630   905  254  281  284
  4636N  5810W
SYDNEY              390 275/ 77  425 354   83   14   644   822  251  277  282
  4609N  6003W
HALIFAX             390 278/ 75  425 362  159   26   710   663  242  266  273
  4455N  6324W
YARMOUTH            390 281/ 68  425 371  132   21   731   531  241  262  269
  4350N  6605W
CYQM                390 282/ 61  425 386   53   08   739   478  229  249  256
  4315N  6700W
DAVEY               390 284/ 57  425 388   29   05   744   449  232  251  258
  4257N  6731W
NANTUCKET           390 285/ 49  425 396  150   23   807   299  228  246  252
  4117N  7002W
091R/79 JFK         390 286/ 43  425 388   97   15   822   202  254  269  272
  4050N  7206W
KENNEDY             390 284/ 41  425 387   77   12   834   125  261  274  276
  4038N  7346W
COYLE               390 283/ 36  425 412   58   08   842    67  212  223  228
  3949N  7426W
KENTON              390 288/ 31  425 406   61   09   851     6  235  245  248
  3914N  7531W
DOVER               370 289/ 27  425 443    6   01   852     0  155  164  167
  3908N  7528W
   FWF  -52   WF1  -48   WF2  -56   ETP  455   PG 011 TOGW 310  STD
A1 MCGUIRE             283/ 27 425 435   84 0012  KWRI
  1-0852 101760  2-0033 005073  3-0925 106833  4-0012 003544
  5-0045 006936  6-0015 002500  7-1037 119813  8-000000
  10-001900  11-121713  B/O-104260
A2 ANDREWS             281/ 22 425 405   78 0012  KADW
  1-0852 101760  2-0033 005073  3-0925 106833  4-0012 003544
  5-0045 006936  6-0015 002500  7-1037 119813  8-000000
  10-001900  11-121713  B/O-104260
A3 LANGLEY             299/ 13 425 427  138 0019  KLFI
  1-0852 101760  2-0033 005073  3-0925 106833  4-0019 005093
  5-0045 006936  6-0015 002500  7-1044 121362  8-000000
  10-001900  11-123262  B/O-104260
```

Example 6

# METEOROLOGICAL SUPPORT TO WHITE SANDS MISSILE RANGE

Harold M. Richart

Atmospheric Sciences Laboratory
US Army Electronics Command
White Sands Missile Range, New Mexico

## Abstract

White Sands Missile Range, New Mexico, a national missile range, is engaged in research, development, test, and evaluation activities involving a wide variety of ballistic and guided missiles, related systems, and other research efforts. Requirements for meteorological data, from the surface to the outer limits of the atmosphere, are discussed. Techniques and instrumentation for provision of these data include the conventional, the nonconventional, and the unique. The role of the Atmospheric Sciences Laboratory in providing meteorological support is described.

## INTRODUCTION

The highly instrumented White Sands Missile Range (WSMR), the only national land range, is operated by the US Army in the support of research, development, test, and evaluation of a variety of systems and projects, including atmospheric research.


PHOTO 1 - MAP, WHITE SANDS MISSILE RANGE

WSMR, approximately 40 by 100 miles, encompasses the Tularose basin and is bounded by mountain ranges on the west and north, with altitudes ranging from 3900 feet Mean Sea Level (MSL) in the basin to 9100 feet MSL at the highest peak. A slightly higher mountain range lies a few miles to the east. Additional land space required for tests of higher-performance missiles is made available through co-use land.

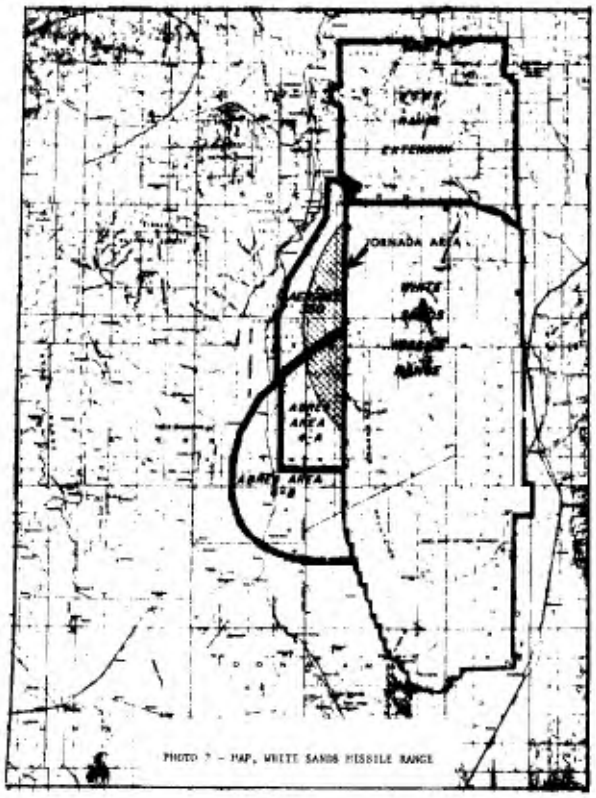


PHOTO 7 - MAP, WHITE SANDS MISSILE RANGE

A northern extension adds approximately 1400 square miles, while adjoining land to the west adds another 1300 square miles, giving a total of 6700 square miles of available land area for missile and payload testing.

Not all missile launches occur at WSMR proper. Since 1963, off-range launches have been made from a variety of locations. Del Rio, Texas, was the location for the Air Force Hound Dog missile launches.

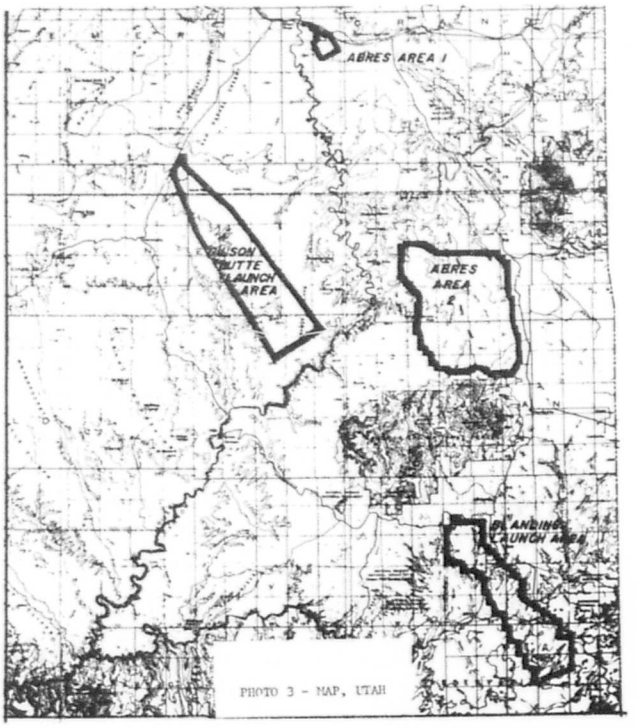


PHOTO 3 - MAP, UTAH

Blanding and Gilson Butte, Utah, have been the sites of 94 launches of the Army Pershing missile; Green River, Utah, is the launch location for the Air Force Athena, the Advanced Ballistic Reentry System (ABRES).


PHOTO 4 - ATHENA TRAJECTORY

One hundred twenty-three Athenas have been launched from the Utah Launch Complex to impact on WSMR for the free world's longest overland flight, 400 nautical miles, of an unguided missile.

Programs using WSMR facilities and the Atmospheric Sciences Laboratory's (ASL) meteorological support services include ground and air weapons systems, defense systems, descent systems (both drag and thrust retardation), ballistic reentry systems, guidance systems of all types, missile-borne research projects in astronomy, laser research, and others. Because of the mild, semi-arid climate of WSMR, optical tracking is seldom difficult; mission cancellation because of weather is an infrequent occurrence. Since WSMR is a land range, recovery of payloads or missile parts is easily and quickly accomplished, providing a tremendous bonus for the experimenter. There are more than 1000 active instrumentation sites, connected by 1200 miles of roads, 60,000 miles of wire and cable, and 340 microwave and radio channels.

The ASL complex at WSMR is ideally located for the conduct of atmospheric research. Unrestricted air space, 4000 square miles, permits the accomplishment of a wide variety of atmospheric measurements and experiments between the earth's surface and the outer limits of the atmosphere. ASL conducts investigations in ballistics applications, atmospheric variabilities in time and space, and sensing techniques from the surface to 110 km, all as applied to support of WSMR and the Army.

WSMR is more highly instrumented for the study of atmospheric conditions than any other comparable area in the United States. Several well-instrumented meteorological towers and a micrometeorology instrumentation array (T Array) provide means for conducting research on atmospheric motions and stability over several types of terrain. Wind and temperature data are routinely collected to 60 km by six rawinsonde stations and one meteorological rocket site. Wind data to 80 km are collected with a slightly different meteorological rocket.

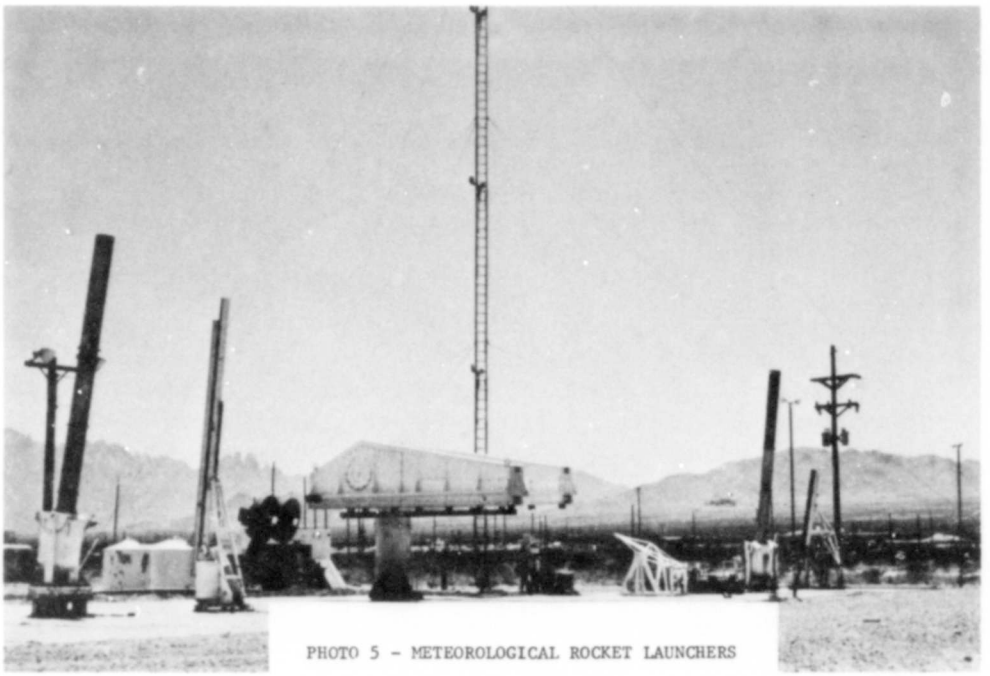

PHOTO 5 - METEOROLOGICAL ROCKET LAUNCHERS

Before the calendar year is ended, ASL will have a Meteor Trail Tracking Radar System in operation to provide wind data from 80 to 110 km. It is believed that there is no other area in the world where meteorological data are routinely available from the surface to 110 km.

## METEOROLOGICAL REQUIREMENTS

Data collected range from the simple surface observations to missile impact locations, using conventional or ASL-developed special-purpose systems and techniques in reduction or derivation. These data are applied by ASL elements, range elements, or test program personnel as necessary for all stages of RDT&E. Wind and temperature, and the derived values of density, refractive index, speed of sound, and other parameters may be required to evaluate a reentry body; similar values may be needed for an exact determination of the performance of a new missile, or a new descent system.

Approximately 75 permanent stations on WSMR and 7 permanent remote stations in Arizona, Utah, and New Mexico are available for data collection.

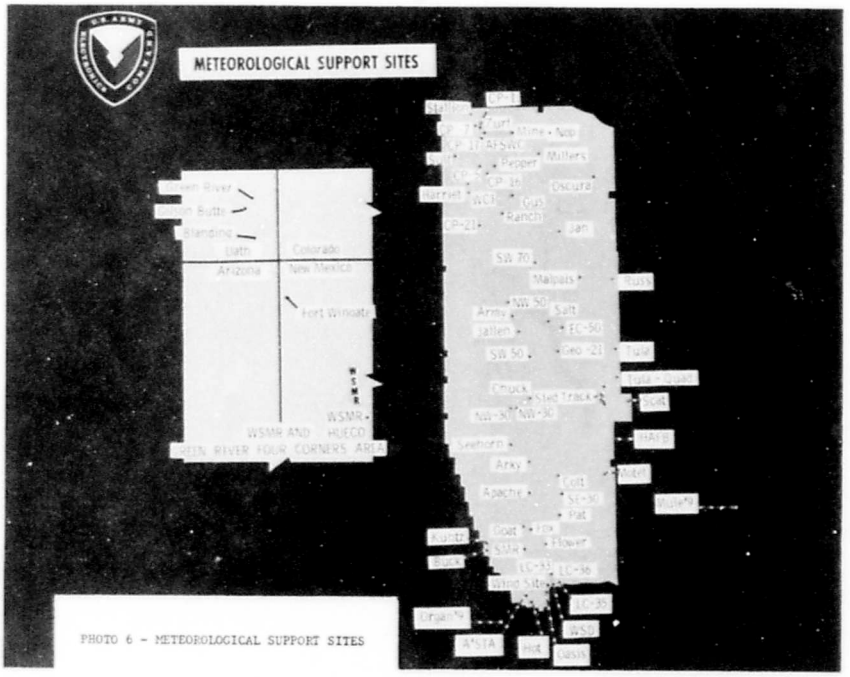


PHOTO 6 - METEOROLOGICAL SUPPORT SITES

Three self-contained mobile rawinsonde/surface observation units are operated as required in the states of Texas, New Mexico, Colorado, and Utah. Ninety military and 34 DA civilian personnel, with a supporting meteorological data collection contract, are directly involved in range support. End product output of 20 military and 92 civilian personnel in other areas of ASL is directed toward techniques and application.

Meteorologists provide general and special weather forecasts for all meteorological parameters required by programs operating at WSMR. The general forecast is unique in that it departs from the conventional terminology. Since optics are important to most of the test programs, sky cover is specific in that the tenths of coverage are given for each type of cloud, as well as the time and height of the cloud coverage. Winds aloft are forecast to 100,000 feet on a routine twice-daily basis. Winds to 140,000 feet are forecast for high-altitude constant-level balloon flights, and winds to altitudes of 235,000 feet are

forecast for the launching of missiles such as the Athena and Aerobee-350. Weather warnings are issued for any atmospheric condition which might endanger life or property or which might jeopardize successful completion of a range operation. The earth's local static-electric field is continuously monitored at the base weather station and in the major launch areas during operations to provide projects with an additional safety factor, a knowledge of potential thunderstorm activity.

Professional meteorological consultation services are provided to test programs requiring meteorological support services at WSMR or that are planning to utilize WSMR facilities for future RDT&E programs. These consultant services generally cover the entire scope of meteorology—atmospheric effects, techniques of applying meteorological data, instrumentation available for data collection. and recommendations for the data and techniques useful to any particular project.

The ballistics meteorological services provided consist of the determination and analysis of atmospheric effects upon missile performance, and prelaunch prediction of missile trajectories and impact points. These predictions (impact predictions) involve a thorough and accurate measurement and analysis of wind conditions through predetermined layers of the atmosphere.

Real-time impact predictions[1-10] developed and applied by ASL personnel are performed at WSMR if vehicle wind response requires simulation of trajectories through measured wind fields to obtain launcher settings more rapidly than provided by manual impact prediction techniques. Examples of missions requiring real-time support are Athena flights from Green River and hi-altitude research vehicles such as the Aerobee-350 with an apogee near 300 miles. Real-time procedures require ballistics-meteorologist services at the launch point for verification of wind-data inputs to the computer and at the computer center for validation of computed layer-winds and derived launcher-settings.

PHOTO 7 - 500 FOOT TOWER

Low-level wind-field measurements for real-time application are obtained from 500-foot towers instrumented at eight levels, with local analog plots and digital sampling at one per second, and from the T-9 Automatic Pibal Tracking System[11,12], with local analog plots and digital sampling at four per second.

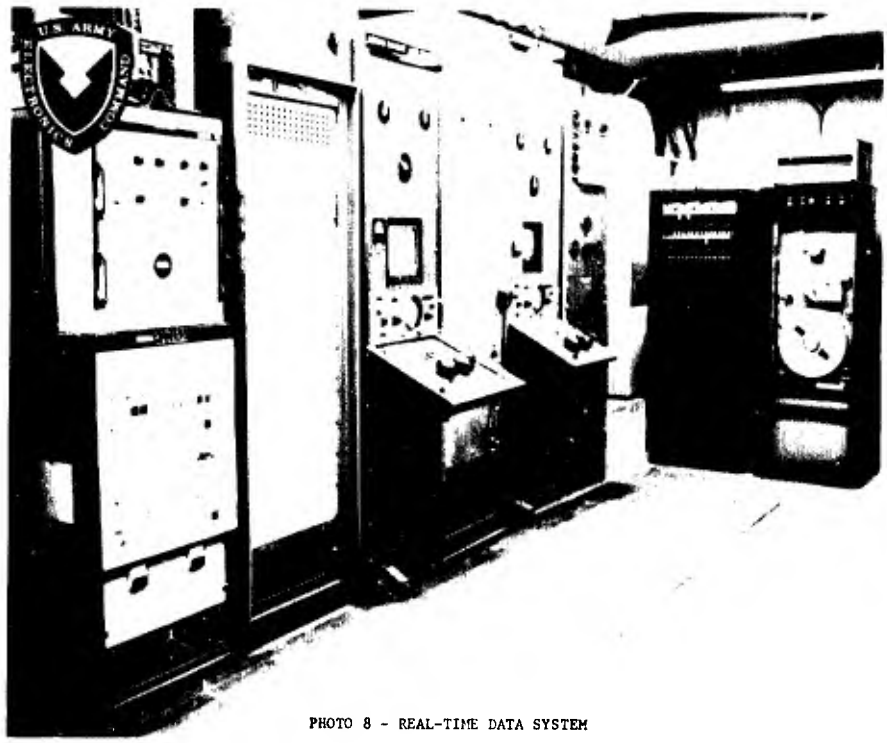


PHOTO 8 - REAL-TIME DATA SYSTEM

All digital data are formatted and transmitted to a high-speed digital computer for processing. Upper-level wind data to altitudes above 200,000 feet MSL are obtained from either of two systems. One method employs real-time computer input of FPS-16 radar tracking data from a balloon-borne ascending target and from a descending target carried aloft by a meteorological rocket. The second method obtains wind data through standard rawinsonde techniques and manual reduction of the information obtained from the radar track of the rocket-borne target. Application of wind data to a trajectory simulation produces a launcher setting which will compensate for the existing wind field to achieve desired project goals. Computer output also includes predicted trajectory velocity vectors, velocities and space points as functions of time, which are presented to project personnel and to the missile flight surveillance officers for performance evaluation during the missile flight.

The field technique of impact prediction[12-16] utilizes tower and pibal wind values from analog plots at the missile launch site and wind data from local rawinsonde observations. Weighting factors are then applied to these measured winds, and compensating launcher settings are determined by using missile response characteristics derived from theoretical trajectory simulations. In addition, space-point determinations for experimental events are derived as required by users. The primary factors in the computations for launcher settings are total ballistic-wind effect, unit-wind effect, coriolis, and tower-tilt effects on the missile. The missile flight safety officer is provided with the predicted trajectory, pertinent space points, and missile velocity vectors prior to launch for use in missile performance evaluations during flights.

In either system, firm firing recommendations (go or no-go) are presented by the ballistics meteorologist (Impact Predictor) to the project, WSMR range controller, and missile flight safety officer. This recommendation forecasts the probability of the successful achievement of the mission objectives under existing and predicted atmospheric conditions.

Many of the meteorological systems employed at WSMR are age-proven, such as the GMD rawinsonde set, the wiresondes, the 500-foot tower with multilevel sensing, the meteorological rocketsonde, and the surface observing equipment. Much productive effort has been made by ASL elements in the development and improvement of meteorological rocket hardware[17,18], data knowledge and techniques[19-21]. Equally as important is the investigative effort in the area of low-level wind-field characteristics[22-27], as this has influenced the processing techniques and produced improved meteorological support to projects.

One system developed by ASL is the T-9 Automatic Pibal Tracking System, which uses the radar (T-9) from the T-38 Fire-Control System (Anti-aircraft).

PHOTO 9 - MOBILE & FIXED T-9 RADAR SYSTEM

The T-9 radar, operating at 3-cm wavelength and 40 kilowatts peak power, has a maximum tracking range of 26,000 yards. In application, the radar tracks a balloon-borne shaped-aluminum-foil target and will consistently obtain wind data to more than 10,000 feet above ground when average wind speeds are 30 to 40 miles per hour. The T-9 system uses two-speed servo-systems to position digital encoders and potentiometers for range, azimuth, and elevation data. The encoders are the source of position data for real-time support. The standard radar analog plotting procedures are slightly modified to produce continuous traces of component wind velocity versus altitude.

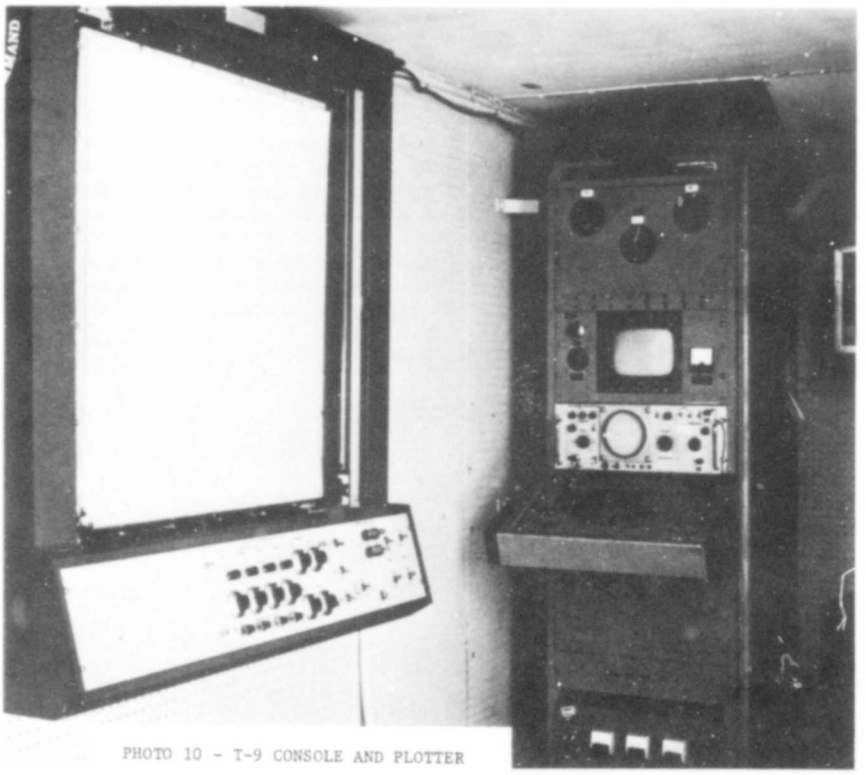

PHOTO 10 - T-9 CONSOLE AND PLOTTER

The T-9 system has been proven reliable and is in ever-increasing demand at WSMR. Specified accuracy is ±2 mph for a wind averaged over 250 feet. Currently, ten fixed-location T-9 systems and five mobile T-9 systems are in use at WSMR, with an additional 11 systems expected to be in operation by the end of FY-71.

Another ASL development, the Sonic Observation of Trajectory and Impact of Missiles (SOTIM), determines the precise impact point of valuable rockets and rocket payloads to permit rapid recovery. SOTIM is a completely passive acoustic system which detects the shock wave generated by an object moving through the atmosphere at speeds greater than the local speed of sound.

Fourteen permanently installed SOTIM sites provide complete coverage of WSMR and surrounding areas. Each site consists of an array of four microphones installed at the corners of a square, 1000 feet on a side, and oriented on true north. As a shock wave travels across the array, it is detected by each microphone and the impulse so generated is transmitted to a central recording station. From the difference in time of arrival at each microphone, the azimuth angle to point of origin may be calculated. Combined with similar information from other sites, trajectory information such as points of origin and impact may be derived with respect to the missile or other object which generated the shock wave. The SOTIM system has proved to be very reliable and has been instrumental in the recovery of many valuable missiles and missile payloads.

## FUTURE REQUIREMENTS

Research and development efforts need ever-increasing detail in meteorological data gathered. The task of providing this meteorological support becomes more difficult because the specialized field of detailed meteorological data acquisition systems is lagging, whereas data acquisition and data processing have been racing ahead in other fields. There has long been a need for faster sample rates, better accuracies in sampling, higher reliabilities, and field versions of laboratory instruments. In a very few years, there will be a requirement for some, if not all, of the following detailed instantaneous vertical and horizontal profiles: temperature, water vapor, index of refraction (optical and electromagnetic), atmospheric motion, turbulence to frequencies of 500 Hz, transmissivity (to

coherent and noncoherent radiation), precipitation-droplet size, ozone content, pollutant concentrations, and others.

All people in the field of meteorology can take pride in the growth of knowledge in their field, the development of the existing systems and the successes they have produced as well as the support provided, whether it be a local or global forecast, a crop-dusting, or lunar voyage; yet no one is willing to stop here. All the knowledge that is collectively possessed is but a fraction of what can be learned. The support that is provided today must continue to become more accurate, more detailed, and more applicable. To achieve this goal, ASL plans to automate all its data collection and processing within the next five years.

## REFERENCES


1. Duncan, L. D., and Henry Rachele, "Real-Time Meteorological System for Firing of Unguided Rockets," February 1966, AD 482 326.
2. Duncan, L. D. and B. F. Engebos, "Techniques for Computing Launcher Settings for Unguided Rockets," September 1966, AD 642 856.
3. Duncan, L. D., "Basic Considerations in the Development of an Unguided Rocket Trajectory Simulation Model," September 1966, AD 642 855.
4. D'Arcy, Edward M., "Some Applications of Wind to Unguided Rocket Impact Prediction," March 1967, AD 653 001.
5. Walters, Randall K., "Numerical Integration Methods for Ballistic Rocket Trajectory Simulation Programs," June 1967, AD 658 064.
6. Duncan, Louis D., and Bernard F. Engebos, "A Six-Degree-of-Freedom Digital Computer Program for Trajectory Simulation," October 1967.
7. Engebos, B. F., and L. D. Duncan, "Real-Time Computations of Pilot-Balloon Winds," March 1968.
8. D'Arcy, Edward M., and Henry Rachele, "Proposed Prelaunch Real-Time Impact Prediction System for the Aerobee-350 Rocket," May 1969.
9. Duncan, L. D., and Bernard F. Engebos, "A Rapidly Converging Iterative Technique for Computing Wind Compensation Launcher Settings for Unguided Rockets," July 1969.
10. Walters, Randall K., and Bernard F. Engebos, "An Improved Method of Error Control for Runge-Kutta Numerical Integration," October 1968.
11. Jacobs, Willie N., "Automatic Pibal Tracking System," May 1968, AD 674 180.
12. Kubinski, Stanley F., "A Comparative Evaluation of the Automatic Tracking Pilot-Balloon Wind Measuring System," April 1967, AD 654 991.
13. Dunaway, Gordon L., "A Wind-Weighting Technique to Predict Velocity Vector Azimuth Angles for Unguided Rockets," December 1969.
14. Engebos, Bernard F., and Duncan, Louis D., "A Nomogram for Field Determination of Launcher Angles for Unguided Rockets," October 1966, AD 644 819.
15. Dunaway, G. L., and Mary Ann B. Seagraves, "Launcher Settings Versus Jack Settings for Aerobee-150 Launchers - Launch Complex 35, White Sands Missile Range, New Mexico," August 1967.
16. Dunaway, Gordon L., "A Practical Field Wind-Compensation Technique for Unguided Rockets," August 1968, AD 680 177.
17. Ballard, Harold N., "The Thermistor Measurement of Temperature in the 30-65 KM Atmospheric Region," November 1969.
18. Avara, E. P., and B. T. Miers, "A Data-Reduction Technique for Meteorological Wind Data above 30 Kilometers," December 1967, AD 667 918.
19. Rachele, Henry, and L. D. Duncan, "The Desirability of Using a Fast Sampling Rate for Computing Wind Velocity from Pilot-Balloon Data," July 1966, AD 640 157.
20. Kays, Marvin, and R. O. Olsen, "Improved Rocketsonde Parachute-derived Wind Profiles," October 1966, AD 644 818.
21. Miers, B. T., and R. O. Olsen, "Short-Term Density Variations Over White Sands Missile Range," October 1969.
22. Monahan, H. H., M. Armendariz, and V. D. Lang, "Estimates of Wind Variability Between 100 and 900 Meters," April 1969.
23. Armendariz, Manuel, Laurence J. Rider, and Frank V. Hansen, "Turbulent Characteristics in the Surface Boundary Layer," November 1968.

24. Rider, Laurence J., Manuel Armendariz, and Frank V. Hansen, "A Study of Wind and Temperature Variability at White Sands Missile Range, New Mexico," September 1968, AD 680 172.
25. Armendariz, Manuel, and Virgil D. Lang, "Wind Correlation and Variability in Time and Space," July 1968, AD 674 179.
26. Rider, Laurence J., and Manuel Armendariz, "A Comparison of Simultaneous Wind Profiles Derived from Smooth and Roughened Spheres," September 1967.
26. Armendariz, M., and H. Rachele, "Determination of a Representative Wind Profile from Balloon Data," January 1967, AD 649 131.

# THE USE OF COMPUTER PRODUCTS IN SEVERE-WEATHER FORECASTING

Robert C. Miller (Col, USAF, Ret)

Arthur Bidner, Lt Col, USAF

Air Force Global Weather Central
Offutt Air Force Base, Nebraska

## INTRODUCTION

During the past 20 years most of the effort toward numerical weather prediction has been focused on the large-scale hemispheric features. The practicing forecaster has, of course, profited from these efforts, but the great benefits, in terms of more precise and accurate forecasts of severe-weather occurrences, have not been clearly identifiable.

The Air Force Air Weather Service has not only recognized this problem but has made marked progress in using numerical techniques to improve both the accuracy and the lead time of severe-weather warnings. This has been accomplished at the Air Force Global Weather Central by utilizing computers to collect, edit, analyze, forecast and display the information required by the severe weather forecaster.

It is obvious that those parameters most important to the forecasting of tornadoes and severe thunderstorms are not those of the general hemispheric circulation, but those of the meso-circulation. For the first time we are using the computer to detect and forecast conditions conducive to these destructive storms — and we are doing it in time to provide reliable warnings to some 550 military locations for vital decisions and protective actions. We feel certain these procedures are improving our credibility in the eyes of the user, which is an important achievement in itself.

In this presentation I will review the problems involved in forecasting tornadoes and severe thunderstorms with damaging winds and/or hail. I will explain those computerized tools used in such forecasts at the AFGWC, with particular emphasis on the Automated Severe Weather Threat (SWEAT) Index conceived and programmed at AFGWC. Finally I will present a recent example of the use of automated products in forecasting one of this summer's most-severe weather outbreaks.

## COMPUTER PRODUCTS AND SEVERE-WEATHER FORECASTS

The conditions sufficient and necessary for the development of tornadoes and severe thunderstorms, their associated destructive phenomena and the meteorological parameters utilized in forecasting them, have been discussed in detail in two previous publications, references (1) and (2). A summary of the more important parameters include:

1. Stability of the air column.
2. The low-level moisture field.
3. The vertical shear between 850 and 500 mbs.
4. The low-level jet.
5. Mid-tropospheric jets, horizontal-shear zones and diffluent patterns.
6. 500-mb thermal fields.

7. 700-mb moisture fields.

8. 850-mb temperature fields.

The difficulty of identifying these parameters in any given situation and forecasting their movement in time and space can be appreciated by any practicing forecaster. Prior to the relocation of the AWS Military Weather Warning Center from Kansas City, Missouri to the Air Force Global Weather Central at Offutt AFB, Nebraska, the prognoses of the various parameters was a time-consuming and laborious task with success dependent on the experience and skill of the individual forecaster. Today, however, the AFGWC environmental data base stored in the UNIVAC 1108 computer system provides the AFGWC severe-weather forecaster not only current analyses of the parameters mentioned but with 12-and 24-hour surface, 850, 700, and 500-mb fine-mesh wind, contour, moisture and temperature prognostic fields for the U.S. area. For example, the fine-mesh Boundary-Layer Model (BLM) provides him with timely and accurate 12- and 24-hour forecast fields of temperature and moisture at 900 meters, wind fields at 50 meters and at 600 meters. This boundary-layer forecast model, which is the subject of another paper being presented by Lt Col Hadeen, also provides detailed information at other intermediate levels. We have chosen the levels mentioned above as most significant for severe-weather purposes.

In addition, the forecaster is provided with a printout of the current Severe-Weather Threat (SWEAT) Index analysis, plus 12-, 24- and 36-hour prognoses of the SWEAT field. The SWEAT computation is given in attachment 1. This is a particularly valuable tool since the index combines weighted values of the five most important parameters conducive to the development of tornadoes and severe thunderstorms and is an invaluable aid in indicating areas of potential severe activity. The forecaster may also request, through a Selective-Display Model (SDM), any other information he may require from the AFGWC data base. The ready availability of these computerized products has resulted in marked improvement in the capability of the AFGWC severe weather unit to provide more timely and accurate forecasts to the field. Although the unit has, this year, a fewer number of experienced severe-weather forecasters, verification figures since activation on 1 February 1970 have improved dramatically when compared month-for-month with previous years. To cite one example — in April of this year 91% of all tornado areas issued verified compared with a previous seven year high of 75%. We firmly believe this improvement is directly attributable to the AFGWC computer data-base products.

## CASE STUDY USING COMPUTER OUTPUT

One excellent example of the utilization of computerized current data and prognostic charts occurred on the 14th of July 1970. A widespread outbreak of tornadoes, severe thunderstorms with damaging winds and hail up to four inches in diameter broke out over portions of Southeastern South Dakota, Southwestern Minnesota, Eastern Nebraska and West-central Iowa during the afternoon and evening causing many injuries and damage in excess of 10 million dollars. To illustrate the routine use of our data-base products I will show several charts, three depicting a composite of the most important parameters and SWEAT fields and a fourth showing the activity actually reported. Figure 1 is the composite chart made from the 14 July 1200Z data base and represents current conditions. These are based upon the U.S. selected level RAOB data available one hour after 1200Z. Figure 2 is a composite chart made from the 12-hour (150000Z) prognostic data base fields available about 1500Z on the 14th of July. Figure 3 is the composite chart made from the actual 0000Z data 15 July and Figure 4 shows the forecast area issued at 1700Z on the 14th of July with the subsequent verification. The excellence of the computer products in this particular storm situation is obvious, but is not unusual. The severe-weather forecasters at AFGWC have developed a very high degree of confidence in the numerical products produced from the AFGWC data base.

## REFERENCES

1. "Forecasting the Degree of Intensity of Severe Thunderstorms," Miller, R.C., In: Preprints of papers presented at the Sixth conference on Severe Local Storms, Chicago, Illinois, April 1969.

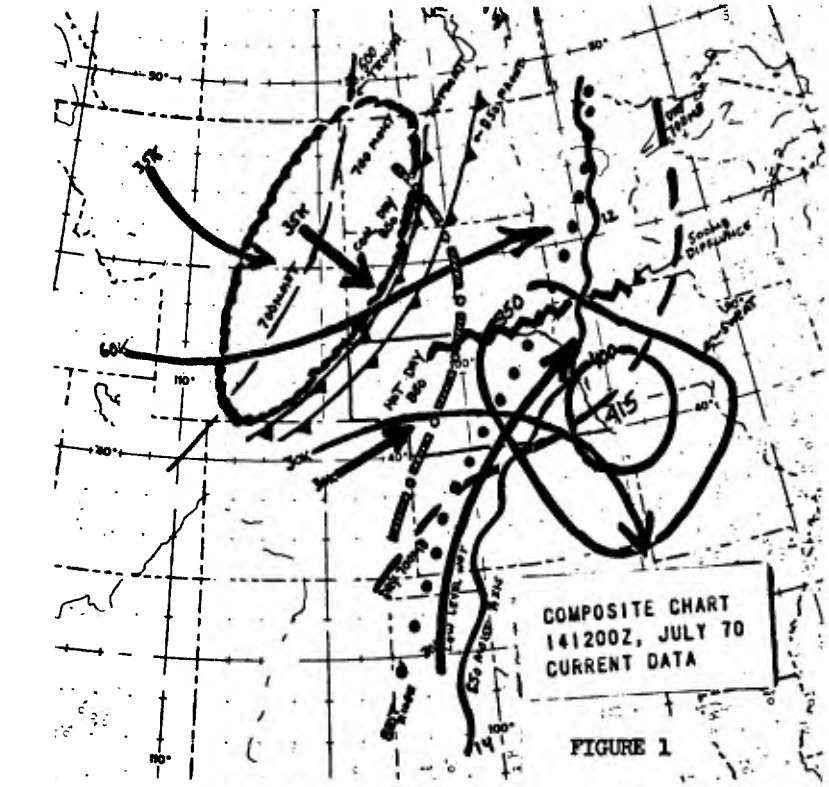


FIGURE 1

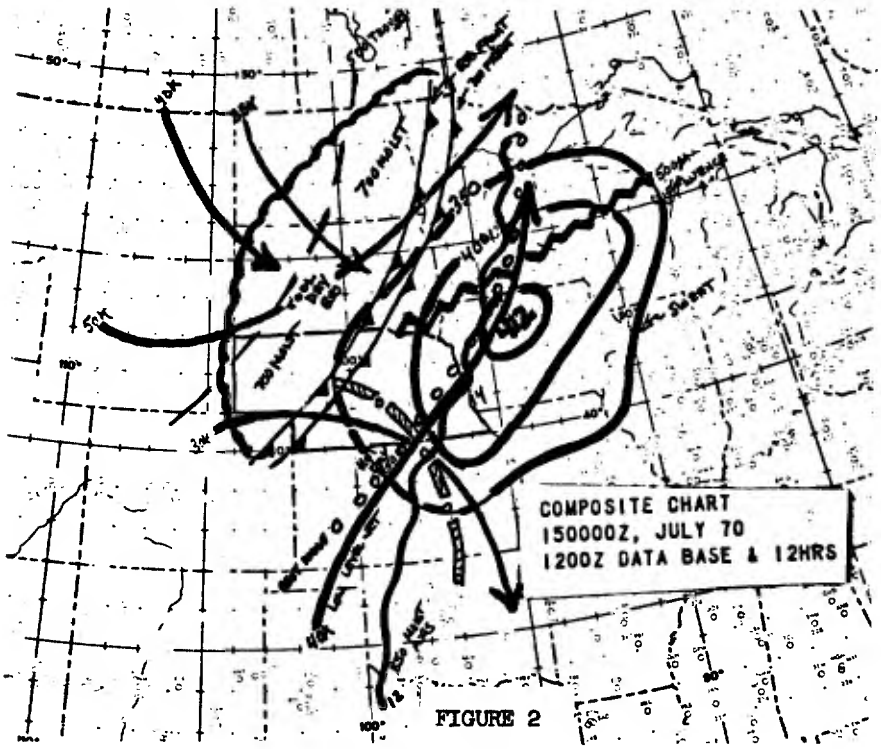


FIGURE 2

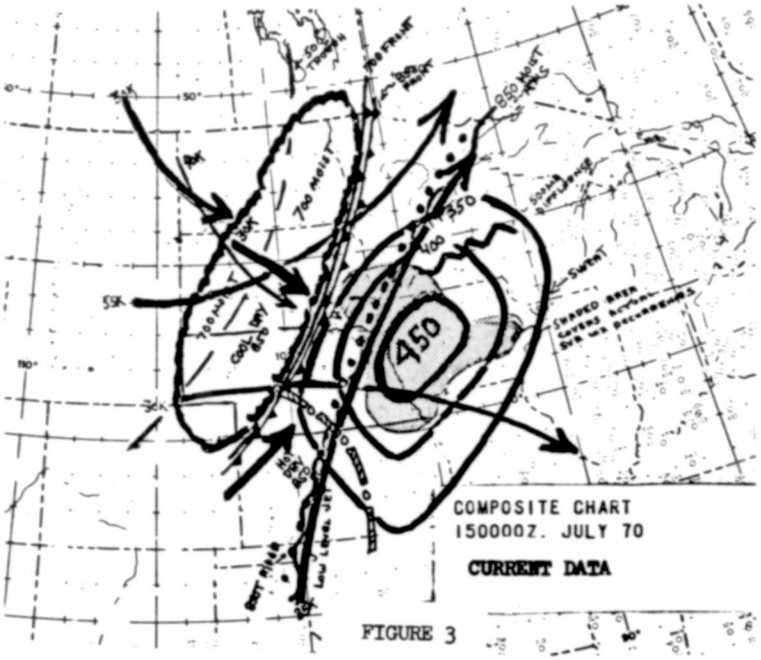


FIGURE 3

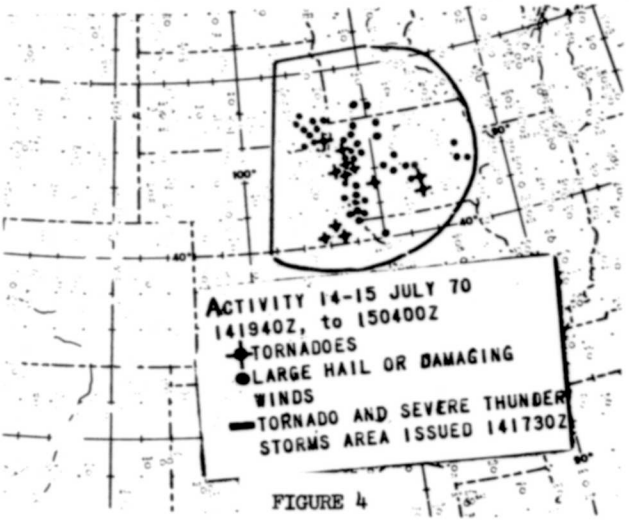


FIGURE 4

2. Notes on Analysis and Severe-Storm Forecasting Procedures of the Military Weather Warning Center, Miller, R. C., Technical Report 200, Air Weather Service (MAC) USAF, July 1967.

ATTACHMENTS

1. "The AFGWC Severe-Weather Threat (SWEAT) Index, A Preliminary Report," Bidner, A., Lt Col, Air Force Global Weather Central, Offutt AFB, Nebraska.

# THE AFGWC SEVERE-WEATHER-THREAT (SWEAT) INDEX (A PRELIMINARY REPORT)

Arthur Bidner Lt Col, USAF

Air Force Global Weather Central
Offutt Air Force Base, Nebraska

## INTRODUCTION

AWS Severe Weather Bulletins WWXX, WWXX1 and WWXX3 are being prepared at AFGWC with the benefit of new computer forecast aids. The most important of these is the SEVERE-WEATHER-THREAT (SWEAT) index, which has been developed to assist in the forecasting of critical convective weather—tornadoes and severe thunderstorms. Although in initial stages of development, this computer prepared index has shown considerable skill, with a resulting increase in AFGWC forecaster confidence in objective severe weather techniques. This article is intended to provide detachment forecasters with preliminary information on this technique.

The requirement for an empirical index to specify and predict areas of potential severe convective weather has long been recognized. The need for such an index stems from the following limitations in the present "state of the art".

a. Reliable operational dynamic models capable of forecasting very small-scale features such as tornadoes (or even small parent cyclones) still appear to be a long way off.

b. The forecast procudures which were used by the Military Weather Warning Center (MWWC) at Kansas City (described in AWSTR 200), limited the forecast period to approximately 12 hours, since they required most of the effort to be expended on analysis. Centralized forecasts of these unique parameters were not available in facsimile circuits, and additional efforts were required to prepare manual forecasts. Automated production of operational forecasts at Kansas City was limited by the capabilities of the computer system. The same constraint prevented any expansion of severe-weather forecasts outside the U.S. area.

c. The procedures in AWSTR 200 are only semi-objective. The constant turnover of MWWC forecaster personnel (usually concentrated in the summer months) with the attendant loss of almost irreplaceable expertise in this esoteric area of forecasting, required an ever-present and very intensive training effort to keep the severe-weather forecasting functions at a consistently high level of goodness. A new approach was needed to augment experience with objectivity.

The transfer of the MWWC function to the Air Force Global Weather Central (AFGWC) provided us with the opportunity to apply unique resources to the problem. Here were available, for the first time, the proper combination of ingredients: a vastly improved current and predicted environmental data base with the required meteorological know-how, programming expertise, and computer hardware. The bulk of the research in the development of the SEVERE-WEATHER-THREAT (SWEAT) Index is being done by Mr Robert C. Miller. Most of the computer programming is being done by Capt Edward P. Malavase.

Case studies collected through the years at the MWWC provided the foundation for this work. Based on a study of 328 tornadoes and using experience gained in daily forecasting, we determined which parameters to consider in such an index. We also had a good idea of the relative weight to be assigned to each. We exercised the following constraints in developing our first version of the SWEAT index.

Attachment 1

a. The index must be computed from U.S. selected-level RAOB data (SLAMS) available approx 1 hour after observation time. (This allows us to have an automated plot of SWEAT at one hour and 15 minutes after RAOB time, and gives us a means of rapidly appraising the current air mass potential).

b. The index must be computed from fields currently stored in the AFGWC prediction data base. (This facilitates automated progs of the SWEAT index without a major revamping of the data base).

c. The parameterization must use reported and predicted values directly, rather than rely on complex pattern recognition, or other derived parameters.

The initial SWEAT index using the above constraints and our empirically derived weighting factors was:

$$I = 12D + 20(T-49) + 2f_8 + f_5 \qquad (1)$$

where I = SWEAT index

D = 850-mb dew point in degrees Celsius, positive values only. (If D is negative, D = 0 and the term drops out).

T ="Total total" in degrees Celsius. The "Total total" is the sum of the 850-mb temperature and dew point minus twice the 500-mb temperature. (If T= 49, T = 49 and the term drops out).

$f_8$ = speed of the 850-mb wind knots.

$f_5$ = speed of the 500-mb winds in knots.

Note that no term may be negative and the SWEAT index (I) is always positive. Application of this formula to 86 past tornado and severe-thunderstorm cases resulted in a distribution of SWEAT versus observed weather shown in Table I.

Table I

SWEAT VS WEATHER FOR TWO DIFFERENT CLASS INTERVALS

| SWEAT | 200 | 2-300 | 3-400 | 4-500 | 5-600 | TOTAL |
|---|---|---|---|---|---|---|
| TORNADO CASES | 0 | 0 | 7 | 26 | 14 | 47 |
| SVR TSTM CASES | 0 | 2 | 14 | 18 | 5 | 39 |

| SWEAT | 250 | 250-300 | 350-400 | 400-450 | 450-500 | 500-600 | TOTAL |
|---|---|---|---|---|---|---|---|
| TORNADO CASES | 0 | 0 | 7 | 12 | 14 | 14 | 47 |
| SVR TSTM CASES | 0 | 7 | 9 | 6 | 12 | 5 | 39 |

From the distribution in Table I it appears that the SWEAT-index threshold value for tornadoes is about 350, and for severe thunderstorms is about 250. Remember that we are here considering only cases where severe weather was known to have occurred. Nothing can be inferred here about SWEAT "false-alarm" rates. It must be emphasized, however, that the SWEAT index is only an indication of the potential for severe weather. A high SWEAT index for a given time (either observed or predicted) does not mean that severe weather is occurring or will occur. Some type of triggering action is necessary to realize this potential. Experience has shown that although high SWEAT values can occur in the U.S. during the morning (12Z) without concurrent severe-convective weather, this potential is usually realized if the predicted values for the afternoon and evening (00Z) remain high. On the other hand, low observed values of SWEAT almost certainly means there is no severe-weather occurring, but SWEAT values can increase dramatically during a 12-hour forecast period.

Additional parameters are being considered for inclusion in this index, and one, the directional shear between the 500-mb and 850-mb wind, is now being evaluated. Initially, it was included in the plotted data, but not in the automated analysis and prognostic fields. The daily comparison of plots and fields provided an opportunity to monitor and evaluate the contribution of this additional term. The directional-shear term changes the SWEAT calculation to

$$I = 12D + 20(T-49) + 2f_8 + f_5 + 125(S + 0.2) \qquad (2)$$

Where S = sin (500-mb wind direction − 850-mb wind direction) and the remainder of the terms are the same as in equation 1. If the 850-mb wind is not in the range 130 through 250 degrees, or the 500-mb wind is not in the range 210 through 310 degrees or the 500-mb direction minus the 850-mb wind direction is less than zero, S = -0.2 and the term drops out.

This term can contribute a maximum of 150 to the index and the new threshold value for severe thunderstorms appears to be about 300, and for tornadoes about 425. Further experience with the new computations may result in some shift in these thresholds, but a major revision is unlikely. Our initial experience with the new index shows that it specifies severe convective weather better than the initial index which had no shear term. The word "severe" is employed because the original SWEAT index was not developed to specify or predict ordinary thunderstorms, and with the addition of still another non-stability parameter (the directional shear) it becomes an even more unlikely tool for ordinary thunderstorm specification. (This is because the wind field is a major discriminator between ordinary and severe-thunderstorm situations). For ordinary thunderstorms, then, it appears best to continue to use some stability index, preferably the Lifted Index.

The next step will be to substitute terrain-referenced levels for pressure levels, particularly in the lower atmosphere. Using the analysis and forecast data from the AFGWC Boundary-Layer Model, we plan to replace the 850-mb moisture with the moisture in the lower 900 meters above the ground, and replace the 850-mb wind with a wind at 900 meters above ground level. This will give a "floating" base and give a more reliable index in high-terrain areas. The index will be retained in approximately its present form however, for use outside the U.S. where there are no Boundary-Layer Model analyses and forecasts. It will also continue to be used to evaluate the modified SWEAT Index.

# PROCESSING OF ITOS SCANNING-RADIOMETER DATA

C. L. Bristor

National Environmental Satellite Center
Suitland, Maryland

## Abstract

The automated handling of scanning radiometer data being obtained from the first Improved TIROS Operational Satellite (ITOS-1) is described. Sensor signals are traced from the spacecraft through the data processing facility with a description of the transformation of raw digitized data into calibrated and mapped imagery. Beginning efforts toward the extraction of quantitative products are discussed along with plans for expansion of the product line.

## INTRODUCTION

TIROS-M, a NASA spacecraft, was launched January 27, 1970 and was transferred to ESSA for routine use as the first vehicle in the Improved TIROS Operational Satellite (ITOS) series. Like the previous ESSA series, it carries vidicon cameras, but it is somewhat larger, has more power, and has a new stabilization system. Although still spin stabilized, there are now two counter rotating masses - one dense flywheel spinning at some 130 rpm and the approximate 4 foot payload cube spinning at one revolution per orbital period. The resulting earth oriented platform permits the mounting of separately rotated imaging scanners. And their availability provides the potential for the extraction of more quantitative image products — both in the visual and infrared portions of the spectrum. In the remainder of this report, current activities will be described whereby raw ITOS scanner signals are automatically converted into several forms. Despite the compromising effects of coherent noise now present in some of the data, a substantial effort is underway toward the enlargement of the product line and the increasing of its utility in both qualitative and quantitative applications. In the following sections, treatment of the raw data will be discussed along with their earth location and analytical manipulation into operationally useful formats.

## DATA SOURCE

The quasi-polar, retrograde orbit of ITOS-1 provides sun synchronous earth viewing with northbound equator crossings near 2:30 PM local sun time. With a mean orbital altitude of 790 nautical miles and data acquisition facilities at Wallops Island, Virginia and near Fairbanks, Alaska, opportunities for obtaining information stored onboard the satellite occur on all but 2-3 orbital passes each day. Since both day and night infrared scanning is obtainable in addition to visual channel coverage, considerable quantities of data must be stored onboard — especially when acquisition opportunities lapse. And, although two tape recorders are available, care must be taken to utilize unrecorded data obtained directly during readout before blind passes so as to minimize gaps in coverage. Further details concerning operational options and constraints, as well as overall spacecraft details, are available from NASA (1).

The two-channel scanning radiometer (SR) provides infrared information in the 10.5-12.5 micron water vapor "window" and .52-.73 micron information in the visible range. Both channels receive energy from the same mirror which rotates at 48 rpm and views a swath from horizon-to-horizon passing directly beneath the spacecraft and oriented perpendicular to the orbital path. In terms of spatial resolution, the instantaneous nadir view in the infrared is 4 nautical miles in diameter and half that amount in the visible channel. A technical memorandom is available with more details concerning the scanner and the direct and recorded modes of data acquisition (2).

Once the scanner data are acquired on the ground, they are relayed by broadband microwave transmission link to the data processing facility at Suitland, Maryland.

## RAW-DATA INGESTION

A new Digital Data-Handling System (DDHS) has been installed at Suitland for the receipt and preprocessing of much of the raw data arriving from the ITOS spacecraft. This is a dual facility, largely computer controlled, in order to minimize the effects of temporary hardware failure and human error. Incoming data can be held on analog tape recorders or accepted directly into the digitizer/computer processing facility. A portion of the equipment is shown in Figure 1.

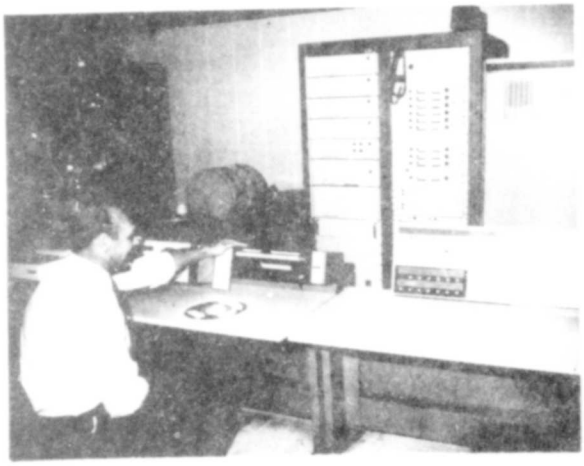

Figure 1. A portion of the ITOS Digital Data-Handling System (DDHS). Ingest and preprocessing computer consoles and specialized digitizing equipment are shown.

Figure 2. A view of the DDHS mode selection and signal-monitoring console.

Linkage to the microwave terminal and an analog tape recorder are shown (far left) along with the data ingestor computer console (with operator) and the adjacent console of the preprocessor computer. Two central equipment racks beyond the consoles contain signal detectors (discriminators, demodulators), analog-to-digital converters, synchronizing detectors, formatting registers and related electronic hardware. Most of the primary components shown are duplicated in order to reinforce operational dependability. The overall mission load is shared between components, but on-line tasks receive priority when partial outage forces a limited performance posture.

Operating mode selection and the assignment of certain component combinations is accomplished by push button selection on a console shown in Figure 2. This unique component provides a focal point for the operation. It includes facility for communication with the data acquisition stations and with those involved in spacecraft operation and control. Oscilloscope signal monitoring and indicator lights assist the operator in assessing the status of the processing activity.

Apart from six digital tape units, the system presently contains five random access disk storage units. A novel feature of the system is the exchange controller which permits communication between any disk unit and any of the four computers (3). This permits one off-line preprocessor to work on a newly ingested raw data base while the on-line ingestor/preprocessor dual facility quickly shifts to a new data-acquisition mission.

Only two operating modes are of interest in connection with the arrival of raw scanner data. These are indicated in Figure 3. In the upper portion, SR information, obtained from the spacecraft tape recorder, arrives at Suitland as a frequency modulated signal stream. It is converted by the FM discriminator into an analog voltage which varies as a function of the energy impinging upon the sensor via the scanning mirror. Fixed reference signals - so called "porch" and "step wedge" patterns — are also injected into the signal stream within the spacecraft in order to mark specific positions of the scan mirror with respect to the spacecraft mounting platform. Synchronizing circuitry detects these unique signal features and provides an interrupt pulse to the ingest computer. By this means, earth scanning response is sampled at a high rate, and certain housekeeping signals (spacecraft temperature, time, spacecraft performance

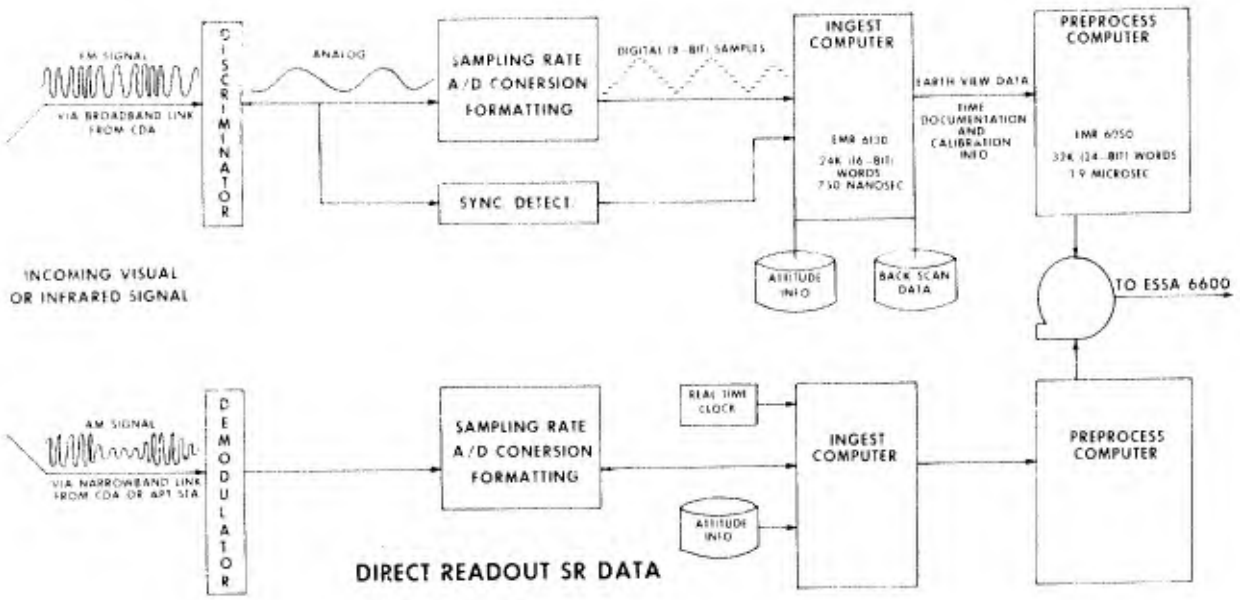


Figure 3. Scanning Radiometer (SR) signal ingestion and preprocessing steps carried out in the DDHS.

telemetry, and space response) obtained during non-earth scanning ("back scan") are sampled at a much reduced rate. The smaller ingest computer interacts to manage this operation. The low volume back-scan data is held on disk and the higher-volume image data is passed to the larger preprocessing computer for eventual recording on tape. At present rates, some 1300 (8-bit) samples are obtained from each channel during earth scan. With some 8,000 usable earth scans (daytime visual and IR both day and night) obtained each orbital period, the total volume of image data to be collected amounts to approximately $10^9$ bits per day.

In the direct readout mode, coverage is obtained during the limited period of contact with the spacecraft. Here the information arrives as an amplitude modulated signal in a format designed for local image-recording receivers. Such signals, relayed to Suitland, may also be processed in a manner similar to that described above. In this case, the entire stream is digitized at the desired earth-view data rate without an electronic synchronizing detector. The porch and stairstep features are then identified and the earth viewing samples separated out by computer software. Also, since the information is arriving directly from the spacecraft, time from the local GMT clock is appended to the data in the ingest computer. In either ingestion mode, the raw data is organized in a common format with all auxiliary information necessary for the following processing steps.

## PREPROCESSING AND SIGNAL CONDITIONING

A sample photo recording of direct transmission ITOS infrared scan data has recently appeared in the literature (4) and other samples are shown in Figures 4 and 5. Here, daytime IR scans are compared with interspersed direct-readout vidicon imagery. The semi-independent information obtainable from the coincident visual and infrared views is evident. Although different recording devices do not produce identical display aspect ratios, the equivalency between image features is readily apparent. Visual-channel image features (lower sectors) having somewhat similar brightness response are seen to have decidedly different radiating temperatures.

For the automated and quantitative processing of such scanner data, certain preprocessing steps are necessary. First, raw sample counts must be converted to physically meaningful units through calibration relationships. They are then normalized to compensate for response changes resulting from the changing viewing angle. For the visual channel data, these efforts are in a preliminary stage. Radiance values must be related to equivalent black-body values and checked against available targets in order to assure meaningful albedo measurements. Response must also

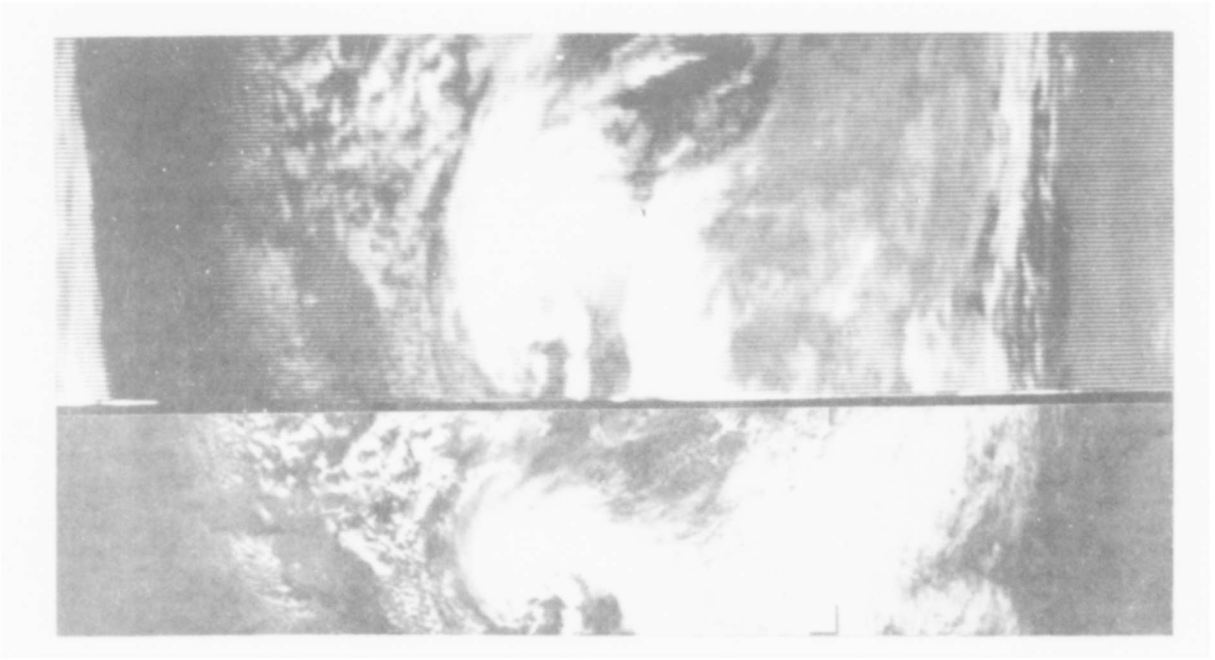

Figure 4. Cyclonic situation over northeast United States at 1925 GMT on August 20, 1970, as viewed by the ITOS-1 APT camera (lower) and in the infrared by the SR (upper) in direct recording mode.

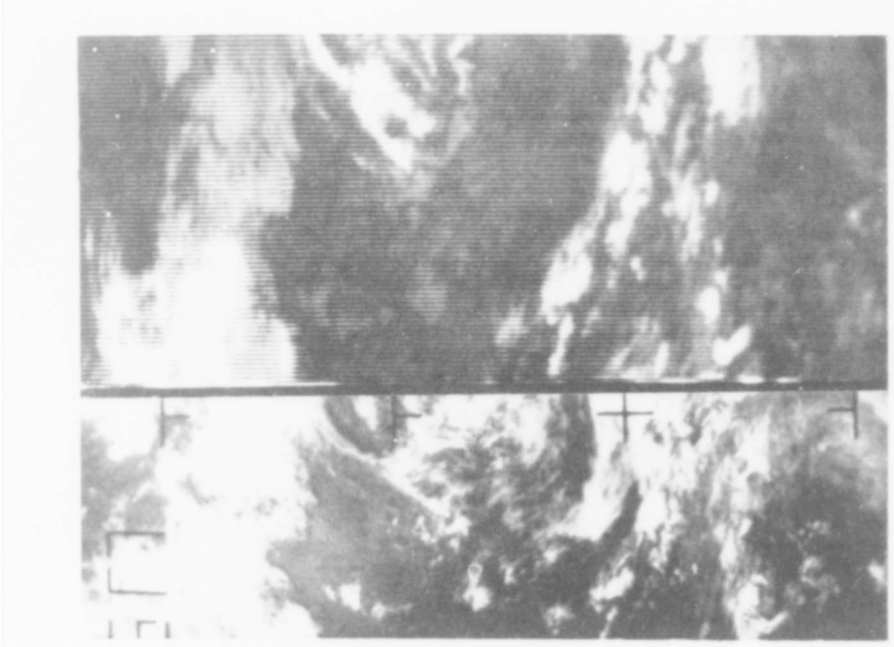

**Figure 5. Cloud features over the western North Atlantic at 1800 GMT on September 10, 1970, again obtained from APT and SR as in Figure 4.**

be adjusted for illumination variations before intercomparisons (across the image scene and frame scene-to-scene) become meaningful. Here the approach being taken is similar to that for the correction of scanned imagery obtained from geostationary satellites. In the initial effort, correction will be made for solar zenith angle without regard for azimuthal relationships between incident and reflected rays (5).

In the infrared case, prelaunch calibration curves establish the relationship between raw voltage response and effective-target radiating temperature, all as a function of sensing-element temperature and other signal handling constraints (6). Because of non-linearity in response, the 0-255 count range provided by 8-bit sampling yields better precision in high temperature response — about 1/3 degree Celsius per count increment in the warmest meteorological range and about one degree in the coldest range. Response normalization for the infrared channel deals with the variation in absorption as a function of atmospheric path length. The current "limb darkening" algorithm makes such corrections based on viewing zenith angle relationships as recently described in a paper by Smith et al. (7). The final calibrated response values are retained as 8-bit samples but in coded form. Each count represents half-degree increments in the warm range and full-degree increments in the colder portion. In this way, the greater available count range is more effectively utilized for the limited meteorological-temperature range.

Before earth location of the scan imagery can begin, the sample population of each scan swath must be aligned with the earth disk. Since space viewing response differs substantially from the coldest earth-viewing response, horizon profiles are well marked. Beginning of earth scan is thereby established through simple thresholding logic. Further use of the earth-horizon information is taken up in the following section.

## EARTH LOCATION OF SCAN DATA

Spacecraft attitude and position as well as scan sample angular relationships are required before the image data can be properly earth located. The nadir angle increment (at the spacecraft) which encompasses one sample step along the scan swath is specified by the rotational speed of the scanning mirror and the speed of the sampling rate controller. The calculated increment can be verified by noting the horizon-to-horizon earth viewing sample population with known spacecraft altitude. The profile in the upper portion of Figure 6, for example, displays 500 samples

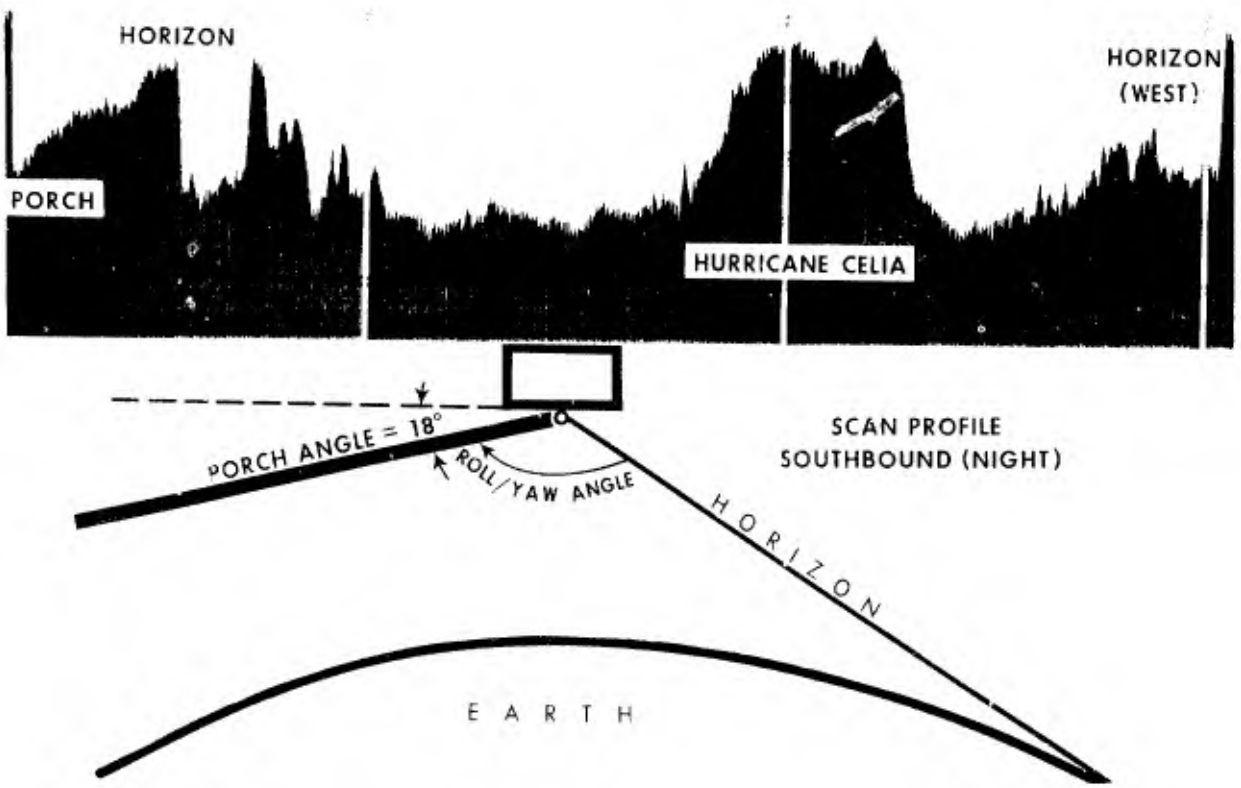


Figure 6. SR profile (upper) through Celia obtained from ITOS-1 at 0220 local time prior to the hurricane's movement into the Texas coast on August 3, 1970. The lower sketch defines the spacecraft roll/yaw attitude angle as measured from the porch to the west horizon.

between vertical coordinate markers for a total of over 1250 samples between horizons. Separate horizon detection also permits use of SR data for attitude determination by counting samples from the west horizon to the porch, the roll/yaw angle can be measured as indicated in the lower sketch. Since the porch signal is injected at a known mirror-spin phase angle, a measure of spacecraft baseplate orientation is thereby obtained. In the lower sketch of Figure 7, the

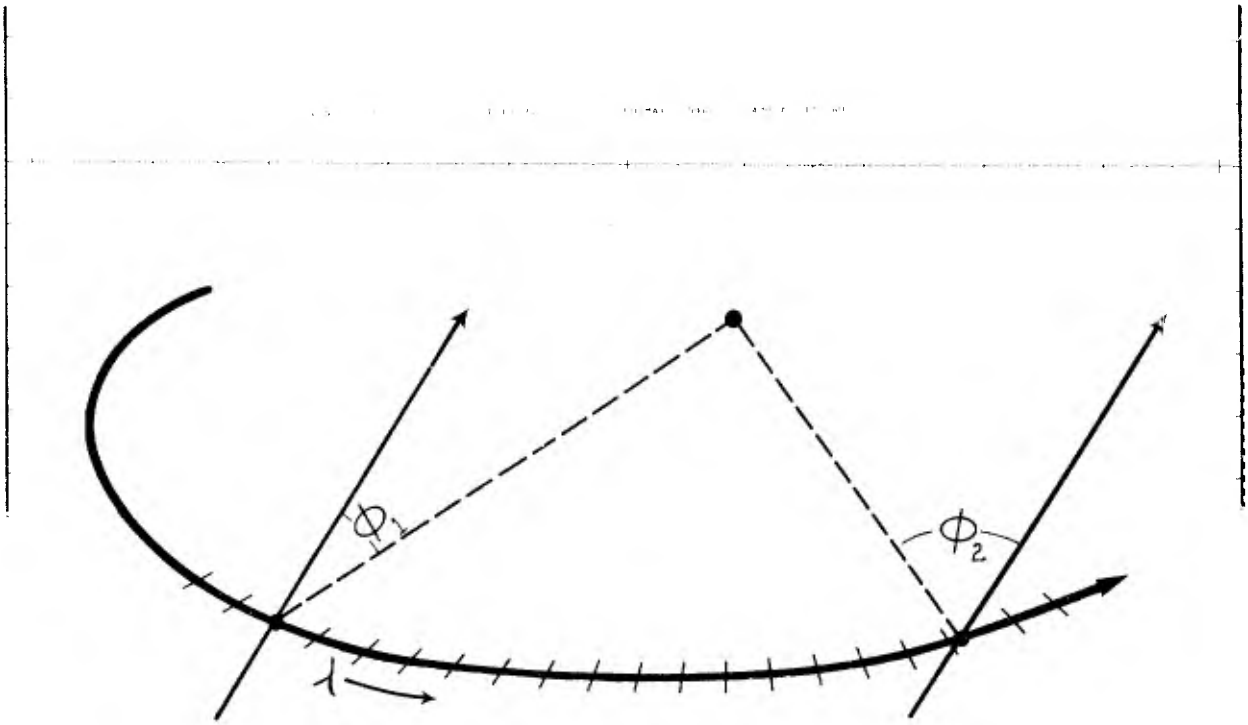


Figure 7. Typical graphic computer output (above) showing roll/yaw spacecraft attitude measurements obtained from SR data on one orbital pass. The fitted curve yields the change from roll to yaw as a function of orbital phase angle (lambda) as illustrated in the lower sketch.

radial component of this angle (designated phi) is shown for two positions of the total spin vector within the orbital phase domain (lambda). It is seen that if the total tilt of the spin vector is measured by $phi_1$ (roll), then, at another position $90^o$ along the orbital track, $phi_2$ will indicate perpendicularity and all tilt will be contained in a tangential component as yaw.

In the upper plot, phi is plotted as a departure of the spin axis from orbit normal. Each dot represents an average of measurements obtained from 16 successive scan lines. Data from an entire orbital pass is plotted in this typical facsimile display. The accompanying sine curve is generated from the data through a least squares fit. In orbital coordinates, the spin vector is thereby expressed in terms of maximum roll (phimax) and the corresponding orbital phase position (lambda). With known orbital characteristics, the spin axis can also be expressed in celestial coordinates. As with earlier spin-stabilized TIROS spacecraft, the earth location of image data utilizes spin-axis predictions based upon persistence.

Spacecraft position determination is also carried out as with earlier satellites, through an orbital prediction package using orbital elements supplied by NASA. As mentioned earlier, relative time is reported along with the SR data during the backscan portion of each scan revolution. Through knowledge of the precise time when this relative timer was reset to zero, the conversion to absolute time is made for each scan. Entering the orbital prediction with the appropriate time, one obtains the three dimensional position vector for the spacecraft.

## MAPPING

Mapping logic for the ITOS scanners was developed in parallel with that now being employed in the experimental mapping of geostationary-spacecraft scan imagery (8). Since geometric calculations for each data sample would be economically prohibitive, the computations are limited to an open lattice of "benchpoints." At present, such points are selected for every 32nd earth-

viewing sample on every 8th line. Roll/yaw attitude components and spacecraft position components are recomputed for each new benchpoint scan line. With data samples synchronized to the earth disk, and earth coordinates available for the benchpoints, the placement of the samples in the map matrix can begin.

In the benchpoint calculations, latitude/longitude positions on the oblate earth are transformed into equivalent i, j coordinates in a square mesh placed upon the desired map projection. The current mesh for the polar stereographic projection contains 2048 x 2048 elements per hemisphere, and the columns are aligned parallel to the 80°W meridian in accordance with Numerical Weather Prediction (NWP) convention.

The actual mapping algorithm is programmed in machine language since the relocation of individual samples is a highly iterative process requiring maximum efficiency. With benchpoints spaced at binary intervals, the linear interpolator logic for relocation involves only binary shifting and does not utilize more costly multiply instructions. Computing time requirements are strongly affected by the amount of incoming data and by the number of map array positions which can be held in high-speed memory, and also by the efficiency with which data flow to and from peripheral storage can be buffered. Present programs map scan data on the 6600 in about 24 minutes (wall-clock time) per single-channel orbital pass. With extended core storage and improved input/output channelization, the outlook is for substantial time reduction to, perhaps, 18 minutes for the equivalent work.

The map-mesh size is slightly less than the 4 n.mi. sample resolution at the equator but degrades to four times that area at the pole. Present logic places the first eligible sample in a map-mesh square, and, where several samples may be eligible, this tends to introduce jitter. One alternate approach selects the most eligible sample (9). Another approach reduces the mesh size until no competition exists. However, this approach is more costly in memory requirements, and filling the voids in foreshortened areas complicates matters. Present plans call for continuance of the present mesh and procedures for the global mapping of visual and both night and day infrared data. Limited sectors will be mapped at finer mesh for special higher-latitude applications. Consideration is also being given to alternate mapping schemes (particularly with overlapped IR sampling) whereby the mean, mode, or other expression of the eligible samples is mapped in each mesh square. In this way, products which depend upon populations of values in image sectors (rather than on precise juxtaposition relationships), may attain improved quantitative significance.

## PRODUCTS

A recent 2048 x 2048-array polar-mapped image is shown in Figure 8. Tests products of this type are currently in preparation for real-time operations now projected for mid-October. They are produced on a photofacsimile recorder having 200 line-per-inch resolution and about 30 effective gray shades. Once-per-day images of this type are produced for both hemispheres for operational and archival use and also as a check on the mapping operation.

Unfortunately, a substantial noise component appears in the image data. The noise is currently having a substantial impact on the utility of the data for both qualitative and quantitative applications. Since mid-August, a considerable diagnostic software effort has been underway in order to measure the noise and understand its impact upon the products to be generated from the mapped information. An interim report is being prepared (10). An early diagnostic noise display is presented in Figure 9. Here, the taped SR response is obtained from a homogenous target prior to the launch of ITOS-1. Several hundred samples on each scan are replicated in eight display lines for each of some 120 scans in order to obtain this enhanced display. The quasi-coherent quality of the noise indicates a tendency for repetition every fourth line. Meanwhile, hardware experts have considered the evidence in terms of spacecraft design and have focused attention on the onboard tape recorders. The design of special ground-based filter circuitry is now in progress as a means of removing the noise. With the expectation that an accompanying speed control (flutter and wow) channel contains the same noise pattern, circuitry is being configured to use this signal for corrective compensation of the taped sensor data. Preliminary tests are encouraging.

Once data quality is improved, a growing product line is anticipated. The primary operational display will be produced on a pass-by-pass basis for local use and for facsimile transmission. A sample facsimile sector is shown in Figure 10. Such 800-line transmissions (at 96 lpm) are projected for standard weather facsimile networks and for possible distribution via satellite rebroadcast (WEFAX).

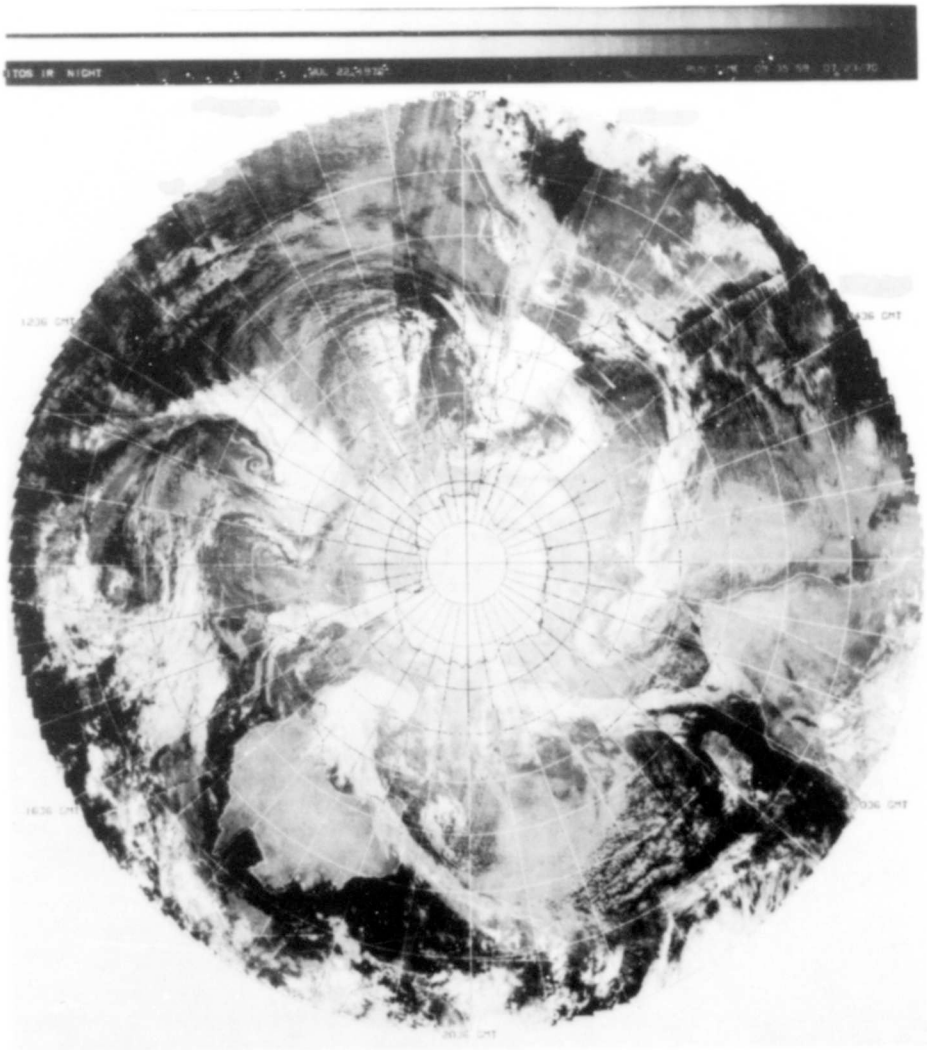

Figure 8. Nighttime SR data for July 22, 1970 in polar-stereographic mapped form for the Southern Hemisphere. Coherent noise in the raw data appears as streaks which tend to parallel the orbital track.

Another visual product combines infrared temperature data and 3-dimensional temperature/height profiles available from NWP grid-point analyses. The result is a "clear-low-middle-high" cloud analysis chart. Such a four shade chart is displayed in Figure 11. Again, the effect of noise is evident – particularly in the clear/low-cloud realm. With limited gray-shade capability on facsimile receivers, charts of this sort may be more usable than full gray-shade images.

Apart from visual products, the extraction of sea-surface temperatures from mapped IR data provides one of the more challenging quantitative applications (7). Operational software for such production is now available, and tests are underway using noisy and experimentally filtered data in order to assess the influence of noise on the final product. A sample product is shown in Figures 12 and 13. Here, temperatures have been extracted from data recorded on the less noisy ITOS-1 tape recorder. Apart from the potential for direct input to NWP analyses, this sample suggests the utility of such a visual analysis as an aid in hurricane trajectory determination.

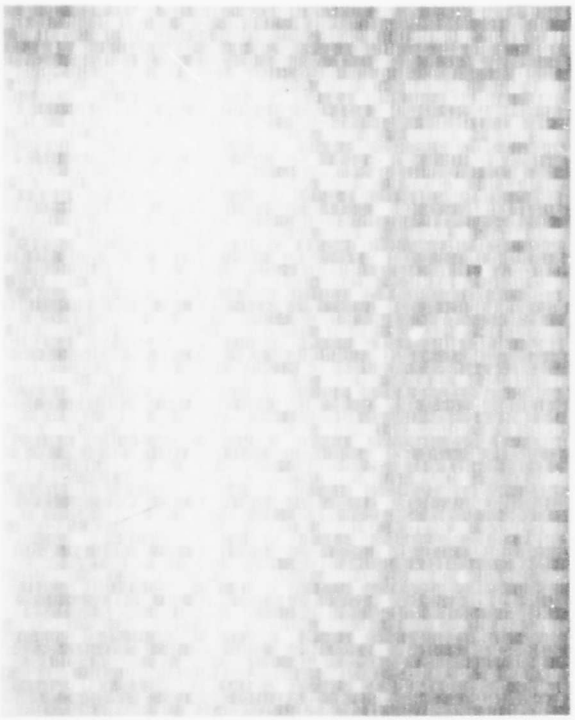

Figure 9. Enhanced display of noise pattern obtained from taped SR signals. This recording of a homogenous target was made prior to the launch of ITOS-1.

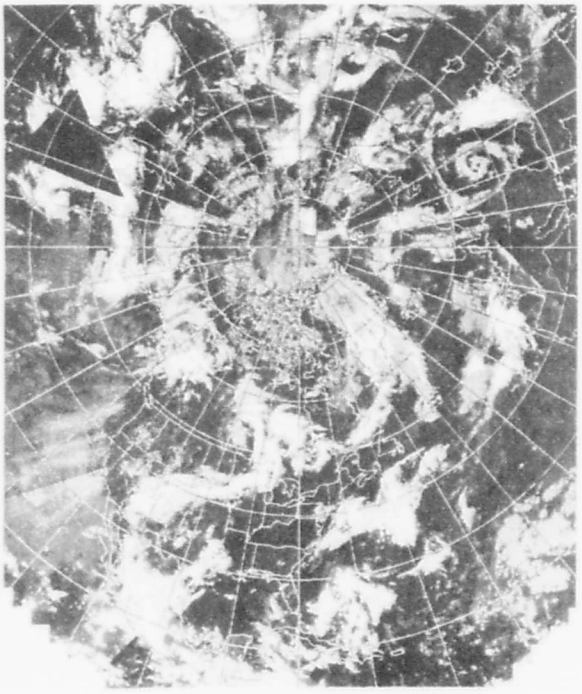

Figure 11. Three-dimensional mapped cloud field obtained by combining IR temperature response and temperature profiles obtained at NWP grid points. Only four gray shades are employed to indicate clear, low, middle and high clouds in order of ascending brightness.

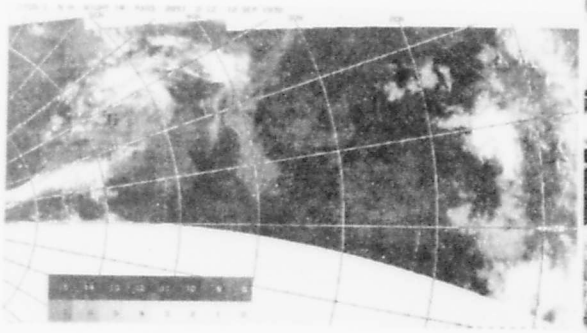

Figure 10. Single orbital pass mapped IR image reproduced from facsimile copy. The format of this Middle East scene (obtained on Sept. 12, 1970) is representative of pass-by-pass production now projected to begin during October 1970.

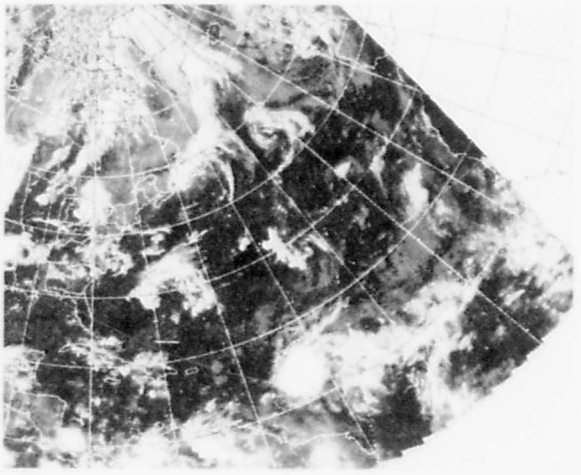

Figure 12. Tropical storm Dorothy as viewed by the ITOS-1 IR scanner on August 19, 1970. The nighttime data near and to the west of the storm was stored on the less noisy tape recorder.

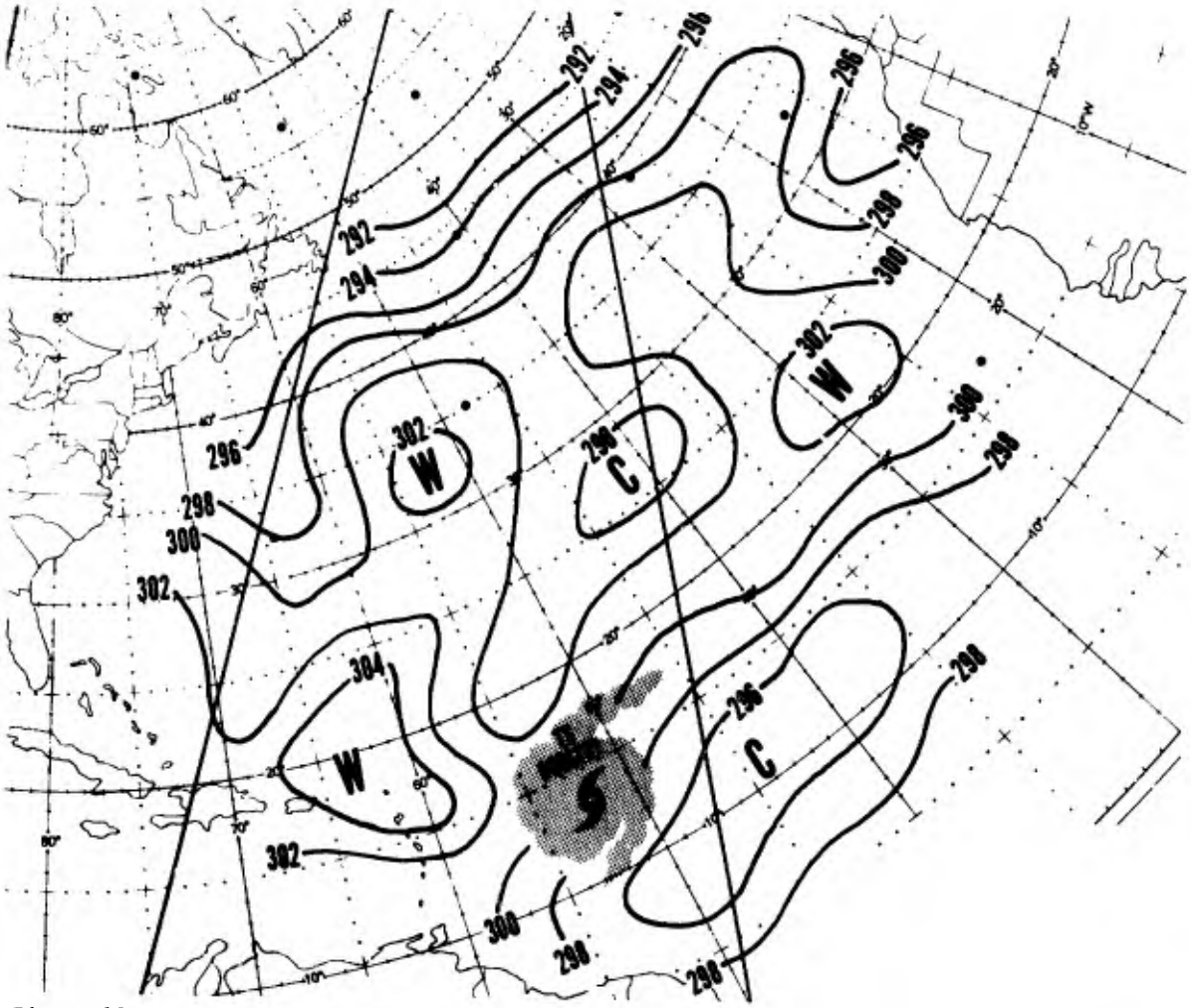


Figure 13. Some 56 sea-surface temperature measurements were obtained within the indicated trapazoidal sector obtained from the less noisy tape recorder data displayed in Figure 12. A substantial gradient is indicated with warmer water to the west along the path of the disturbance.

## OUTLOOK

This report constitutes a brief overview of present SR data processing activities. With a good quality mapped data base, many other product extraction efforts appear feasible. Combinations of visual and IR imagery with digitized radar data may provide more insight in severe storm forecasting. A pilot effort is beginning. Multiday combinations may provide improved ability to monitor the movement and changes in sea ice, and the more quantitative image data will enhance present synoptic/climatology efforts. Day and night mapped infrared images may yield more objective measures of the displacement and growth of synoptic disturbances — particularly in the tropics. Care must be exercised in the commitment of developmental resources in these areas. Computer production efficiency as well as software effort must be weighed against the value of information extracted.

## ACKNOWLEDGMENTS

This paper represents a brief, preliminary version of a multichapter report intended to provide the potential user of ITOS SR with considerable insight and specific technical information. Credit belongs to the twenty or more professionals within the NESC Data Processing and Analysis Division whose efforts are herein summarized.

## REFERENCES


1. U. S. Goddard Space Flight Center, NASA, "ITOS Night-Day Meteorological Satellite," U. S. Government Printing Office, Washington, D. C., 1970.

2. Albert, E. G., "The Improved TIROS Operational Satellite, "ESSA Technical Memorandum NESCTM-7 (with Supplement I.), U. S. Department of Commerce, National Environmental Satellite Center, Washington, D. C., reprinted January 1970.

3. Kahwajy, F. T., "Digital Data-Handling System Equipment Description," Manuscript Report, National Environmental Satellite Center, Washington, D. C., August 1970.

4. Rao, P. Krishna, "ITOS-1 View of the Eastern United States," Cover Picture, Bulletin of the American Meteorological Society, Vol. 51, No. 2, February 1970.

5. Taylor, V. R., "Brightness Normalization of ATS-1 Data," ESSA Technical Memorandum NESCTM-24, U. S. Department of Commerce, National Environmental Satellite Center, Washington, D. C., October 1970.

6. RCA Astro Electronics Division, "Alignment and Calibration Data for TIROS-M Meteorological Satellite," Technical Handbook produced for Goddard Space Flight Center, NASA, Washington, D. C., October 1969.

7. Smith, W. L., Rao, P. K., Koffler, R, and Curtis, W. R., "The Determination of Sea Surface Temperature from Satellite High-Resolution Infrared Window Radiation Measurements," Monthly Weather Review, Vol. 98, No. 8, August 1970.

8. Doolittle, R. C., Bristor, C. L., Lauritson, L., "Mapping of Geostationary Satellite Pictures - An Operational Experiment," ESSA Technical Memorandum NESCTM-20, U. S. Department of Commerce, National Environmental Satellite Center, Washington, D. C., March 1970.

9. Roth, R. C., "A Data-Selection Procedure for the Rectification and Mapping of Digitized Data," Technical Memorandum AFGWC 69-1, Air Weather Service, Offutt AFB, Nebraska, December 1969.

10. Leese, J., "ITOS Scanning Radiometer Noise Analysis," Manuscript Report, National Environmental Satellite Center, Washington, D. C., October 1970.

# THOUGHTS ON THE SECOND DECADE OF NAVY SATELLITE-DATA APPLICATIONS

Commander Kenneth W. Ruggles, USN

Navy Weather Research Facility
Detachment Suitland
(Project FAMOS)
Hillcrest Heights, Maryland 20031

Abstract

The central collection and use of meteorological satellite data is examined from the viewpoint of a user in the field. The question, "How can the vast amount of centrally collected and processed satellite data impact the weather forecast?", is posed. The use of satellite data in numerical analysis and prognosis schemes is shown to be an inadequate approach toward the optimum use of these data. The user is then alternatively faced with the yet-to-be-solved problem of satellite data logistics.

From a highly pragmatic point of view, the sole justification for present meteorological support activities is to provide directed environmental counsel. The value of the rendered service is measured directly in terms of how accurately and efficiently the counsel meets the user's needs. This is the frame of reference I should like to take in discussing the past and pondering the future of weather satellite data in support of Navy users. While my comments are expressed specifically in terms of the Navy's satellite data problems, I propose that the Navy problem is not unique and is only a small manifestation of the greater problem of the entire meteorological community in applying satellite technology.

A Navy user may be any one of a number of organizations, each with a unique environmental problem. Many such organizations operate in the "silent" regions of the world, devoid of conventional meteorological data. Counsel provided such users may be simply numbers for digestion by a fire-control computer, or it may be a complex word picture delivered in verbal or written form. In almost every instance, however, the counsel involves the description and space-time evaluation of weather parameters whose dimensions are spatially thirty miles or less and temporally one hour or less. This is a weather forecast.

Weather satellites—as we know them today—have been configured with two methods of data dissemination. Data are provided directly to a local user through the satellite's direct-readout system, or information can be stored aboard the satellite and then disgorged to a central collection center—in our case the National Environmental Satellite Center (NESC) at Suitland, Maryland.

Early operational satellite systems, such as the TIROS system, provided primarily a single product—photographs of the Earth and its atmosphere. Local readout of these photographs provided an efficient, timely depiction of weather parameters applicable to a directed weather forecast and usually provided the forecaster with all the satellite information needed to formulate his forecast. In terms of efficient support to the user, central information collection could offer very little advantage over the direct readout product. Central data also posed—and still does pose—formidable problems. The user must extract, from a veritable mountain of centrally processed satellite information, those data which are uniquely applicable to his needs. He must then devise some method of transporting these data for use at some operating location. Early in the TIROS era the Navy recognized that the problems with central

satellite data far outweighed the advantages and, accordingly, placed its emphasis on the employment of direct-readout products.

With the launch of ITOS-1 in January 1970, a new generation of satellites and sensors introduced fresh problems in satellite-data handling. While holding promise of greatly improved descriptions of the atmosphere, sophisticated radiometric sensing demands the kind of data processing not normally available to a local user. Local data are still available, but are diminished in impact by an increasing amount of information available only to a central collection point. Whereas, during the TIROS era, the user could conveniently ignore centrally collected data, the ITOS era now confronts him with the problems associated with central data processing and distribution.

Returning to the initial frame of reference, the obvious question now becomes, "How can the vast amount of centrally collected and processed satellite data impact the weather forecast?"

Fig. 1 depicts two possible paths for data to pass from the satellite to the user. In one case the satellite impacts the forecast through an improved numerical process, while in the second instance the responsibility for use of satellite data remains with the field forecaster. The use of satellite data in numerical analysis and prognosis is certainly an attractive path, provided numerical grids of suitable resolution exist to retain significant satellite data.

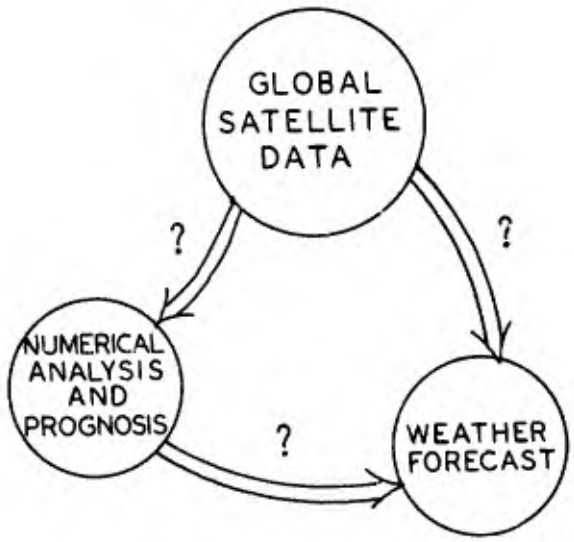


Fig. 1. How can the vast amount of centrally collected and processed satellite data impact the weather forecast?

Recourse to higher resolution numerical grids is often suggested as the total answer to the problem of bringing the expected denser data coverage to bear on the forecast. However, the expected data coverage itself is dependent on the resolution of the computation grid and will vary inversely with this resolution. To illustrate, a meteorological analysis is intended to be an instantaneous snapshot of the atmosphere at a given time. If it were, say, a 500-mb analysis, then with perfect rigor we would require every radiosonde observation accepted into the analysis to have been taken at exactly 500 mb at exactly the analysis time. Similarly, the only valid satellite data would be those sampled directly below the satellite at map time, defining a single point in the analysis. Clearly, if we exercised such rigor we would effectively eliminate the meteorological data base. Therefore, standards are relaxed in order to inject reasonable amounts of data into the analysis. This is justified on the basis of the coarse grid resolution. Now we reverse the argument and say that there is a need for higher space or time resolution in the computational grid, so we must reassess our standards for accepting data into an analysis.

To quantify the impact of higher resolution grids on satellite data, consider the simple case of a meteorological feature of scale greater than two grid intervals imbedded in a mean zonal flow of 10 m $sec^{-1}$ at 500 mb. (The wind is chosen as reasonable, based on [1], while the scale represents the smallest feature that can be defined in a finite grid based on Nyquist considerations [2].) If we choose to accept as valid data over a time interval represented by the time it takes for an imbedded feature to travel a selected fraction of a grid interval, then the acceptable data window would be as shown in Fig. 2.

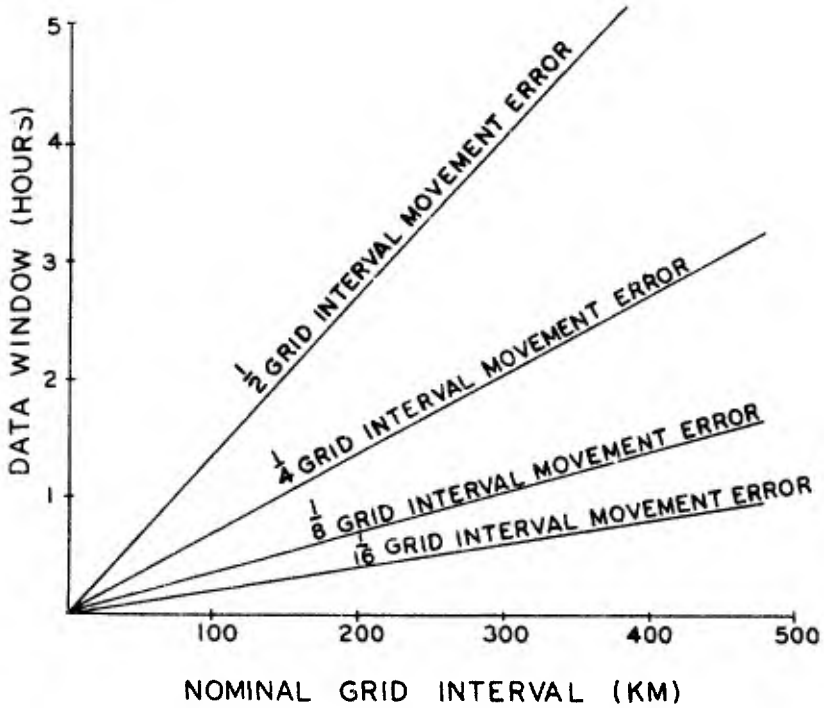


Fig. 2. Allowable data window as a function of computational grid interval for indicated system location error with $\tilde{u}$ = 10 m $sec^{-1}$.

Translating this into terms of the nominal number of polar-orbiting satellites required to provide global coverage, we arrive at Fig. 3.

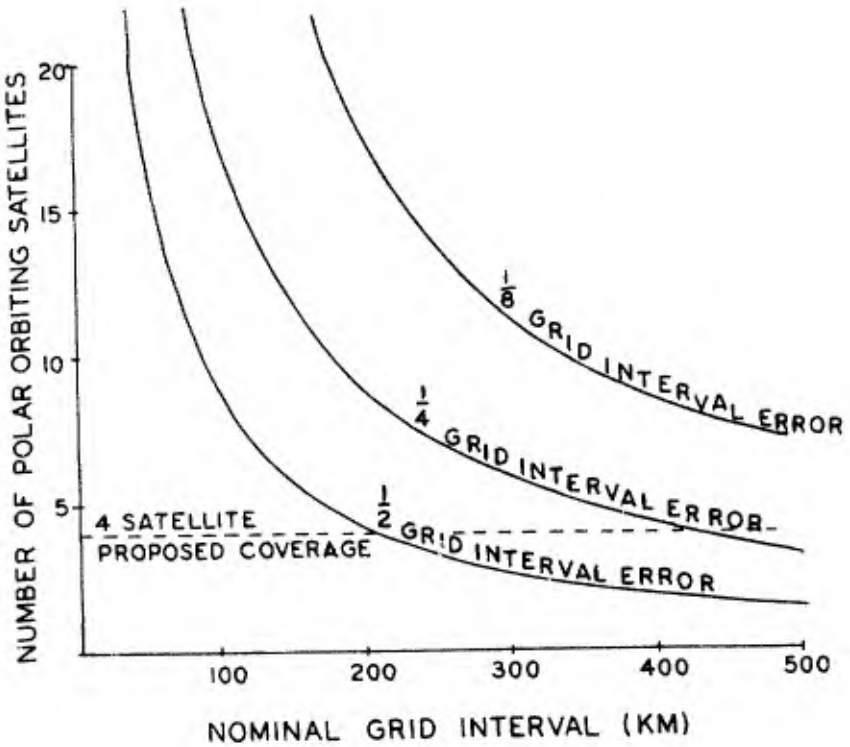


Fig. 3. Number of satellites required to provide global data coverage as a function of nominal grid interval for indicated movement errors.

Based on planned observations using four satellites, the allowable size of a computational grid falls far short of the forecast scale needed to make a meaningful forecast. While theory and improved computational power of future computers may not limit grid resolution, certainly the economics of establishing the data base to support such grids will be the prime factor which dictates the ultimate resolution of numerical schemes.

Therefore, while the satellite data will impact the forecast through an improved numerical product, we must still rely on the field forecaster for judgments involving sub-grid scale phenomena. This means that the field forecaster must be provided with satellite data appropriate for his use.

In the global Navy environment the scope of Fleet environmental data support is fundamentally limited by communications. Given this constraint, the alternatives are (1) take the forecaster to the data, or (2) provide him with tailored data packaging capable of supporting his local forecast requirements. The first alternative is the cheap approach, but does it provide counsel responsive to user needs? It removes the face-to-face dialogue so essential to tailoring a forecast to user needs, and it separates the forecaster from his most important piece of data—a glance out the window at his local sky. Finally, we are all too familiar with the malady of logarithmic vision, where the problems immediately surrounding us appear comparatively far more pressing than those thousands of miles away. Therefore, while cheap, this approach is grossly inefficient because it does not meet the user's needs. This leaves the alternative of bringing the data to the forecaster. How we are to do this on a global scale requires

imagination and innovation. I submit that this is the major problem in the use of satellite data. The past decade has been devoted to developing satellite observing resources. I propose that the major thrust of the next decade be in the area of learning to use these resources efficiently.

## References


1. Lorenz, Edward N., 1967: The nature and theory of the general circulation of the atmosphere. World Meteorological Organization, p. 35.

2. Bendat, Julius S. and A. G. Piersol, 1966: Measurement and analysis of random data. John Wiley & Sons, New York, p. 288.

# APPLICATION OF SATELLITE DATA TO AN AUTOMATED NEPHANALYSIS AND FORECASTING PROGRAM

Ralph W. Collins, Major, USAF
and
Allen R. Coburn, Major, USAF

Air Force Global Weather Central
Offutt Air Force Base, Nebraska

## Abstract

The concept of the numerical analysis and forecasting of cloud parameters at the Air Force Global Weather Central (AFGWC) is discussed briefly. The general logic of the AFGWC grid-mesh nephanalysis program is described. Details of the manner in which video data from satellites are used in the automated analysis to include: digitization, compaction, conversion, correction and integration with other data. Some limitations of the video data are mentioned. The logic and methods of forecasting cloudiness on both 1/8-mesh and 1/2-mesh scales are presented. The report concludes with a short outline of planned improvements to the automated analysis-forecasting system.

## 1. INTRODUCTION

The Air Force Global Weather Central (AFGWC) provides real-time world-wide environmental support to the DOD and other government agencies. An integral part of this support is the timely analysis and prognosis of cloud parameters which include percent total cloudiness, percent cloudiness by layer, and type of cloud. AFGWC has numerically analysed and forecast cloudiness on a synoptic scale since 1962 (Jensen [3] and Edson [2]); however, operational needs have long dictated that the resolution be increased. The long-life meteorological satellites produced great masses of cloud data. Operational requirements demand a technique which could assimilate this data and transform it into a data base for timely applications to DOD problems. The advent of the third-generation computer made possible the development of such a technique to produce these high-resolution analyses and forecasts.

The result of this development is an automated system for the analysis and forecasting of cloud parameters. This system integrates the data from satellites and earthbased sensors and the forecasts from the dynamic prediction models. This report will discuss the concepts and methods used in the computer programs for the analysis (3DNEPH) and for the prognosis (FIVLYR and HRCP). Verification statistics are presented comparing the prognosis to the analysis. The last section of the report contains a brief description of current and planned research.

## 2. CONCEPT

The AFGWC nephanalysis program was developed for the purpose of objectively integrating satellite-sensed data (Figure 1) with other types of conventionally-sensed data to produce a high-resolution, three-dimensional analysis of clouds in the atmosphere. The automated program is a stream of processors, several of which were developed to fully utilize the tremendous amount of satellite data without unnecessarily compromising quantity or quality. The program design allows new types of data, as they become available, to be integrated into

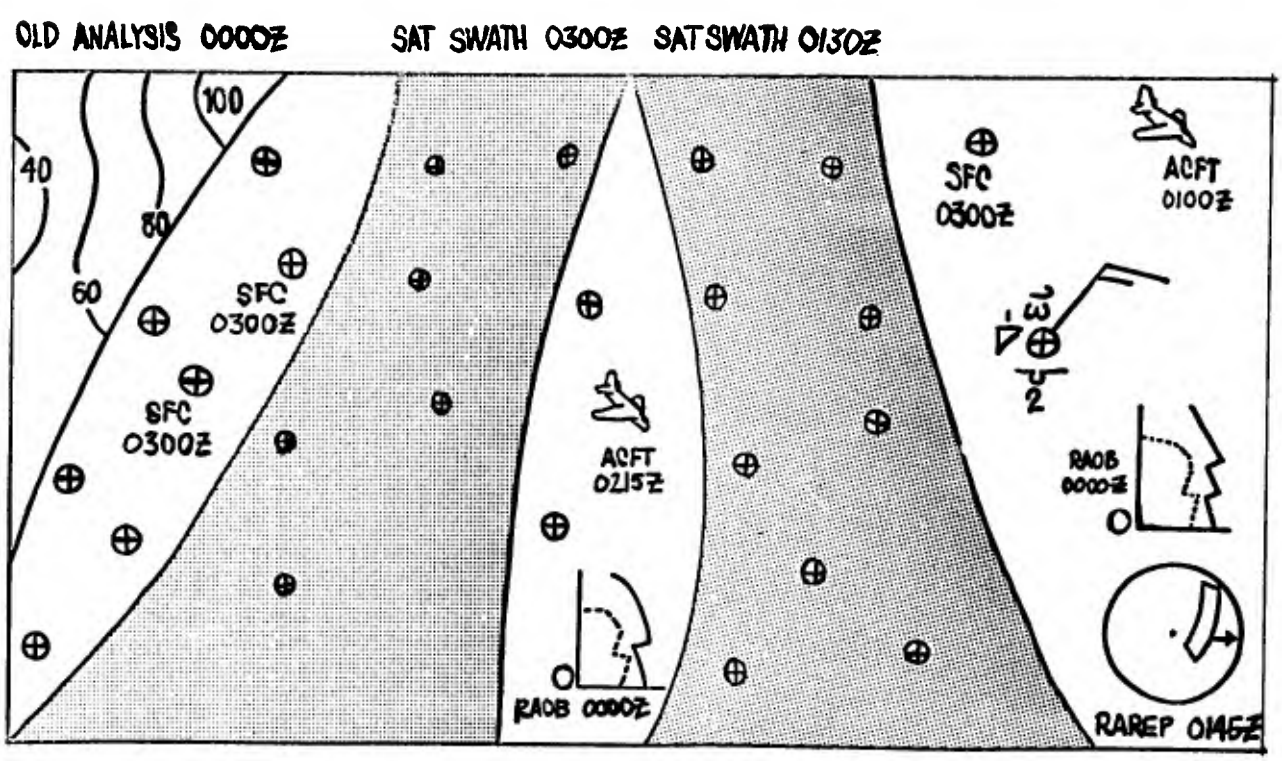


FIGURE 1 DATA RESOLUTION

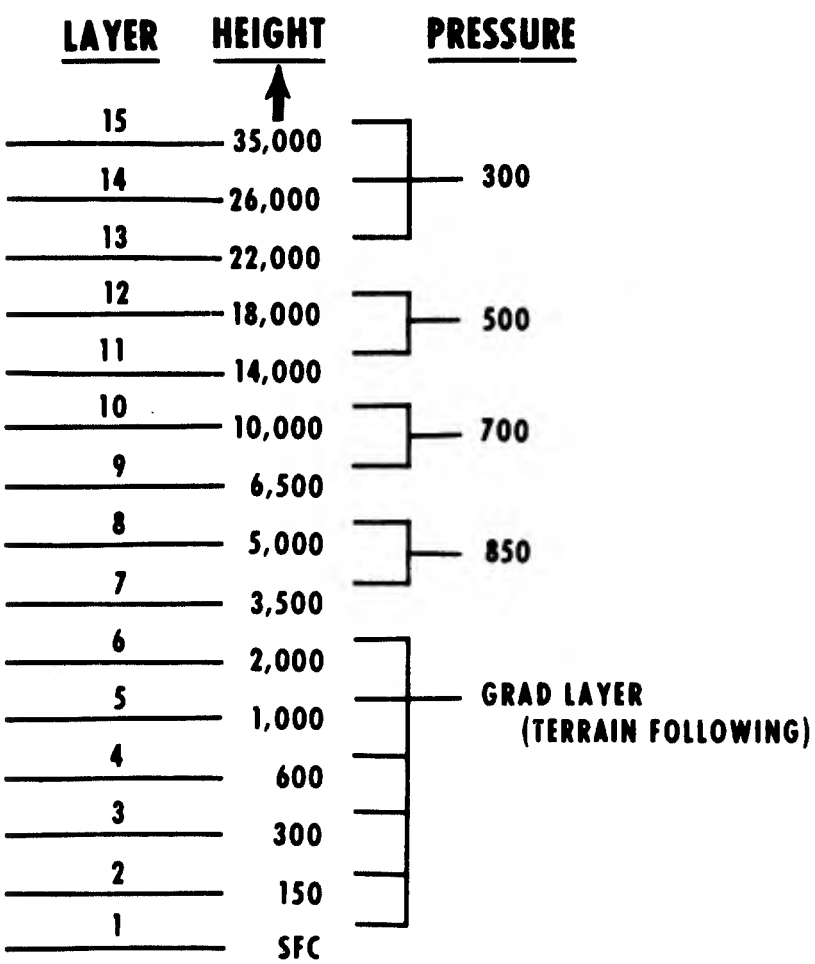


FIGURE 3. CLOUD MODEL LEVELS

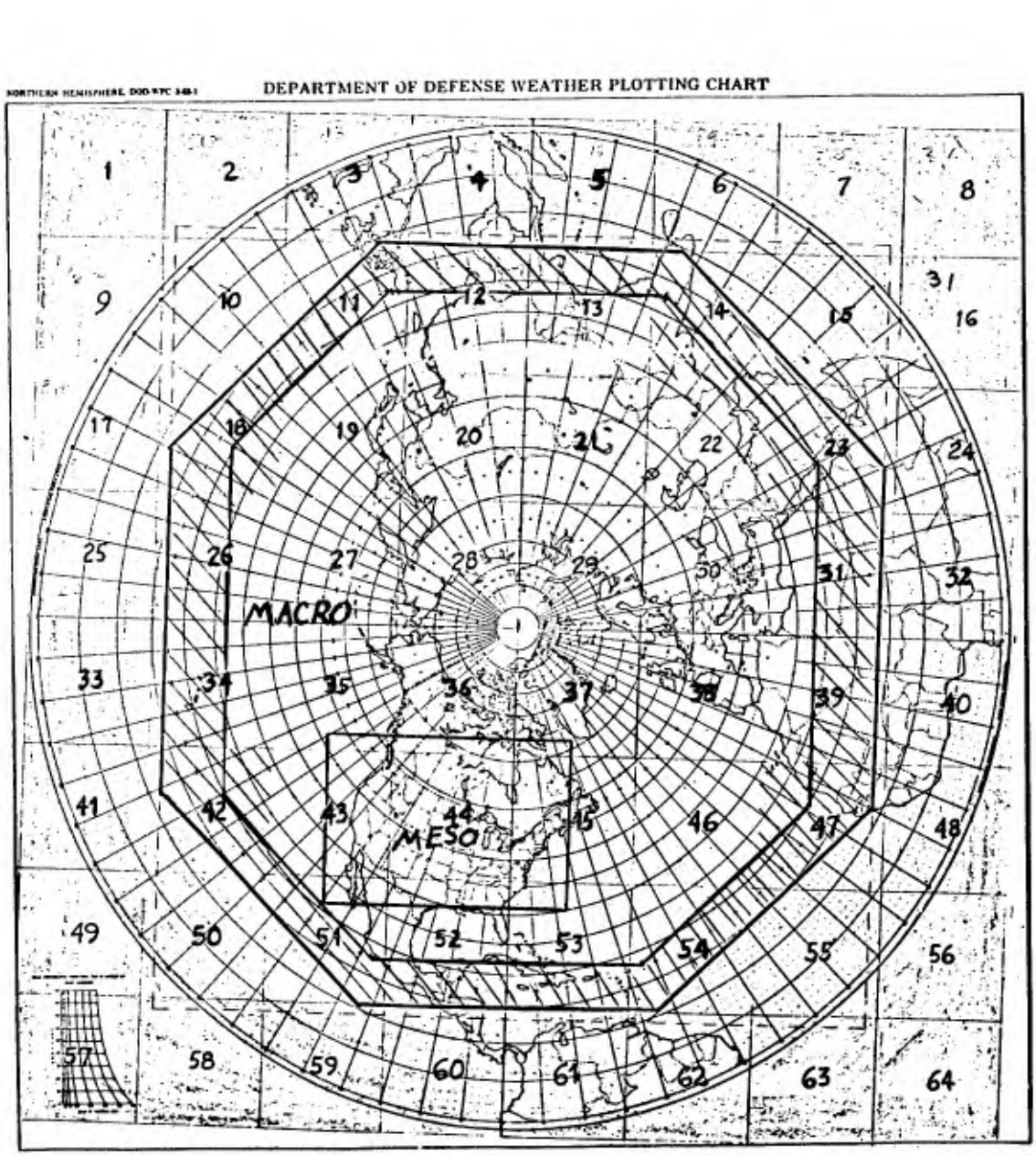


FIGURE 2 GRID AREAS

the operational system with a minimum amount of programming maintenance. This provides the essential capability for future growth. The 3DNEPH program was developed with the basic premise that timely, hemispheric satellite data would be available every six hours in the AFGWC data base.

The generalized, satellite rectification and normalization program produces high-resolution satellite data which enables the 3DNEPH program to numerically produce reliable cloud data. The capability to analyze or forecast for a limited as well as for a hemispheric area is basic to the design of the programs (Figure 2). There are quality-control features and modules which detect existing problems in the input data as well as in the analyses. These problems are identified to a monitoring analyst who has the capability to perform a non-scheduled update of the analysis or forecast over a limited area (window).

Finally, primary emphasis was placed upon the production of a timely and operationally useful analysis and forecast. It is not enough to know the total coverage at a point unless the height and depth of the clouds is also known. The integration and decision processes are geared to the fact that layered cloud information is necessary in order for the forecast models to run. Although total coverage from video data is the input data from the satellite, it must be placed at the correct height so that the overlayed vertical-motion fields can be applied to produce layered forecast cloud-fields. A by-product of the forecast technique is the computation of total coverage.

The analysis and forecast cloud-system utilizes a horizontal grid spacing of approximately 25 nautical miles. The programs analyze and forecast for 15 layers in the vertical (from the earth's surface to 40,000 feet MSL) with higher-resolution layers near the surface (depth of 150 feet in layer 1) and lower-resolution layers at the top of the model (depth of 5000 feet in layer 15) (Figure 3).

## 3. 3DNEPHANALYSIS

There are three major functions of this program:

(1) Input valid data and preprocess this data into a useable format which includes information concerning timeliness, position and source.

(2) Rank conventional data according to timeliness, source and position.

(3) Integrate satellite data, conventional data and the continuity field.

The video-data processor numerically converts the raw satellite-brightness values into meaningful cloud data in four essential steps: digitization, statistical processing, background-brightness correction and making decisions of integration. These data are voltage responses of the radiance (brightness) from the field of view. The analog signals have a voltage range of 1.25 - 5.00 volts and are passed through a digitizer which converts the voltage traces to trains of digital values ranging from 0 to 63.

The sampling rate allows a spatial resolution of satellite brightness values of 1.7 nautical miles at the equator and 3.4 nautical miles at the pole. The satellite brightness data are rectified (positioned to a standard map projection) and normalized (calibrated and corrected such that the response at any point is as though the point were at the sub-satellite point at local noon).

The sampling rate of the digitizer produces eight unique brightness values between two adjacent grid points on the 1/8 AFGWC grid, thus there are 64 brightness values surrounding each grid point.

The Display Package program computes the three statistical parameters of average brightness $\bar{B}$, variability V, and the range of the samples R, for each grid point and stores these in the data base. The first parameter $\bar{B}$, is calculated according to the equation:

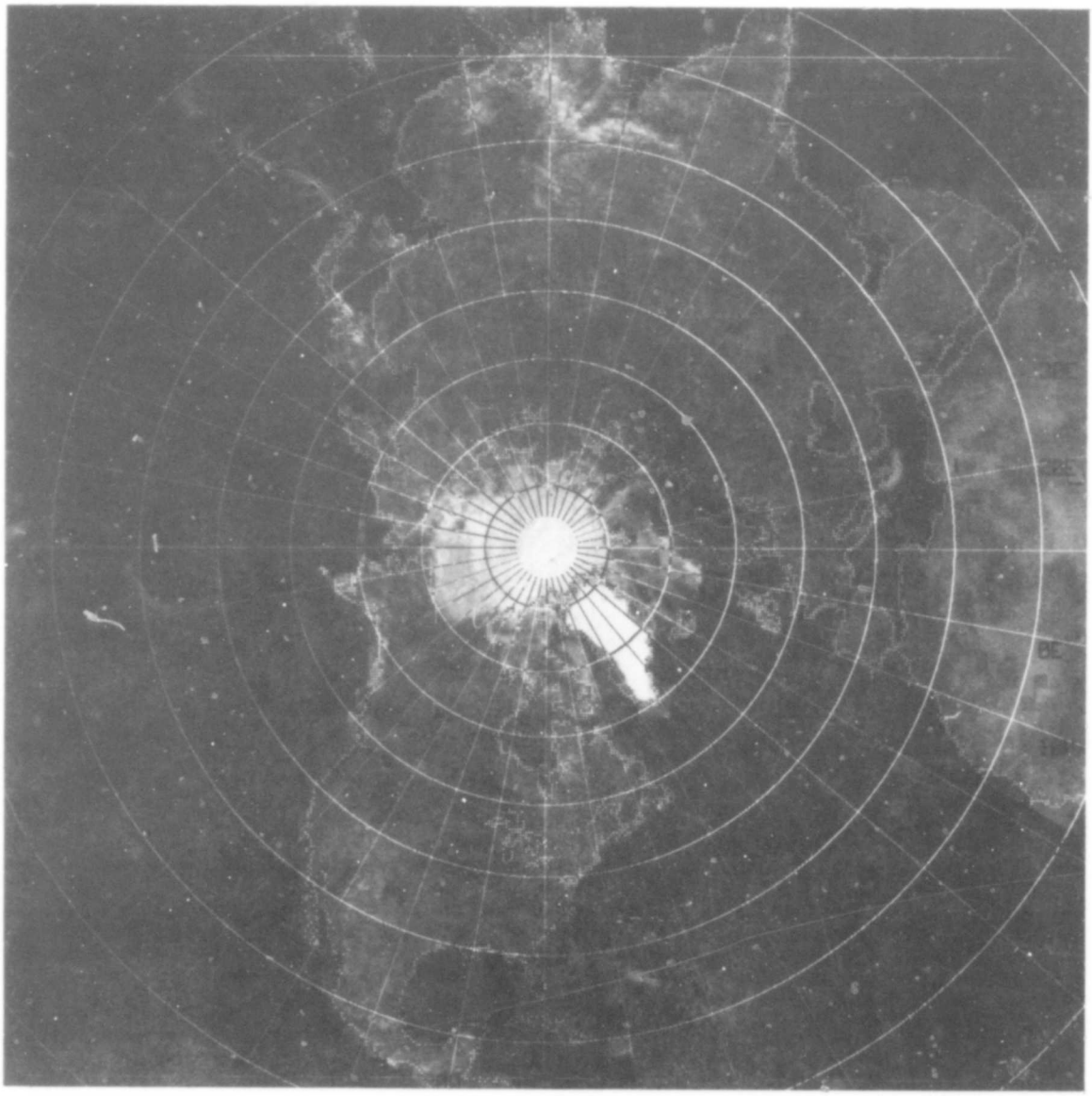

FIG.4. BACKGROUND BRIGHTNESS MAP NORTHERN HEMISPHERE DISPLAY TIME 03012 05 AUG 70 1/60.0 POLAR

$$V = \frac{\sum_{i=1}^{N} B_i}{N}, \qquad (1)$$

where $B_i$ = unique brightness value of a sample (Range: 0 - 63) and

N = number of samples (N must be greater than 40). The second parameter, V, is calculated according to the expression:

$$V = \frac{\sum_{i=1}^{N} (B_i - \bar{B})}{N}. \qquad (2)$$

The third parameter, R, is calculated according to the equation:

$$R = B_i(\text{Max}) - B_i(\text{Min}), \qquad (3)$$

where $B_i(\text{Max})$ = maximum brightness value and all samples and
$B_i(\text{Min})$ = minimum brightness value of all samples.

Video-data statistical parameters are stored in the data base in the form of quarter-orbit strips which run from the equator to the north pole. The data base consists of a maximum of 18 quarter-orbit strips. Each strip is a 128 ✖ 272 data array with the statistical parameter packed into one computer word per grid point. The 3DNEPH program retrieves the statistical video data every three hours.

The video-data processor next uses the average brightness values to update a background-brightness field. This field is a running 7-day minimum of the average brightness values. In performing this update, steps are necessary to insure that erroneous data are not permitted to give unrepresentatively low values of the background brightness. Such a value might result from mislocated data and would remain in the background-brightness field for seven days. To preclude this event the background-brightness value at any grid point is not permitted to decrease by more than two shades of gray (on a 1 - 63 scale) within a 36-hour period. This prevents the inclusion of erroneous data and at the same time permits the background-brightness field to be responsive to changes such as result from melting snow fields, etc. The AFGWC background-brightness field is similar to the NESS composite minimum-brightness charts except that the full range of brightness values (1 - 63) are retained (i.e., no enhancement techniques are used). The average brightness values ($\bar{B}$) are adjusted for existing surface conditions (sand, snow, etc.) using the background-brightness values (Figure 4). The adjusted average brightness values, A, are computed from the equation:

$$A = (\bar{B} - M7)F_B, \qquad (4)$$

where $\bar{B}$ = current average brightness,
M7 = background brightness, and
$F_B$ = background-brightness-range factors.

The full range of possible background-brightness values is divided into three classes which occur over various important surface conditions. In the case of the ESSA 9 satellite, the background-brightness-range factor is computed for each of the three classes as follows:

For dark backgrounds (0 - 16),

$$F_B = 62/(63 - M7) \qquad (5a)$$

For intermediate backgrounds (17 - 35),

$$F_B = \left[\frac{62}{63 - B_D}\right]\left[\frac{B_I - M_7}{B_I - B_D}\right] \qquad (5b)$$

where $B_D$ = brightness value (empirically determined) which differentiates between brightest desert areas and darker terrain (for ESSA 9 $B_D$ = 17), and

$B_I$ = brightness value (empirically determined) which defines the lowest limit of snow-cover conditions (for ESSA 9 $B_I$ = 35).

For bright backgrounds (35 - 62),

$$F_B = 0. \qquad (5c)$$

Figure 5 shows the values of background brightness for ESSA 9 satellite with descriptive levels indicated.

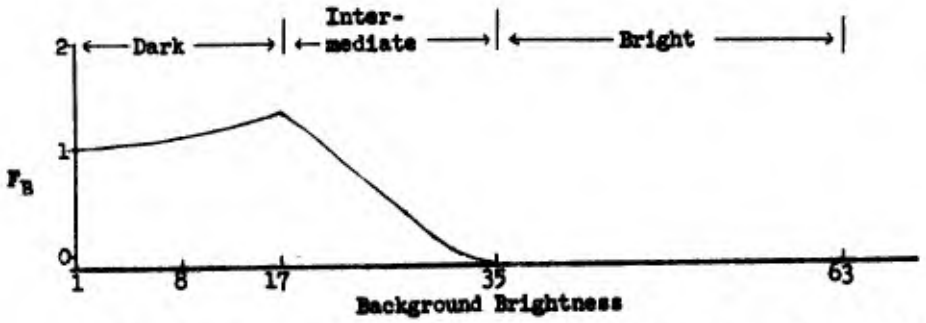


**Figure 5. Background-Brightness Conversion to Range Factor ($F_B$)**

The adjusted average brightness values are then used to compute the percent of total cloudiness, T, according to the equation (Figure 6):

$$T = A\ \left[4 + A\ (C + DA)\right], \qquad (6)$$

where $C = (300 - 8U)/U^2$,
$D = -(4 + 2UC)/(3 + U^2)$, and
U = the upper limit of validity of the equation (for ESSA 9 data U - 45)

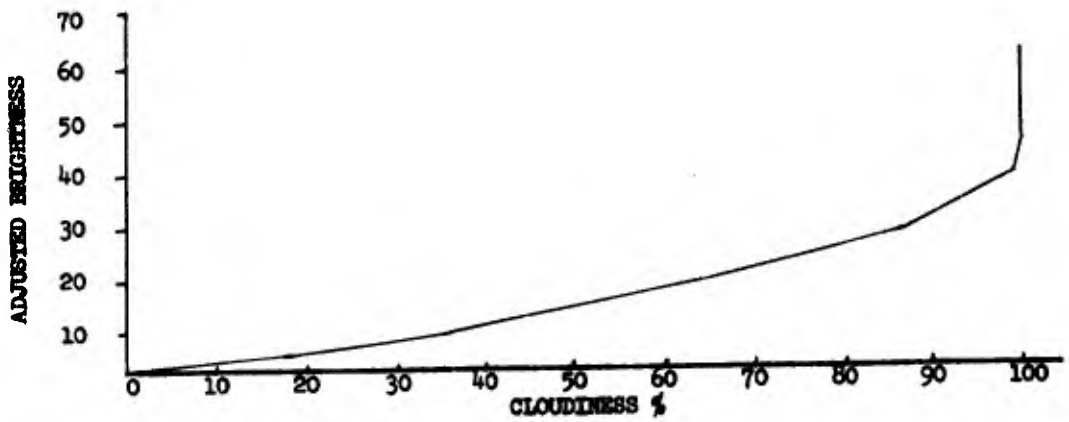


**Figure 6. Brightness vs Clouds**

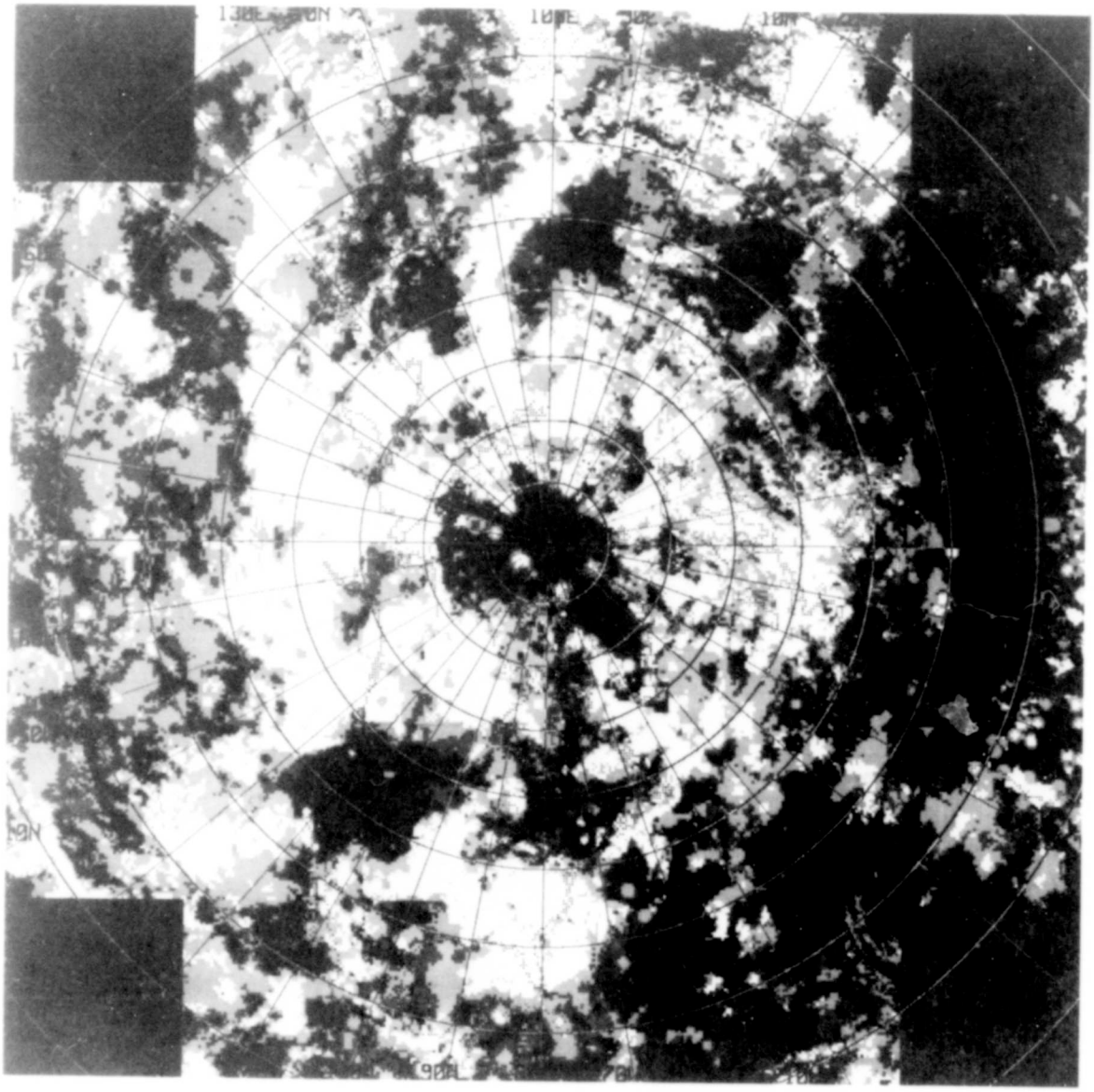

FIG 7. ANALYSIS TOTAL CLOUD ANALYSIS TIME 12002 10 AUG 70 1/60.0 POLAR MAP NORTHERN HEMISPHERE

For adjusted gray shades above 45 the cloud amount is set to 100%.

The type of cloud is determined from the adjusted brightness, A, and the variability V, using the following set of decisions:

(1) If $V \geq 3$, the type of cloud is defined to be cumulus.

(2) If $V < 3$, and $A \geq 56$, the type of cloud is defined to be cumulonimbus.

(3) If $V < 3$, and $A < 56$, the type of cloud is defined to be stratus.

The processor now mosaics all of the satellite data into another 512 x 512 grid array. The following parameters are packed into one computer word per grid point: adjusted average-brightness value, initial variability, initial range of samples, a timing parameter (to be used later in the decisions on ranking), cloud type, and the percent of total cloudiness.

Data must be ranked according to timeliness and data source, so that only the best information is used in the analysis. Video data provide only two types of information: total coverage and type of cloud. In the conversion of the statistical parameters of the brightness field to a total-cloud-cover estimate, several known limitations of the video data are recognized and accounted for in the decisions made in the program. The three significant limitations accounted for in the program are:

(1) Single-layered thin clouds at any level are often not "seen" in the video data.

(2) Single-layered scattered cumulus clouds smaller in diameter than two miles are usually not "seen" in the video data.

(3) Over bright backgrounds the estimate of cloud amount from video brightness becomes more difficult and in some cases unreliable.

In view of the limitations listed above, the following decisions are used in the integration of the video data with conventional data:

(1) When the satellite data is timely (less than two hours old at analysis time) and when the total estimated cloud cover is greater than 4/8, the satellite total coverage overrides all other data in the analysis.

(2) When a single layer of cirrus clouds is reported in the conventional data the satellite data overrides all other total-coverage data.

(3) When a single layer of scattered clouds is reported in the conventional data the reported surface total coverage overrides the satellite total coverage. If no conventional data is available to report total coverage, then the satellite estimate is used with one exception. For areas where the background-brightness values are in the intermediate range (characteristic of brightest desert region), values of one and two eighths coverage are set to zero. Thus, over desert regions, satellite-total-cloud coverage will never be one or two eighths coverage.

If for any point on the grid, no timely data is available, then the three-hour-old analysis field is used as the best analysis of the present cloud conditions.

Type of cloud data, derived from satellite data, are used only when a single layer of clouds is reported at a grid point. These data will replace all other types of conventional data except timely surface reports.

The final processor contains the final set of decision trees which determine the relative importance of the various types of data in producing the final analysis fields. These decision trees were purposely placed in the final

processor so that as new types of data become available, changes to the ranking and ordering of data types would have to be made in only one of the processors. The primary functions of the final processor are:

(1) Determination of continuity fields and

(2) Determination of total coverage.

Two sources of information are available to produce the continuity fields: Three-hour-old analysis (persistence) and the three-hour 1/8-mesh forecast.

Since the 3DNEPH program is currently executed every three hours in the production cycle, the persistence fields are always available in the data base. A number of case studies have shown that the differences between persistence and the three-hour forecast were small. There are persistence fields for 22 parameters which are available for use as continuity fields. Fields for all 22 parameters must be available to the final processor. The parameters and their respective units are listed below:

| Parameters | Units |
|---|---|
| *Total coverage | percent |
| *Minimum base | feet AGL |
| *Maximum top | feet AGL |
| Surface present-weather | coded value |
| Low-cloud type | coded value |
| Middle-cloud type | coded value |
| High-cloud type | coded value |
| *Coverage for 15 layers | percent |

The 1/8-mesh forecast fields are available for 18 of the parameters listed above (quantities marked with an asterisk). Data from cloud forecast fields are used when available to produce continuity fields. Persistence is used only for those parameters (present weather, cloud types) for which forecast fields are never available, and where cloud forecast fields are not available. Results have shown that the continuity fields are at least 80% reliable.

The second function of the final processor is to determine the total cloud coverage through the integration (using decision trees) of conventionally-sensed and satellite-sensed total-cloud-cover data with the continuity-field data (the term conventionally-sensed total-cloud-cover data includes data obtained from Raobs and aircraft reports). Figure 7 is an example of the finished product. Timeliness of data is a very important factors. In addition, a modification of Barnes' [1] technique is utilized to spread the influence of each conventionally-sensed report of total cloud cover. The radius of influence varies between 2 - 6 grid distances. Equations (7) and (8) are used to determine the weighting function at each grid point within the influence region of report.

$$R_s = 25/D_r, \tag{7}$$

where $R_s$ = scan radius and

$D_r$ = a value calculated for each grid point at which a report is located. This value is a function of the number of reports within a distance of four grid points.

$$W = {}^{1}\Big/ \left[1 + 48(R/R_s)^2\right], \tag{8}$$

where W = the weighting function used to modify a grid-point value and

R = the distance of the grid point from the location of the report.

## 4. FORECASTING

As previously mentioned, the forecasting problem is complicated by the fact that there is no capability to operate on the total cloud coverage which is our best data source. The model must operate on specific layers. The best known predictor for cloudiness is the time-integrated vertical motion. A variety of vertical-motion forecasts are available at the AFGWC, but none, of course, have the 15-level, eighth-mesh resolution. The AFGWC Six-level and the PE models store vertical motion at the standard levels of 850, 700, 500, and 300 mb for a whole-mesh grid. The PE also forecasts vertical motion for the 600m AGL. The Limited-Area Meso-Mesh (LAMM) model forecasts in certain windows for the same pressure levels with twice the horizontal resolution. The Boundary-Layer Model (BLM) produces a vertical motion forecast for eight levels nearest the surface in the same windows and with the same resolution as the LAMM. The Multilevel-Cloud Model (MCM) itself computes a vertical motion forecast at the 600m AGL using dynamic-model winds, its own temperature forecasts, terrain, and the diurnal cycle. Basically, the MCM is designed to select the best of these various vertical-motion forecasts, depending on the area, time, and height of the desired cloud forecast, to modify the satellite-oriented nephanalysis.

The MCM does this on two different scales of space and time. First, a forecast is produced for short-range, high-resolution use. This is the HRCP program which maintains the eighth-mesh, 15-level resolution and is capable of forecasting for 3, 6, or 9 hours. This module applies the time-integrated vertical motion to the cloudiness at each point and level in the analysis (with no advection of clouds). Vertical motion fields are interpolated in the horizontal to the eighth-mesh scale. But in the vertical there is no interpolation; the program applies the vertical-motion field that is closest to the level of interest. The exception to this rule is in the boundary layer which is taken to be the lower six levels. In this layer, if BLM forecasts are not available, the 600m AGL vertical motion is interpolated by a simple linear profile which assumes the vertical motion to be zero at the surface.

Second, a forecast is produced for the intermediate-range time period, i.e., out to 24 hours. This is the FIVLYR program, and this program forecasts cloudiness on a half-mesh scale at five levels: 600m AGL, 850, 700, 500, and 300 mb. The problem of differing scales of the various mathematical models plagues this module in reverse. That is, the resolution of the vertical-motion forecasts is similar to the resolution of the cloudiness forecast, but the intelligence in the nephanalysis, which has already condensed the satellite data, has to be condensed even further. In each layer, for each half-mesh point, the nearest 25 eighth-mesh points are averaged. Then a weighted average is done for each of the desired five levels in the vertical. The resulting half-mesh, five-level array serves as the initial condition for the FIVLYR program.

At first glance one might think the original intelligence furnished by the satellite has been so diluted as to be of questionable value, but this is not true. Each eighth-mesh grid point represents approximately 625 $mi^2$. The cloudiness of this area is better represented by considering all the 64 pieces of video data than by arbitrarily selecting any one piece. In addition, the compaction process produces intelligence about the type of cloud. Similarly on the half-mesh scale, we can compact the 25 eighth-mesh points to produce a better representation of the 10,000 $mi^2$ area that can be done with any one-eighth-mesh point. However, most important by far is the fact that the satellite furnishes data for initial conditions over vast regions where we have no other data source.

To produce a forecast from these initial conditions the FIVLYR advects the cloudiness parameter and modifies it with the integrated vertical motion. The

advection is accomplished in the following manner. The three components of the forecast wind are integrated with time to determine the origin point of the parcel of air which is currently at the grid point and pressure level where cloudiness forecast is needed. Then the cloudiness value in the initial field at the origin point (using three dimensional interpolation) is brought to the grid point and level where the forecast is desired. Finally, this cloudiness value is modified by the time-integrated vertical motion as in the HRCP.

Therefore, the basic difference between the HRCP and FIVLYR is that the HRCP modifies cloudiness in situ while the FIVLYR advects the cloudiness. The short-range, high-resolution HRCP concentrates on maintaining local effects and integrity of the analysis. It is designed to just "push" persistence in the right direction. On the other hand, the intermediate-range FIVLYR must move the cloudiness as the systems move in 12 to 24 hours.

Statistics have been computed for the eighth-mesh forecast for the months of February, May and June. Table 1 presents monthly average statistics for the period for the total cloudiness and selected layers. Total cloudiness is a weighted sum of the layers.

| | FEB 70 | | | MAY 70 | | | JUN 70 | | |
|---|---|---|---|---|---|---|---|---|---|
| LEVEL | E | E | RMSE | E | E | RMSE | E | E | RMSE |
| 3 | 1.58 | 3.90 | | 0.91 | 2.65 | 12.71 | 0.61 | 2.90 | 13.25 |
| 5 | 1.21 | 9.75 | | 2.47 | 10.87 | 25.32 | 1.19 | 10.48 | 24.79 |
| 7 | -1.01 | 13.57 | | -4.57 | 17.52 | 31.06 | -6.62 | 18.98 | 30.38 |
| 9 | 1.61 | 14.91 | | -1.60 | 16.24 | 29.13 | -5.55 | 16.83 | 28.68 |
| 11 | 3.37 | 18.76 | | 1.49 | 18.45 | 29.85 | -2.41 | 17.53 | 28.28 |
| 14 | 1.62 | 18.92 | | 0.27 | 18.68 | 28.55 | -2.53 | 18.72 | 25.30 |
| TOTAL | 7.91 | 21.83 | | 5.55 | 24.38 | 33.35 | 0.84 | 25.14 | 34.24 |

**Table 1. Verification of the High-Resolution Cloud Prog**

Levels 7, 9, 11, and 14 (free-atmosphere representation) generally over forecast in February and under forecast in May and June. This may be a seasonal characteristic of the vertical-motion forecast of the dynamic model.

Total cloudiness is biased consistently toward over-forecasting more than any of the individual layers.

These statistics do not include some improvements already discussed in this paper and included in the current operational model.

## 5. FUTURE PLANS

Computer programs are presently being developed to process high-resolution infrared radiation (HRIR) data from meteorological satellites of the ITOS series. HRIR data will be processed in a manner similar to video data. The analog signal will be digitized on a scale from 0 - 63. The digitized data represent flux densities of infrared radiation sensed by the scanning radiometer in the 8-12 micron range. These data will be corrected for standard atmospheric absorption and calibrated with the instrumental response curves before being converted into temperatures.

The HRIR data will be interpreted by constructing a frequency distribution from the 64 digitized "infrared brightness values" mapped into each 1/8 GWC

grid point. Modes in the frequency distribution of brightness values are converted to effective radiating temperatures, are interpreted as tops of cloud layers, and located vertically in the analysis model. Programs are also under development for estimating total cloud cover from the frequency table.

With an average resolution of 1.5 degrees Celsius in the IR data, it is apparent that even this high-resolution data the errors in estimating the height of the radiating surface will continue to be in the realm of 500 - 1000 feet at low levels of the atmosphere and as much as 3000 - 5000 feet at the cirrus-cloud levels.

The coding of the objective analysis of the IR data has made it necessary to develop a high-resolution (1/8-grid mesh) surface-temperature data base for use in the final decision processor. In an effort to improve the decisions of total coverage, a running 7-day maximum temperature field will be maintained and used to determine the surface response temperatures.

The field of IR gradients will be maintained in order to test the possible uses of this type of data.

The routine which computes total cloudiness is empirical. Experimentation is being conducted to remove the bias of this computation since the various level forecasts do not exhibit this tendency.

The diurnal capability of the MCM and the BLM must be fully exploited to produce cumulus, stratus and fog.

Statistics must be accumulated and evaluated to determine the effect of the improvements already implemented.

## REFERENCES

1. Barnes, S. L., "A Technique for Maximizing Details in Numerical Weather Map Analysis," Journal of Applied Meteorology, 3(4): 396-409, Aug 1964.

2. Edson, H., "Numerical Cloud and Icing Forecasts," Scientific Services Technical Note 13, 3rd Weather Wing, Offutt Air Force Base, Omaha, Nebraska, 61 pp., Sep 1965.

3. Jensen, C. E., "Prediction of Large-Scale Cloudiness and Airframe Icing Conditions by Machine Methods," Journal of Applied Meteorology, 2(3): 337-344, June 1963.

# THE APPLICATIONS OF THE NIMBUS METEOROLOGICAL-SATELLITE DATA

Lewis J. Allison

Goddard Space Flight Center
Greenbelt, Maryland

## Abstract

Since the initial launch of Nimbus 1 on 28 August 1964, eight radiometric and three television systems with improved spatial and spectral resolution have been flown by the Nimbus satellite program.

Meteorological parameters such as high-resolution cloud cover and heights, vertical temperature, humidity and ozone profiles, total ozone content, jet-stream detection and high-level winds derived from tracked balloons have been obtained daily on a near-global basis.

In addition, important applications of the Nimbus data have been found in the fields of oceanography, hydrology, geology, forestry and ice reconnaissance. Selected examples of these geophysical applications and related sensor systems are briefly discussed in this paper.

## INTRODUCTION

The Nimbus 1 meteorological satellite which was first successfully launched in August 1964 was a new concept in spacecraft design. It and its successors, Nimbus 2, 3, and 4 carried many more radiometers than the older TIROS series which sensed different parts of the electromagnetic spectrum and hence permitted more detailed research investigations of the earth's atmosphere.

The purpose of this paper is to illustrate the application of the Nimbus satellite data to both old and new scientific technologies and to discuss briefly the present sensor systems.

## THE NIMBUS-4 SPACECRAFT SYSTEM

Figure 1 shows the basic Nimbus 4 spacecraft configuration which includes the solar paddles, attitude-control systems, the modular ring containing thermal-control shutters and nine sensor sub-systems (Nimbus-4 Users' Guide, 1970). The satellite provided a stable platform at approximately 1100-km height from which these new sensors could be earth oriented with $\pm 1°$ accuracy. The experimental data, recorded twice daily at local noon and midnight during the 107 minute sun-synchronous polar orbits were transmitted to ground stations at Fairbanks, Alaska, and Rosman, North Carolina, and processed by the experimenters at the Goddard Space Flight Center, Greenbelt, Maryland, prior to analysis.

## SCIENTIFIC APPLICATIONS OF NIMBUS DATA

### 1. Oceanography

One of the initial applications of the Nimbus High-Resolution Infrared Radiometer (HRIR) was in the field of oceanography. This single-channel scanning radiometer contained a lead-selenide (PbSe) photoconductive cell which was radiation-cooled to -75°C and operated in the 3.5-4.2$\mu$ "atmospheric-window" region. The aperture of the instrument was 0.5 degree, thus the area viewed from 1100 km has the approximate dimensions 9 X 9 km at the sub-satellite

point. The radiometer scan-mirror continuously rotated the field of view of the detector through 360 degrees in a plane normal to the orbital path. The detector therefore viewed the housing cavity, outer space, earth, outer space, and returned to view the housing cavity. The outer-space level served as a zero reference and together with the radiometer housing (typically 290°K) provided for an in-flight check of calibration. In the "atmospheric window," there is still present slight atmospheric attenuation due primarily to water vapor and carbon dioxide and a correction of a few degrees Kelvin may have to be applied to the measured equivalent-blackbody temperature to yield the thermometric temperature of the viewed sea-surface (Warnecke et al., 1969; Kreins and Allison, 1970).

The Temperature-Humidity Infrared Radiometer (THIR), a two-channel scanning bolometer radiometer, was designed to provide day and night cloud-top and surface temperatures from the 10.5-12.5μ window channel, and moisture content from the upper troposphere in the 6.5-7.0μ region. Ground resolution is 8 km for the 10-12μ channel and 22 km for the water-vapor channel. The scan-mirror rotation and on-board calibration is similar to the HRIR system. Atmospheric attenuation corrections have been estimated to be smaller for this instrument than for the HRIR and are presently being evaluated with "ground-truth" data.

Figure 2 shows the north wall of the Gulf Stream through the use of Nimbus 4 THIR data on the left and the Nimbus 2 HRIR on the right. Note the "whiter" hence cooler Labrador Current and "darker-warmer" Gulf-Stream water shown in this daytime photofacsimile filmstrip of THIR analog data (Fig. 2a). A 10°K change over 20 km in the 2 June 1966 nighttime HRIR grid-print map analysis (Fig. 2b) easily delineated the north wall of the Gulf Stream. This position was confirmed by U.S. Navy radiometer-equipped aircraft on the same night (Warnecke, et al., 1969). Infrared imagery from aircraft, ships, and satellites are being studied at the U. S. Navy Oceanographic Office to track the meanders of the Gulf Stream and to develop a thermal-structure prediction model (Smith et al., 1970).

Figure 3 shows the sea-surface temperature patterns detected by the Nimbus 2 HRIR during two periods of the southwest monsoon in the Arabian Sea. Figure 3a shows the early stages of cold water upwelling (dotted area: <23°C) along the Somali Coast on 8 June 1966. By July 6, 1966, this small area of cold water had enlarged to form a fully-developed anticyclonic gyre south of Socotra (Fig. 3b). This surface-upwelling feature had been detected previously by Allison and Kennedy, 1967 with Nimbus 1 HRIR data. Figure 4 shows the confirmation of this localized circulation-feature with ship data collected by Bruce, 1968 during the International Indian Ocean Expedition (1963-1965) and further documented with dynamical studies by Duing, 1969. Figure 5 shows two oceanographic cross-sections analyzed by Szekielda, 1970, from composite research-ship data obtained from the National Oceanographic Data Center, Washington, D.C. On the right, Fig. 5b, is a sea-temperature chart showing the rise of cold water in the vertical. At the left, Fig. 5a, is the reactive phosphate content showing the rise of biological nutrients to the surface during the same upwelling process. Because the spatial distribution of these two parameters is similar, it would be possible to predict the nutrient distribution at the surface with satellite-derived sea-surface temperatures. If the response time of the phytoplankton growth to nutrients and fish growth to phytoplankton content is known, the oceanographic food chain could be forecast under certain conditions in this region. With the successful expansion of the United States purse-seine fishing fleets from the eastern Pacific to the eastern Atlantic, increased interest is now being placed on the Indian Ocean with its specialized oceanographic conditions for future fishery operations (21st Tuna Conference, 1970).

## 2. Hydrology

### Ice and Snow Boundaries

Satellite imagery has important application in the field of hydrology. At present, there is only limited knowledge of the global amounts of annual or perennial snow and ice cover, river and lake discharge (National Academy of Sciences, National Research Council, 1969; Barnes and Bowley, 1970).

Since a large portion of the world's water supply is stored in the form of snow cover, especially in mountainous regions, photo-interpretive studies of satellite television pictures of snow cover and ice concentrations have been made. However, previous satellite snow-and ice-mapping techniques were limited by the resolution and other characteristics of the National Oceanic and Atmospheric Administration (NOAA) vidicon television system (Mc Lain, 1970). The Nimbus-3 and-4 Image-Dissector Camera System (IDCS) has overcome some of these inadequacies.

It has the ability to sense a greater dynamic light range (about 100:1), has a high signal-to-noise ratio by using a photomultiplier tube, has a direct relationship between light flux input and electron-current output and avoids the troubles of a mechanical shutter (Nimbus-IV Users' Guide, 1970). The IDCS video frame consists of 800 scan lines, requires 200 seconds of cycling time and from orbital altitude of 600 n. miles, the ground resolution is approximately 1 to 2 miles at the sub-satellite point. The IDCS data can be recorded for transmission to Fairbanks, Alaska and Rosman, N.C. and has a direct read-out APT mode of operation.

Figure 6 and 7 shows ice and snow concentration boundaries in the Greenland, Baffin Bay and Hudson Bay areas as recorded by the Nimbus-3 IDCS in April 1969. A comparison of the climatological ice fields in April (U.S. Navy H. O. Pub. 705, 1968) to IDCS data in April 1969 in Fig. 6a and b, shows that the ice fields extent in the Greenland Sea was further south than normal. Leads or open water breaks in the ice, snow, ice floes and a line of demarcation between >30% and <30% woodland are shown under clear sky conditions in Fig. 7a and b.

The U. S. Navy has used both the real-time and stored-playback capability of the IDCS to provide ice predictions and ship tracks for U.S. Coast Guard ice breakers and MSTS ships on summertime resupply routes to Baffin Island and Thule, Greenland. In addition, the historic journey of the tanker Manhattan through the northwest passage to Prudhoe Bay, Alaska in August 1969 was assisted by ice observations made from satellite photography (Mariners Weather Log, 1969).

Flood Conditions

Figure 8 demonstrates the usefulness of Nimbus data to show a hydrological sequence of basic importance to the economy of Egypt. Figure 8a is a Nimbus-3 IDCS picture of the Nile River on which an arrow points to the Aswan High Dam location during pre-flood stage 26 May 1969. Figure 8c shows a Nimbus-3 HRIR (day) picture recorded in the 0.7 to 1.3μ spectral region during the Nile's flood stage on 11 Sept. 1969. Note the darker, swollen area of the Lake Nasser Resevoir, south of the dam (arrow). The Aswan Dam which rises 364 ft above the Nile riverbed caused water to flood 400 miles southwestward in the Lake Nasser Resevoir, the waters of which will irrigate 1.3 million acres of arid land, Fig. 8b.

Vegetative and Hydrological Features

The Nimbus-3 daytime HRIR photofacsimile imagery has been very useful in showing the contrast between vegetated and bare surfaces, sand and rock outcroppings, open water and land surface and major plant associations.

Figure 9 shows a transect of Nimbus-3 daytime HRIR data on 15 April 1969 over Africa from the Ivory Coast to the Mediterranean Sea (MacLeod, 1970). The 5-mile ground resolution of this sensor grossly delineates the darker tropical rain forests and tall grass savannahs, the lighter desert steppes, the highly reflective Sahara desert sands, the darker saline marshes (Chott Melri) and Lake Chad.

Figure 10 shows a simultaneous view by two different Nimbus-4 sensors of western, central and southern Indian and Pakistan during orbit 13, 9 April 1970. The dark Arabian Sea, the highly reflective land surface and the bright line of clouds are shown in the Nimbus IDCS picture (Fig. 10a). The Nimbus THIR photofacsimile picture (Fig. 10b) shows the opposite pictorial effect in that the Arabian Sea appears lighter (cooler), the land appears darker (warmer) but the clouds appear the same in both pictures. The clouds remain white because they are located higher in the atmosphere hence radiate with a colder equivalent-blackbody temperature than the sea surface below. The Earth Resources Technology Satellites, A and B, to be launched in 1972-73 will produce much higher-resolution registered images in the visible spectrum (200-300 ft ) and 1000-ft resolution recorded simultaneously by multi-spectral sensors in the near-infrared spectrum. A 100 by 100 n. mile swath of data will be recorded during each orbit and the same ground location will be viewed every 18 days over the North American continent and coastal waters (Nordberg and Scull, 1970). Color-processed ERTS data will be compared to aircraft balloon and surface ground-truth data for detailed studies by research groups in agriculture, forestry, geology, hydrology, coastal oceanography and biology and the monitoring of ecological systems.

## 3. Geology

The principal fields of applied geology are exploration for oil, gas, minerals and engineering construction. Space photography, particularly Gemini and Apollo imagery, have indicated some very promising possibilities but were deficient in solar illumination due to a lack of optimum sun angle (National Academy of Sciences, 1969). However, studies conducted by Pouquet, 1969, delineated major structural geological features over Saudi Arabia as shown by Nimbus-3 daytime HRIR (Fig. 11a). The Arabian Shield shown in the western portion consists of darker igneous and metamorphic rocks overlain by volcanic and sedimentary surfaces. This area is bordered on the east by the interior homocline, a 400-km wide belt of lighter-toned limestone, shale and sandstone. Erosion and deposits of sediments in the lower areas produced a hook-shaped pattern. Extensive areas of wind-blown sand are shown in the north and south portions of the homocline. The three other major structural provinces shown in this figure have been confirmed by tectonic maps (Fig. 11b) and provide an excellent tool to supplement large-scale aircraft photos and interfacial geological field studies (Blodget, 1970).

## 4. Vulcanology

An example of an active effusive volcanic eruption occurred at Surtsey, Iceland on 27 August 1966, Figure 12a (Friedman and Williams, 1970). This volcanic island which appeared on the sea surface in November 1963 had a discontinuous, complex and unpredictable eruptive history until July 1967. Lava temperatures of 1130°C were measured by airborne surveys on successive nights in August 1966. Figure 12b shows the 310°K $T_{BB}$ spike in the analog trace recorded by the Nimbus 2 HRIR on the night of 22 August 1966. This feature was also recorded during 6 other nighttime orbits (Williams and Friedman, 1970). A comparison of the corrected satellite data to air-ground measurements indicated that the satellite radiometer recorded 3-4% of the estimated total thermal yield of the volcano.

Figure 13 shows the eruption of the Beerenberg volcano on Jan Mayen Island, northeast of Iceland, on 21 September 1970, as recorded by Nimbus 4 IDCS. The ash plume shown in the dashed rectangular area extended 200 miles to the southeast. Other active volcanoes such as Hekla, Iceland; Mauna Loa, Hawaii; Mt. Ranier, Washington are being monitored from satellite data by the U. S. Geological Survey in addition to conventional aircraft/ground instrumentation.

## 5. Meteorology

### Radiation Balance

Studies of planetary radiation balance have been carried out in the 1950's using conventional surface and upper air data (London, 1957; Houghton, 1954). Recent results from analyses of Nimbus-2 and -3 Medium-Resolution Radiometer (MRIR) data sensing in the 0.2-4.0μ (solar radiation) and 5-30μ (emitted thermal-radiation) regions have revised the original estimate of 35% global planetary albedo to 29-31% and the mean planetary temperature from 252°K to 254°K (Bandeen, 1968; Raschke and Bandeen, 1970). In Figure 14, net radiation flux (cal $cm^{-2}$ $min^{-1}$) at the top of the atmosphere is depicted for a 15-day period (1-15 July 1966). The light-grey tone delineates areas of excess net flux or regions in the northern hemisphere where more flux is absorbed than emitted. The dark-grey tone covers areas of deficient net flux or regions in the winter hemisphere where outgoing exceeds incoming radiation. The geographic distribution of radiation balance and its variation in time is very important in the study of the exchange of energy and momentum over the globe by the atmosphere and the oceans.

### Tropical-Storm Detection

Nimbus HRIR data has been processed by computer and analyzed for meteorological research purposes for several years (Warnecke et al., 1968, 1969; Hubert et al., 1968; Rao, 1970 and Hawkins, 1970). In order to speed up the tedious human analysis, a new system of data processing by color-display enhancement has been initiated by our laboratory with the Westinghouse Electric Corp., Baltimore, Md. This system processes HRIR data from the Nimbus Meteorological Radiation Tape (NMRT) through the Application Technology Satellite Operations Center at Goddard Space Flight Center (Westinghouse Electric Corp., 1968, Kreins and Allison, 1970). Figure 15a shows the hand-analysis of Hurricane Camille at the peak of its destructiveness at midnight, 18 August 1969 just as it crossed the Gulf Coast near New Orleans (De Angelis, 1969). The color-enhanced version of the black and white print, Fig. 15b, was shown at the conference.

The highest cirrus clouds (coldest $T_{BB}$ values) were color-coded blue to green (<220°K to 250°K). Middle-altitude clouds were yellow to orange (250°K to 270°K) and low clouds were pink to red (270°K to 290°K). The surface of the Gulf of Mexico was indicated by the warmest (grey-toned) $T_{BB}$ values 290° to >300°K.

The color print can be processed to a color negative in approximately two hours while the hand analysis from a computer-produced grid-print map took two days to draw using the same temperature intervals. This time saving has proved to be a great advantage for a detailed "quick look" during meteorological, oceanographic and geomorphological research studies.

Balloon and Buoy Tracking

The Interrogation Recording and Location System (IRLS) was designed to determine the position of remote-sensor platforms by propogation delay measurements and to gather platform sensor data which is stored in the IRLS for relay to ground-acquisition sites.

Fig. 16 shows the generalized system concept (Cote, 1969). Two interrogations per orbit are obtained by IRLS from each platform such as a moving balloon, buoy, ship or fixed platform. Locational coordinates are derived from range measurements which in turn yield solutions based upon intersections of range loci with the earth's surface.

Fig. 17 shows the tracking data for a fixed NAVOCEANO buoy which was accidently cut loose from its mooring south of Puerto Rico. It was recovered 2 1/2 weeks later by the U. S. Coast Guard from exact location data supplied from the Nimbus-3 satellite.

The inherent theoretical accuracy of the IRLS range system is $\pm$1.5 km. However serious sources of error such as one nautical mile per day can accumulate from uncertainties in orbital prediction and ambiguity in position (±5° lat.) due to the long (12-hour) interrogation periods. A total of thirteen balloons at the 50-and 30-mb level have been tracked successfully during June-July 1970 for the purpose of determining wind velocities at these levels (Fig. 18). T-3 ice-island movements, the migration track of an elk, data relays from buoys and ships all have been successfully implemented by IRLS. Future plans include receipt of volcano-temperature information from Mt. Ranier, geomagnetic data from Antarctica and underwater data from a buoy instrument trains.

Remote Sounding of the Atmosphere

One of the most successful of the Nimbus atmospheric sounders was the Satellite Infrared Spectrometer (SIRS) designed by D. Wark and D. Hilleary of the National Environmental Satellite Service of NOAA (Wark and Hilleary, 1969). The SIRS-B Nimbus-4 instrument measured the infrared radiation leaving the atmosphere in 14 spectral intervals in the $CO_2$ and $H_2O$ vapor bands. Measured radiances are related to the temperature and water-vapor profile in the atmosphere (Nimbus-4 User's Guide, 1970). Basic design changes were made to improve the SIRS-A Nimbus-3 instrument. The field of view was decreased, the scan angle was increased horizontally to 37° and the spectral resolution improved so that $H_2O$ vapor content could be derived. Figure 19 shows a SIRS B-Keywest, Florida, radiosonde comparison of mixing ratio for April 8, 1970 and good agreement is shown. The SIRS temperature-profile data were used operationally by the National Meteorological Center since 1969 and validations of the forecasts have shown that a relatively small improvement in the analysis by SIRS data can produce a relatively large improvement downstream in a medium-range prediction of 24 to 72 hours (Wark, 1970; Smith, et al., 1970).

The Infrared Interferometer Spectrometer (IRIS) utilizes a Michelson interferometer which operates between 6 to 25μ (Figure 20a). Included within this spectral interval are the 15μ, $CO_2$ band, Fig. 20b, the 9.6μ, Fig. 20c, $O_3$ band and the 6.3μ water-vapor absorption band, Fig. 20d (Nimbus-IV Users' Guide, 1970). Temperature as a function of height may be inferred from the absorption bands of a uniformly mixed gas such as $CO_2$. Spectral radiance observed by the satellite at various wavelengths corresponds to different height intervals. A mathematical inversion-program is used to derive the profiles of vertical temperature, ozone, and water-vapor content; examples are shown (Fig. 20 left to right) on 10 April 1970 (Conrath et al., 1970, Prabhakara, 1970a, Hanel and Conrath, 1970).

A daily map of total ozone content on 27 April 1969 is shown (Fig. 21) where $O_3$ data filling at 150-km field of view was plotted at 5°-latitude intervals and spaced approximately 28° longitude at the equator. Note the large wave-patterns shown by the ozone content isopleths in both hemispheres (Prabhakara et al., 1970 (b)).

A preliminary comparison was made between the total ozone content of the IRIS and the Backscatter Ultraviolet Spectrometer (BUV) along one orbit on April 15, 1970 (Heath, 1970). Good agreement was found (±5%) from approximately 70°N to 50°S. The BUV monitors the spatial distribution of $O_3$ by measuring the intensity of ultraviolet radiation backscattered from the earth's atmosphere in 12 wavelengths in the 2500-to 3400-angstrom region (Nimbus-IV Users' Guide, 1970). This technique is completely different than the IRIS system yet the results were similar.

A comparison of the ozone-content data was made with a standard 300-mb-level chart (Fig. 22a and b). In areas where strong vertically-tilted troughs persisted, maxima of $O_3$ concentrations were indicated and conversely minimums of $O_3$ content related to strong upper-ridge positions. In addition, a newly designated "full-latitude wave" was noted in both the ozone and 300 mb data. This large amplitude trough extended from 80° to 90°N to 10° to 20°S. The trans-equatorial cloudiness associated with this type of wave is shown on 29 April 1969 (Fig. 23) with daytime HRIR data.

50-and 10-mb temperature charts were drawn from the IRIS data, an example of which is shown in Figures 24 and 25 for 27 April 1969. Note the alternating bands of cold temperatures (213°K and colder-shaded) in the 50 mb chart (Fig. 24) and the simpler gradual warm-to-cold gradient shown at the 10-mb level (Fig. 25). A study of these IRIS-derived temperatures from 100 mb to 10 mb during the 1969 southwest monsoon over India has delineated the temperature field associated with the high-level easterly jet (Prabhakara et al., 1971).

Further research using IRIS data over India should provide a better understanding of the tropical stratospheric flow and its coupling to the lower-tropospheric monsoonal circulation.

## CONCLUSION

The Nimbus satellite program has provided an excellent test platform for the development of many new sensor systems. The data from these instruments have proved to be invaluable for the future implementation of the Global Atmospheric Research Program and World Weather Watch Program of the 1970's and to other geophysical regimes.

## ACKNOWLEDGEMENTS

The author wishes to thank Dr. Raymond Wexler, Goddard Space Flight Center for his helpful comments and suggestions in the review of this paper and is grateful to Allied Research Associates, Concord, Mass., for providing several figures used in this paper.

## REFERENCES

1. Allison, L.J. and J. S. Kennedy, 1967: An Evaluation of Sea Surface Temperature as Measured by the Nimbus I High Resolution Infrared Radiometer, NASA TN D-4078, Goddard Space Flight Center, Greenbelt, Md., 25 pp.
2. Bandeen, W. R., 1968: Experimental Approaches to Remote Atmospheric Probing in the Infrared from Satellites, NASA X-622-68-146, Goddard Space Flight Center, Greenbelt, Md., 50 pp.
3. Barnes, J. C. and C. J. Bowley, 1970: The Use of Environmental Satellite Data for Mapping Annual Snow - Extent Decrease in the Western United States, Final Report 8G-72-F, Allied Research Assoc., Inc., Concord, Mass.
4. Blodgett, H., 1970: Private correspondence.
5. Bruce, J.G., 1963: Comparison of Near Surface Dynamic Topography During the Two Monsoons in the Western Indian Ocean, Deep-Sea Research, Vol. 15, Pergamon Press, Great Britain, pp. 665 to 677.
6. Conrath, B. J., R. A. Hanel, V. G. Kunde and C. Prabhakara, 1970: The Infrared Interferometer Experiment on Nimbus 3, Journal of Geophysical Research, Vol. 75, No. 30, pp. 5831 to 5857.

7. Cote, C., 1969: The Interrogation Recording and Location System (IRLS) Experiment, NASA X-733-69-336, Goddard Space Flight Center, Greenbelt, Md., pp. 21.
8. De Angelis, R. M., 1969: Hurricane Camille, August 5-22, 1969, U. S. Dept. of Commerce, NOAA, Climatological Data, National Summary, Vol. 20, No. 8.
9. Duing, W., 1970: The Monsoon Regime of the Currents of the Indian Ocean, International Indian Ocean Expedition Oceanographic Monographs No. 1, East-West Center Press, Honolulu, Hawaii, pp. 68.
10. Friedman, J. D. and R. S. Williams, Jr., 1970: Comparison of 1968 and 1966 infrared imagery of Surtsey, in Surtsey Research Progress Report V, The Surtsey Research Society, Reykjavik, Iceland, pp. 88-92.
11. Hanel, R. A. and B.J. Conrath, 1970: Thermal Emission Spectra of the Earth and Atmosphere from the Nimbus 4 Michelson Interferometer Experiment, Nature, Vol. 228, pp. 143-145.
12. Hawkins, R. S., 1970: Interpretation and Application of Nimbus High Resolution Infrared Radiometer Data for Southeast Asia, AFCRL-69-0485, Environmental Research Paper No. 308, Office of Aerospace Research, U. S. Air Force, pp. 18.
13. Heath, D., 1970: Private correspondence.
14. Houghton, H.G., 1954: On the Annual Heat Balance of the Northern Hemisphere, J. Meteor. 11, pp. 3-9.
15. Hubert, L.F., A. Timchalk and S. Fritz, 1969: Estimating Maximum Wind Speed of Tropical Storms from High Resolution Infrared Data, National Environmental Satellite Center, NOAA Technical Report NESC 50, 33 pp.
16. Kreins, E. R. and L. J. Allison, 1970: Color Enhancement of Nimbus High Resolution Infrared Radiometer Data, Applied Optics, Vol. 9, No. 3, pp. 681-686.
17. London, J., 1957: A study of atmospheric heat balance. Final Report; Contract AF 19(122) 165 Res. Div., College of Engineering, New York Univ., 99 pp.
18. MacLeod, N. H., 1970: Ecological Interpretation of Nimbus III HRIR Data, NASA X-652-70-98, Goddard Space Flight Center, Greenbelt, Md., 10 pp.
19. Mariners Weather Log, 1969: Historic Journey of the Manhattan, Vol. 13, No. 6, November 1969, pp. 259-261.
20. McClain, E. P., 1970: Applications of Environmental Satellite Data to Oceanography and Hydrology, ESSA Tech. Memo NESCTM 19, 12 pp.
21. National Academy of Sciences, National Research Council, 1969: Useful Applications of Earth-Oriented Satellites - Summary of Panel Reports, 92 pp.
22. Nimbus-IV Users' Guide, 1970: National Space Science Data Center, Goddard Space Flight Center, NASA, Greenbelt, Md., 214 pp.
23. Nordberg, W. and W. Scull, 1970: ERTS A and B Presentation to Northeast Region Technical Committee, 24-25 March 1970, Goddard Space Flight Center, Greenbelt, Md., 26 pp.
24. Pouquet, J., 1969: Geopedological Features Derived from Satellite Measurements in the 3.4-4.2μ and 0.7-1.3μ Spectral Regions, NASA X-622-69-437 (Preprint) pp. 27.
25. Prabhakara, C., B. J. Conrath and R. A. Hanel, 1970(a): Remote Sensing of Atmospheric Ozone Using the 9.6μ Band, Journal of Atmospheric Sciences, Vol. 27, No. 4, pp. 689-697.
26. Prabhakara, C., B. J. Conrath, L. J. Allison, J. Steranka, 1970(b): Seasonal and Geographic Variations of Atmospheric Ozone Derived from Nimbus 3, NASA TN (in preparation), Goddard Space Flight Center, Greenbelt, Md.
27. Prabhakara, C. J. Steranka, L. J. Allison and B. J. Conrath, 1971: Nimbus-3 Satellite Study of the Tropical Easterly Jet Stream over India During the 1969 Monsoon (to be presented at the Symposium on Indian Ocean and Adjacent Seas, January 12-18, 1971, Cochin, India).
28. Raschke, E. and W. R. Bandeen, 1970: The Radiation Balance of the Planet Earth from Radiation Measurements of the Satellite Nimbus II, Journal of Applied Meteorology, Vol. 9, No. 2, pp. 215-238.
29. Rao, P.K., 1970: Estimating Cloud Amount and Height from Satellite Infrared Radiation Data, NOAA Technical Report NESC 54, pp. 11.
30. Smith, W. L., H. M. Woolf and W. J. Jacob, 1970: A Regression Method for Obtaining Real-Time Temperature and Geopotential Height Profiles from Satellite Spectrometer Measurements and its Application to Nimbus 3 SIRS Observations, Monthly Weather Review, Vol. 98, No. 8, August 1970, pp. 582-603.
31. Smith, W. L., P. K. Rao, R. Koffler and W. R. Curtis, 1970: The Determination of Sea Surface Temperature from Satellite High Resolution Infrared Window Radiation Measurements, Monthly Weather Review, Vol. 98, No. 8, pp. 604-611.

32. Szekielda, K.H., 1970: Unpublished data.
33. Twenty-first Tuna Conference, 1970: Proceedings, Lake Arrowhead, California, October 12-14, 1970. U. S. Dept. of Commerce, National Oceanographic and Atmospheric Administration, National Marine Fisheries Service, Fishery-Oceanography Center, La Jolla, California.
34. U.S. Navy Hydrographic Office, 1968: H.O. Publication No. 705, Oceanographic Atlas of the Polar Seas, Part II, Arctic, U.S.N.H.O., Washington, D. C., 149 pp.
35. Wark, D. Q. and D. T. Hilleary, 1969: Atmospheric Temperature: Successful Test of Remote Probing, Science, Vol. 165, No. 3899, pp. 1256-1258.
36. Wark, D., 1970: SIRS: An Experiment to Measure the Free Air Temperature from a Satellite, Applied Optics, Vol. 9, No. 8, p. 1761-1766.
37. Warnecke, G., L.J. Allison, E. R. Kreins and L.M. McMillin, 1968: A Satellite View of Typhoon Marie 1966 Development, NASA TN D-4757, National Aeronautics and Space Administration, Wash., D.C., pp. 94.
38. Warnecke, G., L.M. McMillin and L.J. Allison, 1969: Ocean Current and Sea Surface Temperature Observations from Meteorological Satellites, NASA TN D-5142, Goddard Space Flight Center, Greenbelt, Md., pp. 47.
39. Westinghouse Electric Corporation, 1968: ATS-1 SSCC Data Reduction and Analysis, Contract No. NAS5-11513, Final Report, Defense and Space Center, Baltimore, Md.
40. Williams, R. S. and Friedman, J. D., 1970: Satellite Observation of Effusive Volcanism, British Interplanetary Society Journal, Vol. 23, No. 6, pp. 441-450.

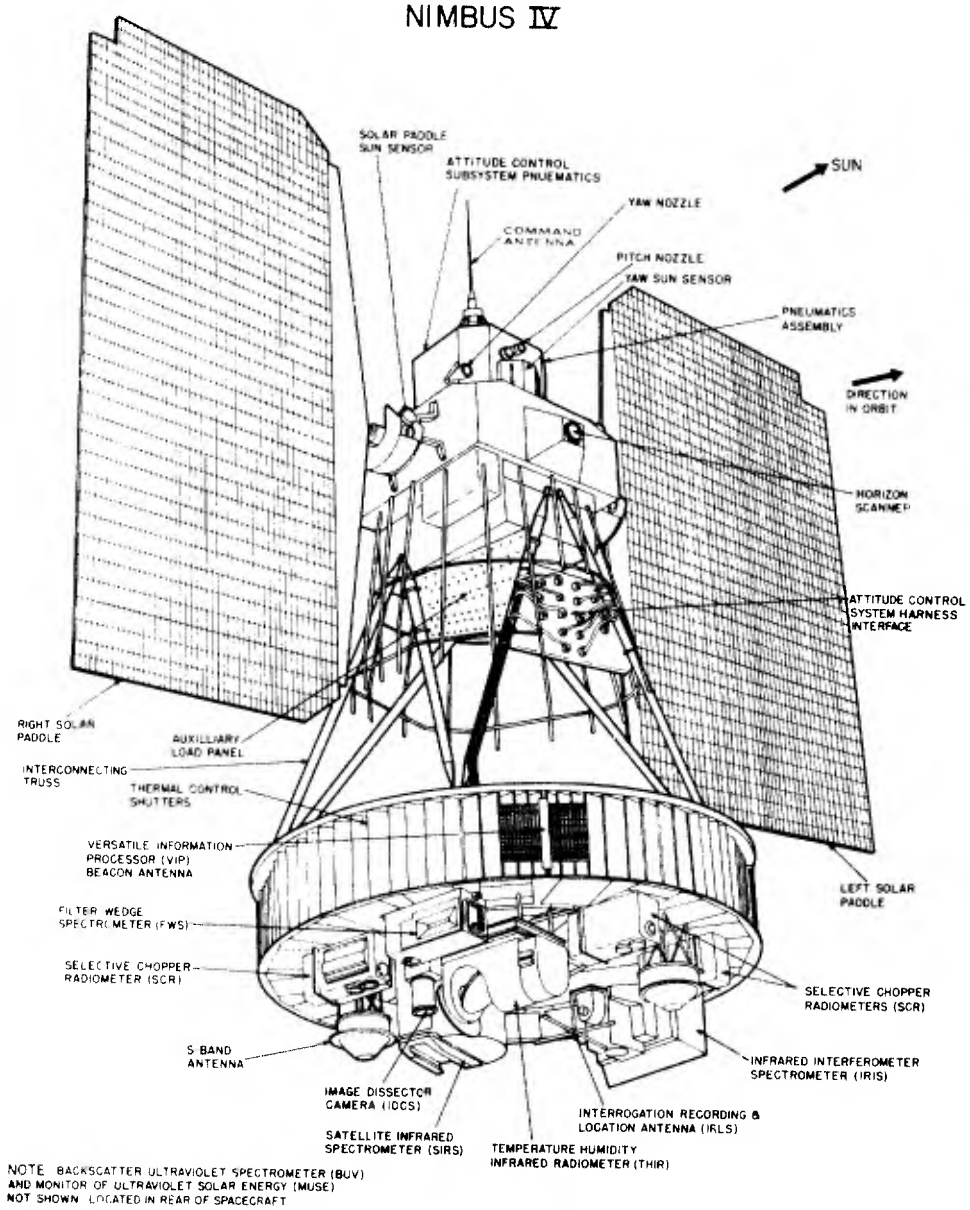


**Figure 1 - Nimbus-4 spacecraft configuration.**

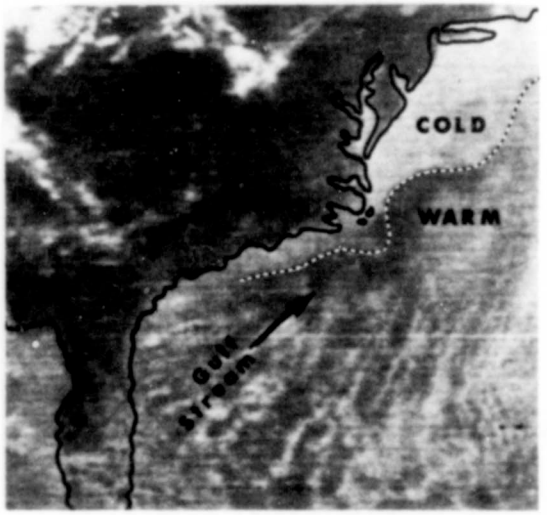


(a)

NIMBUS IV THIR (11.5μ)
ORBIT 5 (DAY)
8 APRIL 1970

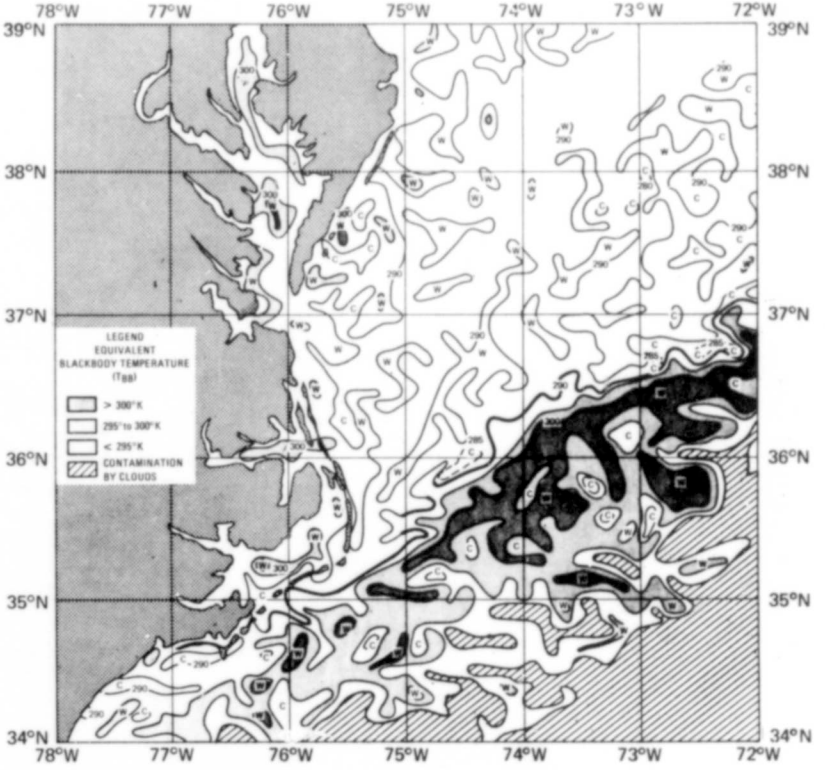


(b)

NIMBUS II HRIR (3.5-4.2μ)
ORBIT 238 (NIGHT)
2 JUNE 1966

Figure 2 - Remote detection of the Gulf Stream north-wall boundary.
a) Nimbus-4, THIR, Orbit 5 (day), 11.5μ-data, 8 April 1970.
b) Nimbus-2, HRIR, Orbit 238 (night) 3.5-4.2μ, 2 June 1966.

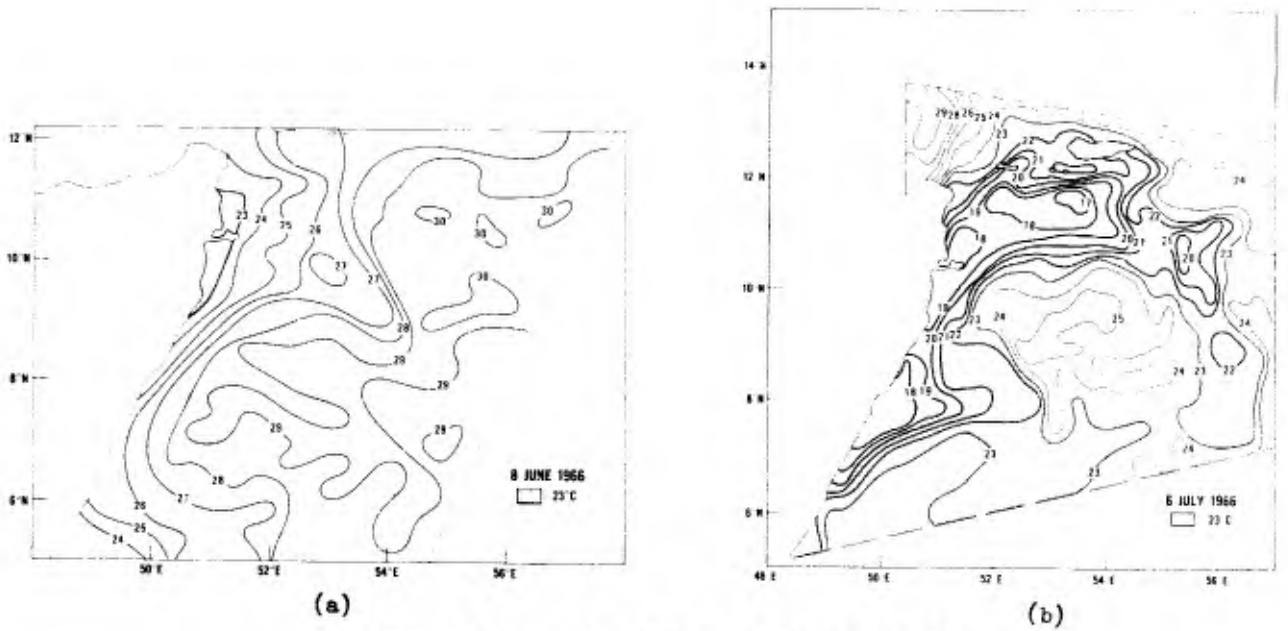


**UPWELLING ALONG THE SOMALI COAST**

**NIMBUS II HIGH RESOLUTION INFRARED RADIOMETER**

**(3.5 TO 4.2$\mu$)**

Figure 3 - Remote detection of upwelling along the Somali Coast, Africa, Nimbus-2, HRIR.
a) Orbit 744 (night), 8 June 1966.
b) Orbit 1120 (night), 6 July 1966.
(Warnecke et al., 1969)

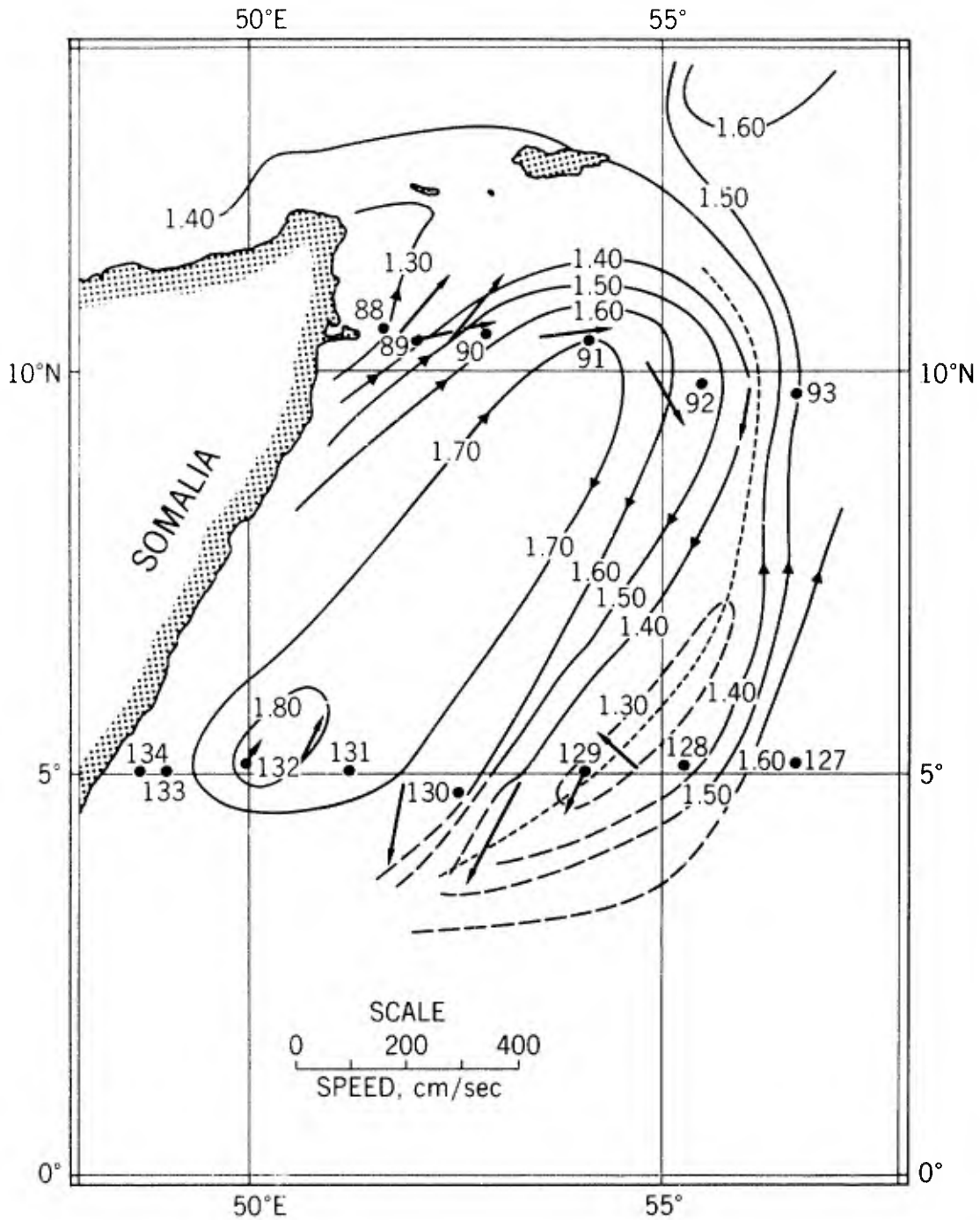


Figure 4 - Surface-current vectors along the Somali Coast during the summer southwest monsoon, 1963-1964 obtained from set of Atlantis II and other direct measurements (Bruce, 1968).

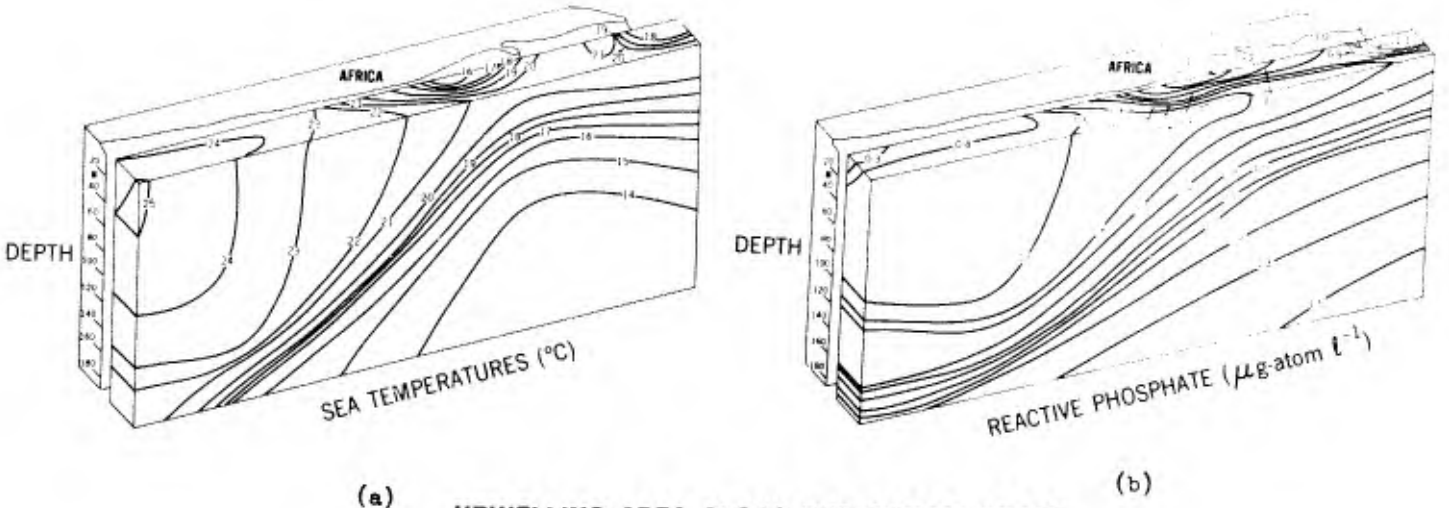


Figure 5 - Physical oceanographic properties, along the Somali Coast, Africa, during the southwest monsoon.
a) Vertical cross-section of sea temperatures (°C).
b) Vertical cross-section of reactive phosphate
(μg . atom ($^{-1}$)
(Szekielda, 1970)

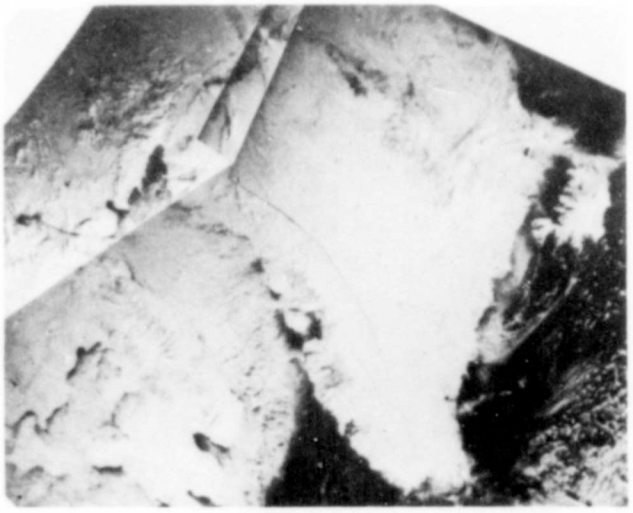

(a)

**NIMBUS III IDCS**
**15 APRIL 1969**

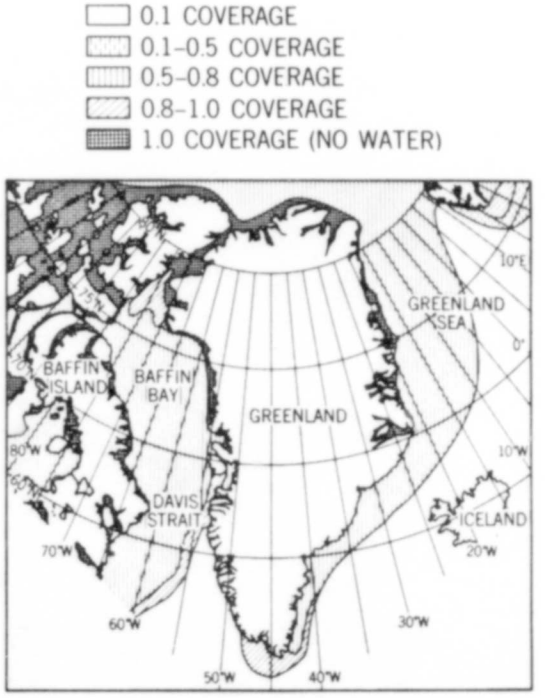


(b)

**ICE CONCENTRATION**
**APRIL**

Figure 6 - Ice and snow boundaries
a) Nimbus-3, IDCS, 15 April 1969
b) April climatological ice concentration for Greenland area (H.O. Pub. 705, 1968)

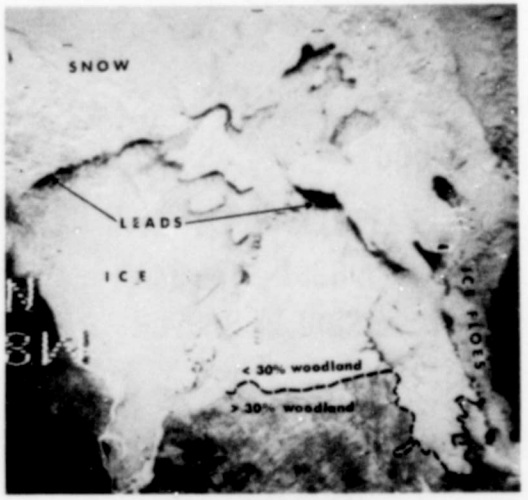


(a) NIMBUS III IDCS
30 APRIL 1969

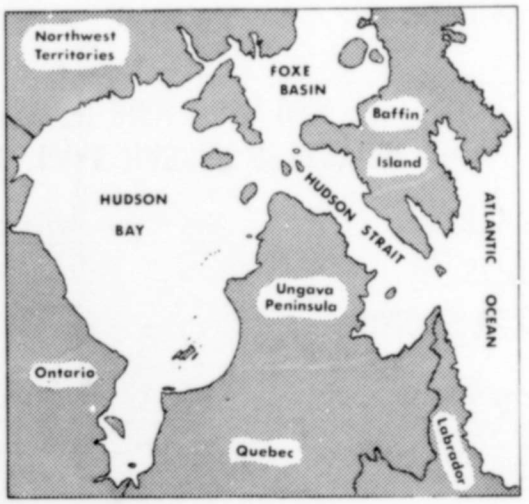


(b)

# ICE–SNOW AND VEGETATION BOUNDARIES

Figure 7 - Ice, snow and vegetation boundaries
a) Nimbus-3, IDCS, 30 April 1969
b) Geographic map of Hudson Bay area
(Allied Research Associates)

NIMBUS III IDCS
26 MAY 1969
(PRE-FLOOD STAGE)

(a)

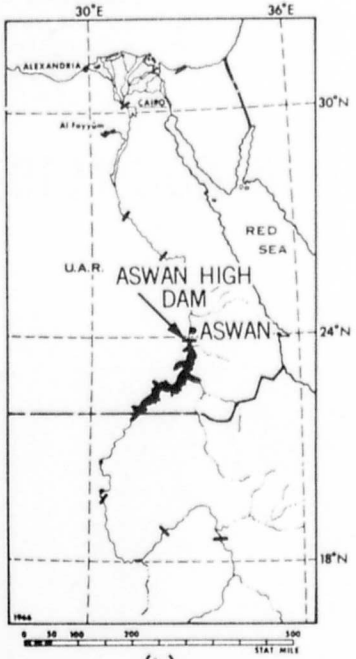


(b)

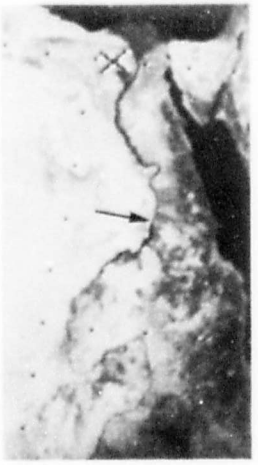

NIMBUS III DAY (HRIR)
11 SEPT 1969
(FLOOD STAGE)

(c)

**FLOODING OF THE LAKE NASSER RESERVOIR AT THE ASWAN HIGH DAM, UAR**

Figure 8 - Aswan High Dam - Lake Nasser Reservoir, UAR
a) Pre-flood stage, Nimbus 3, IDCS, 26 May 1969
b) Map of Lake Nasser area
c) Flood-stage, Nimbus 3 HRIR (day) 11 Sept. 1969
(Allied Research Associates)

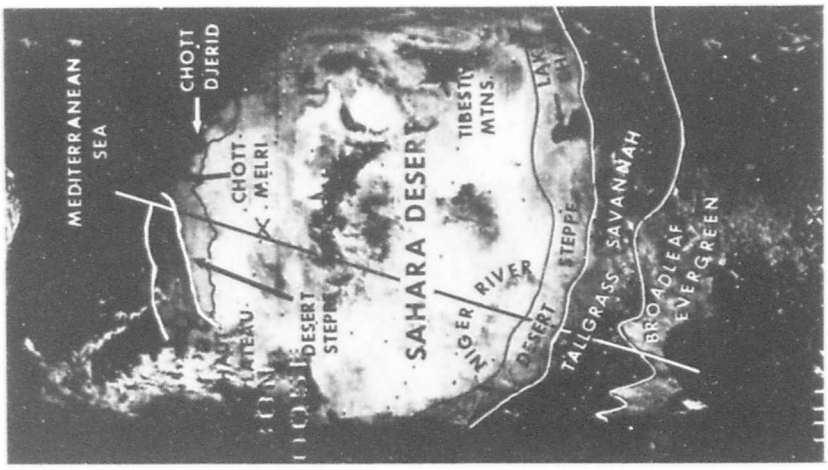


Figure 9 - Nimbus-3 HRIR (day), Orbit 16 on 15 April 1969 showing a transect over areas of broadleaf evergeen, rain forests, tall-grass savannah, desert steppe, desert, saline marshes, and Lake Chad.

(a)

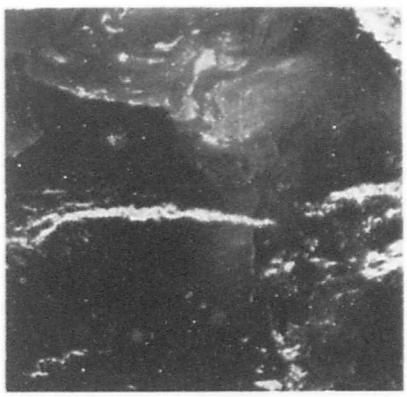

(b)

Figure 10 - A simultaneous daytime view of India, Pakistan and the Arabian Sea by two Nimbus-4 sensors.
a) Nimbus-4, IDCS, Orbit 13, 9 April 1970
b) Nimbus-4, THIR (day), Orbit 13, 9 April 1970

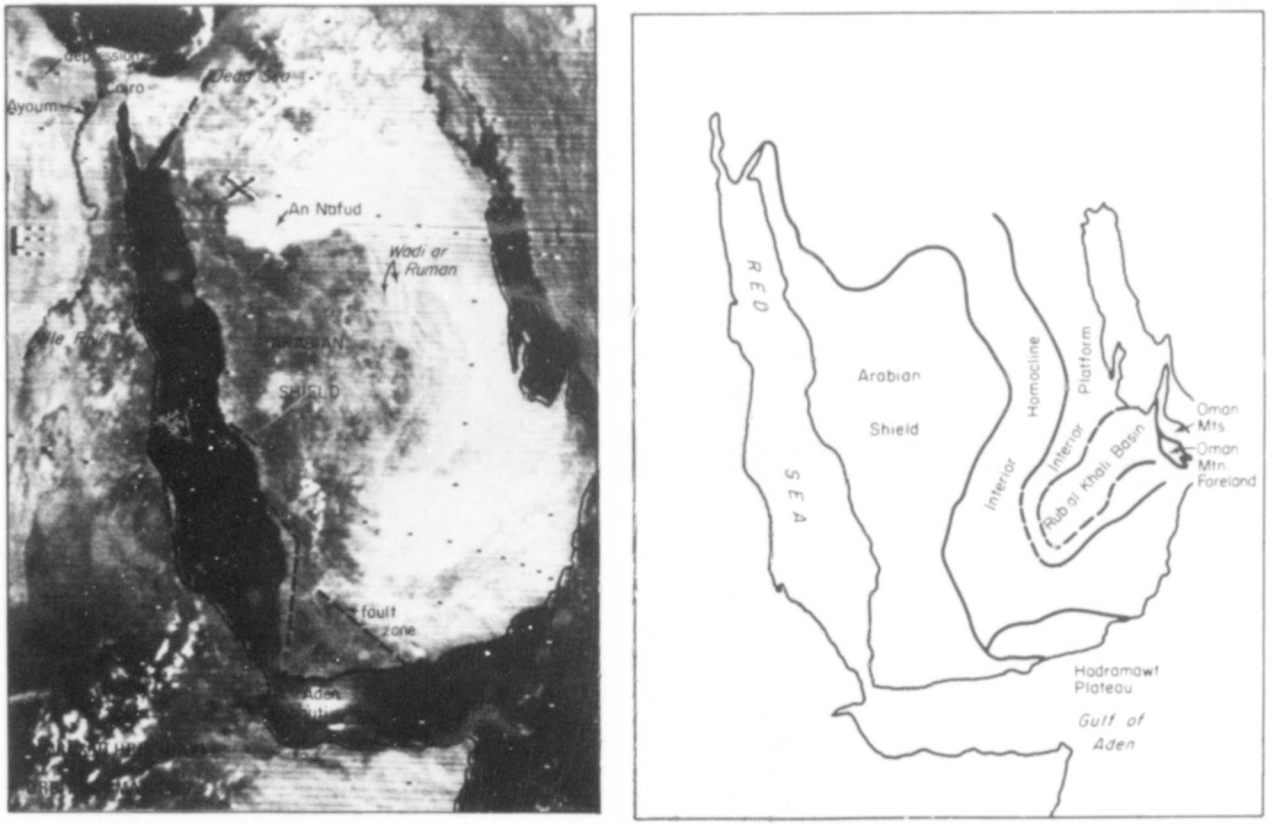


Figure 11 - a) Nimbus-3, HRIR (day), Orbit 42, 2 May 1969
b) Tectonic Map of Saudi Arabia (U.S.G.S.)

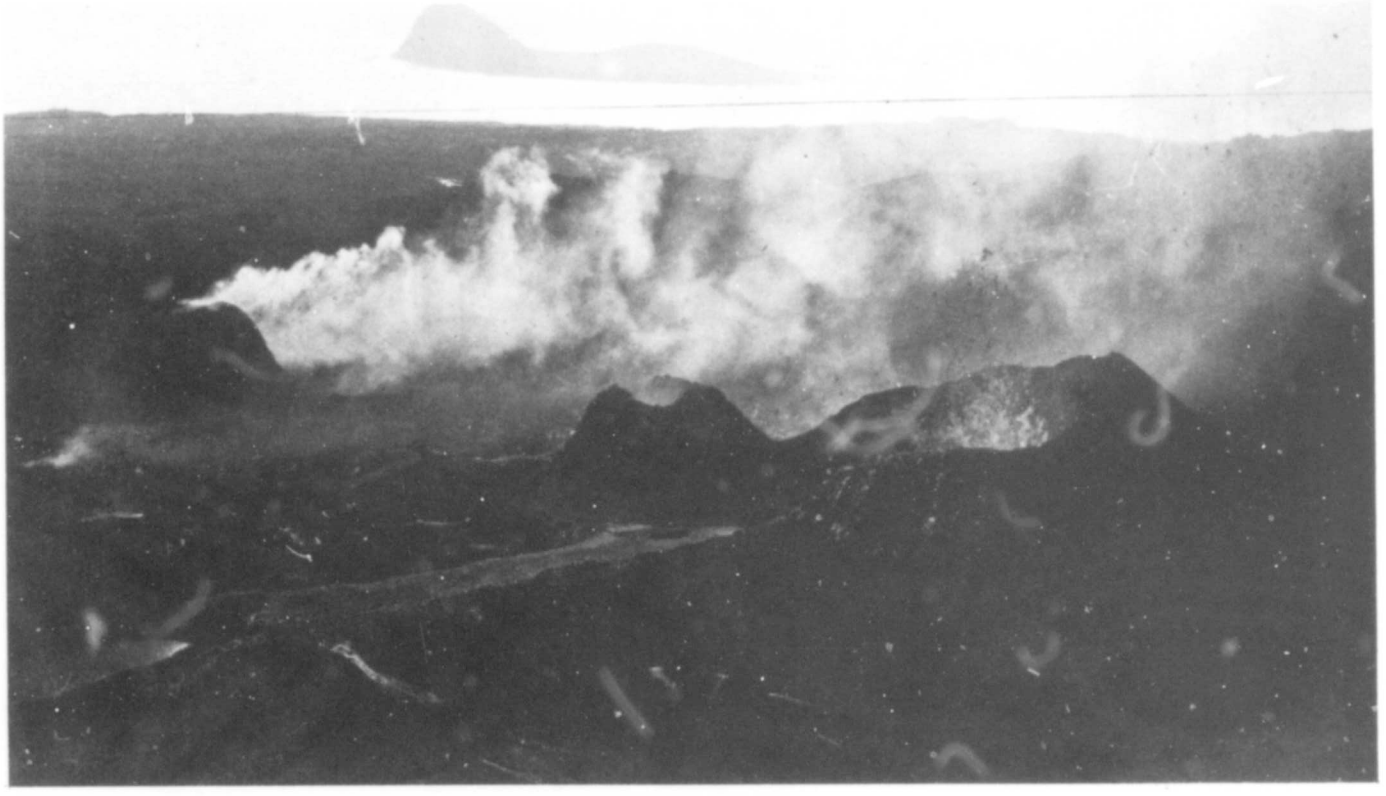

Figure 12 - a) Photo of the Surtur-I crater row, Surtsey, Iceland, on 27 August 1966, 1800 GMT, Jolnir in the backgrou
(R. S. Williams, Jr.)

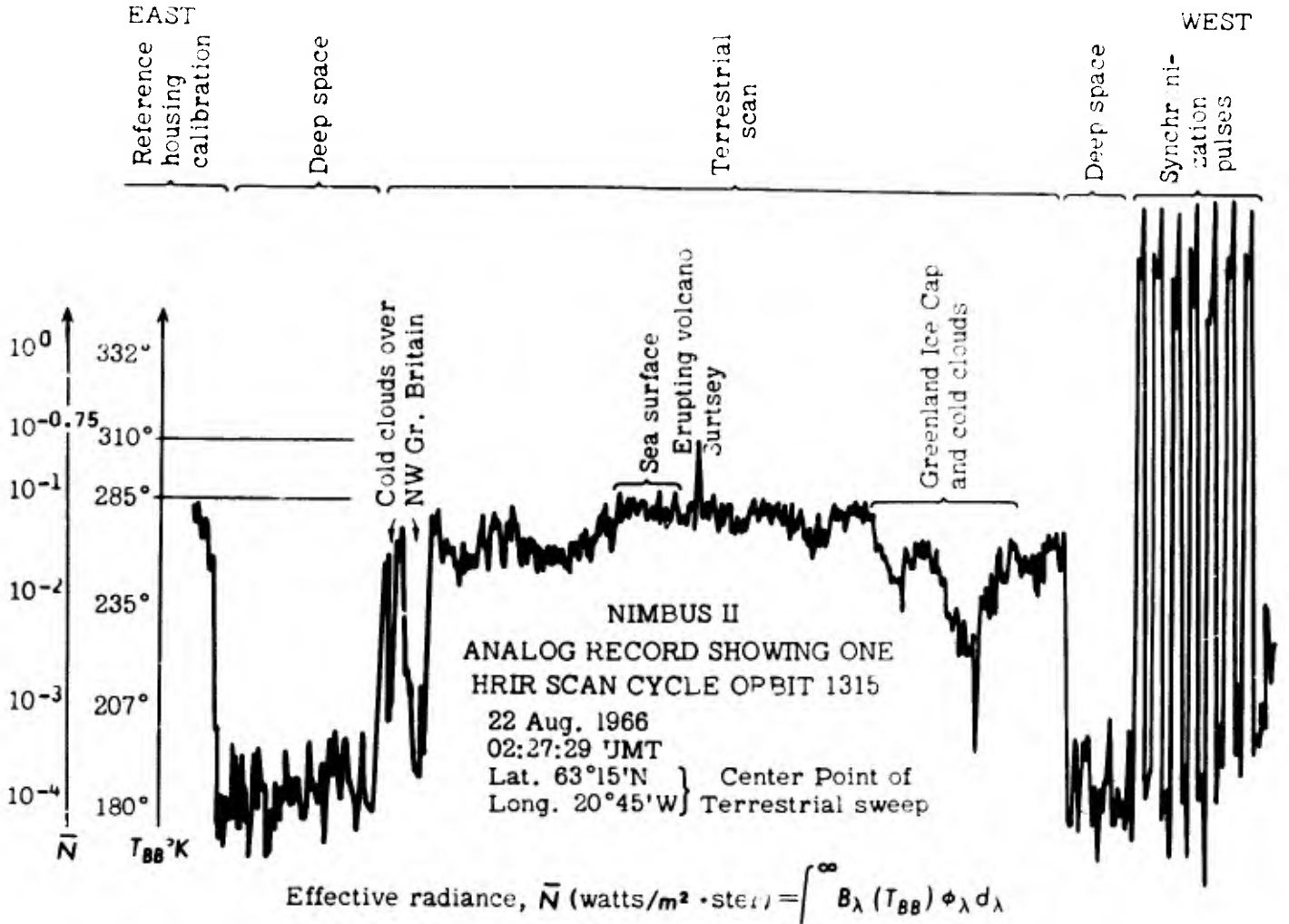


Effective radiance, $\bar{N}$ (watts/$m^2$ · ste.) $= \int_0^\infty B_\lambda (T_{BB})\, \phi_\lambda\, d_\lambda$

Where $B_\lambda$ = Planck function $T_{BB}$ = Equivalent blackbody Temperature in °K $\phi_\lambda$ = Effective spectral response (about 3.4 to 4.1$\mu$)

**Figure-12b) Nimbus-2 HRIR analog record, Orbit 1315, 22 August 1966, 02:27:29 GMT showing 310°K $T_{BB}$ spike over the Surtsey Volcano, Iceland.**

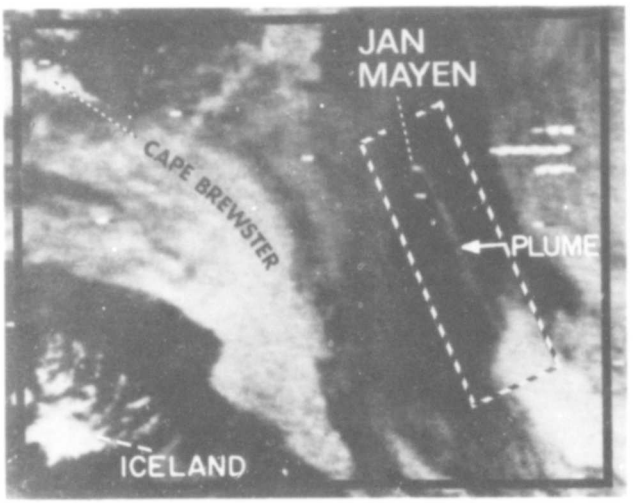


Figure 13 - **The eruption of the Beerenberg volcano on Jan Mayen Island at noon 21 September 1970 as recorded by Nimbus-4 IDCS.**
**(Allied Research Associates)**

ASH PLUME FROM BEERENBERG VOLCANO

This new eruption of the Beerenberg Volcano on Jan Mayen Island was first observed on the night of 20 September 1970. By noon on 21 September, when this Nimbus 4 IDCS picture was taken, the ash plume (within the rectangular area) extended more than 200 miles to the southeast.

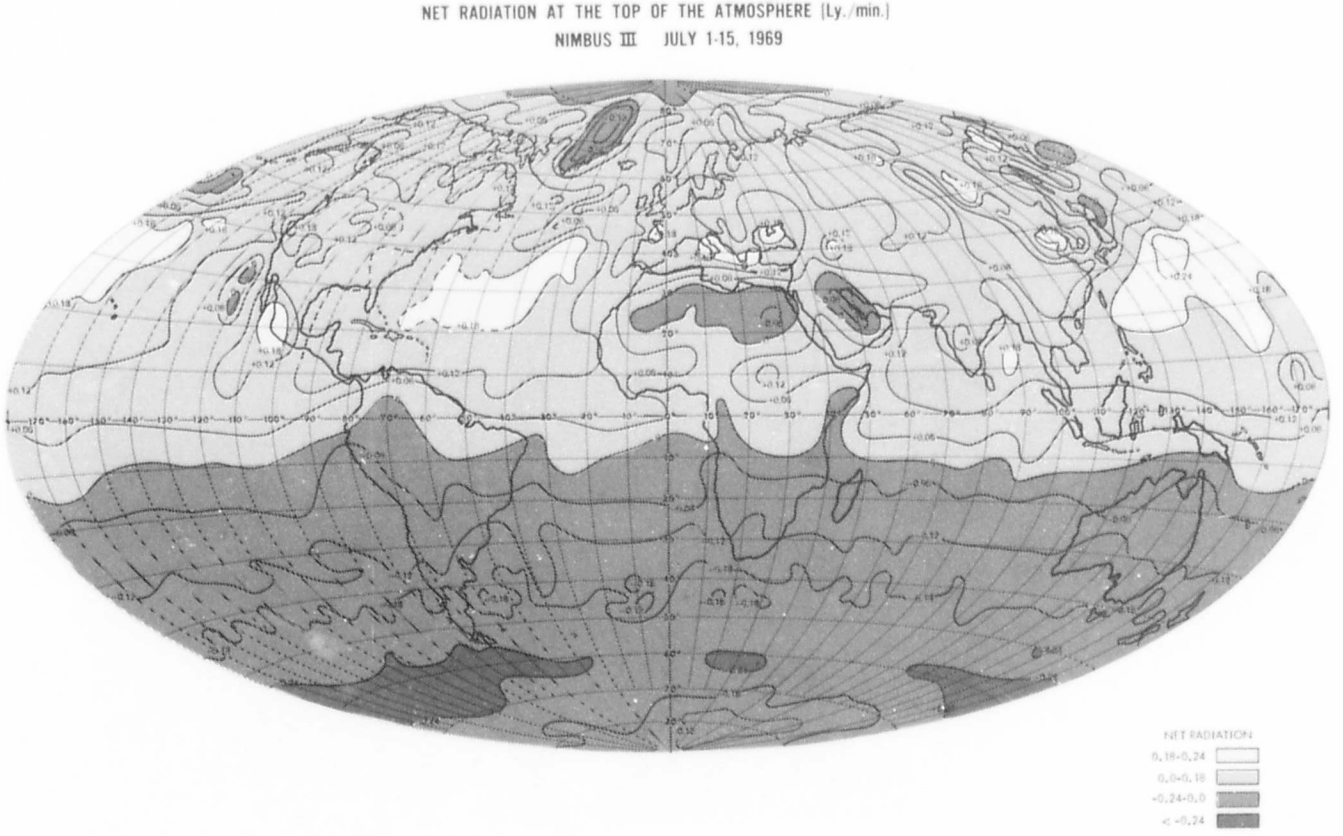


Figure 14 - Net radiation at the top of the atmosphere (ly ./mn), Nimbus 3, July 1-15, 1969.

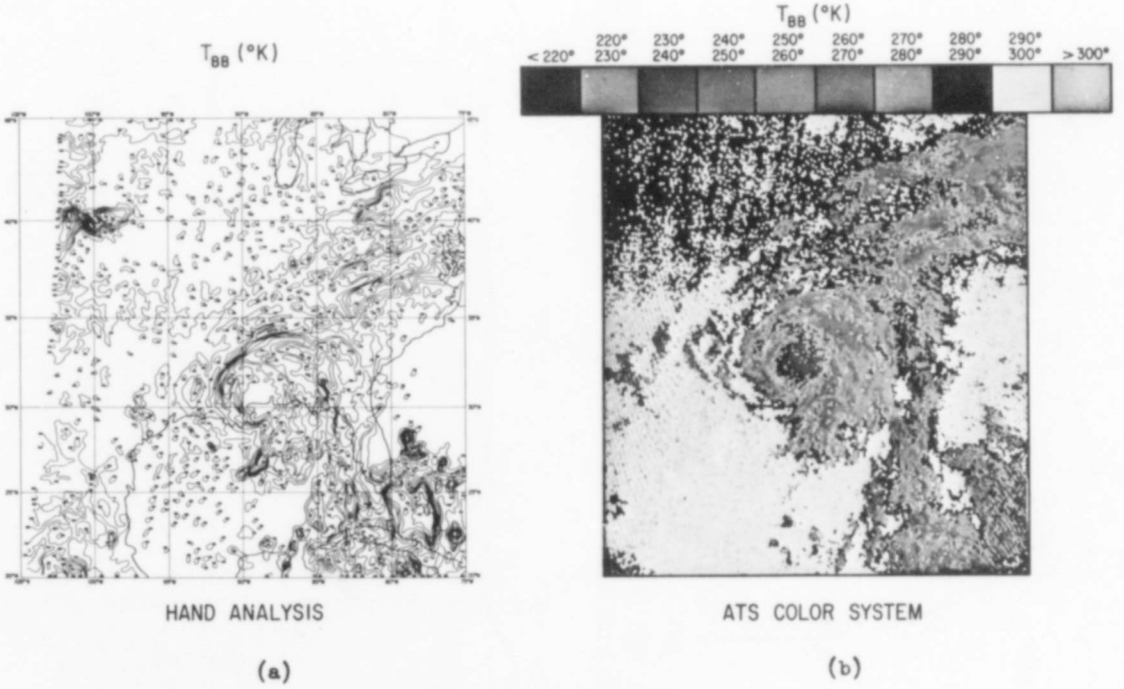


HURRICANE CAMILLE
NIMBUS III HRIR
AUGUST 18, 1969

Figure 15 - a) Nimbus-3 HRIR, orbit 1695, hand analysis of grid-print map, August 18, 1969 ($T_{BB}$ °K).
b) Nimbus-3 HRIR, orbit 1695, color analysis by the ATS ground station process.

# INTERROGATION, RECORDING, AND LOCATION SYSTEM (IRLS)

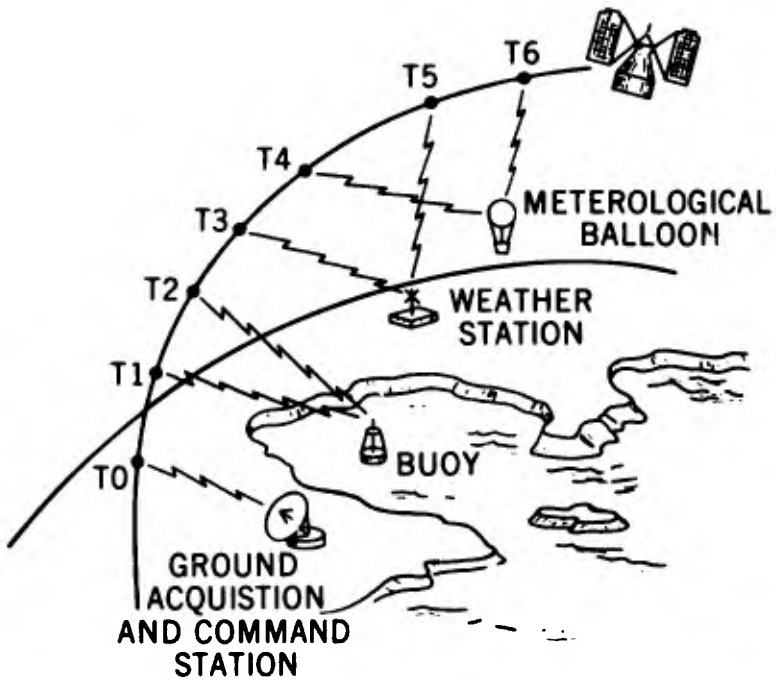


Figure 16 - Interrogation Recording and Location System (IRLS) Nimbus-3 system concept.

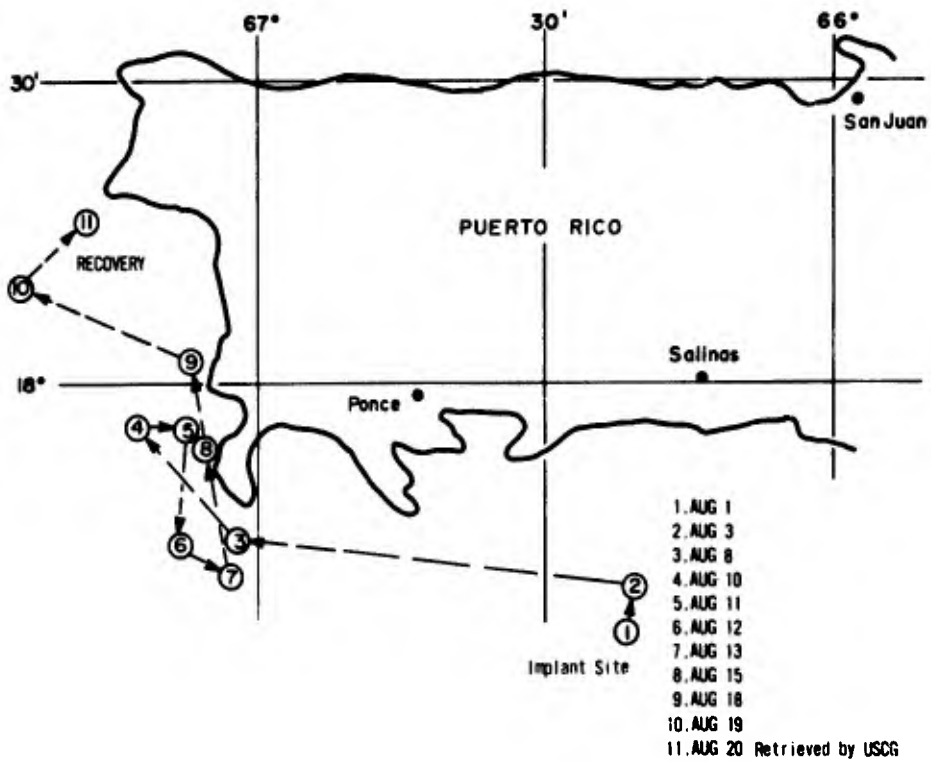


Figure 17 - Nimbus-3 IRLS tracking data for free drifting buoy.

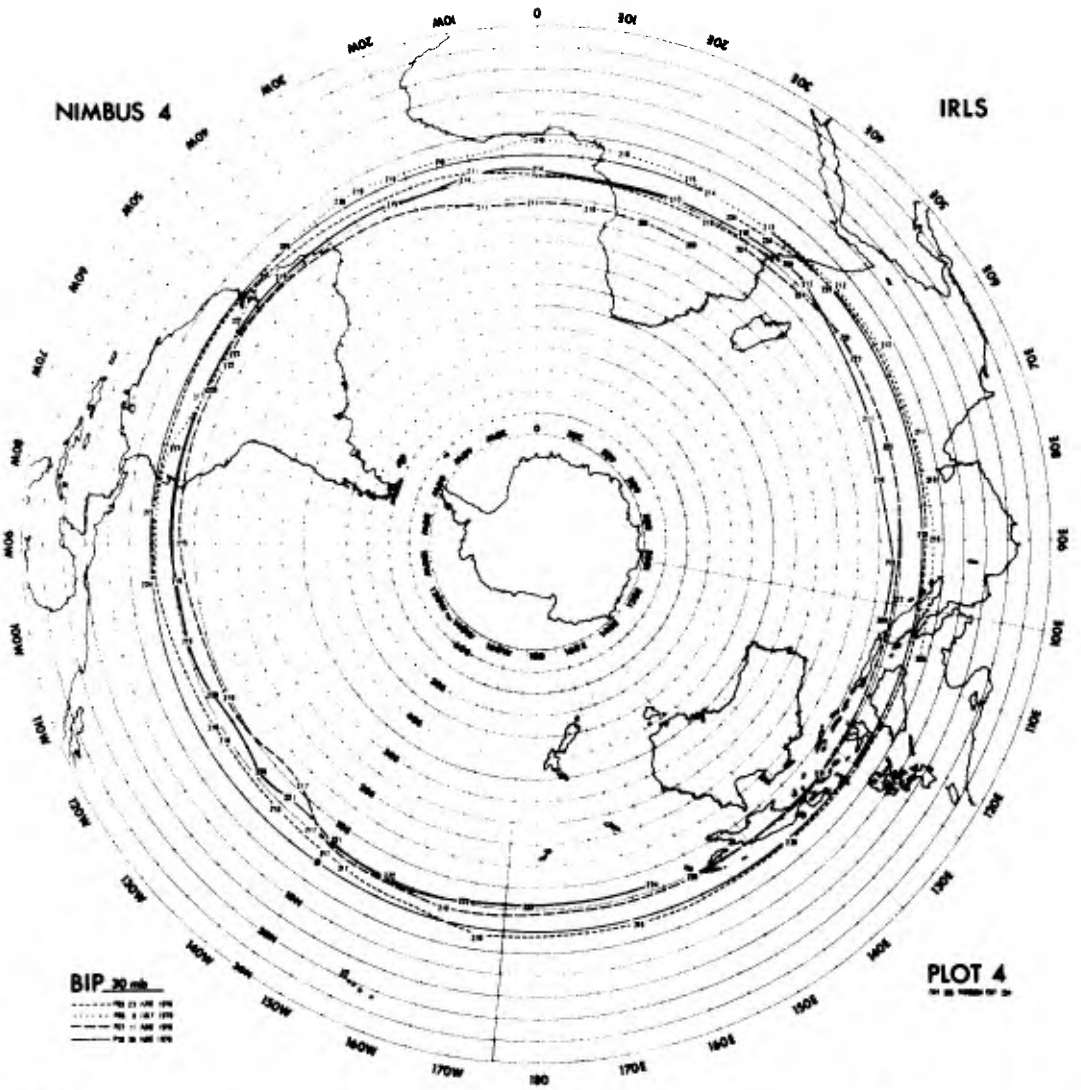


Figure 18 - Plot of balloon instrument-package tracked by Nimbus-4 IRLS at the 30-mb level.

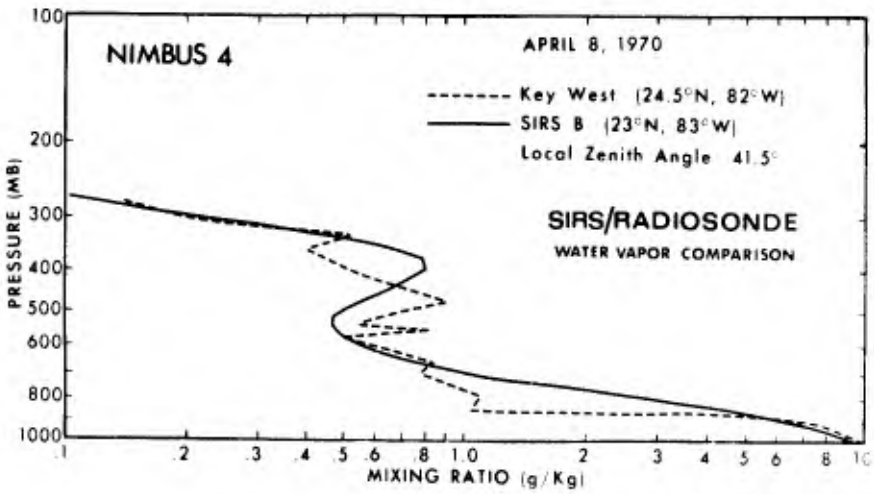


Figure 19 - Nimbus-4, SIRS-B/Radiosonde Comparison of Mixing Ratio (g/Kg) on 8 April 1970 over Key West, Florida.

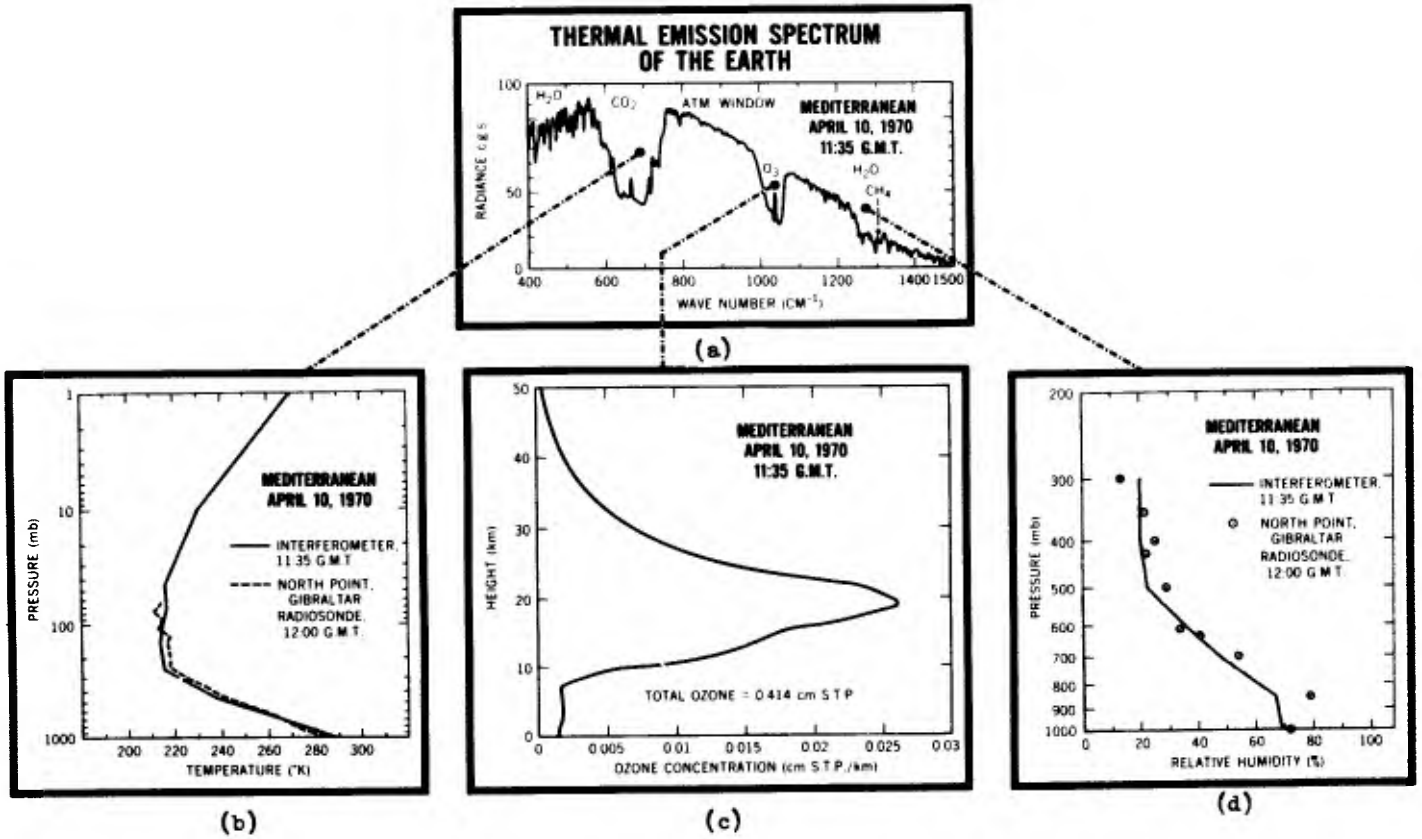


**Figure 20 - a)** Thermal-emission spectrum of the earth (Mediterranean area) Nimbus-4, IRIS, Orbit 29, 10 April 1970.

**b)** Comparison of Gibraltar radiosonde temperature-profile and Nimbus-4 IRIS temperature profile, orbit 29, 10 April 1970

**c)** Vertical profile of ozone concentration over the Mediterranean Sea, Nimbus 4, IRIS orbit 29, 10 April 1970

**d)** Comparison of Gibraltar radiosonde relative-humidity profile of Nimbus-4 IRIS relative-humidity profile, Orbit 29, 10 April 1970.

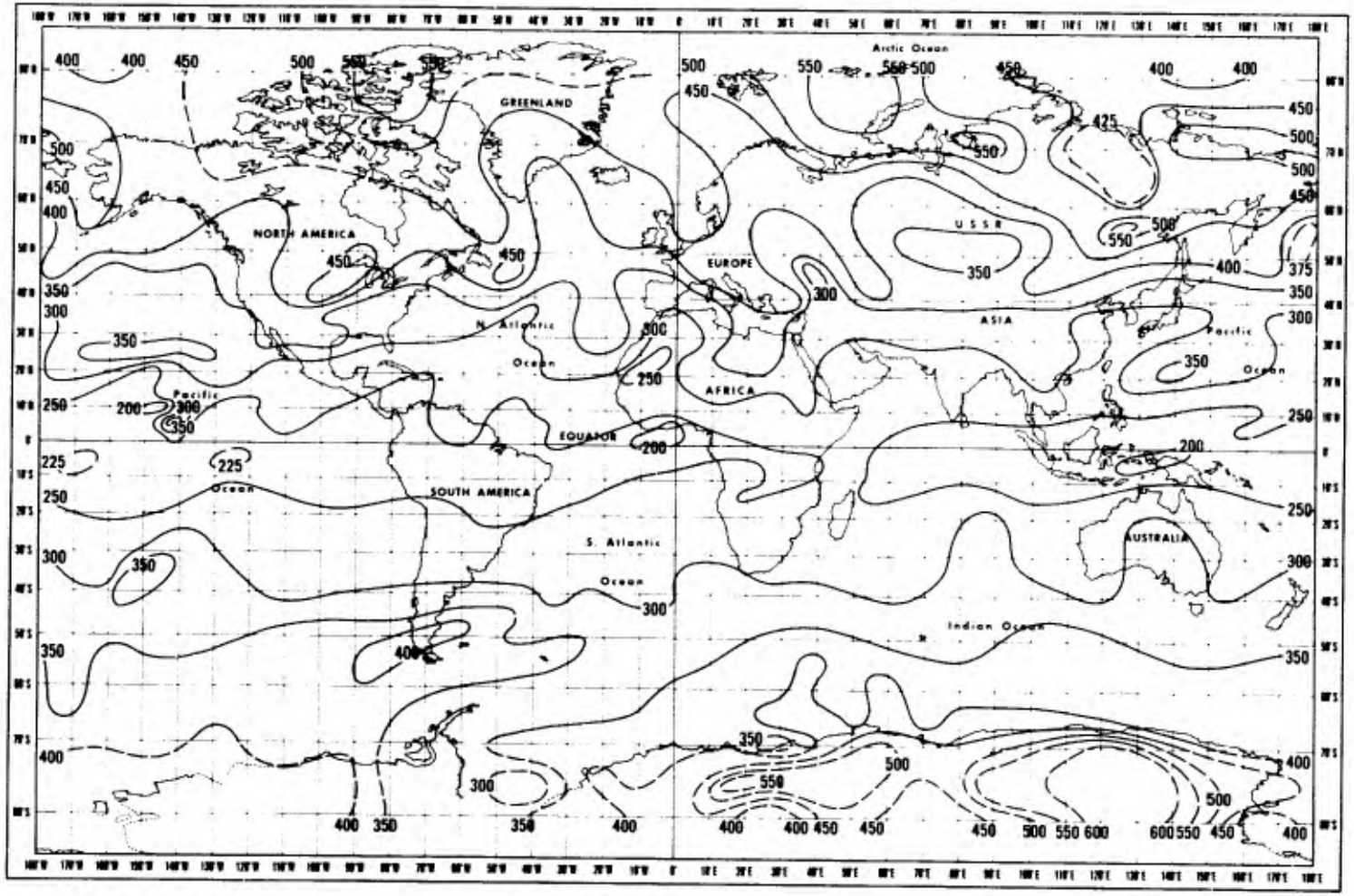


Figure 21 - Total ozone content ($10^{-3}$ cm STP), Nimbus 3 IRIS, 27 April 1969.

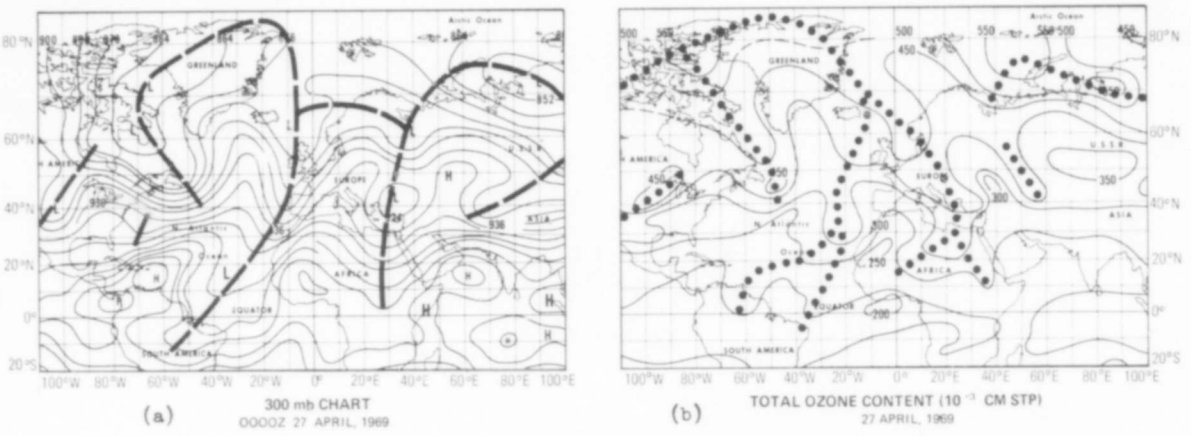


Figure 22 - a) 300-mb chart, 0000 GMT, 27 April 1969 (dashed lines indicate trough positions).
b) Nimbus-3, IRIS total ozone content ($10^{-3}$ cm STP), 27 April 1969 (dotted lines indicate areas of increased ozone content).

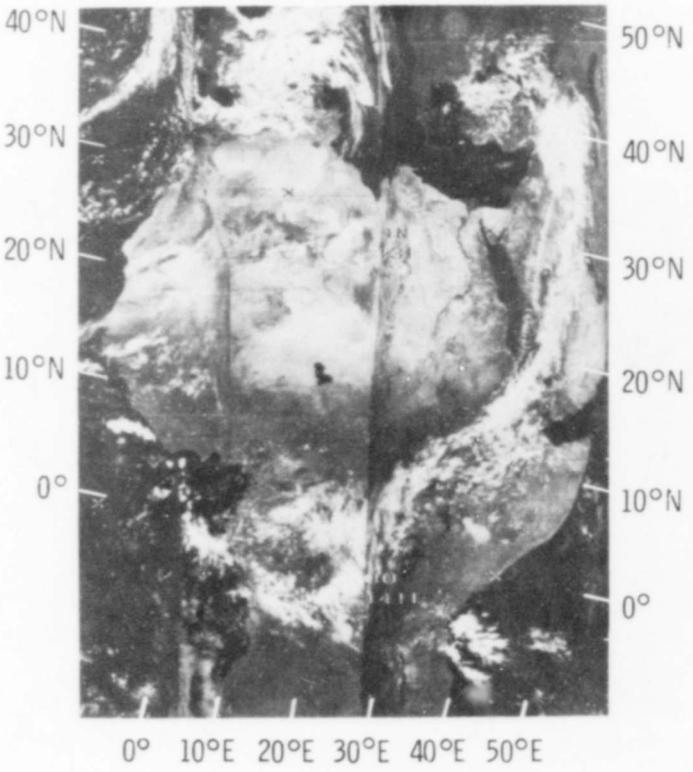


Figure 23 - Nimbus-3, HRIR (day) orbits 202, 203, 204, 29 April 1969 showing the cloudiness related to a "full latitude wave" extending from central Africa, northward to Saudi Arabia and Turkey.

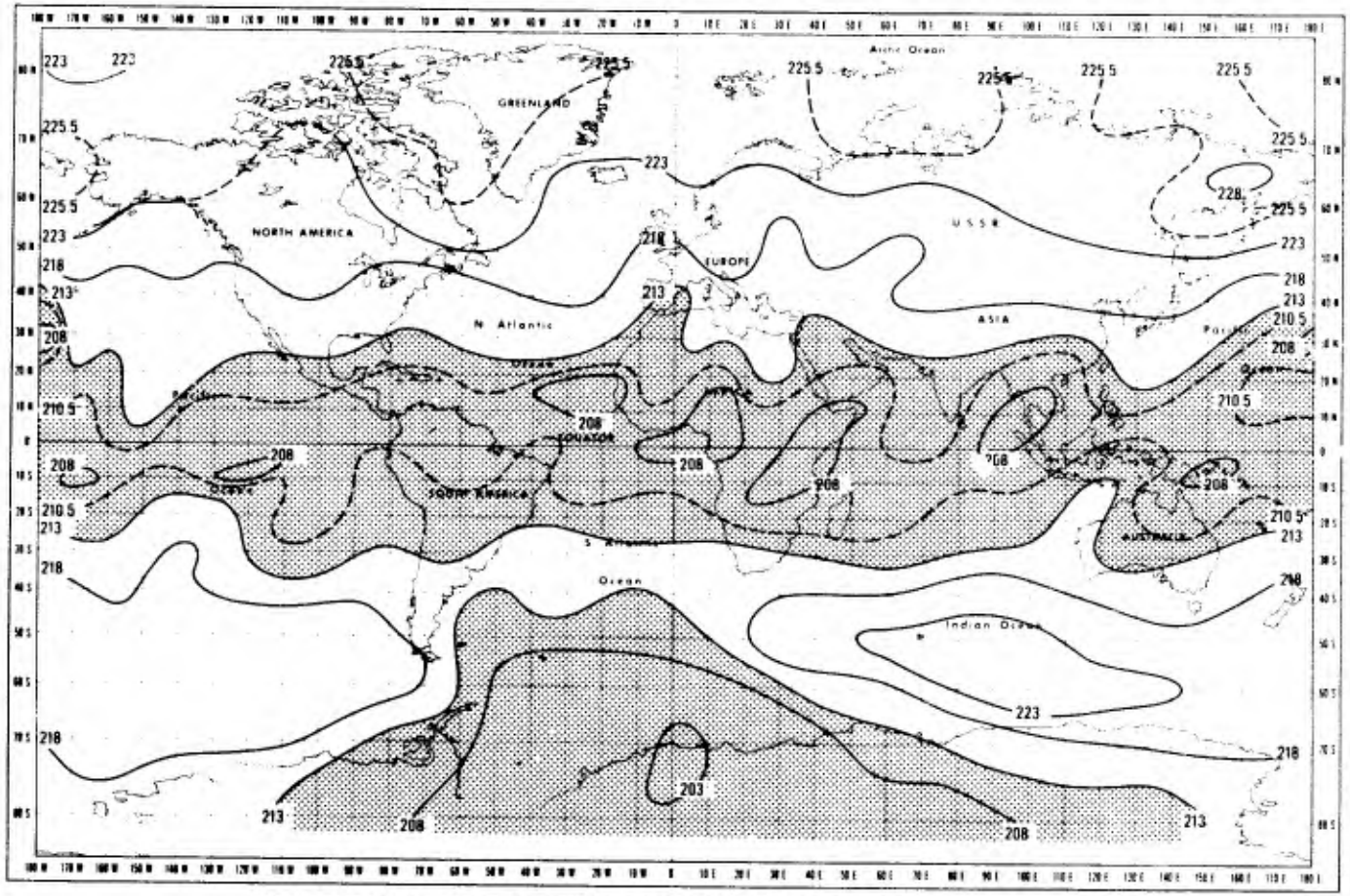


50 MB TEMPERATURES (°K) NIMBUS III IRIS APRIL 27, 1969

**Figure 24 - 50-mb temperatures as derived from Nimbus-3, IRIS data, April 27, 1969**

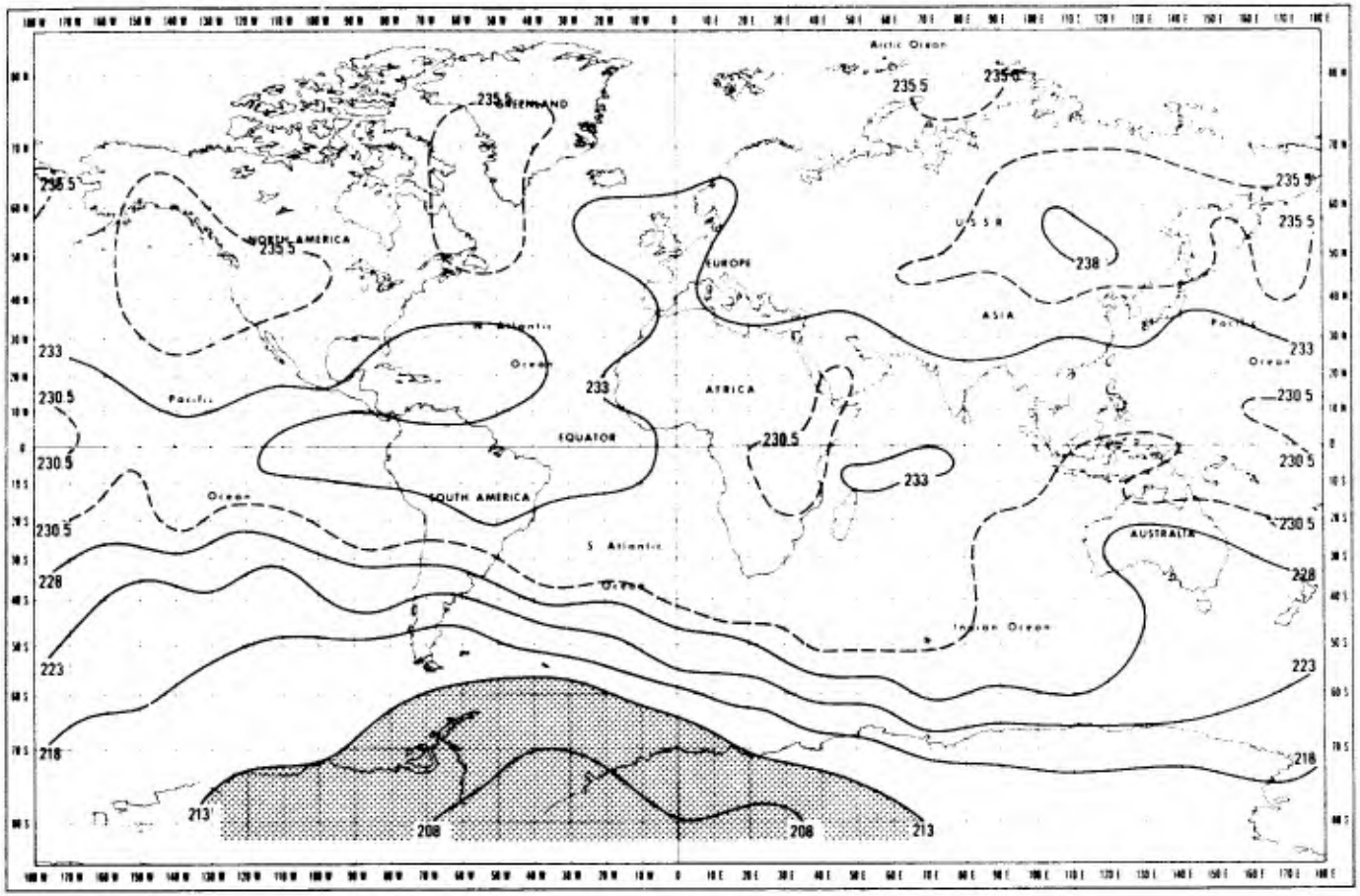


**Figure 25 - 10-mb temperatures as derived from Nimbus-3 IRIS data, April 27, 1969**

# AUTOMATED PRODUCTION OF GLOBAL CLOUD-CLIMATOLOGY BASED ON SATELLITE DATA

Donald B. Miller, Major - USAF

USAF Environmental Technical Applications Center
Washington, D. C.

## Abstract

The mesoscale archive of satellite brightness data may be converted into daily estimates of total cloud amount ($N_s$) using the automated technique described. The method applies empirical weights to the frequencies of five relative brightness classes according to their relative contribution to total cloud cover. The cloud amounts are reckoned over a square 40km on side which is an area comparable to that viewed by the conventional surface observation of total sky cover ($N_t$).

Several comparisons between $N_s$ and $N_t$ values are made in order to show the relation between satellite derived climatological values and conventional observations.

The system for processing the existing archive of mesoscale brightness data (since January 1967) into a climatology of global $N_s$ values is illustrated. Products to be derived from the climatology are also described and illustrated.

## INTRODUCTION

The mesoscale archive of satellite television data represents a valuable source of information about the cloudiness of the earth. To be most useful, the distribution of brightness values contained in this archive should be converted to a conventional measure such as cloud "cover" or "amount." Total sky cover ($N_t$) as estimated by a surface observer in octas or tenths is the standard meteorological measure of cloudiness. The mesoscale satellite-data area (about 40km on a side) approximates that viewed by a surface observer. The establishment of an estimate of total cloud amount from satellite data ($N_s$) permits the use of the existing three years of mesoscale ESSA-vidicon data as a climatological data-base. The mesoscale data provides some 400,000 daily estimates of cloud amount for the entire earth, compared to only about 7,500 estimates based on conventional observations. Leese, et al, (11), Salomonson (18), and Moller and Raschke (15), have critically examined recent work on estimating cloud amounts from satellite data and Crowe (8) is preparing a comprehensive review of the literature. Previous efforts to reduce satellite-derived cloud amounts to climatological information utilized either the daily hand-drawn nephanalyses prepared by the National Environmental Satellite Center (7, 17, 9), or other subjective methods (21, 1). Except for human bias and error (22), a careful subjective analysis represents a good estimate of cloud amount from satellite observations. However, because of the enormous volume of satellite data, it is uneconomical to enlist an army of analysts to reduce pictorial-brightness data to estimates of cloud amount. An automated technique for estimating total cloud amounts from satellite data and the compilation of these estimates into a climatology are described herein.

The mesoscale archive and products of digitized video data from ESSA satellites are described by Booth and Taylor (2, 3). The brightness data which makes up the original full-resolution population are "brightness normalized" (19) for camera-system nonlinearities and inequalities in solar illumination. The mesoscale data array is produced by reducing full-resolution mapped arrays (5, 6). Each resulting mesoscale spot represents an 8x8 block of full-resolution data; its area is 1/64th of an NWP grid square (see Fig. 1). The original relative-brightness range of 15 values is divided into 5 equal classes and a frequency count is made of each class from the original 64-spot population. These 5-class "histograms" comprise the daily mesoscale archive.

The mesoscale archive preserves a measure of the population of brightness values and their distribution through the 5-class frequency counts. These histograms reflect the integrated earth-cloud scene as sensed by the vidicon system over the 40km squares. To estimate total-cloud amount automatically, using the 5-class histograms, a procedure which simulates visual methods of estimation was developed (15). A "probalistic" or weighting scheme is used to weight each of the 5-classes according to their most likely contribution to the estimate of total-cloud amount. The weighting scheme was derived empirically by comparing $N_s$ values with visual estimates from pictures and by comparing $N_s$ values with surface observations ($N_t$). The $N_s$ and $N_t$ values were compared over ocean areas unaffected by sunglint and over land areas unaffected by ice, snow or sand reflections. The empirical phase of the study derived or "tuned" the weights until reasonable results began to appear. The weights which provide good cloud amount estimates from ESSA 7 and ESSA 9 data are listed in Table 1.

Table 1

| Original Brightness-Range | Class | Contribution to Total-Cloud Amount | Weights (ESSA 7 and 9) |
|---|---|---|---|
| 0, 1, 2 | 1 | 0% | 0 |
| 3, 4, 5 | 2 | 25% | 2 |
| 6, 7, 8 | 3 | 88% | 7 |
| 9,10,11 | 4 | 100% | 8 |
| 12,13,14 | 5 | 100% | 8 |

The brightness values in class 1 most likely are not due to clouds, therefore, this class is given a weight of 0 percent in the counting scheme. Brightness values in class 2 may be partly due to clouds and partly due to background. This is the "gray" area of the cloud-no-cloud decision. The empirical evidence suggests that 25 percent of the frequencies of class 2 can be due to clouds. Class 3 is a brightness range in which 88 percent of the values are due to clouds. Brightness values in classes 4 and 5 are most likely due entirely to clouds, therefore they are counted as being 100 percent due to clouds.

With the preceding assumptions, the total-cloud amount of a mesoscale square ($N_s$) can be derived from the brightness class frequencies by the equation:

$$N_s = \sum_{i=1}^{5} W_i f_i / 64 \qquad (1)$$

Where:

$N_s$ are the total cloud amounts (octas)

$f_i$ are the frequencies of the 5 brightness-value classes

$W_i$ are the weights in Table 1

Figure 3 illustrates the results of applying Equation (1) to the satellite data for April 15, 1969.

The mesoscale archive and products of digitized video data from ESSA satellites are described by Booth and Taylor (2, 3). The brightness data which makes up the original full-resolution population are "brightness normalized" (19) for camera-system nonlinearities and inequalities in solar illumination. The mesoscale data array is produced by reducing full-resolution mapped arrays (5, 6). Each resulting mesoscale spot represents an 8x8 block of full-resolution data; its area is 1/64th of an NWP grid square (see Fig. 1). The original relative-brightness range of 15 values is divided into 5 equal classes and a frequency count is made of each class from the original 64-spot population. These 5-class "histograms" comprise the daily mesoscale archive.

The mesoscale archive preserves a measure of the population of brightness values and their distribution through the 5-class frequency counts. These histograms reflect the integrated earth-cloud scene as sensed by the vidicon system over the 40km squares. To estimate total-cloud amount automatically, using the 5-class histograms, a procedure which simulates visual methods of estimation was developed (15). A "probalistic" or weighting scheme is used to weight each of the 5-classes according to their most likely contribution to the estimate of total-cloud amount. The weighting scheme was derived empirically by comparing $N_s$ values with visual estimates from pictures and by comparing $N_s$ values with surface observations ($N_t$). The $N_s$ and $N_t$ values were compared over ocean areas unaffected by sunglint and over land areas unaffected by ice, snow or sand reflections. The empirical phase of the study derived or "tuned" the weights until reasonable results began to appear. The weights which provide good cloud amount estimates from ESSA 7 and ESSA 9 data are listed in Table 1.

Table 1

| Original Brightness-Range | Class | Contribution to Total-Cloud Amount | Weights (ESSA 7 and 9) |
|---|---|---|---|
| 0, 1, 2 | 1 | 0% | 0 |
| 3, 4, 5 | 2 | 25% | 2 |
| 6, 7, 8 | 3 | 88% | 7 |
| 9,10,11 | 4 | 100% | 8 |
| 12,13,14 | 5 | 100% | 8 |

The brightness values in class 1 most likely are not due to clouds, therefore, this class is given a weight of 0 percent in the counting scheme. Brightness values in class 2 may be partly due to clouds and partly due to background. This is the "gray" area of the cloud-no-cloud decision. The empirical evidence suggests that 25 percent of the frequencies of class 2 can be due to clouds. Class 3 is a brightness range in which 88 percent of the values are due to clouds. Brightness values in classes 4 and 5 are most likely due entirely to clouds, therefore they are counted as being 100 percent due to clouds.

With the preceding assumptions, the total-cloud amount of a mesoscale square ($N_s$) can be derived from the brightness class frequencies by the equation:

$$N_s = \sum_{i=1}^{5} W_i f_i / 64 \qquad (1)$$

Where:

$N_s$ are the total cloud amounts (octas)

$f_i$ are the frequencies of the 5 brightness-value classes

$W_i$ are the weights in Table 1

Figure 3 illustrates the results of applying Equation (1) to the satellite data for April 15, 1969.

## THE BACKGROUND-BRIGHTNESS PROBLEM

The technique of minimizing the effects of cloudiness by constructing composite minimum-brightness charts is described by Booth and Taylor (2, 3). By saving only the minimum response at each mesoscale spot for a selected number of days, the permanent or background brightness is retained. McClain and Baker (10) have used composite minimum charts to delineate the snow line over the North American Continent. Miller (12, 13) discusses the applications of composite minimums for estimation of background-brightness fields. To isolate the brightness due to reflections from ice, snow and sand, the minimum values of daily cloud amounts for a multiday period are retained. This multiday composite minimum ($C_m$) field represents residual or background-brightness measured in units of cloud amount. Subtracting the $C_m$ field from the daily fields of $N_s$ ($N_s - C_m = N_s^*$) leaves values which are due to clouds alone ($N_s^*$). In the summer and winter months, 30-day composite minimum values suffice to estimate the background. In spring and fall, shorter and selected periods of 5- or 10-day minima may be used to account for rapid snow fall or snow melt as the seasons change. Figures 2a and 2b show the results of subtracting the 30-day $C_m$ values for April 1969 from the $N_s$ field of April 15, 1969.

Ice, snow and clouds appear equally "bright" in the satellite-brightness data. There is little hope of recovering cloud amounts over large expanses of snow and ice. The $C_m$ fields can be used to indicate those permanent areas of background brightness over which cloud amounts cannot be retrieved. Figure 4 shows the mean cloudiness for January 1969 with the black areas over the continents superimposed from the January 30-day minimum composite. The shades of gray in the picture reflect increasing mean-cloud amount from black (clear) to 8 octas (white) except in the black areas over the continents where the permanent background features have been masked out by the black shading.

The desert sands and other highly reflective terrain features do show a lesser brightness response in the vidicon data than do clouds. Differences between $C_m$ values due to sand and daily $N_s$ values should provide good estimates of cloudiness over the deserts. Note how the cloud band over Egypt in Fig. 2a remains in Fig. 2b after the 30-day $C_m$ values are subtracted. Experimentation with solutions to the problem of extracting useful cloud-amount estimates over desert areas is continuing.

## COMPARISON OF $N_s$ and $N_t$ VALUES

The ESSA series of satellites view mainland China within plus or minus 2 hours of 0600 GMT each day. The area bounded by approximately 20N to 50N latitudes and 95E to 130E longitudes contains some 400 weather stations which provide synoptic observations. These observations have been indexed relative to 1/8 NWP grid mesh (14). Comparisons between $N_s$ and $N_t$ values have been made on a point to point, eighth for eighth basis.

The comparison procedure compares the 0600 GMT $N_t$ value at a 1/8 NWP grid point with the $N_s$ value derived from the satellite data. To minimize time-differences and gridding errors in the satellite data, a "best of five" matching procedure is used to select the $N_s$ value for the comparison. Each $N_t$ value is compared with the $N_s$ value at its grid-point location and with each $N_s$ value at adjacent mesoscale locations up and down, left and right in the grid system. This is a nominal 20km "search" around the $N_t$ grid point for the $N_s$ value which best matches the reported total-cloud amount. Figures 5a and 5b illustrate the statistics derived from the $N_s$ and $N_t$ "best of five" comparisons.

The statistics indicate that $N_s$ values underestimate the low-cloud amounts because the vidicon camera system cannot "sense" small amounts of small cumulus. Similarly the vidicon cannot detect thin cirrus as evidenced by the comparisons made with cirrus and without cirrus being reported by the surface observer. Table 2 is a contingency table for comparison of $N_s$ and $N_t$ values for April 1969 over China. Along the diagonal $N_t = N_s$ 50% of the cases and $N_t$ compared within $\pm$ 1 octa 73% of the time.

Table 2

| $N_t$ \ $N_s$ | 0 | 1 | 2 | 3 | 4 | 5 | 6 | 7 | 8 | Total ($N_t$) |
|---|---|---|---|---|---|---|---|---|---|---|
| 0 | 793 | 94 | 58 | 2 | 0 | 1 | 1 | 0 | 0 | 949 |
| 1 | 366 | 352 | 50 | 5 | 2 | 0 | 0 | 0 | 0 | 775 |
| 2 | 160 | 154 | 217 | 32 | 3 | 7 | 1 | 1 | 0 | 575 |
| 3 | 49 | 56 | 88 | 69 | 17 | 2 | 1 | 1 | 0 | 283 |
| 4 | 27 | 31 | 33 | 27 | 28 | 10 | 3 | 1 | 0 | 160 |
| 5 | 32 | 46 | 47 | 23 | 37 | 49 | 28 | 5 | 0 | 267 |
| 6 | 65 | 65 | 138 | 66 | 44 | 85 | 130 | 33 | 2 | 628 |
| 7 | 60 | 117 | 229 | 172 | 177 | 205 | 288 | 889 | 78 | 2215 |
| 8 | 43 | 40 | 73 | 63 | 72 | 74 | 111 | 569 | 1734 | 2779 |
| Total ($N_s$) | 1595 | 955 | 933 | 459 | 380 | 433 | 563 | 1499 | 1814 | 8631 |

$N_t = N_s$: 50%  $Nt = \pm 1/8\ N_s$: 73%

April 1969

Figure 6 depicts comparisons of $N_s$ and $N_t$ for April 1967, 1968, and 1969 with a 3 year average by percentage frequencies of each octa of total cloud amount. The area of comparison is again mainland China. The $N_s$ values account for about 10% less of the 8 octas coverage and about 10% more 0 octas coverage than conventional surface observations. Part of the difference is due to the surface observer's tendency to overestimate cloud amounts and part of the difference is due to the inability of the satellite's television camera to "see" all the clouds. It is encouraging to note that the shapes of the distributions are quite similar. These preliminary comparisons indicate that there is a good, practical agreement between $N_s$ and $N_t$. The automated $N_s$ values are at least as good as those which can be derived by eye from satellite pictures.

## AUTOMATED PRODUCTION OF SATELLITE CLOUD-AMOUNT CLIMATOLOGY

Figure 7 diagrams the system which is in progress for processing the available record (January 1967 to the present) of mesoscale satellite data for a climatology of total-cloud amount. Daily (about 1400 local time) total-cloud amount values are derived for every 40km square on the sunlit portion of the earth. Fig. 8 depicts the current status of the climatology program.

Data for March and April 1967 through 1970 representing the frequency of occurrence of $N_s$ values of 2 octas or less were provided the Weather Bureau's Space Flight Section for planning the splashdown for Apollo 13. The satellite data agreed well with the limited conventional climatology for the remote splashdown site. Fig. 9 is a 30-day mean cloud amount for June 1969 (background included) with octas represented by the gray scale as indicated. The whitest area around the pole and over Greenland and Northern Canada is snow. The sands of Arabian and Sahara Deserts also appear as bright as clouds. Fig. 10 portrays histograms of the frequency of $N_s$ values around Washington, D. C. in May of 1969. Washington is the middle histogram and the surrounding histograms are for the adjacent 40km squares (north is at the top). The histograms verify the fact that spring is a nice time to visit our capitol. This type of histogram can be produced by months and by multiyear summaries by month for every 40km square on the earth. Fig. 11 is a display of percent frequency of scattered (0-2 octas) cloudiness over Southeast Asia.

## ACKNOWLEDGMENTS

Mr. A. L. Booth, NESC, prepared the initial computer programs (4) which have since been modified and adapted by Capt. R. Feddes, ETAC. CMSgt. R. Miller assisted in the selection of the weights and the initial evaluation of the automated cloud amount computations. TSgt. L. Rockwood and SSgt. P. Wagner manage the submission of the computer jobs and manage the hundreds of magnetic tapes. TSgt. D. Grage and SSgt. P. Wagner prepared the figures. The entire project is conducted with the full cooperation of Mr. C. L. Bristor, Chief of the Data Processing and Analysis Division of the National Environmental Satellite Center, whose many services are gratefully acknowledged.

## References

1. Barnes, J. C. and Chang, D., "Accurate Cloud Cover Determination and Its Effects on Albedo Computations," Final Report, Contract No. NAS5-10478, Allied Research Assoc., Concord, Massachusetts, 1969.

2. Booth, A. L. and Taylor, V. R., "Mesoscale Archive and Products of Digitized Video Data from ESSA Satellites, "ESSA Technical Memorandum NESC TM-9, National Environmental Satellite Center, Washington, D. C., 1968.

3. Booth, A. L. and Taylor, V. R., "Mesoscale Archive and Computer Products of Digitized Video Data from ESSA Satellites," Bull. Amer. Meteor. Soc., 50, 431-438, 1969.

4. Booth, A. L., "AVCS Total Cloud Amount Software Package," Programmer Note 134, Unpublished Manuscript, National Environmental Satellite Center, Washington, D. C., 1970.

5. Bristor, C. L., "Computer Processing of Satellite Cloud Pictures," ESSA Technical Memorandum NESC TM-3, National Environmental Satellite Center, Washington, D. C., 1968.

6. Bristor, C. L., Callicott, W. M. and Bradford, R. E., "Operational Processing of Satellite Pictures by Computer," Monthly Weather Review, 94, 515-527, 1966.

7. Clapp, P. F., "Northern Hemisphere Cloud Cover for Selected Late Fall Seasons Using TIROS Nephanalyses," ESSA Technical Memorandum WBTM NMC 44, National Meteorological Center, Washington, D. C., 1968.

8. Crowe, M., "Cloud Cover Determination from Satellites," Manuscript in preparation. National Environmental Satellite Center, Washington, D. C., 1970.

9. Godshall, F. A., Allison, L. J., Kreins, F. R. and Warnecke, G., "Examples of the Usefulness of Satellite Data in General Atmospheric Research - Part II, "An Atlas of Average Cloud Cover Over the Tropical Pacific Ocean, NASA TR G-958, Goddard Space Flight Center, Greenbelt, Maryland, 1969.

10. McClain, E. P., and Baker, D. R., "Experimental Large Scale Snow and Ice Mapping with Composite Minimum Brightness Charts," ESSA Technical Memorandum, NESC TM-12, National Environmental Satellite Center, Washington, D. C., 1969.

11. Leese, J. A., Booth, A. L. and Godshall, F. A., "Archiving and Climatological Applications of Meteorological Satellite Data," working paper for WMO Commission for Climatology. (To be published as a WMO Tech. Report.)

12. Miller, D. B., "The Background Brightness Problem," Unpublished Manuscript. USAF Environmental Technical Applications Center, Washington, D. C., 5 pp. 1969.

13. Miller, D. B., "A Method for Estimating Total Cloud Amount from Full Resolution, 63 Brightness Scale Mapped Satellite Data," Unpublished Manuscript, USAF Environmental Technical Applications Center, Washington, D. C., 8 pp. 1970.

14. Miller, D. B., McCollum, R. D., and O'Reilly, P. J., "Satellite Versus Surface Estimates of Total Cloud Cover," in preparation, USAF Environmental Technical Applications Center, Washington, D. C., 1970.

15. Miller, D. B., Booth, A. L., and Miller, R. E., "An Automated Method of Estimating Total Cloud Amount from Mesoscale Satellite Data," Extended Abstracts, Symposium on Tropical Meteorology, Univ. of Hawaii, 1970.

16. Moller, F. and Raschke, E., "Problems of Meteorological Observations from Satellites," Space Sc. Review, 9, 90-148, 1969.

17. Sadler, J. C., "Average Cloudiness in the Tropics from Satellite Observations," East West Center Press, Honolulu, Hawaii, 1968.

18. Salomonson, V. V., "Cloud Statistics in Earth Resources Technology Satellite (ERTS) Mission Planning," Preprint X0622-69-386. Goddard Space Flight Center, NASA, Greenbelt, Maryland, 1969.

19. Schwalb, A. and Gross, J., "Vidicon Data Limitations," ESSA Technical Memorandum, NESC TM-17, 22 pp., 1969.

20. Sherr, P. E., Glaser, A. H., Barnes, J. C., and Willand, J. H., "World-Wide Cloud Cover Distributions for Use in Computer Simulations," NASA Contract Report NASA CR-61226, Contract No. NAS 8-21040, Allied Research Assoc., Inc., Concord, Massachusetts, 140 pp., 1968.

21. Young, M. J., "Variability in Estimating Total Cloud Cover from Satellite Pictures," J. Appl. Meteor., 6, 573-579, 1967.

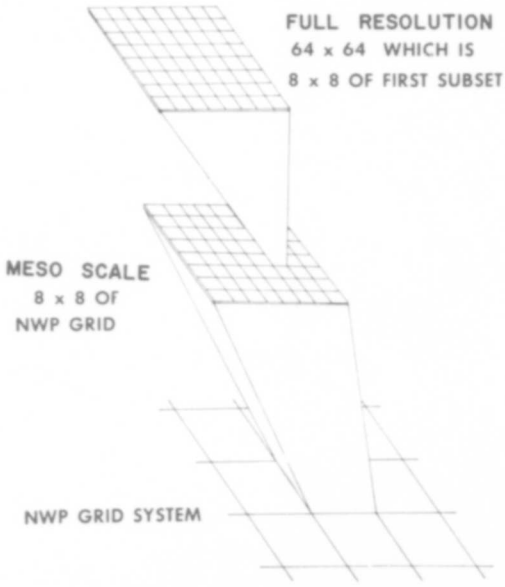


FIG. 1. RELATIONSHIPS BETWEEN THE FULL-RESOLUTION, MESOSCALE AND NWP SPATIAL RESOLUTIONS ARE SHOWN ABOVE. THE MESOSCALE ARCHIVE CONSISTS OF HISTOGRAMS IN 5 CLASSES OF THE ORIGNAL 0-14 RELATIVE-BRIGHTNESS RANGE. THE HISTOGRAMS ARE DERIVED FROM THE 8X8 "BOX" (64 VALUES) OF THE ORIGINAL FULL-RESOLUTION VIDEO DATA.

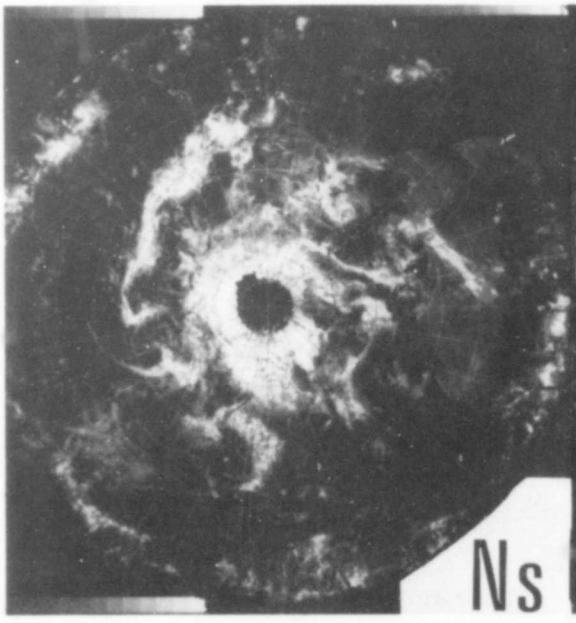


APRIL 15, 1969

FIG. 2A. THE TOTAL EARTH-CLOUD SCENE REPRESENTED IN THE MESO-SCALE RESOLUTION. NOTE HOW THE ICE AND SNOW OF THE ARTIC AND THE SANDS OF THE SAHARA APPEAR AS BRIGHT AS CLOUDS.

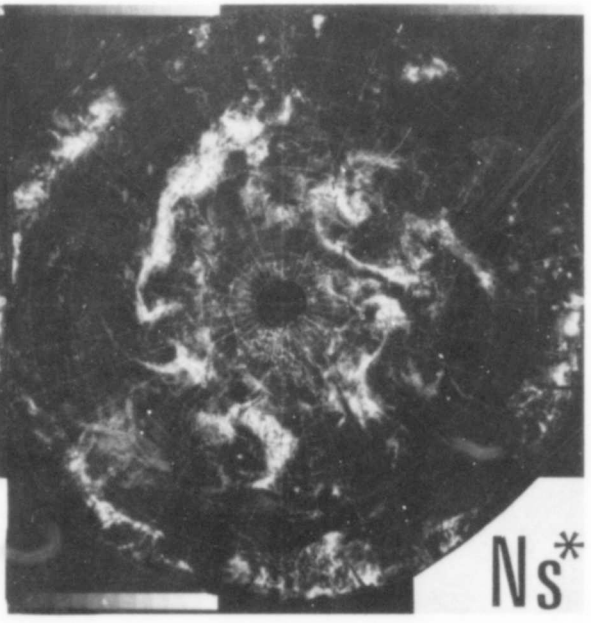


APRIL, 15, 1969

FIG. 2B. THE 30-DAY COMPOSITE MINIMUM-CLOUD AMOUNTS (Cm) FOR APRIL 1969 WERE SUBTRACED FROM THE CLOUD AMOUNTS REPRESTENTED BY FIG. 2A (Ns) FOR APRIL 15, 1969. THE EFFECTS OF ICE, SNOW AND SAND ARE REMOVED SO THAT ONLY CLOUDI-NESS IS PORTRAYED (Ns*)

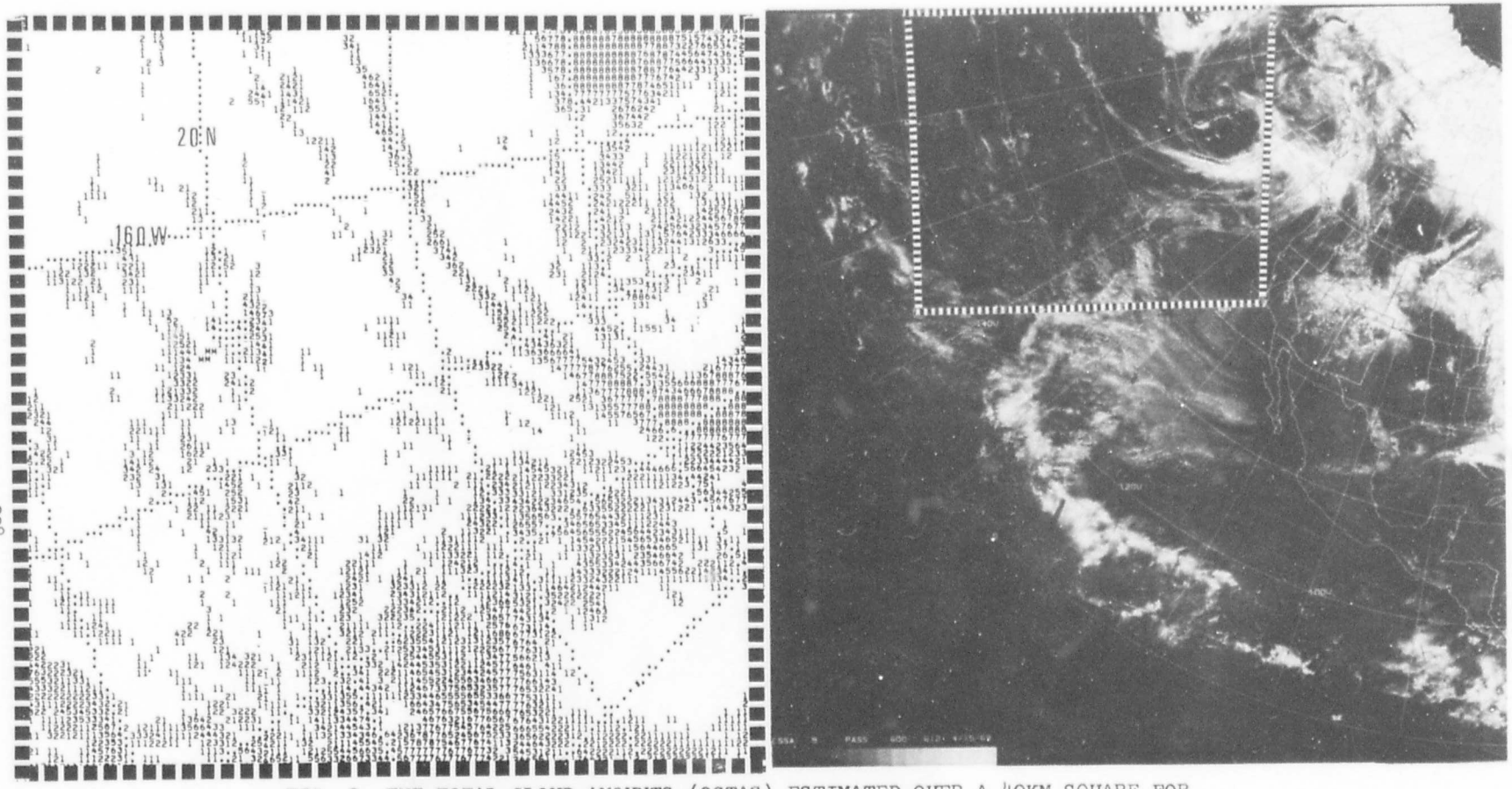


FIG. 3. THE TOTAL CLOUD AMOUNTS (OCTAS) ESTIMATED OVER A 40KM SQUARE FOR APRIL 15, 1969 ARE SHOWN ON THE LEFT. BLANKS INDICATE ZERO EIGHTHS OR CLEAR SKIES AND "M"'S INDICATE DATA VOID AREAS. THE FULL RESOLUTION PICTURE FOR THE SAME DAY APPEARS ON THE RIGHT.

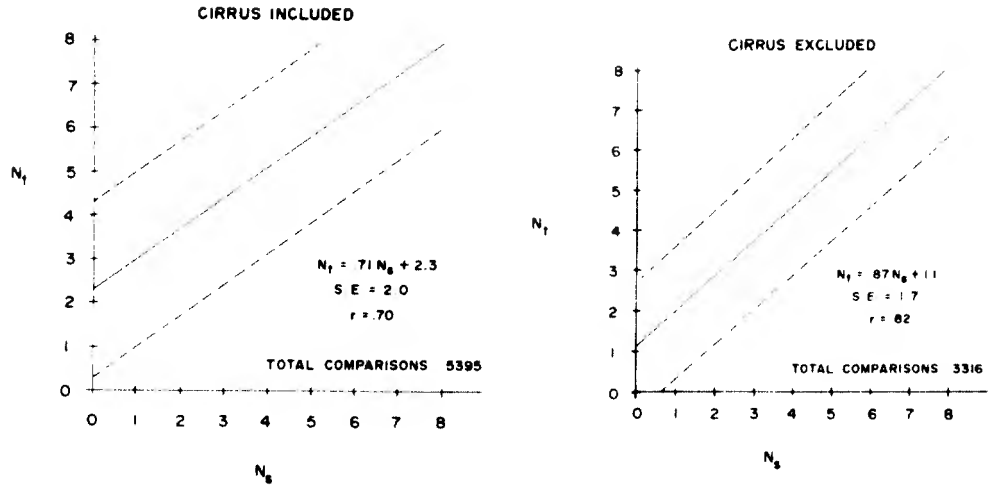


FIGURE 5A. COMPARISON OF $N_s$ AND $N_t$ FOR 12 DAYS SELECTED FROM A 10-MONTH PERIOD (JAN-OCT) IN 1969. AREA OF COMPARISON IS MAINLAND CHINA, 0600 GMT OBSERVATIONS.

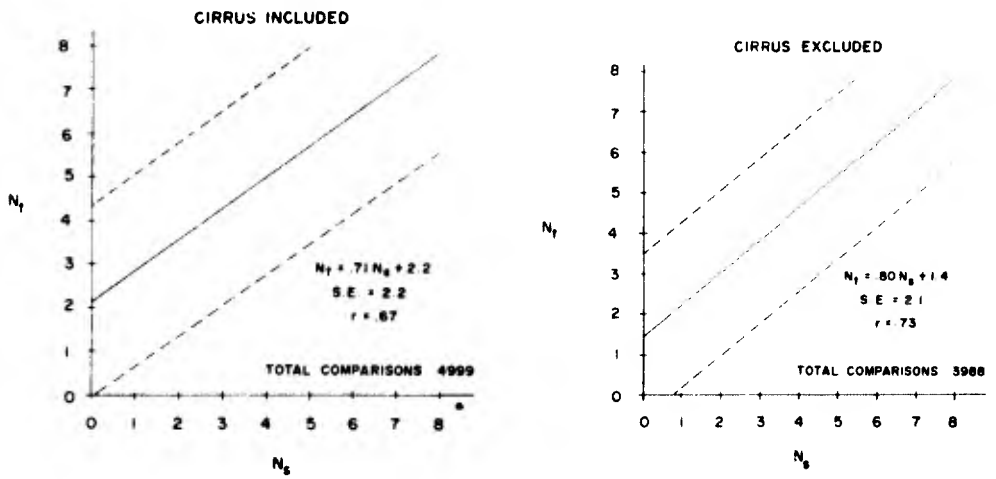


FIGURE 5B. COMPARISONS OF $N_s$ AND $N_t$ FOR THE PERIOD 2-13 APRIL 1968. AREA AND TIMES OF $N_s$ DATA ARE THE SAME AS IN FIGURE 5A.

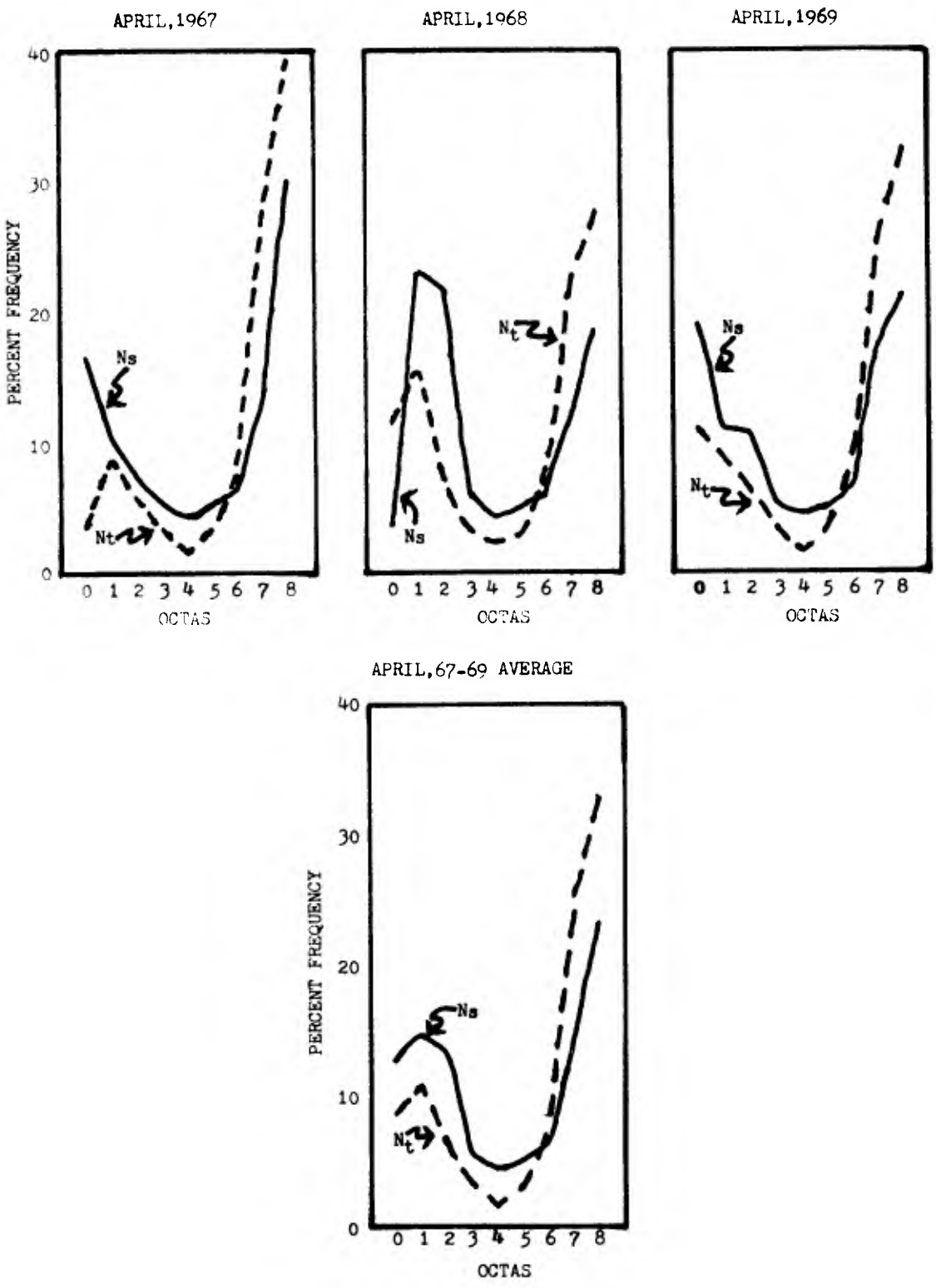


FIGURE 6. COMPARISON OF $N_s$ AND $N_t$ FOR THE MONTHS OF APRIL 1967, 1968, AND 1969. MORE $N_s$ VALUES OCCUR IN THE LOW-CLOUD AMOUNTS (0 TO 2 OCTAS) AND FEWER Ns VALUES OCCUR IN THE HIGHER-CLOUD AMOUNTS (6 TO 8 OCTAS). AREA OF COMPARISON IS MAINLAND CHINA, 0600 GMT OBSERVATIONS.

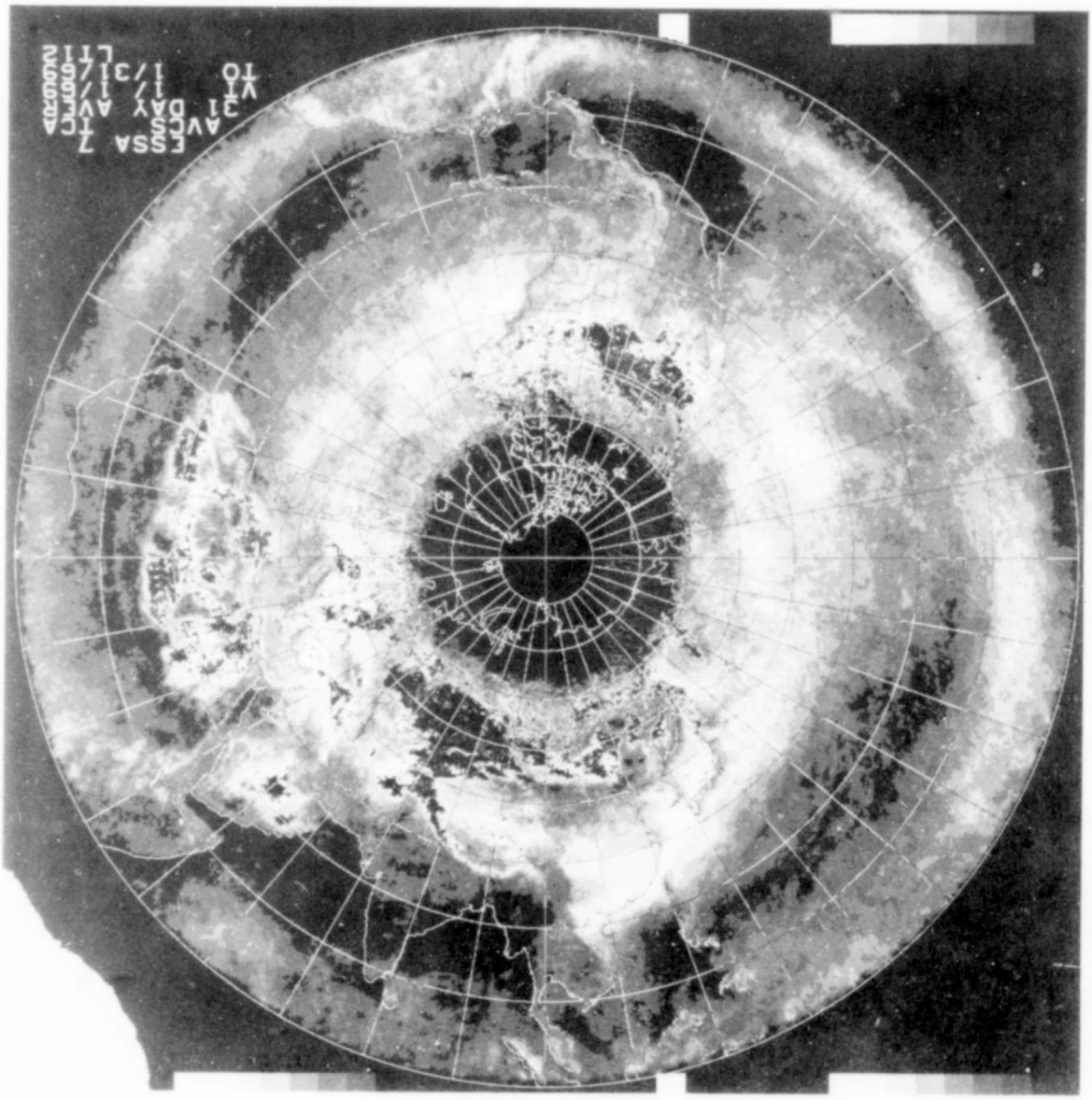


FIGURE 4. MEAN TOTAL-CLOUD AMOUNT FOR JANUARY 1969. EACH GREY SHADE REPRESENTS INCREASING CLOUD AMOUNT FROM BLACK (CLEAR) TO WHITE (OVERCAST OR 8 OCTAS). THE BLACK AREAS OVER THE NORTHERN PARTS ON THE CONTINENTS AND OVER THE DESERT REGIONS OF ARABIA AND AFRICA ARE DERIVED FROM THE 30-DAY $C_m$ VALUES FOR JANUARY. WITHIN THESE BLACK AREAS THE CLOUD AMOUNTS COULD NOT BE ESTIMATED BECAUSE THE BACKGROUND WAS BRIGHT ENOUGH TO BE CONFUSED AS CLOUDS.

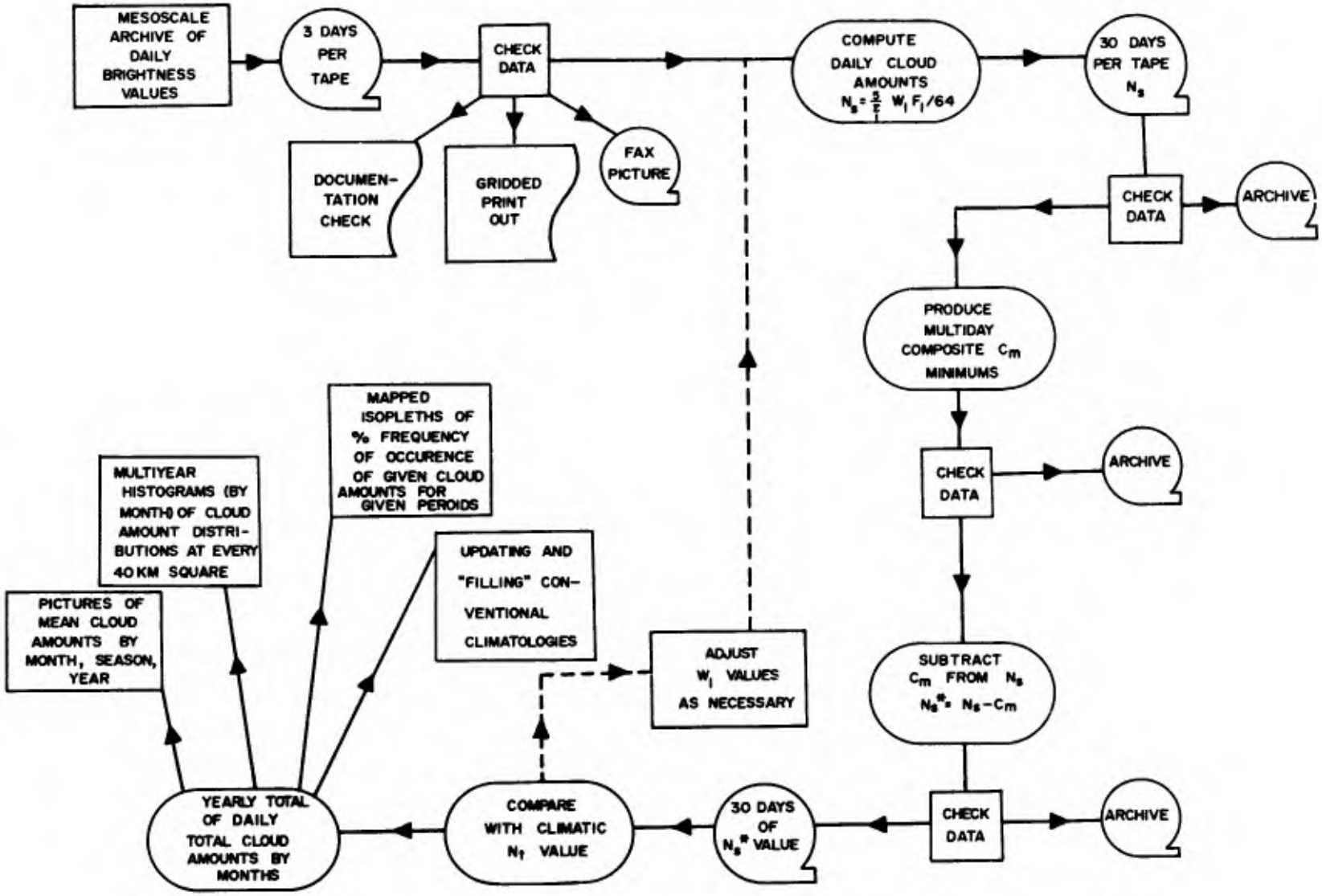


FIG. 7. PRODUCTION OF A CLIMATOLOGY OF TOTAL-CLOUD AMOUNT FROM THE MESOSCALE ARCHIVE OF SATELLITE DATA

# TOTAL CLOUD AMOUNT CLIMATOLOGY STATUS

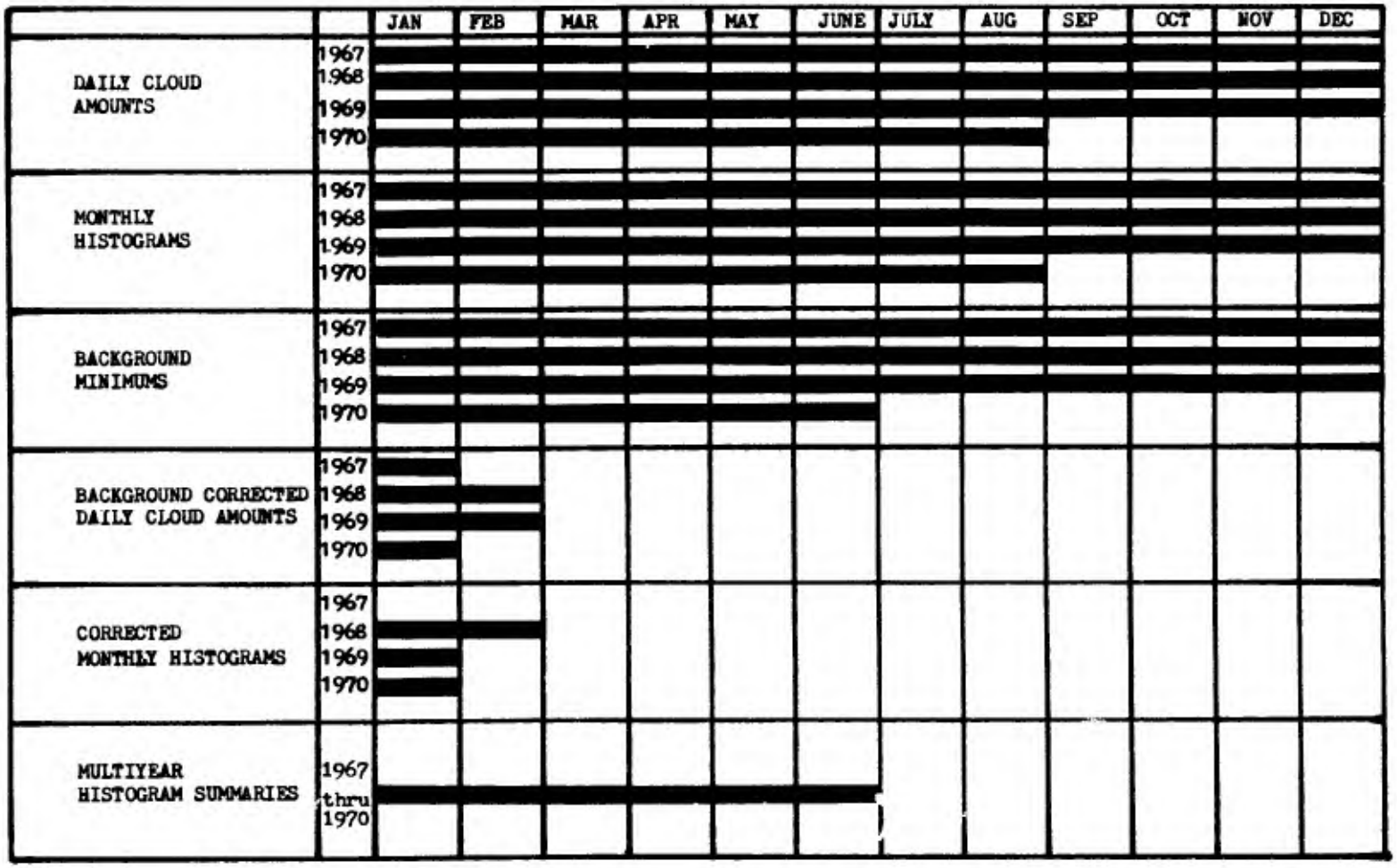


FIGURE 8. STATUS OF THE PRODUCTION OF THE CLIMATOLOGY OF TOTAL-CLOUD AMOUNTS FROM SATELLITE DATA.

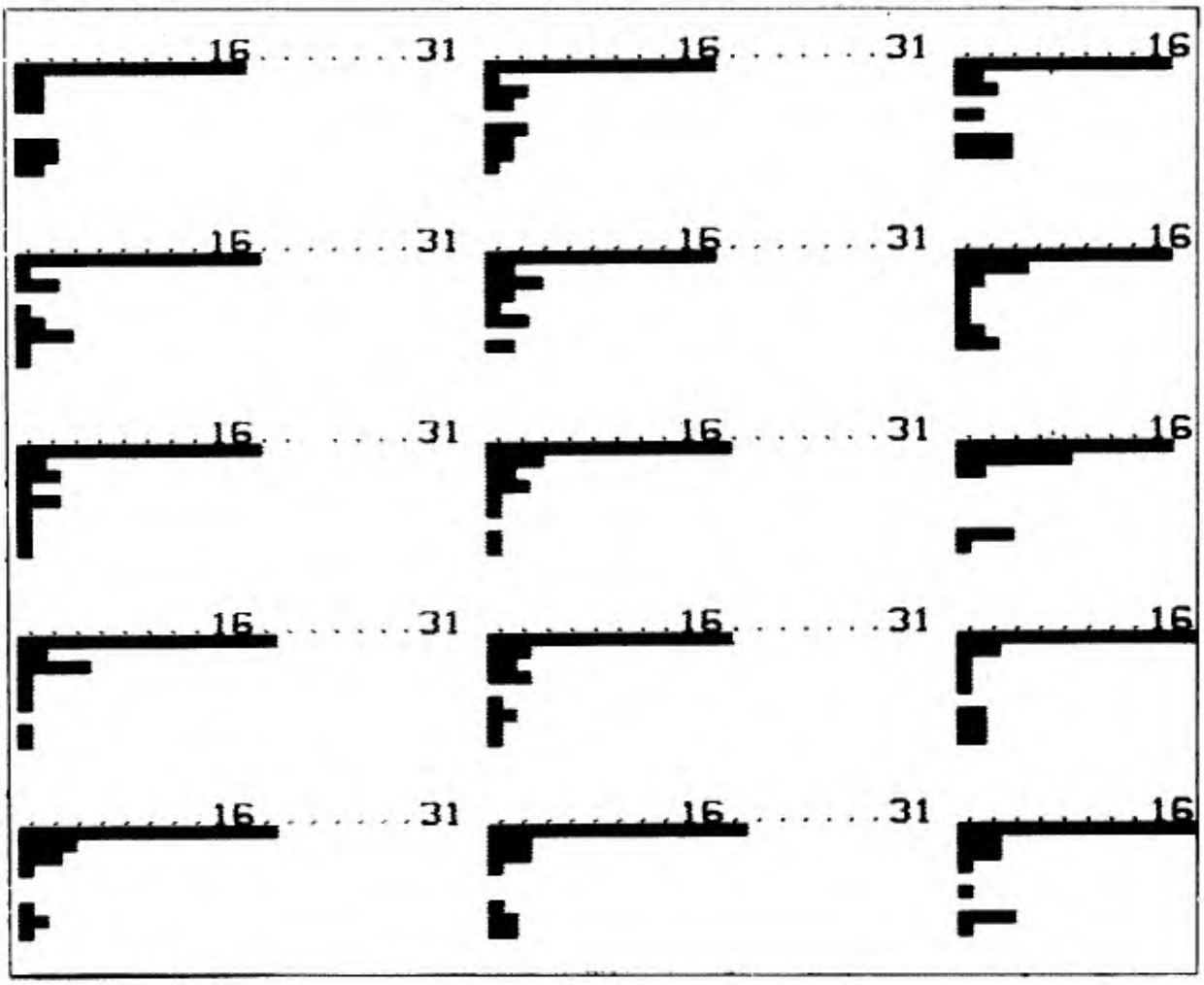


FIGURE 10. HISTOGRAMS OF TOTAL-CLOUD AMOUNT FOR WASHINGTON, DC AREA, MAY 1969. THE CENTER HISTOGRAM IS WASHINGTON, DC, THE OTHERS ARE 30 N.MI. APART WITH NORTH AT THE TOP OF THE FIGURE. THE FREQUENCIES (ABSCISSA) ARE IN DAYS AND THE CLOUD AMOUNTS INCREASE FROM 0 OCTAS TO 8 OCTAS VERTICALLY DOWN THE PAGE.

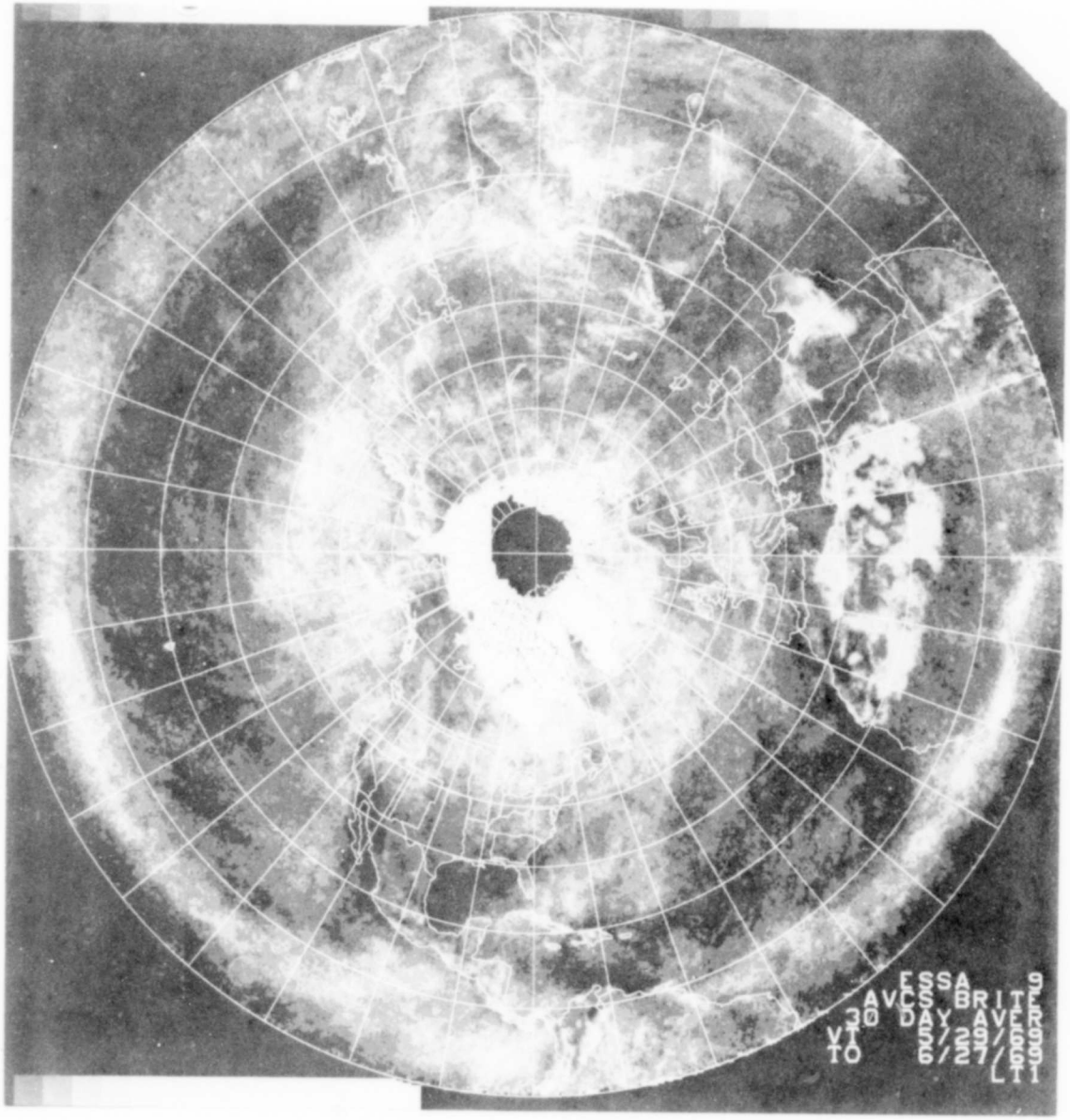


FIGURE 9. MEAN TOTAL-CLOUD AMOUNT JUNE 1969. AMOUNTS INDICATED BY GREY SHADES FROM BLACK (0 AND 1 OCTAS) TO WHITE (7 AND 8 OCTAS). SNOW, ICE, AND DESERT BACKGROUND NOT REMOVED.

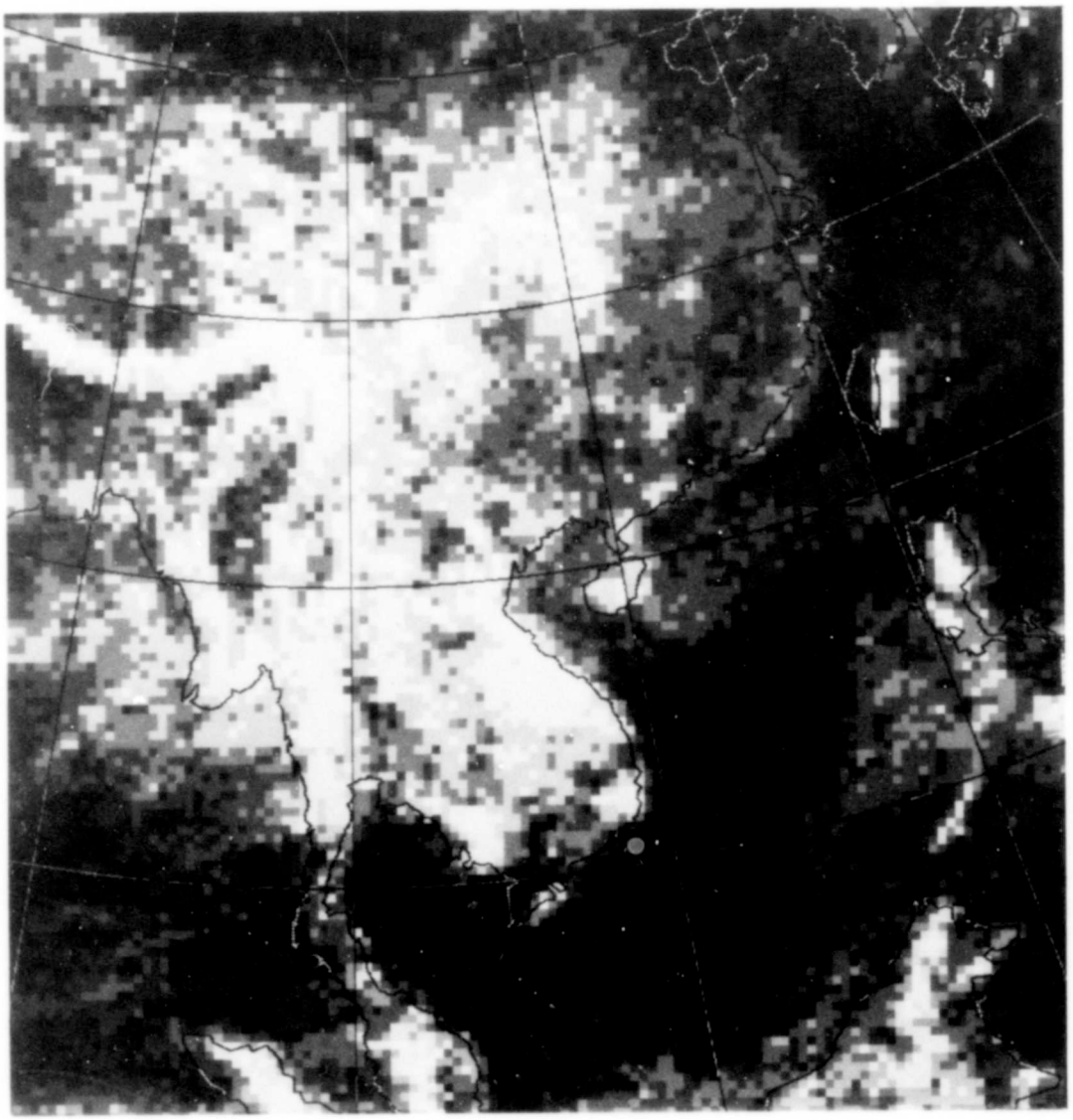

FIGURE 11. PERCENTAGE FREQUENCY OF SCATTERED CLOUDINESS (2 OCTAS OR LESS) OVER SOUTHEAST ASIA, OCTOBER 1967. GREY SHADES ARE IN 10% INTERVALS FROM BLACK (90 TO 100%) TO WHITE (0 TO 10%).

# CLIMATE MODIFICATION & NATIONAL SECURITY

R. R. Rapp

The Rand Corporation
Santa Monica, California

The climate of the earth has not always been as it is now. Geologic records indicate that there have been long periods of quasi-stable climates that are different from what we know today. There is every reason to believe that changes could occur in the future. Our knowledge of what caused the past variances in climate is very sketchy and we do not have a well developed methodology for anticipating future changes. There may be natural events — changes in the output energy of the sun, changes in the form and shape of the oceans and continents on the earth which could cause changes in the climate. But there are also possibilities that the activities of man will change the climate.

At one time, not too long ago, we could speak rather glibly of man versus nature, and talk about "natural" events and "manmade" events. We had some rather strong ideas that there was a great difference in that things were either "natural" or "manmade." But the explosive growth of the human population and its growing use of energy has made this kind of distinction difficult to take seriously in this day and age. Man is having a very definite influence on not only his local surroundings, but the whole nature of the planet. Man is part of nature and his activities are very likely to influence the future course of the natural environment of the earth. Many of man's works result in deleterious effects on the environment.

Most such changes are likely to be inadvertent. The desire for more power and energy may cause man to use fossil fuels to produce heat, to produce waste, and this might influence the climate of the earth. Actions to alter the face of the earth in some major way for some beneficial purpose could alter the climate of the earth in a harmful way. The important point is, that today we have the technology and the available energy to make vast changes in the face of the globe and the composition of the atmosphere. These changes could very well affect the climate in which we live. Finally, we must not overlook the small, but finite, possibility that deliberate attempts might be made to alter the climate of the world to the detriment of the United States. I do not think this is a very likely situation, but it is a possibility. I think the more likely threat to our national security is the possibility that changes will be made to improve a bad situation somewhere in the world that might have a deleterious effect on the climate of the United States.

The question then arise, if we are really concerned about the possibility that man might affect the climate of the earth, what can we do about it? What are the problems? What are the possible solutions? How should we proceed to look at the problems of the possibility of climatic change? One approach, of course, is to try to look into the past and try to discern from geological records what climatic changes occurred, and deduce the causes of such climatic regime. This is a very difficult task. There have been some minor climatic fluctuations in the recorded past, but long records are not quantitative and we have only gross qualitative descriptions of what happened. There is very little information on possible causes, so our study of past climates can only be an attempt to define them more precisely, and then to speculate on the causes.

Another method which has been proposed to study the climate is by means of numerical simulation. The concept of numerical prediction, which was first raised by Richardson fifty years ago, has been developed to a high degree. There are certain problems of numerical prediction which are well in hand, and you have heard quite a bit about some of these at this conference. All of the numerical prediction methods, however, run into the difficulty of the predictability problem which has been discussed so well by Ed Lorenz.

Lorenz advances the proposition that "...certainly formally deterministic fluid systems which possess many scales of motion are observationally indistinguishable from indeterministic systems; specifically, that two states of the system differing initially by a small "observational error" will evolve into two states differing as greatly as randomly chosen states within a finite time

interval..."[1] He goes on to demonstrate and quantify this proposition for a simple model which has no forcing functions and no dissipation. This type of error amplification has been demonstrated by the exercise of other models.[2] We are not so much concerned with this type of error as we are with the ability of the model to discriminate between the ensembles from which the randomly chosen states are selected. Thus we have set about to determine the changes in the mean state of a model of the atmosphere with different boundary conditions and different initial conditions. Our preliminary results indicate that the mean circulation for a period 30 to 60 days after the ice was removed from the Arctic Ocean was significantly different from the runs with the ice present. We have not, as yet, explored the impact of this change on the climate.

A great many problems of numerical simulations are well under control. The work of the Geophysical Fluid Dynamics Lab, ESSA,[3] is an outstanding example of the fidelity with which numerical models can be made to represent the way the real atmosphere behaves. The basic problems of numerical integrations on the sphere have essentially been solved. There are other problems that have not been solved. There are problems of scale, problems of the resolution with which we can calculate in order to determine the effect of small scale motions on the general circulation. There are also problems of physical processes for which we do not have a thorough understanding. And so, although we believe at the present time we have numerical models which are sufficiently realistic to be able to reproduce the climatic features we observe today, we cannot assume, apriori, that these models are sufficiently accurate to properly reflect changes which might alter the climate. We therefore have a twofold problem. One is to exercise the models we do have, and the other is to improve the models.

In the process of exercising the models we do have, what we are essentially doing, is asking the question, What changes in climate would result from the successful completion of a large project? I have already alluded to the effect of removing the ice from the Arctic Ocean. There have been many speculations that, if one did this the ice would not return, or at least not very rapidly, and that the climate could be drastically altered.[4] There is serious talk of some large hydrologic projects — changing the course of rivers, creating lakes where there are now deserts. We would like to estimate the effect this kind of operation would have on the climate. What might happen if some of the large ocean currents were diverted? What would result if films were developed to retard the evaporation of water over large ocean areas? Some of these projects might be undertaken with a very definite beneficial end in mind, and result in serious climatic problems. On the other hand, it is not inconceivable that, if a scheme were available which could change the climate, it might be used in a malicious fashion.

So finally, what is our approach to this whole problem of climatic simulation for national security? We want to find out primarily what changes in the face of the earth or in the content of the atmosphere would have an effect on the climate. We approach this problem by trying to exercise numerical models where the simple insertion of a few statements in numerical programs changes the face of the earth or the content or the condition of the atmosphere, and then look to see what the resulting change in the circulation would be. I've already alluded to the fact that our models are really not tuned finely enough so that we can be sure that the changes we see are actually the changes that would occur. Some of our parametric representations of certain processes might, under the new situation, be inadequate, and we could ge the wrong result. This is an open question — one which we are addressing first in our program at Rand.

With the numerical models now in use we are faced with another serious dilemna. They are run for several months to determine the change. Obviously, climate is not determined by several months. What one really wants to do is look at years. With our present generation of computing machines the time and expense to run for many years is just too great — we do not have computing power to run current step-by-step integrations for long periods of time. There are two ways out of this dilemna. One is to build bigger and better computing machines. ARPA has funded the development of ILLIAC IV, which will be used to try to make long runs of a step-by-step integration of the numerical model. We at Rand are trying to be ready with the programming and the model. We want to be ready to go on ILLIAC IV with this kind of numerical simulation as soon as ILLIAC IV is operating.

But there is another way of looking at this problem which will require more study and more finesse, and that is to try to find ways where we can simulate the gross climatic features without doing the step-by-step, day-by-day weather prediction. There are a good many people interested in this and several approaches to this problem. One way is through use of harmonic analysis[5] — that is to try to filter out the small scale from the large scale and try to learn how to get the really gross effects without detailed study of the smaller scale. Another is the simple sort of zonal averaging such as MacCracken[6] has produced. It is a rather detailed computation scheme, but it works on a zonally averaged two-dimensional model of the atmosphere. There are difficulties with all these schemes, but we believe that all conceivable approaches must be pursued.

The Rand program in climate dynamics has been underway for about one year. It is at present divided into nine subprojects. The first project we undertook was to try to determine whether or not the predictability problem that Lorenz has raised would hamper our approach. We have made quite a few runs with the Mintz-Arakawa(7) 2-level model changing the boundary conditions by running with present conditions and then taking the ice-out of the Arctic basin. We have repeated these runs with randomly distributed temperature errors in order to discover whether the mean changes were discernible through the errors introduced by the randomly changed temperatures. The results of this are just beginning to come in and they indicate that indeed the mean circulation has been changed and that the random errors do not obscure the changes in the mean conditions. This work should be finished within the next 6 to 8 months with a rather complete report on our findings.

In the second project we are continuing with many other global circulation model experiments which we will not necessarily worry about the statistical validations but will simply assume that the changes shown by the model indicate the direction of the change. At present these are being run with the Mintz-Arakawa 2-level global circulation model with a 4x5 degree grid resolution. One experiment which has been run is the removal of the cold Eastern Tropical Pacific surface waters to compare with the work of Bjerknes.(8) Arakawa and Mintz are in the process of completing a 3-level model, the third level being a boundary layer and it is believed that this will greatly increase the fidelity of the model. We are also looking to the possibility of going to a much finer resolution than these experiments. In the meantime until the 3-level model is ready, we will continue with the 2-level model and make changes which have been suggested that might alter the climate.

The third project is on ocean models. One of the big deficiencies of the Mintz-Arakawa model, indeed most of the global circulation models, is that the ocean is not allowed to react in the same way that the atmosphere is. We have developed a barotropic ocean model which has been tested and reported on. We are in the process now of running this barotropic model for the world ocean. At the same time we have done some research and made some analyses to devise a baroclinic model with relatively few layers. This, we hope to mate with the Arakawa-Mintz 3-level model in order to produce a model which will allow the ocean to change with the changing atmosphere and the atmosphere to react to the changing ocean.

The fourth project is a study of the effect on atmospheric radiation of turbidity and cloudiness. This is an area where the theoretical background is not sufficient to make a really good parameterization of the effects on the atmosphere. We have not gone deeply into this as yet. It is at present in the study stage and we hope within a year to get some positive results for correcting some of the possible deficiencies in the current model.

Our fifth project deals with the smaller scale convective cloud model. One of the great problems of global modeling is the inclusion of suitably parameterized models of small scale convection. The fine grid which we hope to achieve should resolve synoptic scale disturbances, but below that there is not much hope that we can resolve such things as convective clouds. Since they are so important in redistributing heat and moisture in the vertical we are carrying out model of cumulus convection in order to try to learn more about the heat and moisture transport by convective clouds. We hope eventually to develop a 3-dimensional model so that we will also be able to look at the effect of the transport of momentum by convective clouds.

Our sixth project is on numerical methods. We note that since the beginning of numerical weather prediction the approach to numerically integrating the equations of motion has been a series of finite different schemes. These have been developed to a high degree but the whole problem of numerical analysis remains something of an art and not completely developed to a science. A new method which instead of using finite differences uses a curve fitting approach and then solves the curve fit equation explicitly. It is known as Galerkin's method, it is complex, and we do not know whether it would provide any advantage over the current method but we're looking at it and we hope in a year to have a report on the possible utility of this method.

I mentioned earlier that the full scale model even one as simple as the Mintz-Arakawa model uses a tremendous amount of time to step along in short time steps to produce results for the order of months or years. Our seventh project is to look at other approaches. At present the interest is centered on the zonally average model developed by MacCrackin at LRL. We have programmed this. We are comparing it with the Mintz-Arakawa model. We are studying it for possible improvement and we'll decide very soon whether such an approach to very long term climatic models is feasible.

Our eighth project continues with the study of climate as it has been recorded or deduced. We believe that one of the ways we can bolster our confidence in a numerical solution is to try to reproduce some of the climatic changes that have occurred in the past. In order to do this we must, of course, know what changes have occurred and has some way of describing what we think

caused these changes. As we developed theories of climatic change we will try them on numerical modeling. If, indeed, our proposed suggestions for why the climatic change occurred produce what we think happened, then we will have additional confidence in our method of numerical solution.

And finally, we are preparing to use the ILLIAC IV as soon as somebody throws the switch. We have already completed a programming of the cumulus cloud model developed by Murray. We chose this as a checkout program because this model has been programmed for many versions of many different machines and it will provide a measure of what we can expect from the ILLIAC IV. Moreover, the kind of mathematics that are used in the convective cloud model and the number of grid points is very similar to what we would have in a global circulation model. Since the cloud mode has already been checked out and ready to go, we are going to turn our programmers to the job of programming the Mintz-Arakawa model. We believe that as soon as a good documentation is available that we can turn our programmers loose, and that when the 3-level model comes along there will be no difficulty in converting to the 3-level model.

So those nine projects make up the Rand program. It is not complete. You will note that we do not have a project on the harmonic analysis approach to long term climate. Perhaps that will come, but we believe that there are others in the country who are perhaps more capable than we to proceed with that. You will note that there are many small scale features that we have not addressed. We have no work going on at Rand in transfer of heat and momentum and energy from the surface of the earth into the atmosphere. We believe this is important but again we think there is competence elsewhere in the country that could be turned to these problems.

And so the Rand program on climate dynamics for environmental security starts with the concept that the U.S. might be harmed either inadvertently or maliciously by changes in the climate that we must find out how to anticipate change in the climate. There is much work to be done to develop a methodology estimate how the climate might change or be changed.

## REFERENCES


1. Lorenz, E. N., "Studies of Atmospheric Predictability," Massachusetts Institute of Technology, Final Report, Statistical Forecasting Project, February 1969.

2. NAC-NRC, "The Feasibility of a Global Observation and Analysis Experiment," Prepared by Panel on International Meteorological Programs as report to NAS Comm. on Atmos. Sci., 1966.

3. Manabe, S., et al,,"Simulated Climatology of a General Circulation Model with a Hydrologic Cycle. III. Effects of Increased Horizontal Computational Resolution," Monthly Weather Review, Vol. 98, No. 3, 1970.

4. Fletcher, J. O., Influence of Arctic Pack Ice on Climate In: Soviet Data on the Arctic Heat Budget and its Climatic Influence, The Rand Corporation, Santa Monica, California, 1966.

5. Saltzman, Barry, "Large-Scale Atmospheric Energetics in the Wave-Number Domain," Reviews of Geophysics and Space Physics, Vol. 8, No. 2, 1970.

6. MacCracken, M., "Ice Age Theory Analysis by Computer Model Simulation," Ph.D. Thesis, University of California, Davis, 1968.

7. Mintz, Yale, "Very Long-Term Global Integration of the Primitive Equations of Atmospheric Motion," WMO-IUGG Symposium on Research and Development Aspects of Long Range Forecasting, Boulder, Colorado, 1964.

8. Bjerknes, J., Studies in Climate Dynamics for Environmental Security: Large-Scale Ocean/Atmosphere Interaction Resulting from Variable Heat Transfer at the Equator, The Rand Corporation, Santa Monica, California, RM-6353-ARPA, August 1970.

# SIMULATION OF ECOLOGICAL SYSTEMS

Amos Eddy

Meteorology
University of Oklahoma
Norman, Oklahoma

Abstract

An ecosystem simulation model is described and some of the problems in adapting this model to a digital computer are discussed. The implications of running such a stochastic process for an extended period of evolution are reviewed briefly. Applications of the system to the solution of resource management problems are proposed.

## Introduction

One object of this project is to represent a mesoscale ecosystem by means of a computer simulation model and to study the evolution of such a system over a period of a quarter century. The model is fundamentally stochastic. By this is meant that interest centers on the statistical properties of the field of variables, while interaction between variables is primarily governed by conditional probabilities. Although some deterministic components are used (for example, the city heat island circulation system is a "conventional" dynamic model), they are controlled by the stochastically produced environment in which they are imbedded.

Another object is to study the variations in the evolution of such an ecosystem which results from subjecting:

a. the interactions to various sets of limiting constraints (resource management practices) under the same initial conditions, and
b. the initial data to varieties of noise and other sampling problems.

The third object is to upgrade the educational background of both our students and ourselves.

A one sentence description of the historical background of the project would explain that the work began in 1968 with a class of graduate students programing a simple grass-grasshopper-rainfall ecosystem (Eddy, 1969), progressed through an urban-rural model (Parton and Eddy, 1970) which used synthesized data, and is currently being made realistic through the incorporation of real observed data and more comprehensive submodels.

At the present time we are adapting our model to the Houston-Dallas-San Antonio ecosystem (Fig. 1). We deliberately include more than one city and more than one watershed. However, data for testing our urban submodel is coming from Houston, while Trinity River data is being used to test our hydrology subroutine. Reservoirs and municipal sewage input on the Trinity are being studied with respect to water-resource quantity and quality management practices. Data from the Houston Model Cities Program and local census data are used to characterize many of the human attributes.

Our group has expanded to include medical doctors, range management specialists, agricultural economists, town planners, meteorologists and biologists. This group is not only interdisciplinary but it is also inter-university and inter-state.

## CONCEPTUAL PROBLEMS

Some of the interesting problems which arise when one attempts to model an ecosystem are the following:

a. The scales on which the phenomena involved must be represented range from smaller than centimeters to larger than hundred of kilometers and from shorter than seconds to longer than decades. (One malaria-inducing insect can destroy a community of humans under a particular set of conditions.)
b. Provision must be made for the adequate description in both space and time on a digital computer system of all the physical and biological variables which are necessary in a probabilistic sense to the successful representation of the ecosystem.
c. Since there is no possibility of dealing explicitly with identified individual components of the system, manipulation must be done with ensembles of individuals. Here the groups must be selected to be large enough to have stable statistical characteristics and small enough to represent groups having common basic properties (stationarity).
d. Actions taken by the biological variables must be associated with their attributes. Just as the average momentum of an air parcel at a particular time will give an indication of its direction of movement, so the average wealth of a group of people will give an indication of its tendency to move to more desireable living conditions, and hunger will produce a tendency to seek food.
e. Although an individual component is normally not identified in the system evolutionary process, he must be indentifiable for a variety of reasons. Perhaps the most cogent one would be that it is for the explicit purpose of developing humans with increasingly better life styles through optimal systems management that this simulation model is being developed. Thus, it must be possible to identify an individual in space and time and characterize him by a complete set of attributes even though he remains

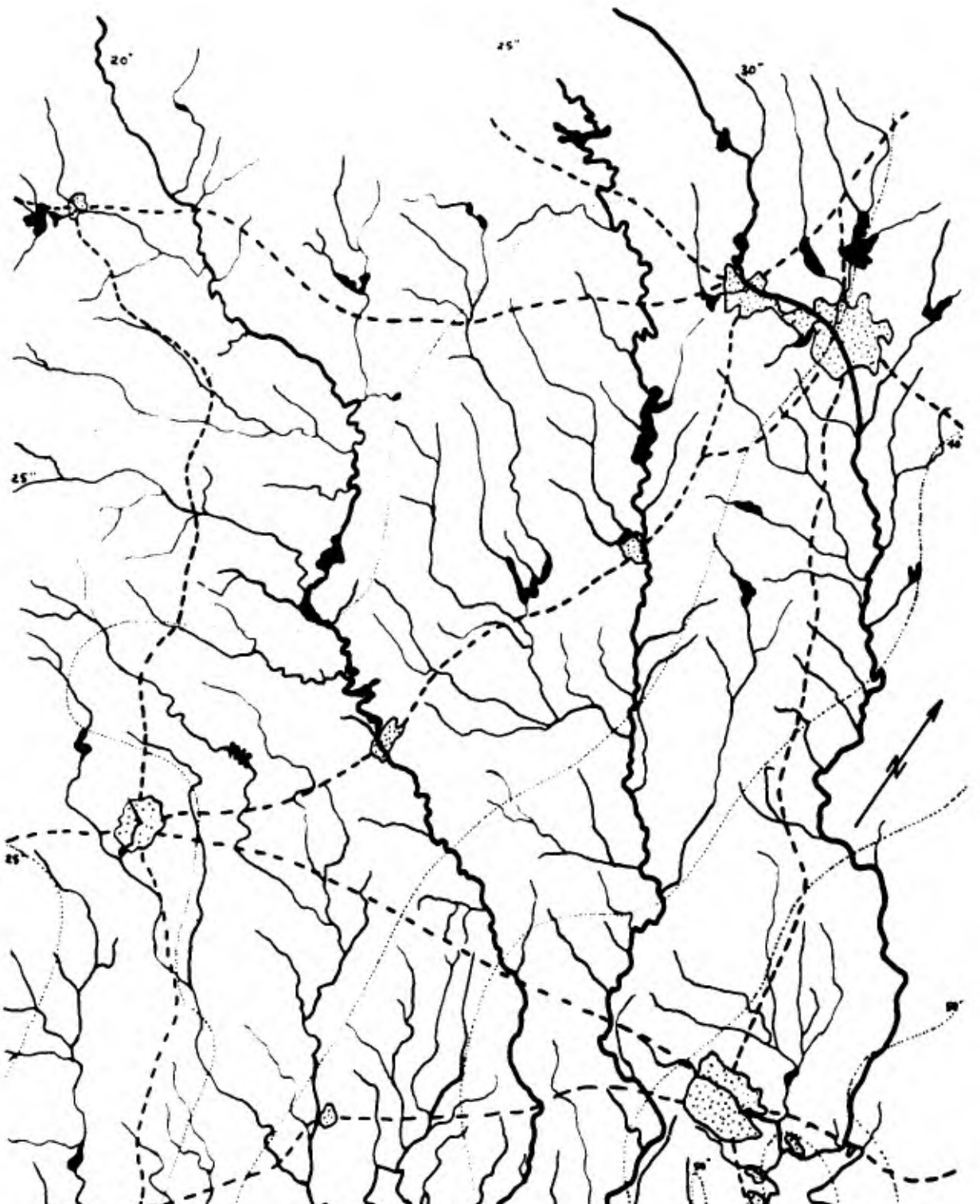

Fig. 1: Houston-Dallas-San Antonio Ecosystem

fundamentally a "statistical man."

f. Natural discontinuities appear between "colonies" of biological species and these discontinuities move in response to stress across the boundaries (ecotones). In a manner analogous to the analysis of airmasses which are delineated by fronts, we have circumscribed the boundaries of our city suburbs with identified dynamic zones of stress. These boundaries move in response to, for example, population density gradients across them while the character of the population inside each suburb is represented by a homogeneous set of attributes. People can diffuse across a suburb boundary into an adjacent suburb in a manner which makes this ecotonal "line" a mixing zone reminiscent of those along weather fronts.

g. The amount of observational data required is enormous; consequently, data must be just sufficient to provide required information—no more and no less. A balance of critical information content in all variable fields must be maintained—it is not economical to define one field to six significant figures while another field is controlling the evolution of the system and can only be defined to three significant figures.

h. The psychology of actual model building as a mutual project of men drawn from a variety of professions is difficult. Not only is this problem the most difficult one to resolve, but also its resolution may represent the most important contribution of any such project.

i. The ecosystem which we are studying is very much man dominated. The manner in which human decisions can affect the evolution of the various components of the ecosystem is a matter of prime interest. We wish to demonstrate the variety of possible futures (including those which are optional under various constraints) which can evolve from particular sets of management policies.

## STRUCTURE OF THE MODEL

The model comprises a set of scientific submodels which operate a common field of variables but which are controlled through lists of parameters specified by a decision making management routine. Fig. 2 shows schematically a representative sample of the model. The central decision making routine keeps track of the "current" state of the fields of variables, some of which are shown in the outer ring. At certain times it will insue edicts to the central ring of subroutines; i.e., it might tell:

a. the botany routine to cut the hay or plant a crop,
b. the zoology routine to move cows from pasture to feed lots,
c. the hydrology routine to irrigate the crops,
d. the urban routine to clean up its sewage, or
e. an industry to cut back on its air pollution.

Since it is beyond the scope of this paper to discuss all the variables and their interactions in details, a brief description of a representative

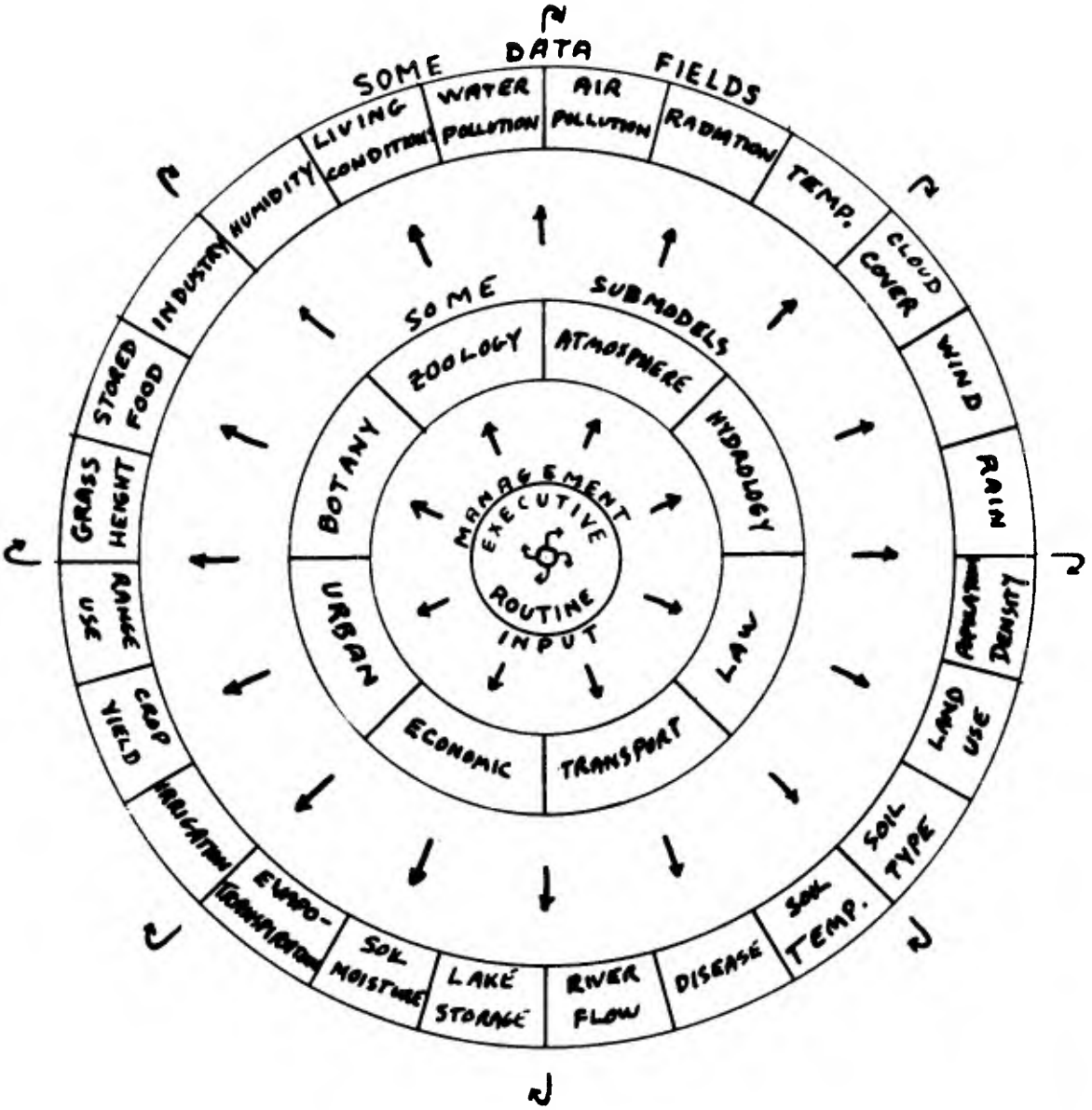


Fig. 2: Schematic of a Representative Portion of Model

sample of the submodels will be used to indicate the structure of the system.

## ATMOSPHERIC SUBMODEL

Five years of climatological data from Oklahoma City have been used to verify the ability of the atmospheric model to produce climatically realistic predictions.

Mean wind speeds and directions are forecast using stochastic transition matrices. Local variations from the mean wind are produced, for example, in the vicinity of urban areas using a dynamic mesoscale "heat island" type of circulation model. Mean relative humidity is a statistical function of wind direction.

Temperature is forecast using a radiation flux-divergence model (Myrup, 1969) which is a "deterministic" function of cloud, temperature, wind, lapse rate, humidity and solar position. A portion of this radiative heating goes to evaporating water, another to warming the soil and some of it to sensible heat which raises the air temperature. A portion of the solar insolation is also used in the botany routine for photosynthesis.

Rainfall occurrence is predicted from a set of first order Markov processes which have been stratified with respect to relative humidity. If rain is to occur, it can be either a Nimbo Stratus type or a shower type. The mean over the ecosystem is drawn from the statistical climatology.

The Nimbo-Stratus type rain is first given a geographical trend and then a two-dimensional Poisson distribution with respect to local intensity.

Showers are given a geographical bias with respect to occurrence, and their shape and intensity are constrained using empirical "area-depth" relationships (Court, 1961).

Air pollution patterns are produced using identified sources and a modified Pasquill-Gifford statistical-dynamical prediction model. Fig. 3 shows the set of principle $SO_2$ sources and a possible cummulative air pollution pattern for Houston over a particular stochastically produced sequence of meteorological conditions.

## HYDROLOGY SUBMODEL

The hydrology submodel is based on empirical relationships standard to the profession. Variables which are manipulated are:

a. runoff
b. potential evapotranspiration
c. actual evaporation over water and land soil and evapotranspiration over crops.
d. soil moisture
e. recharge
f. lake level
g. river flow rate

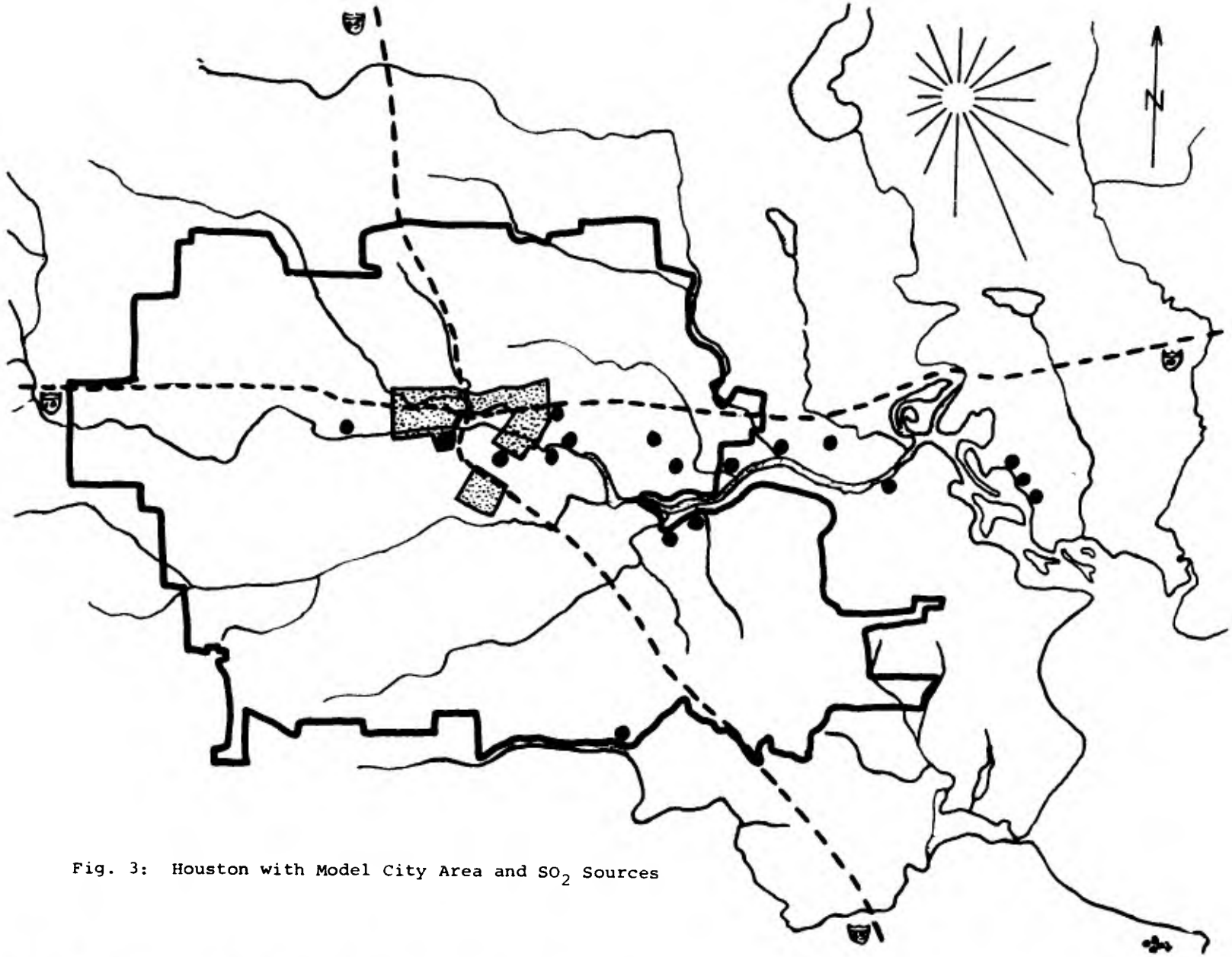


Fig. 3: Houston with Model City Area and $SO_2$ Sources

h. irrigation
i. water pollution

Fig. 4 gives an idea of the geographical characteristics of one watershed, the Trinity, and also an indication of the sampling networks available.

The purpose of including this brief description of the hydrology submodel is to make explicit some of the interactions necessary between the various segments of the ecosystem. The runoff results from the rain produced in the atmosphere model while the evapotranspiration is intimately connected with the botany subroutine. Irrigation is controlled by the executive routine and the lake water sees municipal use. The imagination of the reader can likely supply many of the other interactions required.

## POPULATION DYNAMICS

The movement of individuals or groups of individuals of a zoological character must perforce be possible in the type of simulation model being examined. Even though one may not know why an individual moves (relocates) from point A to point B, it is often the case that migration of populations (grouping, crowds) of individuals can be correlated to environmental conditions. We have provided for several types of population dynamics varying from the directed relocation of cattle herds as a result of range management practices, to the relocation of familes from one section of the city to a remote newly opened and more desireable suburb. Still another one of the principle mechanisms will be described here briefly as it is of a fundamental character and is directly recognizable as a typical geophysical diffusion process.

Suppose an individual currently located at point P of Fig. 5 is being considered for a geographical relocation. We calculate that he has a certain desire to move to a better environmental condition ($\nabla E$) and also that he has a certain ability to move (M). We have derived E, for example, from a combination of population density, housing conditions, air pollution and racial factors, and have derived M from a combination of wealth and education.

An ellipse whose ellipticity is related to M is placed so that a focal point lies over the point P with the major axis pointing along the gradient of E. A pair of random numbers is drawn from an appropriate distribution and the individual is moved to his new position. He has an equiprobable chance of landing anywhere on the ellipse shown dashed in Fig. 5. The ellipse shown is one of an "infinite" set of equiprobable destination patterns. It is clear that on the average the population will "diffuse" toward the right although any individual may go any direction at a particular time step.

Through the use of this mechanism we are able to endow our zoological creatures with a pseudo-intelligence and still allow for individual idiosyncracies.

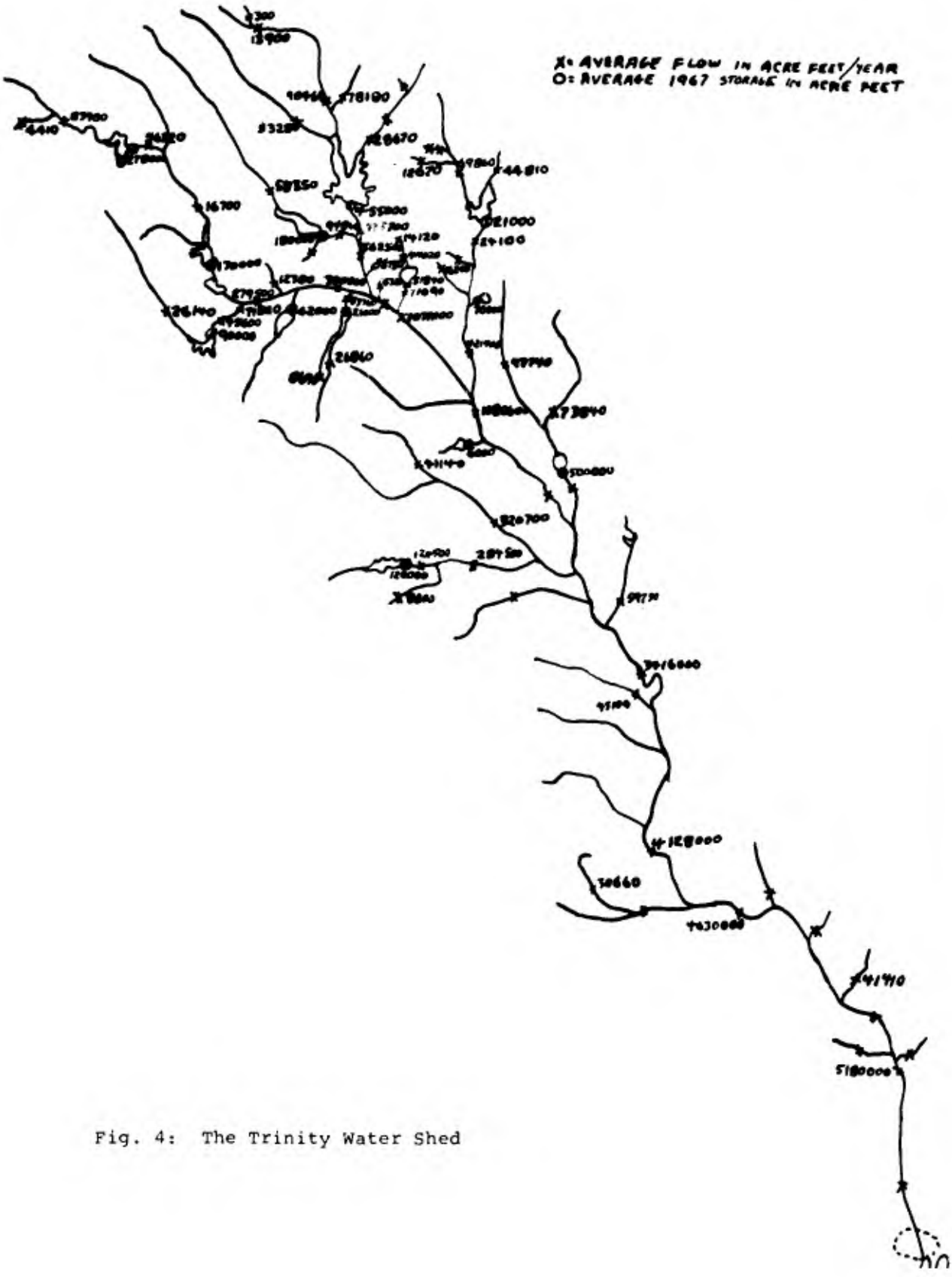


Fig. 4: The Trinity Water Shed

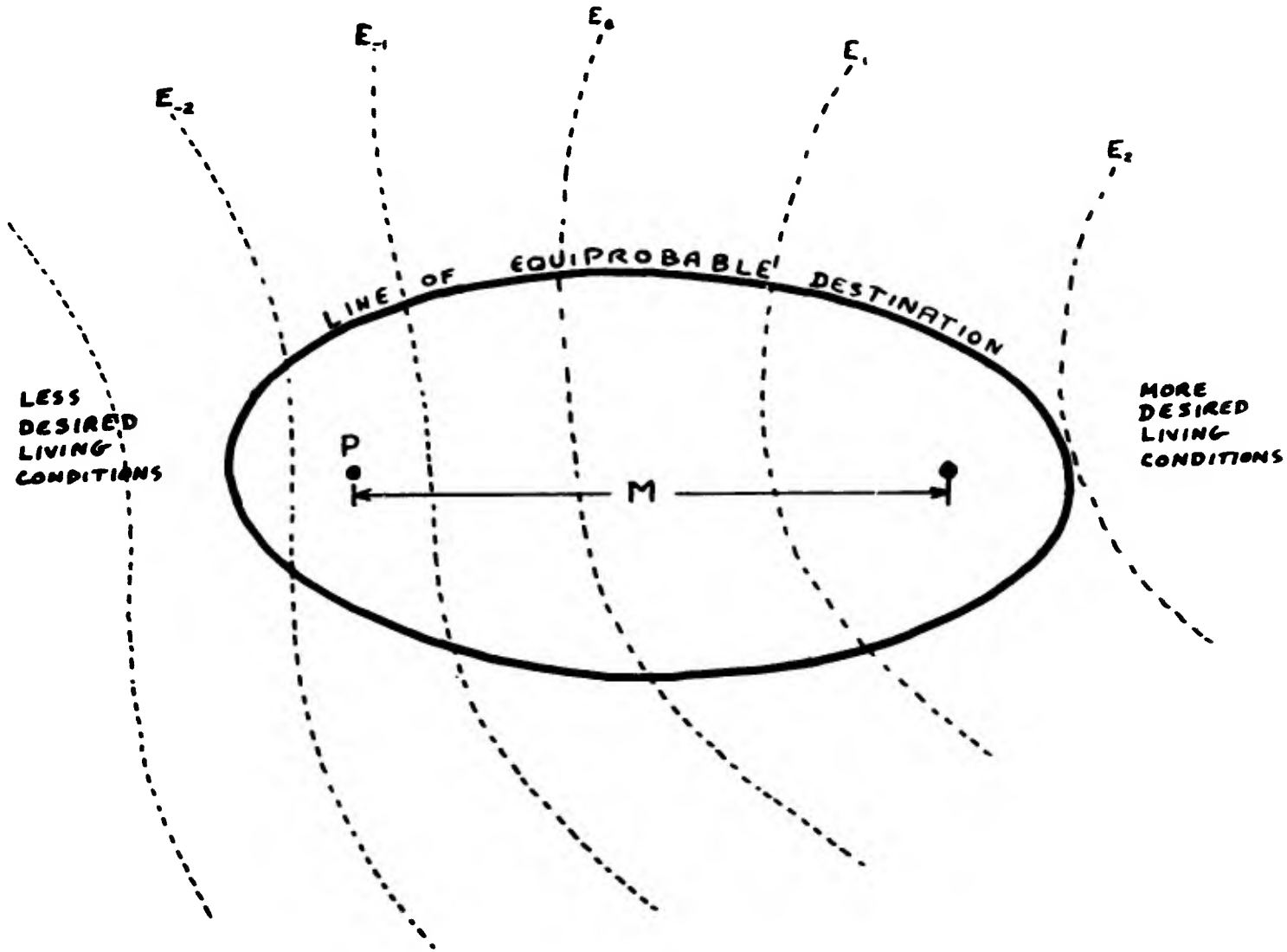


Fig. 5: Population Dynamics Schematic

## DECISION-MAKING ROUTINE

This routine provides the means by which a variety of resource management procedures can be tested and associated life styles which evolve as logical consequences can be evaluated. How is the current drift of human population from farm to city correlated with irrigation policies? How does a city develop as a result of the configuration of rapid transit systems? Is it better to buy imported water and grow wheat or to retrain farmers to be industrial workers, sell their manufactured products as exports and buy imported wheat?

Consider an atomic power plant large enough to service the Dallas-Fort Worth area. Suppose it is cooled by water from the surrounding reservoir. Evaporation from this cooling could amount to some 20,000 acre feet per year—enough to run a small city. What would be the implications of building the power plant on the coast and shipping the power to Dallas-Fort Worth? The advantage would be a saving in fresh water as the Gulf of Mexico water could be used for cooling. Apart from the line losses of power, could an ecological disaster occur to the marine life affected by the local rise in temperature of the water returned from the power plant?

While it is fairly straightforward to effect such decision making in an optimal manner using economic criteria, it is somewhat more involved to try to produce relative utility functions which can represent desired life styles of people. A good deal of work remains to be done in this area. Any reduction in water pollution and air pollution can be brought about; however, what will be the cost to the life styles of the people? If the pollution is not cleaned up, what will be the cost to the overall ecosystem? How do you decide the relative values of a second car for a family versus a healthier forest? Suppose one considers the optimum life styles for all components of the bioshpere. Is it possible that an optimal condition would call for the disappearance of the human species? To what extent can we say, "What is good for humanity is good for the biosphere?" Our executive subroutine requires answers to this type of questions.

## PRESENTATION OF RESULTS

Because of the volume of results which need to be examined for purposes of studying the evolution of the various components of the ecosystem model, extensive use has been made of storage scope output. In particular, movies have been made from the patterns evolving on the scope. As many scientists have already found, the three dimensional (x,y,t) view of an evolving pattern can accelerate scientific diagnoses by a quantum jump.

We have found that the movie output of our results has allowed us to reach other scientific disciplines and decision making management groups in a manner not possible before. We intend to exploit this discovery by making technology provide something which is vital to interdisciplinary research—a common language.

## APPLICATIONS

One clear application of our model is to produce optimal resource management practices. A secondary application derives from the ability of a scientist from one discipline to test his modelling efforts under the influence of dynamic boundary-conditions imposed by models from other impinging disciplines.

## ACKNOWLEDGEMENTS

Most of the programing and the detailed incorporation of observable data to the model described have been performed by Mr. William J. Parton as a part of his dissertation research in the Meteorology Department of the University of Oklahoma. The overall character of the model has been the result of a group effort directed by the author over the past two years. Computer time has been made available by the National Center for Atmospheric Research under the funding of the National Science Foundation.

## REFERENCES

Court, Arnold, 1961: "Area Depth Rainfall Formulas", J. of Geophys. Research, Vol. 66, No. 6, pp. 1823-1831.

Eddy, Amos, 1969: "A Meteorologically Oriented Computer Model of an Ecosystem", Trans. N. Y. Acad. SC., Series II, Vol. 31, No. 6, pp. 618-628.

Myrup, Leonard, 1969: "A Numerical Model of the Urban Heat Island", J. Appl. Meteorology, Vol. 8, pp. 908-918.

Parton, W. J. and Eddy, Amos, 1970: "A Numerical Model of Human Population Dynamics Influenced by a Polluted Environment", AMS Proceedings of the Second National Conference on Weather Modification, pp. 248-252.

# SIMULATION OF WEATHER-SENSITIVE MILITARY OPERATIONS

Ralph E. Huschke

Department of Environmental Sciences
The Rand Corporation
Santa Monica, California

## ABSTRACT

Based on, and illustrated by, experience in designing a computer model of a weather-sensitive STRICOM operation, a set of guidelines is suggested for building simulation models of military operations for the purpose of quantifying the value of weather services. Results from the STRICOM model are presented as an argument supporting the desirability for the weather services to engage in this kind of analysis.

## I. INTRODUCTION

This paper is being given because its subject — simulation of weather-sensitive military operations — is a real and current problem which should be of special concern to the weather services.

Basically, the problem is that military operations (systems, tactics, etc.) are being analyzed more and more by computer simulation (modeling) techniques; many of the operations being modeled are highly sensitive to weather; and few, if any, of these models contain an adequate weather representation. This was brought home to us meteorologists at Rand about two years ago when several operational models — addressing different operations and stemming from different groups within Rand — all seemed to mature about the same time. One thing that all these models had in common was the total absence of any weather factors. One analyst, in briefing the results of his model concerning maintenance scheduling for tactical aircraft in Vietnam, stated flatly that the results would probably have been significantly different had weather been taken into account. The users of another model, designed to evaluate the effectiveness of interdiction campaigns against lines-of-communication networks, admitted that their failure to include weather seriously eroded their confidence in tne results.

Why does this sort of thing happen? I believe that either of two simple answers explain the majority of these cases: either (1) the model designers initially do not credit weather as being a significant variable, and hence ignore it; or (2) they have so much respect for the complexity of weather that they choose not to allow it to complicate their model. Whatever the reason, it turns out to be next to impossible to insert weather into a model after it has been built. If weather sensitivity is a significant factor in an operation, and that operation is being modeled, then the weather effects have to be built into the original model.

I stated at the beginning that this problem should be of special concern to you, the weather services. Here's why. First, the provision of the meteorological know-how and data that has to go into these simulation models is obviously a weather-service job. Of course, if the model builders continue discounting the weather factor until it's too late, then there is little that the weather services can do. But I suspect that requests for this kind of assistance will be more frequent in the future.

Second, there is an important and self-serving reason for weather services to be concerned. The concepts of operational modeling lend themselves to demonstrating the *value of weather service* in the kinds of quantitative terms that the customer understands — costs, kill probabilities, number of targets destroyed, time to do a job, etc. If you accept that is is worthwhile to evaluate weather service in terms of operational contributions, then the weather service themselves, or their advocates, will have to perform such evaluations.

We at Rand had such an opportunity as participants in the recent Mission Analysis of the Air Weather Service (AWS). An overall objective of the Mission Analysis was to quantify AWS contributions to Air Force operations. Three different types of operation were selected for intensive study, and Rand agreed to examine the interface between the AWS and the U.S. Strike Command (STRICOM). We suspected from the start that any quantification would probably have to come from some form of computer model. [1]

I would like to pass on to you some of the lessons learned by us in this effort. I've drawn up a set of guidelines which should be generally applicable to the modeling of a variety of weather-sensitive operations. I will illustrate each guideline from our own modeling experience. And, finally, I will show you a sample of results so that you may judge for yourselves whether or not the substantial effort involved is warranted.

One final comment by way of introduction — if it is weather *service* that you wish to evaluate, then the simulation must involve *decisions* based on that service. Weather service has value only insofar as it improves operational decisions. Therefore, this kind of simulation must include not only the effects of weather on an operation, but also the effects of weather forecasts on an operational decision.

## II. GUIDELINES FOR WEATHER/DECISION MODELING

### 1. Learn the operation from the operator's standpoint.

This cannot be overstressed. The model must have credibility and this is the only way to get it. For a decision model in particular, it is very important to understand in some detail how the decision-maker arrives at critical decisions. What resources has he to work with, typically, and how do they vary with "scenario?"* To what extent is he dependent on collateral decisions made by others? What are the realistic time constraints on the operation? At what points does he depend upon weather service inputs to his thought processes? What are his options as functions of time and/or scenario? What value system is imposed upon him from above (e.g.: target priorities, minimum sortie rates), and what value system may he employ at his level? What is the objective of the operation; how do the component activities contribute to reaching this objective; and how does the value of their contributions vary according to scenario?

The STRICOM operation, while compact in the time dimension, is quite complex in terms of the variety and distribution of military forces that have to be coordinated. Figure 1 is a simplified geographical schematic of a typical strike operation, showing various force elements initially scattered throughout the United States, which have to be marshaled, supported, and transported, ultimately arriving at the point or points from which the assault is launched (e.g.: a final staging base and a forward operating base). The assault itself is normally conceived of as requring a paradrop of troops to establish an airhead in the objective area, followed as soon as possible by the airlanding of reinforcement and supporting forces — all of which may require the support of fighter aircraft operating from a forward operating base.

The entire operation may take from several weeks to several days, depending on urgency. Flexibility is high and command responsibility is quite diffused during the marshaling phase. By the time for the final launch decision, little flexibility is left and responsibility is strongly concentrated in the JTF Commander. Although the JTF Commander has overall responsibility for the entire operation and its ultimate success, it is clear that he places highest priority on accomplishing a successful H-Hour assault.

### 2. Determine acceptable measures of operational effectiveness.

Every operation has, at least theoretically, a quantitative goal. The simplest goal for a single operation is to "succeed," in which case the decision-maker tries to earn a "1" instead of a "0." If such a simple operation is repetitive, the decision-maker's performance may be judged by the relative frequency of successes; and if time is a factor, then the least time needed to attain a certain probability of success might be an acceptable measure of performance. Most often, however, the effectiveness of even a single operation is measurable on a scale: fraction of total target value destroyed; casualties inflicted; percent reduction of network throughput; miles of penetration into enemy territory; and so on. Further, these usually have to be modified by [one or more other factors]$^{-1}$, such as per day, per sortie, per friendly

*Throughout this paper, the term "scenario" will be used to connote the political and military environment of an operation, that is, the location, urgency, level of conflict, enemy strengths and weaknesses, etc.

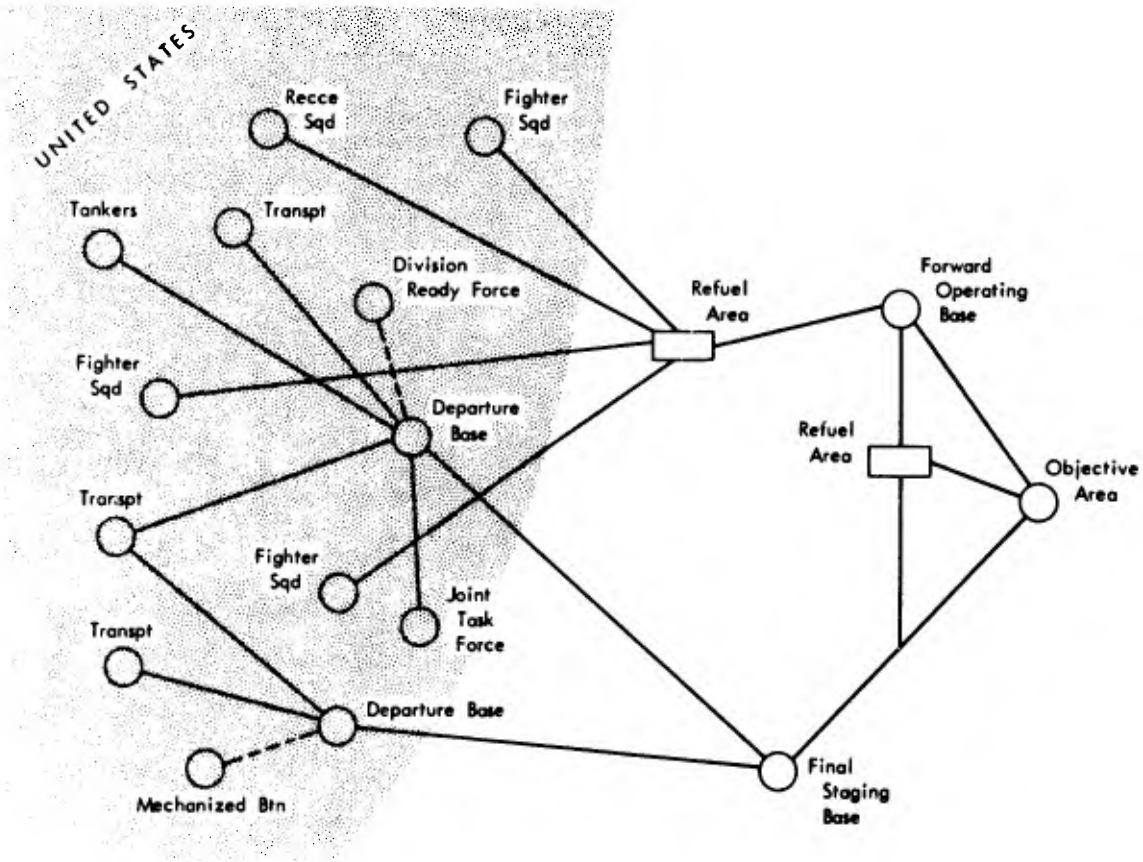


Fig. 1 — Schematic diagram of a typical STRICOM operation.

casualty, per dollar. The number of meaningful combinations of such quantities is very large. (Fortunately, many are easily transformed from one to another.)

The point is that the measure of effectiveness that will show up in the results of the model must be one that can be understood and accepted by the operator — he is not at all interested in a forecaster's skill score or the RMS error of the 500-mb prog. (It is for the weather service to draw the connection between the latter and their contributions to operations.)

The STRICOM case is rather clearly one of "succeed" or "fail." In the kind of emergency to which STRICOM would be called upon to respond, their mission would be quite straightforward and the opportunity for a "partial" success quite limited — at least, STRICOM personnel accept this rationale as being legitimate. Further, the success of the mission is highly dependent on the success of the H-Hour assault; a mission might fail after a successful initial assault, but the reverse would seldom be true. Time would often be an important factor in that the allowable waiting period before launching an assault would be limited. Therefore, the simplest acceptable measure of the effectiveness of the STRICOM operation — and the one that we used — is the probability of a successful assault as a function of the number of days of allotted time to initiate the assault.

3. Simplify the operation within the bounds of credibility.

This is the key problem in actually designing a model. A compromise must be drawn between real-life complexity and computational practicality. This is a delicate process, for the natural tendency of the operator is to retain as much realistic complexity as possible to make the model "believable" to him, while the tendency of the analyst is to oversimplify for the sake of computational ease and to facilitate interpreting the results. The ensuing give-and-take must be endured, for in the end, both must be reasonably well satisfied.

In the course of simplication, the analyst must become very scenario-minded — "If I eliminate this part of the operation from the model, am I eliminating a relevant class of scenarios?"

In the end, the relevance of the scenarios to which the model can be applied will determine a large part of its acceptability.

Many operations are large and involved. Many time-dependent decisions are made concerning widely scattered activities, each of which bear to a greater or lesser degree on the eventual outcome of the operation. Yet, a *complete* model is *not* necessary to yield useful information and may, in fact, hamper a useful interpretation of the results. Ideally, the operation should be scaled down just to that point where the operator can still claim it as his own. (This may even mean leaving some things in that you know will have little effect on the results.) A strong motivation for us, the weather services, to minimize the dimensions of the operation is the fact that time and space relationships determine the amount and sophistication of weather data required by the model. In fact, data limitations will often enough dictate simplifications that you would prefer not to make.

The real complexity of a STRICOM operation is illustrated in Fig. 2, in which the time and space histories of all the force elements are charted from D - 3 through D-Day. It is not necessary to explain this chart in detail for the purposes of this paper — the chart is simply a device to examine the fine structure of the operation. The lower case letters stand for activities that have various kinds and degrees of weather sensitivity (the numbers stand for locations), and for each of which some form of weather forecast is required. There are well over 100 on this diagram.

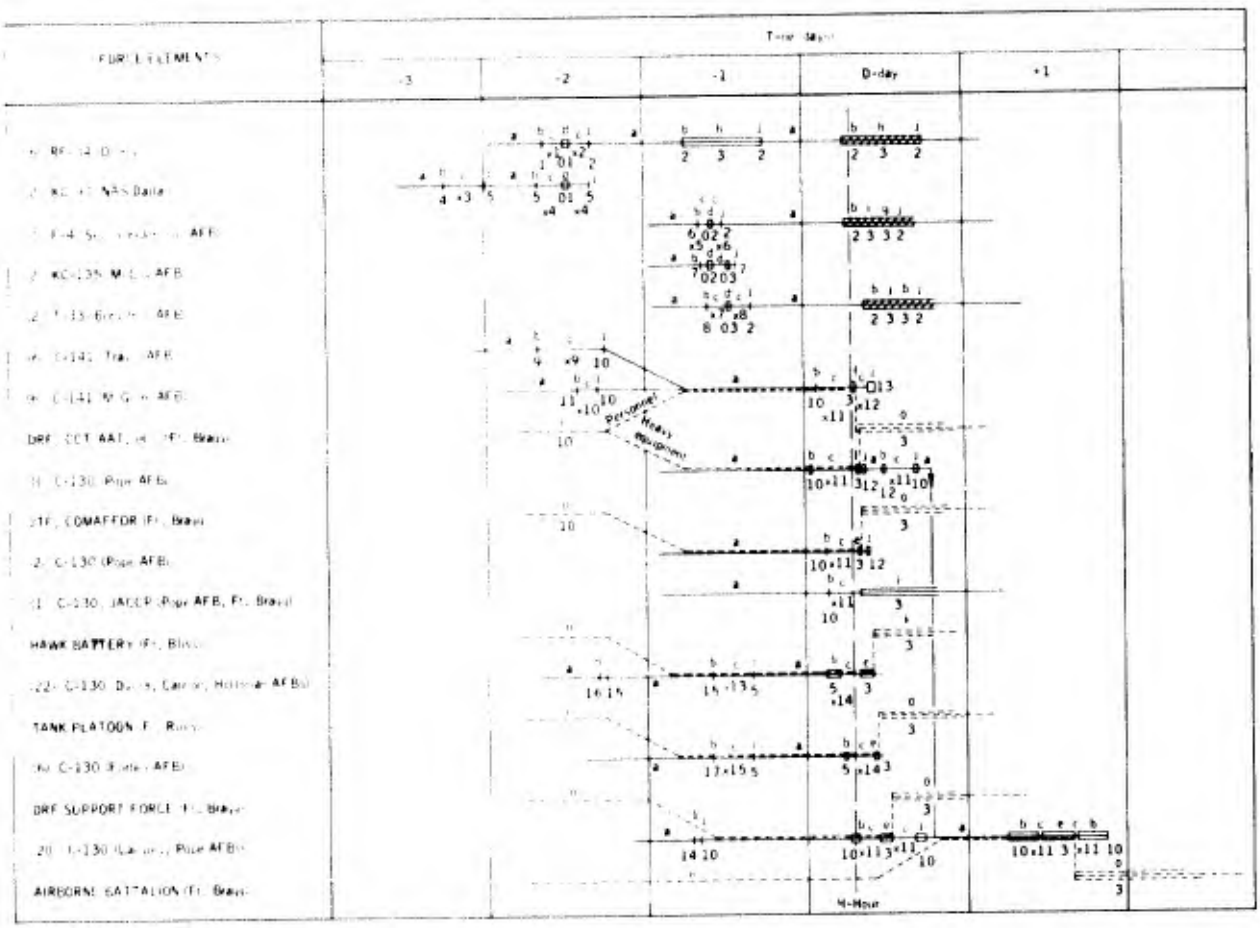


Fig. 2 — Time schematic of a typical STRICOM operation (based on Exercise BOLD SHOT/BRIM FIRE 2-69)

The first question in our simplification problem was obvious. Could we justify omitting *all* of the activities that occur during the marshaling phase (D - 3 to D - 1)? We were told that, in STRICOM exercises, weather problems during the marshaling phase were often bothersome, but seldom caused critical delays or altered assault plans. In a real emergency situation, there would be even greater flexibility to circumvent weather problems as the task force is being assembled. Hence, it was acceptable for us to concentrate on

the assault itself. This meant that the time points of greatest interest were H-Hour (actually, from about H - 1 to H + 3) and some prior hour at which the crucial weather forecast was issued. The locations of interest were the objective area and possibly a final staging base for the troops and transports, and a forward operating base for the fighter aircraft — the latter depending on the types of activities to be included in the model.

By various means (interviews, questionnaires, direct observation, etc.), an acceptable minimum list of assault-related weather-sensitive activities was determined:

(1) The flight of the troop transports from the final staging base to the objective area;
(2) the paradrop at H-Hour;
(3) combat air patrol;
(4) close air support;
(5) the airland of supporting forces and equipment; and
(6) the ground battle.

It was later determined that two of these (the first and last) could not be handled because climatological data could not adequately describe enroute flight weather and soil trafficability. Their omission weakened the model, but not to an unacceptable degree.

4. Look for credible constraints on flexibility.

That the decision-maker must have some flexibility is axiomatic, but it is helpful in simulation studies to keep his options down to a workable minimum. The real operational world, it turns out, is not as flexible as it might be. It is undoubtedly true that many cases of operational rigidity serve to reduce the potential value of weather service — but this is a separate topic in itself, to which modeling techniques might be profitably applied.

At the time of the final decision whether or not to launch a strike assault, the STRICOM JTF Commander can no longer significantly alter the tactical plan. He must go with the personnel, weapon systems, and operations plan on hand, or not go. Further, he has no choice as to *where* the assault will take place; there would seldom be a secondary objective area far enough from the primary to warrant an assumption of significantly different weather conditions. Therefore, his decision simplifies to one of "go" or "delay."

Delay for how long? The typical paradrop assault requires a maximum amount of daylight for accomplishing the ground-battle objectives, and hence H-Hour is nearly always scheduled for the first light of day. The Commander might consider a delay of two or three hours, but if it appeared necessary to wait longer than that for acceptable conditions, he would choose to wait until H-Hour on the next day, i.e., a 24-hour delay. Since the climatological records available for most areas of interest in our model were of 3-hourly surface weather observations, we were forced to define H-Hour weather as that reported in the first 3-hourly observation at or after local sunrise. Hence, we were unable explicitly to consider hourly changes that would affect a short-term delay, and the delay option was restricted to 24 hours only.

In addition to these operational constraints, we impose two more simplifications on the decision process: (1) the Commander has accurate intelligence information, and (2) he believes the weather forecast.

5. Simplify and quantify nonweather decision motivations.

How often we are admonished that weather isn't the only thing that affects operational decisions. True — so some attempt has to be made to account for at least the major nonweather decision criteria. Typically, some probable target value destroyed would have to be played against a probable cost (e.g., attrition), and their ratio would enter into a decision rule that would also include a weather forecast. The change of values and costs with time will often be a significant factor. In a model of a protracted operation, effects on systems availability, such as maintenance and attrition, may have to be considered as decision criteria. In general, the identification and quantification of these nonweather factors require thorough coordination with the operator.

In an operation involving several coordinated weather-sensitive activities and adjudged by a simple succeed-or-fail criterion (as we modeled the STRICOM operation), the basic nonweather factor is the relative importance of the different H-Hour activities as a function of the scenario. By interview and questionnaire, we gained insight into the

way a "composite" JTF Commander would assign importance values to the activities. On a scale of 0 to 10, the importance values reflect the following meanings:

0 = This activity has no relevance in this operation; it is totally unimportant.
1-3 = It would be nice to have this capability "just in case," but this operation can very likely proceed unhampered without it.
4-6 = The absence (or failure) of this activity would probably create hardship, but the likelihood of overall operational success is still high.
7-9 = This capability is very important; to proceed in the face of its probable failure implies extreme urgency, or that all other factors are nearly ideal, or both.
10 = If this activity fails, the entire operation can be expected to fail.

In addition, these operational importance values are additive, that is, the sums of the values for two or more activities are interpretable on the scale given above.

6. Quantify weather effects on each component activity.

There is very little quantitative guidance available to help with this necessary task. Scales or thresholds of weather effects, with rare exception, are arbitrary -- at best, reasoned and experienced guesses at the way weather affects an operation, activity, or weapon system. They vary with the arbiter and his sources of information. It is very important, therefore, to allow weather effects to be a *variable* input to a model. Many operators will have a more or less formalized quantification of weather effects built into their standard operating procedures. This is the logical starting place to develop an appropriate quantification for the model. Usually, the S.O.P. weather thresholds will be overly simple and often will have an aura of traditionality about them. They will always bear careful scrutiny; and any attempts to alter and/or sophisticate them will (and should) lead to some intensive dialogue with the operator.

With the continued paucity of hard data from field tests of weather effects, it becomes tempting to try to calculate weather effects as a "model within a model." A case in point would be the problem of visual target acquisition, where the weather effect is very complex and the total problem is further complicated by such things as target size and contrast, background clutter, aircraft altitude and speed, sun angle and look angle, etc. A model which accounts for the major of these factors, including the atmosphere, might be imbedded in a larger model of a tactical bombing operation.

The detailed rationale for weather-effect quantification used in the STRICOM model is given in Ref. 1 and will not be repeated here. We decided on a two-threshold system -- one separating "unfavorable" from "marginal" conditions, the other separating "marginal" from "favorable," where (imprecisely) "unfavorable" implies a high probability of failure due to weather, and "favorable" implies a high probability that weather will have little deleterious effect. The weather elements and thresholds thereof for each of the four H-Hour activities are shown in Table 1.

7. Determine a method for approximating forecasting skills.

This is a problem which, in itself, warrants a great deal more data collection and analysis than has yet been applied to it. The pros and cons of various methods of forecast verification is a large and old subject in meteorology. We shall not get deeply into it here — but the fact of the matter is that available forecast verification data do not lend themselves readily to the realistic simulation of weather forecasting skills.

I would like to suggest that most forecast simulation schemes will require three main ingredients:

(1) a completely objective "standard" forecasting method.
(2) a means of measuring the skill of actual forecasting relative to the standard; and
(3) a means of relating skill to other factors which can be either logically assumed or objectively derived.

The first of these is the least problematic — a "persistence forecast" for any one or combination of weather events can be straightforwardly calculated from a good set of climatological records. This includes, as a useful example, the probabilities of persistence forecasts for

| Event Designator | Class Intervals of Weather Events | Favorability of Weather Conditions According to Activity | | | | |
|---|---|---|---|---|---|---|
| | OBJECTIVE AREA | | | | | |
| u,u′,x,a | Ceiling (ft) and Visibility (mi) | Paradrop | Airland | CAS: Dive Bomb | CAS: Low-Level | CAP |
| 1 | . . . ceiling < 300 or visibility < 1 | unfavorable | unfavorable | unfavorable | unfavorable | unfavorable |
| 2 | ceiling ≥ 300 and visibility ≥ 1 and ceiling < 600 or visibility < 2 | | marginal | | marginal | |
| 3 | ceiling ≥ 1,000 and visibility ≥ 2 and ceiling < 1,500 or visibility < 3 | marginal | favorable | marginal | favorable | marginal |
| 4 | ceiling ≥ 1,500 and visibility ≥ 3 and ceiling < 5,000 or visibility < 5 | favorable | | favorable | | favorable |
| 5 | ceiling ≥ 5,000 and visibility ≥ 5 and ceiling < 10,000 | | | | | |
| 6 | ceiling ≥ 10,000 and visibility ≥ 5 . . . | | | | | |
| | OBJECTIVE AREA | | | | | |
| v,v′,v,b | Surface Wind (knots) | Paradrop | Airland | N. A. | | N. A. |
| 1 | . . . wind > 40 | unfavorable | unfavorable | | | |
| 2 | 40 ≥ wind > 25 | | marginal | | | |
| 3 | 25 ≥ wind > 15 | marginal | favorable | | | |
| 4 | 15 ≥ wind . . . | favorable | | | | |
| | FORWARD OPERATING BASE | | | | | |
| w,w′,z,c | Ceiling (ft) and Visibility (mi) | | | CAS: Dive Bomb | CAS: Low-Level | CAP |
| 1 | . . . ceiling < 300 or visibility < 1 | N. A. | N. A. | unfavorable | unfavorable | unfavorable |
| 2 | ceiling ≥ 300 and visibility ≥ 1 and ceiling < 1,000 or visibility < 2 | | | marginal | marginal | marginal |
| 3 | ceiling ≥ 1,000 and visibility ≥ 2 . . . | | | favorable | favorable | favorable |

Table 1 — Summary of weather thresholds used in STRICOM weather/decision model.

all possible combinations of pertinent weather events, given that a certain combination of events occurred at verification time.

The second ingredient is, today, the most problematic. For one thing, insufficient weather elements are included in routine, compatible, forecast verification programs. Are wind, temperature, cloud amount, or precipitation forecasts made with the same "skill" as ceiling and visibility forecasts? Second, those forecasts subject to verification are apt to be too "routine" to be representative of forecasting skill motivated by operational pressures. Third, the old question of forecast bias induced by the mere existence of a scoring system still needs to be examined. One approach that could solve at least part of this problem would be a continuous program of sampling from a variety of forecast types and locations. The result would be a climatology of forecast data, compiled so as to be compatible in content and format with a standard data base of actual observations. The analysis of forecasting skill could then

proceed in a very comprehensive manner by computer techniques.

The third ingredient, the relating of skill to "other factors" would also be enhanced by the above-suggested forecast data base. It is well known now that skill is a function of the frequency of occurrence of the weather condition being forecast. Are there more subtle climatic influences on skill? Or influences related to availability of observing and forecasting systems? Or influences related to operational situations? Are we measuring skill correctly?

For the STRICOM weather/decision model, AFCRL studied short-range ceiling-and-visibility forecast verifications for detachments of the 8th Weather Squadron, AWS, and calculated skill scores, S:

$$S = \frac{Pr\{a=u\} - Pr\{x=u\}}{Pr\{u\} - Pr\{x=u\}} \quad ,$$

where a is the actual forecast weather event, x is the persistence forecast event, and u is the observed event. (S measures the fraction of the gap between persistence and perfect forecasts that is closed by the forecasters.) Skill scores (for 12-hour forecasts) were plotted against the occurrence probabilities of weather events, and a linear least-squares fit was calculated, which is shown in Fig. 3 as "average 8WS capability." Figure 3 also shows several variations in forecasting skill which we estimated using the plotted S *vs.* Pr{u} points as a guide. From these functions, which relate Pr{a=u} only to Pr{u} and Pr{x=u}, the probabilities of correct AWS forecasts can be calculated directly from climatological records. These probabilities are those that appear on the diagonal of a forecast verification matrix (forecast *vs.* observed events). For the off-diagonal, incorrect forecast probabilities, the residual probability for each row was distributed according to an arbitrary weighting system based on a qualitative study of actual verification matrices.

9. Establish decision rules and effectiveness criteria.

The decision-maker makes "rational" decisions; that is, under the given constraints, the decision is such that he thinks he is maximizing the measure of operational effectiveness. In real life, all of the inputs to his decision are uncertain — intelligence estimates, personnel and system performance, weather forecasts — but in the kind of model being discussed, the principal uncertainty, if not the only one, should be the weather forecast. If the objective is to evaluate weather service contributions, nonweather-related uncertainties would complicate and becloud the results. (On the other hand, for those operational models designed to study tactical and systems alternatives, the nonweather uncertainties — varying kill probabilities, attrition rates, etc. — should be explicit. Unfortunately, I know of no such model that adequately treats also the effects of weather or forecasts.)

Decision rules, then, combine the quantified nonweather decision criteria (discussed earlier) with weather forecasts. They should be formulated so that a decision based on a correct forecast does maximize the measure of operational effectiveness, which means that the results of the operation are judged by the same criteria as those used by the decision-maker.

Hence, the operational importance values are used in two ways in the STRICOM model. First, they represent the *true* nature of things: if an activity is given an importance value of 10, the failure of that activity results in the failure of the entire operation. Second, they represent the JTF Commander's *assessment* of the situation: if the weather forecast is unfavorable for an activity having an importance value of 10, he will elect to delay the operation. The importance values are actually factors by which the consequences of unfavorable weather are weighted. Thus, as indicated in Fig. 4, for favorable weather, a weight of zero applies, and for marginal weather, some weight between zero and the importance value is appropriate.

In Fig. 4, take weather class "c" as an example. Paradrop weather is predicted to be *marginal*. The weight of 5 implies that problems will be encountered that would not exist were the weather ideal; yet, in themselves, those problems would probably not result in the *failure* of the mission. However, the CAS weather forecast is *unfavorable* (for dive bombing), and the CAS importance value of 6 predicts additional problems which, along with the paradrop problems, results in an overall prediction of mission failure ($5 + 6 \geq 10$). A slightly more *favorable* weather forecast, class "d," predicts no paradrop difficulties, and even though CAP weather is still forecast to be *unfavorable* and CAS weather *marginal*, the overall risk appears small enough to warrant a *go* ($6 + 2 < 10$).

When the weather classes represent weather that occurs at H-Hour (rather than predicted weather), the same rules determine *success* or *failure* of the mission.

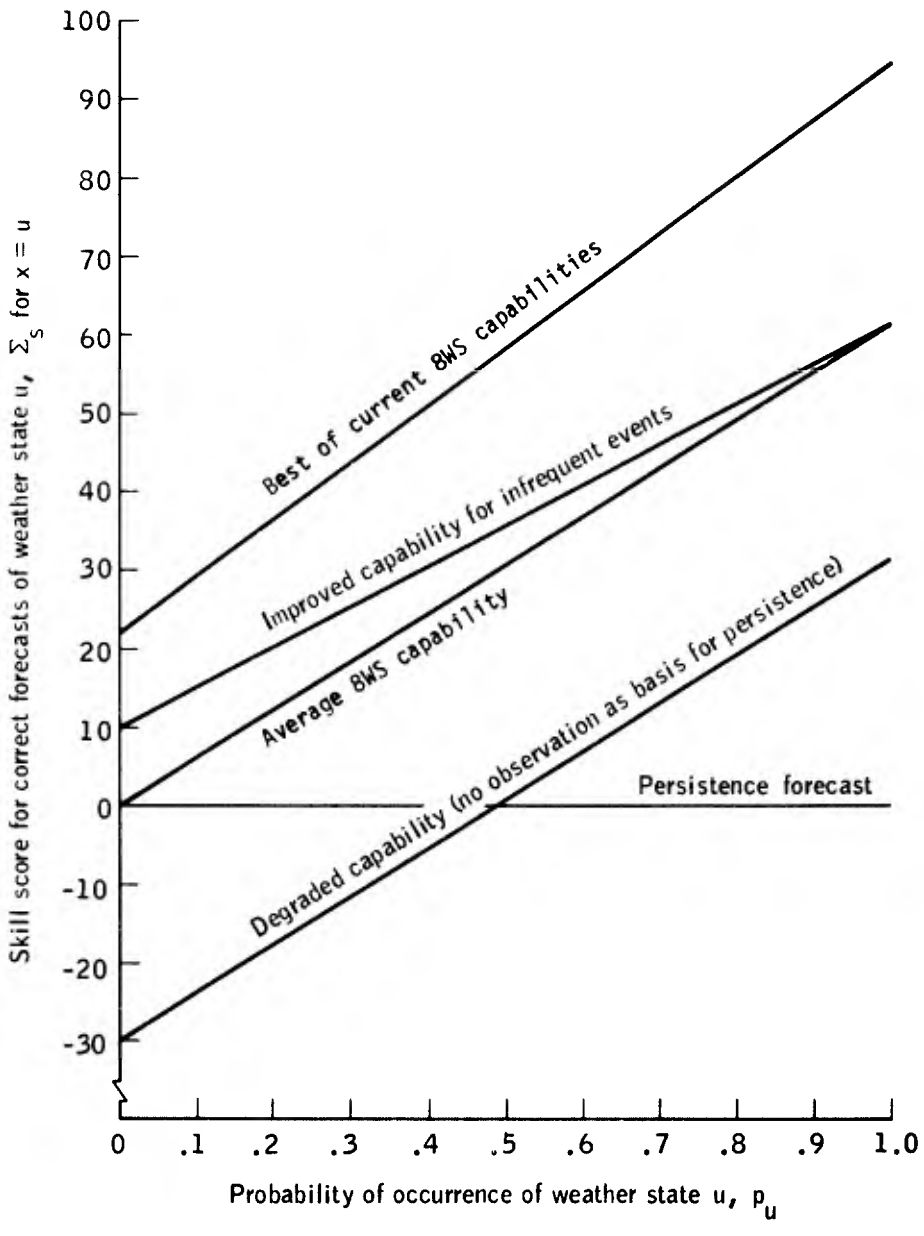


Fig. 3 -- Representations of forecaster skill as employed in STRICOM weather/decision model.

The model calculates estimated probabilities of mission success for missions having been allotted N days for initiation. On every day prior to Day N, a decision is made either to *go* or to *delay* one day. Whenever the decision is to *go*, the mission either *succeeds* or *fails*; and when the mission is a *failure*, there is no further opportunity to make it a *success*. A *delay* decision on Day n, prior to Day N - 1, allows the opportunity for another decision to be made on Day n + 1. A *delay* decision on Day N - 1 is tantamount to a *go* decision on Day N, the last allotted day to initiate the mission.

The basic probabilities that are needed to compile the *success/failure* results can be thought of as filling a 2×2×2 matrix, as illustrated in Fig. 5. (The column under "Delay 1 Day" is a double column to reflect the two modes of a *delay* decision as explained in the previous paragraph.) Each cell represents a different combination of decision and operational conditions; for each a probability is computed; and for each there is a specific implication in terms of a mission *success* or *failure*. These implications are noted in the cells.

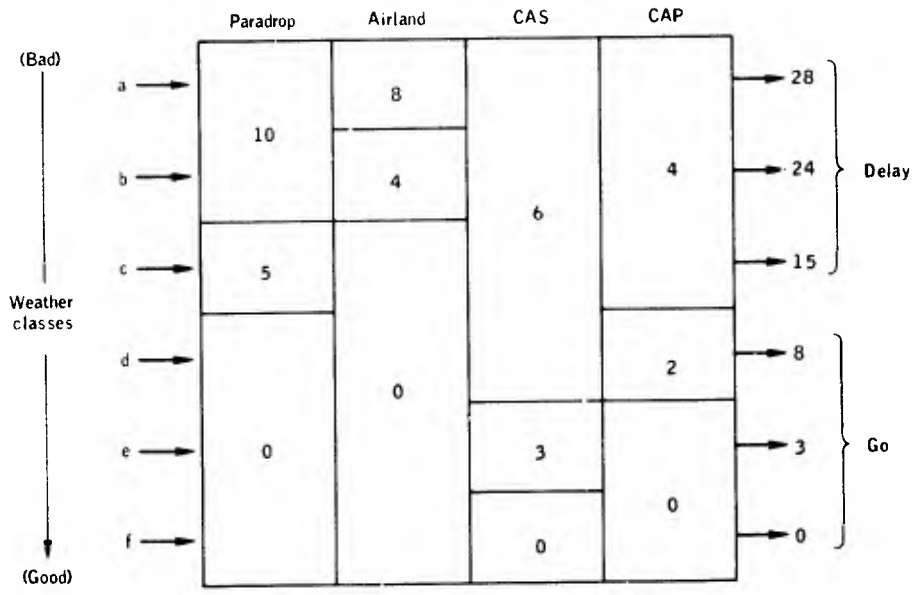


Fig. 4 — Illustration of the way weather forecasts and operational importance values are combined to produce decisions in STRICOM weather/decision model. (Explanation in text.)

| Operational Conditions | | Decision | | |
|---|---|---|---|---|
| | | | Delay 1 Day | |
| Day n | Day n + 1 | Go on Day n | n < N - 1 (Decide again on Day n = n + 1) | n = N - 1 (Go on Day N) |
| favorable | favorable | 000 success | 100 missed opportunity | 100 success |
| | unfavorable | 001 success | 101 missed opportunity | 101 failure |
| unfavorable | favorable | 010 failure | 110 averted failure | 110 success |
| | unfavorable | 011 failure | 111 averted failure | 111 failure |

Fig. 5 — Implications of result probabilities for STRICOM weather/decision model.

10. Write credible scenarios to fit the model.

This is the final test of the model's acceptability. No matter what type of operation is being simulated, some class of experiences or threats (scenarios) has inspired the entire effort. Many simplifications have been made, but room was left to vary a number of input quantities which purport to represent scenarios -- locations, times of year, threat levels, target values, force composition, etc. These inputs now have to be translated back into written scenarios, not necessarily complex or detailed, but in the operator's language so that he may have confidence that the output of the model pertains to *his* kind of operational problem.

Table 2 contains four abbreviated scenarios which were "run" on the STRICOM weather/decision model. Any of these scenarios can be applied to several different geopolitical arenas where strike operations could conceivably be required in the future. These scenarios only "set the stage," and their sole purpose is to supply the rationale for quantifying the operational importance values. For a model as simple as ours, no additional detail is warranted.

| Situation and Operational Importance | Operational Importance Value | | | |
|---|---|---|---|---|
| | Para-Drop | Air-land | CAS | CAP |
| Situation 1: (Major assault — strong air and ground resistance.) Enemy holds airfield. Paratroops essential to secure airhead. Airland required as soon as possible after H-Hour to provide mechanized forces. Enemy ground strength makes CAS very important, and enemy air power makes CAP essential. | 10 | 8 | 8 | 10 |
| Situation 2: (Evacuation — weak air and ground resistance.) Enemy strength at airhead probably not sufficient to deny direct airland, but prior paradrop desirable as insurance. Airland required for immediate evacuation of U.S. nationals. Fighter aircraft probably not required except as psychological adjunctof the assault. | 5 | 10 | 2 | 4 |
| Situation 3: (Major non-airhead assault — strong ground but weak air resistance.) Objective is to engage enemy with paratroops near a drop zone that is some distance from an airhead. Enemy ground resistance expected to be heavy; therefore CAS is essential. Airland subsequent to H-Hour and not in battle area. Enemy has no air power, hence CAP not required. | 10 | 0 | 10 | 0 |
| Situation 4: (Evacuation — runway barricaded but otherwise minimal resistance.) Runway to be used for airland is barricaded with debris. Paratroops must clear this, because primary objective is immediate evacuation of U.S. nationals. No enemy air power, and light ground resistance is expected. | 10 | 10 | 2 | 0 |

Table 2 -- SUMMARY OF SITUATIONAL SCENARIOS EMPLOYED IN STRICOM STUDY

## III. RESULTS FROM THE STRICOM MODEL

The final four figures (Figs. 6 to 9) show a sample of results from the STRICOM simulation study, emphasizing the sensitivity of the model to variations in some of the basic input quantities — time of year, scenario, force structure. Sensitivity to forecasting skill and alloted time is shown on each of the graphs.

The vertical scale is the "probability of success" calculated by the model. *What the model actually calculates is the probability that a correct decision will be made based on weather-forecast information that crudely relates military system performance to weather conditions.* The potential contribution of the Air Weather Service is bounded on the bottom by the mission-success probability in the complete absence of weather forecasts and at the top by the success

probability given perfect forecasting. In the figures, the "no forecast" curve is drawn on the assumption that the decision would always be to launch the assault at the first opportunity regardless of weather information; hence it is a horizontal line having the value of the unconditional probability of success on the first day. The "perfect forecast" curve represents the unrealizable maximum contribution of weather service. The fact that perfect forecasting does not guarantee operational success — even in this model which contains no nonweather uncertainties — is the consequence of the persistence of unfavorable conditions throughout the entire period (the allotted time) during which the mission could be attempted. The shaded area represents a realistic range of weather forecasting capabilities, bounded on the bottom by the "degraded" capability (see Fig. 3), and at the top by the "best" demonstrated skill in the verification data. All "forecasts" shown in these results are for a 12-hour prognostic interval.

Finally, some care must be used in interpreting the horizontal "allotted time" scales -- that is, for example, the success probabilities shown for 3 days allotted time are those that would accrue if the mission had to be attempted within 3 days; they are *not* the success probabilities by the third day of a mission that has 7 days allotted time.

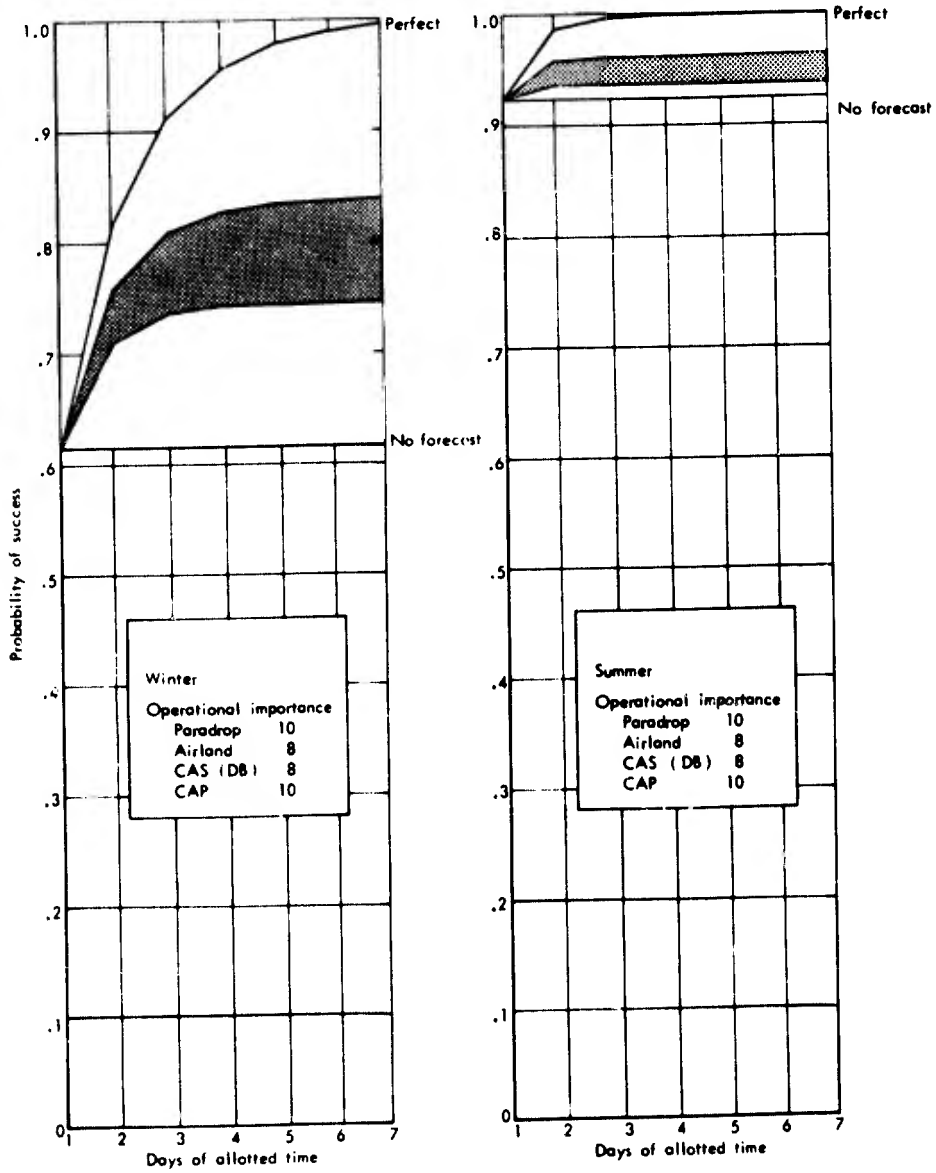


Fig. 6 — STRICOM model results emphasizing seasonal variation in success probabilities.

Figure 6 emphasizes the *seasonal*, or climatic, variability of the contribution of weather forecasting to mission success. The location, scenario, and systems and tactics employed are the same in both graphs. This figure clearly shows that the operational value of weather service is a function of climate — seasonal weather. In the winter at this location, the approximate "best" forecasting service adds 20 to 22 percent success probability, over no forecasting, for operations allowed 3 to 7 days for completion. In summer, the "best" contribution adds only about 4 percent from the second day on. The allocation of the best possible weather-service manpower and systems to the winter operation could obviously pay significant dividends. The potential payoff for a similar meteorological effort in the summer case would be much smaller.

In Fig. 7 it is shown that weather-service value varies as a function of operational objectives and enemy resistance — the scenario. The location and time of year are the same in both graphs. The basic message quantified by this set of results is an intuitively obvious one: the operational value of weather forecasting increases with the operational value of weather-sensitive activities (need to use weather-sensitive systems).

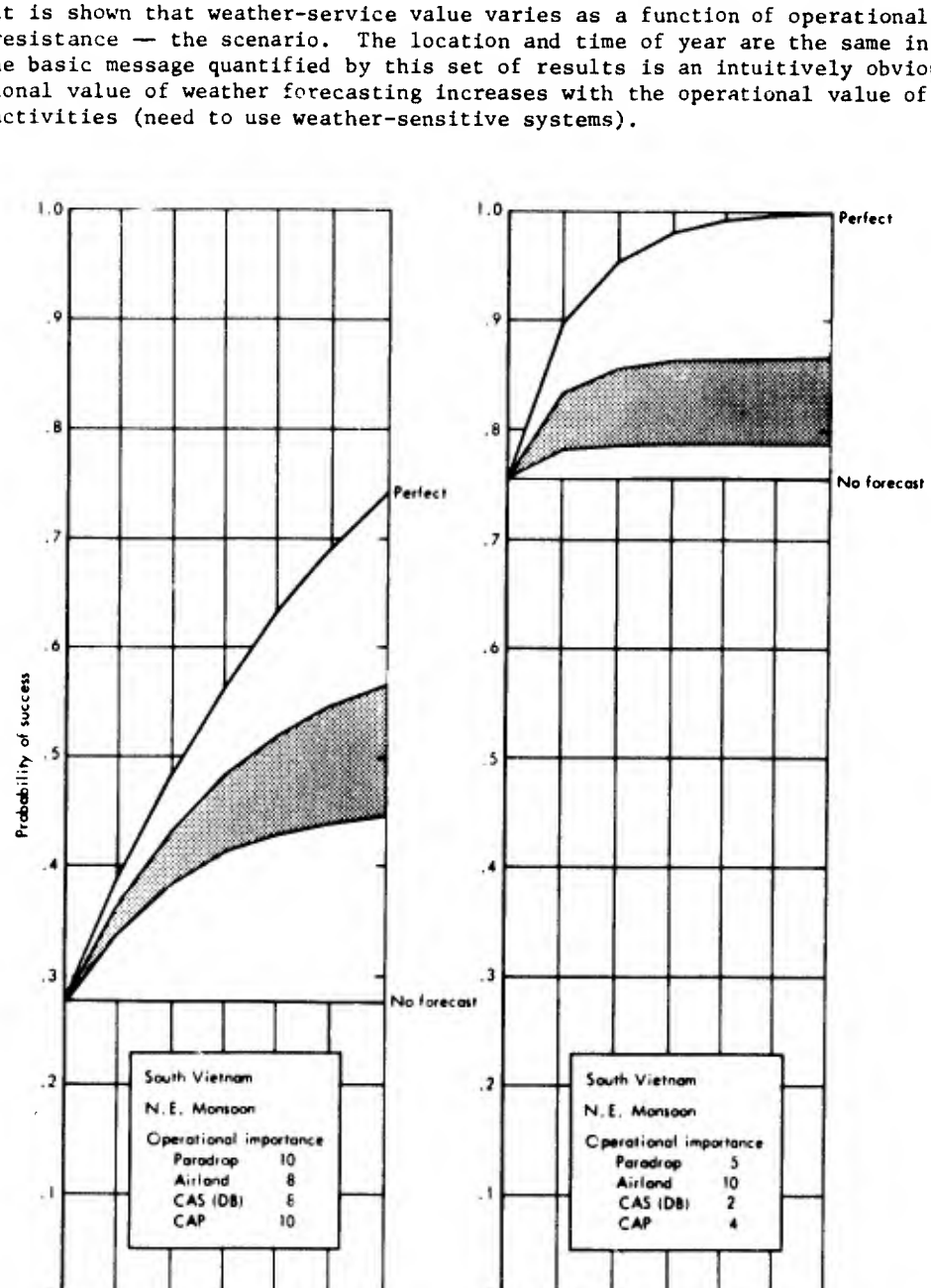


Fig. 7 — STRICOM model results emphasizing differences in success probabilities due to two different scenarios.

Figure 8 shows how the use of a less weather-sensitive system, low-level bombing instead of dive bombing for close air support, can result in an appreciable gain in the unconditional probability of success in certain climates — a gain from 33 percent to 64 percent in this case.

Figure 9, however, illustrates a subtle, but perhaps important complexity in tradeoffs between weather-forecasting skill and "bad-weather" weapon systems. The location, the scenario, and the CAS systems are the same as in Fig. 8; the season is different. Given an allotted time of 3 days or more, *the indicated probability of success with any degree of forecasting skill is greater for the more "weather-sensitive" divebomb system than for the low-level system.* It is possible that this apparent contradiction is simply a misleading consequence of the way in which forecasts are generated by the model. It is possible that the skill of STRICOM forecasters — or any forecasters intimately engaged in a strike operation — is not properly represented by the model; that is, they might be less "optimistic" or have a greater respect for infrequent weather events. It is also possible that these results are realistic. Whatever

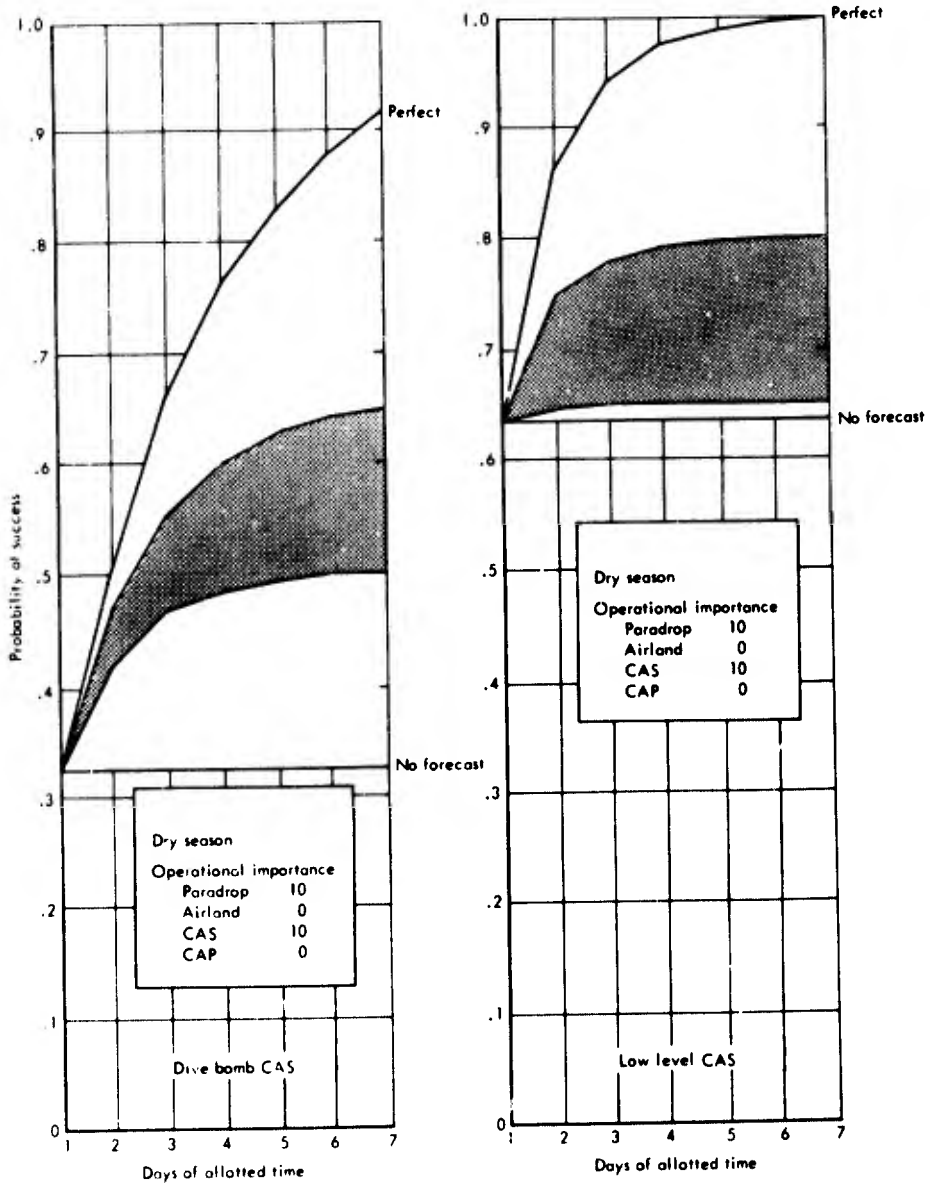


Fig. 8 — STRICOM model results emphasizing differences in success probabilities resulting solely from different CAS bombing systems.

the case, these implications for the competitive value of weather service as a contributor to operational effectiveness should be taken seriously enough to spur on continued study. For the present, these implications should at least help to crystallize what has been an amorphous and insubstantial appreciation of weather-service value.

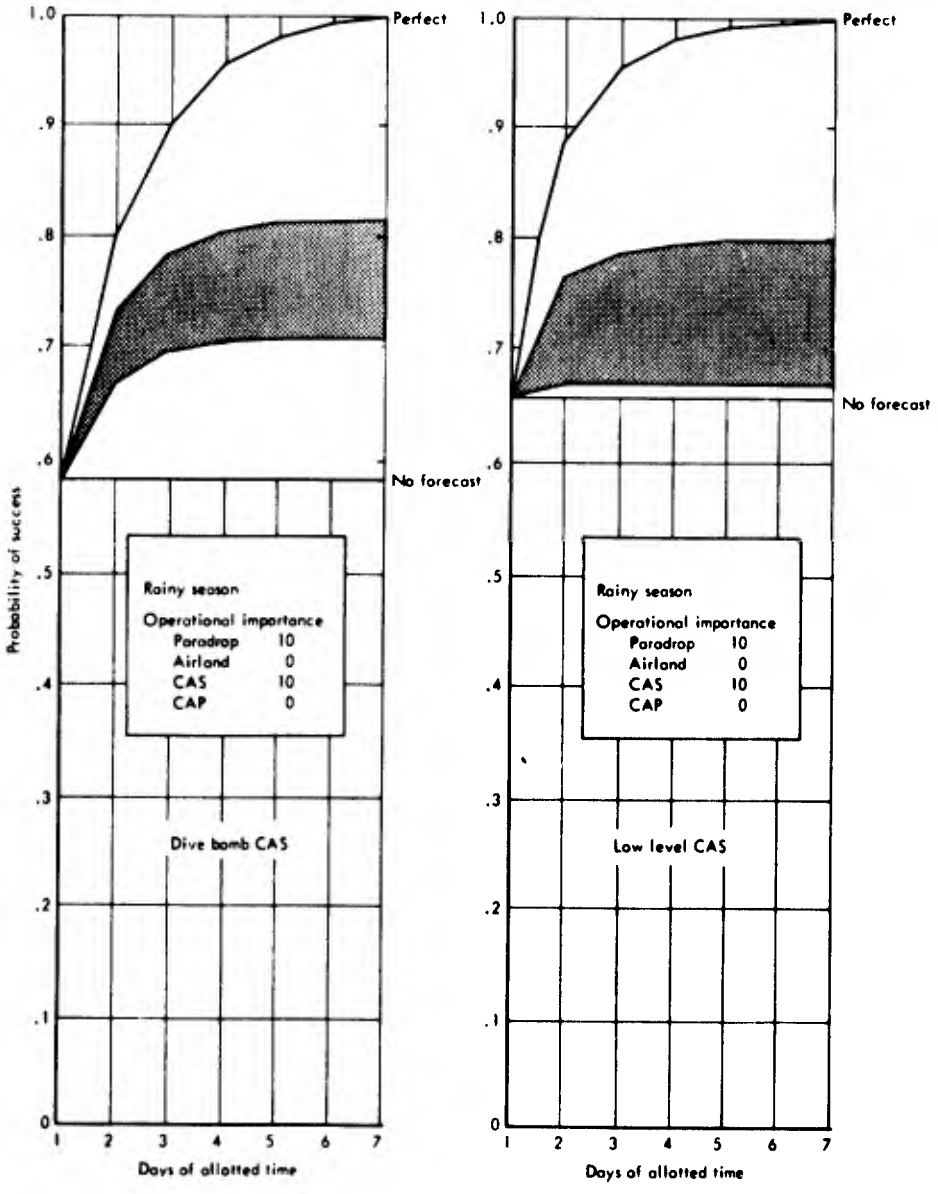


Fig. 9 — Same as Fig. 8 in all respects except that time of year is rainy season instead of dry season.

## REFERENCE

1. Huschke, R. E. and R. R. Rapp. "Weather Service Contribution to STRICOM Operations: A Survey, a Model, and Results." Final Report on Phase I for Air Weather Service Mission Analysis, R-542-PR, The Rand Corporation, Santa Monica, Calif., September 1970.

# ENVIRONMENTAL SIMULATION IN AIR-POLLUTION CONTROL

George C. Holzworth*

Division of Meteorology
National Air Pollution Control Administration
Public Health Service
U. S. DEPARTMENT OF HEALTH, EDUCATION, AND WELFARE

Abstract

The program that the National Air Pollution Control Administration is actively pursuing nationally to protect and enhance the quality of the Nation's air resources is reviewed. In connection with plans to prevent and alleviate air-pollution episodes, the air pollution potential advisory service of the U. S. Weather Bureau is described, particularly in respect to forecast procedures and automation thereof. Research is in progress to quantify the national advisories as well as to increase their lead time.

The type of simulation discussed is mainly concerned with large scale or general features of dispersion in the planetary boundary layer. As a prelude, it would be in order to review the program that the National Air Pollution Control Administration (NAPCA) is following nationally to protect and enhance the quality of the Nation's air resources.

Figure 1 shows the overall course of action being pursued on a regional basis, as specified by the Air Quality Act of 1967 (PL 90-148, 1967). The Department of Health, Education, and Welfare (HEW), i.e., NAPCA:

- o Designates air quality control regions based on meteorological-topographical factors, urban-industrial concentrations, jurisdictional boundaries, etc., in consultation with State and local officials.
- o Develops air quality criteria that serve as a basis for establishing air quality standards.
- o Prepares reports on control techniques for pollutants for which criteria are developed.

Upon publication of <u>both</u> air quality criteria and control techniques for a specified type of pollutant, each State that encompasses all or part of an air quality control region must follow this timetable:

- o Within 90 days, indicate their intent to adopt applicable air quality standards.
- o Within 180 days after the above 90-day period, adopt air quality standards, after holding public hearings, and submit the standards to HEW for review.
- o Within 180 days after the above 180-day period, adopt a plan to achieve the adopted air quality standards, and submit the plan to HEW for review.

---

* On assignment from National Oceanic and Atmospheric Administration, U. S. Department of Commerce

Then the States or regions proceed, under the Air Quality Act, with steps necessary to reach the established standards. By Executive Order 11507, the President has directed that all Federal installations will set outstanding examples in complying with government regulations to control pollution.

The current state of development of the national program is as follows:

- Sixty air quality control regions encompassing 70 percent of the population, have been designated and 85 more are in process or under consideration.
- Air quality criteria and applicable control techniques have been published for particulate matter (NAPCA AP-49, 1969; NAPCA AP-51, 1969) sulfur oxides (NAPCA AP-50, 1969; NAPCA AP-52, 1969), carbon monoxide (NAPCA AP-62, 1970; NAPCA AP-65, 1970; NAPCA AP-66, 1970), photochemical oxidants (NAPCA AP-63, 1970; NAPCA AP-66, 1970; NAPCA AP-68, 1970) and hydrocarbons (NAPCA AP-64, 1970; NAPCA AP-66, 1970; NAPCA AP-68, 1970).
- Air quality standards for particulate matter and sulfur oxides have been approved by HEW for 22 air quality control regions.
- Implementation plans have been submitted to HEW for 9 air quality control regions.
- Legislation is moving through Congress to set national emission standards for automobiles and trucks, and to otherwise speed implementation of the Act.

A very important requirement of each implementation plan is a system for curtailing pollutant emissions on an interim basis whenever necessary to prevent or alleviate the occurrence of episodes of high pollutant concentrations. As used here, an episode is usually interpreted as lasting at least one to two days. Warning systems for air pollution episodes are usually built around "alert levels" corresponding to different degrees of severity of the problem. These alert levels consider air quality data as well as meteorological factors. For example:

- First level may indicate early presence of adverse meteorological conditions.
- Second level may reflect occurrence of pollutant concentrations approaching undesirable levels, which with continuation of adverse meteorological conditions could trigger curtailment of emissions.
- Final level may call for immediate shutdown of all appropriate sources.

In developing implementation plans, emphasis is on preventing the occurrence of undesirable pollutant concentrations. In this regard, use is being made of the high air pollution potential advisory service of the U. S. Weather Bureau (Gross, 1970). This service, which was initially developed and operated for several years by ESSA research meteorologists assigned to NAPCA, is intended to advise responsible officials of impending episodes of limited dispersion conditons like those generally associated with objectionable levels of relatively slow reacting pollutants in medium and large cities. Because of obvious problems in dealing nationally with small scale phenomena over cities, the meteorological potential is evaluated in terms of large scale or general features of dispersion over areas at least as large as 16 degrees$^2$ of latitude-longitude. The meteorological potential for air pollution episodes has been stressed because pollutant concentrations depend critically upon local transport and diffusion conditions as well as pollutant emission rates, certain emission conditions, and atmospheric transformations of most pollutants.

Air-pollution-potential advisories are transmitted daily over teletype service C at 1220 EST. The message says "none today", or specifies the boundaries of forecast areas of high potential, or, if an area exists from the previous day, modification may be indicated. More recently the message has included a narrative discussion of the forecast and estimates of mixing height and wind speed (to be discussed) for upper air stations. By prior arrangement, the forecasts are transmitted to air pollution control authorities and the public by local Weather Bureau offices.

Early research on forecasting high air-pollution potential examined and extended the studies of stagnating anticyclones (Korshover, 1967); the Donora, Pennsylvania, episode of October 26 to 30, 1948 (Schrenk et al., 1949); the London episode of December 5 to 8, 1952 (Douglas and Stewart, 1953); and the air pollution forecasting service developed for the Tennessee Valley Authority (Kleinsasser and Wanta, 1956). The usual synoptic feature found with widespread stagnation lasting over several days was the slow-moving anticyclone. The original forecast criteria were as follows:

- Surface wind speeds less than 8 kts.
- Below the 500-mb level all upper air wind speeds 25 kts or less.
- Subsidence below the 600-mb level.
- Above conditions met over a minimum area of 16 degrees$^2$ of latitude-longitude (58,000 nautical miles$^2$) and expected to continue for 36 hours or more.

The first real-time forecasts of high air-pollution potential were experimental and were made in the autumn seasons of 1957, 1958, and 1959 for the eastern United States. Following the success of these experiments (Niemeyer, 1960; Boettger, 1961), judged largely by comparisons of 24-hour samples of airborne particulate material, the forecast service became operational for the United States east of the Rockies on August 1, 1960, and for the 48 contiguous states on October 1, 1963. On July 10, 1967, the National Meteorological Center (NMC) assumed operation of the forecasting service. Since before the transfer, research to improve these forecasts has continued at both NAPCA and NMC. Although the main purpose of the national air-pollution potential advisory service has not been changed over the years, the forecast procedures or criteria have gone through a number of developments. Much progress has been made in comparison with the original forecast criteria. This is largely due to the utilization and adaption of NMC's computer products and techniques. The essential elements of the current forecasting procedure are as follows:

STAGNATION AREA GUIDELINES

- Wind speed at 5000 ft above station 10 m sec$^{-1}$ or less.
- Twelve-hour temperature <u>decrease</u> at 5000 ft above station 5°C or less.
- Absolute vorticity at 500 mb 10 x $10^{-5}$ sec$^{-1}$ or less.
- Twelve-hour 500-mb vorticity change + 3 x $10^{-5}$ sec$^{-1}$ or less.
- No significant precipitation.

HIGH AIR POLLUTION POTENTIAL CRITERIA

- Stagnation area guidelines substantially satisfied.
- Morning urban mixing height 500 m or less and average wind speed through mixing layer 4 m sec$^{-1}$ or less.
- Afternoon ventilation (mixing height x average wind speed) 6000 m$^2$ sec$^{-1}$ or less and wind speed 4 m sec$^{-1}$ or less.
- Initial forecast high air-pollution potential area at least 58000 nautical miles$^2$.
- Above criteria expected to be satisfied for at least 36 hours after forecast issued (1320 EST).

Stagnation area guidelines are intended to delineate areas of relatively quiescent weather. Values of the stagnation guidelines are generated in NMC's numerical forecasts based on the 6-layer primitive-equation model and initial data for 0000Z. The values

are evaluated in the computer in terms of an index that specifies the elements not satisfied. The computer prints 12-hour maps of the index value at each upper air station from 1200Z today to 1200Z day after tomorrow. These maps become available at 1030 EST. Other parameters such as boundary layer wind speed, 850-mb vertical velocity, and lifted index are being considered for inclusion in the stagnation index. Also, a new method of objectively specifying the occurrence of significant precipitation is being developed.

High air-pollution potential criteria are the main elements of the forecasting procedure. These criteria are indicative of limited vertical mixing and horizontal transport. As indicated, the stagnation area guidelines need only be substantially or roughly satisfied. However, large-scale stagnation is very unlikely when any of the specified limits are greatly exceeded.

Morning and afternoon mixing heights and mixing-layer average wind speeds, based on the 1200Z rawinsonde observation, are calculated on the computer for each upper air station. The mixing height is the height above the ground through which relatively vigorous vertical mixing is assumed. The morning urban mixing-height is calculated as the height above the station where the potential temperature of the surface minimum temperature plus 5°C intersects the observed temperature profile. The "plus 5°C" allows for the urban heat island during the first few hours after sunrise; plus 3°C is used for soundings made in urban areas. Although this technique for estimating morning mixing heights over cities is a crude approximation of a complex phenomenon, it has proven highly useful in large scale considerations of high air-pollution potential For example, in high-potential situations morning mixing heights are often less than 100 meters. The afternoon mixing height is defined as for the morning, except the forecast maximum surface temperature is used instead of the minimum plus 5°C. In view of the assumptions implicit in mixing height calculations, the calculations are most valid in areas where changes in the synoptic features are not large, e.g., as given by stagnation-area guidelines. Average wind speeds in the mixing layers include surface speeds and are arithmetic averages.

Mixing heights and average wind speeds for yesterday afternoon are also calculated; they are based on observed surface maximum temperatures and observed 0000Z winds aloft. This information is particularly useful because, if yesterday's ventilation criterion of 6000 $m^2$ $sec^{-1}$ or less was satisfied, the criterion is increased to 8000 $m^2$ $sec^{-1}$. It is reasoned that, after a duration of near-critical conditions for at least one day, this criterion should be relaxed.

Thus, in addition to the maps of stagnation index the computer also prints out maps of mixing height and average wind speed for three times: yesterday afternoon (observed), this morning (observed), and this afternoon (forecast). These maps become available at 1030 EST. Forecasts of mixing heights and wind speeds for tomorrow have been generated experimentally but they have been less reliable than persistence. Since September 8, 1970, maps with mixing height and average wind-speed isopleths and stagnation areas have been transmitted daily over the Forecast Office Facsimile (FOFAX) circuit at 1340 EST (Tech. Proc. Bull. 52, 1970).

Figure 2 shows the surface weather map for August 29, 1969, near the middle of a forecast episode of high air-pollution potential that began August 23 and ended September 1, 1969. This was a rather long episode for the eastern United States. Also shown is the forecast high pollution-potential area for the afternoon of the 29th and the envelope of all forecast areas during the episode.

Figure 3 shows the 500-mb map corresponding to Figure 3. It may be inferred from Figures 3 and 4 that the stagnation guidelines were very well conformed with over most of the United States. In addition, the high-potential criteria were satisfied exceptionally well in the forecast area. While pollutant concentrations during this episode caused some concern, they did not generally reach levels that might be expected purely on the basis of general meteorological considerations.

In terms of the forecast procedure briefly discussed and outlined, national advisories of high air-pollution potential may be interpreted as indicating areas with a high probability for occurrence of large-scale meteorological conditions that have generally been associated with objectionable levels of slow reacting pollutants in medium and

large cities. Pollutant concentrations are very commonly measured at a point. As such, they are highly dependent upon local and small scale details of pollutant emission, and atmospheric transport and diffusion, all of which are highly variable in space and time over cities. In addition, many common pollutants undergo atmospheric transformations. Clearly, such phenomena can only be effectively dealt with in real time at the local level. This problem has been recognized by the Weather Bureau and NAPCA who have supported the establishment and operation of Environmental Meteorological Support Units (EMSU). The main duties of the EMSUs are:

- To take low-level (to 700-mb) soundings of wind and temperature profiles from within cities.
- To provide advice on meteorological situations and forecasts of meteorological parameters pertinent to local air pollution problems.

At present there are five EMSUs, one each at New York, Philadelphia, Washington, St. Louis, and Chicago. Establishment of additional units is under consideration.

Up to this point, the meteorological conditions for high air-pollution potential have been stressed. However, it is very important to emphasize that the underlying reason for the entire effort is concern for the public's health and welfare. In this context, the fact that criteria for high potential may not have been completely satisfied has not precluded the issuance of an advisory under general conditions of obviously deteriorating air quality.

Two modifications to the national air-pollution-potential forecasting service that would add greatly to the usefulness of the forecasts are:

- An increase in the lead time of the forecasts.
- Provision of quantitative values of the meteorological potential.

Hopefully, the former can be achieved through extension of the stagnation area concept and developing improvements in NMC's forecast products. An experimental effort toward the latter is being made along the lines of a very simple model of dispersion over urban areas (Miller and Holzworth, 1967). In this model the theoretical city-wide average pollutant concentration ($\bar{\chi}$, gm $m^{-3}$) normalized for uniform average-area-emission rate ($\bar{Q}$, gm $m^{-2}$ $sec^{-1}$) is a function of the mixing height (m), average wind speed through the mixing layer (m $sec^{-1}$), and city size or along-wind distance across the city (m). The main assumptions of this model are:

- Steady state conditions prevail.
- Emissions occur at ground level and are uniform over the city.
- Pollutants are non-reactive.
- Lateral diffusion is neglected.
- Vertical diffusion from each infinitesimal source conforms to the Gaussian distribution out to a travel time, which is a function of the rate of vertical diffusion and the mixing height; thereafter, pollutants are uniformly distributed in the vertical.

Thus, based on this model, the potential for urban air pollution is considered quantitatively in terms of meteorological variables. Figure 4 shows the daily values of morning and afternoon average normalized concentration ($\bar{\chi}/\bar{Q}$, sec $m^{-1}$) for a 40-km city during the high air-pollution-potential episode of August 23 to September 1, 1969 (see Figure 2). Each $\bar{\chi}/\bar{Q}$ value shown is the average for all upper-air stations in the forecast high-potential area. Also shown are the corresponding upper decile, upper quartile, and median $\bar{\chi}/\bar{Q}$ values based on climatological records for five summers. All daily values of morning $\bar{\chi}/\bar{Q}$ were well above the climatological medians, most were well above the upper quartiles, and two were above the upper deciles. For the episode as a whole, the morning $\bar{\chi}/\bar{Q}$ values

averaged about 150 sec $m^{-1}$, somewhat above the corresponding upper-quartile value and more than four times the median. Afternoon $\bar{\chi}/\bar{Q}$ values are much lower and less variable than morning values. During the episode, all afternoon $\bar{\chi}/\bar{Q}$ values, except one, were at or above the climatological upper-quartile values. This method of quantitatively appraising the (large-scale) meteorological potential for air pollution will be pursued further.

## Summary

An important objective of the National Air Pollution Control Administration is curtailing pollutant emissions on an interim basis whenever necessary to prevent or alleviate the occurrence of episodes of high pollutant concentrations. The national air-pollution-potential forecasting service has been developed to advise of adverse meteorological conditions that have been associated with episodes of objectionable levels of air quality. These forecasts should properly be recognized as large-scale guidance information whose usefulness can be enhanced considerably by refinements in terms of each particular local situation.

## References

Boettger, C.M., 1961: Air pollution east of the Rocky Mountains: fall 1959, Bull. Amer. Meteor. Soc., 42, 615-620.

Douglas, C.M.K., and K.H. Stewart, 1953: London fog of December 5-8, 1952, Meteor. Mag., 82, No. 969, 67-71.

Gross, E., 1970: The national air pollution-potential forecast program, ESSA Tech.Memo. WBTM NMC 47, U.S. Wea. Bur., Washington, D.C., 28 pp.

Korshover, J., 1967: Climatology of stagnating anticyclones east of the Rocky Mountains, 1936-1965, Public Health Service Publication No. 999-AP-34, Cincinnati, Ohio, 15, pp.

Kleinsasser, T.W. and R.C. Wanta, 1956: The development of a forecasting service for use in air-pollution control, Preprint (presented at the Air Pollution Control Association Meeting in Buffalo, New York, May 21, 1956.)

Miller, M.E. and G.C. Holzworth, 1967: An atmospheric-diffusion model for metropolitan areas, J. Air Pollution Control Assoc., 17, 46-50.

National Air Pollution Control Administration Publication No. AP-49, 1969: Air-quality criteria for particulate matter, U.S. Government Printing Office, Washington, D.C.

National Air Pollution Control Administration Publication No. AP-50, 1969: Air-quality criteria for sulfur oxides, U.S. Government Printing Office, Washington, D.C.

National Air Pollution Control Administration Publication No. AP-51, 1969: Control techniques for particulate air pollutants, U.S. Government Printing Office, Washington, D.C.

National Air Pollutio. Control Administration Publication No. AP-52, 1969: Control techniques for sulfur-oxide air pollutants, U.S. Government Printing Office, Washington, D.C.

National Air Pollution Control Administration Publication No. AP-62, 1970: Air-quality criteria for carbon monoxide, U.S. Government Printing Office, Washington, D.C.

National Air Pollution Control Administration Publication No. AP-63, 1970: Air-quality criteria for photochemical oxidants, U.S. Government Printing Office, Washington, D.C.

National Air Pollution Control Administration Publication No. AP-64, 1970: Air quality criteria for hydrocarbons, U.S. Government Printing Office, Washington, D.C.

National Air Pollution Control Administration Publication No. AP-65, 1970: Control techniques for carbon monoxide emissions from stationary sources, U.S. Government Printing Office, Washington, D.C.

National Air Pollution Control Administration Publication No. AP-66, 1970: Control techniques for carbon monoxide, nitrogen oxide, and hydrocarbon emissions from mobile sources, U.S. Government Printing Office, Washington, D.C.

National Air Pollution Control Administration Publication No. AP-68, 1970: Control techniques for hydrocarbon and organic solvent emissions from stationary sources, U.S. Government Printing Office, Washington, D.C.

Niemeyer, L.E., 1960: Forecasting air pollution potential, Mon. Wea. Rev., 88, 88-96.

Public Law 90-148 (81 Stat. 485), amending the Clean Air Act, as amended (77 Stat. 392, 77 Stat. 992), 1967: Air Quality Act of 1967.

Schrenk, H.H., H. Hieman, G.D. Clayton, W.M. Gafafer and H. Wexler, 1949: Air pollution in Donora, Pa., Public Health Service Bulletin No. 306, U.S. Government Printing Office, Washington, D.C., 173 pp.

Technical Procedures Bulletin No. 52, 1970: Facsimile display of air-pollution potential, Weather Analysis and Prediction Division, U.S. Wea. Bur., Silver Springs, Maryland.

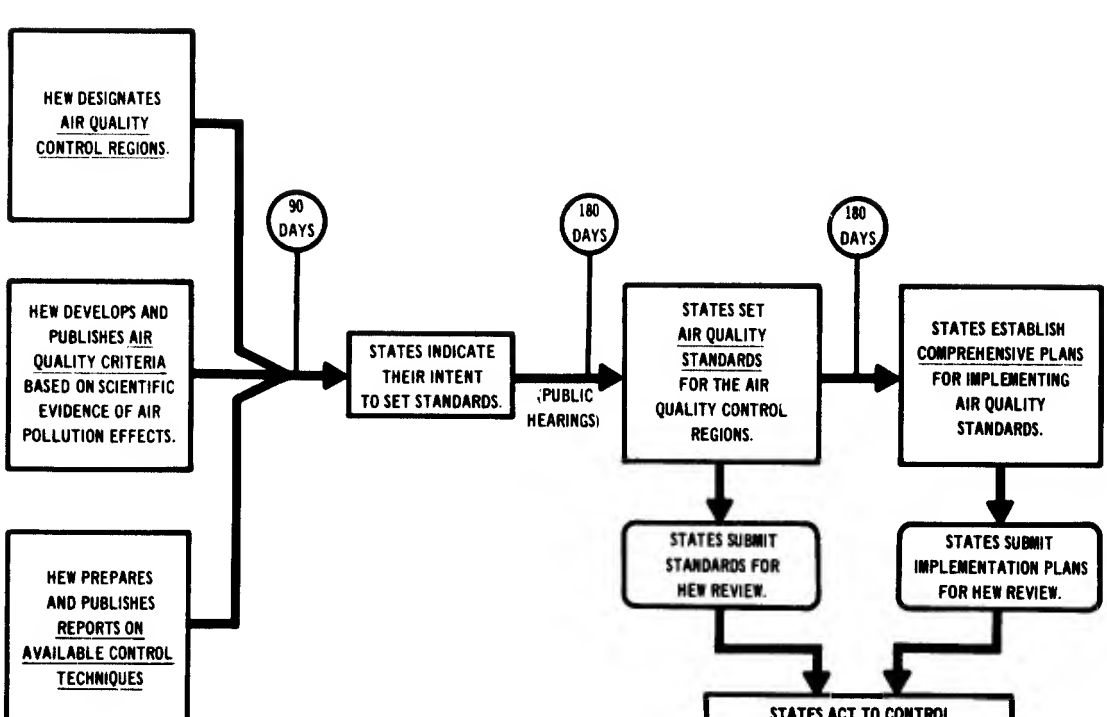


Figure 1. Flow diagram for action to control air pollution on regional basis, under Air Quality Act.

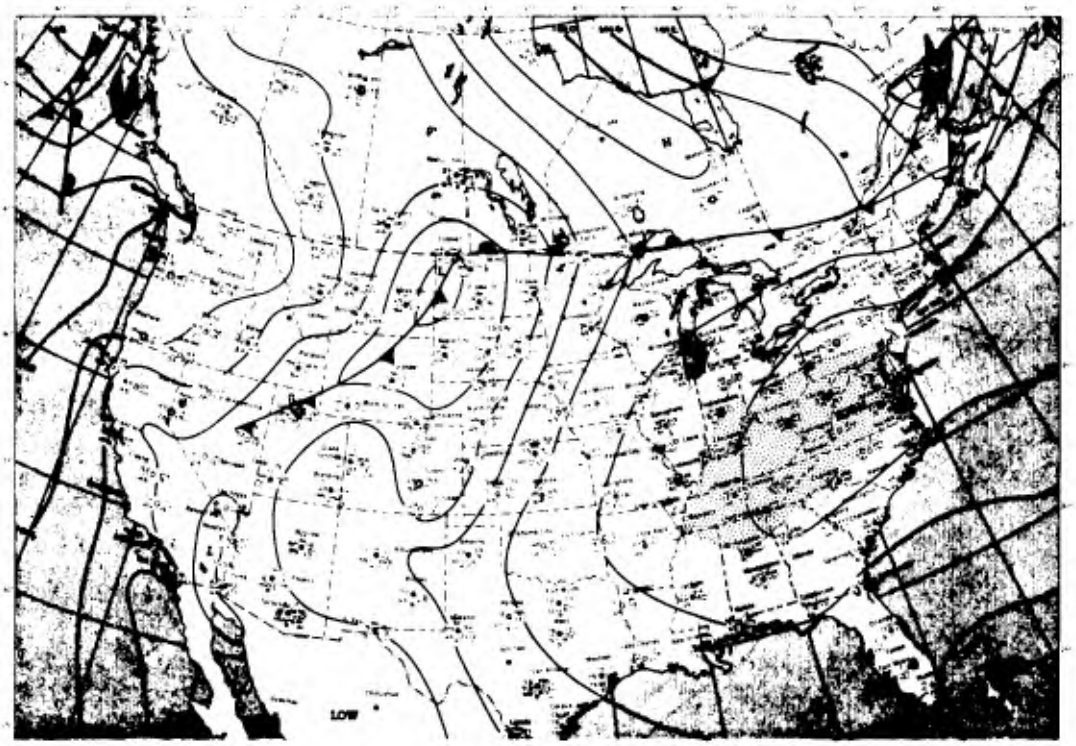


Figure 2. Surface weather map showing forecast high air pollution potential area valid on August 29, 1969, and total area covered by daily forecasts during episode from August 23 to September 1, 1969

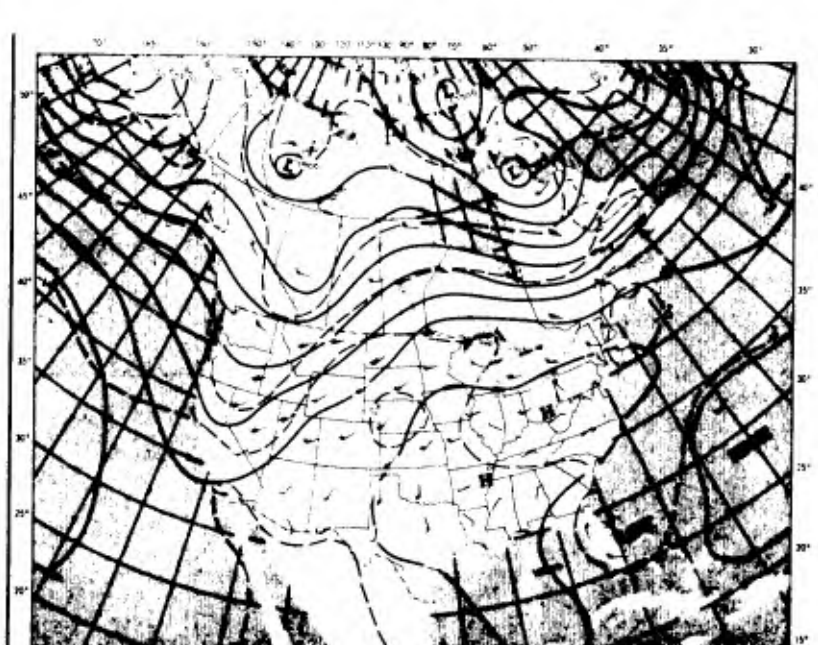


Figure 3. 500-mb map corresponding to surface map of Figure 2.

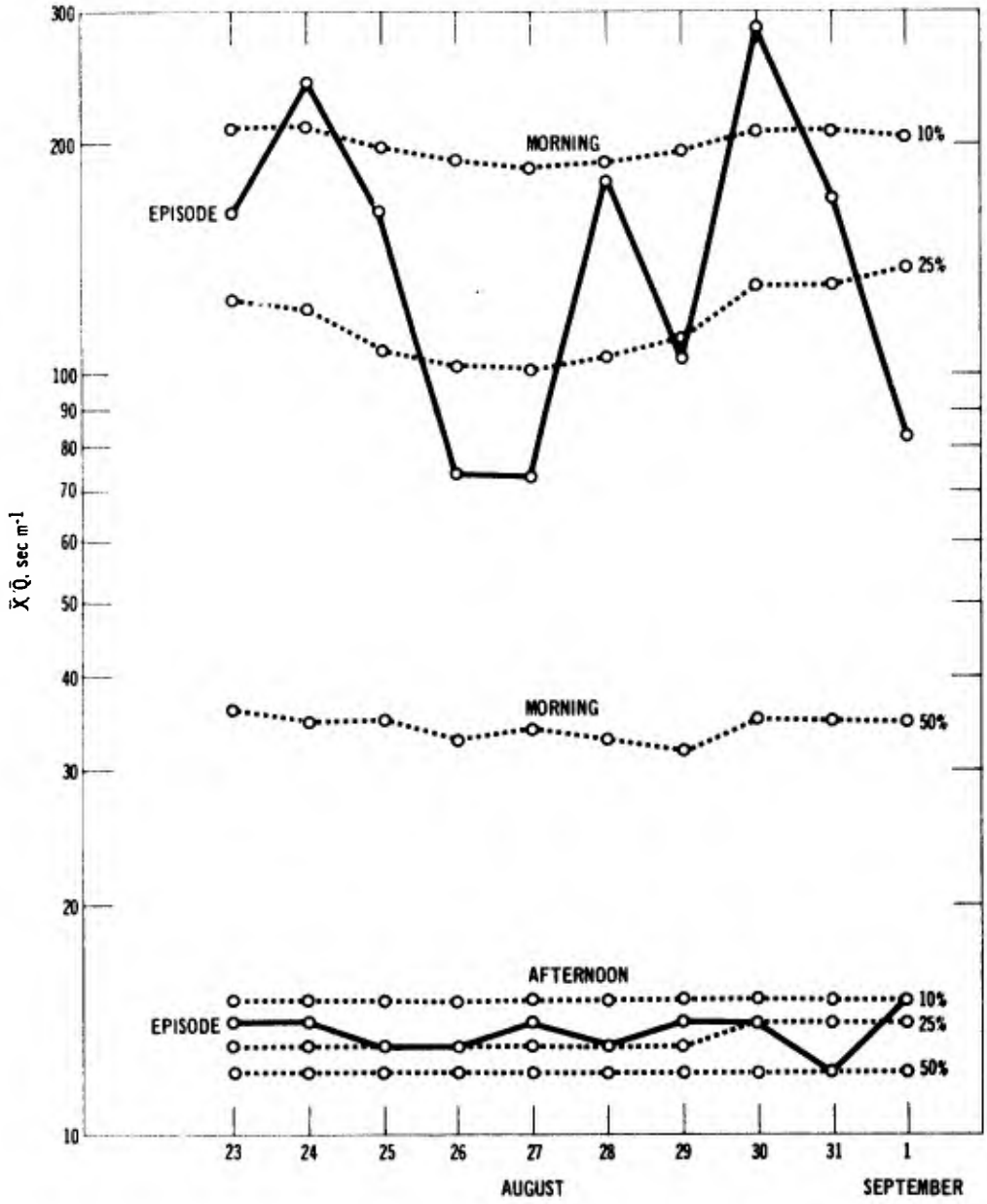


Figure 4. Daily morning and afternoon values of $\bar{X}/\bar{Q}$ (see text) averaged for all upper air stations in daily forecast area of high air pollution potential and corresponding upper percentile values of $\bar{X}/\bar{Q}$ based on upper-air data for five summers, 1960 - 1964.

# NUMERICAL SIMULATION OF HURRICANE DEVELOPMENT AND STRUCTURE

Stanley L. Rosenthal, Richard A. Anthes and James W. Trout

Environmental Science Services Administration
Atlantic Oceanographic and Meteorological Laboratories
National Hurricane Research Laboratory
Miami, Florida

Abstract

Two numerical models designed to simulate the development of tropical cyclones as well as the structure of these storms in the mature stage are described. The first model makes the assumption of circular symmetry and contains substantial vertical resolution (seven levels). The second model allows for azimuthal variations but has only three layers of vertical resolution. Examples of typical results obtained from each model are presented. The structure of the mature hurricane as simulated by either model is shown to be remarkably good.

## 1. INTRODUCTION

In support of Project STORMFURY, the National Hurricane Research Laboratory, ESSA has been asked to develop theoretical models of the life cycle of tropical cyclones. Two such models have now been designed. The first of these, which makes the assumption of circular symmetry, has yielded extremely interesting results[17]. Hurricanes, however, contain important features which are markedly asymmetric. Among these are spiral rainbands, the upper tropospheric outflow pattern and the interactions with neighboring synoptic systems.

While our ultimate goal is to produce a fully three dimensional model of the hurricane and its environment, this must be recognized as an extremely ambitious endeavor requiring substantial future research. The greatest difficulty is associated with the range of scales which must be considered. A grid increment on the order of 10 km is needed to resolve the storm core. However, this resolution is neither feasible nor desirable for the environment where the proper mesh interval is on the order of 100 km. These considerations lead directly to the concept of a fine mesh, moving with the hurricane center, and embedded in a coarser mesh. It is anticipated that substantial difficulties will be encountered in the development of such a model.

In the meantime, however, we have had some success with an asymmetric model of a stationary, isolated tropical cyclone. This model appears to be the logical first step beyond the circularly symmetric models and, as we will see in Section 3, provides a fairly realistic simulation of several of the asymmetric features of mature hurricanes.

## 2. THE CIRCULARLY SYMMETRIC MODEL

Since the mathematical details of this model are already available [17], only a brief verbal description is given here. The vertical structure of the atmosphere is represented by seven levels; geometric height is the vertical coordinate. The levels correspond to pressures of 1015, 900, 700, 500, 300, 200, and 100 mb in the mean tropical atmosphere. All variables are defined at all levels. The primitive equations are employed with external gravity waves eliminated through a simplification of the continuity equation and the boundary condition that the vertical motion vanish at the top and bottom levels. The radial limit of the computational domain is 440 km and the system is open at this lateral boundary. Boundary conditions here require the horizontal divergence, the vertical component of the relative vorticity and the horizontal gradients of potential temperature and specific humidity be zero. Experiments have been conducted with both 10 km and 20 km radial resolution.

The model simulates convective precipitation (and the macroscale heating due to this latent heat release) as well as the enrichment of the macroscale humidity due to the presence of the cumuli. Convection may originate in any layer provided that the layer has a water-vapor supply from horizontal convergence and that conditional instability exists for parcels lifted from the layer. Nonconvective precipitation is also simulated. Details of the parameterization of the convective adjustments and the calculation of rainfall are given in [17].

The air-sea exchanges of sensible heat, latent heat and momentum are treated by means of the bulk aerodynamic equations.

The numerical aspects of the solution include forward time steps, upstream differencing of advection terms and a partially implicit computational cycle. One exception to this is found in the continuity equation for water vapor where a centered flux form is used for advection terms and the Matsuno [10] method of time integration is employed. Complete details are given in [16].

Vertical transports of horizontal momentum by cumulus-scale motions play a significant role in the macroscale dynamics of the hurricane [6,18]. In a previous paper [18], we have shown that the computational diffusion associated with upstream differencing of vertical-advection terms behaves in a fashion similar to that expected of the cumulus transports. We also showed through controlled numerical experiments that solutions with upstream differencing provide far more realistic results than do solutions with centered differences in which no provision is made for representation of the vertical momentum transports by the cumulus. In the same paper [18], we found the lateral-mixing effects produced by cumulus-scale motions to be adequately represented by the computational diffusion produced by upstream differencing of horizontal-advection terms. This was shown through a series of numerical experiments in which results of computations with centered and upstream formulations were compared. Also, the computational lateral-viscosity coefficients were calculated as a function of space and time and found to be in good agreement with the empirical estimates of lateral-mixing coefficients made by Riehl and Malkus [15] for Hurricane Daisy (1958).

The initial conditions for most experiments consist of a weak, nondivergent vortex in gradient balance. The central pressure is 1013 mb; the maximum surface wind is 7 $m\text{-}sec^{-1}$ at a radius of about 250 km. The initial field of specific humidity varies only with height and corresponds, approximately, to the relative humidities of the mean hurricane season sounding [8].

Figure 1 summarizes the evolution at sea level of a typical experiment. The "organizational" period, consisting of the first four or so days, is characteristic of tropical cyclone models which are initialized with nondivergent winds [1,17]. The first day or so of the computation should be considered as some sort of initialization procedure rather than as a forecast.

It is during this time that the inviscid, adiabatic, balanced system is transformed into a slowly varying system in which friction, divergence and diabatic effects are of importance. The remainder of the organizational period seems to have a counterpart in nature. As has been emphasized by Riehl [14] and others, tropical storms form only in pre-existing disturbances and deepening is usually a slow process which requires several days.

Deepest central pressure and strongest winds occur at 168 hours. These peaks, however, appear to represent "overshooting" of an equilibrium state and a closer approach to a steady state is found between 192 and 216 hours. A fairly slow decay is characteristic of the latter stages of the calculation. This is associated with the increased static stability produced by the upward transport of heat by the cumulus convection. Hurricane-force winds are present from about 144 hours to the end of the calculation. The radius of maximum surface wind decreases rapidly during the deepening period and is more or less constant thereafter.

Figures 2 and 3 show vertical cross sections of wind speed and temperature anomaly during the mature stage (192 hours) and verify the highly realistic nature of the solutions. Figure 4 shows a radial profile of the vertical motion at the 900-mb level (192 hours). The spike at 25 km is analogous to the eye wall. It is noted that virtually all ascent occurs in a narrow ring about the storm center. This is in agreement with the observational evidence [15].

Central pressures obtained from the model are empirically consistent with the maximum wind speeds. This is verified by figure 5 based on the work of Colón [4]. Colón presents a scatter diagram of central pressure versus maximum wind based on a number of tropical storm and hurricane observations in various stages of the life cycle (genesis, maturity, dissipation). The two straight lines on figure 5 are drawn to contain almost all of Colón's data points. Also plotted on the diagram are the data points obtained from one of our calculations. These are seen to fall well within the limits of Colón's data.

Average rainfall rates for the inner 100 km of the circulation of another representative calculation are shown by the bottom section of figure 6. During the mature stage, the total rainfall averages about 25 $cm\text{-}day^{-1}$ or, roughly, ten inches per day which is quite reasonable. The nonconvective rainfall is about two-thirds of the convective precipitation. According to Hawkins and Rubsam [7], radar data gathered in Hurricane Hilda (1964) indicate substantial rain from stratiform clouds. Their observations also indicate that while a large portion of Hilda's circulation contained appreciable rain, active cumulonimbi were present only in the eye wall region. In view of these observations, the partitioning of rain between convective and nonconvective components, as shown by figure 6 is acceptable.

Figure 6 also illustrates the efficiency of the inner 200 km for the same experiment. This quantity is defined in the usual manner [12] as the ratio of the rate of kinetic-energy production to the rate of latent-heat release. The values, during the mature stage, are quite close to the empirical value of 2.7 percent found by Palmén and Riehl [12].

Figure 7 illustrates the kinetic-energy content of various rings of the model storm for the

same experiment. The significance of this figure is that the kinetic energy of each ring reaches a definite maximum. The experiments are, therefore, well behaved and there is not a monatonic increase of kinetic energy with time as was the case with some older models of the tropical cyclone [11,16].

As discussed by Riehl [14], large moisture content to great heights is necessary for tropical cyclones to show significant intensification.

On the other hand, since the depth of the moist layer is tuned to the macroscale motion [14] and increases with low-level convergence, the role of the pre-existing disturbance or "organizational period" may well be the development of the required deep moist layer from a humidity distribution which initially approximates that of the mean tropical atmosphere. If this is indeed the case, a model storm in which the initial moisture content is large should grow to the mature stage more rapidly than does a model storm in which the initial humidity is small.

The two experiments summarized on figure 8 differ only in the initial humidity distributions; experiment W2 begins with the humidity of the mean tropical atmosphere while W6 initially has 90 percent relative humidity everywhere. While the peak surface winds and deepest central pressures are about the same for the two calculations, those for W6 occur about 48 hours earlier than do those for W2. An organizational period of 72 hours is required for development in W2, but only 24 hours is needed in W6.

The rainfall rates and efficiencies for W6 (figure 9) are not greatly different from those for W2 (not shown but similar to W1, figure 6). The maximum efficiency is about the same for the two calculations. The average rainfall is about 10 cm-day$^{-1}$ greater in experiment W2.

As already noted, the primary motivation for the development of these models is to provide theoretical support for Project STORMFURY. The circularly symmetric model has been used in several attempts to simulate the field experiments performed last year on Hurricane Debbie [5]. Details of these calculations will be presented elsewhere [19].

## 3. THE ASYMMETRIC MODEL

While this model has not as yet reached the level of sophistication of the symmetric model, it has yielded results of sufficient interest to warrant the preparation of a detailed report [3]. We will very briefly describe the model here and present a few of the more interesting results.

The vertical structure consists of three layers. The upper two layers are approximately 450 mb thick while the third layer is about 100 mb thick and represents the surface boundary layer. The vertical coordinate is the ratio of pressure to surface pressure [13]. The primitive equations are employed in a form similar to that used by Smagorinsky et. al. [20] for general circulation studies. Cartesian coordinates are used in the horizontal with an irregular boundary approximating a circle with radius 435 km. The system is open at the lateral boundary where boundary conditions require the pressure and temperature to be steady state and the radial shear of the wind vector be zero. The horizontal resolution, for computational economy, is 30 km.

Water vapor is treated implicitly as was the case in the earlier symmetric models [16,21]. The convective adjustments of temperature are made in a fashion nearly identical to that used in a very early version of the symmetric model [16].

The horizontal portion of the finite-difference scheme is similar to that used by Smagorinsky et. al. [20] while the vertical scheme closely resembles that presented by Kurihara and Holloway [9]. Time integration is by Matsuno's scheme [10].

Air-sea exchanges of heat and momentum are treated by use of the bulk aerodynamic equations. Vertical transports of momentum by the cumulus-scale motions have not as yet been incorporated. The lateral mixing of momentum is treated pragmatically by adopting a variable lateral-mixing coefficient similar in form to the computational viscosity coefficient implicit in the circularly symmetric model.

The initial conditions consist of a gradient, nondivergent vortex with maximum winds of 18 m-sec$^{-1}$ at a radius of 240 km. While this is a rather intense initial vortex, tests with a symmetric analogue to the asymmetric model indicated that the ultimate mature state of the storm differed little as initial conditions were varied. The time required to reach this stage was, however, directly dependent on the intensity of the initial vortex. Hence, an initially strong vortex provides a computational economy.

If the initial conditions and the boundary conditions had perfect circular symmetry, the solution would remain circularly symmetric for all time. However, the truncation and roundoff errors associated with the conversion of the initial tangential wind (which is circularly symmetric) to cartesian wind components, as well as the fact that the boundary is not an exact circle, introduces weak asymmetries which are predominantly of wave number 4.

Figure 11 summarizes the history of the central pressure and maximum low-level wind. After an early organizational period, we note a gradual intensification to minimal hurricane strength and then a very nearly steady state until about 120 hours. After 120 hours, the storm again begins to intensify and reaches a peak strength of about 64 m-sec$^{-1}$ and 965 mb central pressure at about 230 hours. Thereafter, the storm fills gradually and the calculation is ended at 260 hours.

During the first 120 hours, the system is very nearly circularly symmetric and there is no indication of spiral rain bands or any great degree of asymmetry in the outflow layer. This is evidenced by figure 11 which shows the upper-tropospheric streamlines at 84 hours and figure 12 which shows the rainfall rates for the same time.

After 120 hours, when the storm again begins to deepen, the situation is altogether different. Figure 13 shows the rainfall pattern at 156 hours and indicates distinct counterparts to hurricane spiral rainbands. The upper-level outflow pattern (figure 14) is now distinctly asymmetric with the bulk of the outflow concentrated in the southeast and northwest quadrants. We also note the presence of two small anticyclonic eddies. This outflow pattern is extremely realistic [1] for a mature hurricane.

The breakdown in symmetry as well as the second period of intensification seem to be closely related to the generation of dynamic instability in the outflow layer. The upper section of figure 15 shows, as a function of time, the minimum value of relative vorticity which can be found anywhere in the upper troposphere. Since the coriolis parameter for this calculation is $5 \times 10^{-5}$ $sec^{-1}$, the minimum absolute vorticity until about 100 hours is very close to zero and, at times, only slightly negative. However, at about 100 hours, the minimum vorticity begins to drop rapidly. This is well before the storm begins the second period of deepening and well before the flow takes on its strongly asymmetric character.

The criteria for dynamic instability may be written $\zeta_a \{2|\mathbf{V}|/R + f\} < 0$ where $\zeta_a$ is the absolute vorticity, $\mathbf{V}$ the horizontal wind vector, R the radius of curvature of the streamlines and f the coriolis parameter. A negative value for the term in brackets corresponds to the presence of anomalous winds. Hence, horizontal parcel displacements may be dynamically unstable with negative absolute vorticity and normal winds or with positive absolute vorticity and anomalous winds.

The appearance of substantial amounts of negative absolute vorticity which begins at about 100 hours, therefore, suggests the possible presence of dynamic instability. Indeed, calculations during the second stage of the storm's life verify that large areas of both anticyclonic absolute vorticity and anomalous winds exist. These regions tend to be associated with each other. However, the patterns are sufficiently out of phase to leave banded regions of dynamic instability (figure 16). The pattern of dynamic instability shown by figure 16 is quite similar to that found by Alaka [2] for the outflow layer of Hurricane Daisy (1958).

Figure 18 summarizes the storm structure at 156 hours. The figure shows vertical cross-sections of the circular averages of tangential wind, radial wind and temperature anomaly. The patterns are similar to those produced by the symmetric model and to those observed in real hurricanes [7]. The outward tilt with height of the tangential-velocity maximum appears to be due to the lack of a parametric representation of the vertical transport of momentum by the cumulus scale motions [18]. The small value of the upper-tropospheric temperature anomaly in comparison to observations [7], and in comparison to that obtained from the symmetric model, is a result of the limited vertical resolution of the asymmetric model. The upper-tropospheric temperatures yielded by the model must be thought of as averages over 450 mb layers.

## REFERENCES


1. Alaka, M.A., "The Occurrence of Anomalous Winds and their Significance," National Hurricane Research Project Report No. 45, U.S. Weather Bureau, Miami, Fla., June 1961, 26 pp.

2. Alaka, M.A., "Instability Aspects of Hurricane Genesis," National Hurricane Research Project Report No. 64, U.S. Weather Bureau, Miami, Fla., June 1963, 23 pp.

3. Anthes, R.A., Rosenthal, S.L., and Trout, J.W., "Preliminary Results from an Asymmetric Model of the Tropical Cyclone," Paper submitted for publication in the Monthly Weather Review.

4. Colón, J.A., "On the Evolution of the Wind Field During the Life Cycle of Tropical Cyclones," National Hurricane Research Project Report No. 65, U.S. Weather Bureau, Miami, Fla., November 1963, 36 pp.

5. Gentry, R.C., "The Modification Experiment on Hurricane Debbie, August 1969," Science, Vol. 168, No. 3930, April 1970, pp 473-475.

6. Gray, W.M., "The Mutual Variation of Wind, Shear, and Baroclinicity in the Cumulus Convective Atmosphere of the Hurricane," Monthly Weather Review, Vol. 95, No. 2, February 1967, pp 55-73.

7. Hawkins, H.F., and Rubsam, D.T., "Hurricane Hilda, 1964: II. Structure and Budgets of the Hurricane on Oct. 1, 1964," Monthly Weather Review, Vol. 96, No. 9, Sept. 1968, pp 617-636.

8. Hebert, P.J., and Jordan, C.L., "Mean Soundings for the Gulf of Mexico Area," National Hurricane Research Project Report No. 30, U.S. Weather Bureau, Miami, Fla., April 1959, 10 pp.

9. Kurihara, Y., and Holloway, L.J., "Numerical Integration of a Nine-Level Global Primitive Equations Model Formulated by the Box Method," Monthly Weather Review, Vol. 95, No. 8, August 1967, pp 509-530.

10. Matsuno, T., "Numerical Integrations of the Primitive Equations by a Simulated Backward Difference Method," Journal of the Meteorological Society of Japan, Vol. 44, No. 1, February 1966, pp 76-83.

11. Ooyama, K., "Numerical Simulation of the Life-Cycle of Tropical Cyclones," NSF Grant No. GA-623, New York University, New York, Dec. 1967, 133 pp.

12. Palmén, E. and Riehl, H., "Budget of Angular Momentum and Energy in Tropical Cyclones," Journal of Meteorology, Vol. 14, No. 2, March 1957, pp 150-159.

13. Phillips, N.A., "A Coordinate System Having Some Special Advantages for Numerical Forecasting," Journal of Meteorology, Vol. 14, No. 2, April 1957, pp 184-185.

14. Riehl, H., Tropical Meteorology, McGraw-Hill, New York, 1954, 392 pp.

15. Riehl, H. and Malkus, J.S., "Some Aspects of Hurricane Daisy, 1958," Tellus, Vol. 13, No. 2, May 1961, pp 181-213.

16. Rosenthal, S.L., "Experiments with a Numerical Model of Tropical Cyclone Development; Some Effects of Radial Resolution," Monthly Weather Review, Vol. 98, No. 2, February 1970, pp 106-120.

17. Rosenthal, S.L., "A Survey of Experimental Results Obtained from a Numerical Model Designed to Simulate Tropical Cyclone Development," ESSA Technical Memorandum ERLTM-NHRL 88, U.S. Department of Commerce, National Hurricane Research Laboratory, Miami, Fla., January 1970, 78 pp.

18. Rosenthal, S.L., "A Circularly Symmetric, Primitive Equation Model of Tropical Cyclone Development Containing an Explicit Water Vapor Cycle," Monthly Weather Review, Vol. 98, No. 9, September 1970 (In Press).

19. Rosenthal, S.L., "A Circularly Symmetric, Primitive Equation Model of Tropical Cyclones and its Response to Artificial Enhancement of the Convective Heating Functions," Monthly Weather Review (In Press).

20. Smagorinsky, J., Manabe, S., and Holloway, J.L., "Numerical Results from a Nine-Level General Circulation Model of the Atmosphere," Monthly Weather Review, Vol. 93, No. 12, December 1965, pp 727-768.

21. Yamasaki, M., "Detailed Analysis of a Tropical Cyclone Simulated with a 13-Layer Model," Papers in Meteorology and Geophysics, Vol. 19, No. 4, December 1963b, pp 559-585.

## ILLUSTRATIONS

| Figure | Caption |
|---|---|
| 1. | Results from Experiment S18. Top: Central pressure as a function of time. Center: Maximum surface wind as a function of time. Bottom: Radii of maximum surface wind; outer limits of hurricane and gale force winds at the surface; radii of maximum 900 mb. vertical motion. |
| 2. | Results from Experiment S18. Cross section of total wind speed at 192 hours. |
| 3. | Results from Experiment S18. Cross section of temperature anomaly at 192 hours. |
| 4. | Results from Experiment S18. Radial profile of 900 mb vertical motion at 192 hours. |
| 5. | Results from Experiment W2. Central pressure plotted against maximum surface |

| Figure | Caption |
|---|---|
| 5. (Contd.) | wind for hours 96, 120, 144 and 168. Parallel sloping lines are drawn to enclose most of Colón's (1963) empirical data points from a large number of tropical cyclones in various stages of life cycle. |
| 6. | Results from Experiment W1. Top: efficiency of the radial interval zero to 200 km. Bottom: average rainfall over the radial interval zero to 100 km. |
| 7. | Results from Experiment W1. Variation with time of the kinetic energy content of various radial intervals. |
| 8. | Top: comparison of central pressure as a function of time for Experiments W2 and W6. Center: comparison of maximum surfacd wind for Experiments W2 and W6. Bottom: results from Experiment W6. Radii of maximum surface wind; inner and outer limits of hurricane force and gale force winds at the surface. |
| 9. | Results from Experiment W6. Top: efficiency of the radial interval zero to 200 km. Bottom: average rainfall over the radial interval zero to 100 km. |
| 10. | Results from an experiment with the asymmetrical model. Top: central pressure as a function of time. Bottom: maximum boundary layer wind as a function of time. |
| 11. | Results from an experiment with the asymmetrical model. Streamline pattern in the upper troposphere at 84 hours. Radial line in the southeast quadrant is marked at intervals of 60 km. |
| 12. | Results from an experiment with the asymmetrical model. Rainfall ($cm\text{-}day^{-1}$) pattern at 84 hours. |
| 13. | Results from an experiment with the asymmetrical model. Rainfall ($cm\text{-}day^{-1}$) pattern at 156 hours. |
| 14. | Results from an experiment with the asymmetrical model. Streamline pattern in the upper troposphere at 156 hours. |
| 15. | Results from an experiment with the asymmetrical model. Top: minimum relative vorticity in the upper troposphere as a function of time. Bottom: maximum temperature anomaly in the upper troposphere as a function of time. |
| 16. | Results from an experiment with the asymmetric model. The upper troposphere at 156 hours. Heavy solid and dashed lines are relative vorticity. Thinner solid and dashed lines are $2\,|\,V|/R$. The dotted region is the area in which the criterion for dynamic instability of horizontal parcel displacement is satisfied. |
| 17. | Results from an experiment with the asymmetric model. Vertical cross sections of circular averages at 156 hours. Top: tangential wind. Center: radial wind. Bottom: temperature anomaly. |

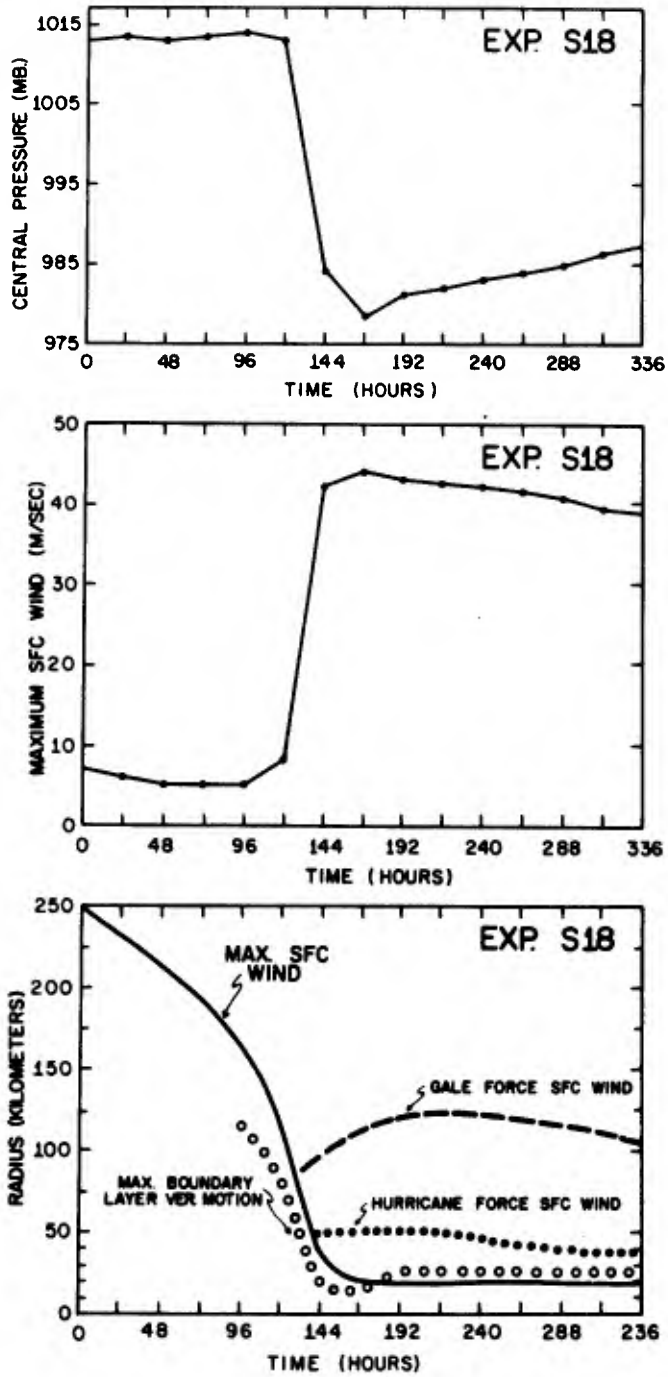


Figure 1. Results from Experiment S18. Top: Central pressure as a function of time. Center: Maximum surface wind as a function of time. Bottom: Radii of maximum surface wind; outer limits of hurricane and gale force winds at the surface; radii of maximum 900-mb vertical motion.

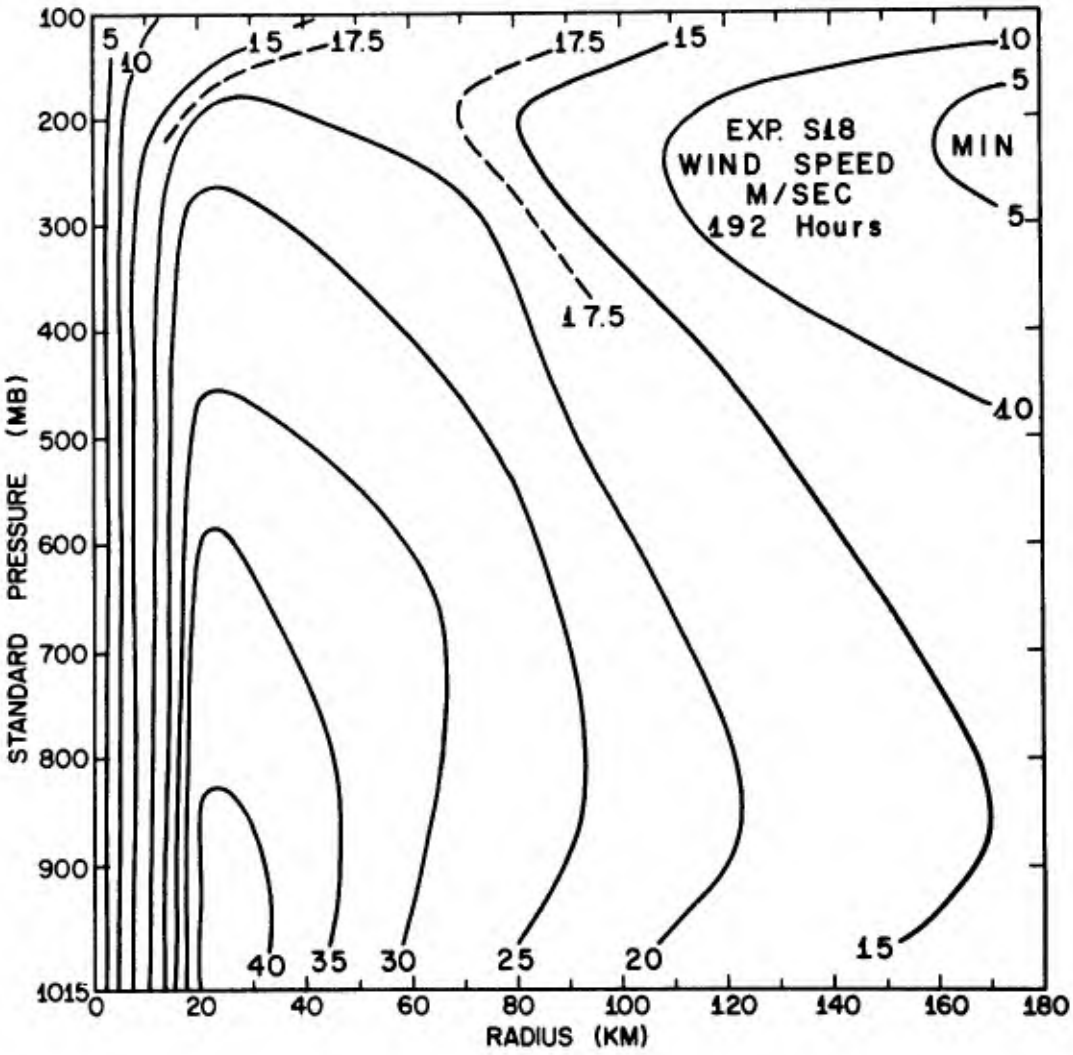


Figure 2. Results from Experiment S18. Cross section of total wind-speed at 192 hours.

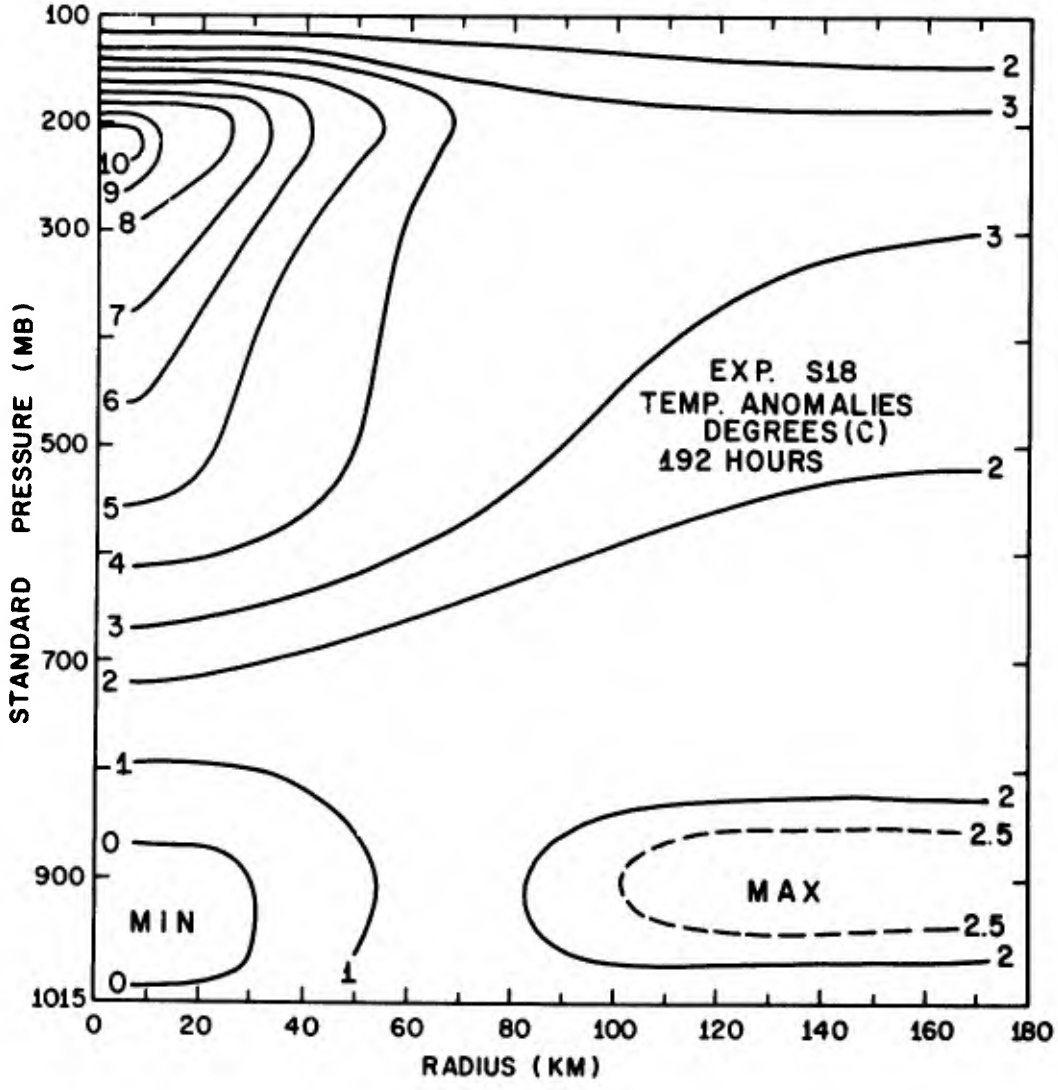


Figure 3. Results from Experiment S18. Cross section of temperature anomaly at 192 hours.

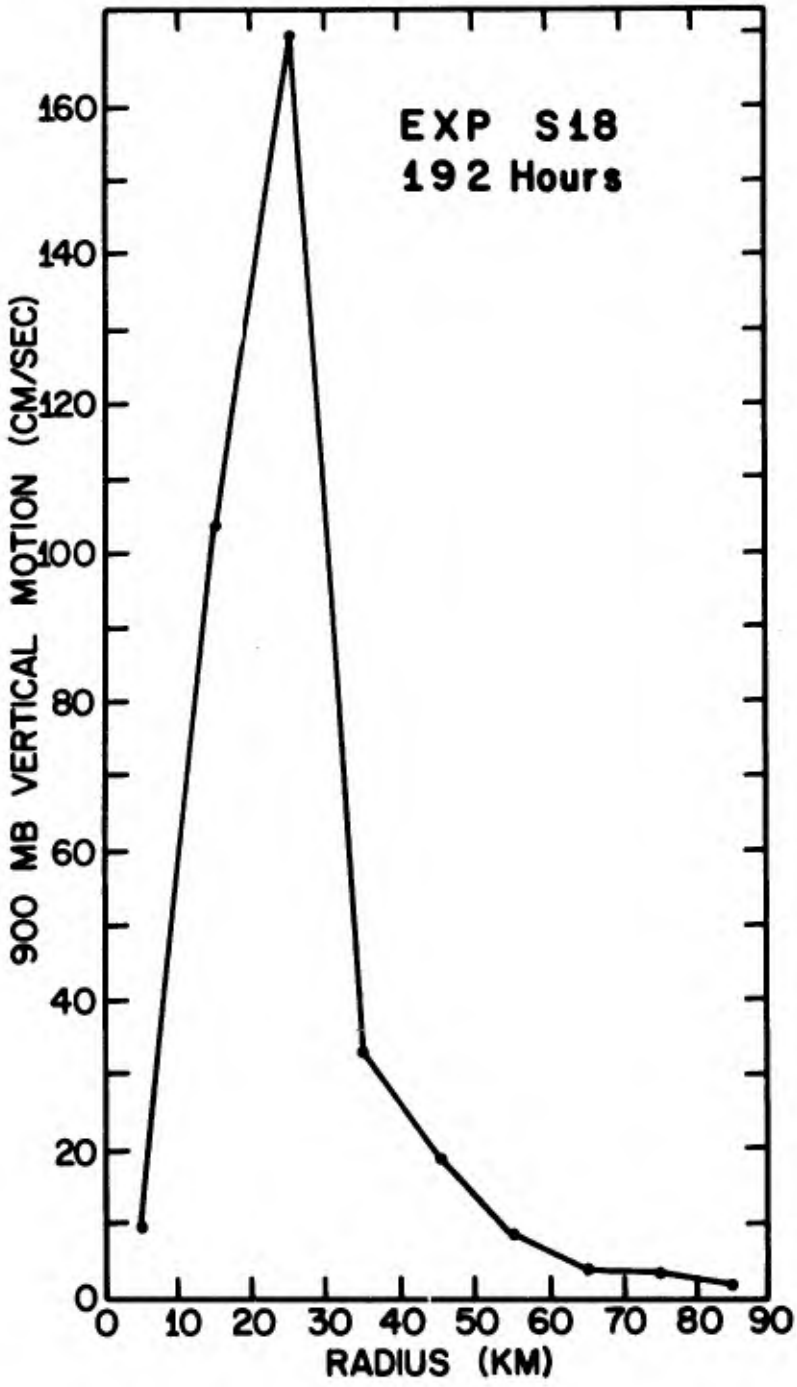


Figure 4. Results from Experiment S18. Radial profile of 900-mb vertical motion at 192 hours.

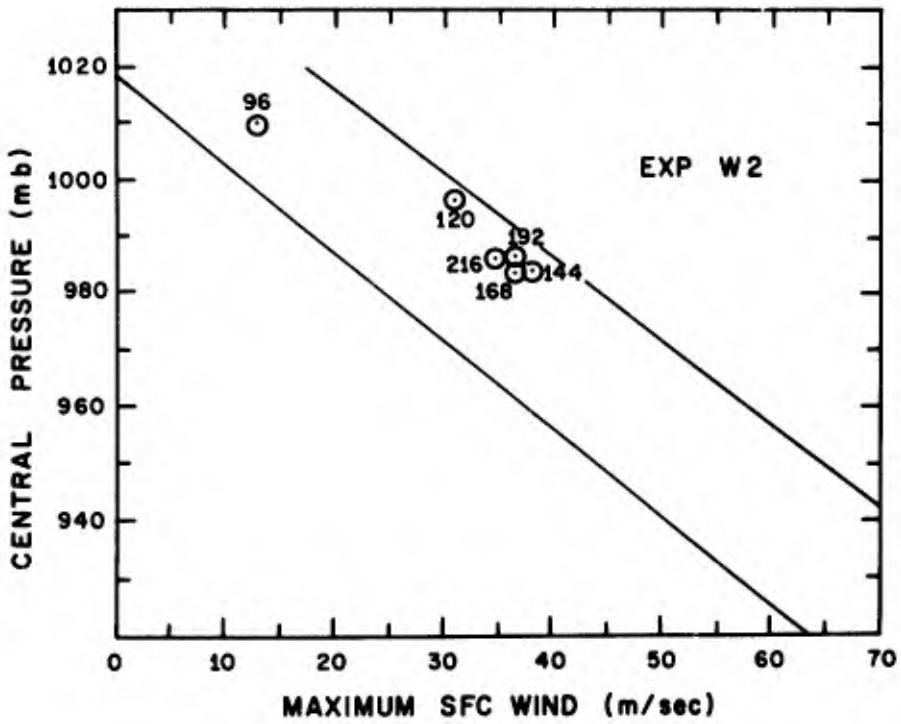


Figure 5. Results from Experiment W2. Central pressure plotted against maximum surface wind for hours 96, 120, 144 and 168. Parallel sloping lines are drawn to enclose most of Colón's (1963) empirical data points from a large number of tropical cyclones in various stages of life cycle.

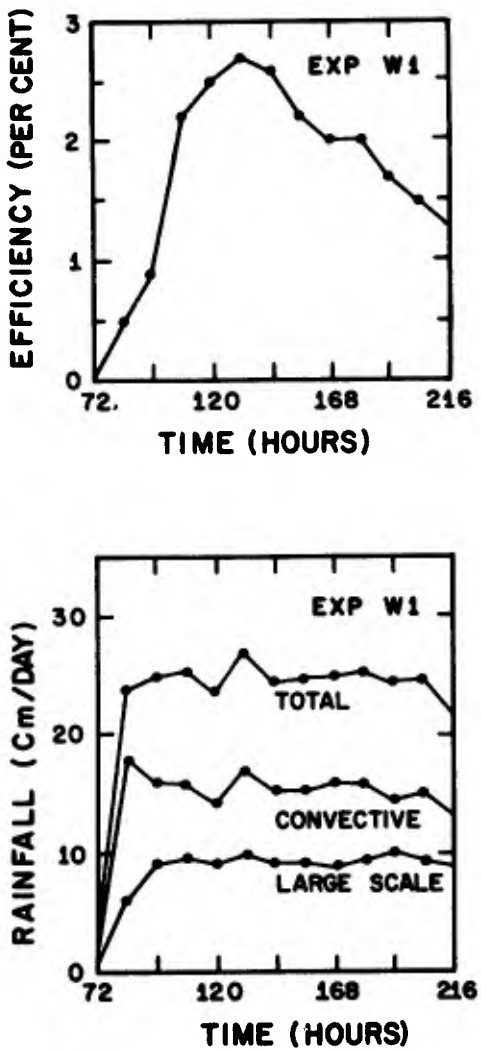


Figure 6. Results from Experiment W1. Top: efficiency of the radial interval zero to 200 km. Bottom: average rainfall over the radial interval zero to 100 km.

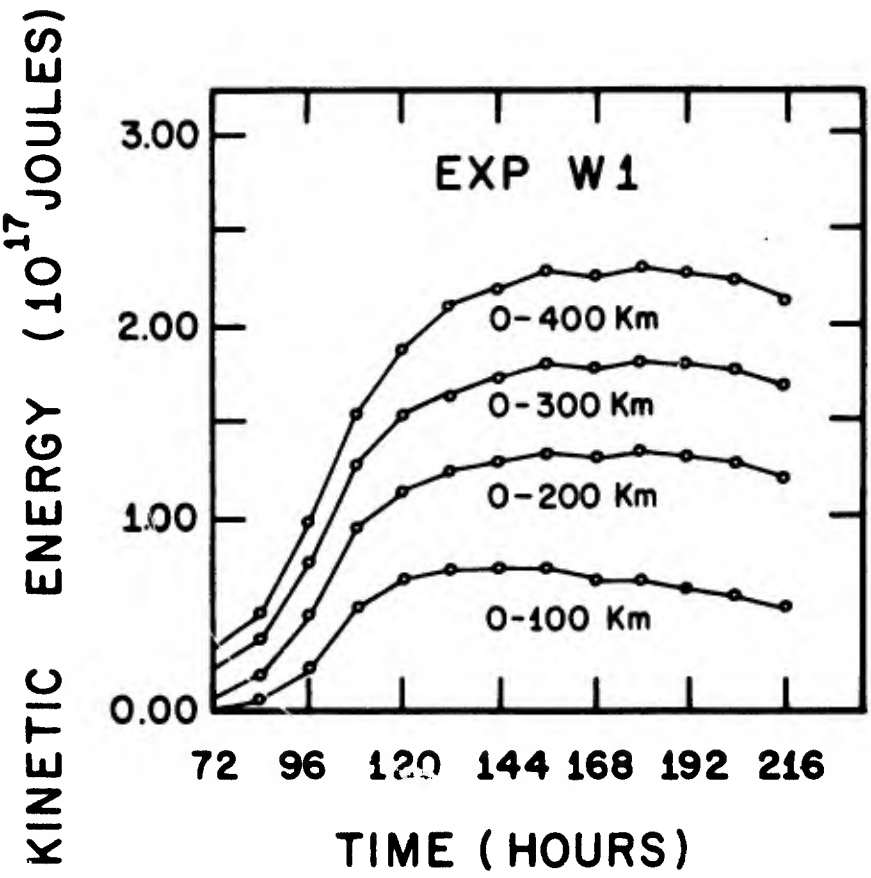


Figure 7. Results from Experiment W1. Variation with time of the kinetic-energy content of various radial intervals.

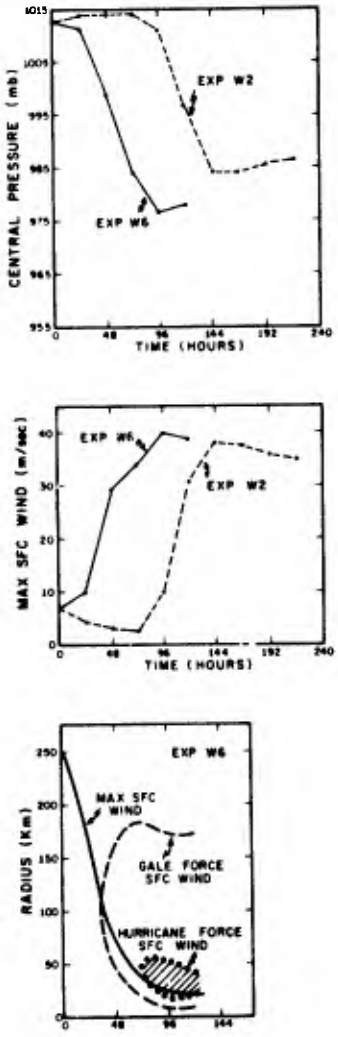


Figure 8: Top: comparison of central pressure as a function of time for Experiments W2 and W6. Center: comparison of maximum surface wind for Experiments W2 and W6. Bottom: results from Experiment W6. Radii of maximum surface wind; inner and outer limits of hurricane force and gale force winds at the surface.

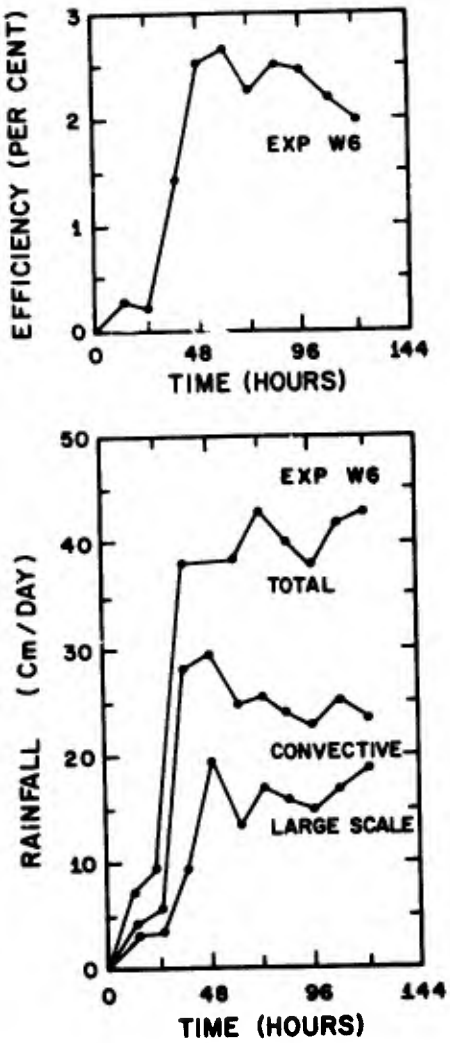


Figure 9: Results from Experiment W6. Top: efficiency of the radial interval zero to 200 km. Bottom: average rainfall over the radial interval zero to 100 km.

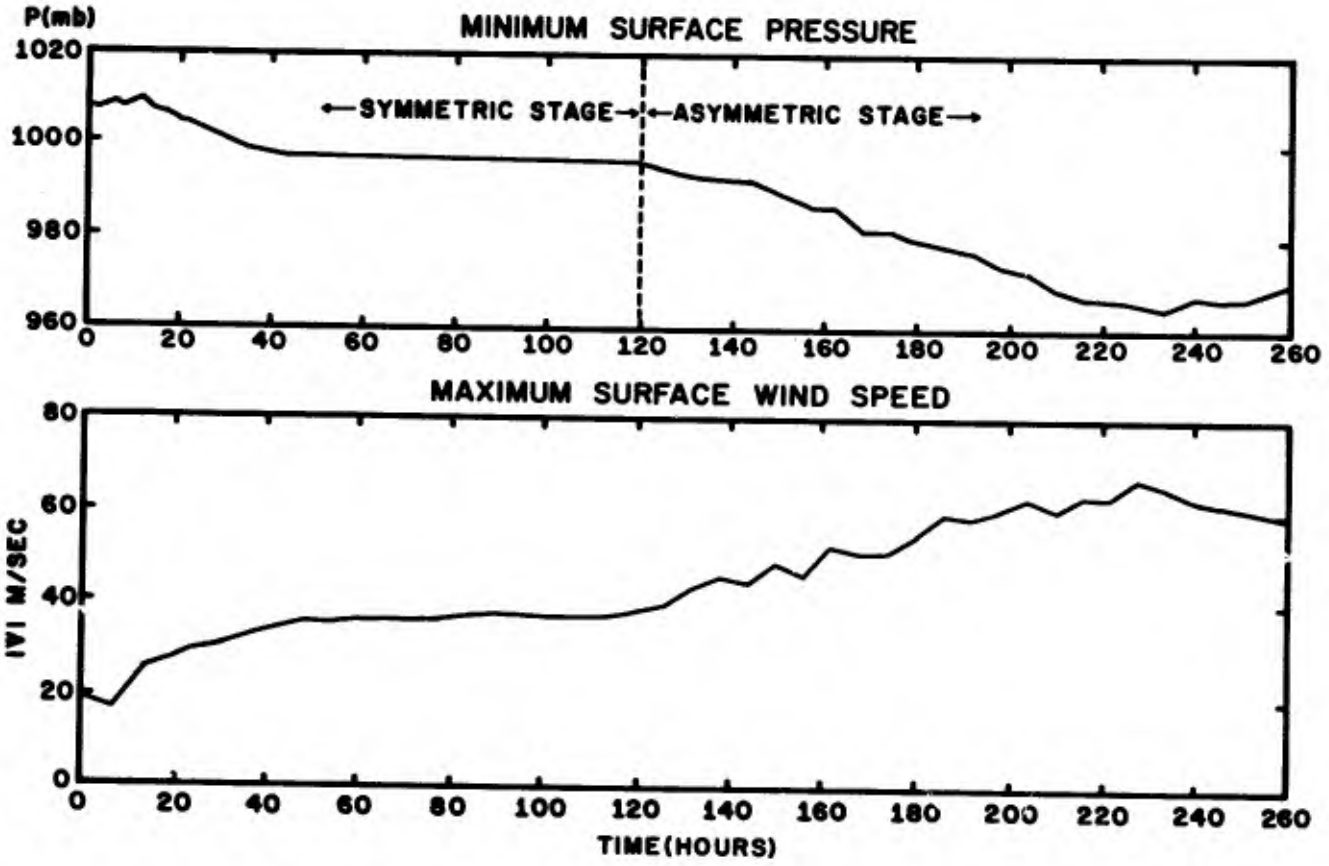


Figure 10. Results from an experiment with the asymmetrical model. Top: central pressure as a function of time. Bottom: maximum boundary-layer wind as a function of time.

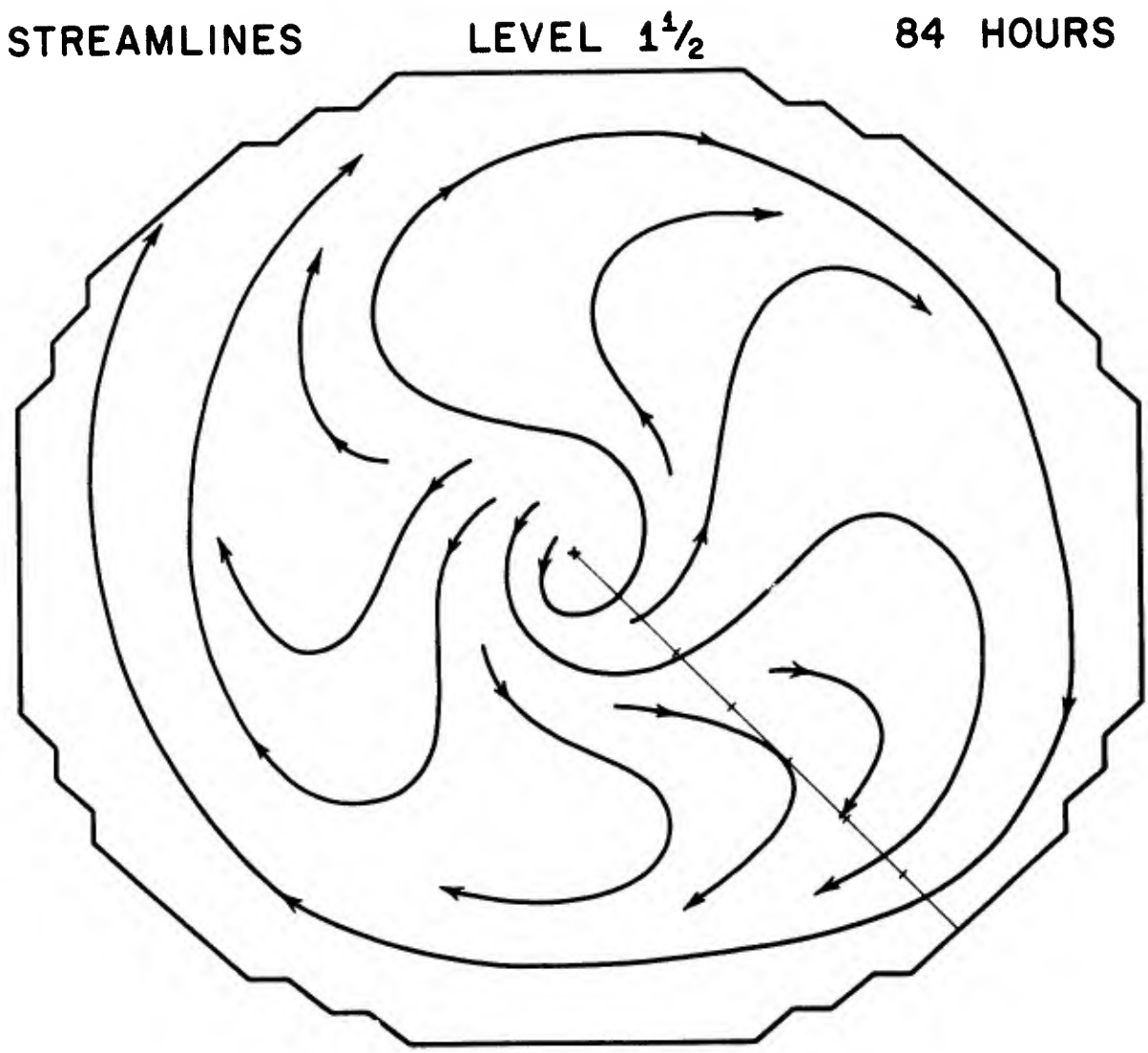


Figure 11. Results from an experiment with the asymmetrical model. Streamline pattern in the upper troposphere at 84 hours. Radial line in the southeast quadrant is marked at intervals of 60 km.

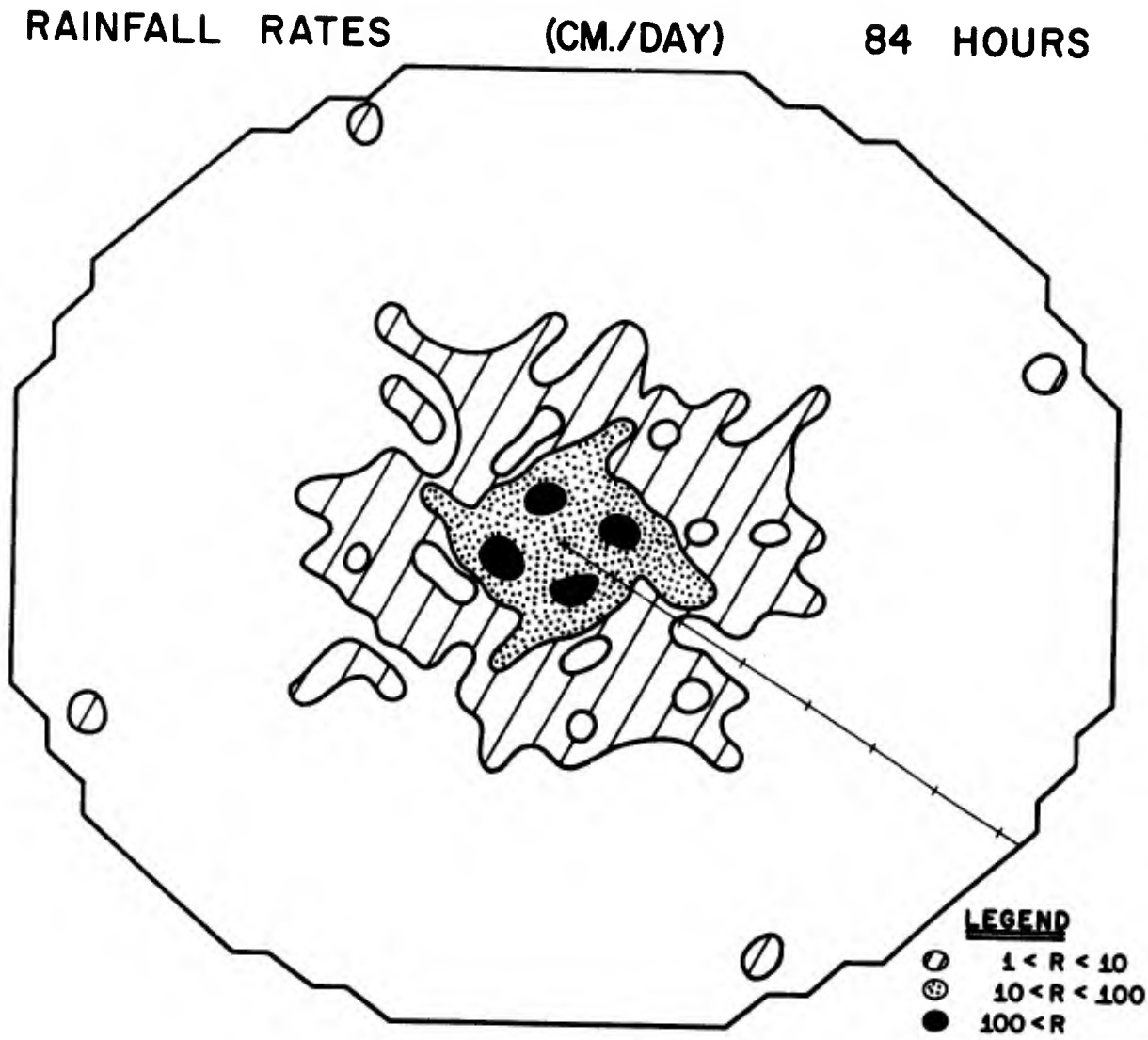


Figure 12. Results from an experiment with the asymmetrical model. Rainfall ($cm\text{-}day^{-1}$) pattern at 84 hours.

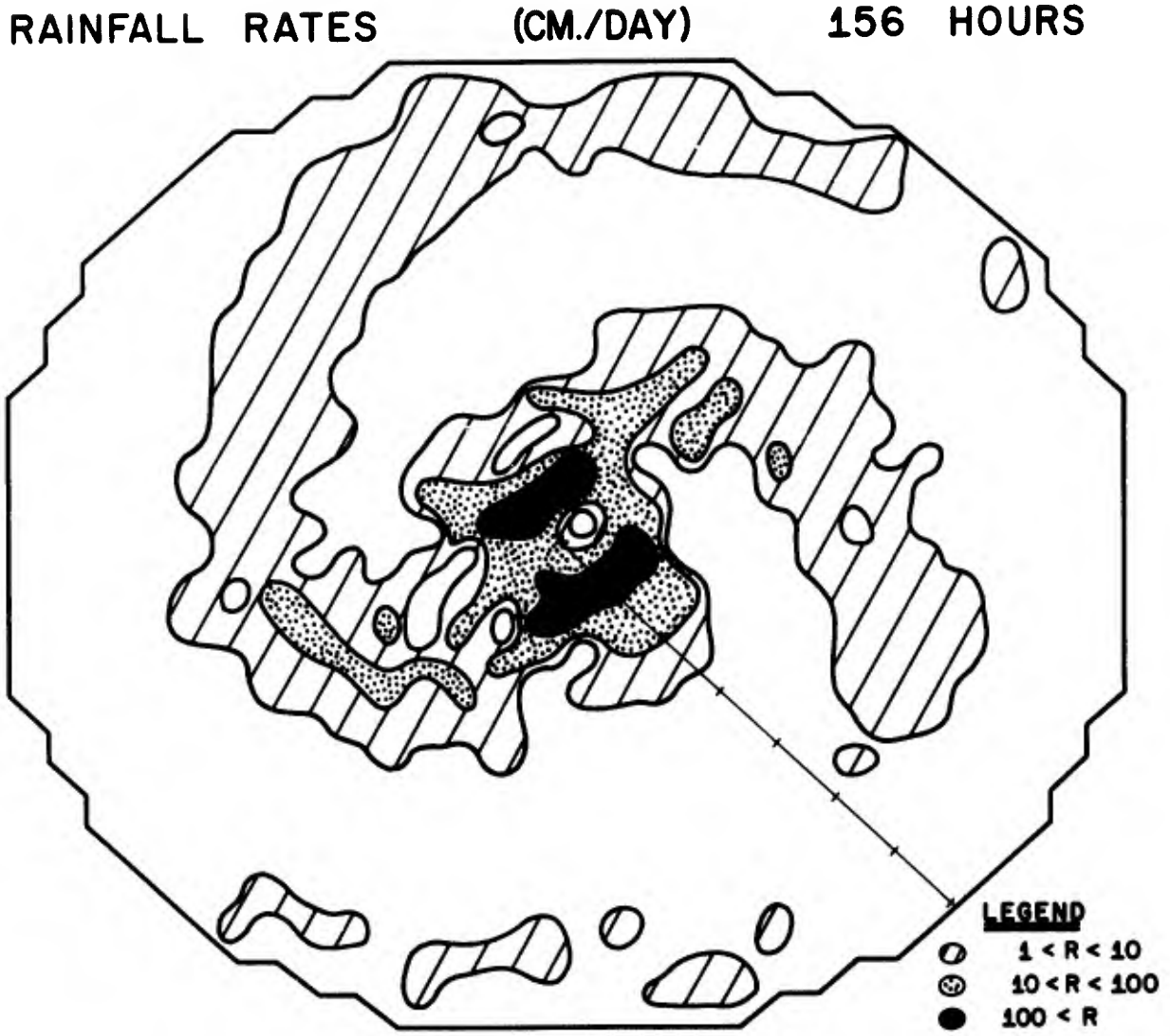


Figure 13. Results from an experiment with the asymmetrical model. Rainfall ($cm\text{-}day^{-1}$) pattern at 156 hours.

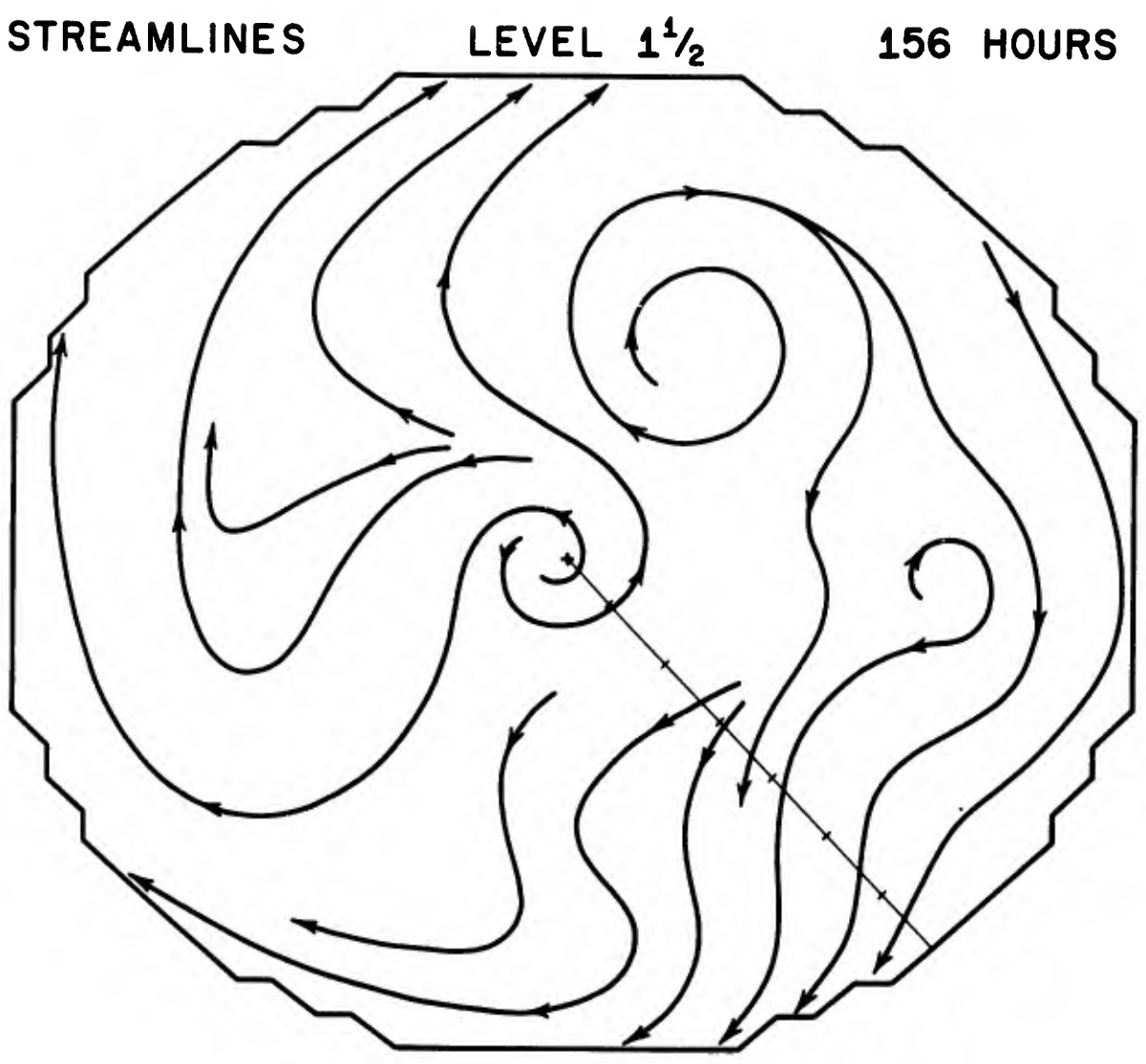


Figure 14. Results from an experiment with the asymmetrical model. Streamline pattern in the upper troposphere at 156 hours.

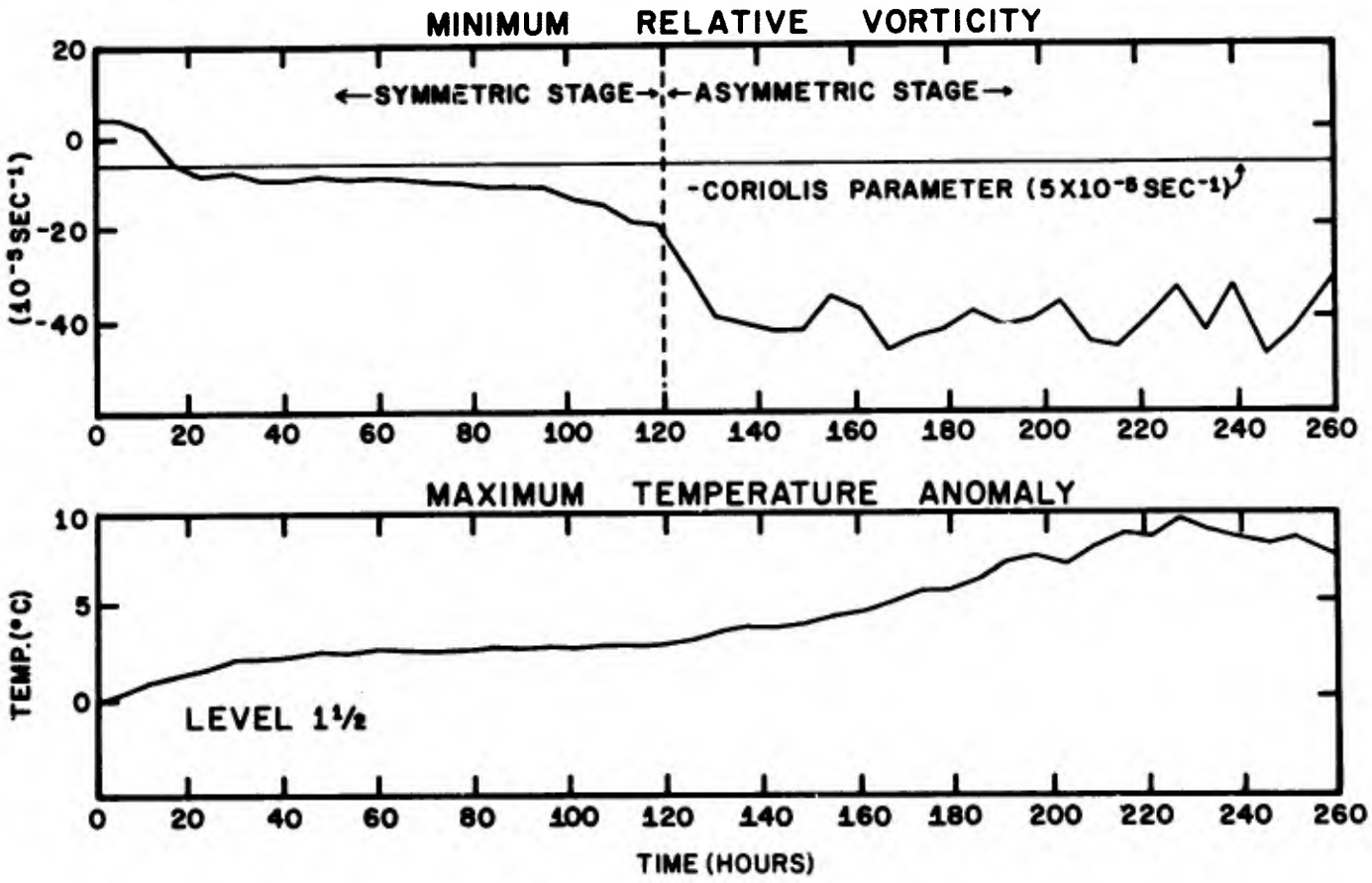


Figure 15. Results from an experiment with the asymmetrical model. Top: minimum relative vorticity in the upper troposphere as a function of time. Bottom: maximum temperature anomaly in the upper troposphere as a function of time.

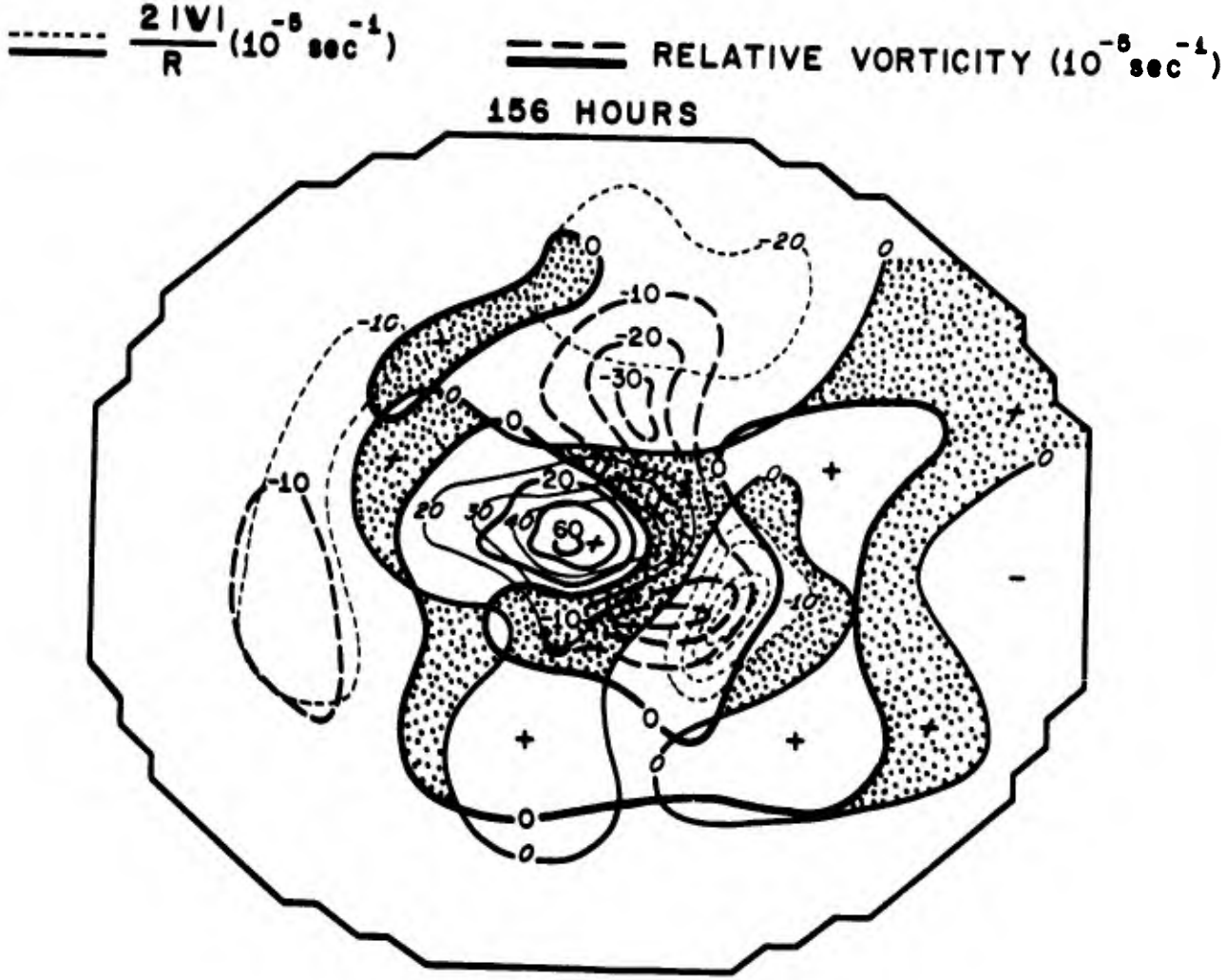


Figure 16. Results from an experiment with the asymmetric model. The upper tropsophere at 156 hours. Heavy solid and lines are relative vorticity. Thinner solid and dashed lines are $2|V|/R$. The dotted region is the area in which the criterion for dynamic instability of horizontal parcel displacement is satisfied.

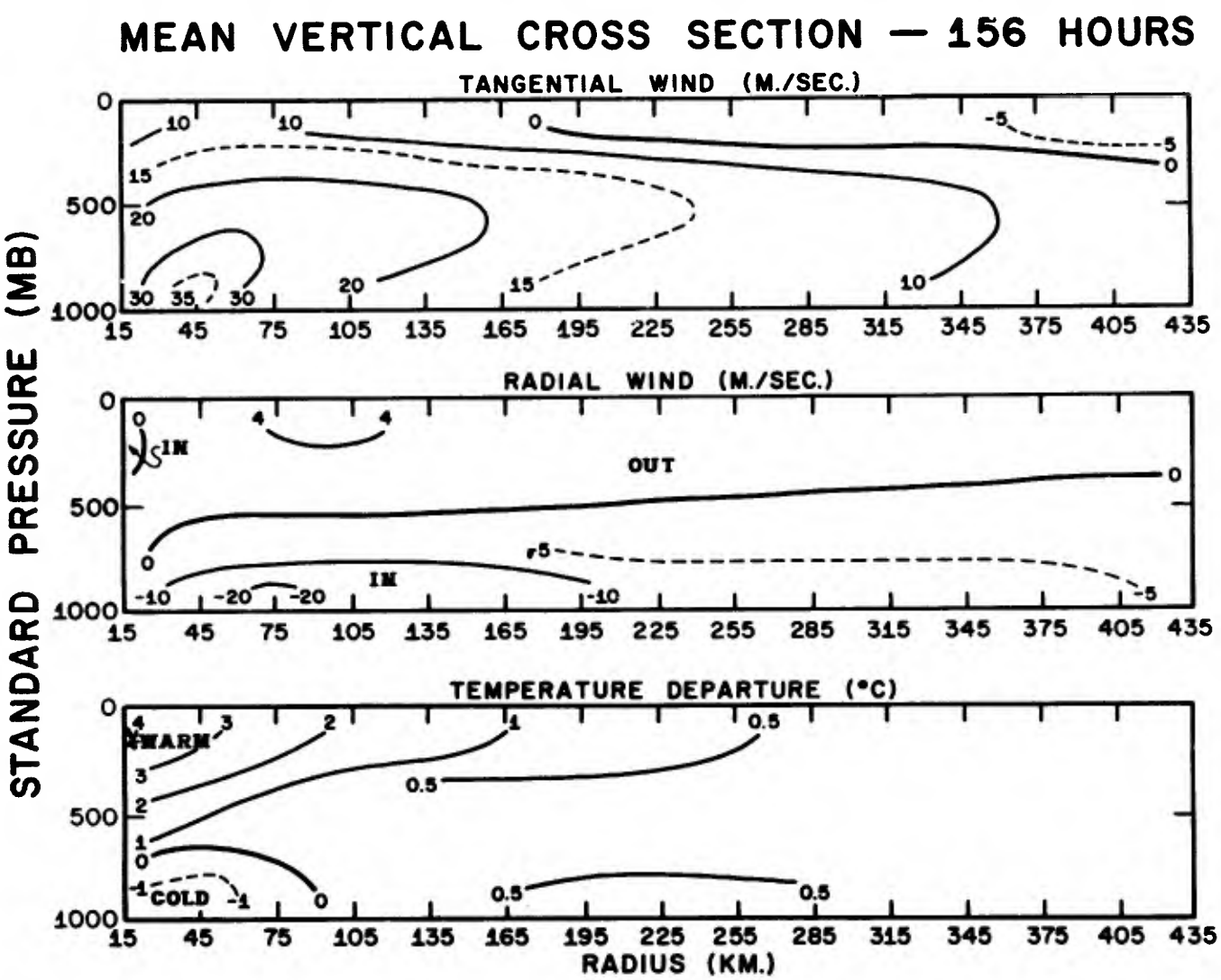


Figure 17. Results from an experiment with the asymmetric model. Vertical cross-sections of circular averages at 156 hours. Top: Tangential wind. Center: Radial wind. Bottom: Temperature anomaly.

## Chairman

Dr. Karl Johannessen, Associate Director of U. S. Weather Bureau, ESSA

## Panel Members

Colonel Daniel Mitchell, Commander, Air Force Global Weather Central
Dr. Fred Schuman, Director, National Meteorological Center
Capt W. Sam Houston, Commander, Fleet Numerical Weather Central
Capt Colin Armstrong, Assistant Commander for Operations, Naval Weather Service Command
Mr. Leonard Snellman, Chief, Scientific Services, Western Region, ESSA/Weather Bureau
Lt Col Glenn Reiter, Chief, Aerospace Sciences Division, 2nd Weather Wing, Air Weather Service

## DISCUSSION

The following is a summary of the panel discussion by producers and users of automated meteorological products on common problems associated with automation. The discussion was based on answers to prepared questions by selected panel members and answers to questions from the floor.

## PREPARED ANSWERS TO THE SET QUESTIONS

### On Requirements for Future Progress in NWP

QUESTION No. 1. In order of priority, what areas have the greatest potential for future progress in NWP considering the practical limitations of current and planned personnel and financial resources, and what is the rationale for your selection: (a) better observational data coverage, (b) increased computer capability, (c) more research on numerical methods, (d) more research on development of more sophisticated and realistic atmospheric models, or (e) other areas?

Shuman. — The list is no less than the areas vital to progress in numerical weather prediction (NWP). The first four — (a) better observations, (b) faster computers, and greater know how in (c) mathematics and (d) physics — are the ones used as the basis for my discussion at the Colorado Springs Conference last year.

"(e) other areas" is an important addition. Numerical weather prediction (NWP) has come to mean more than a rather narrow scientific discipline. It also embraces engineering techniques and, of course, service. In a thorough discussion of progress of NWP it would be difficult indeed to separate it from quality control, automated graphics and communications, and the methods of use and interpretation of NWP products by forecasters (the so-called man-machine mix).

We need not only to know how, but also to do, and the products must be effectively utilized. Anything less is not progress in a service-oriented endeavor.

In the long run, no order of priority can be given to the five areas listed. Each is as essential as the others for continuing progress. Even in a limited time frame, we have never been in a situation where improvements in any one of the areas did not lead to progress. In a limited time frame, however, an order of priority can generally be assigned, although the order will vary from time to time.

The most obvious example was the overriding importance of the computer limitation before the advent of modern electronic high-speed stored-program machinery. Following acquisition of

early versions of such machinery in the early 1950's, a combination of lack of scientific knowledge and know-how in numerical methods was encountered, and remained the controlling factor for several years. This was followed around the turn of the 1960's by a brief period when the most important factor for progress was learning by the forecaster to use the products more effectively. Baroclinic models and machinery to run them coincided rather happily in the early 1960's, but know-how in primitive equation models with high vertical resolution preceded by some five years the machinery on which they could be run operationally (in 1966).

With continuing improvements in the physics of the models, in analysis methods, in automatic communications, and in the observation system (oceanic AIREPs and various kinds of satellite-based observations), we are again in a situation, I believe, where the computer limitation is the most serious one. At this time I place increased computer capability at the top of the list of priorities. We need raw speed to reduce truncation error by reducing the distance between grid points in the horizontal and, we believe, in the vertical as well.

Computer relief is just around the corner, since the so-called fourth-generation computers, some six times faster than the CDC-6600, already exist. Only budgeting, the acquisition process, and reprogramming stand in our way, and such problems should prove soluble within a year or so.

Better observations are second on my list of priorities at this time. Every indication is that dramatic relief of this ancient problem is also near at hand. The Vertical Temperature Profile Radiometer (VTPR) is planned to fly on ITOS-D in early 1972. This promises global six-level temperature coverage, and is an operational system. Experience with early experimental versions of this type of equipment, SIRS-A and SIRS-B aboard Nimbus-3 and Nimbus-4, has been favorable, and much is expected of VTPR. Operational prototypes of geostationary satellites are also due beginning in 1972, and wind observations made by tracking clouds should provide vital information, especially in low latitudes.

I will not order priorities further, but want to say that it is not my intention to recommend a diversion of effort from one area to another by the priorities I have assigned. This is merely an interesting little game I am playing at the behest of the program committee of this Conference. Advances on all fronts must continue if we are to have orderly progress.

QUESTION No. 2. What data sources do we have now that are not being exploited fully? For example, is it necessary or desirable to obtain all AIREPS available at civil airline and governmental flight-control facilities? Can we better use our aircraft-reconnaissance capabilities to cover data-void areas? How can we better use satellite data? What other practical and feasible steps could be taken to increase the timely availability of data for NWP both within the CONUS and worldwide.

Houston. — Since the Navy is primarily interested in analysis/forecasting for ocean areas (typically sparse-data areas), it is vital to get all ship obs, upper-air obs, and AIREPS from these regions, particularly in tropical or subtropical regions where our coverage is worst.

I am convinced that we are receiving only a fraction of the total available surface ship observations and AIREPS. Many AIREPS reported to ARINC (and possibly to military collection stations) die at the collection point. Many commercial ship reports die at the nearest shore radio station or intermediate collection point or never leave the ship. I personnally believe that our surface ship and AIREP coverage could be increased over 100% with a concentrated effort on (a) accepting reports at military and commercial radio stations from anyone with a report to offer and (b) on forwarding collectives into high-speed channels. Funding of the program to reimburse commercial stations and shipboard operators should be increased.

Navy and Air Force reconnaissance flight routines and schedules show a tremendous capability to cover data-void areas. However, the actual number of recco reports which reach Monterey by cutoff time is very low.

Observations from satellites may be the answer to data gathering from ocean areas. However, during one week in July of this year, we received 7 first-quality observations in time for the preliminary analysis.

Recommendations:

1. ARINC links from key commercial collection points direct to AWN terminals.

2. AWS/AACS links from major MAC terminals direct to AWN terminals.

3. Authorization for military radio stations to accept reports from any ship (Naval or civilian).

4. Regularly scheduled recco for the remaining void areas.

5. More control on forwarding of ship reports by Navy and WB collection points.

6. Model changes to make use of asynoptic data.

QUESTION No. 3. What do you envision as the optimum mix of hemispheric or global models and fine-mesh and boundary-layer models to provide the maximum information considering the observational coverage currently available or planned for the near future? Should the fine-mesh models be run completely independently and extended over a larger area to reduce boundary influences in the area of primary interest, or should they be run for the smaller areas of primary interest and tied into the forecast fields from the coarser-grid models?

Mitchell. — The key factors in determining the optimum mix of models with limited computer capabilities must be the operational requirements, the data density, timeliness of data receipt and computer run times. With currently available computers it is impractical to prepare fine-mesh models for an area where we have no operational requirement or where little or no data exists. However, we cannot rely on coarse-mesh models to forecast weather resulting from small scale features for critical operational areas where adequate data is available. Detailed fine-mesh models are required to forecast for airfield terminal weather, point storm warnings, air pollution, etc., while coarse-mesh models are moderately satisfactory for long-range aircraft navigation information.

We at AFGWC have concluded that with current computer capability, coarse-mesh global models augmented by limited area fine-mesh models over land areas where we have extensive operational requirements and adequate data is the optimum mix. Our coarse-mesh 6-level model (GWC grid, approx 200 miles) is run out to 72 hours with a 3+20 data cutoff time. A dry version of Dr. Shuman's PE model is run on the 0600Z and 1800Z data out to 36 hours. A fine-mesh model is run for the U. S. window with a 1+00 cutoff time using SLAM's. This is used for input to the boundary-layer model with a 1/8 GWC grid (approximately 25 mi) for the U. S. A similar schedule is to be followed for the European and Asian windows. We also have a contingency window that can be run for any area of the world.

Given greater computer capacity a global PE model with approximately 100-mile grid spacing with more detail in the boundary layer is ultimately needed.

## On Quality Control of Numerical Products

QUESTION No. 1. Should there be a common quality-control program for standard products prepared by the various centrals, e. g., a standardized program for verification of upper-level prognoses against observed data at various forecast periods?

Armstrong. — There should be quality control of all products, a man-machine mix both at the processing center and at the user inface location. The amount of quality control or effort utilized by verification should and does depend on the individual user's accuracy requirements. At our Fleet Numerical Weather Central we run a RME program between our Navy barotropic model and the Navy's five-level PE Model as described by Lt Kessel. We also run some spot checks against the NMC FAX-chart data which would represent NMC's six-level model. Verification is only one facet of quality control. The verification statistics now being kept by each agency on its own product performance could be used to design common criteria. The approaches are already quite similar, but comparison against each other has always been spotty because fields haven't been exchanged routinely. Forecasts should be compared against each other's analyses as well as against certain high-quality observations, for, as we know, analyses are not necessarily the same.

Houston. — Verification is only one facet of quality control. By all means, there should be common yardsticks for those key products which are common. The verification statistics now being kept by each agency on its own products' performance could be used to design common criteria. The approaches are already quite similar, but comparison against each other has always been spotty because fields haven't been exchanged routinely. Forecasts should be compared against each other's analyses as well as against certain high-quality observations. Quality control of analysis is of vital importance; exchange of preliminary analyses would allow for quality control of input data and may lead to improvements in data exchange.

QUESTION No. 2. What type of quality control of progs is best suited to detect errors or weakness in NWP products for example: objective, subjective, and combinations of objective and subjective?

Snellman. — The type of quality control used should depend on how the NWP products are used. Monitoring the quality of most NWP products and especially horizontal flow patterns can be done, in my opinion, by presently available objective verification schemes. However, it is frequently important to verify limited areas separately. Systematic errors in NWP products are often linked to geographical locations.

I believe that subjective evaluation of NWP products has an important place in an overall quality-control program. A product can consistently verify rather poorly, yet be a useful tool to a forecaster because of the way he uses the product. The 72-hour 500-mb NWP prognosis is an example. This prognosis frequently shows up rather poorly against the verifying chart as regards smaller-scale features; yet when used by a forecaster as an indicator of only the changes in the larger-scale features of the flow, it rates high marks in quality.

Also, there are two types of quality control required — accuracy of product and availability. The former has been discussed above, but the latter is also important. Some subjective control is needed for availability, including missing and illegible products, inadequate labeling, etc.

QUESTION No. 3. What role should field users play in the quality control of centrally-prepared numerical products?

Reiter. — The field should have a very limited quality-control role. First, I will outline the reasons why the centrals should do almost all the quality-control work. At the end I discuss the field-users role.

1. It is not economical to have a large number of field users repeating the same quality-control checks.

2. Field units are not manned for the quality-control function nor do they have the capability to do in-depth checking of computer products.

3. The facility that makes the forecast should do the amending of the forecast rather than having a number of separate field amendments.

4. Not all users of centralized products are meteorologists. There are products that go directly to the operator who has no means to quality control the products.

5. The best data base is at the central. The effective utilization of limited communication facilities restricts the amount of raw data available at the field units.

6. Centers can update their data base and forecasts using specific criteria for each product making use of their computer facilities.

The field units have an obligation and responsibility to notify the center if they discover serious errors especially if these errors would constitute a hazard to the operator. For the first three hours of a forecast period, field forecasters must have the freedom to change the forecast to cover the obvious errors detected in using the center products.

Field forecasters have broader responsibility in regard to use of computer products than is encompassed by the term quality control. That is, as they interpret and modify the machine output to produce forecasts for their customers they must record their reasoning for these modifications so the center meteorologists can develop improved programs for the machine.

There must be communication between the researcher and the field forecasters so the field-users knowledge can be incorporated into research and development efforts [1] .

[1] Fletcher, Robert D.: "Two Outstanding Problems of Modern Meteorology," Bull. Amer. Meteor. Soc., Vol. 37, No. 9, November 1956, pp. 473-476.

---

QUESTION No. 4. What percentage of its resources should a computerized weather central devote to quality control of data, of analyses, of prognoses?

Mitchell. — For any meteorological product quality has to be in terms of its capacity to satisfy an operational requirement, and the meteorological needs of the customers of each center are different. As a matter of fact, the military needs of my many customers are usually illusive, contradictory and demanding — all at the same time!

It is important, however, to realize that a weather product may be high quality for one application, and very low quality for another; for instance, a smoothed forecast wind-field provides good quality winds for navigation, flight, and fuel-consumption planning, but provides low-quality forecasts for meso-scale clouds and precipitation. Judging quality is not easy, particularly if you don't know what your product may be used for.

Quality control in the weather central must consider the prevention, detection and correction of errors in centralized analyses and forecasts. Errors in data is the first consideration and includes the obviously important data-quality control functions in data acquisition, communications handling, data recognition, and data decoding. These are extremely vital functions that must be done at whatever the cost.

The decision on how much to devote to quality control must be made by each center based upon the impact of poor quality on the user. In our case in the Air Force the costs of weather-product quality control are small when compared with the costs resulting from not having quality control — the cost of the loss or degradation of just one of the many exotic weapons systems we support may finance our quality control for several years.

Determining quality control costs is always difficult. A broad guideline is to charge to QC all functions which would not have to be performed if all raw data, production and delivery were perfect, and if this could be guaranteed well in advance of production. Just as the goal of industrial quality-control systems is to improve the product until product-quality inspections are redundant, so should the goal of a center's quality-control system be to eliminate the need for it's error-detection functions.

In summary, the answer to "how much" quality control lies in each individual center's answer to "what for?" and "what if I don't?". In AFGWC's case, where tailored environmental products go direct to the operator, the "what for" answer comes from the operator himself, and anyone who has had military experience knows the answer to "what if I don't!" The answer to what percentage of resources should be devoted to quality control is: Whatever is necessary to assure success in meeting the mission requirements.

Shuman. — The question cannot be answered precisely as posed, but is useful to jog discussion. Quality control is very fuzzily bounded with R&D and general management and supervision, for example. In general, with a given amount of available effort and resources, a balanced effort must be made to maintain quality reliably.

Control of quality is more effective if it is done throughout the operation and organization. If a large block of effort and resources were set aside, specifically marked "quality control," the danger would be run that an attitude of "let George do it" would develop in the rest of the organization.

NMC has, however, small efforts clearly marked "quality control." We have a Quality Control Specialist in the Upper Air Branch, who works closely with Data Acquisition Division of the Weather Bureau. This specialist, using the data banks of the NMC communications computer, keeps a close watch on all rawinsonde data received in the center. In the case of errors or deficiencies detected in U. S. observations, notification is sent to the originator on an observation-by-observation basis. In the case of other observations, correspondence is initiated with foreign services when consistent long-standing deficiencies are recognized.

In the Analysis and Forecast Division, Office of the Chief, there is a group of three people who maintain verification records on key products. Verification statistics are of little use to a center except as a check on quality. About 50% of the effort of Development and Testing Section of Extended Forecast Division can be called quality control. They are heavily involved in verification and testing.

The Senior Duty Meteorologist, who in effect is the real-time chief of the center around the clock, is engaged in quality control at least 90% of the time. He is responsible for everything from timeliness of flow of material and standards of professional judgments by forecasters down to legibility of labels. The Extended Forecast Division crews, being much smaller, do not have a man relatively free of fixed production assignments, but the same problems exist, and a like effort is expended on supervisory quality control.

There are computerized verification programs and checks against errors in all machine programs from initial passage of data through the communications computer, through the analysis and prediction codes, to final exit of information from post-processing codes. These all clearly fall under the process of quality control.

We depend very heavily, by the way, on the field for quality control of our products. About three contacts a day are originated by the field, some written, but most by telephone. Our policy is to fully respond to such contacts, correcting mistakes and complying with requests when feasible, or fully explaining when not. Contacts also come from special interests through Weather Bureau Headquarters, such as aviation interests; and from foreign services through Office of International Affairs, ESSA. All of these are recognized as valuable to quality control of our operation.

We are not a factory turning out automobiles the same day after day. It would be interesting to explore the semantics of the words "quality control" when applied to products made largely with professional help. Professionalism is necessary precisely because each cycle deals with a new weather situation different from all others. Maintenance of quality in a flow of professional judgments, if seems to me, must be primarily the responsibility of the individual professional himself. If we go a step further, and include under "quality control" all activities affecting quality, then the phrase becomes all-inclusive, covering the entire organization.

Houston. — It depends on mission requirements; the most important products require the most quality control. About 10 percent of manpower and 2-5 percent of computer time in each area, should be alloted.

The control should be automated to the greatest possible extent in all three areas; however, for the foreseeable future, human judgment will be required. Automation is most feasible in the control of raw data. Control of analysis/prognosis quality can be (and is) partially automated. At the present time, it is still necessary for experienced scientists to eye-ball products to determine if they "look like the real atmosphere." Many times the product has been transmitted before the quality controller gets around to making his decision. More effort needs to be expended on automated quality control (through better program design and through faster means of quick-look display). Real-time quality control from the user in the field is feasible if proper communication channels and quick-look displays are available. The field user should also be encouraged to provide "feed back" useful to longer-range model changes.

## Exchange of Information Between Computer Facilities

QUESTION No. 1. What steps have been taken or are planned for the real-time exchange of numerical products between your facility and the other major weather centrals to provide mutual backup to protect against catastrophic failure (machine or communications) in one central or for the exchange of specialized products (e. g., outputs from fine-mesh or boundary-layer models, oceanographic data, etc.) on a routine basis?

Shuman. — Under the aegis of the Federal Coordinator for Meteorological Services and Supporting Research a plan [1] was completed last month for massive backup of NMC by the Air Force Global Weather Central (GWC). The backup provided is not complete, but is designed to provide reasonable continuity of facsimile products to field facilities in the event of an extended power outage or computer failure. Outages of less than 12 hours are not covered by the plan, nor is the entire facsimile schedule. Only the National Facsimile Circuit (NAFAX) will be served by GWC. The purpose of the plan is to achieve backup of high priority

products within existing resource constraints. The plan calls for 38 transmissions per day from GWC, including 62 separate fields of variables.

---

1 Federal Plan for Cooperative Backup among Operational Processing Centers. FCM 70-4. U. S. Department of Commerce, Environmental Science Services Administration, Federal Coordinator for Meteorological Services and Supporting Research, Washington, August 1970, i + 8 pp.

---

Houston. — FNWC has initiated a request for a drop on National Fax circuit for the express purpose of comparing our products with NMC products. FNWC and GWC are installing a full-duplex computer-to-computer link for (a) exchange of common products for verification, (b) transmission of unique products to avoid duplication, and (c) emergency backup of raw data sources. FNWC will provide low-level and oceanographic products requested by GWC and will receive unique high-altitude products generated by Offutt.

Mitchell. —

a. With regard to emergency backup:

1. We are providing backup to the USWB facsimile system. This consists of preparing and transmitting charts over WFX 1234 upon notification from NMC. Backup of AFGWC analysis and prognostic charts by NMC has been discussed but no firm plans generated.

2. There are no plans at present for mutual emergency backup between AFGWC and FNWC.

b. With regard to routine exchange of products:

1. Product exchange with the FNWC has been underway for over one year and plans to increase are underway. A 6000 WPM full duplex circuit will be operating between FNWC and AFGWC computer before the end of the year.

2. Facsimile products are received from NMC over the national facsimile net.

QUESTION No. 2. What are the advantages of having representatives from the other weather centrals permanently stationed at each of the three major centrals?

Houston. — The primary advantage to FNWC has been in the area of coordinating raw data and autodin message traffic into and out of the AWN. Of secondary importance to date, has been direct liaison work to keep each other advised of plans and programs. FNWC has been particularly fortunate in having the services of two experienced USAF programmers. Lt Col Long has written Varian display programs which are a breakthrough in real-time quality control by FNWC duty officers.

Mitchell. — A people-exchange program at its best must contribute to a more optimum National effort in environmental support and service. More for less is going to be demanded of us, so although our missions justify our existance we cannot afford to go down parallel paths in the expensive search for our most precious ingredient — knowledge.

More tangible and immediate potential benefits to accrue to each organization include the following:

a. The individuals concerned contribute to the mission of the organization to which he is assigned. He is a producer, not a visitor. He brings the unique talents for which he was selected to bear upon a different set of operational problems.

b. Having worked in a different environment he returns to his own operation with a fresh, less tunneled view. Hopefully, he will be able to contribute to new and better scientific techniques or methods of operation. However, if he does nothing but assist his parent organization avoid pitfalls, he has, in these days of explosive and costly technology, vindicated the exchange program.

c. Representatives acting additionally in a liaison capacity can (1) keep both organizations informed on programs and ideas and (2) facilitate exchange of products and techniques.

The key to a successful program is of course people. They must be the best. I wholeheartedly endorse an exchange program under these conditions. We have had two outstanding representatives from the FNWC since 1969. They have made significant contributions to the AFGWC mission. I am pleased to have them aboard and will welcome any more like them. Dr. Shuman and I have been discussing the details for an exchange program between NMC and AFGWC.

Shuman. — The three U. S. centers should be in close touch with what each other is doing, and an exchange program of visiting scientists would add much to liaison. I believe that is truer now than it has been in the past.

The three centers have now existed long enough that we can look at the situation with some perspective. The duplication which was feared some ten years ago when the three centers were established has materialized to no great degree. Each center has developed its program along lines demanded by its customers. Fleet Numerical Weather Central (FNWC) has specialized in oceanic analysis and prediction and Global Weather Central (GWC) in a highly tailored service including request/reply systems. The National Meteorological Center (NMC) with its broadly-based responsibility has strived for improvement of large-scale prediction models, with I believe some success.

None of the centers need apologize for the progress they have made. In looking around the world one would be hard put to find as good services based on solid hard-won achievements. It seems sometimes that this is more clearly recognized in foreign lands than it is here at home.

But times are changing, and much remains to be done. Each center of the future will need to a greater degree those very elements in which the others have specialized. The ocean and atmosphere will be tied together; request/reply systems will become a necessity if we are not to bury the forecaster further in piles and piles of charts and other materials; models will be going down the scale to serve the long-standing need for local short-range guidance, and up the scale for extended-forecast improvement; both the physics and numerics of models will be improved; positive adjustments to new and better computers, data sources, and collection systems will be made. We are not running out of things to do, and we need all the help we can get. This is not a situation which will be solved by pouring in new resources alone.

A sound first step I believe would be to freshly look to each other for techniques already developed. A program of exchange of visiting scientists would be an important part of improving free exchange of techniques and ideas generally. Such a program has been started with an exchange of people between FNWC and GWC and the establishment of Operating Location H (OL-H) of the Air Force at NMC. NMC is also well along with plans for sending a visiting scientist to GWC. A full exchange, however, will not happen overnight.

People must be carefully chosen, and sometimes trained, and personal preferences play a part, especially in the case of civilians. The trend is clearly in the direction of a complete three-way exchange, however, and will probably be an accepted way of life in the future.

## Problems Related to Centralized Computer Support

QUESTION No. 1. What products that your units are now preparing manually do you feel could be prepared more economically by a computer and with no loss (or with possible gain) in accuracy and timeliness?

Reiter. — There is hardly a limit on what else could be more economically prepared by computer if adequate long-haul communications to the field units were available. The actual limit is determined by the capacity of the computers and what can be sent to the field in a timely manner.

Any forecast that can be prepared by objective techniques could be made economically by computer. The following are examples: — icing, turbulence at all levels, cloud tops and layers, thunderstorm downrush velocities, and stability indices.

For instances, cloud tops are difficult for the field forecaster to handle. There is a lot of observational data available — IR, satellite, visual obs, aircraft reports, etc. The search

for the data and collating of eight to ten sources of information on existing clouds can be mind-boggling. The computer could do a much better job of picturing the current and predicted cloud distribution than our field forecasters.

Recently we completed the computerization of several routine tasks that were impossible to do economically by hand at the European Weather Central. These are good examples: — all synoptic, metar, and aero reports are screened for critical weather phenomena. Hourly bulletins of appropriate significant weather characters are plotted in the geographical location of the reporting station on a 1:10 million map scale. The computer scans approximately 2,000 hourly observations.

Also plotted on 1:10 million scale charts are ceilings and visibilities for the reporting stations. We have found these bulletins extremely useful in preparing sensible-weather predictions, our met watch, and also in our verification of weather advisories.

Real-time presentation of statistical information to the terminal forecaster in the form of graphical print-outs appears to be worthy of study. Our center forecasters must look-up and collate a mass of statistically and dynamically-derived information when preparing their terminal forecasts. A computer prepared pictorial display of the best statistical forecast along with important dynamically-derived parameters would be most helpful.

QUESTION No. 2. What are economics of automated, user-tailored products from a central compared with automated forecaster-guidance products requiring regional and/or local tailoring?

Snellman. — I think that centrally-produced automated products in user-tailored formats can save considerable manpower and facilities at field stations. Upper-wind forecasts for aviation users is an example. However, there are relatively few automated products of this type that are consistently of high enough quality to be acceptable. This is not to say that satisfactory automated products can't be produced. Many can, but most programs needed to produce them would be enormously complicated and require input data not readily available at a central location. Also, there are so many different user requirements that the number of programs needed would not make it feasible, at least for the next decade.

I believe that the best and cheapest way to provide users with adequate weather service is to provide the forecaster dealing with the user (i.e., local or regional forecaster) objectively-prepared guidance products which he tailors to meet user needs. The forecaster is then in a position to serve many users, to know their specific requirements and to fashion his meteorological advice in light of these requirements.

QUESTION NO. 3. What is the optimum method or methods to educate field forecasters on the use, advantages and limitations of centrally-prepared computer products?

Reiter. — All avenues for getting information to the field should be used. Education begins in the schools where information on centralized products and their use must be a part of the curriculum. The schools need to maintain a close-liaison with the centralized facilities so the instruction is current and meaningful.

Numerous publications in the form of tech notes, booklets, manuals, and pamphlets are necessary but not sufficient.

Personal instruction in the field stations in an eye-ball to eye-ball situation under the actual forecasting environment is absolutely necessary. Anyone who has ever spent Christmas eve putting a toy together with a set of instructions any child can understand realizes how effective real-time personalized instruction can be.

Finally, statistics on success and limitations must be made available to the field to build confidence in the products.

## QUESTIONS OR COMMENTS FROM THE FLOOR

Q: Dr. Stackpole, NMC. — Mr. Snellman, does the prediction that the man in the man-machine mix should be in the field mean that forecast centers (not analysis centers) will wither away?

A: Snellman. — As NWP products improve the manual effort at the forecast center should be eliminated. Adaptation of objectively-produced guidance to weather-service requirements should be done by local forecasters who know local terrain effects and requirements. We have already seen the man eliminated from NMC's production of temperature-forecast guidance. Reasons for this opinion are: 1) that local forecasters can learn and adjust to bias and systematic errors of machine products while manual input at central location is a variable and unknown quantity, and 2) the final central man-machine product is frequently too general for local use.

Exceptions would be man-machine central forecasts of hurricanes and severe storms. Here it is best to have a small group of experts at a central using machine outputs to produce rather specific forecast guidance, for these reasons: —

1). Need for consistent forecast over rather large geographical area, and

2). These phenomena occur infrequently at one location, so not feasible for local stations to be "tooled up" continually.

Q: Dr. Kreitzberg (Drexel Inst.). — For at least fifteen years it has been recognized that a substantial interagency effort is required to develop the knowledge, skills, and instrumentation to overcome our inability to forecast sensible weather and other mesoscale phenomena. How and when will we proceed beyond talk, proposals, and plans to implementation of an interagency meso-meteorological research, development and applications project?

A: Dr. Johannessen. — It is true that the many conferences held and some of the grandiose plans which have been prepared relating to mesoscale meteorology are more indicative of the importance attached to the subject than of the progress being made. It appears to be very difficult to get a concerted research effort in mesoscale meteorology off the ground. I feel that perhaps some of the disappointment stems from the tendency to regard mesoscale meteorology as a "system" or a "project." Mesoscale meteorology comprises the whole field of meteorology and progress in this area must come through progress in all branches of meteorology, in handling numerically the dynamics on all scales, in cloud physics, in turbulence transfer processes, and, perhaps more important than anything, through advances in the technology of observing on the mesoscale.

It is wrong, though, to state that no progress has been made. I think that very significant progress has been made. In the area of observing, the ATS series of weather satellites is showing us mesoscale weather as it has never been seen before. One mile space resolution and ten minutes time resolution is squarely in the mesoscale spectrum. The completion of the national weather-radar network is near, and through remoting techniques the detailed radar information is becoming generally available for forecasting purposes in locations away from the radar sites.

I believe that we are on the threshold of a new era in prediction and warning of mesoscale phenomena. The new opportunities have come about through technological advances in other fields than meteorology, as is often the case.

Comment by Mr. Thomas (ESSA/Weather Bureau). — NMC is now receiving more than 75% of marine upper-air data within operational deadlines. Quality control of data differs between national and international sources. Regular QC programs are being conducted to improve data acquisition at centralized facilities. Better coordination of data acquisition / QC efforts is needed between services and user/suppliers.

Q: Prof Elsberry (Naval Postgraduate School). — Do the panel members envision a changing role in education of the forecasters of the 1970s? Will this be a self-education, an organized in-house program, or some other program? Will there be a change in emphasis or in the depth of meteorological education?

A. Mitchell. — Future emphasis will have to be given to training of the Staff Meteorologist in his interface with the operators. Our products will continue to be more centrally prepared and the Staff Meteorologist must state operator requirements and assure that the operator gets adequate service. Internally at AFGWC, we are doing our own training. In many areas, it takes up to (6) six months for the new forecaster to become fully productive. The Air Weather Service does indicate to Hq Air Force special subjects for unique requirements for trainees in the AFIT program. These requirements change as operational techniques and requirements change.

A. Houston. — One aspect of the forecaster's education that must be emphasized more in the future is the understanding of computer programs to produce analysis and progs. This understanding is needed to improve the quality control and feedback function that the forecaster must perform now and for the foreseeable future. More emphasis should also be placed on the ocean-atmosphere interaction.

A. Snellman. — The role of education should remain much the same, namely to develop well-rounded physical scientists. Important changes in present courses are needed. For example the present rather clear distinction between dynamic and synoptic meteorological courses should be eliminated. Much of synoptic meteorology is dynamic meteorology, there is no clear separation now. Increasing emphasis should be put on satellite and radar meteorology. This means giving the student a thorough background in thermodynamics, dynamics, and geography as satellite picture interpretation involves this knowledge. Analysis and forecasting laboratory courses should continue but be drastically modified from present. I'm thinking especially of demonstrating meteorological equations by use of graphics in the laboratory.

In-house and self-education programs are needed due to rapid developments taking place in the science. Additional emphasis should also be placed on statistical analysis and computer science in undergraduate meteorological programs.

A. Armstrong. — I concur with the comments that have been made and feel that we will definitely have to still be strong in the basic preparation in the Navy and the Marine Corps because of our varying types of duty and forecasting aids available at different locations. I would like to review what I believe to be the Navy's present concept and plans for the Seventies. We plan to maintain a strong forecasting course at the Naval Postgraduate School (Monterey) for our officers and the same for our enlisted forecasters at Lakehurst, New Jersey. We plan and are emphasizing at these schools the computer's role and processes used as well as products available. We also have had in existence a two-weeks training course at our main processing center in Monterey. This has only been moderately successful because of the varying backgrounds of attendees. We have used teams of computer experts visiting Weather Centrals, facilities and smaller units, which has been very successful. We plan to continue this program and to complement it with satellite-forecasting experts. We also plan to have a readily updated, usable Computer Products Manual which will provide details of the products. We are updating an existing one at this time. We recommend short technical notes and technical memos issued for field forecaster use. We also recommend a tour or tours at the Fleet Numerical Weather Central Monterey. Emphasis should not change "in depth" but "in breath" as the forecaster will have to absorb more data and training to best utilize his new aids.

Comment by Dr. Gerrity (NMC). — I would like to comment on the significance of Mr. Huschke's paper for the education of meteorologists. Dynamical and statistical forecasting techniques will have to be oriented to provide guidance in the appropriate "probabilistic statement" of uncertainty.

Comment by Mr. Bradley (Drexel Institute). — With the advent of more asynoptic data and computers capable of reducing truncation errors, considerable research will be required on the analysis/initialization/assimilation problem in order that the full benefits shall be realized.

# SUMMARY COMMENTS

Dr. Robert D. Fletcher
Deputy Chief of Staff for Aerospace Sciences
HQ Air Weather Service
Scott Air Force Base, Illinois

The night before last, Senator Mathias spoke of the overriding importance of education in these modern technological days. I wish that he could have attended our meetings here this week. The papers presented by representatives of our military services and of our allied civilian agencies, governmental and non-governmental, have demonstrated that our profession takes a back seat to no one with respect to intelligent imagination and exploitation of the newest of sophisticated developments. The dedication of each participant to the unique requirements of his own organization, combined with his adherence to the highest standards of our science and profession, was truly inspiring.

I hope that each of you will have benefited from having heard of the developmental efforts and experiences of your colleagues. This is true in the case of the Air Weather Service. Hopefully these technical exchanges will help each of us better to understand and appreciate the points of view of the others. Of the benefits of these meetings I'd like to emphasize one which I believe has special potential. This consists of following through with respect to new approaches and ideas which have been expressed here. The Air Weather Service has listened, in the audience, to the expression of a number of new concepts which may be of great benefit to us. On each of these we intend to contact the individual or agency involved for advice and assistance which may lead to our adoption of it. Other offices represented here may wish to do the same.

It's impossible for me, in my job of summarizing the results of the meeting, to select any paper or indeed any session which was outstanding with respect to the others. Monday afternoon was devoted to the subject of automated analysis and forecasting. Continuing research shows promise for increasing the reliability of quantitative precipitation forecasts. New and promising approaches to prognosis of both equatorial and higher-latitude areas were described: persistence for the former, dynamics for the latter, with a "sponged-up" region in between. Use of a highly successful, detailed boundary-layer model was described. It was brought out that spectral models—radically different from those now programmed in our centrals—have considerable promise. Experiments with a very detailed primitive-equation model for a limited area in the tropical Atlantic showed real potential value. A new model explaining, for example, strong winds over the northwest wall of the Gulf Stream was described.

Tuesday morning we concentrated on local-area forecasting. In a discussion on predictability of local-area weather it was emphasized that we need a better handle on our limitations in order to guide the distribution of our resources. We were apprised of the availability of data from a very dense network of raob stations in southeast Asia and were shown beautiful films of selected analyses of these data. A very sophisticated technique for use in 24-hour weather forecasting, utilizing the analog approach, was demonstrated. The all-important role of the man, in his mix with primitive-equation products of a weather central, was clearly pointed out. Progress in automated production of ceiling and visibility forecasts was described.

On Tuesday afternoon emphasis was placed on tailored meteorological support. A sophisticated plan for collecting, editing, and distributing atmospheric data to Army field operations was described in detail with a goal of 1985 for its complete implementation. It was pointed out that condensation-pressure spread, vertical velocity, and potential temperature are predictable and give a good indication of expected weather, but we were cautioned that the data available must be at the same level as the ability to make command decisions. Current techniques for computerizing flight plans in large quantities and for extended areas were presented. In another application, equipment and techniques used in providing support to missile test firings were described. It was brought out that introduction of computer support to severe-weather forecasting has produced significant improvements in such service and that even more benefits are in the offing.

Wednesday morning representatives from several agencies discussed the automated processing and application of satellite data. At the outset it was emphasized that the computer is an absolute necessity because of the vast amounts of data involved. The producers of satellite data described the processing of scanning-radiometer data, monitoring of sea ice, extraction of sea-surface temperatures, upwelling in ocean currents, geological surveys, and other potentials. The users of the data debated the concepts of local and central readouts, and described the uses of satellite data in nephanalysis and prognosis programs and in cloud climatology.

Thursday morning was devoted to environmental simulation. Real progress has been made in simulating large-scale modification; e. g., removal of the Arctic sea ice, and advances are under way with other problems such as putting the ocean into the ocean/atmosphere computer model. We were shown remarkably realistic simulations of hurricanes and had a preview of the very latest results incorporating asymmetry into the hurricane model. The great value of modelling the interplay between weather and operations was brought out, and an example was described in which the quantitative value of weather to a tactical military operation was demonstrated. We were told about the relation between the Federal Government and the States under the provisions of the Air Quality Act, and the role of the meteorologically derived "air-pollution potential" in the overall pollution problem was clarified.

This afternoon we have just concluded a spirited panel discussion on automated meteorological support. The panel was made up of distinguished and experienced computer-output producers and customers and was outstandingly chaired by a self-proclaimed "layman." Matters such as quality control, data needs, research needs, and many others were taken up. Since I cannot summarize this very valuable panel discussion at all adequately, I suggest that the detail which will appear in the proceedings replace my summary in this case. As you know, all who registered and signed up for one will receive a copy.

I hope you will agree with me that this meeting—Texcon 6—has served a useful purpose. The job of organizing and running it has taken many hours of hard work by many individuals. Faced with the spectre of austerity, not to mention the world political situation, we don't know what the future has in store for us. Nevertheless the Army and Air Weather Service have been discussing the prospects of Texcon 7 with the Army as host, and we're talking in terms of a year and a half or two years from now at an Army location which will be announced when plans become firmed up. When they do, we sincerely hope we'll secure the valuable and wholehearted support which you all have provided us on the present occasion.

In closing, and speaking for Gen Best and the AWS, I wish to thank the Naval Weather Service Command for their superlative efforts and cooperation in presenting our 6th Conference, and to express our sincere gratitude to the Naval Academy for their gracious hosting of us here on this beautiful campus. We thank all the speakers for their valuable presentations, the program chairmen for the efficient running of their sessions, and the program coordinators for their helpful efforts. Special thanks are due Mr. Max Edelstein for his wisdom and hard work in acting for the Naval Weather Service side of the house. Mr. Edelstein will thank personally those Navy personnel most active in the program, and AWS wishes to add a warm endorsement to his sentiments. To Col Ed Jess go our thanks and expressions of appreciation for the outstanding managerial job he's done for the AWS. Thanks in advance are given to Mr. Robert Stone for preparation of the Proceedings, a job which will be well done if it's at all like what he's done for us at past meetings. And I want Maj Gary Atkinson, Mr. Val Descamps, Maj Karl Hebenstreit, and Capt John Diercks to know that AWS is extremely appreciative of the long hours of thought and work they have devoted to this conference. Perhaps most important of all, many thanks to the attendees for their being here and for their discussions which have been so valuable to the success of this Technical Exchange Conference. I hope to see all of you at Texcon 7.

Security Classification

## DOCUMENT CONTROL DATA - R & D

*(Security classification of title, body of abstract and indexing annotation must be entered when the overall report is classified)*

| | |
|---|---|
| 1. ORIGINATING ACTIVITY (Corporate author)<br>HQ, AIR WEATHER SERVICE (MAC) | 2a. REPORT SECURITY CLASSIFICATION<br>UNCLASSIFIED<br>2b. GROUP |

3. REPORT TITLE
"Automated Weather Support", Proceedings of the Sixth Technical Exchange Conference, Annapolis, Md., Sep 1970.

4. DESCRIPTIVE NOTES (Type of report and inclusive dates)
Technical Report

5. AUTHOR(S) (First name, middle initial, last name)
Authors of separate articles

| | | |
|---|---|---|
| 6. REPORT DATE<br>April 1971 | 7a. TOTAL NO. OF PAGES<br>392 | 7b. NO. OF REFS |
| 8a. CONTRACT OR GRANT NO.<br>b. PROJECT NO.<br>c.<br>d. | 9a. ORIGINATOR'S REPORT NUMBER(S)<br>AWS Technical Report 242<br>9b. OTHER REPORT NO(S) (Any other numbers that may be assigned this report) | |

10. DISTRIBUTION STATEMENT
Approved for Public Release; Distribution Unlimited.

| | |
|---|---|
| 11. SUPPLEMENTARY NOTES | 12. SPONSORING MILITARY ACTIVITY<br>HQ, Air Weather Service |

13. ABSTRACT

Contains the full texts of all presentations and panel discussions given at the Conference, the subject of which was automated weather support and the problems of the "man-machine mix." Sessions with 4 to 6 presentations each were held on Automated Analysis and Forecasting, Local-Area Forecasting, Tailored Meteorological Support, Automated Processing and Application of Satellite Data, Environmental Simulation, and a Panel on Automated Meteorological Support. Authors represented USAF, Navy, Army, ESSA, Rand Corp., NPCA, and University of Oklahoma.

DD FORM 1 NOV 65 1473



UNCLASSIFIED
Security Classification

MAC-8 AFB, IL 71-17799